

ลักษณะเฉพาะทางอัญมณีวิทยาของคอรันด์มจากแหล่งอภิสสารเวลา
พื้นที่อัญมณีรัตนปุระ ประเทศศรีลังกา



นางสาวณัฐภาณี บัวดี

วิทยานิพนธ์นี้เป็นส่วนหนึ่งของการศึกษาตามหลักสูตรปริญญาวิทยาศาสตรมหาบัณฑิต

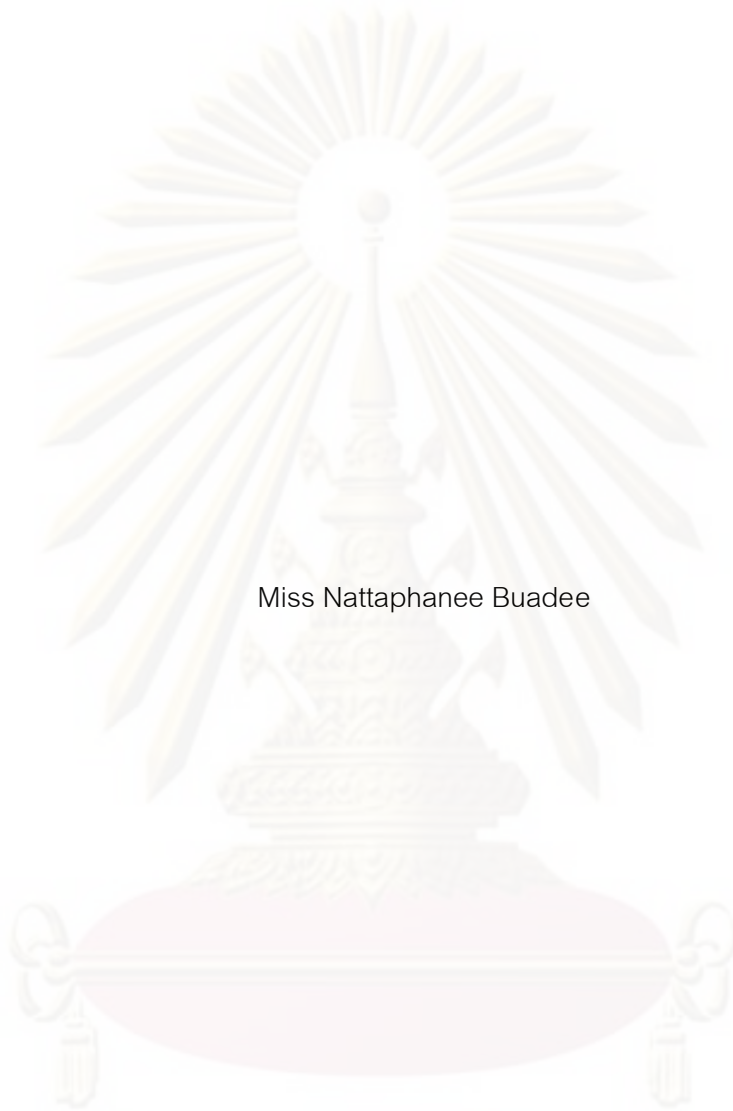
สาขาวิชาธรณีวิทยา ภาควิชาธรณีวิทยา

คณะคณะวิทยาศาสตร์ จุฬาลงกรณ์มหาวิทยาลัย

ปีการศึกษา 2551

ลิขสิทธิ์ของจุฬาลงกรณ์มหาวิทยาลัย

GEMMOLOGICAL CHARACTERISTICS OF CORUNDUM FROM
AWISSAWELLA DEPOSIT, RATNAPURA GEM FIELD, SRI LANKA



Miss Nattaphanee Buadee

A Thesis Submitted in Partial Fulfillment of the Requirements
for the Degree of Master of Science Program in Geology

Department of Geology

Faculty of Science

Chulalongkorn University

Academic Year 2008

Copyright of Chulalongkorn University

Thesis Title GEMMOLOGICAL CHARACTERISTICS OF CORUNDUM
FROM AWISSAWELLA DEPOSIT, RATNAPURA GEM FIELD,
SRI LANKA

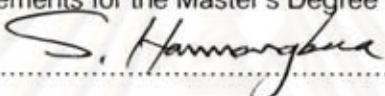
By Miss Nattaphanee Buadee

Field of Study Geology

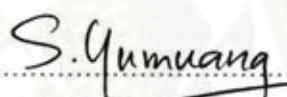
Advisor Assistant Professor Chakkaphan Sutthirat, Ph.D.

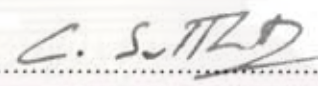
Co-Advisor Associate Professor Visut Pisutha-Armond, Ph.D.

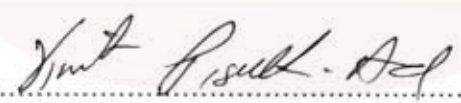
Accepted by the Faculty of Science, Chulalongkorn University in Partial
Fulfillment of the Requirements for the Master's Degree

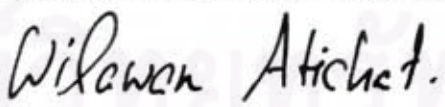
..... Dean of the Faculty of Science
(Professor Supot Hannongbua, Ph.D.rer.nat)


THESIS COMMITTEE

..... Chairman
(Assistant Professor Sombat Yumuang, Ph.D.)

..... Advisor
(Assistant Professor Chakkaphan Sutthirat, Ph.D.)

..... Co-Advisor
(Associate Professor Visut Pisutha-Armond, Ph.D.)

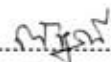


..... External Examiner
(Mrs. Wilawan Atichat)

..... External Examiner
(Mr. Surin Intayot, Ph.D.)

ณัฐภาณี บัวดี : ลักษณะเฉพาะทางอัญมณีวิทยาของคอรัันดัมจากแหล่งอวิสสาเวลลา พื้นที่อัญมณี
รัตนปุระ ประเทศศรีลังกา (GEMMOLOGICAL CHARACTERISTICS OF CORUNDUM FROM
AWISSAWELLA DEPOSIT, RATNAPURA GEM FIELD, SRI LANKA). อ.ที่ปริกษาวิทยานิพนธ์
หลัก: ผศ. ดร.จักรพันธ์ สุทธิรัตน์, อ.ที่ปริกษาวิทยานิพนธ์ร่วม: รศ. ดร.วิสุทธิ พิสุทธิธานนท์ จำนวน
หน้า 100 หน้า.

ปัจจุบันอุตสาหกรรมอัญมณีและเครื่องประดับของไทยมีการนำเข้าพลอยในตระกูลคอรัันดัมเป็นจำนวนมาก
จากหลายแหล่งทั่วโลก โดยประเทศศรีลังกาจัดว่าเป็นแหล่งศักยภาพทางด้านอัญมณี และเป็นที่ยอมรับว่าเป็นแหล่ง
ของทับทิมและแซฟไฟร์ที่มีคุณภาพ ลักษณะทางธรณีวิทยาของประเทศศรีลังกาเป็นส่วนหนึ่งทางตอนใต้ของอนุทวีป
อินเดีย เกิดขึ้นจากการเคลื่อนตัวแยกออกจากกันของแผ่นเปลือกโลกในระดับตื้น ทำให้เกิดเป็นเกาะศรีลังกาที่หินฐาน
ประกอบไปด้วยหินแปรสภาพระดับสูงอายุพรีแคมเบรียน หินฐานของประเทศศรีลังกาแบ่งออกเป็นหน่วยหิน 3 หน่วย
คือ หน่วยหินไฮแลนดคอมเพล็กซ์ หน่วยหินวานนิคอมเพล็กซ์ และหน่วยหินวิจายานคอมเพล็กซ์ แหล่งอวิสสาเวลลา
ตั้งอยู่ทางตะวันออกของกรุงโคลัมโบ ในพื้นที่อัญมณี "รัตนปุระ" ซึ่งเป็นแหล่งอัญมณีที่มีชื่อเสียงของประเทศ โดย
แหล่งอวิสสาเวลลามีความสัมพันธ์กับหน่วยหินไฮแลนดคอมเพล็กซ์

ในการศึกษาครั้งนี้ ตัวอย่างคอรัันดัมจากแหล่งอวิสสาเวลลามีสามารถแบ่งออกเป็น 2 กลุ่ม ตามสีหลักของ
ตัวอย่าง คือ กลุ่มสีเหลือง และกลุ่มสีฟ้า ทั้งสองกลุ่มสีแสดงหย่อมสีสีน้ำเงิน มลทินแร่ที่พบได้แก่ อะพาไทต์ เฟลสปาร์
แคลไซต์ การ์เน็ต ฮีมาไทต์ ไพรอกซีน และไดแอสปอร์ แสดงรูปแบบสเปกตรัมการดูดกลืนรังสีอัลตราไวโอเล็ตถึงอิน
ฟราเรดระยะใกล้ 2 รูปแบบแตกต่างกันตามกลุ่มสี กลุ่มสีเหลืองแสดงสเปกตรัมการดูดกลืนเพิ่มขึ้นอย่างต่อเนื่องไป
ตามช่วงรังสีอัลตราไวโอเล็ต ร่วมกับการดูดกลืนของการแลกเปลี่ยนประจุระหว่างเหล็กสามประจุกับเหล็กสามประจุที่
ตำแหน่ง 450 นาโนเมตร การดูดกลืนของเหล็กสามประจุที่ตำแหน่ง 388 นาโนเมตร และการดูดกลืนของการ
แลกเปลี่ยนประจุระหว่างเหล็กสองประจุกับไทเทเนียมสี่ประจุที่ตำแหน่ง 565 นาโนเมตรซึ่งเกิดจากสีน้ำเงินของหย่อม
สี กลุ่มสีฟ้าแสดงการดูดกลืนของการแลกเปลี่ยนประจุระหว่างเหล็กสองประจุและไทเทเนียมสี่ประจุที่ตำแหน่ง 565
นาโนเมตร การดูดกลืนของเหล็กสามประจุที่ตำแหน่ง 388 นาโนเมตร และการดูดกลืนของโครเมียมสามประจุ
เล็กน้อยที่ตำแหน่ง 412 นาโนเมตรในตัวอย่างที่มีสีฟ้าอมม่วง ผลจากการวิเคราะห์องค์ประกอบธาตุรองรอยโดยการ
วิเคราะห์เชิงคุณภาพ พบว่ามีปริมาณของธาตุเหล็กร้อยละ 0.125 ถึง 0.940 ในกลุ่มสีเหลือง และร้อยละ 0.134 ถึง
0.256 ในกลุ่มสีฟ้า การคำนวณอัตราส่วนอะตอมระหว่างธาตุแมกนีเซียม เหล็ก และไทเทเนียมจากผลการวิเคราะห์
ธาตุรองรอยเชิงปริมาณโดยเครื่องอิเล็กตรอนไมโครโพรบ พบว่าบริเวณสีเหลืองมีปริมาณของธาตุแมกนีเซียมสูง และ
บริเวณที่สีฟ้ามีปริมาณของทั้งสองกลุ่มสีมีปริมาณของธาตุไทเทเนียมและเหล็กสูง โดยมีธาตุแมกนีเซียมมีปริมาณ
ค่อนข้างต่ำ (น้อยกว่าหรือเท่ากับร้อยละ 20) องค์ประกอบและปริมาณของธาตุรองรอยสามารถแยกคอรัันดัมจาก
แหล่งอวิสสาเวลลาออกจากคอรัันดัมที่มีกำเนิดสัมพันธ์กับหินบะซอลต์ได้ และสามารถแยกออกจากคอรัันดัมที่มี
กำเนิดสัมพันธ์กับหินแปรบางแหล่งได้ เช่น คอรัันดัมจากพม่า และซองเกีย พลอยคอรัันดัมจากอวิสสาเวลลามี
ศักยภาพค่อนข้างสูงสำหรับการปรับปรุงคุณภาพสีโดยการเผา กลุ่มสีเหลืองมีสีเหลืองเข้มขึ้นโดยการเผาที่อุณหภูมิ
1,650°C ภายใต้สภาวะบรรยากาศแบบออกซิไดซิง สำหรับตัวอย่างกลุ่มสีฟ้าสามารถเผาได้เป็นสีน้ำเงินโดยการเผาที่
อุณหภูมิ 1,650°C ภายใต้สภาวะบรรยากาศแบบรีดิวซิง

ภาควิชา.....	ธรณีวิทยา.....	ลายมือชื่อนิสิต.....	
สาขาวิชา.....	ธรณีวิทยา.....	ลายมือชื่ออ.ที่ปริกษาวิทยานิพนธ์หลัก.....	
ปีการศึกษา.....	2551.....	ลายมือชื่ออ.ที่ปริกษาวิทยานิพนธ์ร่วม.....	

4872283023 : MAJOR GEOLOGY

KEY WORDS : Awissawella / corundum / deposit / Ratanapura/ sapphire

NATTAPHANEE BUADDEE: GEMMOLOGICAL CHARACTERISTICS OF CORUNDUM FROM AWISSAWELLA DEPOSIT, RATNAPURA GEM FIELD, SRI LANKA. ADVISOR: ASSIST. PROF. CHAKKAPHAN SUTTHIRAT, Ph.D., CO-ADVISOR: ASSOC. PROF. VISUT PISUTHARNOND, Ph.D., 100 pp.

Recently, many gem corundums have been imported from many deposits throughout the world for gem and jewelry industries in Thailand. Among these deposits, Sri Lanka deposits have been very well-known as sources of high quality ruby and blue sapphire. Geologically, Sri Lanka was a southern part of the Indian sub-continent which they appear to have separated due to shallow tectonic movement. Consequently, Sri Lanka Island contains a main basement of highly metamorphosed Precambrian rocks. These basement rocks are subdivided into three major lithological units, namely Highland Complex, Wannu Complex and Vijayan Complex. Awissawella deposit is located on the East of Colombo within the vicinity of "Ratnabura", the most famous gem deposit of the country. These deposits are closely associated with the Highland Complex.

Corundum samples from Awissawella under this study can be divided, on the basis of main body color, into two varieties, i.e., yellow and light blue which both varieties contain blue color patches. Mineral inclusions are apatite, feldspar, calcite, garnet, hematite, pyroxene and diaspore. UV-VIS-NIR absorption spectra show two main different patterns depending on their varieties; yellow variety presents continuous increase of absorption toward the UV region of the spectra with a minor peak of Fe^{3+}/Fe^{3+} pair at 450 nm, Fe^{3+} peak at 388 nm and band of Fe^{2+}/Ti^{4+} pair at 565 nm caused by blue patches. Blue variety usually presents peaks of Fe^{2+}/Ti^{4+} pair at 565 nm, Fe^{3+} peak at 388 nm and small peak of Cr^{3+} at 412 nm in bluish violet samples. Qualitative of trace element analyses show significant Fe_2O_3 contents of 0.125 to 0.940 % in yellow body, 0.134-0.265 % in blue body. Recalculated atomic proportions of quantitative EPMA analyses plotted in a Mg-Fe-Ti ternary diagram show that yellow components are mostly rather high Mg contents whereas blue component in both varieties have high Ti and Fe contents with low Mg contents ($\leq 20\%$). Awissawella corundum samples could be separated based on trace element proportions, from basaltic corundums and some metamorphic corundums such as Myanmar and Songea. Regarding to heating experiments, these corundums have high potential to improve their colors. Yellow variety appear to be intensified by heating at $1,650^{\circ}C$ in oxidizing atmosphere; on the other hand, blue variety can be increased their blue shades by heating at $1,650^{\circ}C$ in reducing atmosphere.

Department : Geology

Student's Signature *Nattaphanee*

Field of Study : Geology

Advisor's Signature *C. S. Thirath*

Academic Year : 2008

Co-Advisor's Signature *Visut Pisutharnond*

ACKNOWLEDGEMENTS

First of all, the author would like to express my sincerest gratitude to my thesis advisor, Assistant Professor Dr. Chakkaphan Sutthirat, Associate Professor Dr. Visut Pisutha-Arnond my co-advisor, for his invaluable advice and supervision throughout the completion of this thesis. Thanks are also extended to, Dr. Surin Inthayot and Ms. Wilawan Atichat: The Director of The Gem and Jewelry Institute of Thailand (Public Organization): GIT for being members of the thesis committee whose comments are especially helpful.

The author sincerely appreciates the Department of Geology, Faculty of Science, Chulalongkorn University for providing sample preparation, electric furnace and Electron Probe Micro-Analyzer (EPMA). And also The Gem and Jewelry Institute of Thailand (Public Organization): GIT for the providing to use laboratory instruments, i.e., Gemological Microscope, Energy Dispersive X-ray Fluorescence Spectrometer (EDXRF) and UV-VIS-NIR Spectrometer etc. The author is very grateful the staff of the GIT Lab for their assistance: Mr. Thanong and Ms. Thitinthree Leelawatanasuk, Miss Sureeporn Pumpeng, Miss Chaniya Somboon and Miss Numravee Susavee. Financial support for this research has been provided by the The Gem and Jewelry Institute of Thailand (Public Organization): GIT.

Finally, specially would like to thank to my family and Mr. Surachat for their kind assistance encouragement and social support.

ศูนย์วิทยทรัพยากร

จุฬาลงกรณ์มหาวิทยาลัย

CONTENTS

	Page
Abstract (Thai).....	iv
Abstract (English).....	v
Acknowledgements.....	vi
Contents.....	vii
List of Tables.....	ix
List of Figures.....	xi
CHAPTER I Introduction.....	1
1.1 General statement.....	1
1.2 Objectives of study.....	3
1.3 Methodology.....	3
1.4 Analytical Techniques.....	6
CHAPTER II Geography, Geology and Gem Deposits of Sri Lanka.....	14
2.1 Geography.....	14
2.2 General Geology.....	15
2.3 Metamorphic Complexes.....	18
2.4 Gem Deposits.....	21
2.5 Awissawella Deposit.....	39
CHAPTER III Awissawella corundum and general characteristics.....	43
3.1 Introduction.....	43
3.2 Color.....	44
3.3 Physical and Gemological properties.....	45
CHAPTER IV Absorption Spectra and Trace Element contents.....	47
4.1 Introduction.....	47
4.2 Fourier Transform Infrared Spectrometry.....	48
4.3 UV-VIS-NIR Spectrometry.....	51
4.4 Semi-Quantitative EDXRF Analyses.....	55
4.5 Quantitative EPMA Analyses.....	57

	Page
CHAPTER V Internal features & Mineral inclusions	64
5.1 Identification.....	64
5.2 Mineral Chemistry.....	69
CHAPTER VI Experimental Heat Treatment	71
6.1 Introduction.....	71
6.2 Color Appearance.....	72
6.3 UV-VIS-NIR Spectra.....	75
6.4 Fourier Transform Infrared Spectra.....	81
CHAPTER VII Discussion and Conclusions	84
7.1 Gem Characteristic and Geographic Origin.....	84
7.2 Potential for Heat Treatment	91
7.3 Conclusions.....	92
References.....	94
Biography.....	100
Appendixes.....	CD
Appendix A) Physical properties and optical properties of Awissawella corundums.....	CD
Appendix B) FTIR spectra of unheat corundums from Awissawella.....	CD
Appendix C) UV-VIS-NIR absorption spectra of unheat Awissawella corundums.....	CD
Appendix D) Chemical composition of Awissawella corundums, obtained by EDXRF.....	CD
Appendix E) Major and Trace element contents of the Awissawella corundums, obtained by EPMA.....	CD
Appendix F) Triangular diagram of atomic proportions between Mg, Ti and Fe of Awissawella corundums.....	CD
Appendix G) UV-VIS-NIR & FTIR spectra after heat treatment of Awissawella corundums.....	CD

LIST OF TABLES

Tables		Page
1.1	Thailand export statistics of precious stones and semi-precious stones in January- December, 2007. (GIT, 2008).....	2
2.1	Chronology of basement rocks in Sri Lanka (Kröner et al., 1991).....	19
2.2	Key gem minerals of Sri Lanka listed by locality. Topographic sheet numbers are keyed to those shown on Figure 2.9 (Dissanayake and Rupasinghe, 1993).....	25
3.1	Summary of physical properties of representative corundum samples from Awissawella, Sri Lanka.....	46
3.2	Summary of optical properties of yellow and light blue sapphire varieties from Awissawella, Sri Lanka.....	46
4.1	Absorption features of chromophores in Awissawella corundum (modified from Themelis, 1992).....	54
4.2	Statistic EDXRF analyses of trace elements contained in Awissawella sapphire samples obtained from model OXFORD, ED 20000.....	55
4.3	Statistic EDXRF analyses of trace elements contained in Awissawella sapphire samples obtained from model EAGLE III.....	56
4.4	Statistics of EPMA analyses of Awissawella sapphire samples obtained from quantitative EPMA and their recalculated atomic portion based on 3(O).....	59
5.1	EPMA analyses of some mineral inclusions found in Awissawella corundums.....	69
5.2	Summary of internal features and mineral inclusions found in each variety of Awissawella corundums under this study.....	70
6.1	Color shades of Awissawella sapphire samples in comparison between before and after heat in oxidizing atmosphere.....	73
6.2	Color shades of Awissawella sapphire samples comparison between before and after reducing heat treatment.....	75

Tables	Page
7.1 Summary of mineral inclusions found in corundums from Awissawella and other metamorphic corundum deposits.....	85
7.2 Trace elements of Awissawella sapphire samples in comparison with those of basaltic and metamorphic sapphires elsewhere. Numbers of samples are present in parentheses.....	88



ศูนย์วิจัยทรัพยากร
จุฬาลงกรณ์มหาวิทยาลัย

LIST OF FIGURES

Figures	Page
1.1	Flowchart showing methodology of this research project..... 6
1.2	Basic gem equipments, including 1. Refractometer, 2. Ultraviolet lamps, 3. Electronic balance and 4. Gemological microscope, all based at the GIT..... 7
1.3	GIA Gem Set belonging to the GIT used for color coding of the sample. 7
1.4	Laser Raman Spectroscope (Model Invia, Ranishaw) belonging to the GIT..... 8
1.5	Hitachi UV-VIS-NIR Spectrophotometer (Model U-4001) based at the GIT.. 9
1.6	UV-VIS-NIR Spectrometer (Model Lambda 950) based at the GIT..... 9
1.7	FTIR Spectrometer (NEXUS 670) based at GIT..... 10
1.8	OXFORD EDXRF spectrometer (model ED 2000) based at the GIT..... 10
1.9	EDXRF spectrometer (model EAGLE III) based at the GIT..... 11
1.10	JEOL Electron Probe Micro-Analyzer (model JXA-8100) based at the Department of Geology, Faculty of Science, Chulalongkorn University... 12
1.11	Three to six samples of Awissawella sapphires are set in resin block for EPMA analyses..... 12
1.12	Linn electrical furnace model HT 1800 Plus VAC Bottom Loader based at the Department of Geology, Faculty of Science, Chulalongkorn University..... 13
2.1	Map of Sri Lanka, show locations of island in the Indian Ocean south-east of India (available from www.sjr.mb.ca/ms/geo/countries/sri/img18.gif)..... 14
2.2	Section across the central part of Sri Lanka showing three distinctive peneplains (Zoysa, 1981)..... 15

Figures	Page	
2.3	Gondwana assembly reconstruction showing location of Pan-African events. Older cratonic blocks of West Gondwana and possible outboard terrains. Pan-African belt: <i>B</i> , Brasiliano; <i>DF</i> , Dom Feliciano; <i>D</i> , Damara; <i>G</i> , Gariiep belt; <i>K</i> , Kaoko belt; <i>L</i> , Lufilian arc; <i>LH</i> , Lützow-Holm Bay; <i>MD</i> , Madagascar; <i>Y</i> , Yamato mountains; <i>R</i> , Ross orogen; <i>S</i> , Saldanian belt; <i>SH</i> , Shackleton Range; <i>SL</i> , Sri Lanka; <i>SR</i> , Sor Rondane mountains; <i>Z</i> , Zambezi belt. Other features: <i>EM</i> , Ellsworth-Whitmore mountains; <i>QML</i> , Queen Maud Land; <i>SF</i> , São Francisco craton (Dissanayake and Chandrajith, 1999).....	16
2.4	The juxtaposition of Sri Lanka, the southern tip of India and Madagascar (encircled) in Gondwana. The central shaded belt indicates the mineral belt within the geosuture (Dissanayake and Chandrajith, 1999).....	17
2.5	Simplified and generalized geological map of Sri Lanka showing major lithotectonic units (Dissanayake and Chandrajith, 1999). The dashed line gives only the proposed boundary.....	19
2.6	Map of Sri Lanka showing the main lithotectonic units and the gem fields studied. The boundary between the Highland Complex and Wannu Complex is uncertain and is denoted by a broken line. The numbered sequences represent the topographic sheets. The palaeopressure contours of the Highland Complex of Sri Lanka in relation to the locations of the gem fields are also shown (Dissanayake and Rupasinghe, 1993).....	23
2.7	A Prospector's Guide Map to Gem Deposits of Sri Lanka. Areas are categorized as "highly probable", "probable", "poor", and "no deposit" on the gem potential (Dissanayake and Rupasinghe, 1993).....	24
2.8	Classification of gem deposits in Sri Lanka with an example of location in each different type (modified after Dissanayake et. al, 2000).....	27

Figures	Page
2.9 The Elahera gem field in northeastern Sri Lanka is noted for its vast production of many gemstone varieties. The main gem mining activity is between the 19- and 24-mile posts (Gunawardene and Rupasinghe, 1986).....	28
2.10 Geological map of the Elahera gem field (Dissanayake and Chandrajith, 1999).....	29
2.11 Geology of the Bakamuna area and the detailed geology of the skarn deposit (Dissanayake et. al, 2000).....	29
2.12 Schematic cross section showing different modes of occurrence of gemstones (Henny, 1999).....	32
2.13 Geological map of the main Ratnapura gem field. Inset shows the location of the Ratnapura and Elahera gem fields in relation to the main lithotectonic units of Sri Lanka (Dissanayake and Chandrajith, 1999).....	35
2.14 A schematic E-W cross section of the Okkampitiya area indicating occurrences of karstic potholes, blind shafts and channels. The enlargements are schematic representations of sedimentary infill in karstic potholes located on the gentle slope (A), on the flood plain (C) and a bifurcating channel (B) (Mathavan et. al, 2000).....	37
2.15 A mined karstic channel in the marble of Okkampitiya gem field (Mathavan et. al, 2000).....	38
2.16 Map of Sri Lanka (Ceylon) showing the location of the important cities, mining areas and Ratnapura gem field including Awissawella, that is located in the Highland South Western Complex. (modified from www.palagems.com/ceylon_sapphire_bancroft.htm).....	40
2.17 Awissawella deposit located close to the mountain which is possible primary source of corundum.....	41
2.18 Mining pits in Awissawella deposit operated by local miners.....	41
2.19 Rock fragments and mineral assemblages, mainly quartz, contained in gravel beds.....	41

Figures	Page
2.20 (a) and (b) Geode-like gravels found in gravel bed that contain corundum; (c) corundum samples and other minerals found in geode-like gravels.....	42
3.1 Corundum sample batch from Awissawella, Sri Lanka.....	43
3.2 Crystal habits in some sapphires from Awissawella.....	44
3.3 Different body colors in yellow variety of samples in which their color codes are based on the GIA Gem Set.....	45
3.4 Different body colors in light blue variety of samples in which their color codes are based on the GIA Gem Set based on the GIA Gem Set.....	45
4.1 FTIR Spectrum of SapAw_13 of yellow variety shows common absorption pattern.....	49
4.2 FTIR Spectrum of SapAw_23 of yellow variety showing declined curve within 3200-3700 cm^{-1} along with strong absorption around 3309 cm^{-1} ...	49
4.3 FTIR Spectrum of SapMa_01 of light blue variety showing declined curve within 3200-3700 cm^{-1} along with strongly absorption curve of C-H stretching	50
4.4 FTIR Spectrum of SapMa_03 of light blue variety shows common absorption pattern	50
4.5 UV-VIS-NIR spectra yellow (SapAw_06) in yellow variety (color code Y2/2) showing absorption peaks due to $\text{Fe}^{3+}/\text{Fe}^{3+}$ pairs and Fe^{3+} at 450 and 388 nm, respectively; besides, blue patch may yield absorption bands due to $\text{Fe}^{2+}/\text{Ti}^{4+}$ IVCT with the maxima about 565 nm.....	52
4.6 UV-VIS-NIR spectra greenish yellow (SapAw_11) in yellow variety (color code gY3/4) showing absorption peaks due to $\text{Fe}^{3+}/\text{Fe}^{3+}$ pairs and Fe^{3+} at 450 and 388 nm, respectively; besides, its light greenish yellow with blue patch may cause absorption bands due to $\text{Fe}^{2+}/\text{Ti}^{4+}$ IVCT with the maxima about 565 nm.....	52

Figures	Page
4.7 UV-VIS-NIR spectra yellow green (SapAw_16) in yellow variety (color code YG/GY 2/1) showing absorption peaks due to $\text{Fe}^{3+}/\text{Fe}^{3+}$ pairs and Fe^{3+} at 450 and 388 nm, respectively; besides, its yellow green with blue patch may cause absorption bands due to $\text{Fe}^{2+}/\text{Ti}^{4+}$ IVCT with the maxima about 565 nm.....	53
4.8 UV-VIS-NIR spectra blue (SapMa_05) in blue variety (color code B5/2) showing of absorption peaks at 388 and 450 nm due to of Fe^{3+} and $\text{Fe}^{3+}/\text{Fe}^{3+}$ pairs, respectively and present of strong absorption band with peaks of $\text{Fe}^{2+}/\text{Ti}^{4+}$ IVCT with maxima at 565 nm is main cause of blue color.....	53
4.9 UV-VIS-NIR spectra violet blue (SapMa_04) in blue variety (color code vB4/3) showing absorption peaks at 388 nm of Fe^{3+} , 377 and 450 nm of $\text{Fe}^{3+}/\text{Fe}^{3+}$ pairs; besides, strong absorption bands with maxima at 565 nm of $\text{Fe}^{2+}/\text{Ti}^{4+}$ IVCT causing blue color are also observed.....	54
4.10 Average of trace elements revealed as symbols obtained by EDXRF and their standard deviations in form of lines.....	57
4.11 Different areas selected for EPMA analyses: (a) Yellow sapphire variety containing yellow body and blue patch zones; (b) Blue sapphire variety with light blue body and blue patch zones.....	58
4.12 Model representing the interaction of trace elements in the system Al-Mg-Fe-Ti (tetrahedron). Sapphires of this composition were heat treated at 1850°C in an oxidizing atmosphere (a) and at 1750°C in a reducing atmosphere (b), Häger (2001).....	62
4.13 Mg-Fe-Ti ternary diagram of 33 yellow variety samples with analyses of two different color zones including 145 points of yellow body and 174 points of blue patch.....	63
4.14 Mg-Fe-Ti ternary diagram of 13 light blue variety samples with two different color zones including 57 points of light blue body and 36 points of blue patch.....	63

Figures	Page
5.1 Cloud inclusions along growth plane in sample SapAw_01 of yellow variety.....	64
5.2 Fingerprints in samples SapAw_03 of yellow variety.....	64
5.3 Negative crystals in sample SapAw_03 of yellow variety.....	65
5.4 Crystal inclusion (apatite) in sample SapAw_09 of yellow variety.....	65
5.5 Opaque mineral (hematite) in sample SapAw_09 of yellow variety.....	65
5.6 Iron-stained fractures and growth line in sample SapMa_05 of light blue variety.....	65
5.7 Raman spectrum of calcite inclusion in sample SapAw_01 of yellow variety with peaks at 1088, 714 and 283 cm^{-1}	66
5.8 Raman spectrum of apatite crystal in sample SapAw_16 of yellow variety with peaks at 963, 580, 448, 430 and 418 cm^{-1}	66
5.9 Raman spectrum of feldspar crystal in sample SapMa_02 present peaks at 1122, 769, 509 and 284 cm^{-1}	67
5.10 Raman spectrum of feldspars inclusion in sample SapMa_03 present peaks at 1122, 769, 509 and 284 cm^{-1}	67
5.11 Raman spectrum of hematite inclusion in sample SapMa_02 present peaks at 1332 and 631 cm^{-1}	68
5.12 Raman spectrum of diaspore inclusion in sample SapMa_06 present peaks at 795, 665, 495 and 446 cm^{-1}	68
6.1 Awissawella corundum samples before and after heating at 1650 $^{\circ}$ C in oxidizing condition; (A) yellow variety (representation of 18 samples), (B) light blue variety (only sample available).....	72
6.2 Awissawella corundums before and after heating at 1650 $^{\circ}$ C in reducing condition; (A) yellow variety (representation of 4 samples), (B) light blue variety (representation of 11 samples).....	74
6.3 UV-VIS spectra (o-ray) of the sample SapAw_21 measured before and after heating experiment at 1,650 $^{\circ}$ C in O ₂ atmosphere for 10 hours soaking time.....	77

Figures	Page
6.4 Residue spectrum of the sample SapAw_21 obtained by subtracting the spectra before heat from that after the experiment as shown in Figure 6.3.....	77
6.5 UV-VIS spectra of the sample SapMa_06 measured before heating experiment. Note the presence of absorption peaks at 450 nm caused by Fe^{3+}/Fe^{3+} pairs are always present along with 388 nm peak of Fe^{3+} and 565 nm peak of Fe^{2+}/Ti^{4+} IVCT band causing of blue color.....	78
6.6 UV-VIS spectra of the sample SapMa_06 after heating experiment at 1,650°C in O_2 atmosphere for 10 hours soaking time. Note the presence of decrease absorption peaks around 565 nm peak of Fe^{2+}/Ti^{4+} IVCT process.....	78
6.7 UV-VIS spectra (o-ray) of the sample SapAw_08 of yellow variety (color code gY2/3) measured before and after heating experiment at 1,650°C in N_2 atmosphere for 5 hours soaking time.....	79
6.8 Residue spectrum of the sample SapAw_08 obtained by subtracting spectra before and after heating experiment as shown in Figure 6.7.....	79
6.9 UV-VIS spectra (o-ray) of the sample SapMa_12 of light blue variety (color code vB3/3) measured before and after heating experiment at 1,650°C in N_2 atmosphere for 5 hours soaking time.....	80
6.10 Residue spectrum of the sample SapMa_09 obtained by subtracting the spectra before and after heating experiment as shown in Figure 6.9.....	80
6.11 FTIR spectra of SapAw_13 of yellow variety before and after heating in oxidizing environment at 1,650°C show disappearance of O-H stretching peak at about 3309 cm^{-1} after heat.....	82
6.12 FTIR spectra of SapMa_06 of light blue variety before and after heating in oxidizing environment at 1,650°C show decreased intensities of CO_2 and C-H stretching absorption peaks after heat.....	82

Figures	Page
6.13 FTIR spectra of SapAw_04 of yellow variety before and after heating in reducing environment at 1,650°C show deduction of O-H stretching peak at about 3309 cm ⁻¹ after heat.....	83
6.14 FTIR Spectra of SapMa_03 of light blue variety before and after heating in reducing environment at 1,650°C show deducted intensity of absorption peaks after heat.....	83
7.1 FTIR spectra comparing between yellow and light blue varieties. (a) FTIR spectra of yellow variety show O-H stretching peak at about 3309 cm ⁻¹ which disappeared after heat treatment. (b) FTIR spectra of light blue variety show the non-existence of such O-H stretching peak either natural or heated stones.....	86
7.2 Plotting Fe ₂ O ₃ + TiO ₂ versus Ga ₂ O ₃ trace composition of Awissawella sapphires samples and sapphires from other basaltic and metamorphic origins.....	89
7.3 Plots of Fe ₂ O ₃ versus Ga ₂ O ₃ of Awissawella sapphire samples and some sapphire with basaltic and metamorphic sapphire.....	90
7.4 Plotting between Fe ₂ O ₃ /Cr ₂ O ₃ and TiO ₂ /Ga ₂ O ₃ of Awissawella sapphire samples, other sapphires in Sri Lanka and some Myanmar and Songea sapphires.....	90
7.5 Trace composition plotting between Fe ₂ O ₃ /Cr ₂ O ₃ and TiO ₂ /Ga ₂ O ₃ of Awissawella sapphires, other Sri Lanka sapphires and some Madagascar sapphires.....	91

CHAPTER I

INTRODUCTION

1.1 General Statement

Nowadays, gem and jewelry industries of Thailand have grown up rapidly; precious and semi-precious stones made income over twelve thousands million baht in 2007 (GIT, 2008; see Table 1.1). Because of such strong growth as well as the fact that there was a rapid reduction of gem resources in the country during the last few decades, rough gem materials from all over the world have to be imported for enhancing, cutting and setting in jewelry before exporting to the world market. Among the important colored stones, corundums (ruby and sapphire) are the most popular gemstones which have been used for jewelry and ornament worldwide. This is an important factor for development of gem and jewelry industry in the country. Many corundum deposits have been discovered around the world. Among these gem deposits, the island of Sri Lanka, often referred as “Jewel Box” of the Indian ocean, still has high potential of new gem deposits although it has long been a major producer of fine-quality gemstones (e.g., corundum, chrysoberyl, zircon, garnet, spinel, topaz, beryl, moonstone, tourmaline, quartz and peridot) for some decades. Therefore, Sri Lanka is an interesting source of gem market and also gemological research.

The major gem locality of Sri Lanka is Ratanapura gem field. Many mining activities have been operated, mostly small scale by local miners, spreading around the area. Recently, Awissawella becomes a new corundum (mostly sapphire) mining area of Ratanapura gem field. However, gem research of this deposit has not been published prior to initiation of this research. This research project was designed to characterize gemological properties of corundum, mostly sapphire, from Awissawella deposit that is very beneficial information for gems industry. Gemological laboratory can applied some information gained from this study to distinguish geographic origin of sapphire that is becoming very hot issue in the international gem trade nowadays. In addition, results of

experimental heat treatment reported herein may lead to reduction of loss in industrial treatment of these sapphires.

Table.1.1 Thailand export statistics of precious and semi-precious stones in January-December, 2007. (GIT, 2008)

Seq.no.	Country	Jan-Dec 2007	
		Value	%
1	United States	3,476,320,385.00	27.14
2	Hong Kong	3,475,563,727.00	27.13
3	India	1,313,861,086.00	10.26
4	Japan	956,658,158.00	7.47
5	Switzerland	848,447,406.00	6.62
6	Italy	333,506,454.00	2.60
7	United Kingdom	324,235,646.00	2.53
8	Germany	259,750,510.00	2.03
9	France	242,596,645.00	1.89
10	Austria	205,674,545.00	1.61
11	Singapore	188,440,893.00	1.47
12	Russian Federation	167,625,323.00	1.31
13	United Arab Emirates	108,748,115.00	0.85
14	Australia	91,962,572.00	0.72
15	Belgium	84,654,273.00	0.66
16	Spain	77,510,789.00	0.61
17	Sri Lanka	74,564,411.00	0.58
18	Israel	70,590,518.00	0.55
19	Cayman Island	62,836,029.00	0.49
20	Canada	56,212,713.00	0.44
21	Vietnam	45,200,463.00	0.35
22	Korea	42,496,624.00	0.33
23	Malaysia	37,884,166.00	0.30
24	Ukraine	35,973,878.00	0.28
25	Lebanon	28,643,109.00	0.22
	Others	199,183,972.00	1.56
	Total	12,809,142,410.00	100.00

1.2 Objectives

Two main objectives were set for this study as following.

1.2.1 To characterize particularly physical properties and internal features of corundum (sapphire) samples from Awissawella deposit, Ratnapura gem field, Sri Lanka

1.2.2 To enhance experimentally the sapphire samples using high temperature furnace.

The study was carried out using both basic and advanced gem-testing instruments. All detailed gemological characteristics were collected such as crystal habit, specific gravity, refractive indices, internal features, absorption spectra and chemical compositions. Results gained from the study are compared to those of other significant localities. Subsequently, characteristics of Awissawella sapphire are pointed out. Perhaps, some characteristics may lead to the understanding of their genesis. In addition, heat treatment and altered features after heating of some samples are additionally included to gain information for the gem industry.

1.3 Methodology

The method of study was consequently designed to reach the target; that can be summarized in Figure 1.1 and described below. Reports of each step are revealed within Chapters II to VII based on appropriated aspects. In addition, introductory of this research project is already described herein this chapter.

1. Literature Reviews: Geology, corundum deposits, corundums in Ratnapura gem fields and other gemological researches of Sri Lanka were initially reviewed. This information gives basic knowledge on geologic setting related to gem genesis, distribution of corundum deposit of the country. It actually led to research plan and experimental design throughout the project and critical discussion in the final part. Crucial information summarized from this step is reported in Chapter II.

2. Samples Collection: All corundum samples from Awissawella were bought directly from the local miners in area which detailed description of the area is reported in

Chapter II. Subsequently, these samples were picked up particularly based on their shape and transparency. In fact, most samples have euhedral crystal.

3. Samples Preparation and Color Grouping: Each rough sample was marked its c-axis observed directly from the crystal form and also using a polariscope before cutting and surface polishing perpendicular and parallel to the c-axis. The polished samples were then taken to the further determination and analyses. Subsequently, prepared samples can be divided in 2 main body varieties, i.e., yellow and light blue as fully described in Chapter III.

4. Determination of Physical and Optical Properties: All polished samples were weighed, photographed, giving color codes by comparison with GIA Gem Set color chart (see Figure 1.3); besides, the basic physical and optical properties were measured initially to confirm the corundum properties of all samples. These basic properties include refractive indices (RI) measured by refractometer, specific gravity (SG) using an electronic balance, color observed under daylight lamp and fluorescence under long wave ultraviolet light (LWUV, 365 nm) and short wave ultraviolet light (SWUV, 254 nm). All of these properties are also reported in Chapter III.

5. Investigation of Internal Features: Internal features were observed firstly under microscope (Figure 1.2) before taking photos and identification of mineral inclusions. Mineral inclusions exposed close to the sample surface were subsequently identified using Laser Raman Spectroscopy (Figure 1.4). In addition, some mineral inclusions were chemically analyzed using Electron Probe Micro-Analyzer (EPMA). All analytical results of internal feature and mineral inclusions are given in Chapter V.

6. Absorption Spectroscopy: Absorption spectra were obtained from Ultraviolet-Visible-Near Infrared (UV-VIS-NIR) spectrophotometer and Fourier Transform Infrared (FTIR) spectrophotometer. The UV-VIS-NIR absorption patterns can indicate causes of color in the samples both before and after heat treatment besides they sometimes support identification of geographic origin. Regarding to FTIR spectroscopy, its information may be useful for identification of heat treatment and investigation of invisible particle embedded as well as chemical bonding in the stone. In this study,

absorption spectra UV-VIS-NIR and FTIR were analyzed for all polished unheated samples. In addition, some samples selected for heat treatment were analyzed absorption spectra from before and after heating for comparison between unheated and heated characteristics in these stones. Therefore, absorption spectroscopy is present in Chapters IV and VI which report on natural properties and treated properties, respectively.

7. Trace Geochemistry: The samples were semi-quantitatively analyzed for major element (Al_2O_3) and particular trace elements (e.g., Fe_2O_3 , TiO_2 , Cr_2O_3 , V_2O_3 and Ga_2O_3) using an Energy Dispersive X-Ray Fluorescence (EDXRF) Spectrometer. In addition, quantitative analyses were carried out using Electron Probe Micro-Analyzer (EPMA) which can perform on the samples in small specific color zones individual samples. EDXRF analyses are actually used to compare with corundums from elsewhere that is more likely suitable for the gem testing laboratory under consideration of geographic origin. On the other hand, quantitative trace elements (EPMA analyses) are used to interpret more specific aspects such as causes of color and potential to enhancement. However, EPMA trace analyses can also be used for aspect of geographic origin if data is available. Most of the trace geochemical analyses are reported in Chapter IV; however, part of the information used for discussion in Chapter VII particularly for the aspect of color cause.

8. Experimental Heat Treatment: Heat treatment experiment was carried out to get additional information that would be useful for the gem industry. The experiment was set using optimum conditions that have been reported by previous researchers which peak temperature was set at 1650°C for both oxidizing and reducing atmospheres. Detailed procedure and result obtained from the experiment are reported and discussed in Chapter VI.

9. Discussions and Conclusions: Consequently, discussions in crucial aspects to serve all objectives are made using data obtained from the research as well as literature. These are included in the last chapter of this report.

10. *Final Report*: Finally, the research report is written and submitted to the department as mentioned above. In addition, a few publications are prepared for conference and journal.

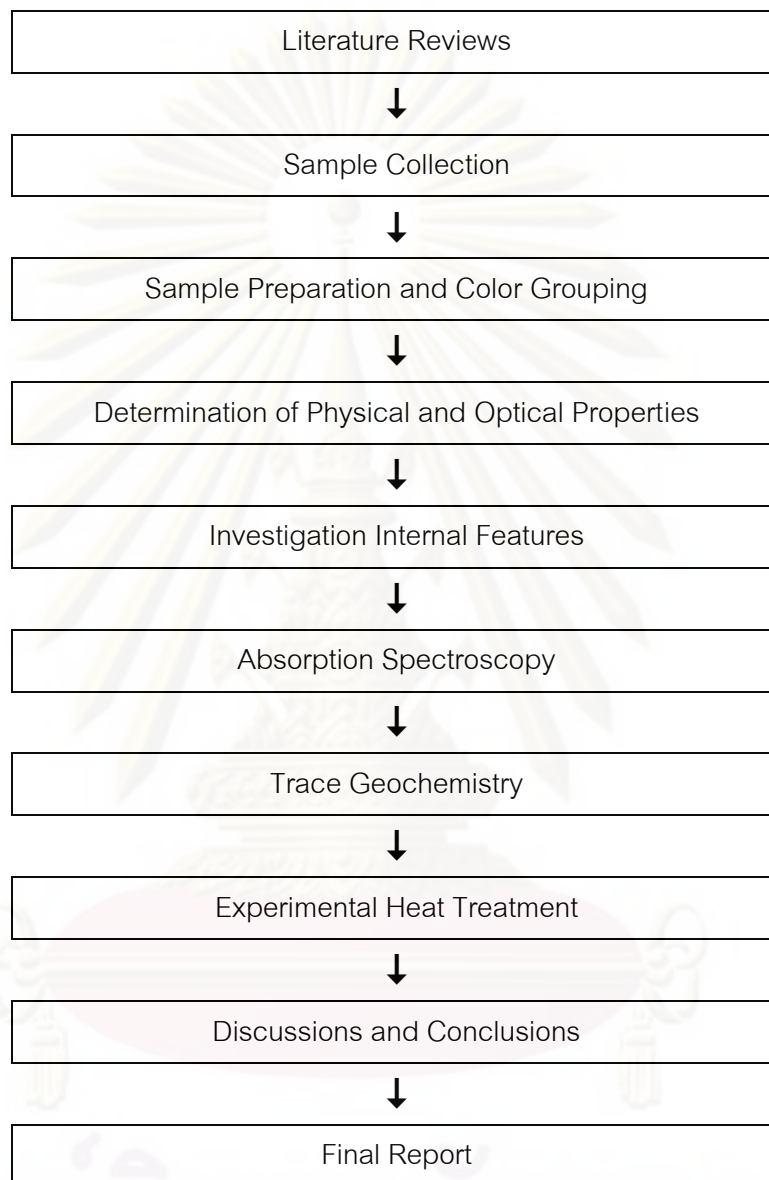


Figure 1.1 Flowchart showing methodology of this research project.

1.4 Analytical Techniques

1. *Basic Gem Equipments*: Physical and optical properties of sapphire samples were collected using the basic gem equipments including refractometer, ultraviolet lamps both long wave (LW) or short wave (SW), electronic balance and gemological

microscope (Figure 1.2). These equipments are based at the Gem and Jewelry Institute of Thailand (GIT).



Figure 1.2 Basic gem equipments, including 1. refractometer, 2. ultraviolet lamps, 3. electronic balance and 4. gemological microscope, all based at the GIT.

2. *GIA Gem Set*: Color of each sapphire sample was coded by comparison with the GIA Gem Set (Figure 1.3) made from colored plastic that has different sides, faceted and flat. The flat side was used during this study because it is more appropriated for polished surface of sapphire samples.



Figure 1.3 GIA Gem Set belonging to the GIT used for color coding of the sample.

3. *Laser Raman Spectroscope*: model Invia, Ranishaw attached with high resolution microscope (Figure 1.4) based at the GIT is engaged to identify mineral inclusions found in the studied samples. Raman spectroscopy is a result of vibrational phenomena of molecular structure activated by light energy. The principal of vibrational spectroscopy is interaction between electrical field associated with photon and changes

induced by vibrational movements in electronic charges distribution within the substance. Raman spectroscopy has been introduced as an analytical tool for mineral identification without preparation. However, it cannot distinguish clearly some mineral inclusions that set deep into sapphire samples. The best result is obtained from mineral inclusions that are exposed or very close to the surfaces of samples.



Figure 1.4 Laser Raman Spectroscope (Model Invia, Ranishaw) belonging to the GIT.

4. *Ultraviolet-Visible Light-Near Infrared (UV-VIS-NIR) Spectrometer*: contains a monochromatic light source generating wavelengths over the range of ultraviolet (UV), visible light (VIS) and near infrared (NIR). Absorption spectra are detected with the photocell and then signal is transferred to display on the monitor. This instrument has double beams. A beam of light is switched between a reference path and a sample path, which are re-combined at the detector, which thus compares the two beams. The signal from the reference path is subtracted from that of the sample path to give a spectrum of the sample. UV-VIS-NIR absorption spectrum may be related to electron transitions of trace elements or other structural defects in sapphires. For this research project, the absorption spectra in UV-VIS-NIR region samples were obtained from the HITACHI UV-VIS-NIR spectrophotometer, model U-4001 (Figure 1.5) and UV-VIS-NIR Spectrometer, Model Lambda 950 (Figure 1.6) which both are based at the GIT. The oriented sample was fixed in the middle of the black plate with 2-2.5 mm diameter slit

and placed into the cell holder. Each sample was measured perpendicular to c-axis for ordinary ray (o-ray) by using polarizing filter.



Figure 1.5 Hitachi UV-VIS-NIR Spectrophotometer (Model U-4001) based at the GIT.



Figure 1.6 UV-VIS-NIR Spectrometer (Model Lambda 950) based at the GIT.

5. *Fourier Transform Infrared (FTIR) Spectrometer*: can be used for recording the absorption or transmission spectra in the range of near to far infrared. The infrared spectra give information about the structures and specific bonding in mineral specimen, such as O-H stretching. Infrared absorption spectra under this study were obtained from FTIR Spectrometer model NEXUS 670 (Figure 1.7) based at the GIT.



Figure 1.7 FTIR Spectrometer (NEXUS 670) based at the GIT.

6. *Energy Dispersive X-ray Fluorescence (EDXRF) Spectrometer*: is a nondestructive analysis method. This technique is an application on energy emission of electrons in atoms. These electrons are excited by X-ray and then they move to the higher energy levels in their own atoms or may be ejected away from their atoms. Subsequently, electrons in the higher energy level will replace the lost electrons; this process must emit energy in particular range. Each element has different atomic weight that leads to dissimilar energy level. Therefore, those different energies can be utilized for determination of chemical constituent of material. Semi-quantitative analyses of major element (Al_2O_3) and trace elements (i.e., Fe_2O_3 , TiO_2 , Cr_2O_3 , V_2O_5 and Ga_2O_3) in sapphire samples were obtained using two EDXRF machines, OXFORD model ED2000 and model EAGLE III at the GIT (Figures 1.8 and 1.9).



Figure 1.8 OXFORD EDXRF spectrometer (model ED 2000) based at the GIT.



Figure 1.9 EDXRF spectrometer (model EAGLE III) based at the GIT.

7. *Electron Probe Micro-Analyzer (EPMA)*: is a quantitatively analytical method which is able to analyze within a certain tiny area in micrometer scale. The electron beam is focused on the surface of a sample and activates electrons around the analytical area; consequently, characteristic X-rays of the sample are produced. The characteristic X-rays are detected at specific wavelengths using appropriate crystals in multiple channels. Intensities of peak count are measured along with back ground before determination of individual element concentrations under automatic ZAF correction. JEOL EPMA (model JXA-8100) (Figure 1.10) based at Department of Geology, Faculty of Science, Chulalongkorn University was engaged for chemical analyses of major and trace compositions of host sapphire sample and major and minor elements of some mineral inclusions found in the sapphire. For trace analyses (including major Al composition) of the sapphire host, condition was set at 20 kV with beam current of about 2.2×10^{-8} A using 2 μm beam with measuring times of 50 seconds for peak count and 20 seconds for background. On the other hand, analytical condition for mineral inclusion was set at 15 kV with about 2.2×10^{-8} A using focused beam (smaller than 1 μm) with measuring times of 30 seconds for peak count and 10 seconds for background. Standards used for calibration are synthetic and natural minerals such as synthetic corundum for Al, synthetic periclase for Mg, synthetic eskolaite for Cr, synthetic Gd-Ga garnet for Ga, jadeite for Na, Fayalite for Fe, wollastonite for Si and Ca, K-feldspar for K etc.

Before EMPA analysis, three to six corundum grains that may contain mineral inclusions were placed into round mold and then filled by resin (Figure 1.11). Subsequently, the samples inclusions were polished until inclusions were exposed to the surface. Unfortunately, some inclusions were gone during polished process.



Figure 1.10 JEOL Electron Probe Micro-Analyzer (model JXA-8100) based at the Department of Geology, Faculty of Science, Chulalongkorn University.

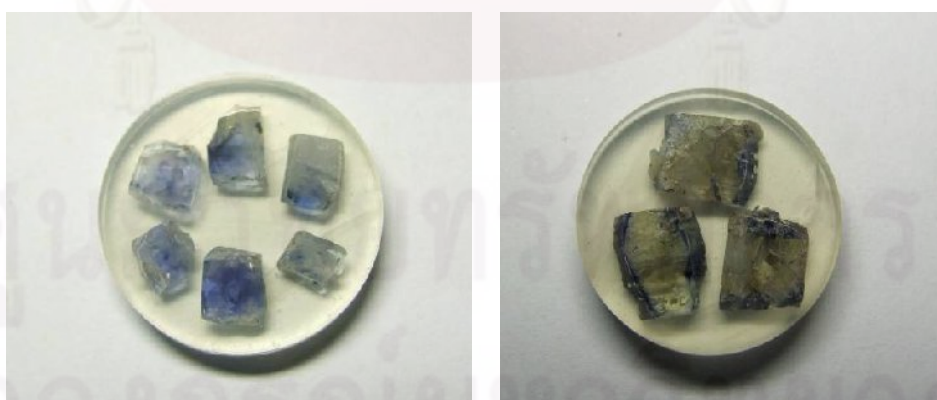


Figure 1.11 Three to six samples of Awissawella sapphires are set in resin block for EPMA analyses.

8. *High Temperature Furnace*: used in this experiment is Linn electrical furnace (model HT 1800 Plus VAC Bottom Loader) (Figure 1.12) based at the Department of Geology, Faculty of Science, Chulalongkorn University. The furnace consists of a heating chamber attached with bottom-side sample loader. U-shaped rods of molybdenumdisilicate (MoSi_2) are used as heating element. A pair of heating rods is hung on the top of the chamber. Heating steps and soaking temperatures are automatically controlled using preset programs. The atmospheric condition in the chamber can be controlled by feeding gas such as pure O_2 , air, pure N_2 throughout the heating and cooling processes.



Figure 1.12 Linn electrical furnace model HT 1800 Plus VAC Bottom Loader based at the Department of Geology, Faculty of Science, Chulalongkorn University.

ศูนย์วิทยทรัพยากร
จุฬาลงกรณ์มหาวิทยาลัย

CHAPTER II

GEOGRAPHY, GEOLOGY AND GEM DEPOSITS OF SRI LANKA

2.1 Geography

Sri Lanka (previously called Ceylon) is situated in the Indian ocean south-east of India (Figure 2.1). It is an island with an area of 25,325 square miles (65,845 km²) bordered by the Indian ocean and is essentially a part of the shield area of peninsular India. Geologically, Sri Lanka is the southern continuation of the Indian sub-continent. It is believed to have separated in recent geological times due to shallow tectonic movement (Rupasinghe et al., 1986).



Figure 2.1 Map of Sri Lanka, show locations of island in the Indian Ocean south-east of India (available from www.sjr.mb.ca/ms/geo/countries/sri/img18.gif).

Topographically, Sri Lanka can be divided into 3 peneplains (Zoysa, 1981). These with their respective elevation above seal level are: 1st Peneplain (from coastal plain to 30 m above sea level); 2nd Peneplain (from 30 to 480 m above sea level); 3rd

Peneplain (from 480 to 720 m above sea level) (see Figure 2.2). It is very important to mention that most of the gem areas are located significantly within the 2nd peneplain.

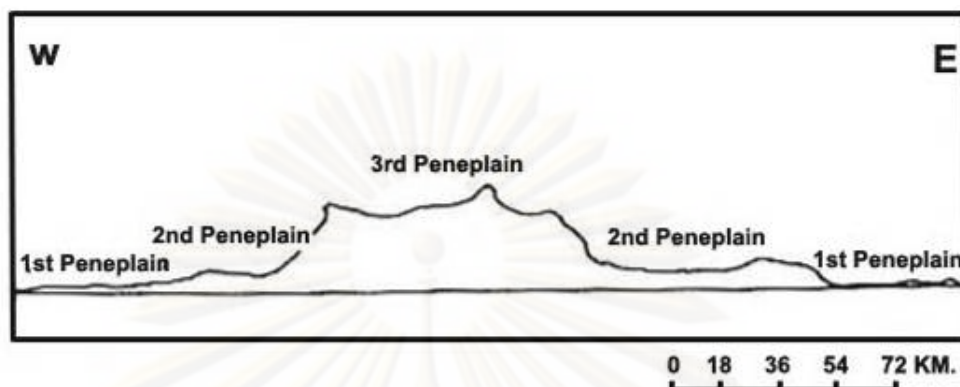


Figure 2.2 Section across the central part of Sri Lanka showing three distinctive peneplains (Zoysa, 1981).

2.2 General Geology

Sri Lanka belongs to a unique geologic position of Gondwana. It is a small island which is an important jigsaw piece of the Gondwana supercontinent. The Gondwana had been marked by collisional events between the component cratons of West Gondwana (i.e., Africa and South America) and East Gondwana (i.e., Australia, Antarctica, India, Sri Lanka and Madagascar). Dissanayake and Chandrajith (1999) correlated geologic features of South India, Sri Lanka, and Madagascar for proper understanding of Pan-African tectonics in East Gondwana; consequently, it brought to position of Sri Lanka within Gondwana (Figure 2.3).

Tectonic and metamorphic evolution of high-grade basement rocks in Sri Lanka can be explained within the frame work of a major Pan-African continental collision event between West Gondwana and East Gondwana (Kröner, 1980, 1991; Kriegsman, 1993). During the collision, the formation of Mozambique belt, one of major suture zones, had been exposing in Sri Lanka as “Highland Complex”. It shows crucially characteristics of a mineralized belt related to gem- and graphite-bearing formations (Munasinghe and Dissanayake, 1982; Dissanayake, 1985). This mineral belt also shows remarkable similarities of lithology and mineralogy to the Kerala Khondalite Belt along the southern

tip of India, south of the Ranotsara shear zone in southeast Madagascar and Mozambique belt in Tanzania.

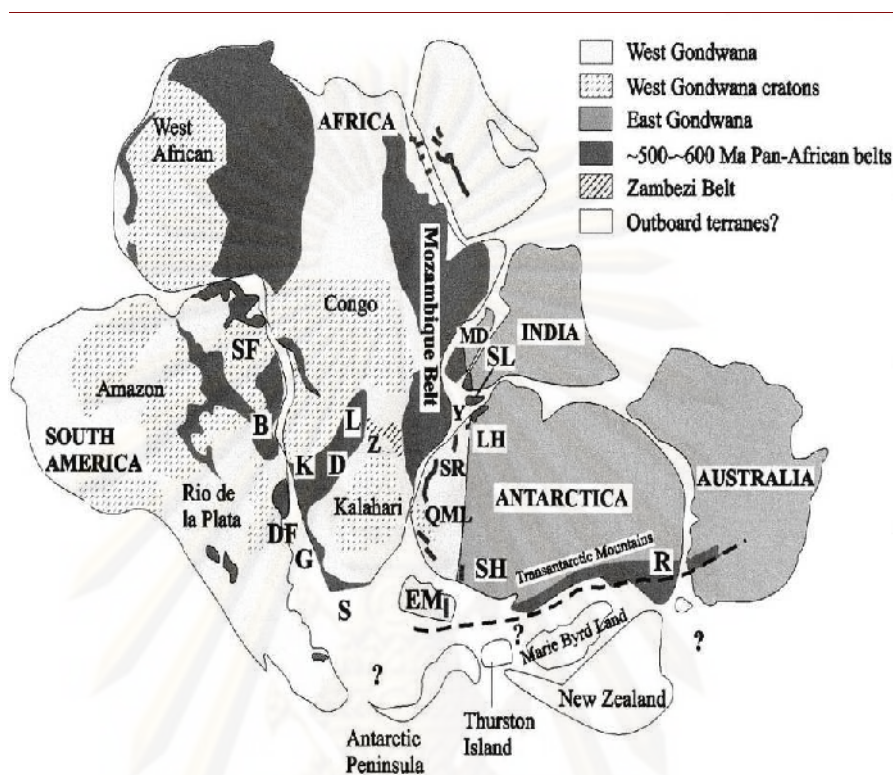


Figure 2.3 Gondwana assembly reconstruction showing location of Pan-African events. Older cratonic blocks of West Gondwana and possible outboard terrains. Pan-African belt: *B*, Brasiliano; *DF*, Dom Feliciano; *D*, Damara; *G*, Gariiep belt; *K*, Kaoko belt; *L*, Lufilian arc; *LH*, Lützow-Holm Bay; *MD*, Madagascar; *Y*, Yamato mountains; *R*, Ross orogen; *S*, Saldanian belt; *SH*, Shackleton Range; *SL*, Sri Lanka; *SR*, Sor Rondane mountains; *Z*, Zambezi belt. Other features: *EM*, Ellsworth-Whitmore mountains; *QML*, Queen Maud Land; *SF*, São Francisco craton (Dissanayake and Chandrajith, 1999).

The correlation between granulites and amphibolites in East Antarctica and Sri Lanka Precambrian by Yoshida and Vitanage (1993) revealed that the Skallen Group of Lützow-Holm area in East Antarctica and the Highland Complex in Sri Lanka are quite similar in lithology that are complexes of orthogneisses, metabasites, quartzites, metapelites and mafic gneisses. These geological and mineralogical features indicate the juxtaposition of Sri Lanka, Madagascar and also Lützow-Helm Bay area of Antarctica.

Dissanayake and Chandrajith (1999) compiled such information and some other literatures and subsequently suggested that a distinct mineralized belt was conclusively running from Antarctica through the Highland Complex of Sri Lanka into Madagascar, Mozambique, Tanzania, and farther north (Figure 2.4). This mineral belt is clearly of Pan-African origin and is now considered to be an important geosuture associated with the main Mozambique Belt and confirming the important position of Sri Lanka in the context of Gondwana.

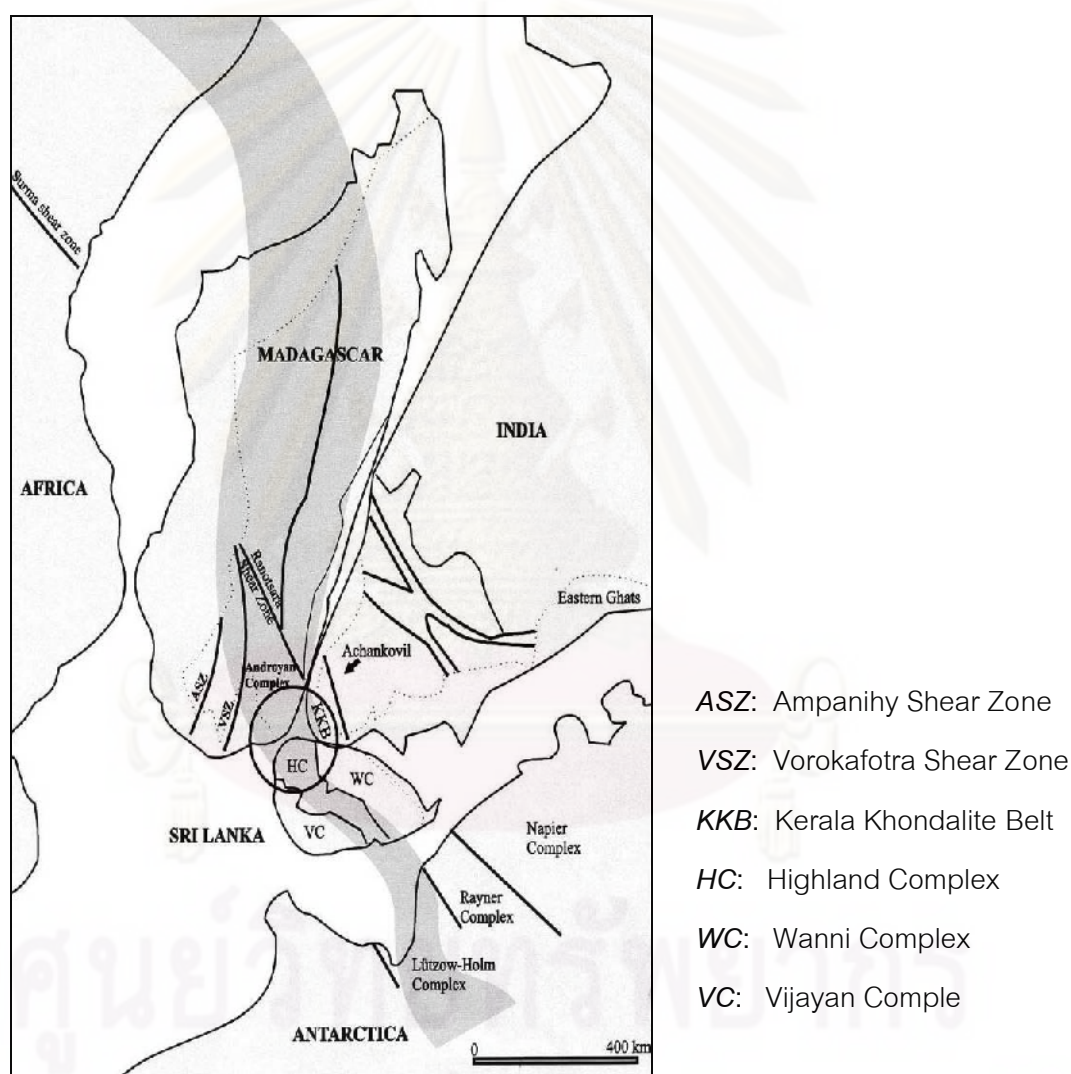


Figure 2.4 The juxtaposition of Sri Lanka, the southern tip of India and Madagascar (encircled) in Gondwana. The central shaded belt indicates the mineral belt within the geosuture (Dissanayake and Chandrajith, 1999).

About 90% of the Sri Lanka basement is characterized by highly metamorphosed Precambrian rocks that are grouped mainly as Proterozoic metasediments up to granulite facies. These rocks vary in compositions and are sometimes intruded by pegmatites and mafic dykes that indicate magmatism processes. The rest of the area consists of Miocene formations, Quaternary deposits and minor unmetamorphosed igneous rocks including late pegmatite. Miocene limestones expose in the north-western area and at a small area of the south-western coastline. Small isolated Jurassic sandstone formations are found at Andigama and Tabbowa. Red earth including Ratnapura bed, coral reefs, beach sands, beach rocks and alluvium are mapped as Quaternary deposits ranging in age from Pleistocene and recent epochs.

2.3 Metamorphic Complexes

Recent studies of the basement rocks have traditionally subdivided the Proterozoic high-grade rocks into three major lithological units, on the basis of rock type, chronologic metamorphic history and metamorphic grade (i.e., Kroner et al., 1991; Dissanayake and Chandrajith, 1999). They are Highland Complex (HC), Wannu Complex (WC) and Vijayan Complex (VC). Moreover, Kadugannawa Complex (KC) is exceptional lithotectonic unit situated on the boundary between HC and WC lithotectonic unit, and among the other prominent geological features of the Vijayan Complex are the small plutons of granites and acid charnockites near the east coast, Kataragama Klippe (KK) and the north-west-trending suite of dolerite dikes at Kallodai, Buttala Klippe (BK). (see Figure 2.5).

ศูนย์วิทยทรัพยากร

จุฬาลงกรณ์มหาวิทยาลัย

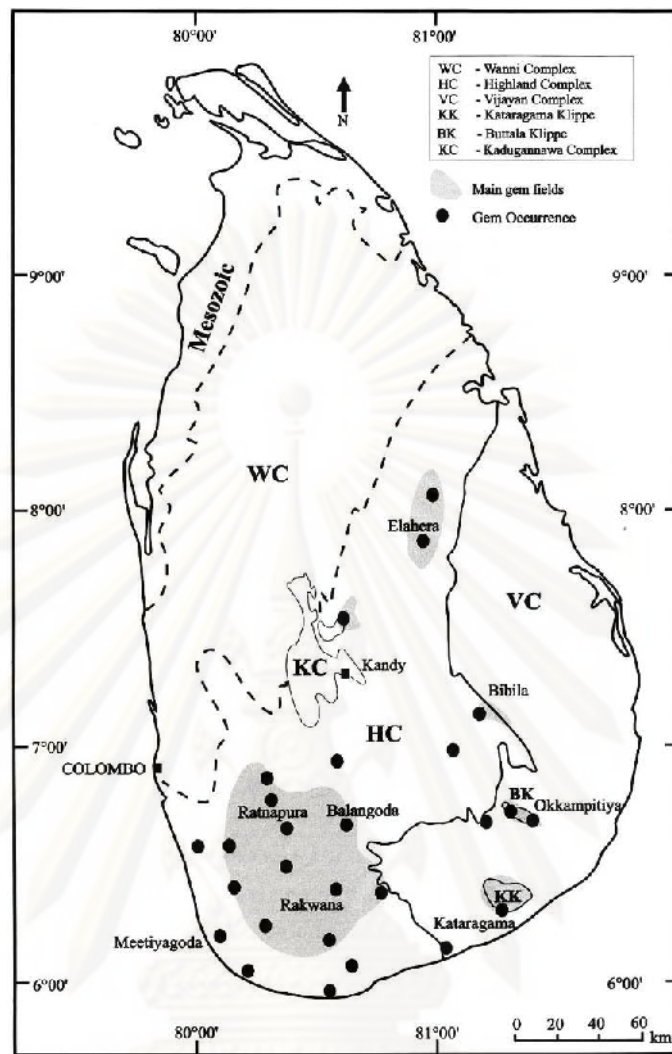


Figure 2.5 Simplified and generalized geological map of Sri Lanka showing major lithotectonic units (Dissanayake and Chandrajith, 1999). The dashed line gives only the proposed boundary.

Table 2.1 Chronology of basement rocks in Sri Lanka (Kröner et al., 1991).

	HC	Wanni Complex	Vijayan
Depositional age of supracrustal	~2000 Ma	~1100 Ma	~1100 Ma
Granitoid intrusives	~665-1942 Ma	~1000-1100 Ma	~1000-1100 Ma
Regional granulite grade	< 665 > 550 Ma	< 665 > 550 Ma	-
Regional amphibolite grade	-	-	~456-591 Ma
<i>In-situ</i> charnockitization	~550 Ma	535-550 Ma	-
Post-tectonic granites	~550-580 Ma	~550 Ma	-
Minor cooling	463-611 Ma	420-524 Ma	-

Highland South Western Complex (HC): This large unit forms as backbone of the Precambrian basement and occupies the entire hill area of the island. Former Highland series and south-western group have been included together and named as Highland South-western Complex (HC) (Cooray, 1984). Deposition of supracrustal rocks took place at about 2000 Ma years ago. About 50% of all rocks in the HC are granitoid origin (regional granulite grade metamorphism at 750-900°C and 8.5-7.5 Kbar); these granitoids range in age from ~1942 Ma to ~650 Ma (Table 2.1). The HC granulite is composed of meta-sedimentary rocks such as quartzite, marbles, calc-silicates and garnet sillimanite-gneisses (khondalite), meta-volcanic suits, mafic to granitic granitoid intrusives and mafic dykes.

Vijayan Complex (VC): exposes along the eastern and southern parts, lying to the east of HC. The depositional age of supracrustal rocks of Vijayan complex is around 1100 Ma. Among the other prominent geological features of the VC, small plutons of granites and acid charnockites are found near the east coast and the north-west-trending suite of dolerite dikes at Kallodai (Dissanayake and Chandrajith, 1999). The VC rocks are mostly characterized by amphibolite facies with peak metamorphism taken around 456-591 Ma (Table 2.1), and the fact that it has not been subjected to granulite facies metamorphism which has been interpreted by Kröner et al. (1991) to mean that the charnockitic bodies within the Vijayan domain are tectonic klippen and/or unfolded or intersliced fragments of the Highland Complex. These are similar to the Kataragama klippe of established HC derivation (Figure 2.5). The Vijayan basement consists of various granitoid gneisses ranging in composition from tonalite to leucogranite and migmatite (Milisenda et al., 1991). Metasedimentary rocks (e.g., metaquartzite and calc-silicate rocks) are found as xenolithic inclusions with minor amount in these gneisses. In contrast to the Wannu Complex, hornblende-bearing calc-alkaline plutonic rocks are common in this unit (Kröner et al., 1991).

Wanni Complex (WC): This rock domain occurs along NW and W edges of the HC (Figure 2.5). The former West Vijayan Complex (Cooray, 1984) has been renamed as the Wannu complex by Kröner et al. (1991). The Wannu complex also has been subjected to the same granulite metamorphism of HC. However, its supracrustal rock deposition

was simultaneous to the Vijayan complex (around 1100 Ma). Paleo-metamorphic pressures of the Wanani complex are lower than that of the HC. Granitoid gneisses, varying from migmatitic to charnockitic gneisses, and minor metasediments are the main rock types in the complex (Kröner et al., 1991). Comparisons of modal ages and paleo-pressure data suggest that this rock unit may belong to an individual metamorphic complex.

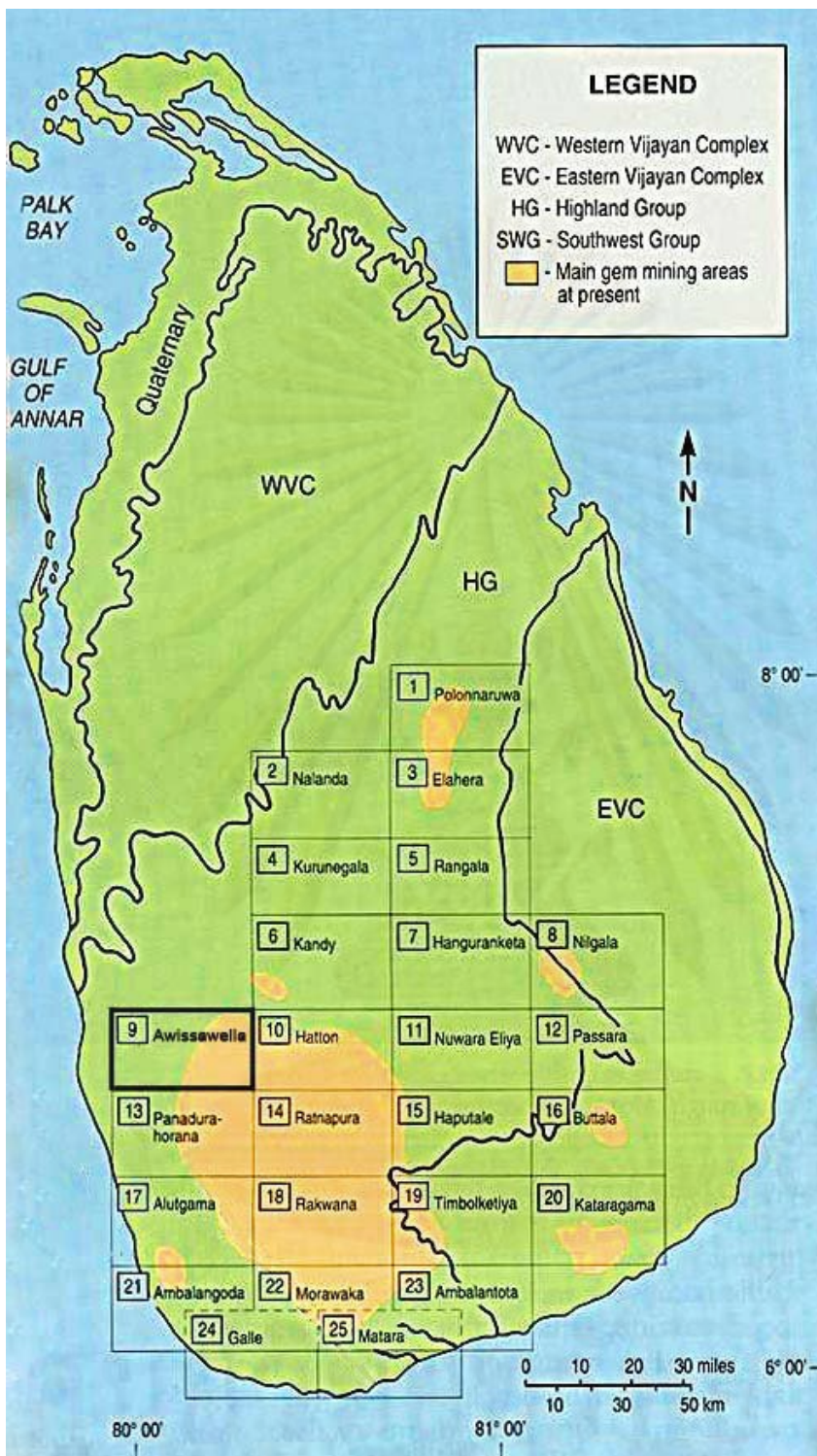
Kadugannawa Complex (KC): is situated within the HC, around Kandy and Peradeniya. This complex has zircon dates (660 to 550 Ma) and Nd model ages (1100 Ma) comparable to the Wannani complex (Kroner et al., 1991). Parts of the Kadugannawa Complex have experienced granulite grade metamorphism (Schenk et al., 1991). However, evidence for a retrogressive event has also been preserved at some locations. The KC is composed of biotite-hornblende and biotite gneisses as well as amphibolites, minor quartzo-feldspathic and pelitic gneisses and metaquartzites. There is no evidence to show that the KC is a nappe structure of the Wannani Complex. Therefore, it is recognized as a differentiated suite of calc-alkaline intrusive rocks intruded into the rocks of HC around 890-1000 Ma ago.

Finally, it should be notified that most gem-bearing areas of Sri Lanka are underlain by the granulite of Highland Complex. Although, some gem occurrences, such as in the Okkampitiya gem field, are found outside the Highland Complex, it is suspected that they originated in the Highland Complex and were later transported by rivers and deposited in this area.

2.4 Gem Deposits

The central granulite HC covering about 30,000 km² of the Sri Lankan island is prospected as the main gem formations. Minor gem occurrences are also discovered in the westernmost VC in the eastern part of the island (Dissanayake et al., 2000). Most of the economic gem deposits are situated in paleoplacers within alluvial gravels of Pleistocene to recent age and are also associated with river and stream systems in the central-southern area of the island. Some researchers have correlated the major periods of gravel deposition with sea level changes and periods of peneplanation. Some gems

are recovered from active fluvial systems, either from recent gravels or from reworked paleoplacers. In some locations, deep shafts sunk in the riverbanks are working on the same gem-bearing gravel bed exposed nearby the river. A few gem deposits are actually located very close to the bedrock source and may form as residual deposits. Karstic cavities within the weathered zone of calcareous metasediments are also high prospective area for pocket deposits in some particular area (Dissanayake and Rupasinghe, 1995). Sri Lanka has the high density of gem deposits in relation to its landmass in the world and production of gems dominates its export earnings from minerals. In 1993, Dissanayake and Rupasinghe had research study to characterize know gem-producing regions and identify potential new areas, using 500 samples of the gem mineral potential of south-central Sri Lanka (Figure 2.6). Based upon the results of this sampling and follow up mineralogical work a set of 4 key criteria were established to categorize the gem mineral potential of south central Sri Lanka. The key criteria defined were: lithology and topography, drainage density, presence of alluvium and heavy mineral concentrations. From the results of the sampling and application of the criteria was devised to categorize the gem bearing potential of the area, ranging from a "No Deposits" class up to a "Highly Probable" class. The distribution of these groups is illustrated in Figure 2.7, which clearly outlines the 3 main gem fields, centered on Ratnapura-Rakwana; Buttala and Elahera. The major gem fields of Sri Lanka lie in the HC terrain (Figure 2.5). In these areas most of the gem exploitation is done in the flood plains and hill slopes characterized by parallel ridge and valley topography. Gem-mining is very rare in the Vijayan Complex except perhaps along and around rivers which have drained the HC terrain. Studies of remote sensing data (e.g., aerial photos and satellite images) from gem-bearing terrain have shown that the locations of many deposits are controlled by structural (primary deposits) and morphotectonic (secondary deposits features). For example, zones of pegmatite dykes are controlled by major faults of other structural lineaments or faults and joints control river valleys and terraces. In Sri Lanka, Gunaratne and Dissanayake (1995) described a good example of such controls on gem deposits in the Bogawantalawa area. They also noted the complex effects of morphotectonic structures in either enhancing or degrading gem deposit formation in some situations.



- 1: Polonnaruwa
- 2: Nalanda
- 3: Elaheera
- 4: Kurunegala
- 5: Rangala
- 6: Kandy
- 7: Hanguranketa
- 8: Nilgala
- 9: Awissawella
- 10: Hatton
- 11: Nuwara Eliya
- 12: Passara
- 13: Panadura-Horana
- 14: Ratnapura
- 15: Haputale
- 16: Buttala
- 17: Alutgama
- 18: Rakwana
- 19: Timbolketiya
- 20: Kataragama
- 21: Ambalangoda
- 22: Morawaka
- 23: Ambalantota
- 24: Galle
- 25: Matara

Figure 2.6 Map of Sri Lanka showing the main lithotectonic units and the gem fields studied. The boundary between the Highland Complex and Wannu Complex is uncertain and is denoted by a broken line. The numbered sequences represent the topographic sheets. The palaeopressure contours of the Highland Complex of Sri Lanka in relation to the locations of the gem fields are also shown (modified after Dissanayake and Rupasinghe, 1993).

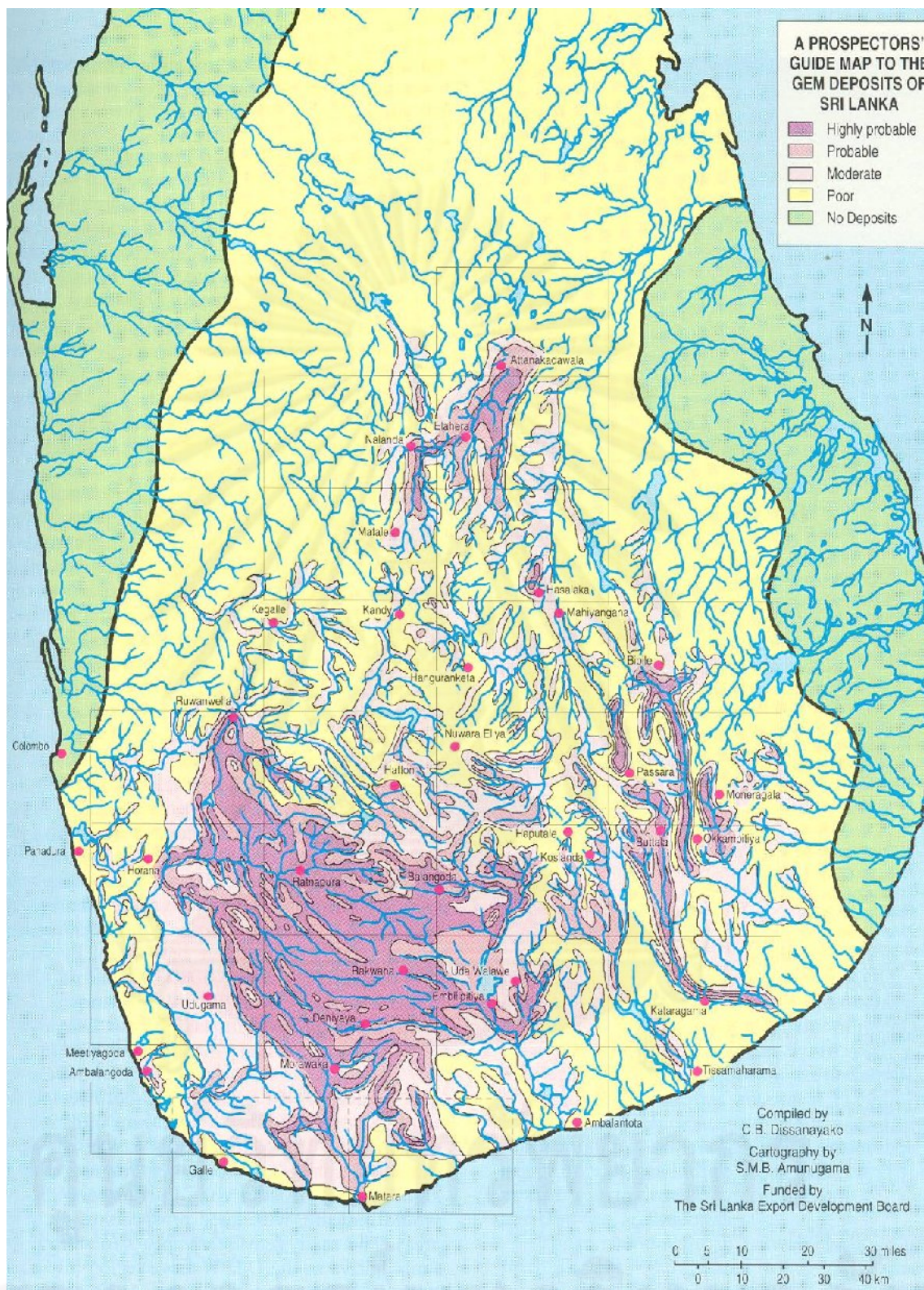


Figure 2.7 A Prospector's Guide Map to Gem Deposits of Sri Lanka. Areas are categorized as "highly probable", "probable", "poor", and "no deposit" on the gem potential (Dissanayake and Rupasinghe, 1993).

Table 2.2 indicates the distribution of gem minerals found in Sri Lanka. The two main gem fields, Ratnapura and Elahera contain a wide variety of gem minerals.

Table 2.2 Key gem minerals of Sri Lanka listed by locality. Topographic sheet numbers are keyed to those shown on Figure 2.6 (Dissanayake and Rupasinghe, 1993).

Topographic Sheet		Gem minerals
No.	Name	
01	Polonnaruwa	corundum, garnet
02	Nalanda	apatite
03	Elahera	chrysoberyl, corundum, garnet, iolite (cordierite), korerupine, sinhalite, sphene, spinel, zircon
04	Kurunegala	amethyst, apatite, citrine, fluorite, iolite (cordierite), topaz, tourmaline
05	Rangala	no known deposits
06	Kandy	amethyst, aquamarine
07	Hanguranketa	corundum
08	Nilgala	corundum, garnet, spinel, tourmaline, zircon
09	Awissawella	amethyst, andalusite, beryl, chrysoberyl, corundum, diopside, epidote, iolite (cordierite), korerupine, garnet, sinhalite, spinel, tourmaline, zircon
10	Hatton	andalusite, corundum, garnet, iolite (cordierite), spinel, topaz
11	Nuwara Eliya	amethyst, corundum, spinel, zircon
12	Passara	corundum, ekanite, garnet, korerupine, spinel, taaffeite, topaz, tourmaline, zircon
13	Panadura-Horana	aquamarine, axinite, beryl, chrysoberyl, corundum, garnet, vesuvianite, phenakite, scapolite, sillimanite, spinel, taaffeite, topaz, tourmaline, zircon
14	Ratnapura	amethyst, andalusite, apatite, beryl, chrysoberyl, citrine, corundum, diamond, danburite, diopside, ekanite, garnet, iolite (cordierite), korerupine, scapolite, sillimanite, sinhalite, spinel, taaffeite, topaz, tourmaline, zircon

Table 2.2 (continue).

Topographic Sheet		Gem minerals
No.	Name	
15	Haputale	andalusite, axinite, beryl, chrysoberyl, corundum, diopside, garnet, vesuvianite, spinel, topaz, tourmaline, zircon
16	Buttala	corundum, ekanite, garnet, spinel, tourmaline
17	Alutgama	chrysoberyl, corundum, spinel, zircon
18	Rakwana	apatite, aquamarine, axinite, beryl, chrysoberyl, corundum, danburite, diopside, ekanite, enstatite, fluorite, garnet, korerupine, spinel, tourmaline, zircon
19	Timbolketiya	garnet
20	Kataragama	corundum, hiddenite (spodumene), sphene, spinel
21	Ambalangoda	moonstone (feldspar)
22	Morawaka	aquamarine, beryl, chrysoberyl, corundum, danburite, diopside, garnet, sillimanite, sphene, spinel, tourmaline, zircon
23	Ambalantota	beryl, chrysoberyl, corundum, garnet, vesuvianite, iolite (cordierite), scapolite, sillimanite, sinhalite, spinel, tourmaline, zircon
24	Galle	beryl, chrysoberyl, corundum, sphene
25	Matara	aquamarine, chrysoberyl, corundum, garnet, zircon

Gem deposits in Sri Lanka can be basically classified as primary and secondary deposits (Figure 2.6). However, more than 90% of the gem mining in Sri Lanka is taken in secondary deposits (e.g., residual, eluvial and alluvial). The primary deposits are grouped within two main rock types, i.e., igneous or metamorphic rocks. Pegmatites are the major type of magmatic (igneous) gem origin in Sri Lanka whereas metamorphic origins can be further subdivided into skarn and aluminous metasedimentary types (Dissanayake et al., 2000) (Figure 2.8). Details of these type deposits are described below.

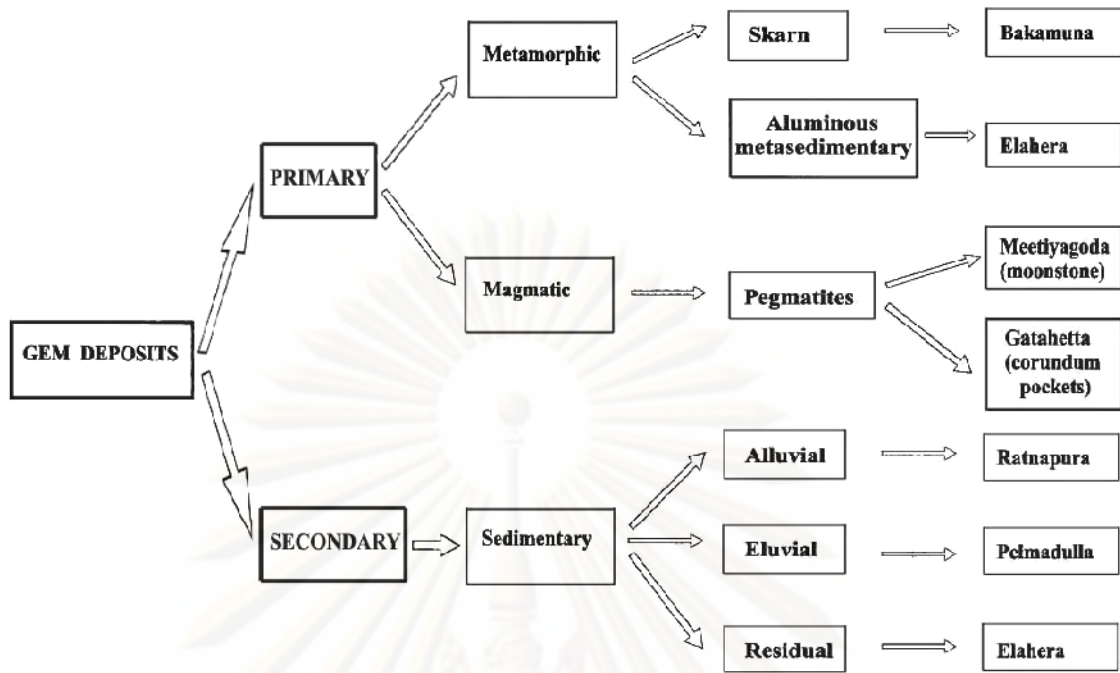
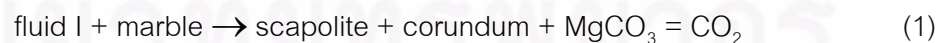


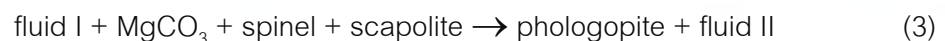
Figure 2.8 Classification of gem deposits in Sri Lanka with an example of location in each different type (modified after Dissanayake et al., 2000).

2.4.1 Skarn Type Deposit

Skarn and carbonate rocks are the major source of gems in Sri Lanka, particularly corundum (both sapphire and ruby) and spinel. Skarn deposits were formed by the reaction of pegmatitic fluids with the marble. Hydraulic fracturing of the rock and an increase in CO_2 pressure and dedolomitization made the rock permeable to these fluids. The reaction between the marble and the fluids proceeded in stages. The initial reactions were dedolomitization and the conversion of calcite to scapolite and precipitation of corundum:



The scapolite and corundum became unstable with the increase in Mg activity in the fluids and hence reacted to form phlogopite and spinel:



The action of secondary fluids (fluid II) which are richer in Al in the fresh marble through reaction 1 caused the precipitation of enhanced quantities of corundum. The limited Mg availability prevented complete conversion of corundum to spinel through reaction 2 (Silva and Siriwardena, 1988).

Ferroaxinite and garnet are also commonly associated with calcium rich skarn deposits. Skarns containing corundum and spinel have been reported from the contact of intrusive granite and marble in Elahera gem fields, it covers approximately 150,000 m² in Matale and Polonnaruwa districts, located in northeastern Sri Lanka (Figures 2.5 and 2.9) and also lie within the Highland Complex and consist mainly of quartzites, marbles and garnet-sillimanite-biotite gneisses (Figure 2.10) (Dissanayake and Chandrajith, 1999) where the granites with pegmatites intruded into marble originating such significant skarn deposits. Moreover, these skarn deposits have also been found in Bakamuna (Figure 2.11), Kolonne and Ohiya (Cooray, 1984; Silva and Siriwardena, 1988; Gunaratne and Dissanayake, 1995).

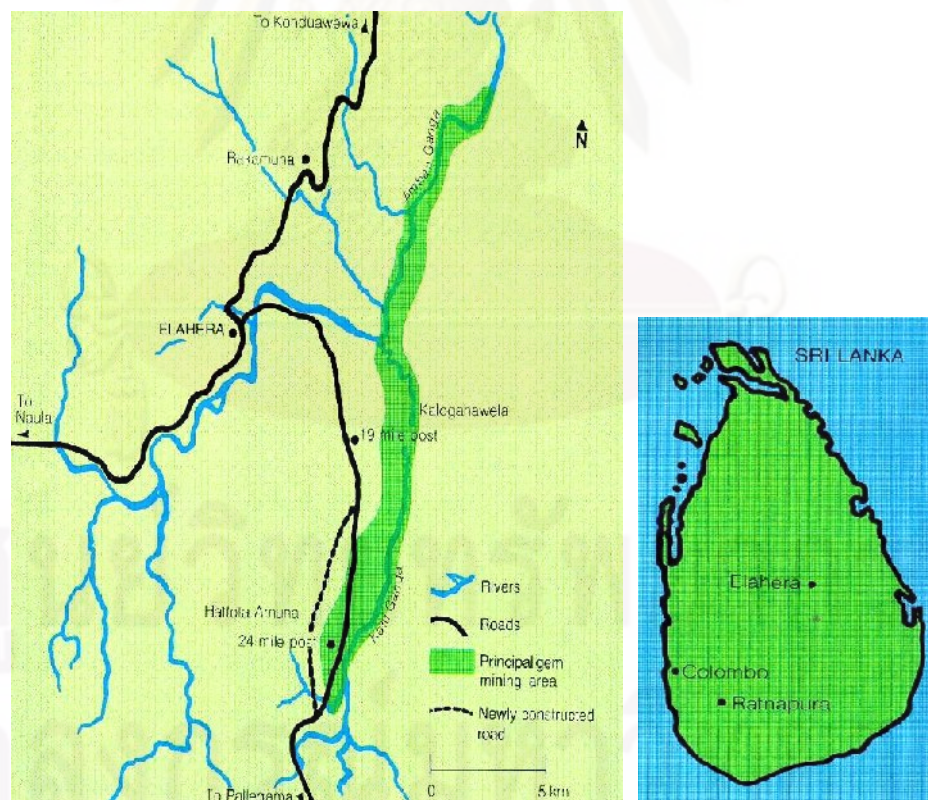


Figure 2.9 The Elahera gem field in northeastern Sri Lanka is noted for its vast production of many gemstone varieties. The main gem mining activity is between the 19- and 24-mile posts (Gunawardene and Rupasinghe, 1986).

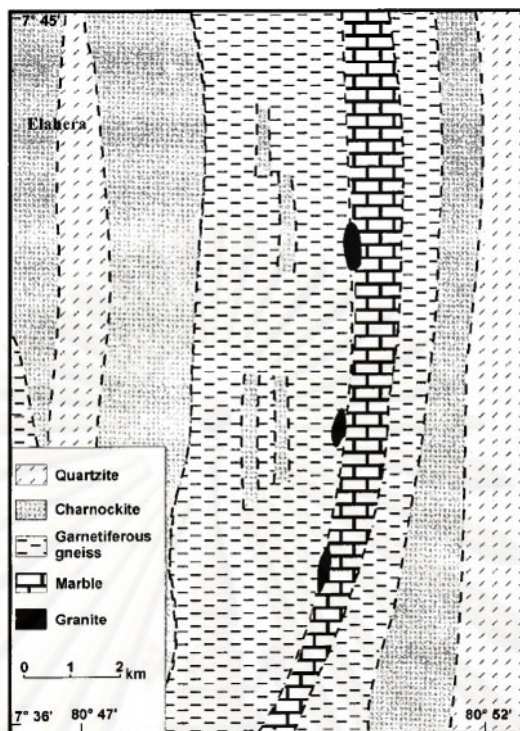


Figure 2.10 Geological map of the Elahera gem field (Dissanayake and Chandrajith, 1999).

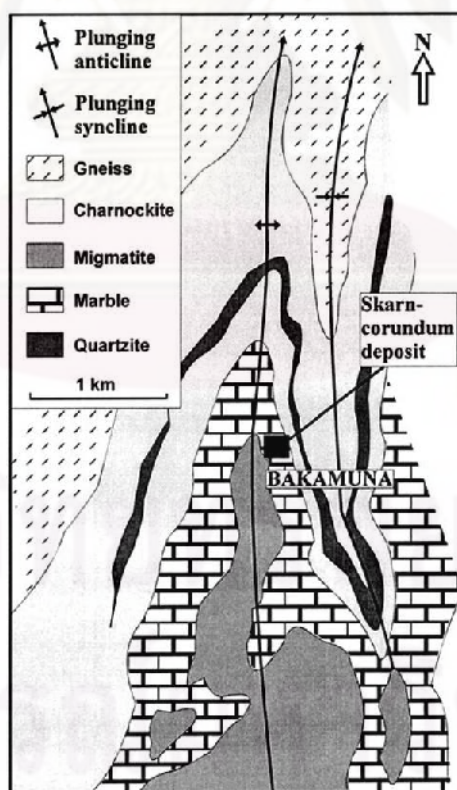


Figure 2.11 Geology of the Bakamuna area and the detailed geology of the skarn deposit (Dissanayake et al., 2000).

2.4.2 Aluminous Metasedimentary Type

One of the characteristic features of the Highland Complex is the abundance of aluminous metasedimentary rocks. These have the chemical composition required for the formation of corundum and other aluminous gem minerals such as garnet, sillimanite and cordierite. In particular many of the metamorphic rocks are enriched in alumina, with some highly aluminous compositions, called khondalites. These contain up to 30% Al_2O_3 and thus are very promising source materials for corundum and other aluminous gem phases. It is clear that in the Highland Complex a combination of the P-T conditions and a suitable chemical composition has yielded voluminous sources for gems of this type. Examples of gem deposits reported or worked from such rocks include corundum recovered from biotite-sillimanite gneiss at Polgahwela, geuda from khondalites near Haldummulla, corundum from Tannahena near Kandy and from Haputale. One particularly fine example of such a deposit containing fine, high quality deep blue-black sapphires from Aparekka near Matara has been described but it seems to have been worked out and its exact location is unclear (Gunaratne and Dissanayake, 1995).

2.4.3 Pegmatitic Deposit

Pegmatites are coarse-grained, acid, granitic intrusions and several suites have been intruded into the metamorphic bedrock of Sri Lanka during several phases of activity throughout the geological evolution of the island. They are also considered as important sources of gem minerals. Beryl and chrysoberyl containing pegmatites have been reported from Buttala area. Be-rich pegmatitic fluids are considered as the source of such gem bearing pegmatites (Rupasinghe et al., 1984). Zircon bearing pegmatites have been recorded from several locations and one such large deposit is found in Balangoda area (Cooray, 1984). Topaz and tourmaline bearing pegmatites are found in the Nawalapitiya (Ranasinghe, 1995) and Elahera areas as well as at Polwatte. One of the best known pegmatitic gem deposits is the moonstone deposit at Meetiyyagoda, southern Sri Lanka where a pegmatite intrudes the metamorphic basement and has been heavily weathered. Similar moonstone deposits have been reported from the areas

around Balangoda and Kundasale and a newer deposit of smoky moonstone was discovered at Imbulpe, east of Ratnapura (Harder, 1992). High quality corundum has been recovered from pegmatites in Moneragala and from the Okkampiitya region. Amethyst has been reported from Kekirawa along with citrine, including a yellow purple bi-coloured variety called ametrine. An unusual occurrence of geode-hosted corundum is found in pegmatites described by Kumaratilleke and Ranasinghe (1992) where well-formed yellow and blue sapphires are found in clay-filled hollows in weathered pegmatites. Such deposits have been reported from Badulla, Moneragala, Awissawella and at Getahetta. This deposit type is described for the sapphire under this study.

2.4.4 Secondary Deposits

Sedimentary (secondary) gem deposits are by far the most importance of all gem deposits in Sri Lanka and were classified by Dahanayake et al. (1980) into residual, eluvial and alluvial types (Figure 2.12). The sedimentary placer gem deposits occur in thin layers or lenses of gravel and sand, termed locally as "*Illam*", in river beds and alluvial plains and on hill slopes and hillsides. Among the most important factors that govern the depositional nature of these gem deposits are the intensity and distance of transportation from the source, by the shapes and sizes of the rock and mineral fragments found and the topographical suitability of the sites for deposition.

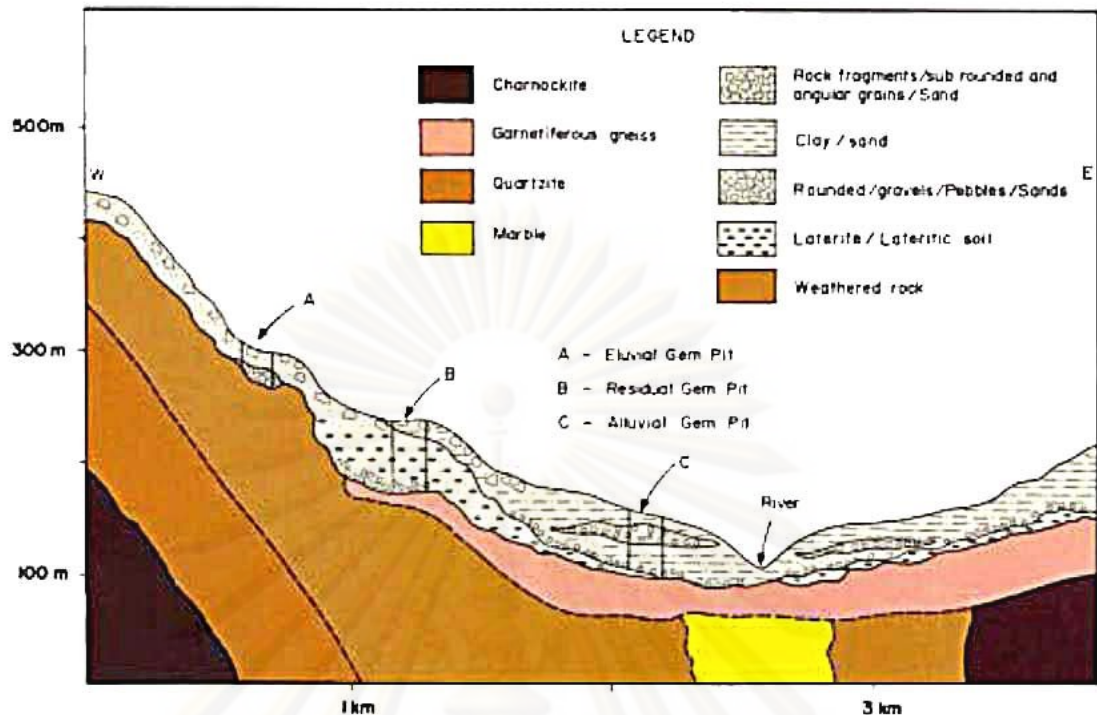


Figure 2.12 Schematic cross section showing different modes of occurrence of gemstones (Henny, 1999).

Residual deposits: These deposits are characterized by layers of sediment containing gem phases mainly deposited *in situ* or very close to nearby primary bedrock sources. Most of these deposits are associated with floodplains of rivers and stream channels and their sources are assumed to be in the close vicinity. A characteristic feature of the residual gem deposits is the presence of layers of alternating sand, clay and laterite with angular rock fragments are a common feature and are found at depths ranging from a few centimeters down to about 10 meters. Gem types are corundum, spinel, garnet, tourmaline, zircon and apatite—mostly conserving the crystal shape. Generally blue sapphires and rubies (corundum) are the major gem stones mined. This type of deposit is the results of *in-situ* weathering of local bedrock or perhaps an early alluvial source which left the resistant gem minerals together with poorly sorted, angular rock debris behind. They are sitting in a clay-sand matrix representing the weathered bedrock. Residual deposits are common in the Elahera gem field. The mode of occurrence of gem pits in Elahera is mostly of the residual type. This region is also characterized by ridge and valley topography in a plunging synclinal structure. The synclinal strike valley is relatively wider and forms a vast flood plain with the major river,

Kalu Ganga, running centrally along the strike. The Kalu Ganga has been major vehicle for transportation of the materials into the valley, resulting in accumulations of deposits on hill slopes as well as along the banks of the river. Elahera gem field produces a wide variety of gem materials, including blue, pink, yellow, violet and “padparadscha” sapphire, marvelous color ranges of spinel, rhodolite and hessonite garnets, chrysoberyls (including alexandrite and chatoyant varieties), many colorless zircon, green and “cognac” tourmaline, brownish green korerupines, near-colorless to yellowish or greenish sinhalites. In addition, many rare stones such as gem epidolite, sillimanite (fibrolite) and taaffeite are also found in the locality rock crystal quartz, amethyst and topaz (Gunawardene and Rupasinghe, 1986).

Eluvial Deposits: This type of deposit mainly results from gem-bearing material transported down slope by mass soil movements usually aided by water action. They are often found on hill slopes and flat areas incised by stream valleys where they often grade into true alluvial deposits making identification difficult. This type of deposit is characterized by angular to sub-rounded nature of the gem minerals and rock fragments set in a clay/sand soil matrix. The gem-bearing sediment for the most part retaining their crystallographic outlines-corundum, spinel, garnet, tourmaline and zircon are trapped under the boulders and cobbles. Generally gem quality stones are blue sapphires and rubies. They are generally localized and not persistent in lateral extent.

Alluvial Deposits: These alluvial gem deposits are the most common deposit type in Sri Lanka (approximately 90% of deposits worked are alluvial) and are typified by the extensive deposits around and within the Ratnapura gem fields in south-central Sri Lanka. As shown in Figure 2.13, except for scattered patches of alluvium, the areas surrounding the main Ratnapura gem field consist of Precambrian metamorphic rocks of charnockite-metasedimentary type. The main rock types are charnockites, garnet-sillimanite granulites, amphibolites and perthite-bearing garnet-biotite granulitic gneisses. Of these, charnockites and pelitic garnet-sillimanite granulites are the most abundant. The occurrence of intrusive rocks of zircon-bearing granites, vein quartz and pegmatites is of particular significance. They occur mostly in old stream terraces and flood plains. Gems transported by fluvial processes, especially by rivers, are deposited

mainly within valleys and floodplains, forming alluvial deposits. The Ratnapura gem field consists of Pleistocene or sub-recent alluvium with patches or streaks of gravel of heavy minerals laid down in flood plains of streams, either in the beds of abandoned tributaries or in talus fans at the foot of steep hill slopes. The heavy minerals including gems have deposited during periods of intense flooding that caused their mechanical removal from their source areas (Dissanayake and Chandrajith, 1999). The gems are found in certain horizons in river and lake deposits that have accumulated into a thickness of about 40 feet in the strike valleys. The most abundant constituent of the gem gravels is quartz in smooth rounded pebbles and cobbles from less than an inch to several inches across. These are accompanied by a variety of smaller detrital grains of gem and rare-earth minerals of a highly immature mature, sometimes retaining their crystal outlines. Heavy minerals and gem type minerals found are corundum, beryl, chrysoberyl, garnet, spinel, tourmaline, feldspar, quartz and zircon. Occasionally, cordierite, andalusite, apatite, kornepine, sinhalite, taaffeite and ekanite are also recognized in the sediments. Important gemstones mined are blue sapphires, fancy sapphires and rubies, alexandrite and cat's eye chrysoberyl and yellow beryl. These deposits can reach to depths of 20-30 meters and usually contain two or three gem-bearing layers. The gem bearing gravel (illam) occurs as layers of different morphologies, thicknesses and extent within active and fossil fluvial systems. It is compositionally variable with sand, clay and pebble layers are found alternatively in these deposits. More than one gem bearing gravel layers belonging to different periods of deposition can be found at any location. There is a broad correlation between the peneplanation surfaces observed in the topography of Sri Lanka and the location of the major alluvial gem deposits suggesting a link between periods of increased fluvial activity in response to changes in sea level, possibly during the last glacial period (Gunaratne and Dissanayake, 1995). A distinctive feature of most alluvial gem deposits in Sri Lanka is the diversity of gem minerals found in deposits with most common phases being found in the majority of alluvial deposits together with local variations. A full description of the illam is given below.

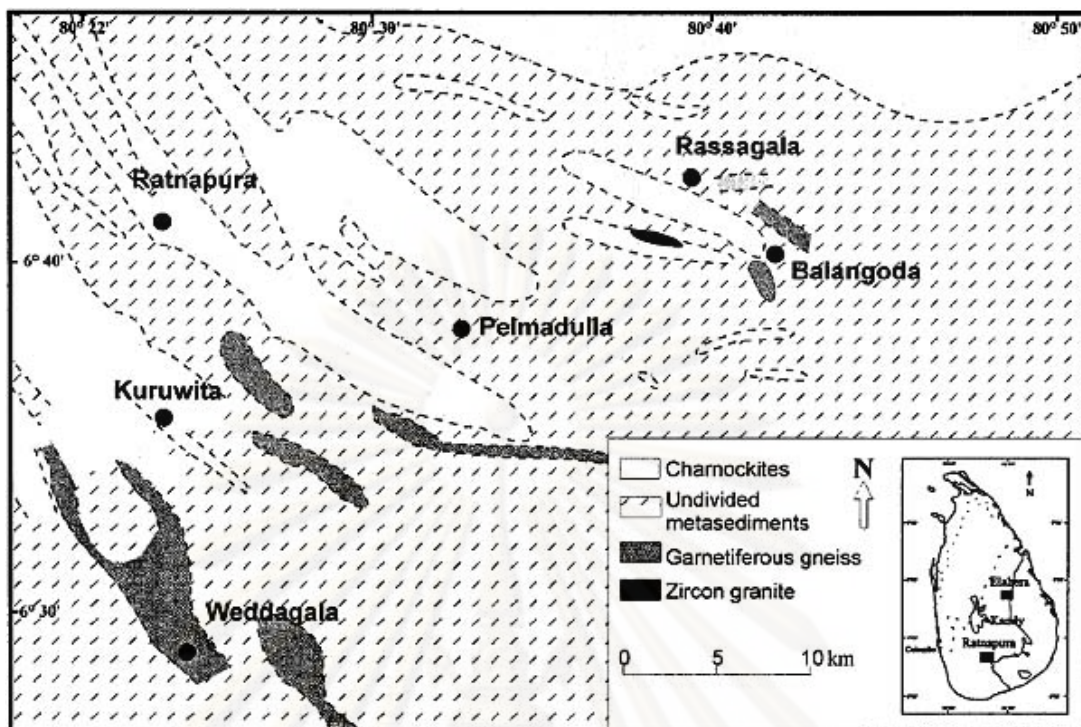


Figure 2.13 Geological map of the main Ratnapura gem field. Inset shows the location of the Ratnapura and Elahera gem fields in relation to the main lithotectonic units of Sri Lanka (Dissanayake et al., 2000).

Illam: The gem-bearing horizon within the residual/eluvial/alluvial deposit sediment is known as the illam. This is generally a 0.5-1.5m thick horizon of gem-bearing gravel capped above and below by blue-green colored clay. However, both from reports and personal observation (Henney, 1999) there is considerable variation in the thickness, extent and composition of the illam, the later of which has appears to have some correlation with the gem content of the gravels. In some areas the illam is shallow (< 3m below the surface), thin (ca. 10-20 cm), generally characterized by quartzose gravels and blue grey clay and is laterally not persistent, presumably occupying depressions in the underlying bedrock surface. At other sites it is several tens of meters (20-30 m) below the surface, 0.5-1.5 m thick and laterally extensive (several 100 m²) and is occasionally repeated with several illam horizons encountered as the shaft or pit is dug. This type of occurrence may represent a buried river valley or flood plain. Generally there is no way to predict multiple bands unless there has been earlier mining in the same area. Gem miners reported however that there is no direct correlation between thickness of the illam and gem content and that the thinnest illam

can yield significant gems whilst the thickest can be barren. In terms of bulk mineralogical composition of the illam there is a broad range from clay dominated to those containing fine-grained sand. The former are generally blue green-grey in color and have high clay content whilst the sandier illams are dark greens, brown and black. Both are often associated with high contents of organic material which releases a pungent odor when the illam is excavated and in fact presents some difficulties when extracting the illam from deeper, poorly ventilated shafts and pits.

There is some evidence, mainly anecdotal, that the sandier illams are more often characterized by higher abundance of "pashpurga" or yellow sapphire and are thus highly sought after and intensely worked when they are located. Illam is not always an alluvial facies and some occurrences are clearly elluvial and residual in origin. In particular the illam exploited for hessonite garnet near Buttala is in residual gravel within karstic hollows in weathered calcareous metasediments. This is a very local deposit and one instance the garnet is worked from the weathered bedrock itself. Mineralogically, the illam is dominated by quartzose material with minor amounts of various resistant phases including opaques. The proportion of "gravel" to fines varies as does the grain size and degree of sorting and rounding within the gravel component.

Okkampitiya Gem Field (Karstic Deposit): The Okkampitiya gem field is situated within the Buttala kippe, which is found near the HC-VC boundary within the VC (Figure 2.5). The combined HC-VC unit was overthrust onto VC, and isolated remnants of the HC rocks occur as 'klippe' or 'outliers' within the VC area. The area is underlain by marble, pelitic gneisses, quartzite, migmatite, basic granulite and minor pegmaties and calc silicate rocks, and these rocks are bounded by Vijayan granitic gneisses to the east. Marble is a dominant lithology within the Okkampitiya region. The marble is composed mainly of calcite and dolomite, other minerals presents in minor amounts include, forsterite, diopside, phlogopite and accessory spinel and apatite. The spinel shows a well-developed octahedral habit occasionally up to 10 mm across and it is often of gem-quality. Forsterite in the marble is usually partly altered. Occasionally, the top of the marble is weathered to beige to buff-colored saprolite zone, composed of microcrystalline carbonate material and coarse calcite fragments. The marble shows

cavernous features in places which are linked to short joints and fractures (<10m). The gem deposits described below provide further evidence of karstification in the marble (Mathavan et al., 2000). In contrast to the other gem fields, in the Okkampitiya gem field many of the gem bearing sediments are enclosed within karstic potholes and channels in marble (Figure 2.14). The sizes of these potholes range from a few decimeters (on the gentle slopes) up to a few meters (on flood plains) while the depth ranges up to 3-4 m (see Figures 2.14 and 2.15). Dissolution of marble by meteoric waters, particularly along joints and fractures, and perhaps subsidence and collapse would have formed the karstic potholes and channels. Perhaps the palaeokarstic process may have played a dominant role in the development of the present alluvial flood plains, and in this respect the gem-bearing sediments have calcite and dolomite as the major constituents besides from quartz.

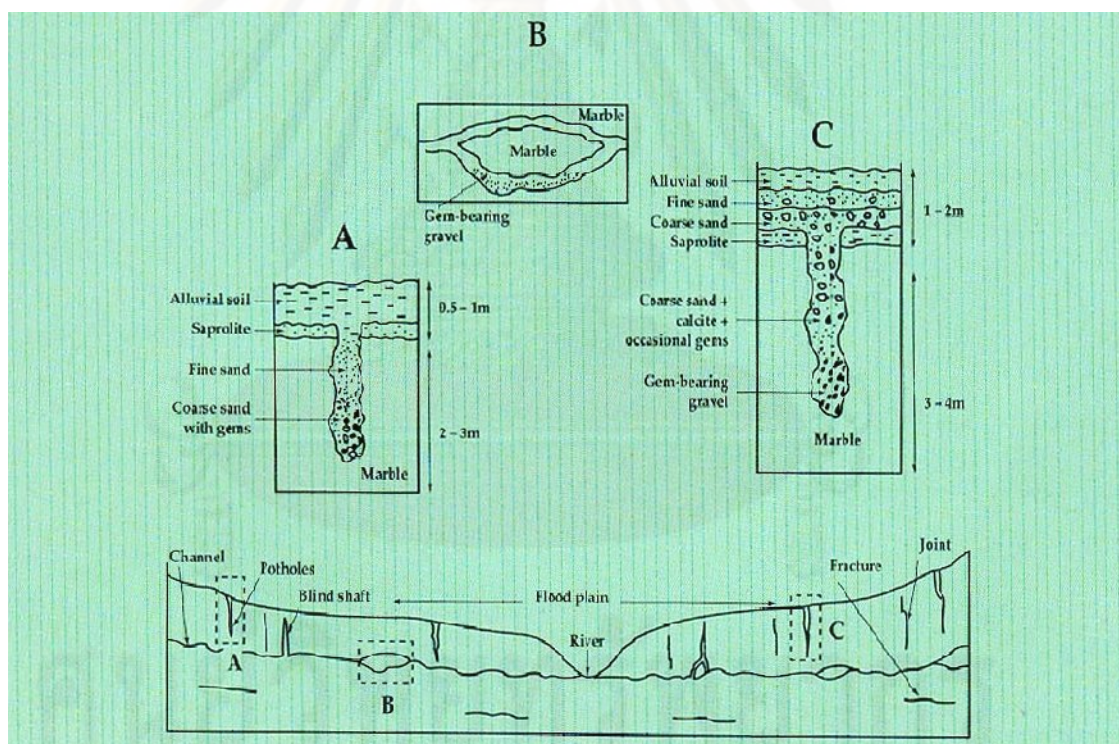


Figure 2.14 A schematic E-W cross section of the Okkampitiya area indicating occurrences of karstic potholes, blind shafts and channels. The enlargements are schematic representations of sedimentary infill in karstic potholes located on the gentle slope (A), on the flood plain (C) and a bifurcating channel (B) (Mathavan et al., 2000).



Figure 2.15 A mined karstic channel in the marble of Okkampitiya gem field (Mathavan et al., 2000).

The dominant gems in the deposits located in the flood plains are geuda-type corundum and sapphires. Their abundance decreases in sites located on the gentle slopes, where spinel and tourmaline are more prominent. The corundums invariably show worn crystal faces or rounded surfaces and the quartz pebbles, which are also present occasionally in the gem sediments, have well rounded shapes. These features either indicate long distance of transport before deposition in the potholes and the channel beds, or they represent reworked older sedimentary deposits. Additionally, swirling of sediments in the potholes could also have contributed the observed rounded features. The rough stratification of the sediments possibly suggests that the karstic plains may have been flooded with gem-bearing sediments. Primary occurrences of corundum in the Okkampitiya area have been observed, but the worn crystal faces of corundum indicate distant provenance further north, possibly from the Bibile region. In contrast to the effects of strong mechanical abrasion shown by corundum, spinel and tourmaline show sharp crystal edges on the spinels and striations remaining on the tourmalines, which are evidence of local provenance. As noted earlier, gem quality spinel occurs in the host marble, and the local pegmatites may have been the source of

the tourmaline. Krastic marble terrains clearly provide important “*sedimentation traps*” for gem-bearing deposits. In addition, small pockets of gemstone-rich deposits, found elsewhere on the island and sometimes referred to as ‘gedi illam’, may have been formed in a similar manner either in marble or related lithologies (Mathavan et al., 2000).

2.5 Awissawella Deposit

Awissawella deposit, the study area, is located about 50 kms east of Colombo. It is a part of Ratnapura gem field as shown in Figure 2.16. Most of Ratnapura gem fields lie in the Highland South Western Complex unit which consists of Precambrian metamorphic rocks. However, gem exploitations have carried out along flood plains and hill slopes characterized by parallel ridge and valley topography (Danhnayake, 1980) in which vast gem field of alluvial and eluvial types are recognized (Dissanayake et al., 2000). For instant, Awissawella deposit is characterized by secondary deposit that has derived from contact metamorphic rock in particular spots along the Highland South Western Complex. All gravels and fine-grained sediments have been transported into alluvial deposits situated very close to the mountainous source (Figure 2.17). Gem mining around Awissawella deposit is typically small scale pitting (Figure 2.18). Corundums are found in the gravel beds at least 2 layers containing shallower than 10 m and deeper than 40 m. Miners dig into gravel bed, then tunnel along that taking all sediments for washing. These gravel beds contain fragmental rocks of gneiss schist, sapphire, quartz, etc. (Figure 2.19). In addition, geode-like gravel containing abundant mica formed as outer crust and often found sapphire accumulated with other minerals in the central hole (Figure 2.20).

ศูนย์วิทยุทรัพยากร

จุฬาลงกรณ์มหาวิทยาลัย

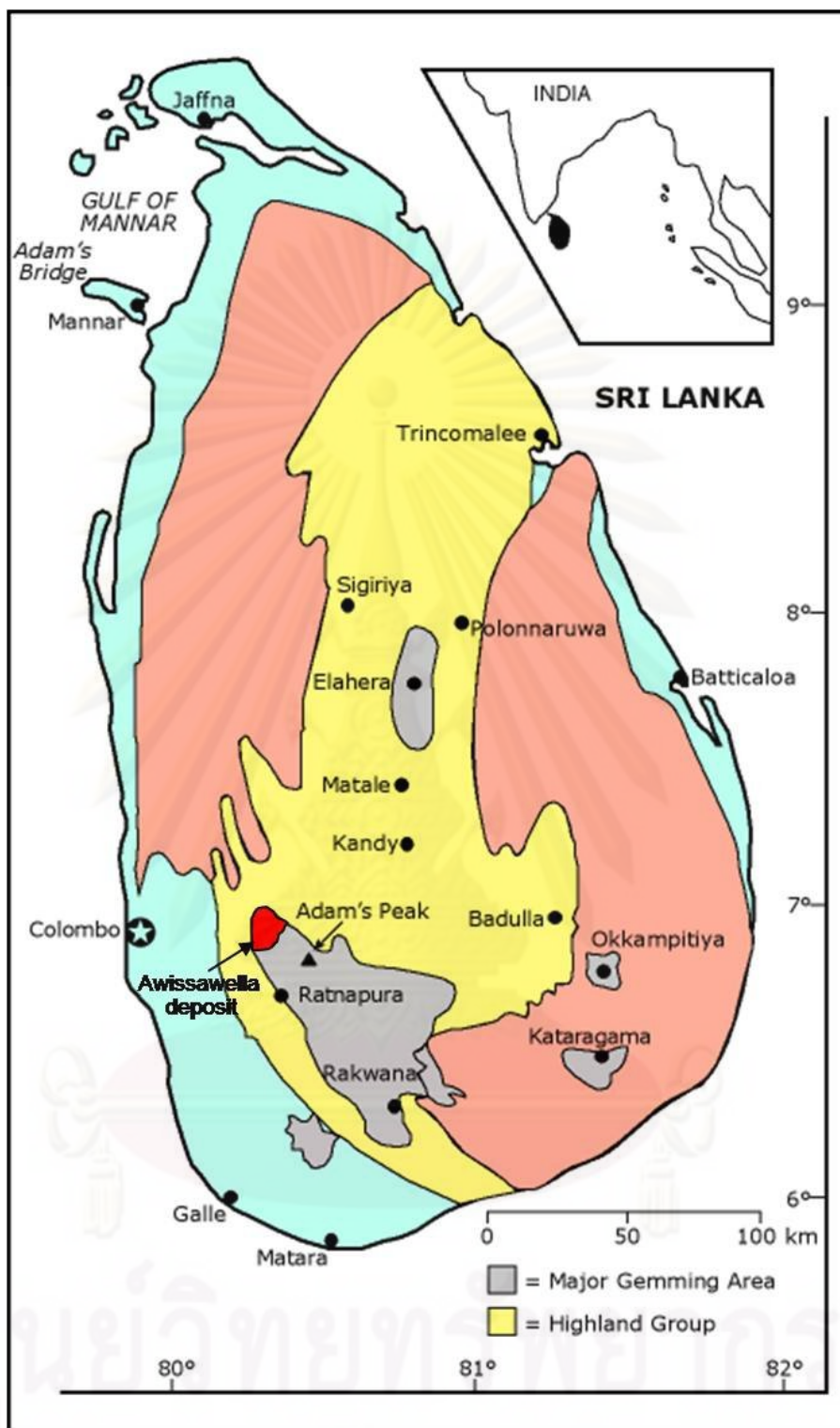


Figure 2.16 Map of Sri Lanka (Ceylon) showing the locations of the important cities, mining areas and Ratnapura gem field including Awissawella, that is located in the Highland South Western Complex (modified from www.palagems.com/ceylon_sapphire_bancroft.htm).



Figure 2.17 Awissawella deposit located close to the mountain which is possible primary source of corundum.



Figure 2.18 Mining pits in Awissawella deposit operated by local miners.



Figure 2.19 Rock fragments and mineral assemblages, mainly quartz, contained in gravel beds.

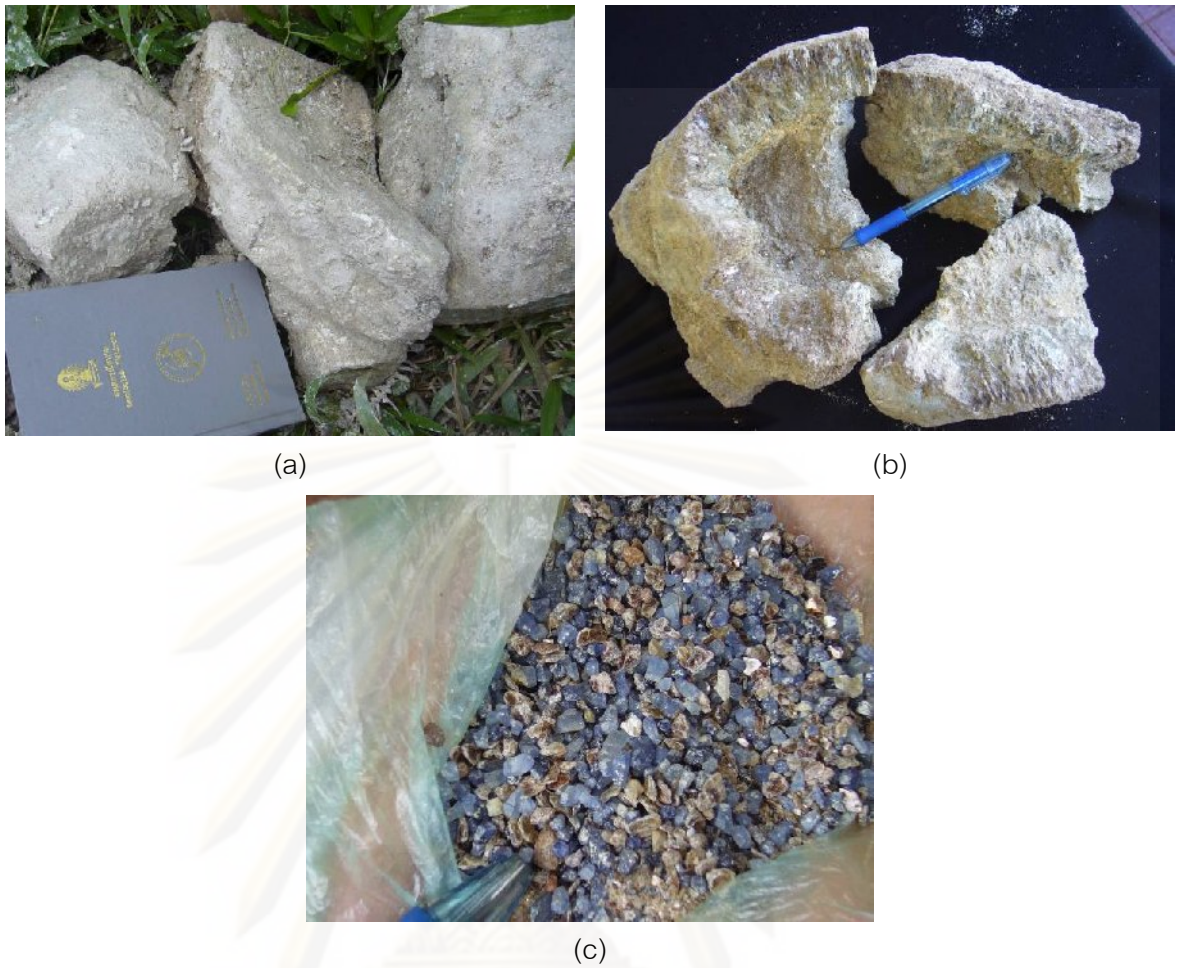


Figure 2.20 (a) and (b) Geode-like gravels found in gravel beds that contain corundum; (c) corundum samples and other minerals found in geode-like gravels.

ศูนย์วิทยทรัพยากร
จุฬาลงกรณ์มหาวิทยาลัย

CHAPTER III

AWISSAWELLA CORUNDUM AND GENERAL CHARACTERISTICS

3.1 Introduction

This chapter reports the general characteristics of corundum from Awissawella deposits in their natural conditions before treatment. All forty six corundum samples were selected to represent whole batch (about 500 stones) (Figure 3.1). The selection was usually based on the variation of color and transparency of these samples. Most of the samples clearly show well-preserved crystal habits such as barrel shape, hexagonal prism and spindle-shaped hexagonal bipyramid (see Figure 3.2). Their weights range from 1.0 to 5.0 carats. Besides, most stones are fractured and partly filled by iron stains. Subsequently, they were cut and polished as flat surfaces perpendicular and parallel to the c-axis before further investigation. Then physical and gemological properties of the samples were observed, measured and recorded. These physical and gemological properties include color, specific gravity (SG), refractive index (RI), fluorescence under long wave (LW) and short wave (SW) of ultraviolet (UV) lamp and internal features. All properties mentioned above were carried out using basic gem testing equipments and some advanced instruments which details will be described in the following sections. For spectroscopic studies and trace compositions results will be reported in the next chapters.



Figure 3.1 Corundum sample batch from Awissawella, Sri Lanka.

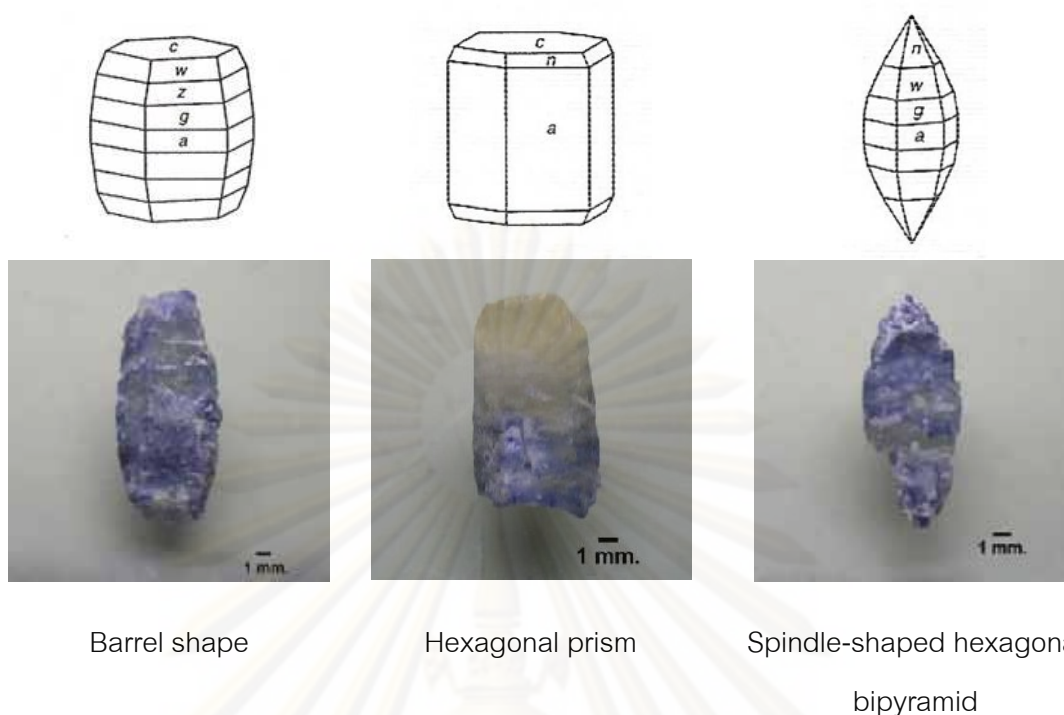


Figure 3.2 Crystal habits in some sapphires from Awissawella.

3.2 Color

The rough samples of Awissawella corundum used in this study are generally blue in color. But after cut and polished, they show some variations of body color and color patch or zoning in all samples. Consequently all 46 samples were separated, based on their body color shades, into two color varieties; the first variety has yellow body with blue patch (SapAw01-SapAw33) and the second variety has light blue body with deeper blue patch (SapMa01-SapMa13) (see Appendix A). Observation was done under standard daylight 6500 K and comparison with GIA Gem Set. GIA Gem Set color specimens were made from plastic: they have 2 different sides (e.g. faceted and flat). Flat side was used during this study because it is more appropriated to the samples.

Color codes of samples obtained from the comparison are summarized as following. Yellow variety is composed of yellow (Y), greenish yellow (gY) and yellow green (YG/GY) (Figure 3.3). Light blue variety is mostly blue (B) and violet blue (vB) (Figure 3.4). Color patch or zoning, both samples in yellow variety and blue variety have blue shades contains blue (B), bluish violet (bV) and violet blue (vB). Comparative results of all color varieties are shown in Appendix A.

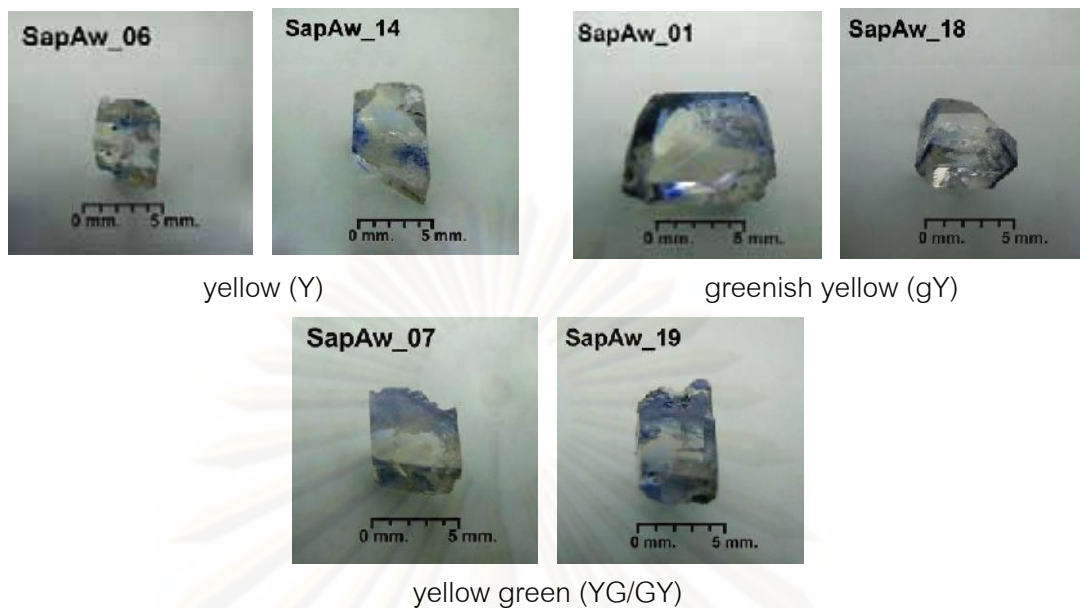


Figure 3.3 Different body colors in yellow variety of samples in which their color codes are based on the GIA Gem Set.



Figure 3.4 Different body colors in light blue variety of samples in which their color codes are based on the GIA Gem Set.

3.3 Physical and Gemological Properties

All of the physical and optical properties are summarized in Tables 3.1-3.2 and details of result are reported in Appendix A.

Table 3.1 Summary of physical properties of representative corundum samples from Awissawella, Sri Lanka.

Varieties	Weight (ct)	SG.	GIA Color Code	
			Body	Patch
Yellow	1.01-9.25	3.90-3.97	Y2/2-Y3/5 gY2/3-gY3/4 YG/GY2/1	B4/2-B7/4 vB4/3-vB7/3 bV7/4- bV8/3
Light blue	1.52-8.02	3.90-3.96	B2/2-B5/2 vB3/3-vB4/3	B3/4-B5/1 vB4/3-vB5/3 bV8/3

Table 3.2 Summary of optical properties of yellow and light blue sapphire varieties from Awissawella, Sri Lanka.

Varieties	Refractive Indices		Bire.	Fluorescence	
	n_e	n_o		LW	SW
Yellow	1.768-1.771	1.760-1.763	0.007-0.009	st. Orange	w. to mo. Orange
Light blue	1.768-1.772	1.761-1.763	0.007-0.009	mo. Orange - mo. Reddish orange	vw. Orange

ศูนย์วิทยทรัพยากร
จุฬาลงกรณ์มหาวิทยาลัย

CHAPTER IV

ABSORPTION SPECTRA AND TRACE ELEMENT CONTENTS

4.1 Introduction

Spectrometry and trace element compositions of sapphire samples are reported herein in this chapter. Spectrometry was analyzed within lengths of infrared and UV-VIS-NIR using Fourier Transform Infrared (FTIR) Spectrometer and UV-VIS-NIR Spectrometer as mentioned in Chapter I. For trace element geochemistry, it was analyzed for both semi-quantitative contents using Energy Dispersive X-ray Fluorescence Spectrometer (EDXRF) and quantitative contents using Electron Probe Micro-Analyzer (EPMA).

The FTIR spectra give information on some structural and bonding of molecules within gem specimen. The transition responsible for IR band is related to molecular vibrations (stretching or bending of bonds). Therefore, infrared absorption is caused by structural vibration determined by bond lengths and bond angles between atoms (Volynets et al., 1972; Baran, 1991; Smith, 1995).

Absorption spectra of corundum and other gemstones are usually investigated within wavelengths ranging between 200 and 1500 nm which are parts of ultraviolet (UV) (10-380 nm), full range of visible light (VIS) (380-780 nm) and parts of near infrared (NIR) (780-2500 nm). UV-VIS-NIR spectroscopy may give information of absorption spectra in this range, which in turn may be related to electron transitions of trace elements or other structural defects in sapphires. The colors in corundum are significantly caused by Cr, Ti and Fe which they usually occur as trace geochemical composition. Trace elements causing colors, known as chromophores, in corundum crucially contain chromium, titanium, iron, vanadium and probably magnesium. Interaction between these elements and main aluminium component can absorb some parts of the visible light, causing distortion even with very narrow ranges; consequently, colors are produced by combination of the rest of visible spectrum.

In addition, non-coloring trace elements, such as gallium, silicon and calcium may also be found in corundum which may in turn be very crucial indication of geographic origin. Therefore, EDXRF analyses have been used to compare statistically among corundums from other places throughout the world which is the main purpose of gem labs for certification of corundum origin. On the other hand, EPMA results are aimed to explain the cause of color and potential for heat treatment of Awissawella corundums; however, they have to be investigated in relation with UV-VIS-NIR spectroscopy.

4.2 Fourier Transform Infrared Spectrometry

Forty six samples of Awissawella corundum representing all color varieties were examined within near- to mid- infrared (IR) spectral region. Each sample was fixed in the middle of a sample holder plate with 0.3 mm diameter slit and placed in the cell holder. Single IR beam was allowed to pass through the sample to detector.

Representative spectra of unheated sapphires from all color varieties are present in Figures 4.1 to 4.4. The observed spectra usually reveal similar absorption patterns within wave number range of 400-4000 cm^{-1} . They contain peaks of CO_2 , probably caused by air and breath at 2360-2365 cm^{-1} and 2340-2350 cm^{-1} , peaks of C-H stretching of hydrocarbon, may be coated along crack and surface, at 2840, 2920, 2950 and 3051 cm^{-1} (Smith, 1995), peaks of H_2O likely from humidity at 3400-3900 cm^{-1} , and only yellow variety samples show band peaks of structural O-H stretching at 3183, 3232 and 3309 cm^{-1} (Volynets et al., 1972). Apart from the common peaks, some samples (Figures 4.2 and 4.3) show extensively declined curve within 3200-3700 cm^{-1} along with strongly absorption curve of C-H stretching. These samples were then taken to examine in detail again. Consequently, many cracks were recognized; these cracks contain iron stain; besides, carbon-containing polishing powder and humidity remained after polishing process may cause such curious curves. However, they are possibly affected by diaspore ($\text{AlO}(\text{OH})$) in the stones. Hydrogen (H) in the environment may diffuse into crystal lattice and combines with oxygen (O) forming $\text{AlO}(\text{OH})$ structure that is invisible even observing under microscope but it can be detected by FTIR at 3309 cm^{-1} absorption peak (Lomthong, 2004).

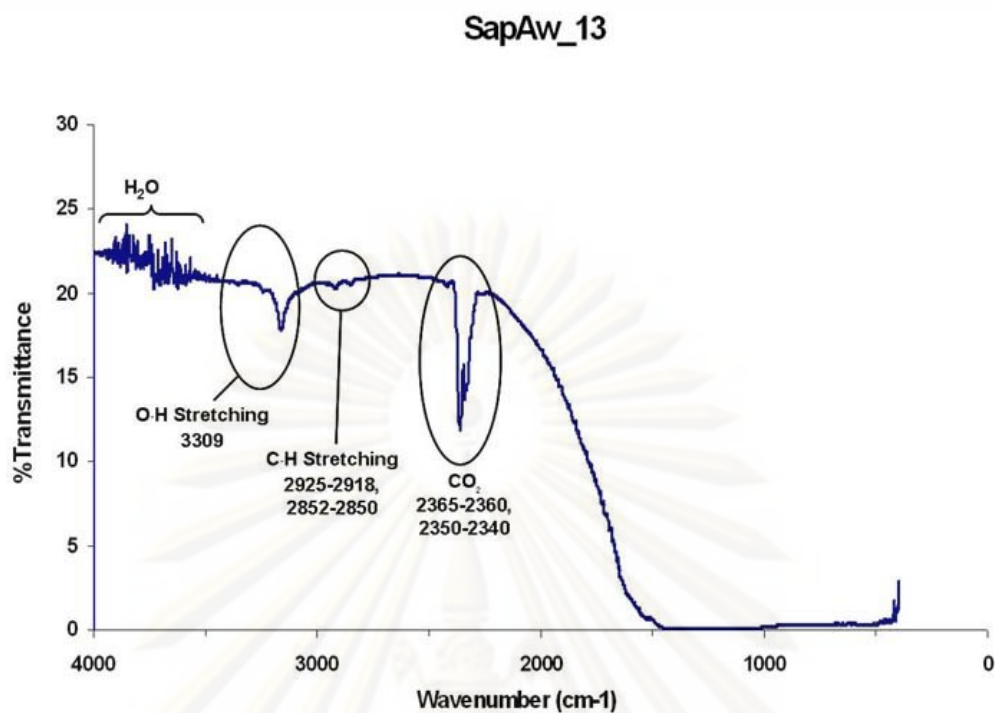


Figure 4.1 FTIR Spectrum of SapAw_13 of yellow variety shows common absorption pattern.

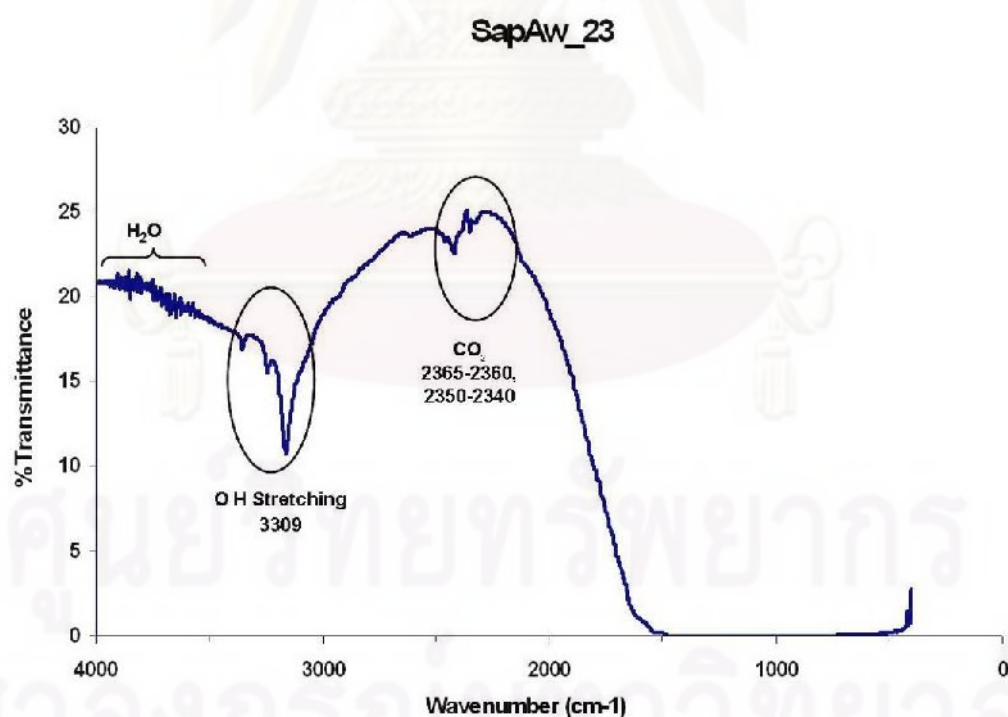


Figure 4.2 FTIR Spectrum of SapAw_23 of yellow variety showing declined curve within 3200-3700 cm⁻¹ along with strong absorption around 3309 cm⁻¹.

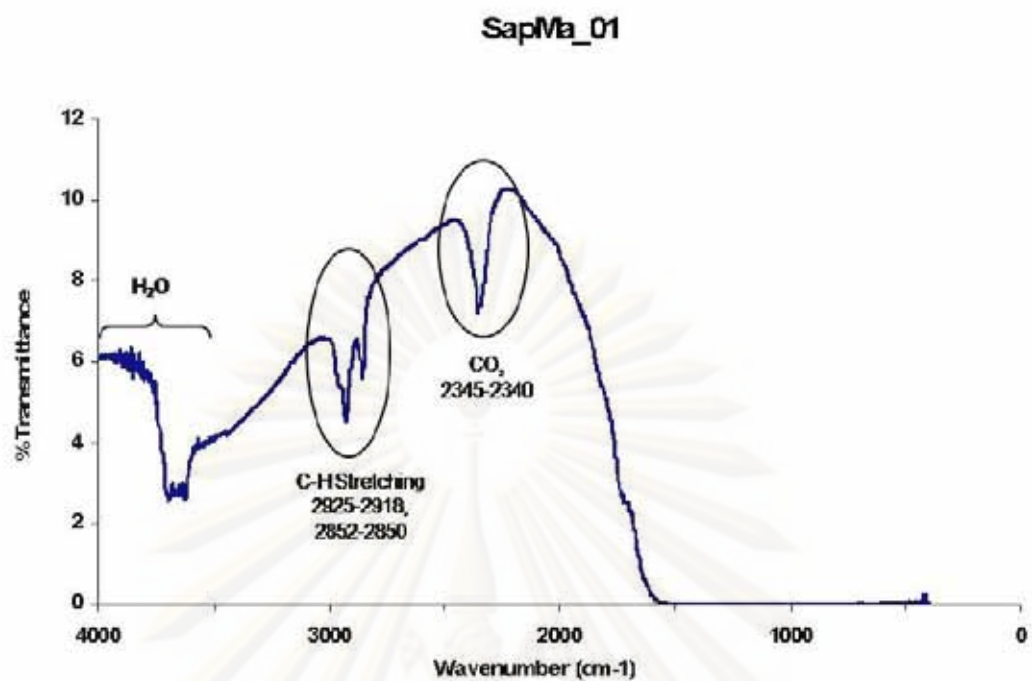


Figure 4.3 FTIR Spectrum of SapMa_01 of light blue variety showing declined curve within $3200\text{-}3700\text{ cm}^{-1}$ along with strongly absorption curve of C-H stretching.

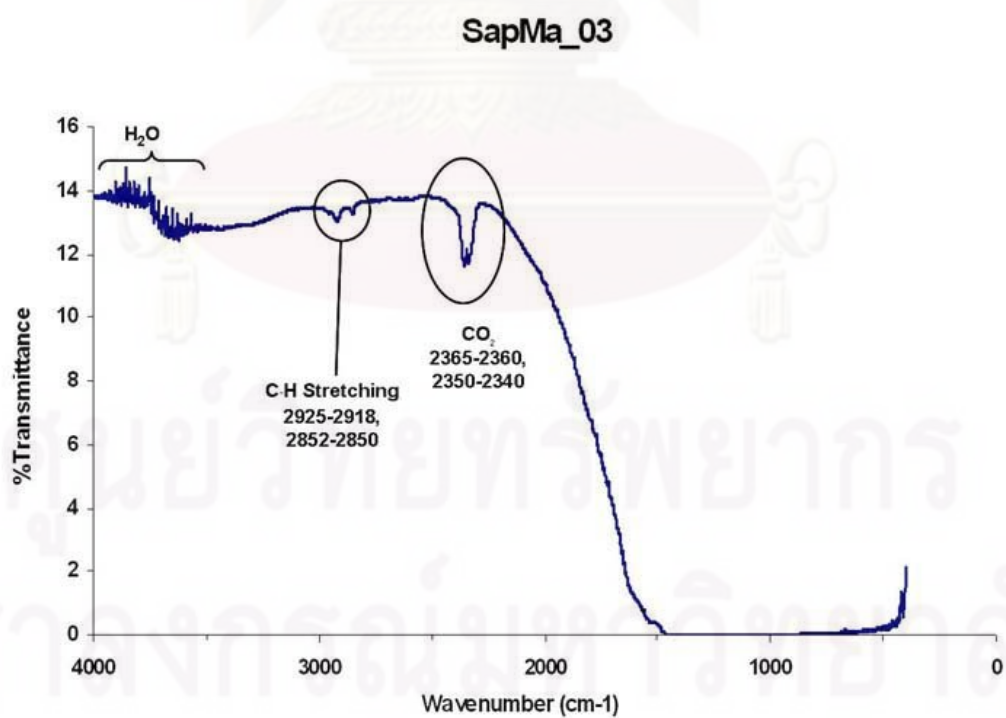


Figure 4.4 FTIR Spectrum of SapMa_03 of light blue variety shows common absorption pattern.

4.3 UV-VIS-NIR Spectrometry

Representative UV-VIS-NIR absorption patterns of both sample varieties from Awissawella are presented in Figures 4.5 to 4.8. All spectra observed from both varieties are summarized in Table 4.1. Comparative results of all color varieties are reported in Appendix C.

Absorption patterns of yellow variety with colors shading from yellow to greenish yellow and yellow green, usually show a continuous increase of absorption toward the UV region of the spectra with a minor peak of $\text{Fe}^{3+}/\text{Fe}^{3+}$ pairs at 450 nm, band of $\text{Fe}^{2+}/\text{Ti}^{4+}$ pairs with maxima at 565 nm and also Fe^{3+} peak at 388 nm (Figures 4.5 to 4.7). These absorption peaks give clearly combination between blue and yellow that make stones appearing yellow to yellow green colors.

Blue variety shading from blue to blue and bluish violet mostly shows absorption patterns quite similar to those observed in the yellow variety. It may be due to green color shades (greenish yellow and yellow green); besides, blue color patches found in the yellow variety are likely caused by similar processes in the blue variety. In general, absorption patterns of blue variety present peak of $\text{Fe}^{3+}/\text{Fe}^{3+}$ pairs at 450 nm, bands of $\text{Fe}^{2+}/\text{Ti}^{4+}$ pairs with maxima at 565 nm and also Fe^{3+} peak at 388 nm and in bluish violet samples usually present small peak of Cr^{3+} at 412 nm (Figures 4.8 and 4.9). However, absorption band with peak at 565 nm of $\text{Fe}^{2+}/\text{Ti}^{4+}$ becomes stronger in blue variety. In addition, peak at 377 nm caused by $\text{Fe}^{3+}/\text{Fe}^{3+}$ pairs (Figure 4.9) is sometime observed in blue sample.

ศูนย์วิทยทรัพยากร

จุฬาลงกรณ์มหาวิทยาลัย

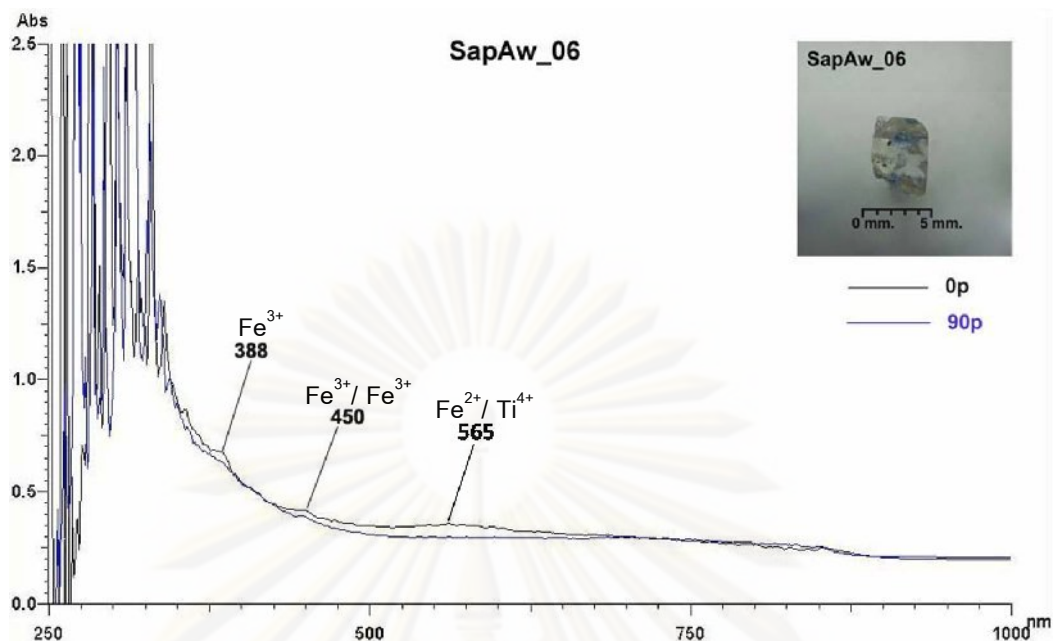


Figure 4.5 UV-VIS-NIR spectra yellow (SapAw_06) in yellow variety (color code Y2/2) showing absorption peaks due to Fe³⁺/Fe³⁺ pairs and Fe³⁺ at 450 and 388 nm, respectively; besides, blue patch may yield absorption bands due to Fe²⁺/Ti⁴⁺ IVCT with the maxima about 565 nm.

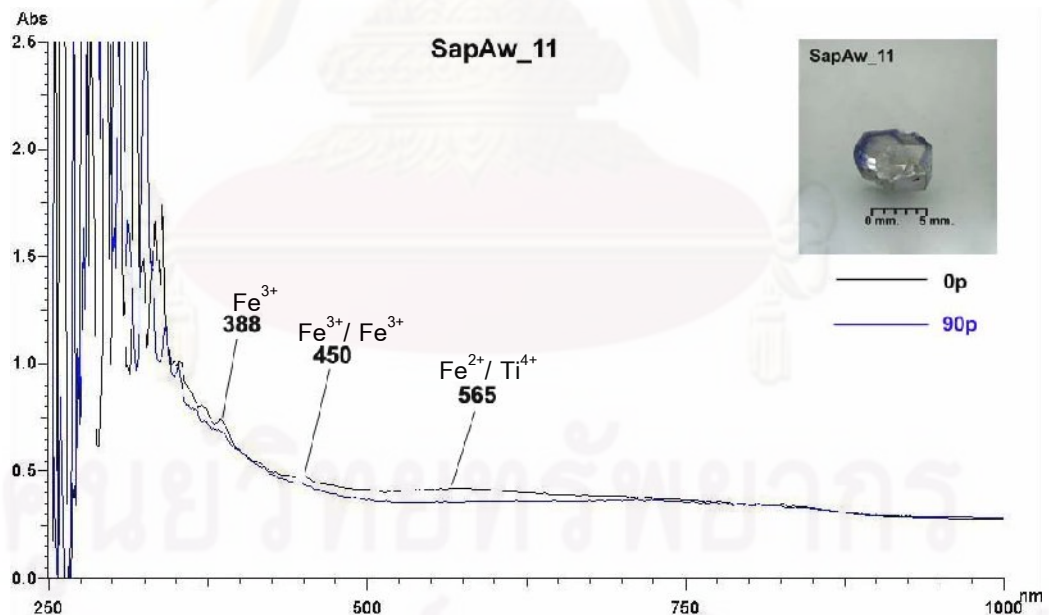


Figure 4.6 UV-VIS-NIR spectra greenish yellow (SapAw_11) in yellow variety (color code gY3/4) showing absorption peaks due to Fe³⁺/Fe³⁺ pairs and Fe³⁺ at 450 and 388 nm, respectively; besides, its light greenish yellow with blue patch may cause absorption bands due to Fe²⁺/Ti⁴⁺ IVCT with the maxima about 565 nm.

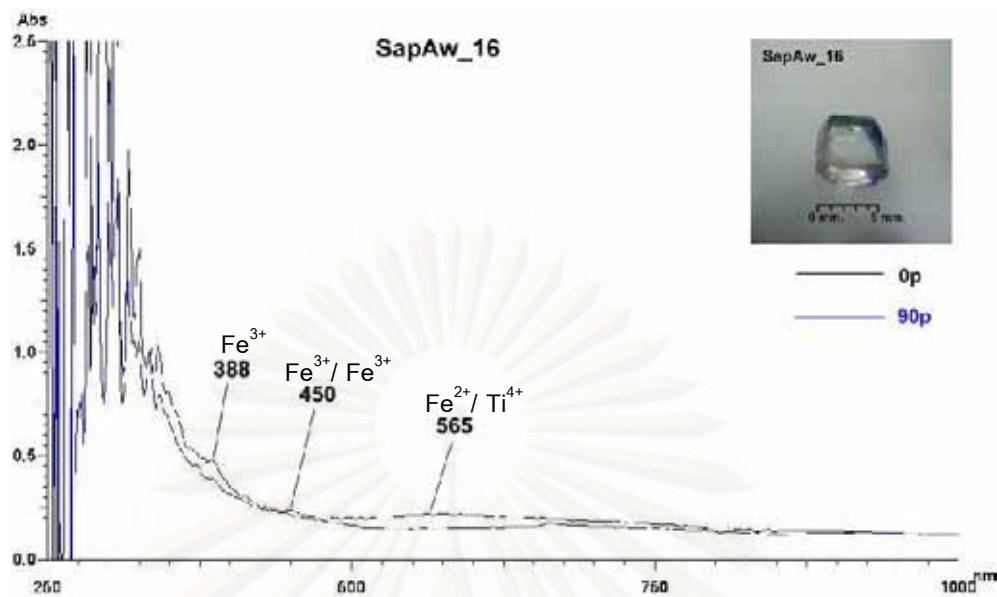


Figure 4.7 UV-VIS-NIR spectra yellow green (SapAw_16) in yellow variety (color code YG/GY 2/1) showing absorption peaks due to Fe³⁺/Fe³⁺ pairs and Fe³⁺ at 450 and 388 nm, respectively; besides, its yellow green with blue patch may cause absorption bands due to Fe²⁺/Ti⁴⁺ IVCT with the maxima about 565 nm.

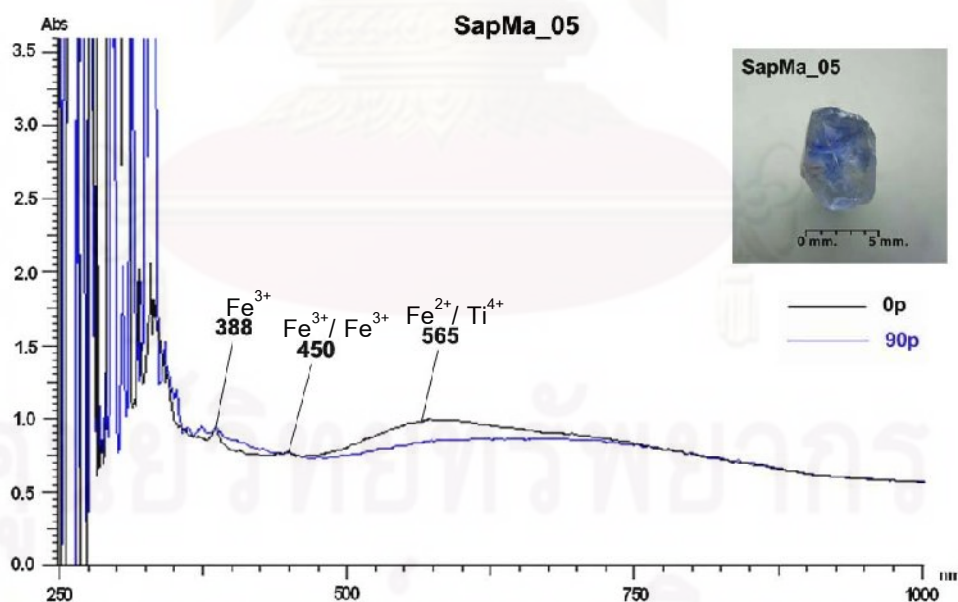


Figure 4.8 UV-VIS-NIR spectra blue (SapMa_05) in blue variety (color code B5/2) showing of absorption peaks at 388 and 450 nm due to of Fe³⁺ and Fe³⁺/Fe³⁺ pairs, respectively and present of strong absorption band with peaks of Fe²⁺/Ti⁴⁺ IVCT with maxima at 565 nm is main cause of blue color.

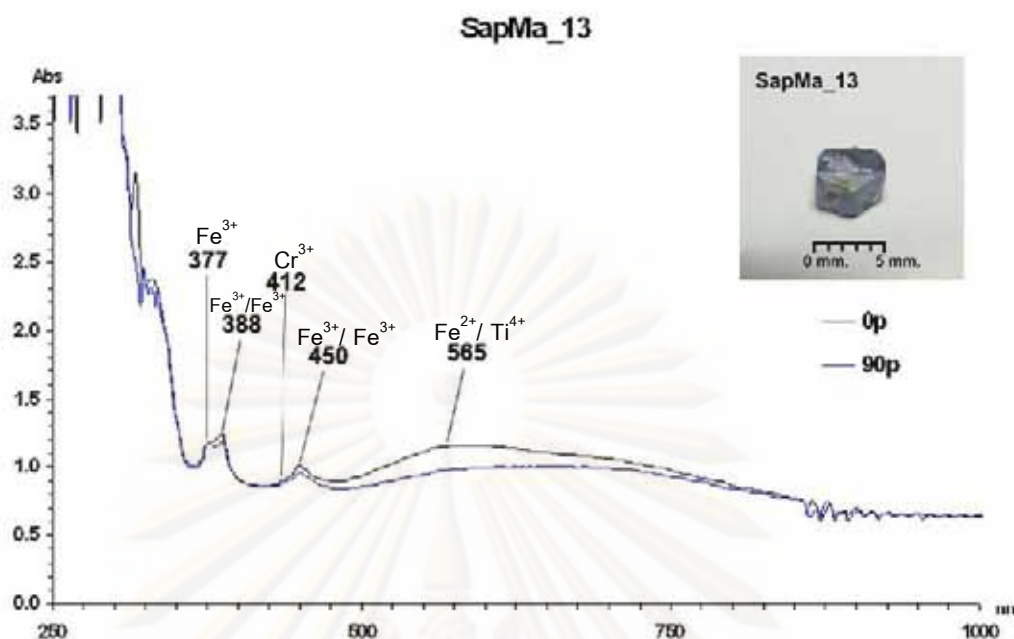


Figure 4.9 UV-VIS-NIR spectra violet blue (SapMa_04) in blue variety (color code vB4/3) showing absorption peaks at 388 nm of Fe^{3+} , 377 and 450 nm of $\text{Fe}^{3+}/\text{Fe}^{3+}$ pairs; besides, strong absorption bands with maxima at 565 nm of $\text{Fe}^{2+}/\text{Ti}^{4+}$ IVCT causing blue color are also observed.

Table 4.1 Absorption features of chromophores in Awissawella corundum (modified from Themelis, 1992).

Peak (nm)	Element	Apparent Color	Color Variety of Awissawella corundums				
			Yellow			Blue	
			Y	gY	YG/GY	B	vB
377	$\text{Fe}^{3+}/\text{Fe}^{3+}$	blue, blue/green, green, yellow	-	-	-	-	✓
388	Fe^{3+}	pink, orange, blue, blue/green, green, yellow, golden/yellow	✓	✓	✓	✓	✓
412	Cr^{3+}	ruby; pink, blue, blue/green	-	weak	-	-	-
450	$\text{Fe}^{3+}/\text{Fe}^{3+}$	pale orange, blue, blue/green, yellow, golden/yellow, green	✓	✓	✓	✓	✓
565	$\text{Fe}^{2+}/\text{Ti}^{4+}$	blue, blue/green sapphires	weak	✓	✓	✓	✓

4.4 Semi-Quantitative EDXRF Analyses

Semi-quantitative trace element analyses of corundum samples were carried out for Fe, Ti, Cr, Ga and V contents using an EDXRF spectrometer, OXFORD model ED2000 and model EAGLE III. The analytical results are summarized in Tables 4.2 and 4.3. The results of all samples are present in Appendix D.

Table 4.2 Statistic EDXRF analyses of trace elements contained in Awissawella sapphire samples obtained from model OXFORD, ED 2000.

Color Variety Wt%	Yellow sapphire variety		Blue sapphire variety	
	Min-Max	Mean±SD	Min-Max	Mean±SD
Fe ₂ O ₃	0.125-0.940	0.340±0.181	0.134-0.265	0.198±0.053
TiO ₂	0.025-0.223	0.087±0.048	0.044-0.130	0.085±0.034
Cr ₂ O ₃	0.000-0.023	0.007±0.007	0.000-0.009	0.002±0.003
Ga ₂ O ₃	0.006-0.014	0.010±0.002	0.010-0.021	0.016±0.004
V ₂ O ₅	0.000-0.037	0.005±0.008	0.001-0.013	0.006±0.004

Results from model OXFORD, ED 2000. are described as below;

The yellow variety contains high iron contents ranging from 0.125 to 0.940% with an average of 0.340% Fe₂O₃. Titanium contents are moderate to low (0.025-0.223% with an average of 0.087% TiO₂). The other elements are mostly low such as ≤0.023% Cr₂O₃, ≤0.014% Ga₂O₃ and ≤0.037% V₂O₅.

The blue variety also appears to have high iron contents (0.134-0.265% with an average of 0.198% Fe₂O₃) while titanium contents are moderate to low contents (0.044-0.130% with an average of 0.085% TiO₂). Besides, contents of chromium (≤0.009% Cr₂O₃), gallium (≤0.021% Ga₂O₃), and vanadium (≤0.013% V₂O₅) are similarly low.

Table 4.3 Statistic EDXRF analyses of trace elements contained in Awissawella sapphire samples obtained from model EAGLE III.

Color Variety Wt%	Yellow sapphire variety		Blue sapphire variety	
	Min-Max	Mean±SD	Min-Max	Mean±SD
Fe ₂ O ₃	0.035-0.315	0.084±0.072	0.040-0.120	0.065±0.031
TiO ₂	0.010-0.200	0.044±0.039	0.020-0.130	0.044±0.045
Cr ₂ O ₃	0.000-0.010	0.006±0.004	0.000-0.210	0.033±0.092
Ga ₂ O ₃	0.000-0.030	0.006±0.008	0.000-0.0870	0.016±0.037
V ₂ O ₅	0.000-0.010	0.007±0.004	0.000-0.015	0.006±0.006

Results from model EAGLE III are described as below;

The yellow variety contains high iron contents ranging from 0.035-0.315% with an average of 0.084% Fe₂O₃. Titanium contents are moderate to low (0.010-0.200% with an average of 0.044% TiO₂, some samples show values up to 0.200%) while other elements contents are low ($\leq 0.010\%$ Cr₂O₃, $\leq 0.030\%$ Ga₂O₃ and $\leq 0.010\%$ V₂O₅).

The blue variety also appears to have high iron contents (0.040-0.120% with an average of 0.065% Fe₂O₃) and moderate to low content of titanium (0.010-0.130% with an average of 0.044%, some samples show values up to 0.130% TiO₂). Other elements are low contents; chromium ($\leq 0.010\%$ some samples show values up to 0.210% Cr₂O₃), gallium ($\leq 0.010\%$, some samples show values up to 0.087% Ga₂O₃), vanadium ($\leq 0.015\%$ V₂O₅).

The result of trace geochemistry in samples from both, model OXFORD, ED2000 and model EAGLE III are counterpart, there are rather high in iron contents, moderate to low in titanium contents and low contents in chromium, gallium and vanadium. Average analyses and their standard deviation (S.D.) of each variety are graphically and Model shown in Figure 4.10. However, analytical errors are clearly large as shown by the error bars in Figure 4.10; therefore EDXRF analyses should not be conclusive evidences.

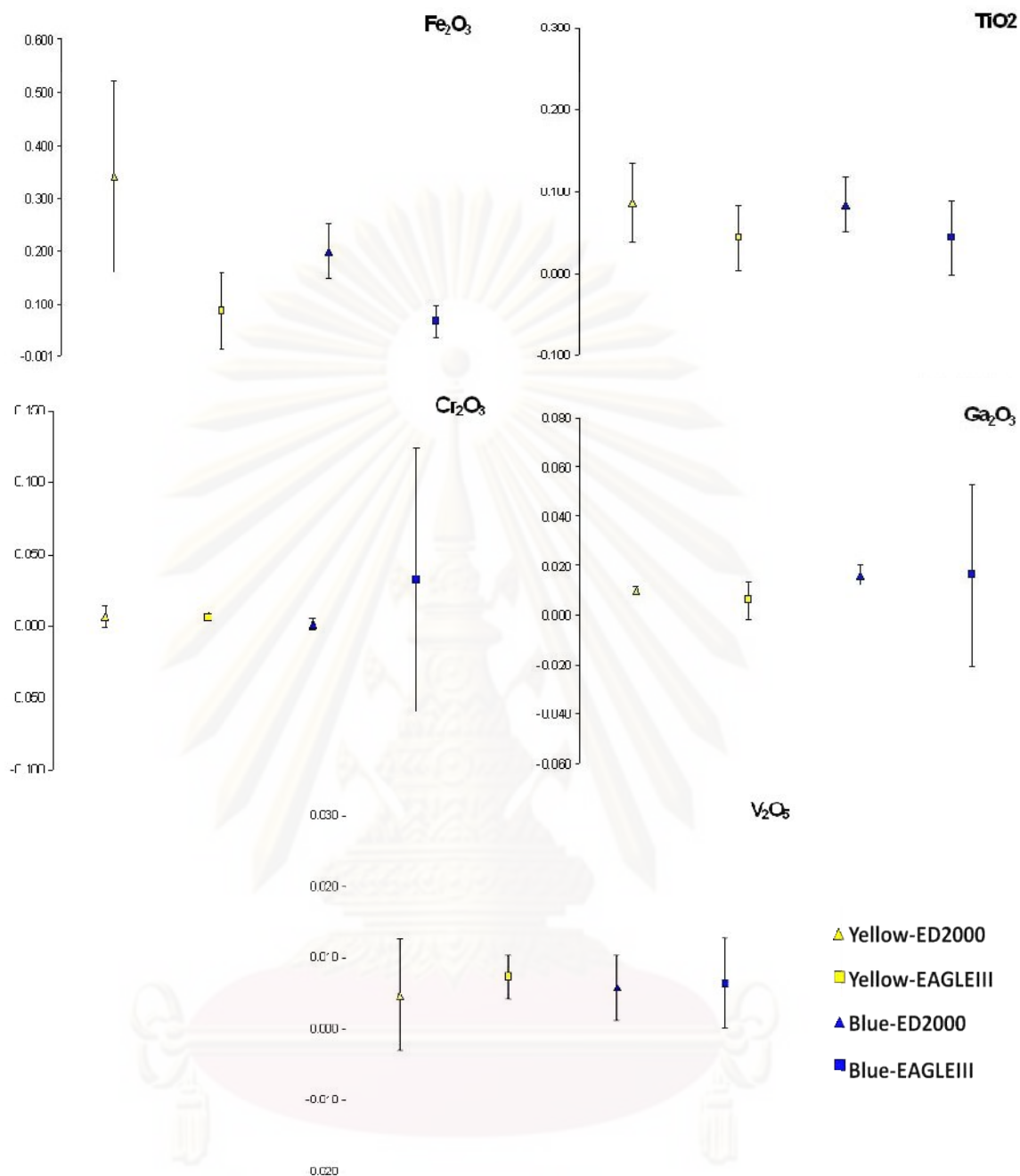


Figure 4.10 Average of trace elements revealed as symbols obtained by EDXRF and their standard deviations in form of lines.

4.5 Quantitative EPMA Analyses

Electron Probe Micro-Analyzer (EPMA) was used to analyze quantitative major and trace geochemistry, i.e., Ti, Cr, Ga, V, Fe, Ca, Mg, Mn and K. Separately analysis along the body color and patch color was designed for all samples. For instant, yellow sapphire variety is divided into 2 main analyzed zones (yellow body and blue patch)

(see Figure 4.11a) whereas blue sapphire variety is also divided into 2 main analyzed zones (light blue body and blue patch) (see Figure 4.11b). Table 4.4 shows statistic EPMA analyses in different color zones of each sapphire variety. Recalculated atomic proportion based on 3 oxygen atoms were carried out and listed in the same Table. The results of all samples are collected in Appendix E.

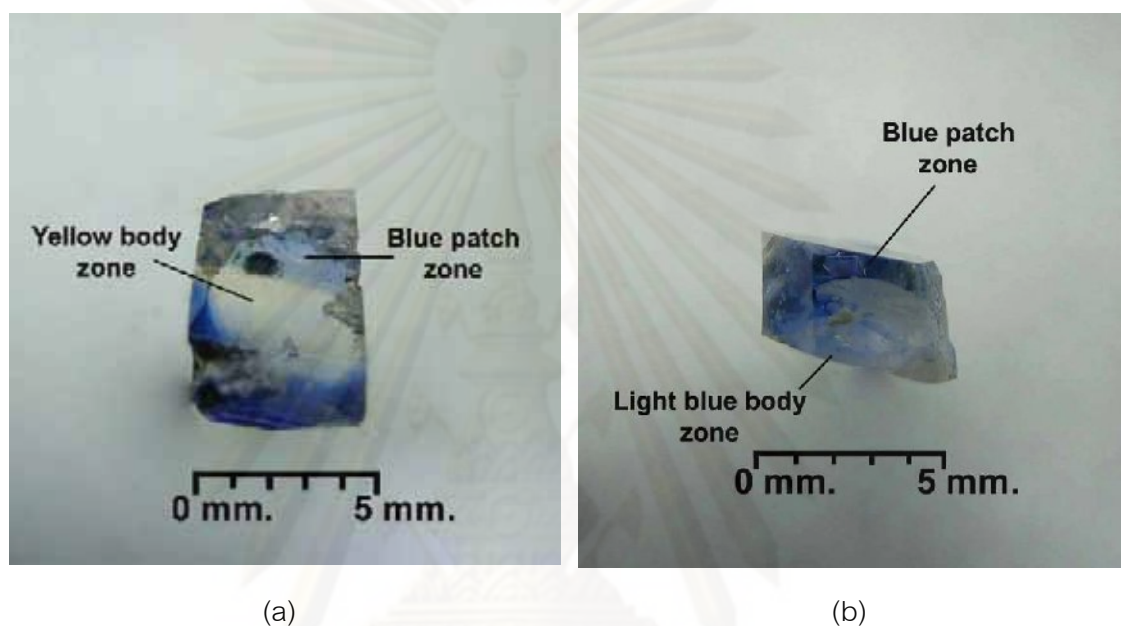


Figure 4.11 Different areas selected for EPMA analyses: (a) Yellow sapphire variety containing yellow body and blue patch zones; (b) Blue sapphire variety with light blue body and blue patch zones.

Table 4.4 Statistics of EPMA analyses of Awissawella sapphire samples obtained from quantitative EPMA and their recalculated atomic portion based on 3(O).

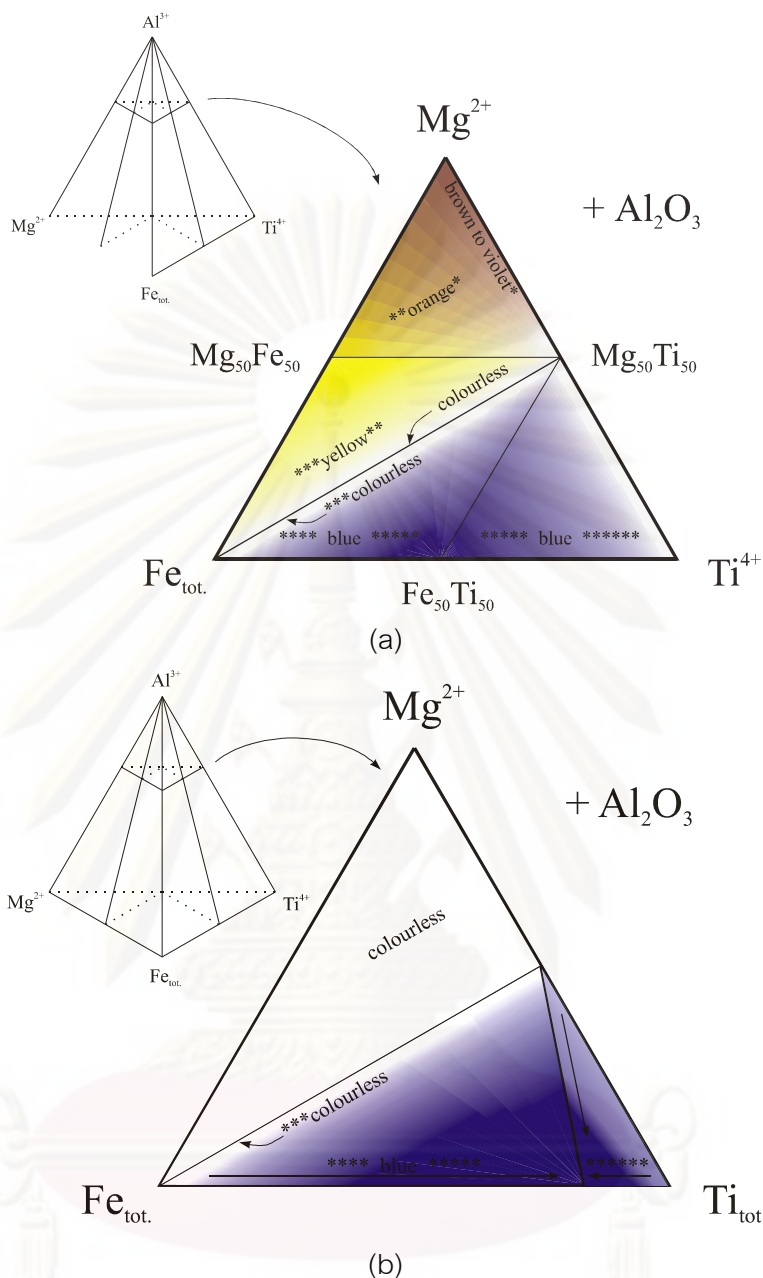
Color variety wt%	Yellow sapphire variety				Blue sapphire variety			
	Yellow Body		Blue Patch		Light blue Body		Blue Patch	
	Min-Max	Mean±SD	Min-Max	Mean±SD	Min-Max	Mean±SD	Min-Max	Mean±SD
Al ₂ O ₃	98.624-101.163	99.956±0.548	98.628-101.376	99.910±0.489	99.561-101.061	99.996±0.420	99.727-101.051	100.090±0.420
SiO ₂	0.000-0.066	0.014±0.012	0.000-0.173	0.017±0.018	0.000-0.067	0.019±0.016	0.000-0.077	0.014±0.017
TiO ₂	0.000-0.244	0.027±0.043	0.000-0.444	0.052±0.046	0.000-0.223	0.064±0.054	0.003-0.147	0.037±0.032
Cr ₂ O ₃	0.000-0.025	0.003±0.005	0.000-0.025	0.003±0.005	0.000-0.023	0.003±0.005	0.000-0.016	0.004±0.005
Ga ₂ O ₃	0.000-0.053	0.010±0.011	0.000-0.039	0.009±0.009	0.000-0.049	0.014±0.011	0.000-0.057	0.014±0.013
V ₂ O ₃	0.000-0.030	0.003±0.006	0.000-0.027	0.003±0.006	0.000-0.034	0.003±0.006	0.000-0.022	0.002±0.006
FeO	0.016-0.206	0.086±0.036	0.000-0.150	0.063±0.027	0.040-0.411	0.111±0.060	0.0160.365	0.132±0.083
CaO	0.000-0.016	0.003±0.004	0.000-0.015	0.003±0.004	0.000-0.015	0.004±0.004	0.000-0.012	0.004±0.003
MgO	0.000-0.032	0.011±0.007	0.000-0.046	0.006±0.006	0.000-0.035	0.010±0.008	0.000-0.044	0.010±0.010
MnO	0.000-0.019	0.002±0.004	0.000-0.020	0.002±0.004	0.000-0.015	0.002±0.004	0.000-0.022	0.004±0.006
K ₂ O	0.000-0.016	0.002±0.003	0.000-0.022	0.003±0.004	0.000-0.010	0.004±0.003	0.000-0.014	0.005±0.004
Total	98.723-101.351	100.118±0.545	98.759-101.650	100.072±0.483	98.791-101.232	100.230±0.403	100.000-101.182	100.315±0.427

Figure 4.4 (continue).

Formula 3(O)								
Al	1.994-1.999	1.998±0.001	1.991-2.000	1.998±0.001	1.993-1.999	1.999±0.001	1.994-1.999	1.997±0.001
Si	0.000-0.001	0.000±0.000	0.000-0.003	0.000±0.000	0.000-0.001	0.000±0.000	0.000-0.001	0.000±0.000
Ti	0.000-0.003	0.000±0.001	0.000-0.006	0.001±0.001	0.000-0.003	0.001±0.001	0.000-0.002	0.000±0.000
Cr	0.000-0.000	0.000±0.000	0.000-0.000	0.000±0.000	0.000-0.000	0.000±0.000	0.000-0.000	0.000±0.000
Ga	0.000-0.001	0.000±0.000	0.000-0.000	0.000±0.000	0.000-0.001	0.000±0.000	0.000-0.001	0.000±0.000
V	0.000-0.000	0.000±0.000	0.000-0.000	0.000±0.000	0.000-0.000	0.000±0.000	0.000-0.000	0.000±0.000
Fe	0.000-0.003	0.001±0.000	0.000-0.002	0.001±0.000	0.001-0.005	0.001±0.001	0.001-0.005	0.002±0.001
Ca	0.000-0.000	0.000±0.000	0.000-0.000	0.000±0.000	0.000-0.000	0.000±0.000	0.000-0.000	0.000±0.000
Mg	0.000-0.001	0.000±0.000	0.000-0.001	0.000±0.000	0.000-0.001	0.000±0.000	0.000-0.001	0.000±0.000
Mn	0.000-0.000	0.000±0.000	0.000-0.000	0.000±0.000	0.000-0.000	0.000±0.000	0.000-0.000	0.000±0.000
K	0.000-0.000	0.000±0.000	0.000-0.000	0.000±0.000	0.000-0.000	0.000±0.000	0.000-0.000	0.000±0.000
Total	1.999-2.000	2.000±0.000	1.998-2.000	2.000±0.000	1.999-2.000	2.000±0.000	1.999-2.000	2.000±0.000

Statistically, the results of all analyses are quite similar within the same color of each sample. As expected, Fe contents in both yellow and blue varieties are higher than the other trace elements. In blue zones, including light blue body in blue variety and blue patch in both varieties, Fe contents are likely higher than those of yellow body of yellow variety. Ti contents are moderate to low in all cases; however, yellow variety seems to contain lower Ti than blue variety besides deeper blue color patch yields higher Ti content. Furthermore, the analyses of Mg contents are rather dominant in yellow body color while contents of Cr, Ga, V, Ca, Mn and K are quite low (Table 4.4). The analytical results also confirm that Awissawella corundums usually contain high Fe content, whereas Cr, Ga and V contents are very low, comparable to the results from EDXRF.

Contents of trace element are significant to color of corundum and relative to absorption spectra. The interaction of Mg, Ti and Fe in creating stable yellow color centers or blue colors is well understood and can be depicted in Figure 4.12 (Höger, 2001). This information is important for the design of experimental heat treatment of each sample reported in Chapter VI. Because of the higher contents of Fe, Ti and Mg against other trace contents in both color varieties, then the Fe, Mg and Ti contents of all the data points were plotted in a ternary diagram. As a result, the recalculated atomic Fe component would make up $\geq 40\%$ and all of data points appear to fall within appropriate colors (Figures 4.13 and 4.14) as they belong in comparison with results of Höger. Mg-Fe-Ti ternary diagram in Figure 4.13 contains analyses of 33 yellow variety samples including 145 data of yellow body zones and 174 data of blue patch zones whereas the same diagram in Figure 4.14 consists of 13 light blue variety analyses including 57 analyses of light blue zone and 36 points of blue patch zones. However, the errors of some selected points under analysis may make some points falling in wrong color zone which may be interfered by the observed color appearance or vice versa.



- | | | | |
|-------|---|-------|---|
| * | colour centre due to Mg | ** | colour centre due to Mg and Fe |
| *** | yellow due to Fe ³⁺ | **** | Fe ²⁺ /Fe ³⁺ -charge transfer green due to Fe ³⁺ |
| ***** | Fe ²⁺ /Ti ⁴⁺ -charge transfer | ***** | precipitation of TiO ₂ |

Figure 4.12 Model representing the interaction of trace elements in the system Al-Mg-Fe-Ti (tetrahedron). Sapphires of this composition were heat treated at 1850°C in an oxidizing atmosphere (a) and at 1750°C in a reducing atmosphere (b), Häger (2001).

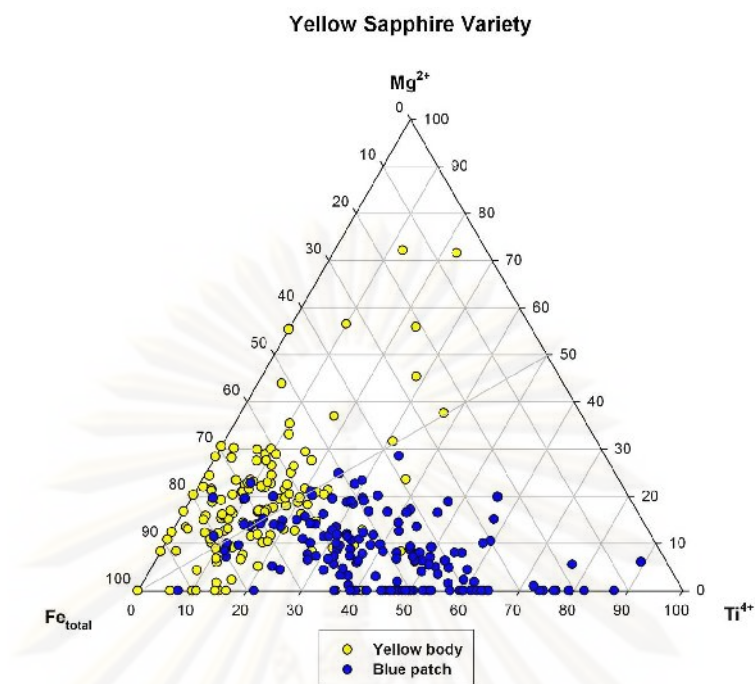


Figure 4.13 Mg-Fe-Ti ternary diagram of 33 yellow variety samples with analyses of two different color zones including 145 points of yellow body and 174 points of blue patch.

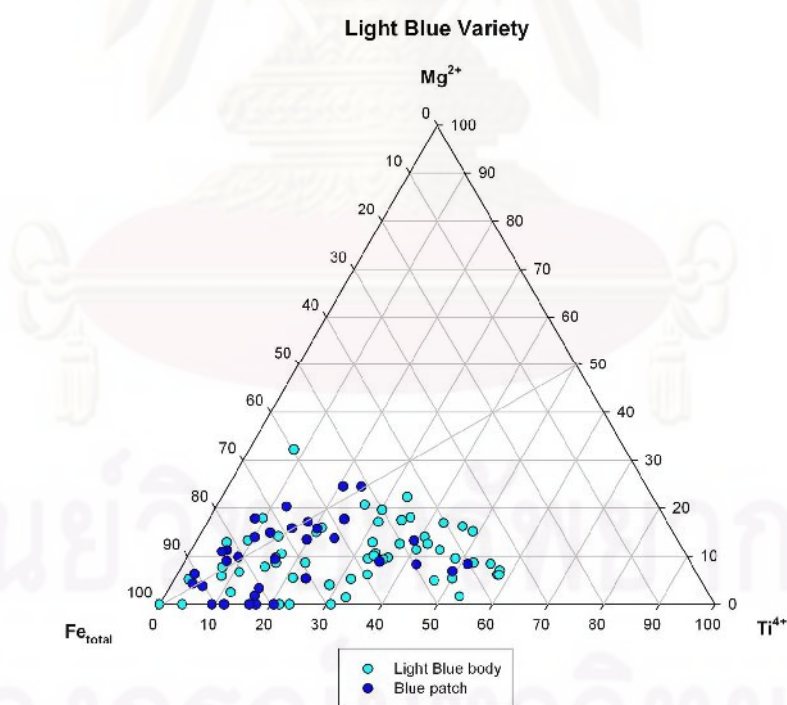


Figure 4.14 Mg-Fe-Ti ternary diagram of 13 light blue variety samples with two different color zones including 57 points of light blue body and 36 points of blue patch.

CHAPTER V

INTERNAL FEATURES AND MINERAL INCLUSIONS

5.1 Identification

Awissawella corundum samples were firstly examined under a binocular gemological microscope for initial investigation of internal features. This examination is aimed to observe all internal features including mineral inclusions. This initial information is very crucial for designing further works (e.g., Raman spectroscopy and analysis of mineral chemistry).

Internal features observed under microscope are generally composed of growth feature with some cloud inclusions, fractures with sometimes strained by iron solution, fingerprints, negative crystals and 2 phase inclusions (see Figures 5.1 to 5.6). Several types of mineral inclusions were additionally identified using Laser Raman Spectroscopy before some representative's mineral inclusions were then selected for chemical analysis using Electron Probe Micro-Analyzer (EPMA).



Figure 5.1 Cloud inclusions along growth plane in sample SapAw_01 of yellow variety.



Figure 5.2 Fingerprints in samples SapAw_03 of yellow variety.

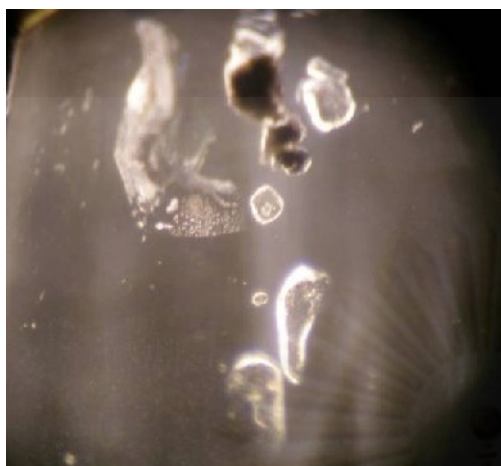


Figure 5.3 Negative crystals in sample SapAw_03 of yellow variety.



Figure 5.4 Crystal inclusion (apatite) in sample SapAw_09 of yellow variety.



Figure 5.5 Opaque mineral (hematite) in sample SapAw_09 of yellow variety.

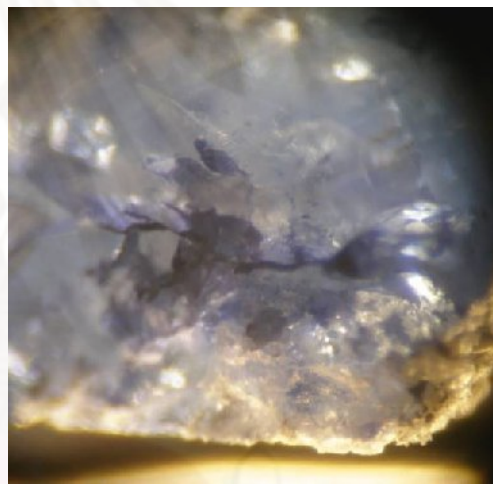


Figure 5.6 Iron-stained fractures and growth line in sample SapMa_05 of light blue variety.

Mineral inclusions embedded close to the sample surfaces were identified using Laser Raman Spectroscopy. As a result, the most common mineral inclusions are apatite, feldspar, calcite, hematite, garnet and diaspore.

Calcite and apatite appear to be the most dominant mineral inclusions which are found in all color varieties. They are usually transparent and colorless (Figures 5.7 and 5.8). Both calcite and apatite inclusions are found as single and aggregate crystals. Feldspar inclusions are present single and aggregate crystals, oval and transparent

crystals (Figures 5.9 and 5.10). Hematite is formed as brown to black opaque inclusions (Figure 5.11). Diaspore is formed as black opaque inclusions (Figure 5.12).

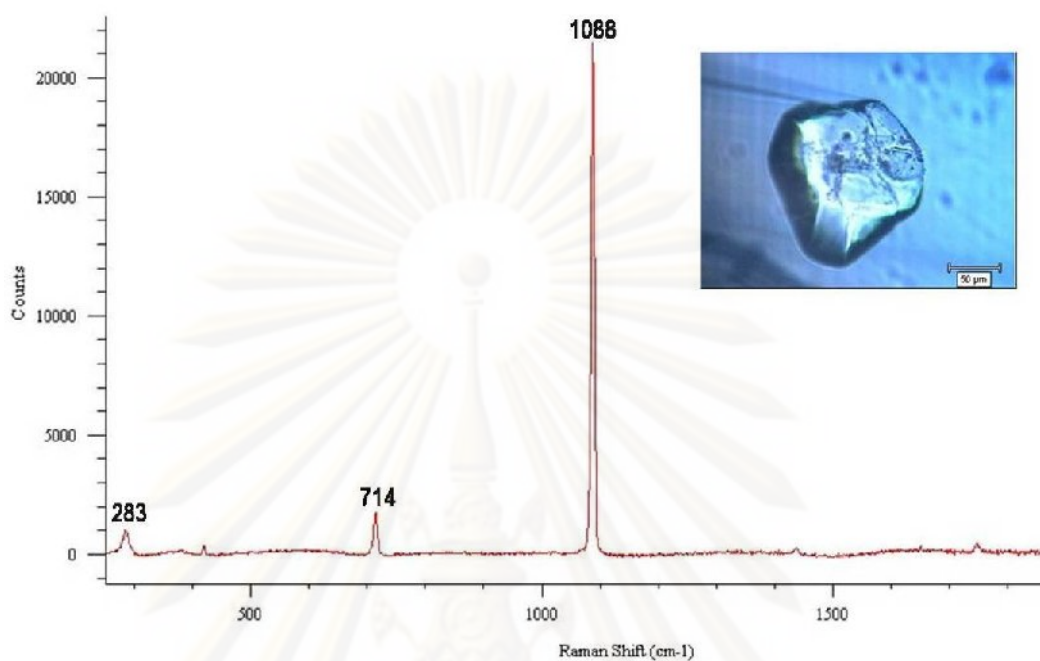


Figure 5.7 Raman spectrum of calcite inclusion in sample SapAw_01 of yellow variety with peaks at 1088, 714 and 283 cm⁻¹.

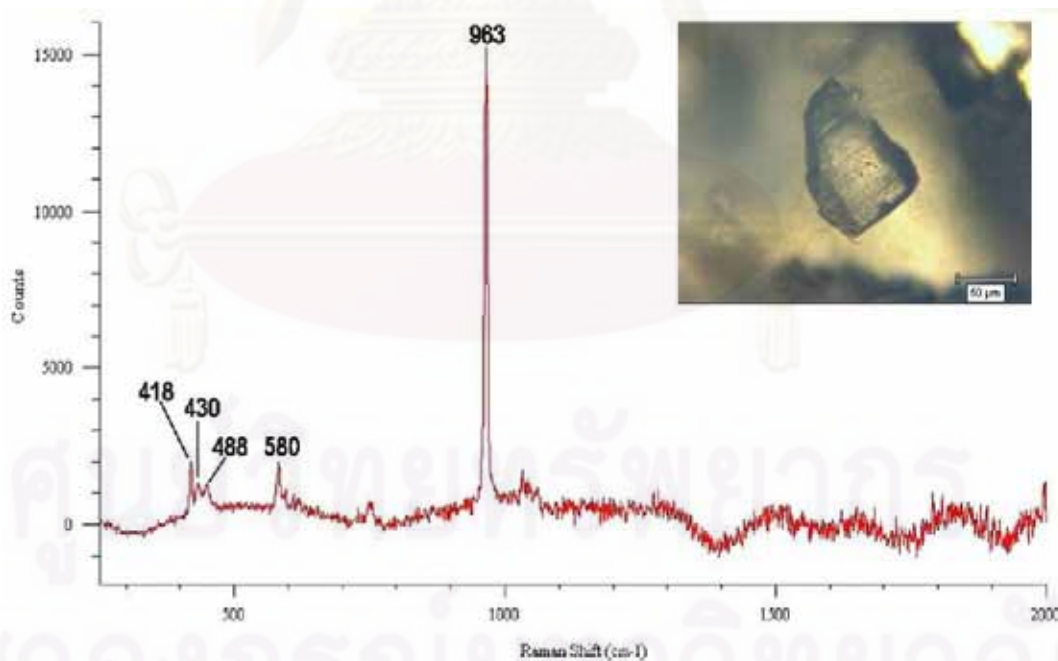


Figure 5.8 Raman spectrum of apatite crystal in sample SapAw_16 of yellow variety with peaks at 963, 580, 448, 430 and 418 cm⁻¹.

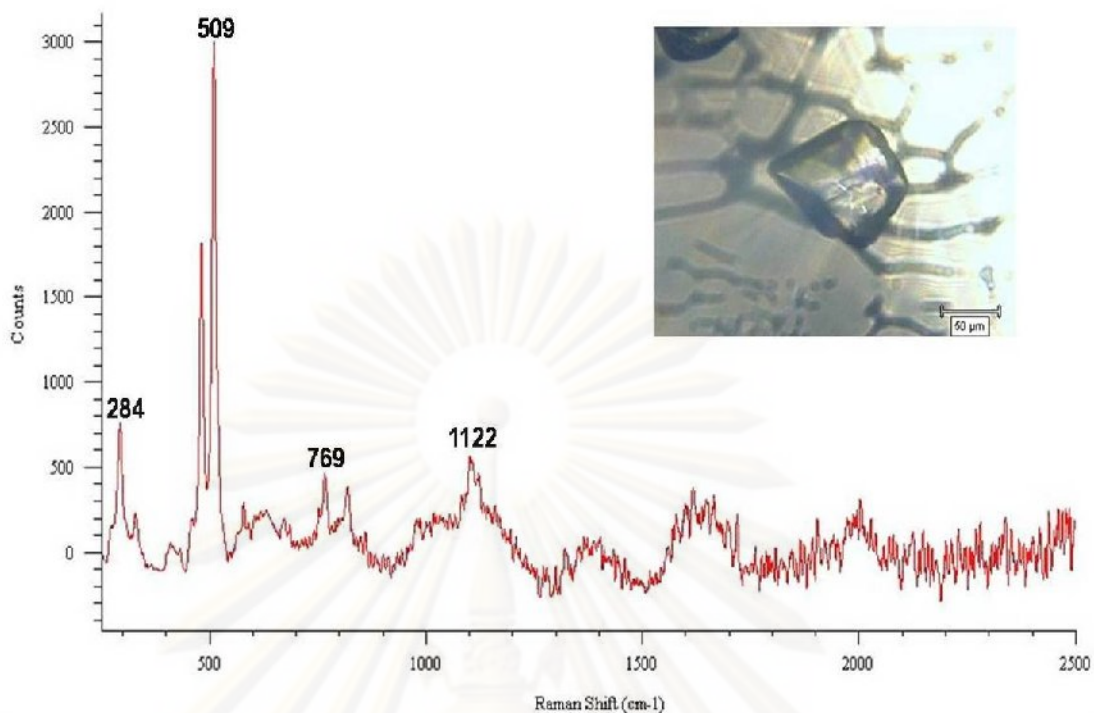


Figure 5.9 Raman spectrum of feldspar crystal in sample SapMa_02 present peaks at 1122, 769, 509 and 284 cm^{-1} .

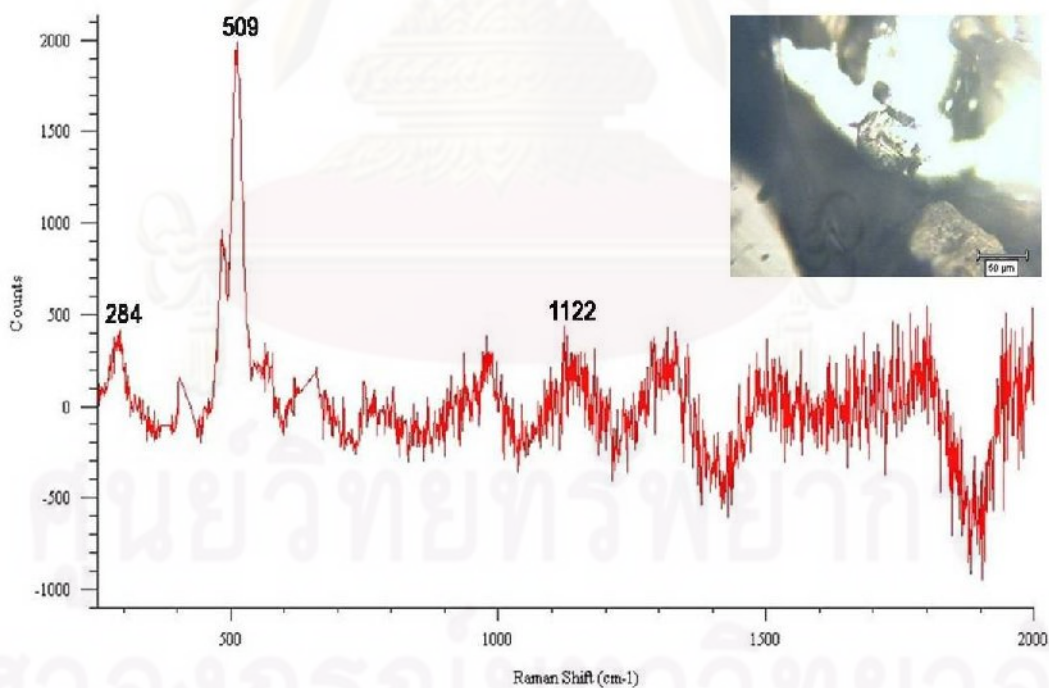


Figure 5.10 Raman spectrum of feldspars inclusion in sample SapMa_03 present peaks at 1122, 769, 509 and 284 cm^{-1} .

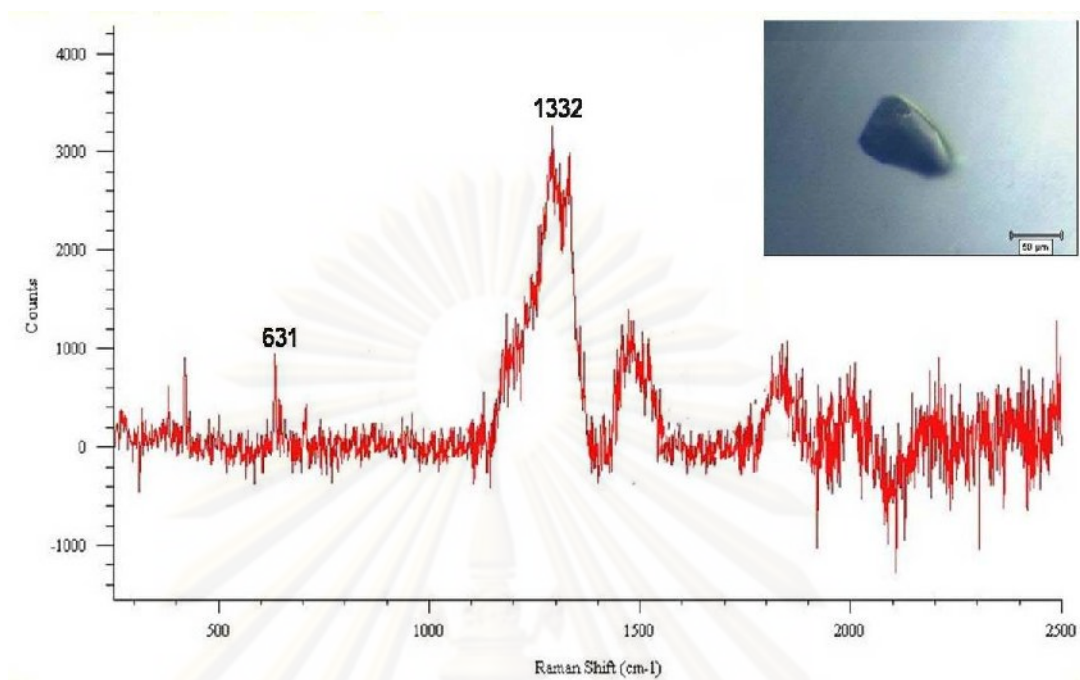


Figure 5.11 Raman spectrum of hematite inclusion in sample SapMa_02 present peaks at 1332 and 631 cm^{-1} .

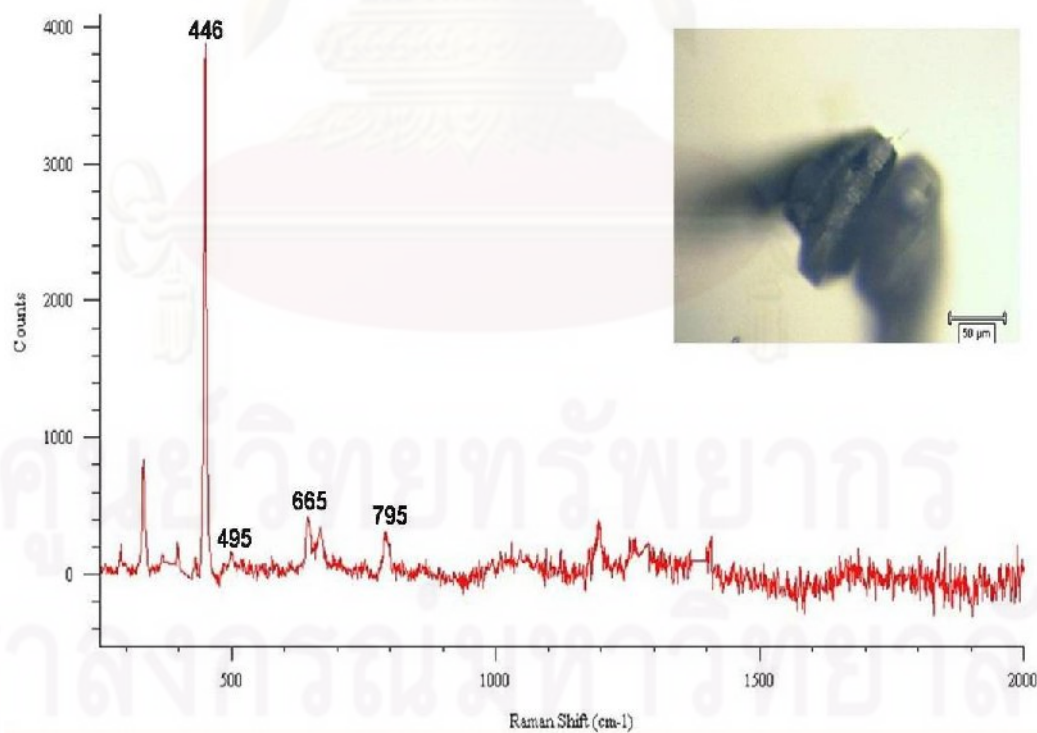


Figure 5.12 Raman spectrum of diaspore inclusion in sample SapMa_06 present peaks at 795, 665, 495 and 446 cm^{-1} .

5.2 Mineral Chemistry

Electron Probe Micro–Analyzer (JEOL JXA-8100) was engaged to analyze mineral inclusions. Most mineral inclusions initially identified by Raman Spectroscopy were selected. Unfortunately, some inclusions were destroyed during polishing process. There were finally garnet, feldspar, pyroxene and calcite available for this analysis (Table 5.1).

All available analyses were recalculated on basis of proper oxygen atoms such as 6(O) for pyroxene, 1(O) for calcite, 8(O) for feldspar and 24(O) for garnet (Table 5.1). These analyses not only confirm Raman analyses but also give more information that will be used for discussion in the last chapter. For instant, mineral chemistry of these inclusions indicates that garnet is rich in pyrope component; feldspar yields about 65-69%Ca and 30-35%Na of mole fraction falling in plagioclase range; calcite is likely pure phases without dolomite component. Pyroxene (enstatite) is really present but it would yield very important data of original source. All internal features found in each color variety of Awissawella corundums under this study are summarized in Table 5.2.

Table 5.1 EPMA analyses of some mineral inclusions found in Awissawella corundums.

Point	Garnet (Pyrope)	Feldspar		Pyroxene (enstatite)	Calcite		
	Aw21-In7	Aw22-In9	Aw33-In8	Ma8-In3	Aw3-In5	Aw8-In17	Aw14-In4
SiO ₂	52.02	51.35	51.97	64.90	0.00	0.03	0.00
TiO ₂	0.00	0.00	0.03	0.00	0.00	0.00	0.00
Al ₂ O ₃	24.18	31.08	30.98	0.55	0.01	0.03	0.05
Cr ₂ O ₃	0.01	0.01	0.00	0.00	0.00	0.00	0.00
FeO _{total}	0.37	0.00	0.01	0.42	0.19	0.20	0.12
MnO	0.00	0.02	0.00	0.00	0.13	0.03	0.04
MgO	22.41	0.00	0.00	34.09	0.14	0.02	0.00
BaO	0.00	0.00	0.00	0.00	0.00	0.04	0.00
CaO	0.01	13.42	13.03	0.02	51.75	53.82	58.29
Na ₂ O	0.02	3.33	3.92	0.01	0.00	0.00	0.00
K ₂ O	0.00	0.09	0.09	0.01	0.00	0.00	0.01
Total	99.02	99.29	100.02	100.00	52.23	54.18	58.51

Table 5.1 (continue).

Formular	24(O)	8(O)		6(O)	1(O) per one mole of CO ₂		
Si	6.916	2.343	2.355	2.140	0.000	0.000	0.000
Ti	0.000	0.000	0.001	0.000	0.000	0.000	0.000
Al	3.788	1.671	1.654	0.021	0.000	0.001	0.001
Cr	0.001	0.000	0.000	0.000	0.000	0.000	0.000
Fe ³⁺	0.000	0.000	0.000	0.000	0.000	0.000	0.000
Fe ²⁺	0.041	0.000	0.000	0.012	0.003	0.003	0.002
Mn	0.000	0.001	0.000	0.000	0.002	0.000	0.001
Mg	4.440	0.000	0.000	1.676	0.004	0.001	0.000
Ba	0.000	0.000	0.000	0.000	0.000	0.000	0.000
Ca	0.000	0.656	0.632	0.001	0.991	0.994	0.996
Na	0.004	0.294	0.345	0.001	0.000	0.000	0.000
K	0.000	0.005	0.005	0.000	0.000	0.000	0.000
Total*	15.190	4.971	4.992	3.850	1.000	1.000	1.000

Table 5.2 Summary of internal features and mineral inclusions found in each variety of Awissawella corundums under this study.

Internal features	Yellow variety	Blue variety
- Fingerprints	✓	✓
- Negative crystal	✓	✓
- 2 phase inclusion	✓	✓
- Minute particles	✓	✓
Crystal inclusions		
- Apatite	✓	✓
- Feldspar	✓	✓
- Calcite	✓	✓
- Garnet (pyrpo)	✓	✓
- Pyroxene (enstatite)	✓	✓
- Hematite	✓	✓
- Diaspore	✓	✓

CHAPTER VI

EXPERIMENTAL HEAT TREATMENT

6.1 Introduction

Color is one of the most important factor of gems' value. Heat treatment has become very useful for enhancement of color and clarity in gemstone industry because good quality gemstones are rare in the nature. Heat treatment without any chemical additive for ruby and sapphire may cause alterations of physical and/or chemical structures that are in turn introducing color and clarity modifications. Each gemstone has its particular molecular structure and may contain different chromophoric elements which absorb light at different energy ranges. Therefore, selective light absorption or transmission spectrum and trace element of corundums can be used to understand their color causing mechanism. Consequently, potential and specify procedure for heat treatment can be assessed to corundum. Experimental heat treatment was therefore designed for this project.

The experiments were carried out using Linn electrical furnace (model HT1800 VAC Bottom Loader). Selective samples for the experiments were firstly considered from their absorption spectra and trace elements as reported in Appendices C and E. These are related to color causing mechanism of corundum. Subsequently two sets of samples were divided for different treatment conditions. They were then placed into an alumina crucible for heating under preset conditions. The first group, contain 18 yellow sapphire samples and 1 light blue sapphire sample, were heated in oxidizing atmosphere by feeding pure O₂ gas with peak temperature at 1650^oC for 10 hours soaking time. The second group, consist of 4 yellow sapphire samples and 11 light blue sapphire samples, were heat-treated under reducing condition by feeding pure N₂ with peak temperature at 1650^oC for 5 hours soaking time. These experimental design were set based on previous experimental reports (e.g., Pattamalai, 2002; Sakkaravej, 2004; Lomthong, 2004; Somboon, 2006) which wished to reach the optimum conditions. Temperatures of both experiments were controlled at the same increasing rates of 4^oC per minute but cooling rate of the first oxidizing heat is much quicker than the other.

After the heating experiments, all samples were photographed and observed the UV-VIS-NIR absorption spectrum again.

6.2 Color Appearance

Oxidizing Experiment: was aimed to remove blue component from the stone. Yellow variety samples show clearly deduction of blue and intensification of yellow components after heating (Figure 6.1A) whereas light blue sample shows just slight change in color which yellow shade is slightly produced after heating (Figure 6.1B). Table 6.1 shows color shades of samples before and after heat treatment in oxidizing condition.



Figure 6.1 Awissawella corundum samples before and after heating at 1650°C in oxidizing condition; (A) yellow variety (representation of 18 samples), (B) light blue variety (only sample available).

Table 6.1 Color shades of Awissawella sapphire samples in comparison between before and after heat in oxidizing atmosphere.

Sample	Body color		Patch color	
	Before	After	Before	After
Yellow sapphire variety				
SapAw_05	gY2/3	Y4/5	vB4/3	gY2/3
SapAw_06	Y2/2	Y4/5	B4/2	gY3/4
SapAw_13	Y2/2	Y4/5	B5/1	B3/3
SapAw_15	Y3/3	Y4/5	vB5/3	B2/2
SapAw_16	YG/GY2/1	Y4/5	B5/1	YG/GY2/1
SapAw_21	YG/GY2/1	Y3/4	vB4/4	gY2/3
SapAw_22	YG/GY2/1	Y3/5	bV8/3	-
SapAw_23	YG/GY2/1	Y5/5	vB5/3	gY2/3
SapAw_24	gY2/3	Y4/5	B7/4	-
SapAw_25	gY2/3	Y3/5	vB5/3	Y2/2
SapAw_26	gY2/3	Y5/4	bV7/4	Y2/2
SapAw_27	YG/GY2/1	Y4/5	B7/4	-
SapAw_28	YG/GY2/1	Y5/4	B5/1	colorless
SapAw_29	gY2/3	Y2/2	vB5/3	Y2/2
SapAw_30	YG/GY2/1	Y3/5	B5/3	B3/3
SapAw_31	gY2/3	Y4/5	vB4/4	-
SapAw_32	YG/GY2/1	Y4/5	B5/2	-
SapAw_33	YG/GY2/1	Y3/5	B5/2	YG/GY2/1
Light blue sapphire				
SapMa_06	B2/2	Y2/2	vB5/3	B4/2

Reducing Experiment: was carried out with intention to intensify blue component. Blue components in most light blue samples are clearly increased but those yellow samples are slightly changed after heating. The later one appears to have pale blue replacement on their yellow body color and blue patches (Figure 6.2). Table 6.2 shows comparison between color shades before and after heat treatment in reducing condition.

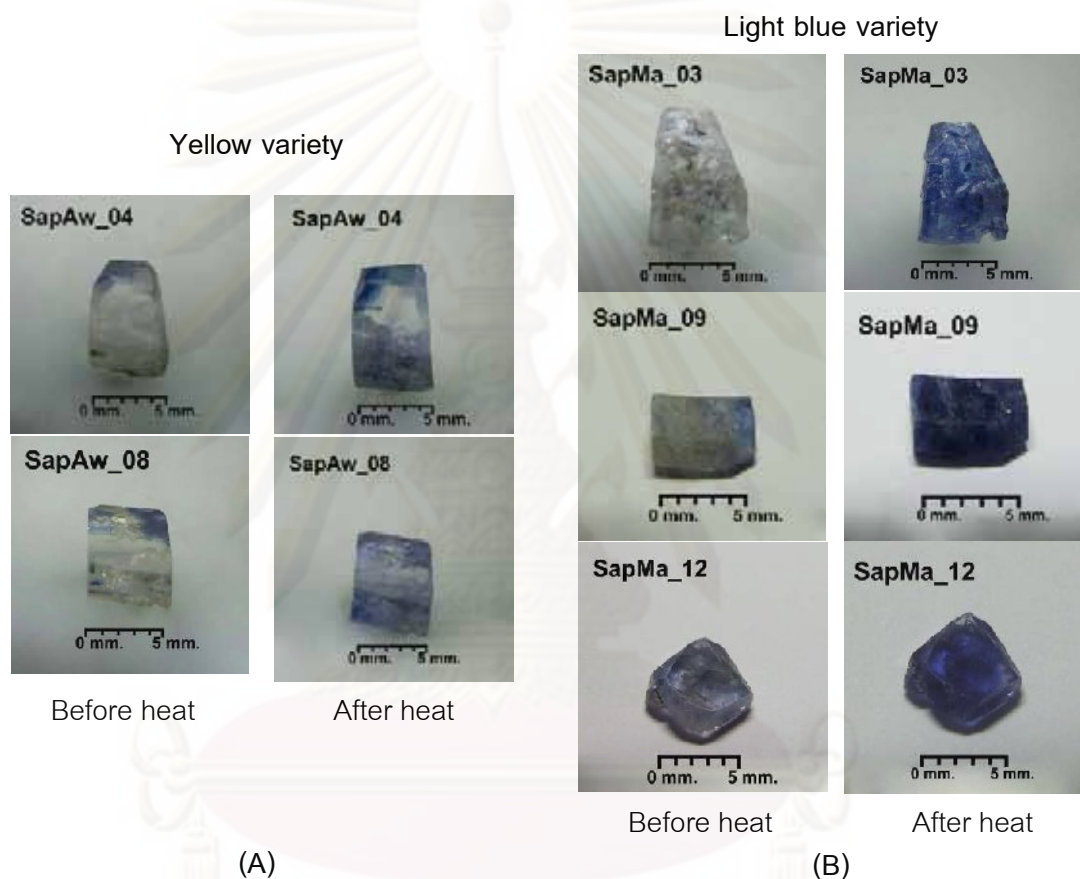


Figure 6.2 Awissawella corundums before and after heating at 1650°C in reducing condition; (A) yellow variety (representation of 4 samples), (B) light blue variety (representation of 11 samples).

Table 6.2 Color shades of Awissawella sapphire samples comparison between before and after reducing heat treatment.

Sample	Body color		Patch color	
	Before	After	Before	After
Yellow sapphire variety				
SapAw_04	Y2/2	B3/1	B7/2	B7/4
SapAw_08	gY2/3	B3/3	vB5/3	vB5/3
SapAw_10	gY2/3	vB2/3	B4/2	bV5/5
SapAw_11	gY3/4	vB2/3	bV7/4	bV6/4
Light blue sapphire				
SapMa_01	B2/2	B8/3	vB5/3	-
SapMa_02	vB3/3	vB5/3	vB4/3	vB7/3
SapMa_03	B3/1	vB7/3	-	-
SapMa_04	B3/1	bV8/3	B5/1	vB4/3
SapMa_05	B5/2	bV6/4	bV8/3	bV2/3
SapMa_07	B3/3	vB7/3	B5/2	vB5/3
SapMa_08	B3/3	vB7/3	vB4/3	vB3/3
SapMa_09	B2/2	B8/3	vB4/4	-
SapMa_10	B4/2	vB5/3	B3/4	vB3/3
SapMa_11	vB3/4	vB5/3	vB5/3	vB3/3
SapMa_12	vB3/3	bV7/4	vB5/3	bV3/4
SapMa_13	vB4/3	B4/2	vB5/3	-

6.3 UV-VIS-NIR Spectra

The UV-VIS absorption spectra (o-ray) of those samples were recorded both before and after the heating experiments. Some selective spectra are displayed in Figures 6.3 to 6.6 and all samples' spectra are shown in Appendix G. UV-VIS spectra of yellow variety samples before experiment mostly show absorption peaks due to Fe^{3+} at 450 and 388 nm, low absorption bands with maxima about 565 nm due to $\text{Fe}^{2+}/\text{Ti}^{4+}$ IVCT process (Figure 6.3). It should be notified that peak assemblage around 850-900 nm are

due to effect of changing lamps. Subtraction of spectra before treatment from those after the heating can be applied to observe more clearly picture of changing. As a result, absorption pattern of Fe^{3+} peak at 388 nm and color center, a continuously increased absorption towards shorter wavelengths with a shoulder at around 460 nm is produced in all yellow sapphires (Figure 6.4). This pattern is generally known to be caused by stable defect centers typical of Sri Lanka yellow sapphire (Pisutha-Arnond et al., 2004; Somboon, 2006). On the other hand, absorption bands with peak about 565 nm are disappeared (Figure 6.4). For light blue variety, before experiment, they usually show absorption peak at 450 nm caused by $\text{Fe}^{3+}/\text{Fe}^{3+}$ pairs together with 388 nm peak of Fe^{3+} and 565 nm peak of $\text{Fe}^{2+}/\text{Ti}^{4+}$ IVCT process (cause of blue color) (Figures 6.5; measured by UV-VIS-NIR spectrophotometer, model U-4001). Decreasing absorption band of $\text{Fe}^{2+}/\text{Ti}^{4+}$ IVCT after the heat treatment (Figures 6.6; measured by UV-VIS-NIR spectrophotometer, Model Lambda 950) is clearly observed from the same sample. However, due to different versions of operating software of both machines, spectrum subtraction could not be carried out.

As expected for the reducing heat in yellow variety (Figures 6.7 to 6.8), most samples shows very slightly increases of absorption band due $\text{Fe}^{2+}/\text{Ti}^{4+}$ IVCT process that causes blue color in sample after the heat treatment. Therefore, residue spectra (obtained from subtraction of spectra measured before treatment from that measured after the heating) show slightly increases absorption band about 565 nm after the heat treatment a flat line. For light blue variety (Figures 6.9 to 6.10), before experiment, all samples show absorption peak at 450 nm caused by $\text{Fe}^{3+}/\text{Fe}^{3+}$ pairs are always present along with 388 nm peak of Fe^{3+} and 565 nm peak of $\text{Fe}^{2+}/\text{Ti}^{4+}$ IVCT band. As the color of most samples show more intensive absorption band of $\text{Fe}^{2+}/\text{Ti}^{4+}$ IVCT process after the heat treatment, the residue spectra show obviously a continuous absorption line with the maxima about 565 nm which is related to more color intensities of samples.

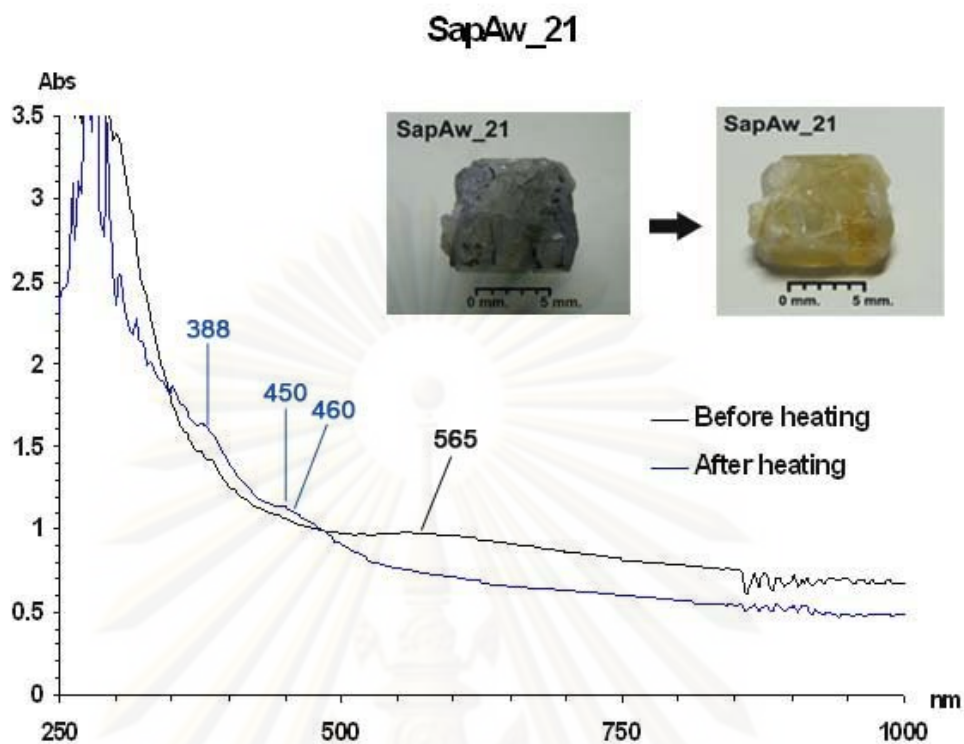


Figure 6.3 UV-VIS spectra (o-ray) of the sample SapAw_21 measured before and after heating experiment at 1,650°C in O₂ atmosphere for 10 hours soaking time.

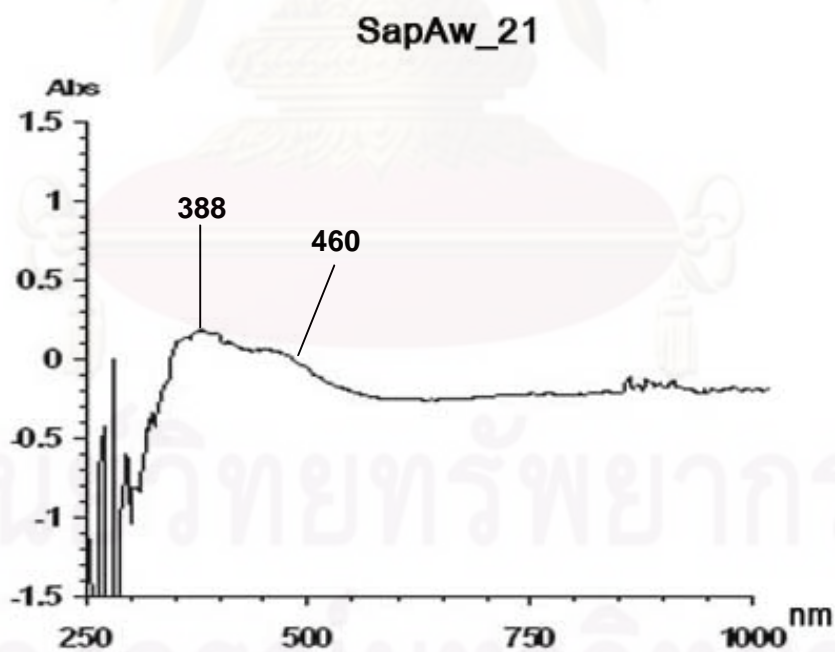


Figure 6.4 Residue spectrum of the sample SapAw_21 obtained by subtracting the spectra before heat from that after the experiment as shown in Figure 6.3.

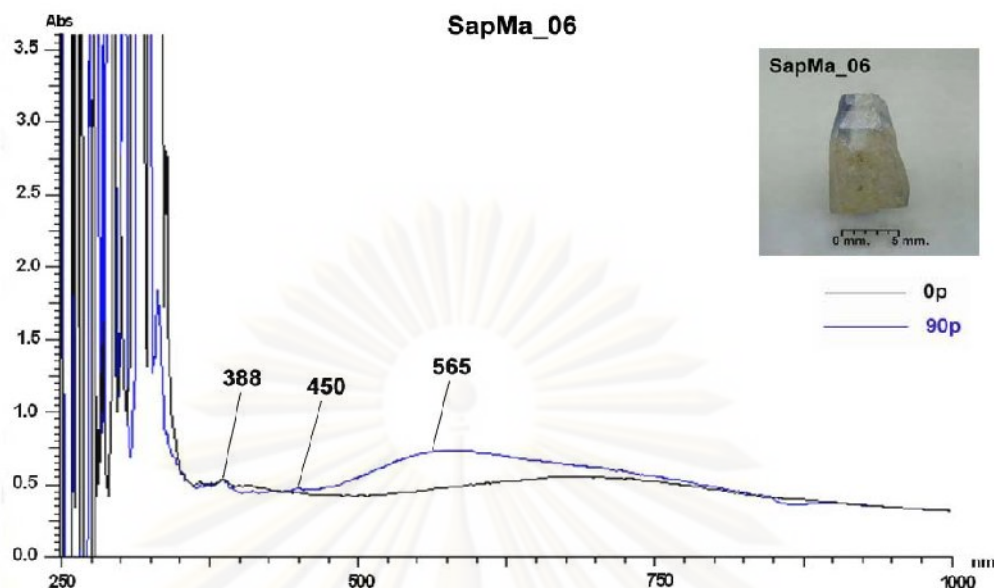


Figure 6.5 UV-VIS spectra of the sample SapMa_06 measured before heating experiment. Note the presence of absorption peaks at 450 nm caused by $\text{Fe}^{3+}/\text{Fe}^{3+}$ pairs are always present along with 388 nm peak of Fe^{3+} and 565 nm peak of $\text{Fe}^{2+}/\text{Ti}^{4+}$ IVCT band causing of blue color.

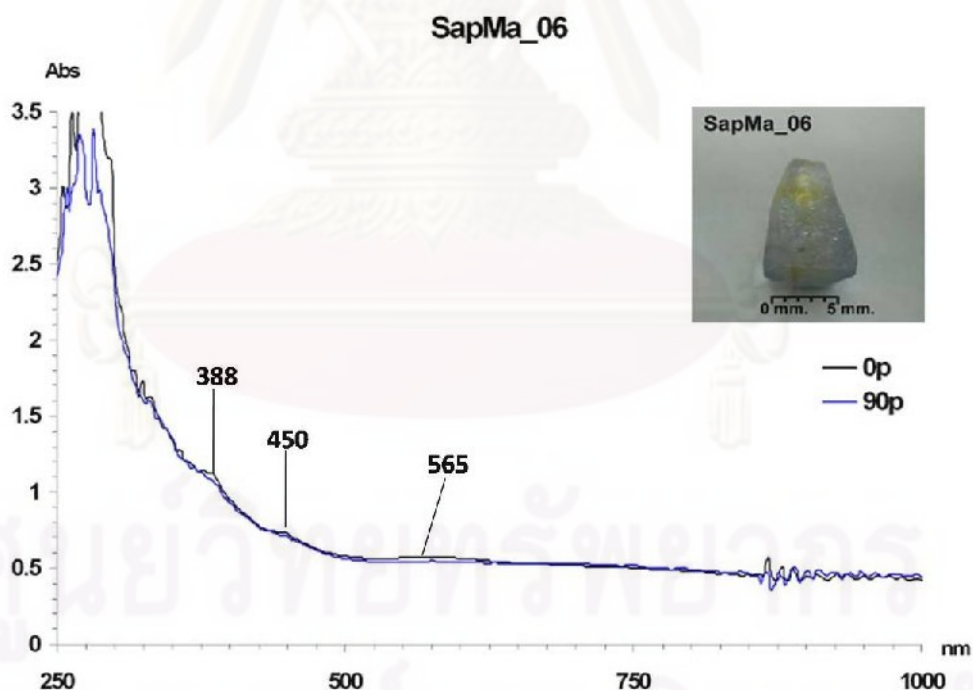


Figure 6.6 UV-VIS spectra of the sample SapMa_06 after heating experiment at 1,650°C in O_2 atmosphere for 10 hours soaking time. Note the presence of decrease absorption peaks around 565 nm peak of $\text{Fe}^{2+}/\text{Ti}^{4+}$ IVCT process.

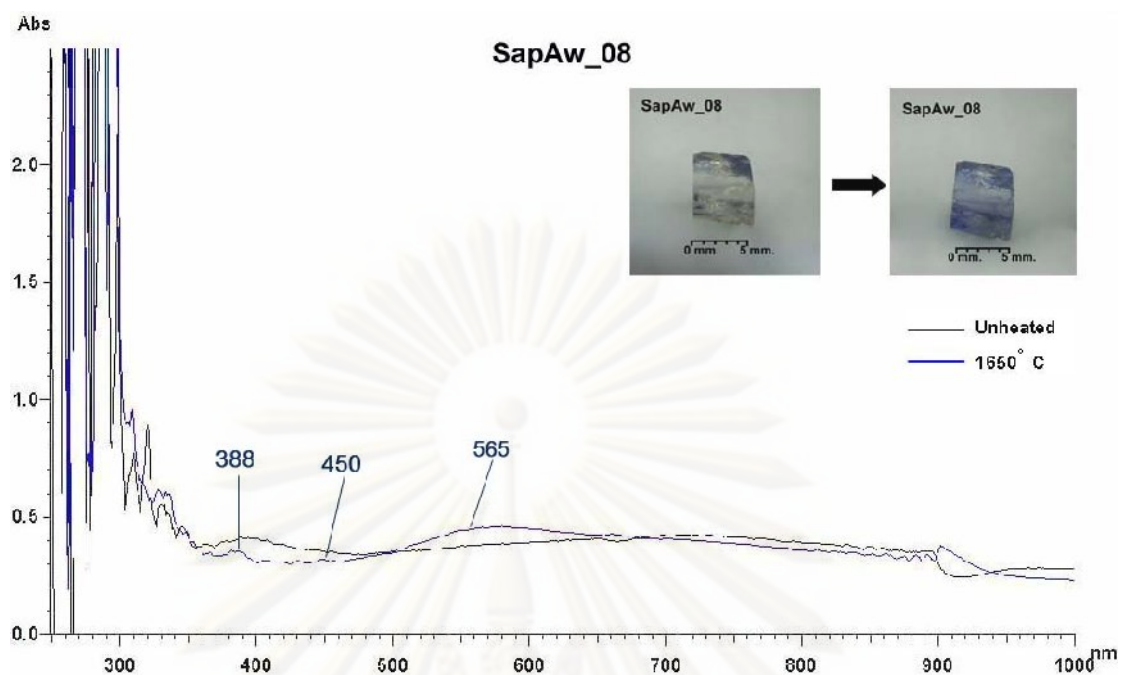


Figure 6.7 UV-VIS spectra (o-ray) of the sample SapAw_08 of yellow variety (color code gY2/3) measured before and after heating experiment at 1,650°C in N₂ atmosphere for 5 hours soaking time.

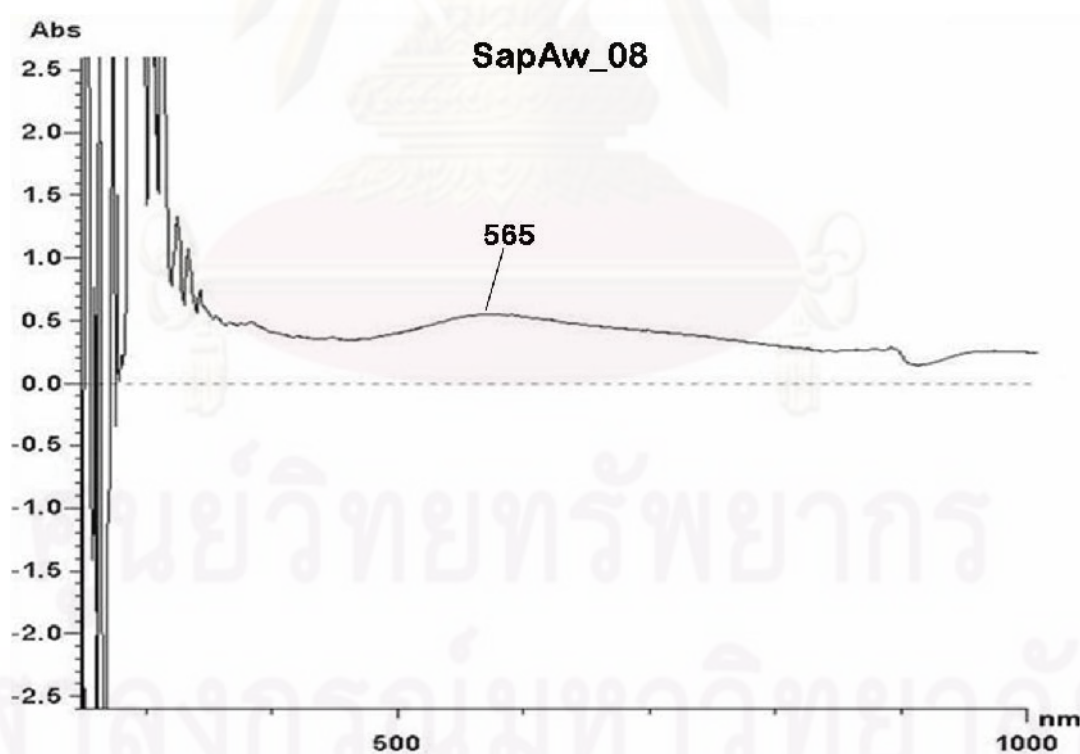


Figure 6.8 Residue spectrum of the sample SapAw_08 obtained by subtracting spectra before and after heating experiment as shown in Figure 6.7.

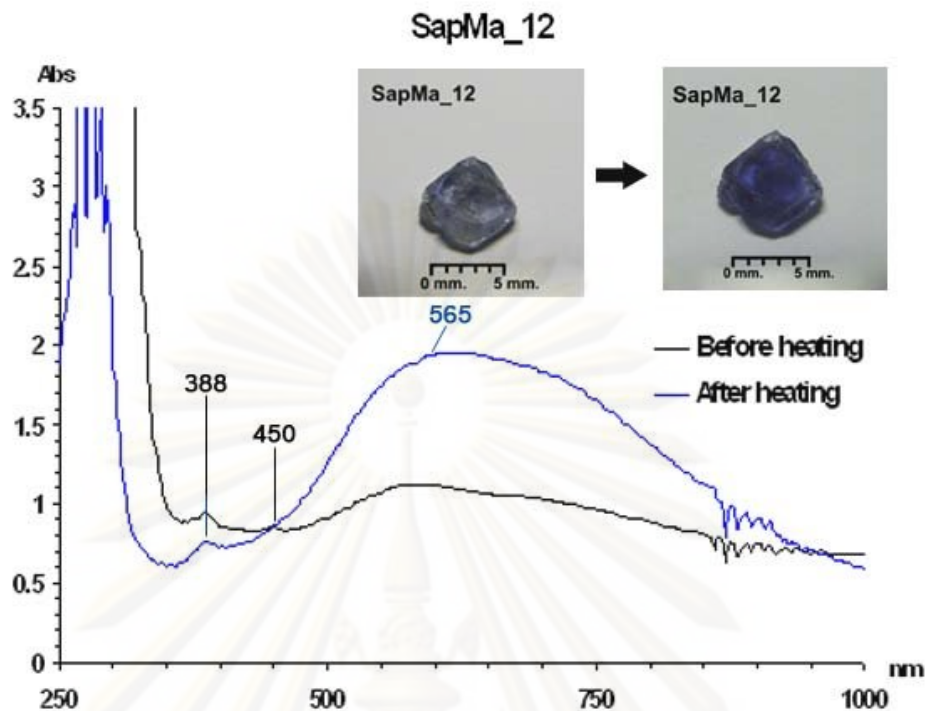


Figure 6.9 UV-VIS spectra (o-ray) of the sample SapMa_12 of light blue variety (color code vB3/3) measured before and after heating experiment at 1,650°C in N_2 atmosphere for 5 hours soaking time.

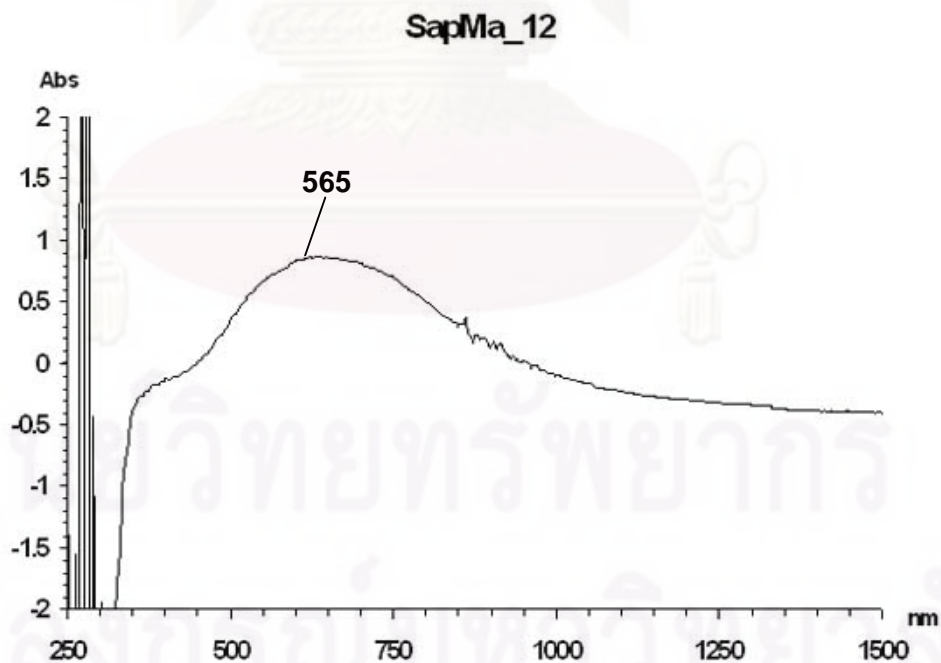


Figure 6.10 Residue spectrum of the sample SapMa_09 obtained by subtracting the spectra before and after heating experiment as shown in Figure 6.9.

6.4 Fourier Transform Infrared Spectra

Representative FTIR spectra of sapphire samples after heat treatment are shown in Figures 6.11 to 6.14, whereas all FTIR spectra collected in this study are reported in Appendix G. In general, all sapphires show absorption patterns of H₂O at 3400-3900 cm⁻¹, pattern of CO₂ at 2345-2540 cm⁻¹, peaks of C-H stretching of hydrocarbon at 2852-2950 and 2925-2918 cm⁻¹. Among these peaks, O-H stretching peak at about 3309 cm⁻¹ is the most crucial for consideration of high temperature treatment, this is because the other peaks are possibly effected by contamination of the stone. For examples, peaks of H₂O and CO₂ may be involved by vapor and air surrounding the sample, whereas C-H stretching peaks would indicate iron stain, carbon polishing powder and organic oil film coated along crack and surface. Volynet et al. (1972) suggested that O-H stretching peak could be appeared and intensified after heating up corundum at high temperatures. However, Sakkaravej (2004) advised the O-H stretching peak in FTIR spectra is uncertainly effected by high temperature treatment. However, they would be possibly effected by diaspore (AlO(OH)) in the stones which it can be detected by FTIR at 3309 cm⁻¹ absorption peak (Lomthong, 2004). Therefore, only O-H stretching peaks will be considered in these analyses. Unheated yellow sapphires showed O-H stretching peak at about 3309 cm⁻¹ that was disappeared after heating both oxidizing and reducing experiments (Figures 6.11 and 6.13). The light blue variety disappear to have O-H stretching peak at 3309 cm⁻¹ in most unheated stone as well as after both heating experiments (Figures 6.12 and 6.14).

ศูนย์วิทยทรัพยากร

จุฬาลงกรณ์มหาวิทยาลัย

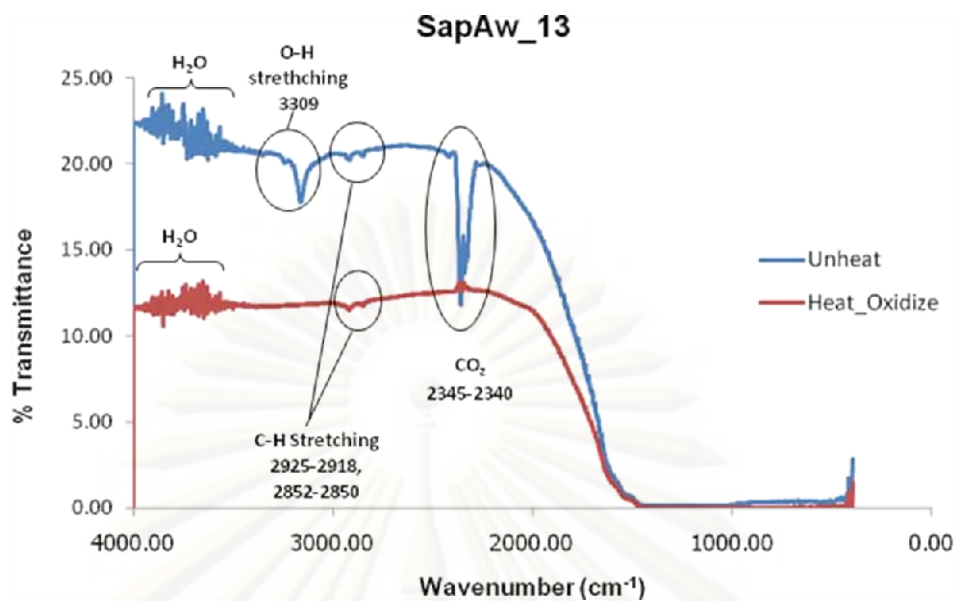


Figure 6.11 FTIR spectra of SapAw_13 of yellow variety before and after heating in oxidizing environment at 1,650°C show disappearance of O-H stretching peak at about 3309 cm⁻¹ after heat.

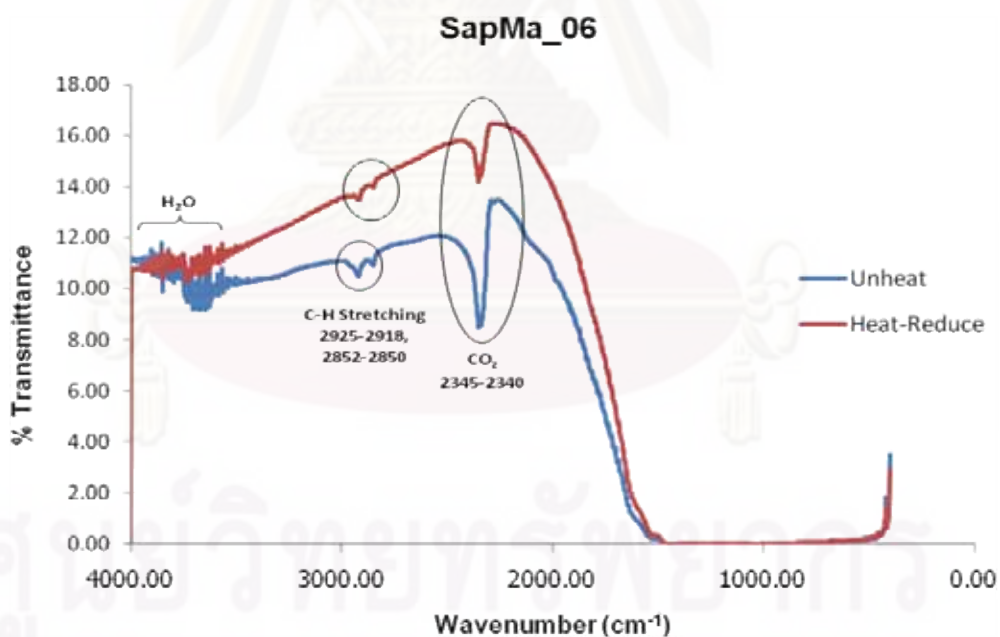


Figure 6.12 FTIR spectra of SapMa_06 of light blue variety before and after heating in oxidizing environment at 1,650°C show decreased intensities of CO₂ and C-H stretching absorption peaks after heat.

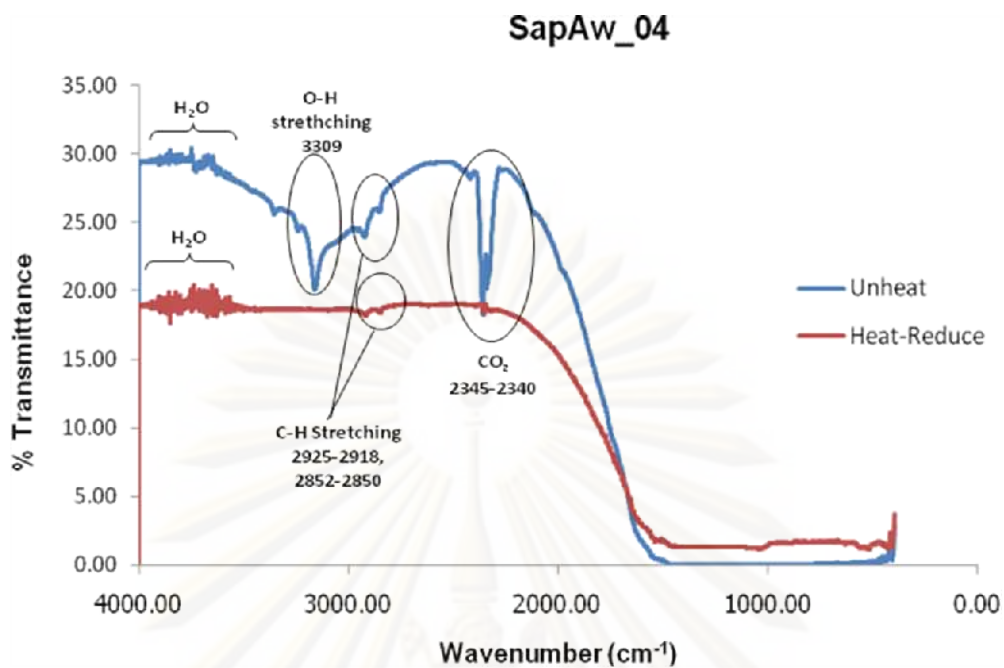


Figure 6.13 FTIR spectra of SapAw_04 of yellow variety before and after heating in reducing environment at 1,650°C show deduction of O-H stretching peak at about 3309 cm⁻¹ after heat.

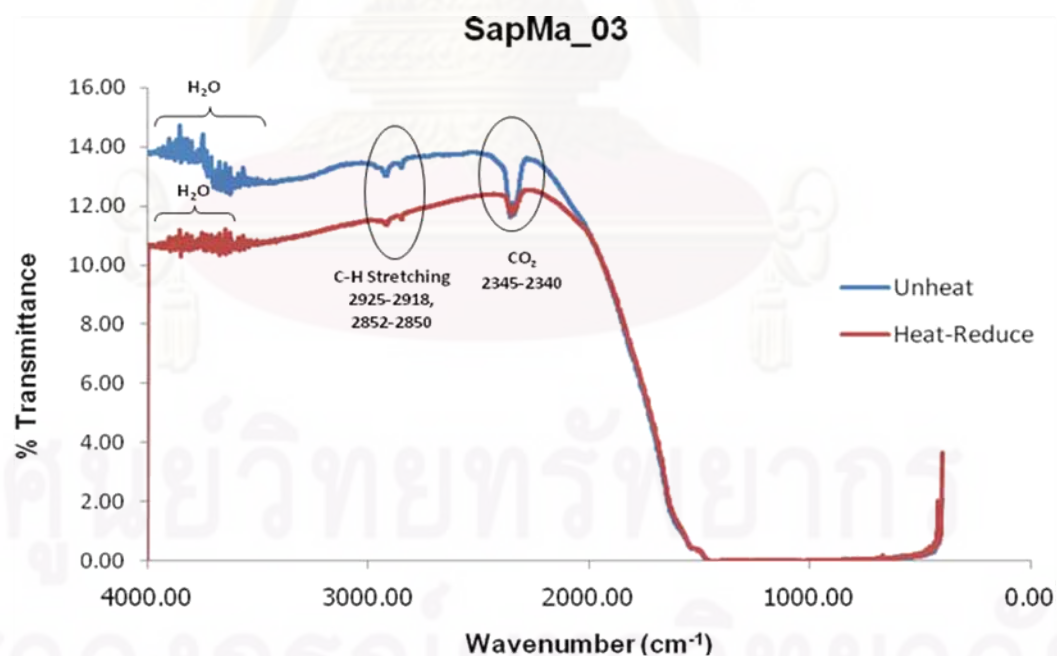


Figure 6.14 FTIR Spectra of SapMa_03 of light blue variety before and after heating in reducing environment at 1,650°C show deducted intensity of absorption peaks after heat.

CHAPTER VII

DISCUSSION AND CONCLUSIONS

7.1 Gem Characteristic and Geographic Origin

Corundum samples from Awissawella under this study mostly show blue color patches or zones that can be divided, based on their body colors, into 2 main color varieties, i.e., yellow and light blue sapphires. Moreover, both sapphire color varieties can also be subdivided into a few subgroups based on detailed color appearances in comparison with the GIA Gem Color Set. Yellow variety is composed of yellow, greenish yellow and yellow green subgroups whereas light blue variety has only blue and violet blue sub groups. They have weights ranging from 1.01 to 9.25 carats for yellow sapphire variety and 1.52 to 8.02 carats for light blue sapphire variety. Specific gravity is approximately 3.90 to 3.97 for all samples, refractive indices are within ranges of 1.768-1.771(n_e), 1.760-1.763(n_o) in yellow sapphire, and 1.768-1.772(n_e), 1.761-1.763(n_o) in light blue sapphire with birefringence of 0.007-0.009. For the fluorescence under ultraviolet lamp, yellow sapphire variety is strong orange under long wave and weak to moderate orange under short wave whereas the light blue variety yields moderate orange to moderate reddish orange under long wave and very weak orange under short wave.

Internal features observed under microscope are generally characterized by fractures filled with iron stain, fingerprints, mineral crystals, negative crystals and two phase inclusions. Mineral inclusions are identified, using Laser Raman Spectroscopy, as apatite, feldspar, calcite, pyroxene (enstatite), hematite and garnet (pyrope). These are compared with mineral inclusions reported from other metamorphic corundums including Umba, Songea, Ilakaka, Madagascar, Mogok, Wellawaya corundums (Hughes, 1997; Intasopa et al., 2002; Wathanakul et al., 2002; Lomtong, 2004; Tipprasert, 2006; www.gubelinlab.com, 2007; www.fieldgemology.org, 2009) in Table 7.1. Apatite inclusions have been found in corundum from many deposits. Several minerals, such as boehmite, brookite, dolomite, epidote, graphite, mica, monazite, paragonite, pyrrhotite, rutile, spinel and zircon, have been reported from others metamorphic corundum but they have not yet been found in Awissawella corundum

under this study. However, Mg-rich pyroxene (enstatite) and Mg-rich garnet (pyrope) are firstly recorded from Awissawella sapphire whereas the other metamorphic corundums usually contain diopside pyroxene and almandine garnet instead (see Table 7.1). This would be the most crucial indication of Awissawella deposit that can be differentiated from the other metamorphic deposits even from other Sri Lankan sapphires. Moreover, it should be notified that dolomite and spinel inclusions have never been observed although Mg-rich pyroxene and garnet are present. It seems to have specific type of primary origin rather than common metamorphic origin.

Moreover, Awissawella corundums can be separated from Myanmar and Songea corundums by trace geochemistry. However, trace geochemistry of Madagascar corundum overlaps that of the Awissawella corundum; nonetheless, mineral inclusions (Table 7.1) of Madagascar corundum (e.g., boehmite, graphite, mica, monazite, paragonite and zircon) are somehow different from those observed in Awissawella corundum, diaspore and pyroxene in particular.

Table 7.1 Summary of mineral inclusions found in corundums from Awissawella and other metamorphic corundum deposits.

Minerals	¹⁺²⁺³⁺⁵ Tanzania	⁴⁺⁵ Madagascar	¹⁺⁵ Myanmar	⁶⁺⁷ Sri Lanka	Awissawella
Apatite	X	X	X	X	X
Boehmit	X	X		X	
Brookite			X		
Calcite	X	X	X		X
Diaspore			X		X
Dolomite	X		X		
Epidote	X				
Feldspar	Andesine	X	X	X	X
Garnet	Almandine	X	Almandine		Pyrope
Graphite	X	X	X	X	
Hematite	X			X	X
Mica	Biotite Muscovite Paragonite	X	X	X	
Monazite	X	X	X	X	
Paragonit	X	X			

Table 7.1 (continue).

Minerals	¹⁺²⁺³⁺⁵ Tanzania	⁴⁺⁵ Madagascar	¹⁺⁵ Myanmar	⁶⁺⁷ Sri Lanka	Awissawella
Pyroxene	Diopside				Enstatite
Pyrrhotit	needles			X	
Rutile	X	X	X	X	
Spinel	X		X	X	
Zircon	X	X	X	X	

¹ Hughes (1997); ² Wathanakul et al. (2002); ³ Lomtong (2004); ⁴ www.gubelinlab.com (2007); ⁵ Intasopa et al. (2002);

⁶ Tipprasert (2006); ⁷ www.fieldgemology.org (2009)

The FTIR spectra of unheated yellow variety samples showed peak of structural O-H stretching at 3309 cm^{-1} in all samples but it did not exist in light blue variety (Figure 7.1). The O-H stretching peak at about 3309 cm^{-1} in natural yellow variety that was also vanished after heating both in oxidizing and reducing experiments. This finding contradicts report of Volynet et al. (1972) suggested that the O-H stretching peak could be appeared and intensified after heating up corundum at high temperatures in reducing atmosphere. However, it may indicate for instant that Awissawella yellow variety appears to have more hydrogen atoms occupying in their structure than those in blue variety.

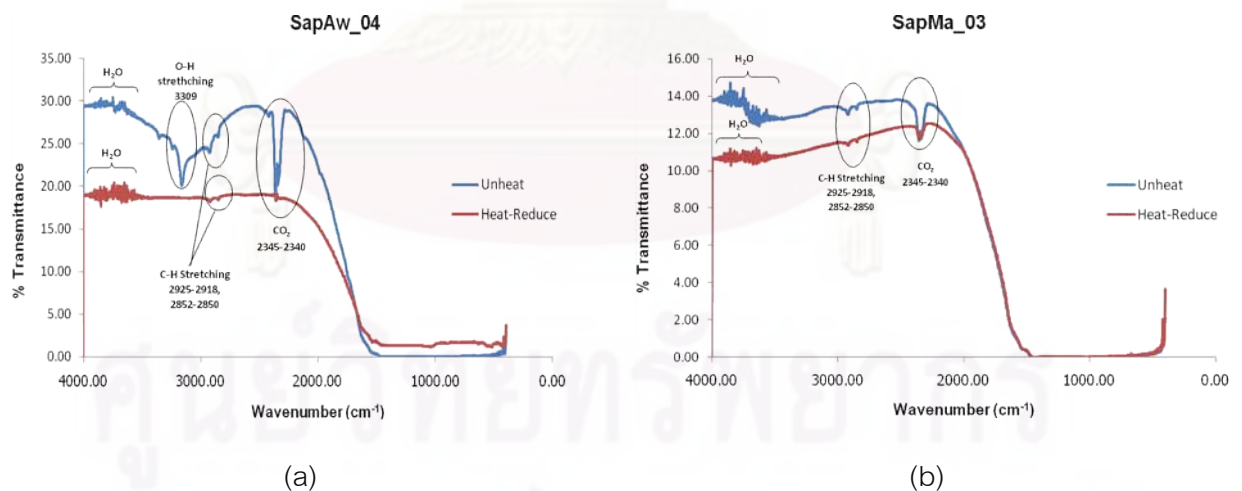


Figure 7.1 FTIR spectra comparing between yellow and light blue varieties. (a) FTIR spectra of yellow variety show O-H stretching peak at about 3309 cm^{-1} which disappeared after heat treatment. (b) FTIR spectra of light blue variety show the non-existence of such O-H stretching peak either natural or heated stones.

The UV-VIS-NIR spectra of Awissawella yellow sapphires show absorption peaks due to Fe^{3+} at 450 and 388 nm and additional absorption bands due to $\text{Fe}^{2+}/\text{Ti}^{4+}$ IVCT process at 565 nm. The latter absorption band appears to cause blue patches in the stone. Light blue samples mostly show absorption patterns quite similar to those observed in the yellow variety but absorption band with peak at 565 nm of $\text{Fe}^{2+}/\text{Ti}^{4+}$ becomes much stronger. In addition, light blue variety in bluish violet samples usually present small peak of Cr^{3+} at 412 nm. These absorption patterns can be used to assess the potential and appropriate condition of heat treatment. However, they have to be concerned along with trace element composition for such propose.

EDXRF analyses of yellow and light blue varieties of Awissawella corundum are compared to some basaltic and metamorphic sapphires which data are kindly provided by the GIT in Table 7.2. As shown in Tables 7.2, the yellow and blue sapphire varieties of Awissawella corundum contain extremely low Fe_2O_3 content as compared to those of basaltic corundums from Thailand and Laos but the contents are similar to those of the metamorphic corundums from Madagascar (Ilakaka and Skaraha), Myanmar and other deposits in Sri Lanka except those from Songea.

Table 7.2 Trace elements of Awissawella sapphire samples in comparison with those of basaltic and metamorphic sapphires elsewhere. Numbers of samples are present in parentheses.

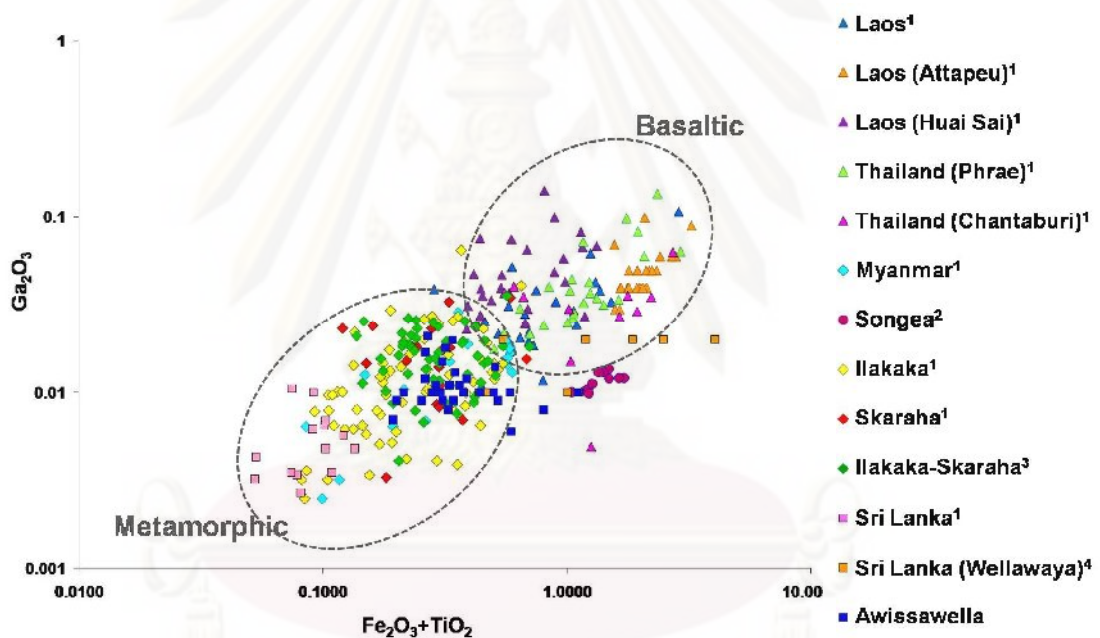
Localities (no.of sample)	Varieties	Trace Elements (Wt.%)			
		TiO ₂	Cr ₂ O ₃	Fe ₂ O ₃	Ga ₂ O ₃
Basaltic					
Chanthaburi ¹ (12)	blue	0.03-0.14	0.00-0.15	0.53-2.67	0.00-0.06
Phrae ¹ (13)	blue	0.01-0.26	0.00-0.41	0.43-2.68	0.02-0.14
Laos ¹ (22)	blue	0.02-0.37	0.00-0.08	0.20-2.54	0.01-0.11
Laos:Attapeu ¹ (23)	blue & green	0.02-0.82	0.00-0.09	1.44-2.43	0.03-0.10
Laos:Huai sai ¹ (31)	blue	0.03-0.34	0.00-0.31	0.30-1.27	0.02-0.14
Metamorphic					
Skaraha ¹ (19)	blue	0.01-0.24	≤0.07	0.09-0.66	≤0.04
Ilakaka ¹ (69)	blue	0.01-0.21	≤0.06	0.05-0.61	≤0.06
Ilakaka-Skaraha ² (51)	blue & violet	0.01-0.27	0.00-0.14	0.10-0.66	≤0.03
Myanmar	blue	0.00-0.24	≤0.01	0.06-0.59	≤0.03
Songea ³ (4)	blue	0.02-0.16	≤0.03	1.13-2.06	≤0.02
Songea ³ (11)	yellow	0.00-0.09	0.00-4.39	0.01-1.69	0.01-1.10
Songea ³ (8)	purple	0.01-0.23	≤0.14	1.01-1.91	≤0.02
Sri Lanka ¹ (14)	blue	0.01-0.03	≤0.05	0.04-0.12	≤0.01
Wellawaya ⁴ (4)	blue	0.30-3.71	≤0.03	0.19-0.36	≤0.02
Awissawella (21)	yellow	0.03-0.22	0.00-0.02	0.13-0.94	0.00-0.01
Awissawella (7)	blue	0.04-0.13	0.00-0.01	0.13-0.27	0.01-0.02

¹ with the courtesy of GIT; ² Sakkaravej, (2004); ³ Lomthong, (2004); ⁴Tipprasert (2006)

Plots of Fe₂O₃+ TiO₂ versus Ga₂O₃ and Fe₂O₃ versus Ga₂O₃ of all color varieties of Awissawella sapphires together with basaltic and metamorphic sapphires from elsewhere are displayed in Figures 7.2 and 7.3, respectively. These plots show clearly that Awissawella sapphires are very close to metamorphic origins of Ilakaka-Skaraha (Madagascar), Myanmar and other deposits in Sri Lanka sapphire.

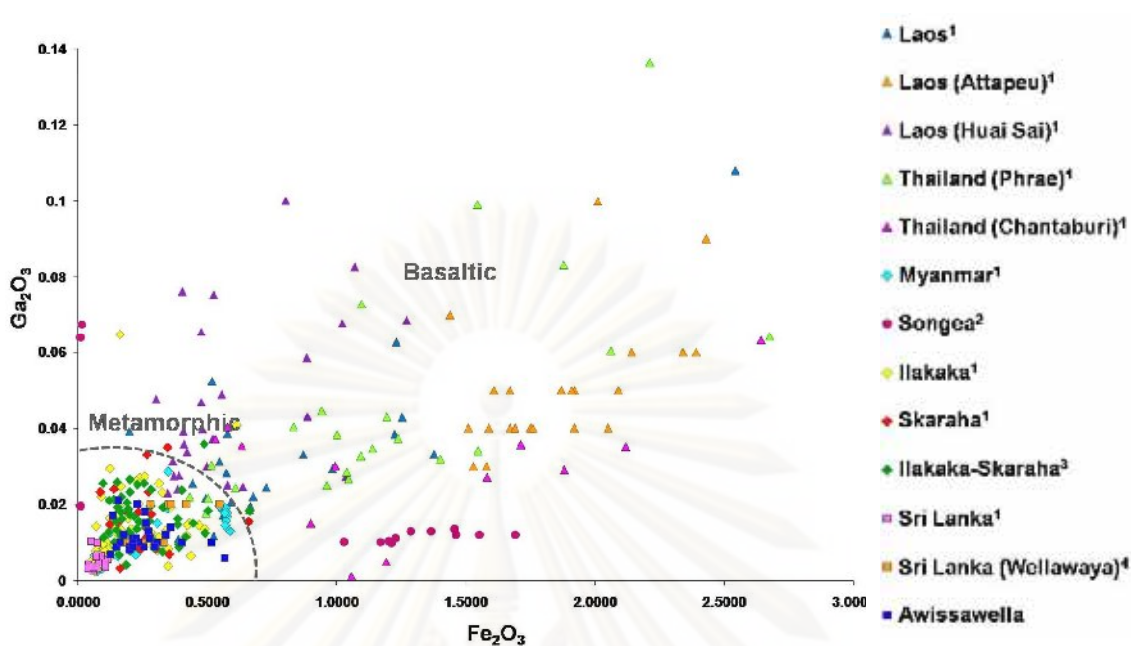
Fe₂O₃/Cr₂O₃ versus TiO₂/Ga₂O₃, as suggested by Sutherland and Schwarz (2001) and Sutherland et al., (2003) for origin determination, of all varieties from Awissawella and other Sri Lanka deposits together with other metamorphic origins are

plotted in Figures 7.4 to 7.5. These plots show clearly that Awissawella sapphires can be separated from Myanmar and Songea sapphires (Figure 7.4), their $\text{Fe}_2\text{O}_3/\text{Cr}_2\text{O}_3$ ratios of both origins are higher than those from Awissawella and other Sri Lanka deposits. But $\text{Fe}_2\text{O}_3/\text{Cr}_2\text{O}_3$ ratios of Madagascar (Ilakaka-Sakaraha) sapphires are similar to the range of Awissawella sapphires (Figure 7.5). In addition, although $\text{Fe}_2\text{O}_3 + \text{TiO}_2$ or Fe_2O_3 contents of Awissawella sapphire similar to Madagascar sapphire, their Ga_2O_3 contents are somewhat lower; therefore, Awissawella sapphires can be separated from Madagascar sapphires using contents of Ga_2O_3 (Figures 7.2 and 7.3 again). Even though, they are not always the case.



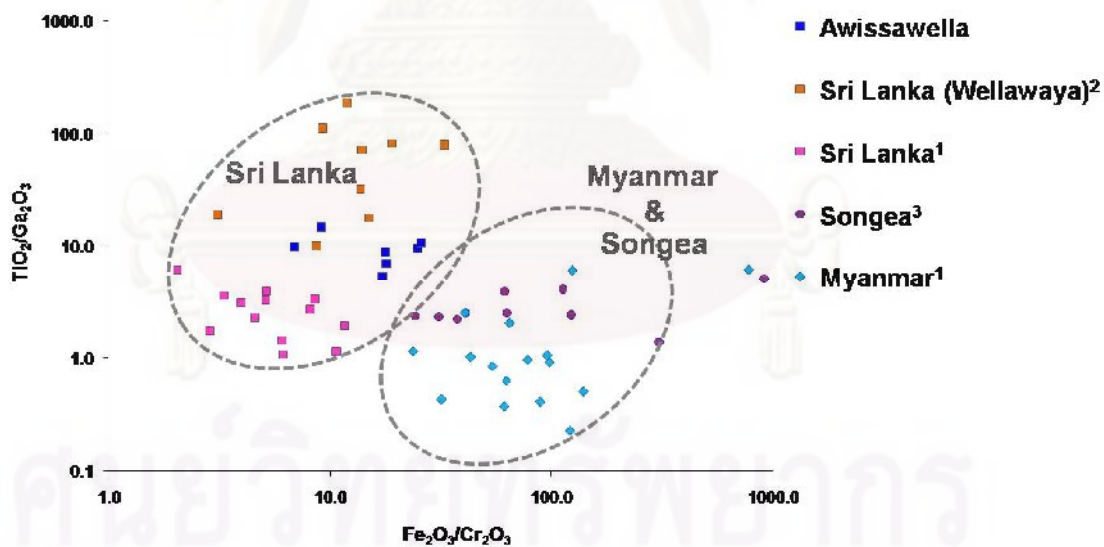
¹ with the courtesy of GIT; ² Lomthong, (2004); ³ Sakkaravej, (2004); ⁴ Tipprasert (2006)

Figure 7.2 Plotting $\text{Fe}_2\text{O}_3 + \text{TiO}_2$ versus Ga_2O_3 trace composition of Awissawella sapphires samples and sapphires from other basaltic and metamorphic origins.



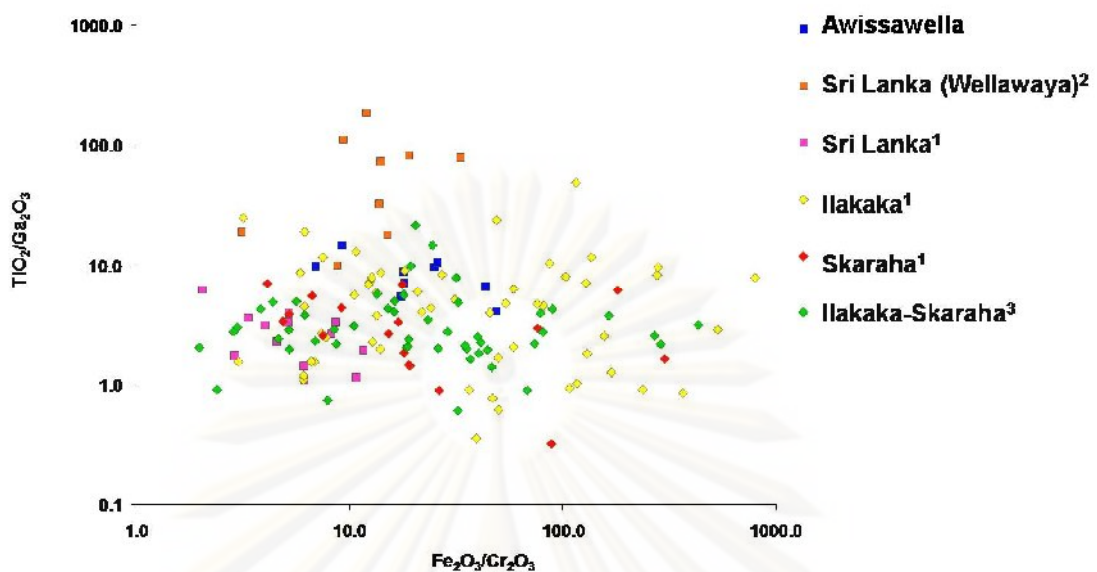
¹ with the courtesy of GIT; ² Lomthong, (2004); ³ Sakkaravej, (2004); ⁴ Tipprasert, (2006)

Figure 7.3 Plots of Fe_2O_3 versus Ga_2O_3 of Awissawella sapphire samples and some sapphire with basaltic and metamorphic sapphire.



¹ with the courtesy of GIT; ² Tipprasert, (2006); ³ Lomthong, (2004)

Figure 7.4 Plotting between Fe_2O_3/Cr_2O_3 and TiO_2/Ga_2O_3 of Awissawella sapphire samples, other sapphires in Sri Lanka and some Myanmar and Songea sapphires.



¹ with the courtesy of GIT; ²Tipprasert, (2006); ³ Sakkaravej

Figure 7.5 Trace composition plotting between $\text{Fe}_2\text{O}_3/\text{Cr}_2\text{O}_3$ and $\text{TiO}_2/\text{Ga}_2\text{O}_3$ of Awissawella sapphires, other Sri Lanka sapphires and some Madagascar sapphires.

For the quantitative EPMA analyses of trace elements, both yellow and light blue varieties present higher Fe contents than the other trace elements. Significant trace elements causing color in corundum are Mg, Ti and Fe which their recalculated atomic proportions are plotted in a ternary diagram (Figures 4.12 to 4.14). Yellow components in yellow sapphire variety are mostly rather high Mg contents; on the other hand, blue component in varieties have high Ti and Fe contents. Moreover, Mg contents are quite low ($\leq 20\%$) in most blue component. This finding agrees well with color-causing model in corundum of Häger (2001).

7.2 Potential for Heat Treatment

Both varieties of Awissawella corundums have potential for heat treatments either in oxidizing condition or reducing condition. However, selection of sapphires must be taken appropriately for proper heating conditions. In oxidizing experiment, the yellow coloration created during the heating process is likely caused by increased Fe^{3+} contents and defect centers stabilized by Mg in the Al_2O_3 structure or the so-called 'stable color centers or Mg-trapped hole color centers'. The UV-VIS spectra of yellow

sapphire samples after treatment in oxidizing experiment show Fe^{3+} peak at 388 nm and a continuous increase in absorption towards shorter wavelengths with a shoulder at around 460 nm. Fe^{3+} may be modified from oxidizing of Fe^{2+} . The last spectral pattern is generally known to be caused by stable defect centers as typical observed from Sri Lanka yellow sapphire (Pisutha-Arnond et al., 2004; Somboon, 2006). In contrast, light blue variety when heated in the oxidizing condition cannot be removed all blue components from the samples because the interaction of trace elements (Mg-Fe-Ti) in the samples have excess of Ti content after the calculation of MgTiO_3 clusters. The excess Ti in combination with Fe could form color-active FeTiO_3 clusters. These clusters create $\text{Fe}^{2+}/\text{Ti}^{4+}$ inter-valence charge transfer absorption bands near 565 nm which are responsible for the blue coloration of Awissawella sapphire. In addition, yellow coloration could not be created clearly in light blue variety after heat in such condition that appears to have the same reason.

In reducing experiment, both varieties of Awissawella corundums can improve the blue component but the light blue variety seems to response better than the yellow variety. The appearance of pale blue replacing yellow body color is subtly observed that may be caused by slightly higher Ti against Mg in the blue patch as recorded by EPMA. Therefore, the pale blue variety is more appropriated to intensify blue component in reducing heat; on the other hand, yellow variety trends to develop better quality of yellow color under reducing heat.

7.3 Conclusions

1. Awissawella rough samples clearly show well-preserved crystal habits such as barrel-shape, hexagonal prism and spindle-shape hexagonal bipyramid that have mainly blue in color. However, some variations of color can be observed after they have been cut. Consequently, they can be separated into yellow variety and light blue variety.

2. The UV-VIS-NIR absorption spectra show two main different patterns depending on their varieties. Yellow variety presents clearly a continuous absorption increasing towards shorter wavelengths forming a shoulder of $\text{Fe}^{3+}/\text{Fe}^{3+}$ pairs at around 450 nm with a Fe^{3+} peak at 388 nm and absorption band of blue patches with peak at

565 nm belonging to $\text{Fe}^{2+}/\text{Ti}^{4+}$ IVCT. Blue variety usually presents high absorption band of $\text{Fe}^{2+}/\text{Ti}^{4+}$ pairs with maxima at 565 nm, peak of $\text{Fe}^{3+}/\text{Fe}^{3+}$ pairs at 450 nm, Fe^{3+} peak at 388 nm and in bluish violet samples usually present small peak of Cr^{3+} at 412 nm.

3. Significant peaks of FTIR spectrum at around 3309 cm^{-1} , caused by structural O-H stretching, present only in yellow variety samples before heat treatment. That may be naturally different from light blue variety which may get higher temperature involvement. Besides, more hydrogen atoms would be more abundant in yellow variety.

4. Based on EDXRF and EPMA analyses, iron is the most dominant trace element in all sapphires. Plots of $\text{TiO}_2 + \text{Fe}_2\text{O}_3$ versus Ga_2O_3 and Fe_2O_3 versus Ga_2O_3 of all Awissawella sapphires suggest metamorphic source origin. In addition, Ga_2O_3 contents in the Awissawella sapphires are obviously lower than those in the Madagascar sapphires (Ilakaka and Sakaraha). The plots of $\text{Fe}_2\text{O}_3/\text{Cr}_2\text{O}_3$ versus $\text{TiO}_2/\text{Ga}_2\text{O}_3$ can separate Awissawella sapphires from other metamorphic source origins such as Myanmar and Songea.

4. The most common mineral inclusions in sapphire sample are apatite and calcite which usually occur as single crystal or cluster. Other mineral inclusions are feldspar, garnet (pyrope), diaspore, pyroxene (enstatite) and hematite.

6. Awissawella corundums have high potential to improve their colors. Yellow variety appears to be intensified by heating at $1,650^\circ\text{C}$ in oxidizing atmosphere; on the other hand, blue variety can be increased blue shades by heating at $1,650^\circ\text{C}$ in reducing atmosphere. These results are clearly explained by their trace chemical compositions.

ศูนย์วิทยทรัพยากร

จุฬาลงกรณ์มหาวิทยาลัย

REFERENCES

- Cooray, P.G. 1984. Introduction of The Geology Of Sri Lanka. Second (Revised Edition), National Museums of Sri Lanka Publication. 340 pp.
- Dahanayake, K. 1980. Modes of occurrence and provenance of gemstones of Sri Lanka. Mineral. Deposits. 15: 81-86.
- Data of mineral inclusions found in corundums from Madagascar. Available from: www.gubelinlab.com (2007, February 25).
- Data of mineral inclusions found in corundums from Sri Lanka. Available from: www.fieldgemology.org (2009, April 10).
- Deer, W. A., Howie, R. A. and Zussman, J. 1992. An introduction to the rock-forming minerals. 549 pp.
- Dissanayake, C.B. 1985. The application of plate tectonics to mineral exploration: discovery of a mineralized belt in Sri Lanka. In Dissanayake, C. B., and Cooray, P.G., eds. Recent advances in the geology of Sri Lanka. CIFEG (International Center for Training and Exchange in the Geosciences, Paris) occasional publication 1985/2(6):.47–57.
- Dissanayake C B. 1995. Prospecting for new gem deposits. Handbook on Geology and Mineral Resources of Sri Lanka. K. Dahanayake (Ed), GEOSAS-II, Colombo, Sri Lanka.
- Dissanayake, C.B. and Chandrajith, R. 1999. Sri Lanka–Madagascar Gondwana Linkage: Evidence for a Pan-African Mineral Belt. The Journal of Geology. 107: 223–235.
- Dissanayake, C.B., Chandrajith R. and Tobschall H.J. 2000. The geology, mineralogy and rare element geochemistry of the gem deposits of Sri Lanka. Bulletin of the Geological Society of Finland. 72(Parts 1–2): 5–20.
- Dissanayake, C.B. and Rupasinghe, M. S. 1993. A Prospectors' Guide Map to The Gem Deposits of Sri Lanka. Gems & Gemology. 03(2): 173-181.

- Dissanayake, C.B. and Rupasinghe, M.S. 1995. Classification of gem deposits of Sri Lanka. Geologie en Mijnbouw. 74: 79–88.
- Emmett, J.L. and Douthit, T.R. 1993. Heat treating the sapphires of Rocks Creek, Montana. Gems & Gemology. 29(4): 250-272.
- Ferguson, J., and Fielding, P.E. 1971. The origins of colours of yellow, green, and blue sapphires. Chemical Physics Letters. 10: 262-265.
- Ferguson, J., and Fielding, P.E. 1972. The origins of the colours of natural yellow, green, and blue sapphires. Aust.J.Chem. 25: 1372-1385.
- Gunaratne, H.S. and Dissanayake, C.B. 1995. Gems and gem deposits of Sri Lanka. Colombo. National Gems and Jewellery Authority. 203 pp.
- Gunawardene, M. and Rupasinghe, M.S. 1986. The Elahera gem field in central Sri Lanka. Gems & Gemmology. 22: 80-95
- Häger, T. 1992. Ergebnisse und "farbhemmende" Spurenelemente in blauen Saphiren. Ber. Dt. Mineral. Ges. Beih. Europ. J. Mineral. 4: 109.
- Häger, T. 1993. Stabilisierung der Farbzentren von gelben natürlichen Saphiren. Ber. Dt. Mineral. Ges. Beih. Europ. J. Mineral. 5: 188.
- Häger, T. 1996. Farbrelebante Wechselwirkungen von Spurenelemente in Korund. Ph.D Thesis, University of Mainz: 170 pp.
- Häger, T. 2001. High temperature treatment of natural corundum. In: Proceeding of the International Workshop on Material Characterization by Solid State Spectroscopy, April 4-10, 2001, Hanoi, Vietnam, 1-10.
- Harder, H. 1992. Smoky Moonstone - A New Variety From Ratnapura, Sri Lanka. Zeitschrift der Deutschen Gemmologischen Gessellschaft. 41(2/3): 69-84.
- Henney, P. 1999. Sri Lanka National factsheet. Best Practice in Small-scale Gemstone Mining DFID Knowledge and Research Project, 57-85.
- Hughes, R.W. 1997. Ruby & Sapphire. Colorado USA: RWH Publishing, Boulder. 511pp.

- Intasopa, S., Atichat, W., Pisutha-Armond, V. and Sriprasert, B. 2002. Inclusions in Corundum: A new approach to the definition of standards for origin determination. Department of Mineral Resource. 223 pp.
- Klein, C. and Hurlbut, Jr.C.S. 1977. Manual of mineralogy. John Wiley & Sons, Inc. 681 pp.
- Kriegsman, L. 1993. Geodynamic evolution of the Pan-African lower crust in Sri Lanka. Geol. Ultraiectnia. 114: 208.
- Kröner, A. 1980. Pan-African crustal evolution. Episodes 1980: 3–8.
- Kröner, A. 1991. Africa linkage of Precambrian Sri Lanka. Geol. Rundsch. 80: 429–440.
- Kröner, A., Cooray, P. G. and Vitanage, P. W. 1991. Lithotectonic subdivision of the Precambrian basement in Sri Lanka. *In* Kröner, A., ed. The crystalline crust of Sri Lanka. Pt. I. Summary of research of the German–Sri Lanka consortium. Geol. Surv. Dept., Sri Lanka Prof. 5: 5–21.
- Kumaratilleke, W.L.D.R.A. and Ranasinghe, U.N. 1992. Unusual Corundum - Bearing Gem Pockets At Avissawella, Getahetta, Sri Lanka. Z. Dt. Gemm. Ges. 41: 7-16.
- Krebs, J.J. and Maisch, W.G. 1971. Exchange effects in optical absorption spectrum of Fe^{3+} in Al_2O_3 . Physical Review B. Vol.4: p.757-769.
- Lehmann, G. and Harder, H. 1970. Optical spectra of di- and trivalent iron in corundum. American Mineralogist. 55: 98-105.
- Lomthong, P. 2004. Characteristics of some corundum from Songea, Tanzania. M.Sc. Thesis. Department of Geology. Faculty of Science. Chulalongkorn University: 92 pp.
- Map of Sri Lanka, show locations of island in the Indian Ocean south-east of India. Available from: www.sjr.mb.ca/ms/geo/countries/sri/img18.gif (2007, March 7).
- Map of Sri Lanka (Ceylon) showing the locations of the important cities, mining areas. Available from: www.palagems.com/ceylon_sapphire_bancroft.htm (2007, May 13).

- Mathavan, V., Kalubandara, S. T. and Fernando, G. W. A. R. 2000. Occurrences of two types of gem deposits in the Okkampitiya gem field, Sri Lanka. Journal of Gemmology. 27(2): 65-72.
- Milisenda, C., Pohl, J.R. and Hofmann, A.W. 1991. Charnockite formation at Kurunegala, Sri Lanka. *In* Kröner, A., ed. The crystalline crust of Sri Lanka. Pt. I. Summary of research of the German–Sri Lanka consortium. Geol. Surv. Dept., Sri Lanka Prof. 5: 141–149.
- Munasinghe, T. and Dissanayke, C.B. 1982. A plate tectonic model for the geological evolution of Sri Lanka. Journal Geol. Soc. India 23: 369–380.
- Nassau, K., 1982. Comment on “Heat treating corundum”. *In*: Editorial forum. Gems & Gemology. 18: 109.
- Nassau, K., 1994. Gemstone Enhancement. 2nd edn. Butterworths, London.
- Nassau, K., and Valente, K. 1987. The seven types of yellow sapphire and their stability to light. Gems & Gemology. 23: 22-231.
- Nikolskaya, L.V., Terekhova, V.M. and Samoilovich, M.I. 1978 On the origin of sapphires with a new heat-treatment technique (part B). Contributions to Gemology. 2: 21-33.
- Pisutha-Arnond, V., Häger, T., Wathanakul, P., and Atichat, W. 2004. Yellow and brown colouration in beryllium treated sapphires. Journal of Gemology. 29(2): 77-103.
- Pisutha-Arnond, V., Wathanakul, P., and Atichat, W., Häger, T., Win, T.T., Leelawatanasuk, T., and Somboon, C. 2003. Beryllium-treated Vietnamese and Mong Hsu rubies. *In*: Hofmeister W., Quang V.X., Doa N.Q., and Nghi T.(eds). *In*: Proceeding of the 2nd International Workshop on Geo-and Material-Science on Gem-Minerals of Vietnam, 1-8 October 2003, Hanoi, 171-175.
- Ranasinghe, P.N.1995. Gold & other mineral resources in Ramboda area. B.Sc. Thesis. University of Peradeniya.

- Rupasinghe, M S., Banerjee, A., Pense, J. and Dissanayke, C.B. 1984. The geochemistry of beryllium and fluorine in the gem fields of Sri Lanka. Mineral Deposita. 19: 86-93
- Rupasinghe, M.S., Senaratne, A. and Dissanayake, C.B. 1986. Light, heavy and rare minerals in washed gem gravels of Sri Lanka. Journal of Gemmology. 20: 177–184.
- Sakkaravej, S. 2004. Thermal enhancement of some blue sapphires from Madagascar. M.Sc. Thesis. Department of Geology. Faculty of Science. Chulalongkorn University: 212 pp.
- Schenk, V., Raase, P. & Schumacher, R. (1991): Metamorphic zonation and P-T history of the Highland Complex in Sri Lanka. In: The Crystalline Crust of Sri Lanka, Part I, Summary of Research of the German-Sri Lankan Consortium (A. Kröner, ed.). Geol. Sun. Dep. Sri Lanka, Prof. 5: 150-163.
- Schmetzer, K., Bosshart, G., and Hänni, H.A., 1983. Naturally coloured and treated yellow and orange-brown sapphires. Journal of Gemmology., 18: 607-622.
- Schmetzer, K. and Medenbach, O. 1988. Examination of three-phase inclusions in colorless, yellow, and blue sapphires from Sri Lanka. Gems & Gemology. 30 (4): 107-111.
- Schmetzer, K. and Schwarz, D. 2004. The causes of colour in untreated, heat treated and diffusion treated orange and pink-orange sapphires a review. Journal of Gemmology. 29(3): 149-182.
- Schmetzer, K., and Schwarz, D. 2005. A microscopy based screening system to identify natural and treated sapphires in the yellow to reddish-orange colour range. Journal of Gemmology. 29(7/8): 407-449.
- Silva, K.K.M.W. and Siriwardena, C.H.E.R. 1988. Geology and the origin of the corundum-bearing skarn at Bakamuna, Sri Lanka. Mineralium Deposita. 23: 816–190.

- Somboon, C. 2006. Yellow coloration in heat-treated natural sapphires. M.Sc. Thesis. Department of Geology. Faculty of Science. Chulalongkorn University: 88 pp.
- Sutherland, F.L. and Schwarz, D. 2001. Origin of gem corundums from basalt fields. The Australian Gemmologist. 21: 30–33.
- Sutherland, F. L., Coenraads, R. R., Schwarz, D., Raynor, L. R., Barron, B. J. and Webb, G. B. 2003. Al-rich diopside in alluvial ruby and corundum-bearing xenoliths, Australian and SE Asian basalt fields. Mineralogical Magazine. 67(4): 717-732.
- Table of Thailand export statistics of precious and semi-precious stones in January-December, 2007. Available from: http://www.git.or.th/thai/gem_and_jewelry_database/gem_and_jewelry_database_index.htm (2008, March 10).
- Themelis, T. 1992. The heat treatment of Ruby and Sapphire, USA: World Graphics Inc, 236 pp.
- Tipprasert, S. 2006. Thermal enhancement and characteristics of sapphires from Wellawaya, Sri Lanka. B.Sc. Thesis. Department of Geology. Faculty of Science. Chulalongkorn University: 55 pp.
- Townsend, M.G. 1968. Visible charge transfer band in blue sapphire. Solid State Commun. 6: 81-83.
- Wathanakul, P., Leelawathanasuk, T., Singhanumrung, S., Pavaro, T., Somboon, S., Sriprasert, B., Lomthong, P. and Sakkaravej, S. 2002. Gemstone research of advance instruments for origin determination. 84 pp.
- Yoshida, M. and Vitange, P. W. 1993. A review of the Precambrian geology of Sri Lanka and its comparion with eight. assembly, evaluation, and dispersal. Rotterdam, Balkema: 97–109.
- Zoysa E.G. 1981. Gem occurrences in Sri Lanka. Journal of the Gemmological Society of Japan. 8(114): 43-49.



APPENDIXES

ศูนย์วิทยทรัพยากร
จุฬาลงกรณ์มหาวิทยาลัย



APPENDIX A

ศูนย์วิทยทรัพยากร
จุฬาลงกรณ์มหาวิทยาลัย

Appendix A Physical properties and optical properties of Awissawella corundums.

Table A-1 Physical and optical properties of yellow sapphire variety from Awissawella, Sri Lanka.





Samples		Weight (ct)	GIA Color		SG.	RI		Bire.	Fluorescence	
			Body	Patch		Max	Min		LW	SW
SapAw_01		2.79	gY2/3	B5/1	3.95	1.768	1.760	0.008	st. Orange	w.Orange
SapAw_02		3.84	YG/GY2/1	vB4/3	3.96	1.771	1.762	0.009	st. Orange	w.Orange
SapAw_03		4.81	YG/GY2/1	B6/2	3.89	1.771	1.763	0.008	st. Orange	w.Orange
SapAw_04		3.39	Y2/2	B7/2	3.97	1.770	1.762	0.008	st. Orange	mo. Orange

Table A-1 (Continue).






Samples	Weight (ct)	GIA Color		SG.	RI		Bire.	Fluorescence	
		Body	Patch		Max	Min		LW	SW
SapAw_05	 2.29	gY2/3	vB4/3	3.93	1.768	1.761	0.007	st. Orange	mo. Orange
SapAw_06	 1.47	Y2/2	B4/2	3.94	1.768	1.760	0.008	st. Orange	mo. Orange
SapAw_07	 1.79	YG/GY2/1	vB7/3	3.95	1.769	1.760	0.009	st. Orange	w.Orange
SapAw_08	 2.75	gY2/3	vB5/3	3.95	1.770	1.761	0.009	st. Orange	w.Orange
SapAw_09	 7.69	YG/GY2/1	vB4/3	3.87	1.768	1.761	0.007	st. Orange	w.Orange

Table A-1 (Continue).

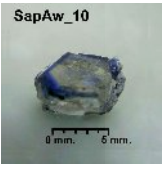
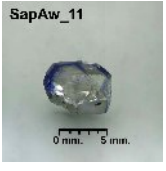



Samples		Weight (ct)	GIA Color		SG.	RI		Bire.	Fluorescence	
			Body	Patch		Max	Min		LW	SW
SapAw_10		6.72	gY2/3	B4/2	3.88	1.770	1.762	0.008	st. Orange	w.Orange
SapAw_11		3.48	gY3/4	bV7/4	3.92	1.769	1.761	0.008	st. Orange	w.Orange
SapAw_12		3.48	Y2/2	vB7/3	3.94	1.770	1.761	0.009	st. Orange	w.Orange
SapAw_13		1.79	Y2/2	B5/1	3.93	1.768	1.760	0.008	st. Orange	w.Orange
SapAw_14		3.34	Y3/5	B4/2	3.95	1.768	1.761	0.007	st. Orange	w.Orange

Table A-1 (Continue).






Samples	Weight (ct)	GIA Color		SG.	RI		Bire.	Fluorescence		
		Body	Patch		Max	Min		LW	SW	
SapAw_15	 SapAw_15 0 mm. 5 mm.	2.33	Y3/3	vB5/3	3.91	1.771	1.762	0.009	st. Orange	w.Orange
SapAw_16	 SapAw_16 0 mm. 5 mm.	1.89	YG/GY2/1	B5/1	3.97	1.770	1.762	0.008	st. Orange	w.Orange
SapAw_17	 SapAw_17 0 mm. 5 mm.	1.76	YG/GY2/1	vB5/3	3.90	1.770	1.762	0.008	st. Orange	mo. Orange
SapAw_18	 SapAw_18 0 mm. 5 mm.	1.53	gY3/4	vB4/3	3.93	1.768	1.760	0.008	st. Orange	w.Orange
SapAw_19	 SapAw_19 0 mm. 5 mm.	2.63	Y3/3	bV8/3	3.88	1.769	1.760	0.009	st. Orange	w.Orange

Table A-1 (Continue).

Samples	Weight (ct)	GIA Color		SG.	RI		Bire.	Fluorescence		
		Body	Patch		Max	Min		LW	SW	
SapAw_20		1.01	gY2/3	B6/2	3.93	1.769	1.762	0.007	st. Orange	w.Orange
SapAw_21		6.57	YG/GY2/1	vB4/4	3.85	1.768	1.761	0.007	st. Orange	w.Orange
SapAw_22		7.91	YG/GY2/1	bV8/3	3.86	1.770	1.762	0.008	st. Orange	w.Orange
SapAw_23		8.46	YG/GY2/1	vB5/3	3.90	1.769	1.761	0.008	st. Orange	w.Orange
SapAw_24		7.97	gY2/3	B7/4	3.85	1.770	1.762	0.008	st. Orange	w.Orange

Table A-1 (Continue).



Samples	Weight (ct)	GIA Color		SG.	RI		Bire.	Fluorescence	
		Body	Patch		Max	Min		LW	SW
SapAw_25	 5.16	gY2/3	vB5/3	3.84	1.770	1.762	0.008	st. Orange	w.Orange
SapAw_26	 8.12	gY2/3	bV7/4	3.85	1.768	1.760	0.008	st. Orange	w.Orange
SapAw_27	 9.25	YG/GY2/1	B7/4	3.87	1.768	1.760	0.008	st. Orange	w.Orange
SapAw_28	 5.05	YG/GY2/1	B5/1	3.92	1.771	1.762	0.009	st. Orange	w.Orange
SapAw_29	 4.89	gY2/3	vB5/3	3.86	1.771	1.763	0.008	st. Orange	w.Orange
SapAw_30	 4.29	YG/GY2/1	B5/3	3.91	1.770	1.762	0.008	st. Orange	w.Orange

Table A-1 (Continue).


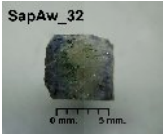

Samples		Weight (ct)	GIA Color		SG.	RI		Bire.	Fluorescence	
			Body	Patch		Max	Min		LW	SW
SapAw_31		4.12	gY2/3	vB4/4	3.84	1.770	1.762	0.008	st. Orange	w.Orange
SapAw_32		5.37	YG/GY2/1	B5/2	3.83	1.768	1.760	0.008	st. Orange	w.Orange
SapAw_33 (SapAwTw_01)		7.14	gY2/3	vB4/3	3.80	1.768	1.761	0.007	st. Orange	w.Orange

Table A-2 Physical and optical properties of blue sapphire variety from Awissawella, Sri Lanka.

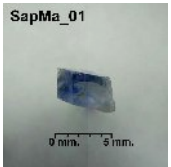




Samples	Weight (ct)	GIA Color		SG.	RI		Bire.	Fluorescence	
		Body	Patch		Max	Min		LW	SW
SapMa_01	 1.52	B2/2	vB5/3	3.96	1.771	1.762	0.009	mo. Redish orange	vw. Orange
SapMa_02	 8.02	vB3/3	vB4/3	3.94	1.769	1.761	0.008	mo. Redish orange	vw. Orange
SapMa_03	 2.69	B3/1	-	3.75	1.772	1.763	0.008	mo. Redish orange	vw. Orange
SapMa_04	 3.35	B3/1	B5/1	3.96	1.770	1.763	0.007	mo. Redish orange	vw. Orange
SapMa_05	 2.18	B5/2	bV8/3	3.91	1.770	1.762	0.008	mo. Redish orange	vw. Orange

Table A-2 (Continue).









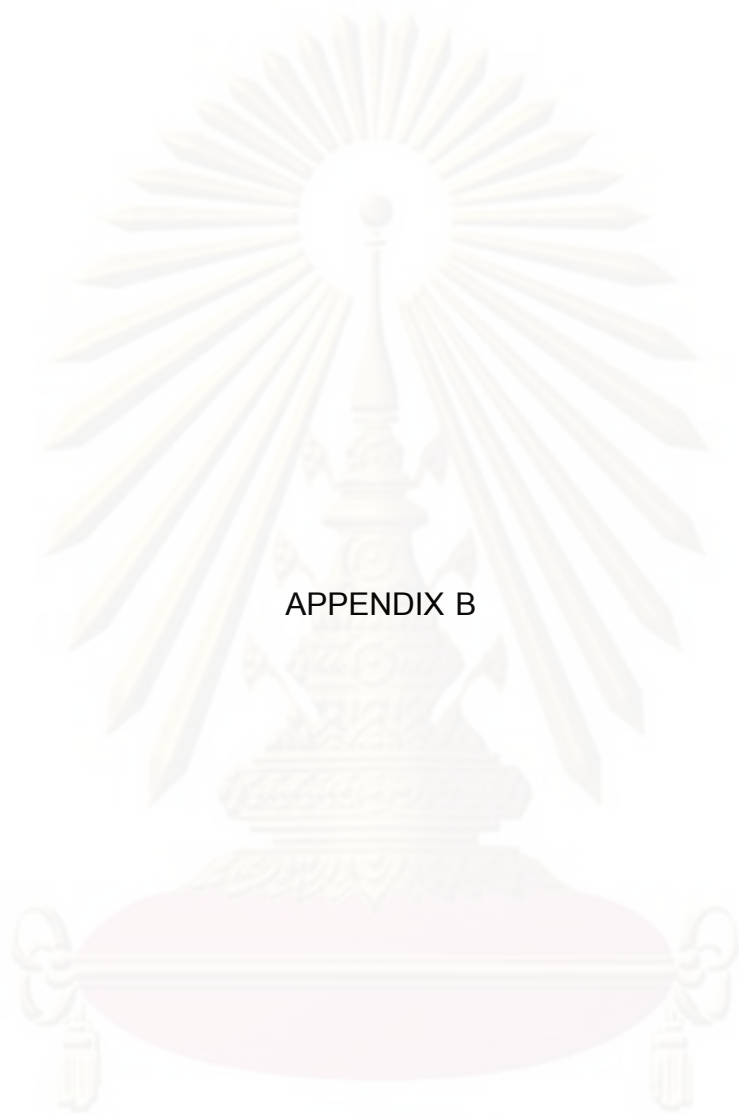
Samples	Weight (ct)	GIA Color		SG.	RI		Bire.	Fluorescence		
		Body	Patch		Max	Min		LW	SW	
SapMa_06	 SapMa_06 0 mm. 5 mm.	2.08	B2/2	vB5/3	3.95	1.768	1.761	0.007	mo. Redish orange	vw. Orange
SapMa_07	 SapMa_07 0 mm. 5 mm.	4.98	B3/3	B5/2	3.94	1.770	1.763	0.007	mo. Orange	vw. Orange
SapMa_08	 SapMa_08 0 mm. 5 mm.	7.69	B3/3	vB4/3	3.86	1.772	1.763	0.008	mo. Redish orange	vw. Orange
SapMa_09	 SapMa_09 0 mm. 5 mm.	2.45	B2/2	vB4/4	3.92	1.770	1.763	0.007	mo. Redish orange	vw. Orange
SapMa_10	 SapMa_10 0 mm. 5 mm.	2.44	B4/2	B3/4	3.82	1.770	1.763	0.007	mo. Redish orange	vw. Orange

Table A-2 (Continue).

Samples		Weight (ct)	GIA Color		SG.	RI		Bire.	Fluorescence	
			Body	Patch		Max	Min		LW	SW
SapMa_11		2.63	vB3/4	vB5/3	3.90	1.772	1.763	0.008	mo. Redish orange	vw. Orange
SapMa_12		2.09	vB3/3	vB5/3	3.94	1.771	1.762	0.009	mo. Redish orange	vw. Orange
SapMa_13		1.56	vB4/3	vB5/3	3.94	1.770	1.762	0.008	mo. Redish orange	vw. Orange



APPENDIX B

ศูนย์วิจัยทรัพยากร
จุฬาลงกรณ์มหาวิทยาลัย

Appendix B FTIR spectra of unheat corundums from Awissawella

Appendix B-1 FTIR spectra of yellow sapphire variety from Awissawella, Sri Lanka

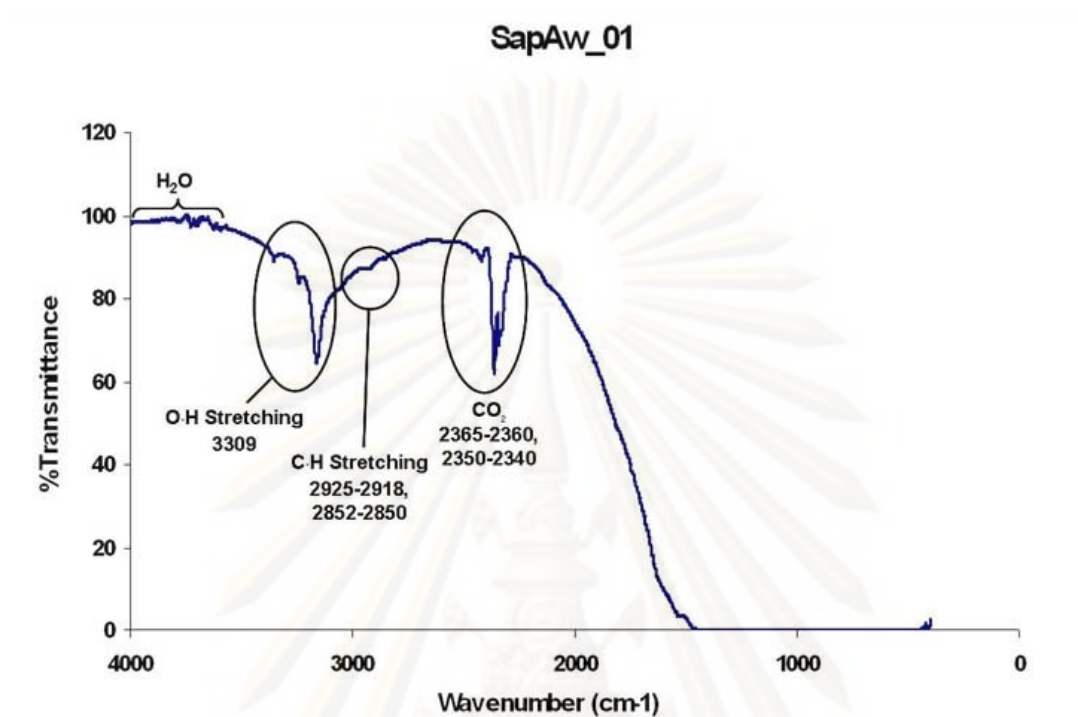


Figure B-1.1 FTIR spectra of the sample SapAw_01

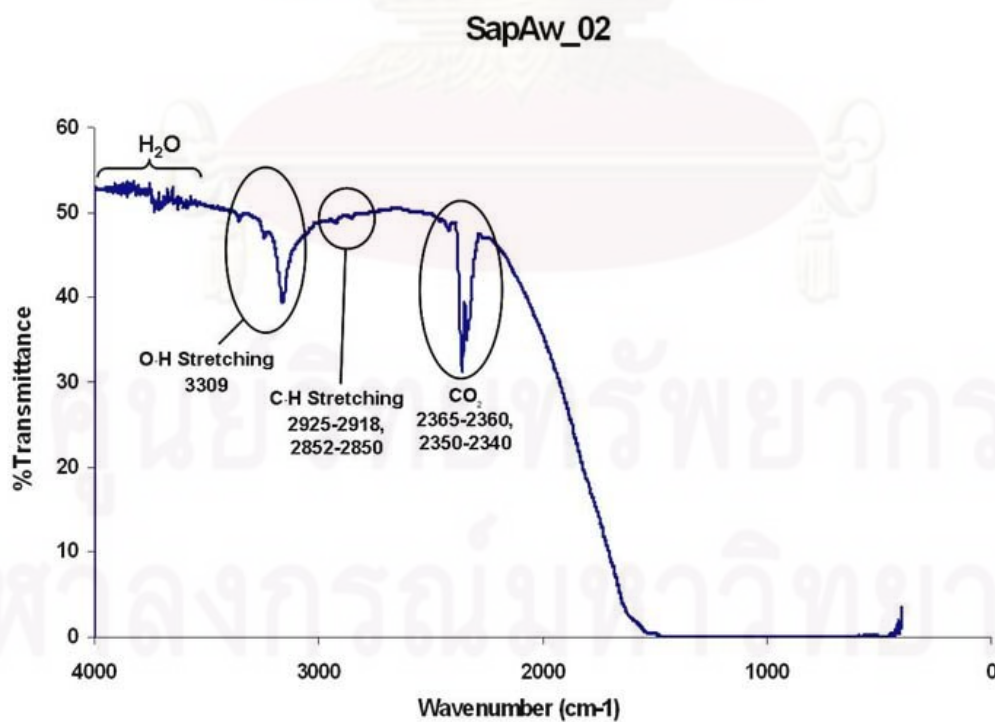


Figure B-1.2 FTIR spectra of the sample SapAw_02

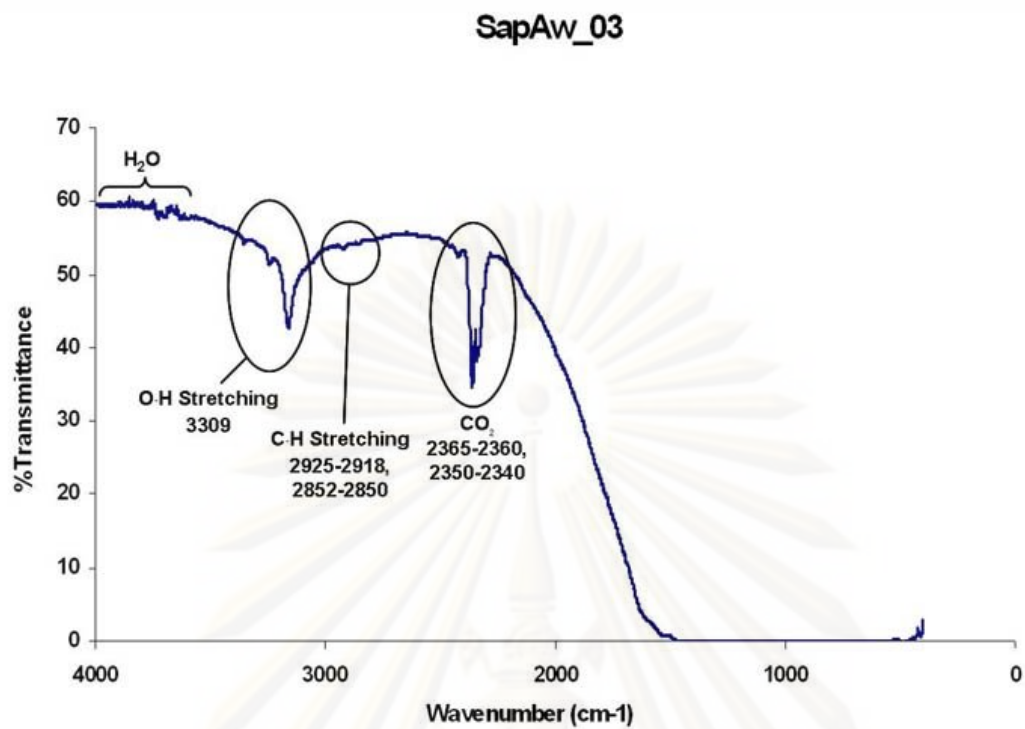


Figure B-1.3 FTIR spectra of the sample SapAw_03

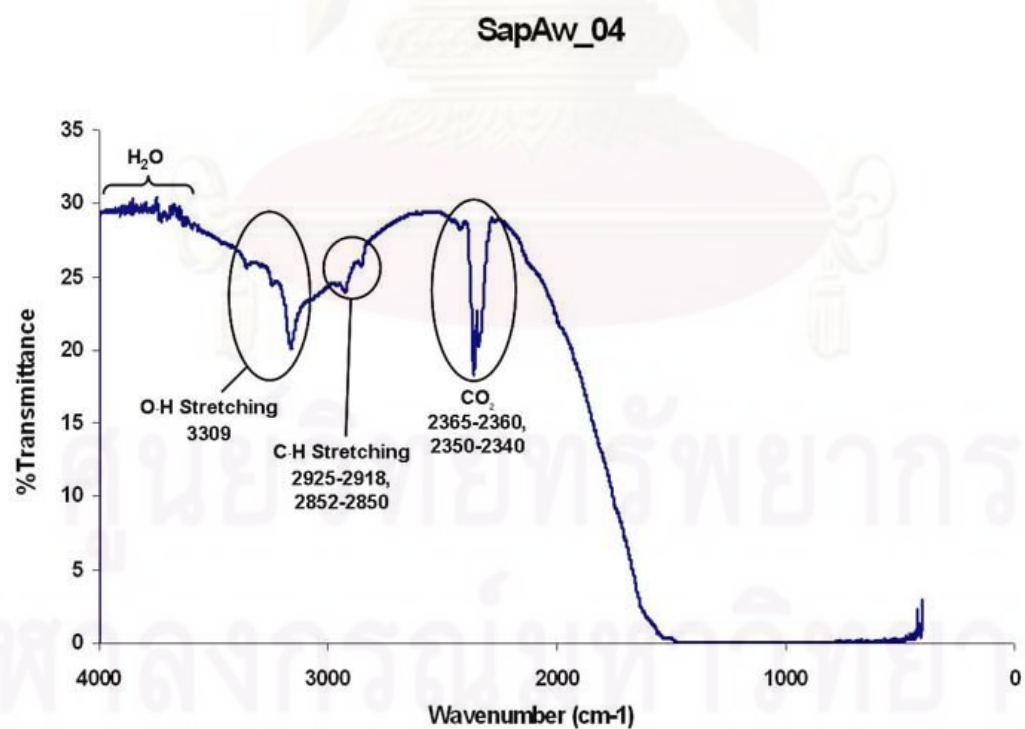


Figure B-1.4 FTIR spectra of the sample SapAw_04

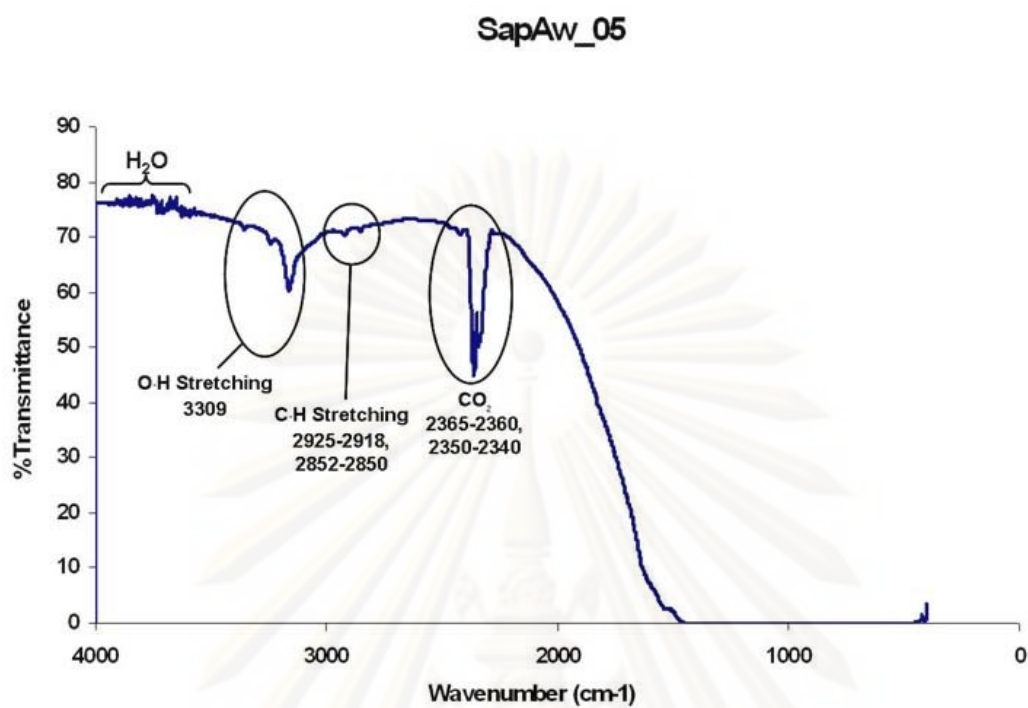


Figure B-1.5 FTIR spectra of the sample SapAw_05

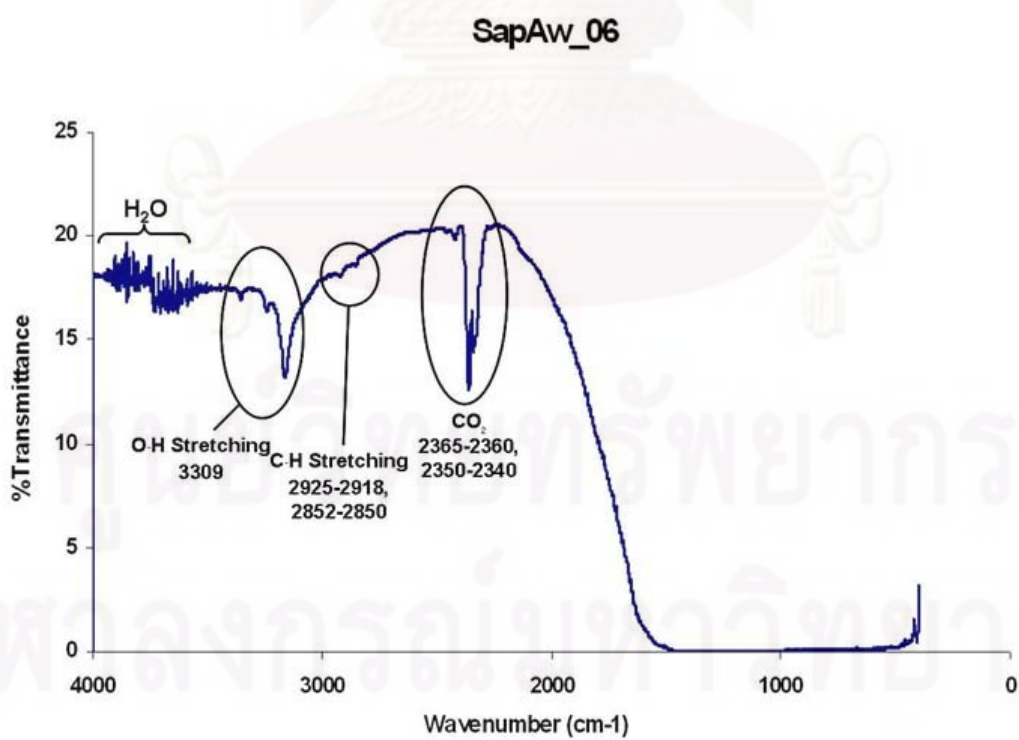


Figure B-1.6 FTIR spectra of the sample SapAw_06

SapAw_07

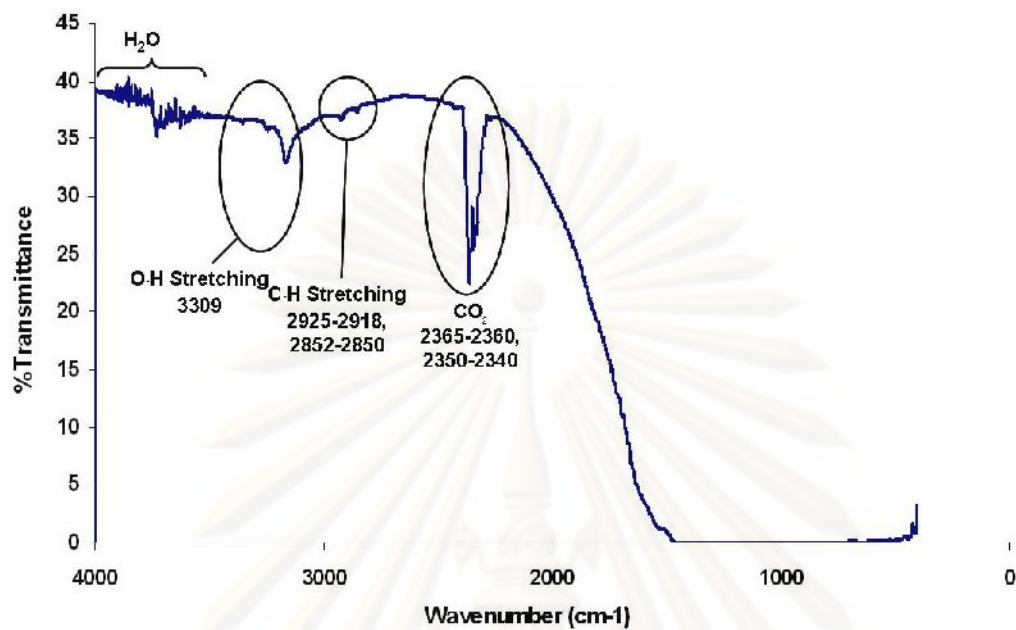


Figure B-1.7 FTIR spectra of the sample SapAw_07

SapAw_08

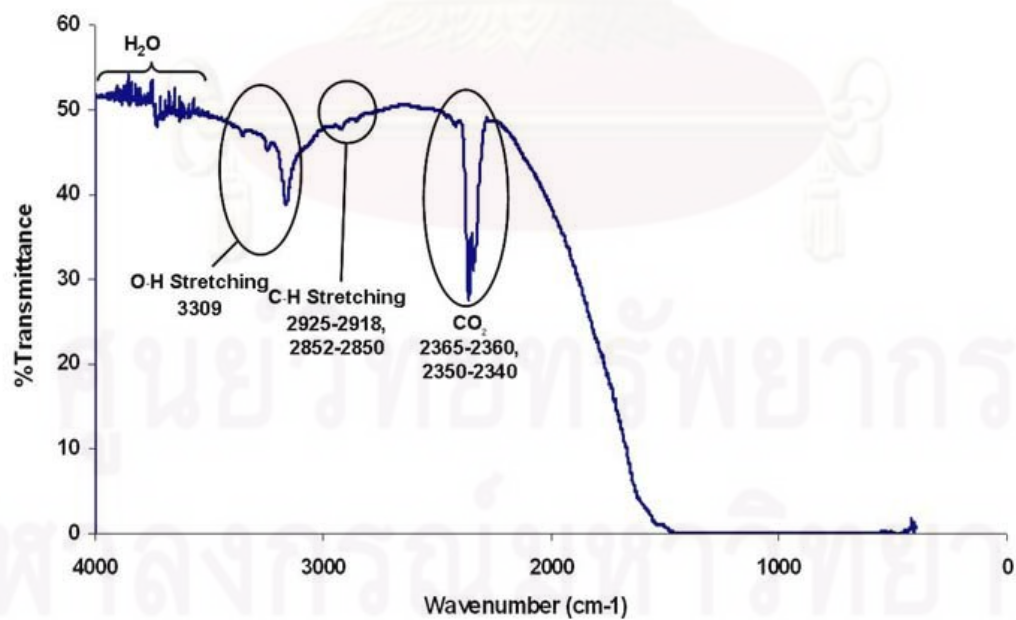


Figure B-1.8 FTIR spectra of the sample SapAw_08

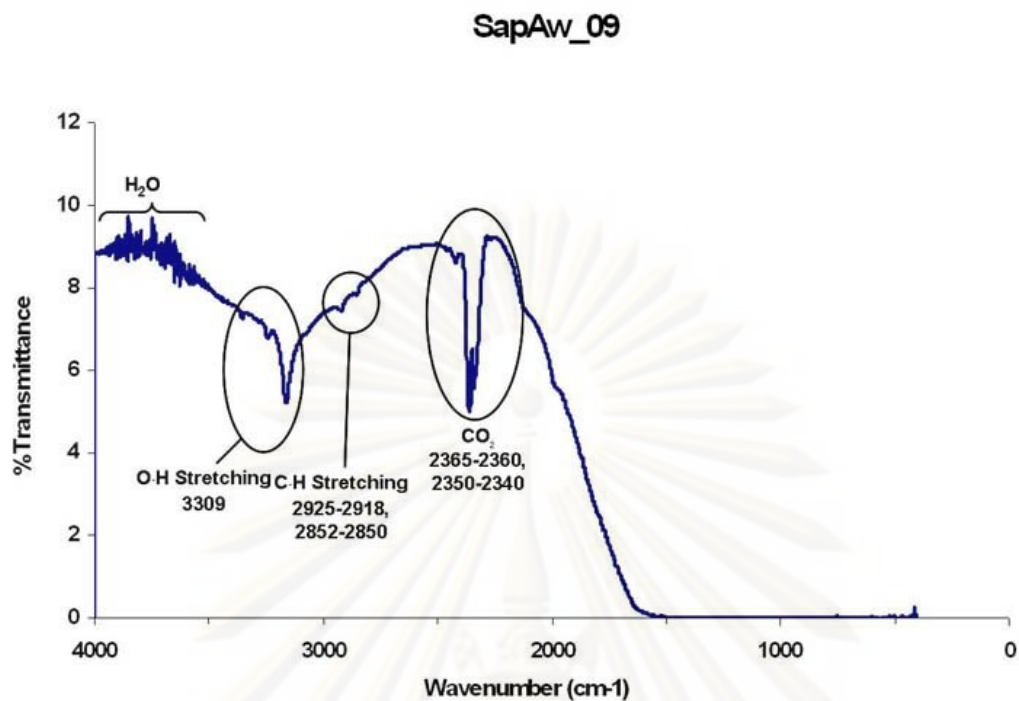


Figure B-1.9 FTIR spectra of the sample SapAw_09

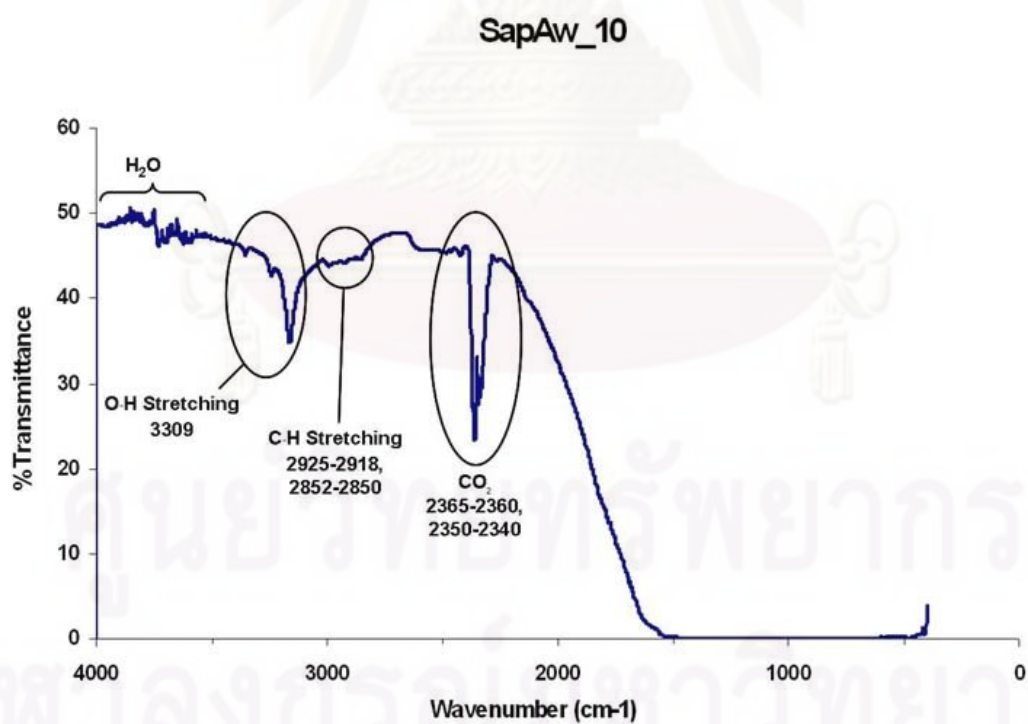


Figure B-1.10 FTIR spectra of the sample SapAw_10

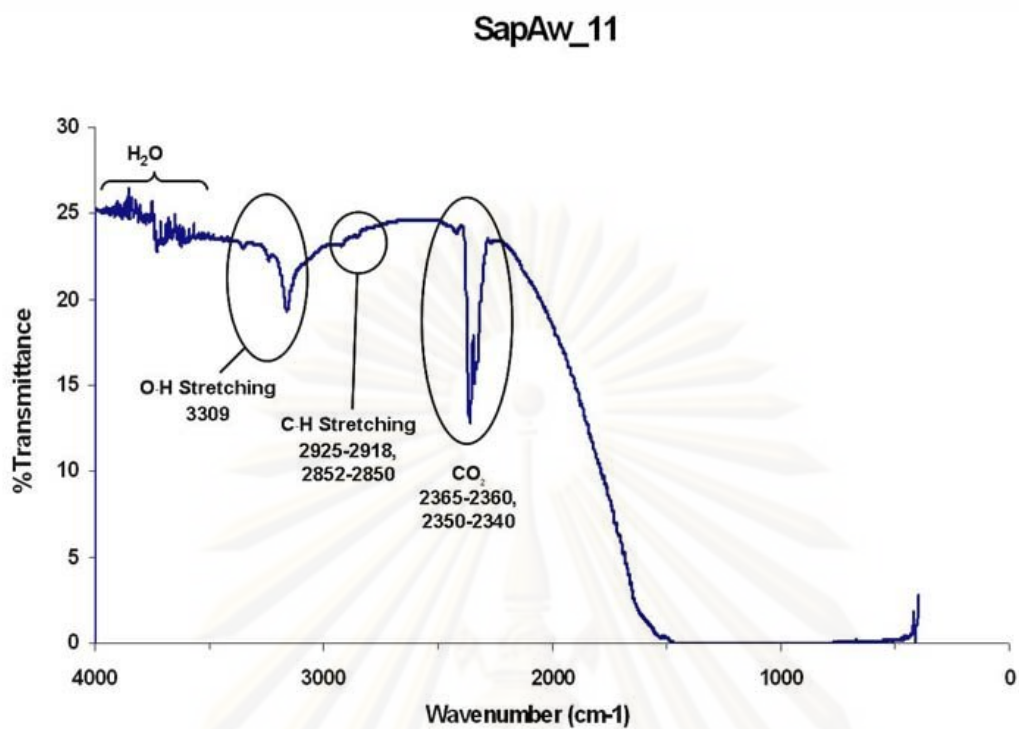


Figure B-1.11 FTIR spectra of the sample SapAw_11

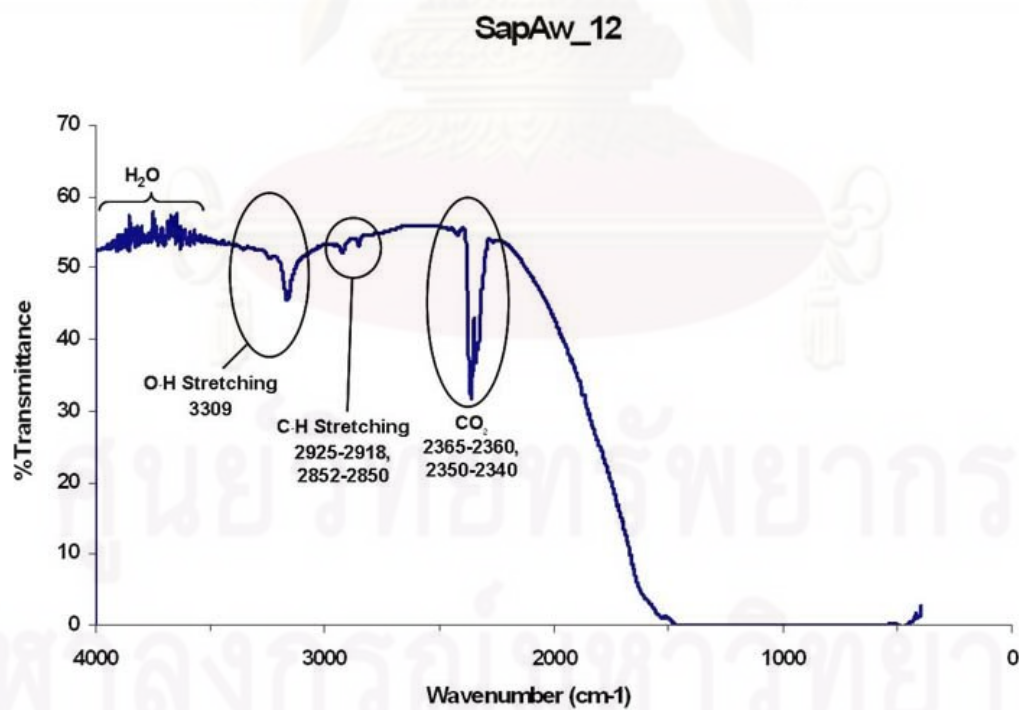


Figure B-1.12 FTIR spectra of the sample SapAw_12

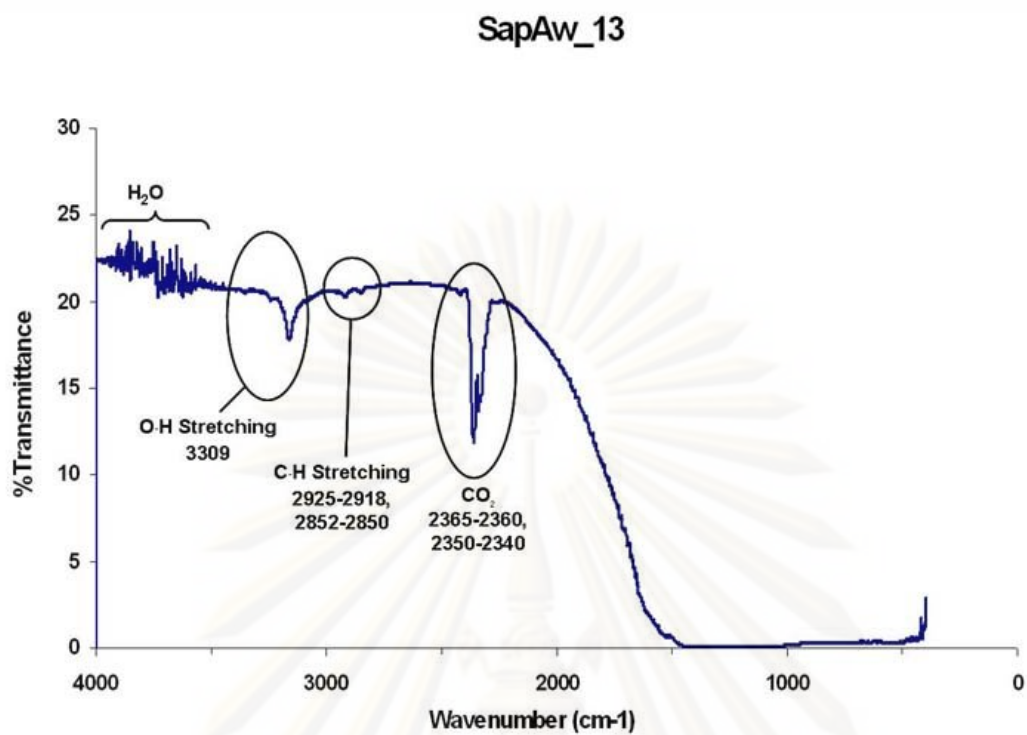


Figure B-1.13 FTIR spectra of the sample SapAw_13

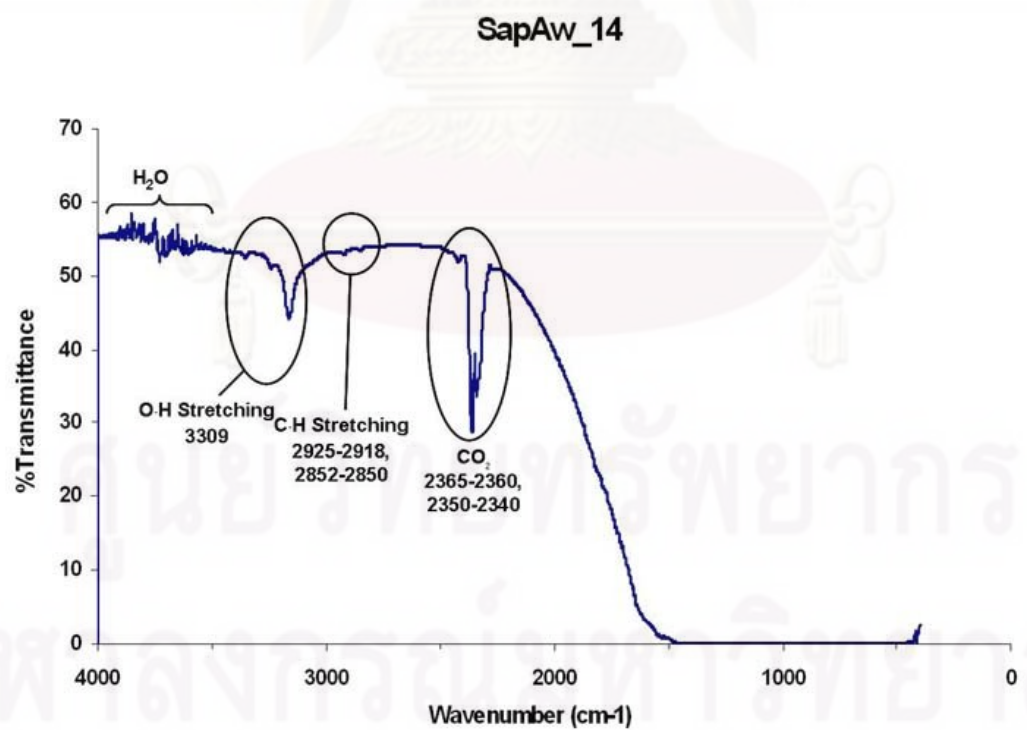


Figure B-1.14 FTIR spectra of the sample SapAw_14

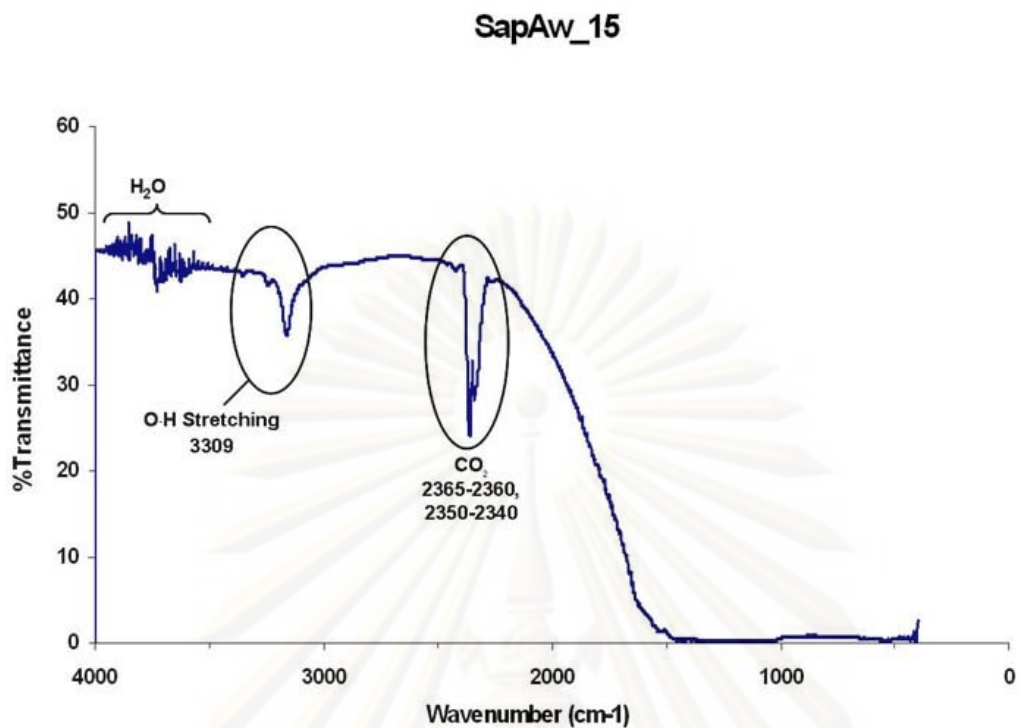


Figure B-1.15 FTIR spectra of the sample SapAw_15

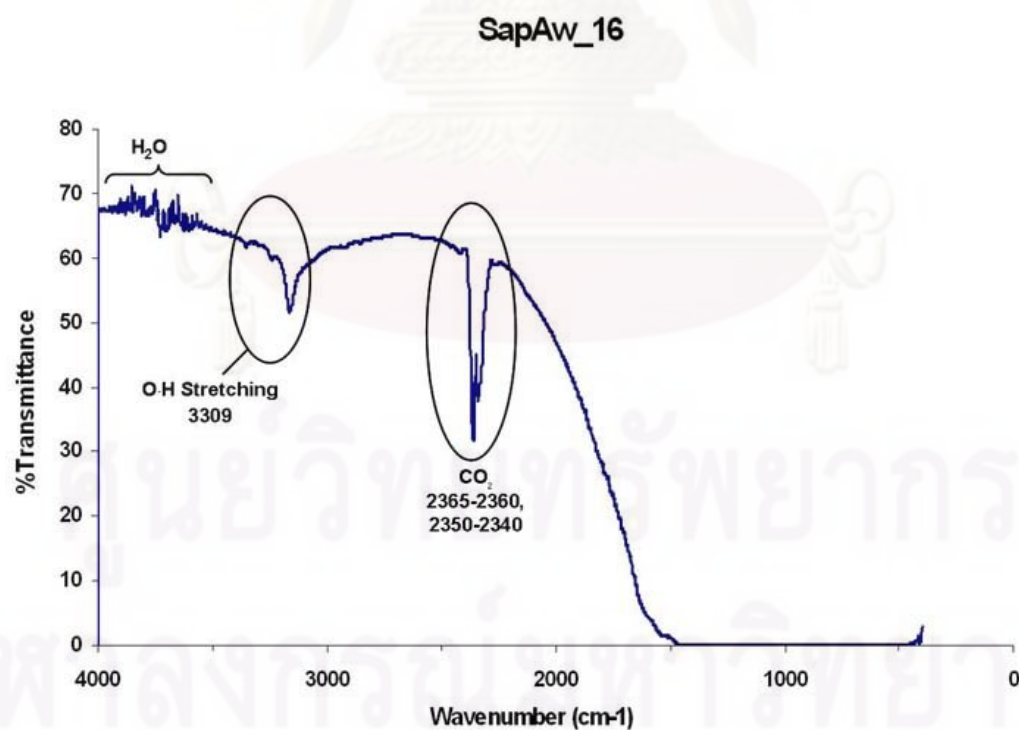


Figure B-1.16 FTIR spectra of the sample SapAw_16

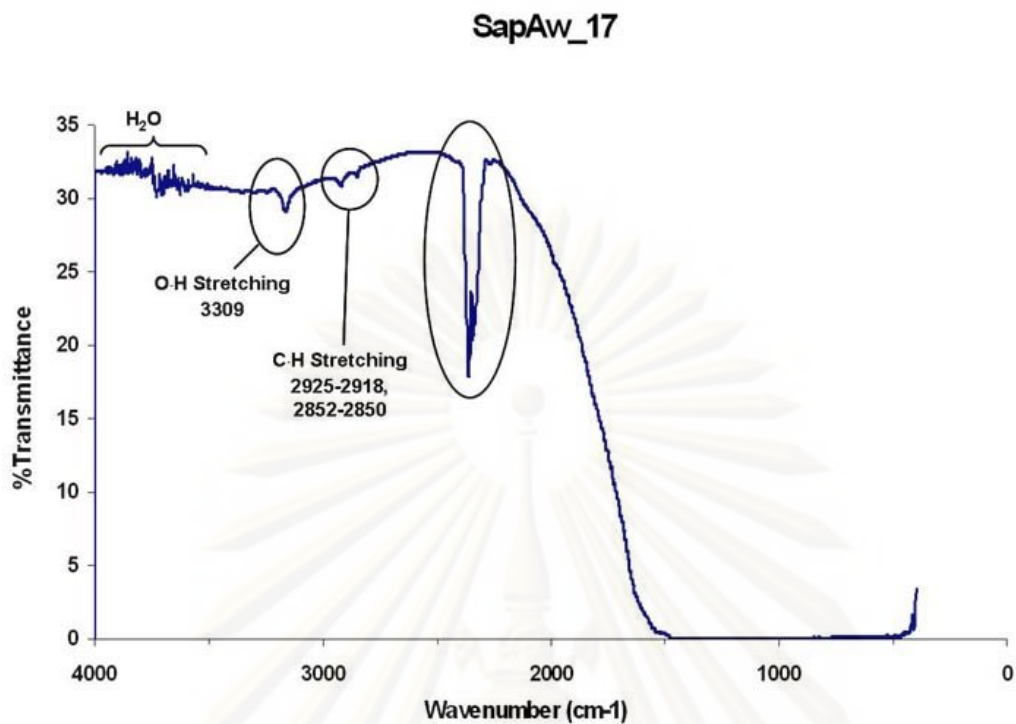


Figure B-1.17 FTIR spectra of the sample SapAw_17

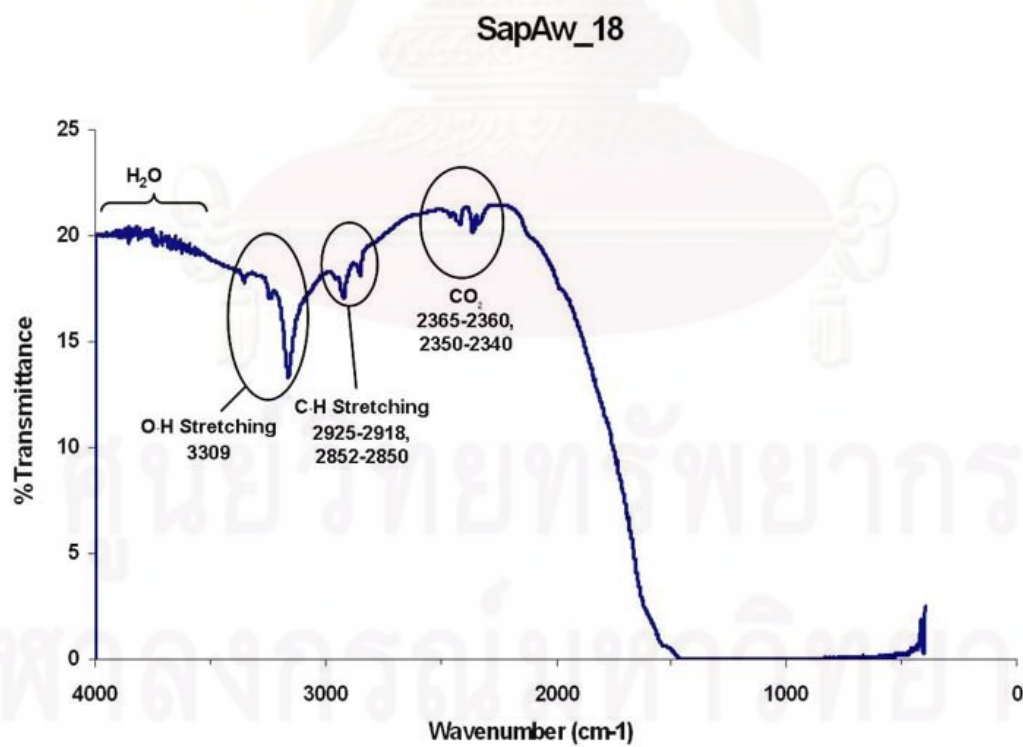


Figure B-1.18 FTIR spectra of the sample SapAw_18

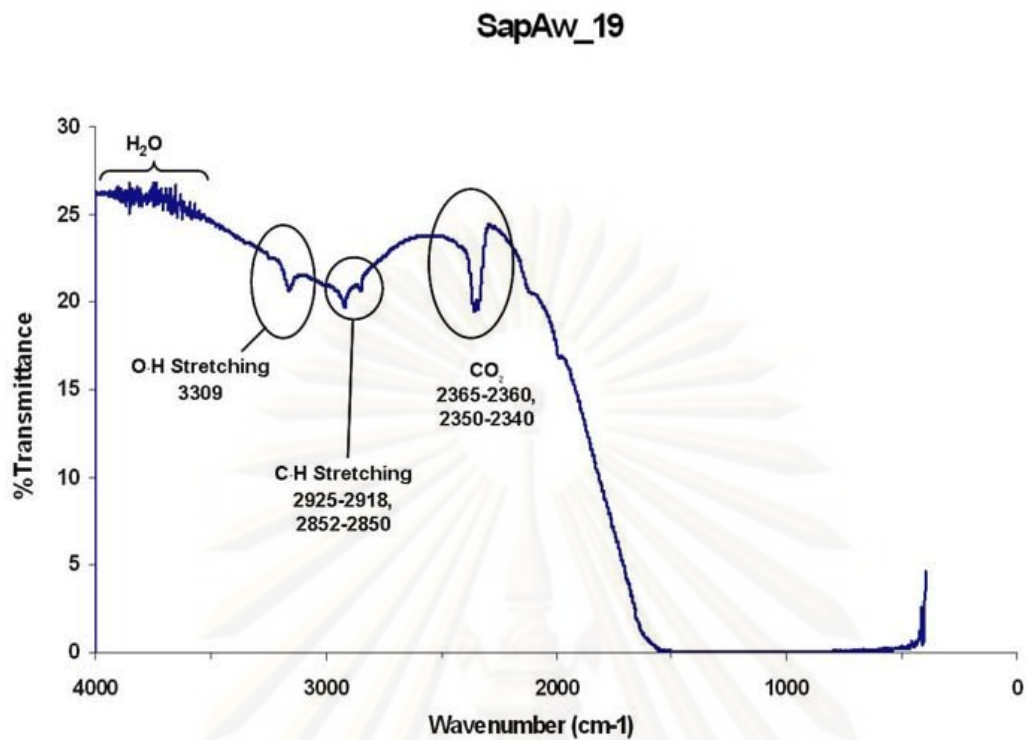


Figure B-1.19 FTIR spectra of the sample SapAw_19

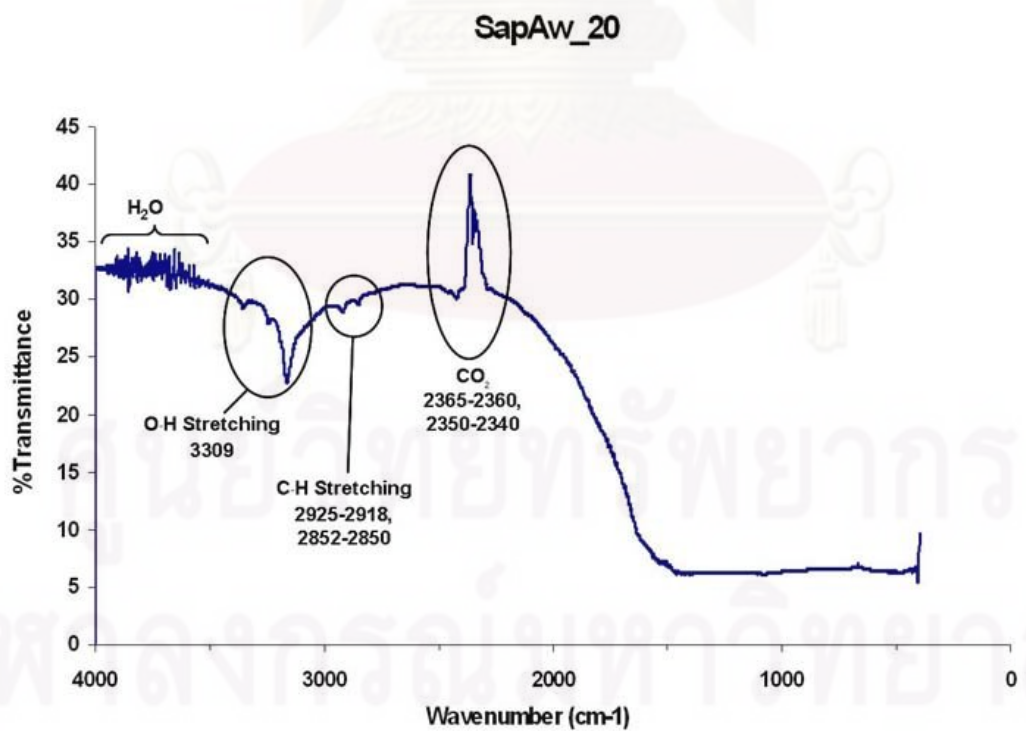


Figure B-1.20 FTIR spectra of the sample SapAw_20

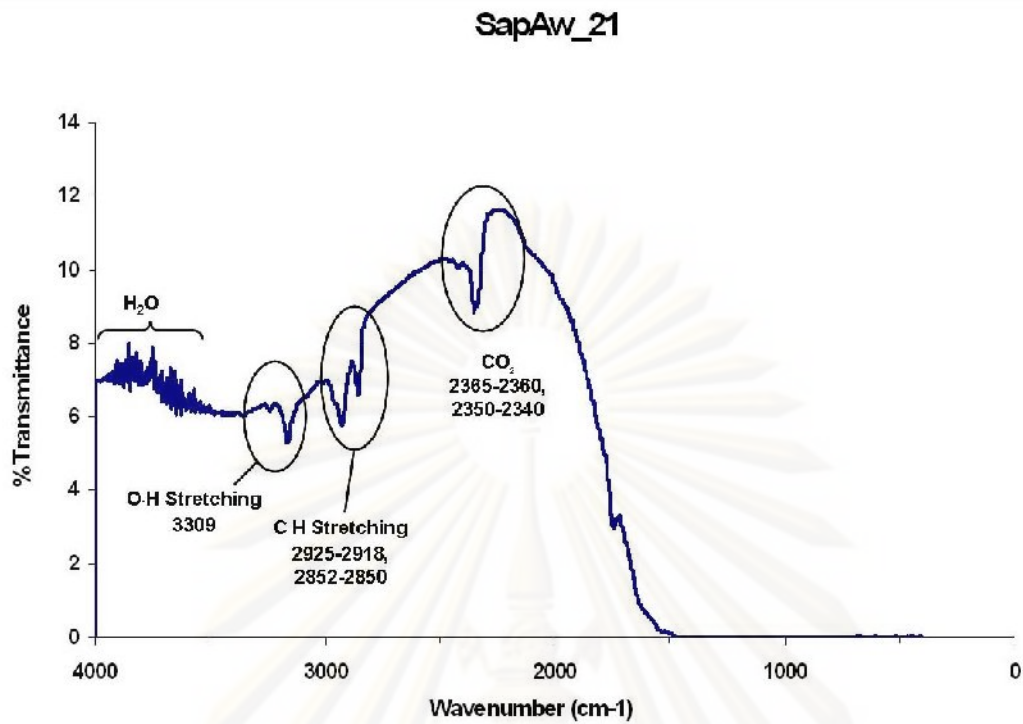


Figure B-1.21 FTIR spectra of the sample SapAw_21

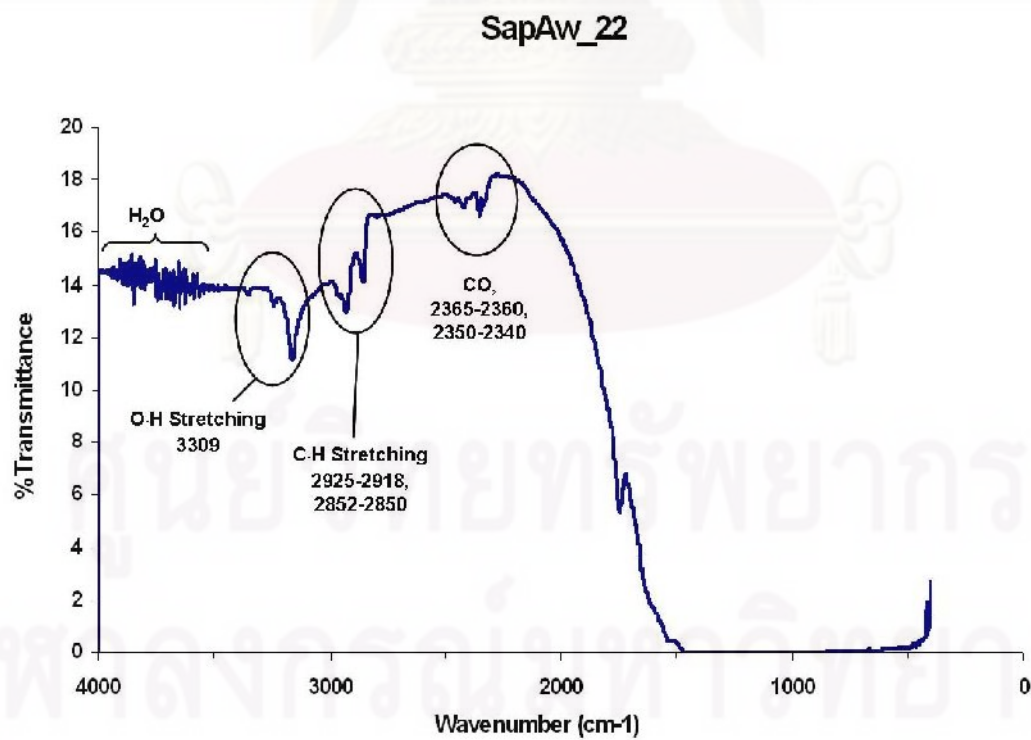


Figure B-1.22 FTIR spectra of the sample SapAw_22

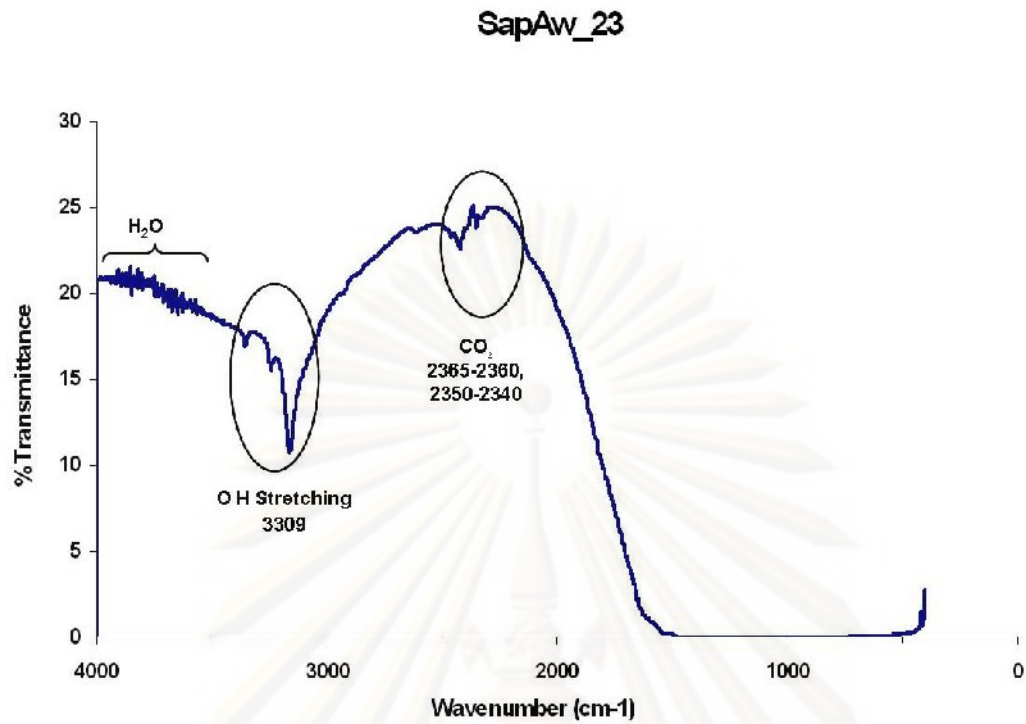


Figure B-1.23 FTIR spectra of the sample SapAw_23

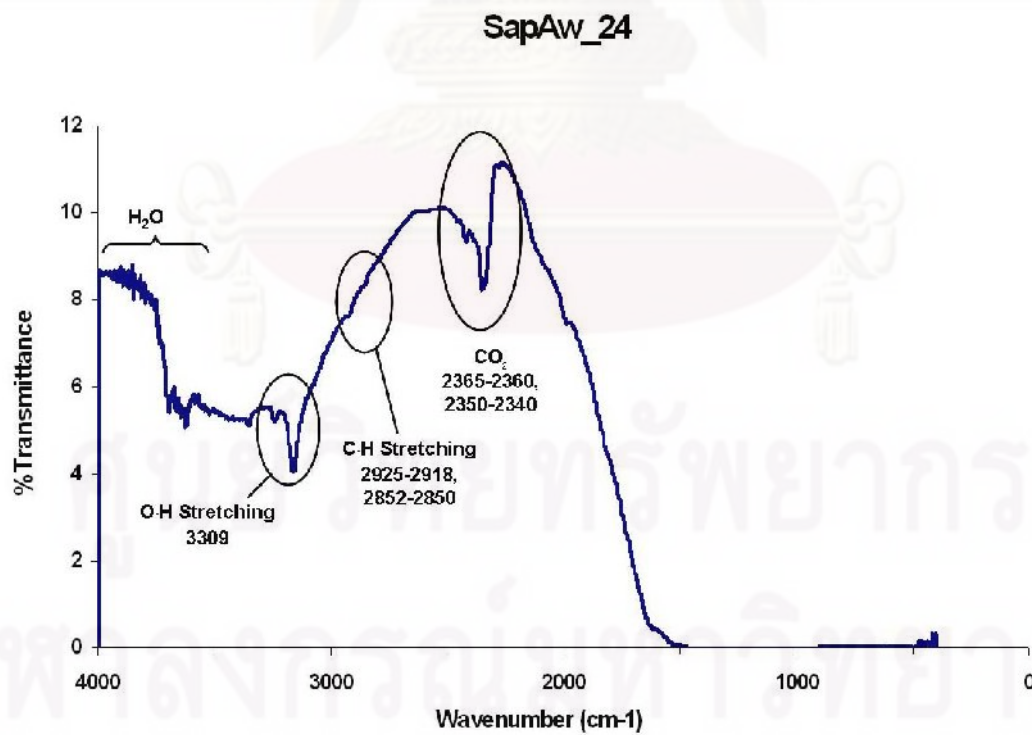


Figure B-1.24 FTIR spectra of the sample SapAw_24

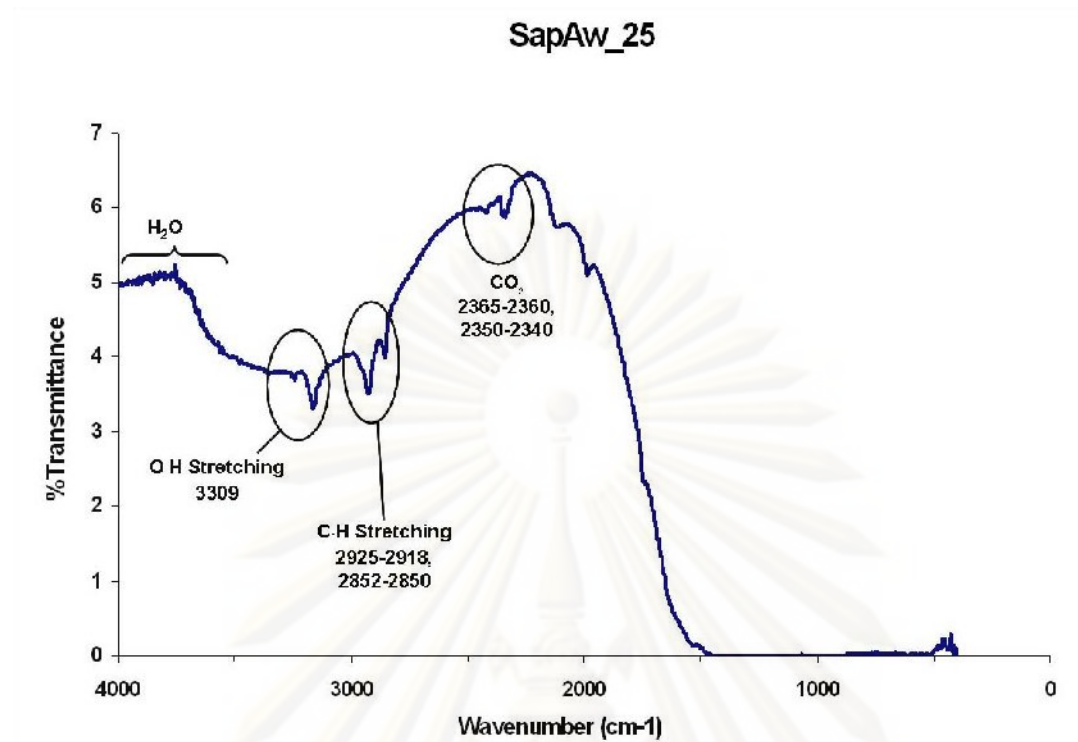


Figure B-1.25 FTIR spectra of the sample SapAw_25

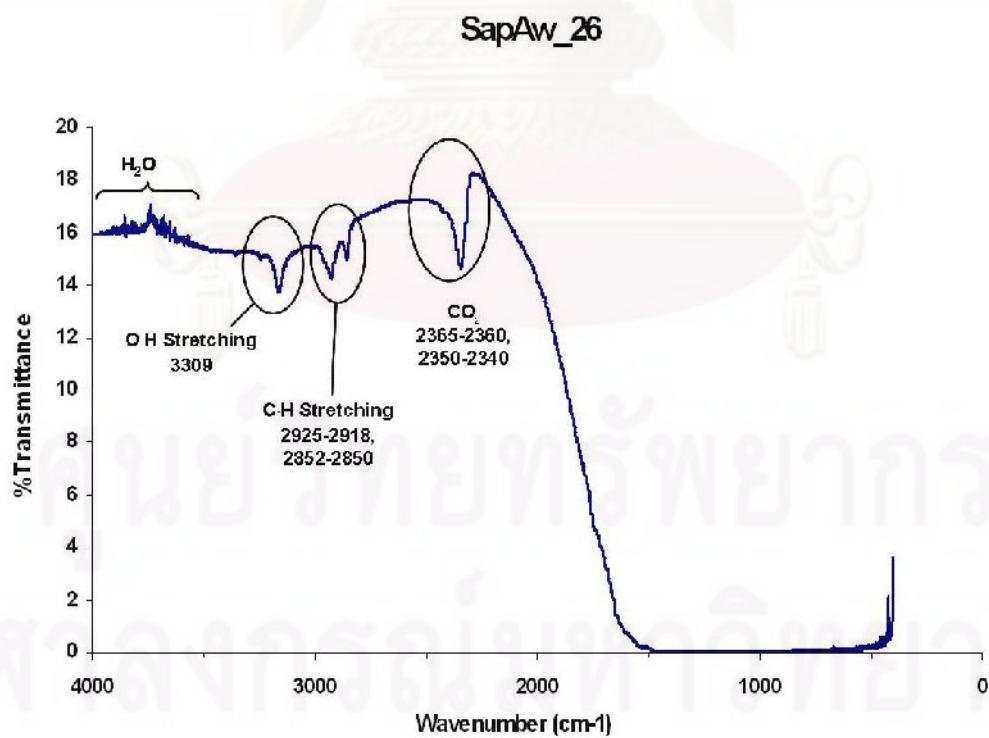


Figure B-1.26 FTIR spectra of the sample SapAw_26

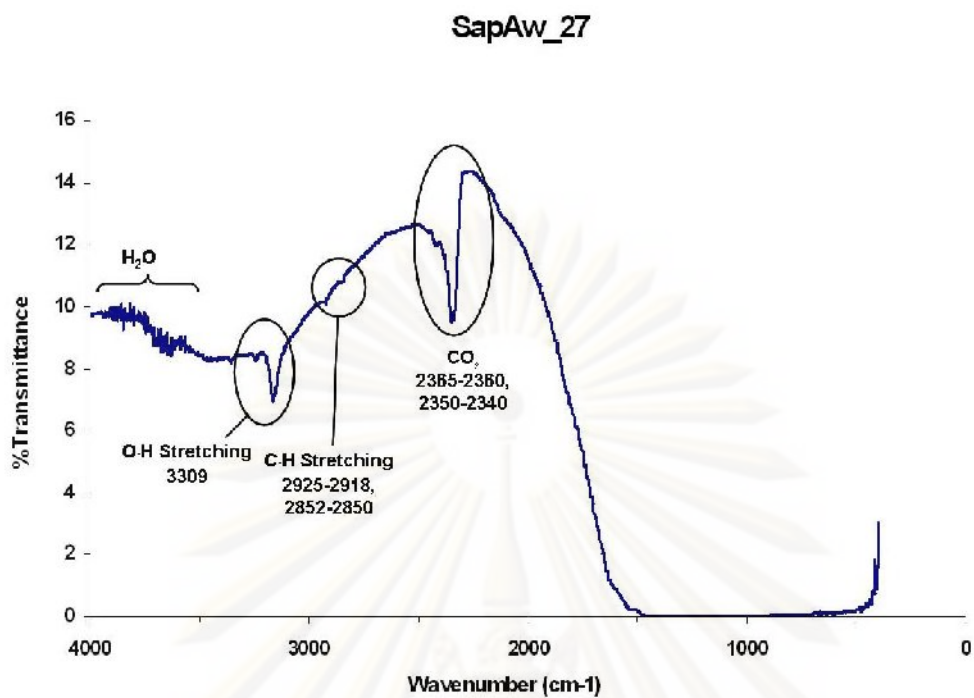


Figure B-1.27 FTIR spectra of the sample SapAw_27

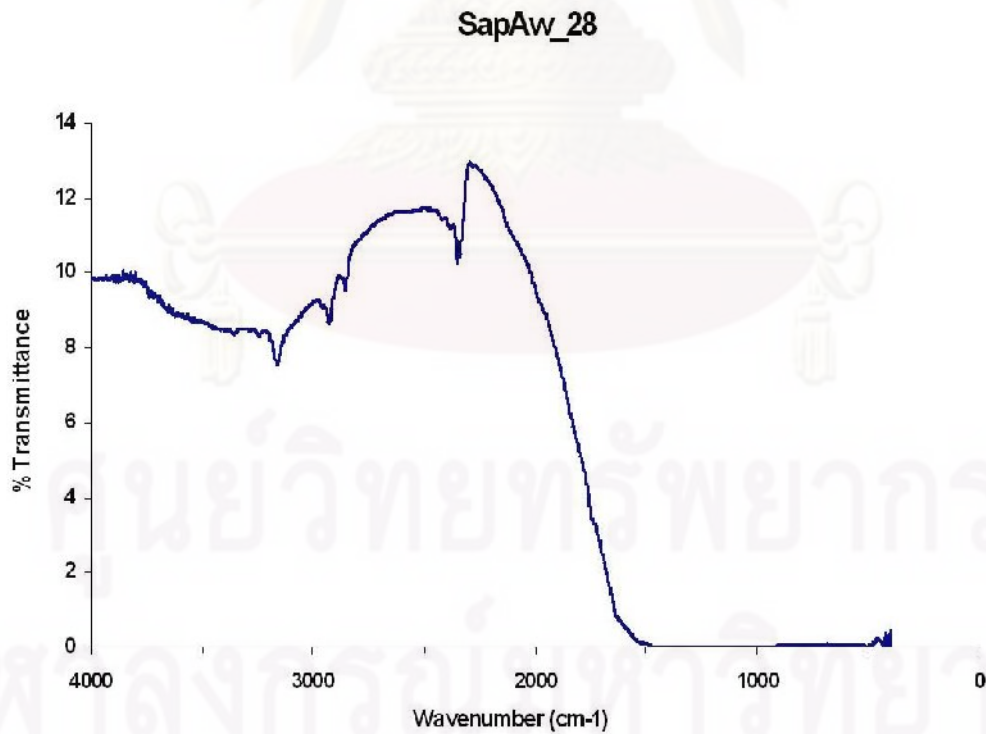


Figure B-1.28 FTIR spectra of the sample SapAw_28

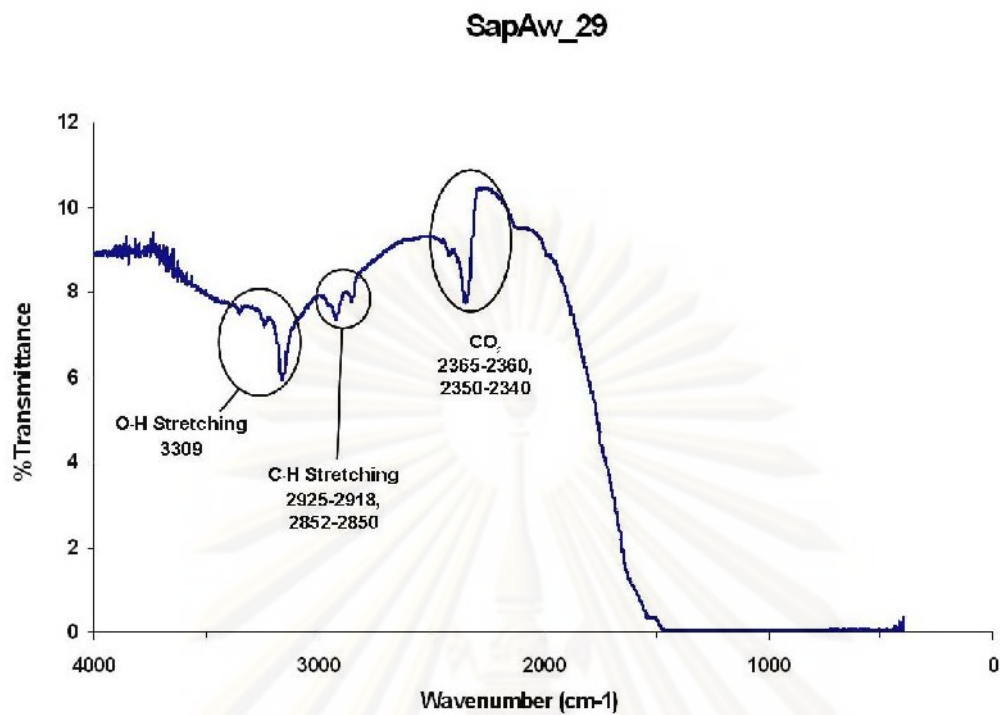


Figure B-1.29 FTIR spectra of the sample SapAw_29

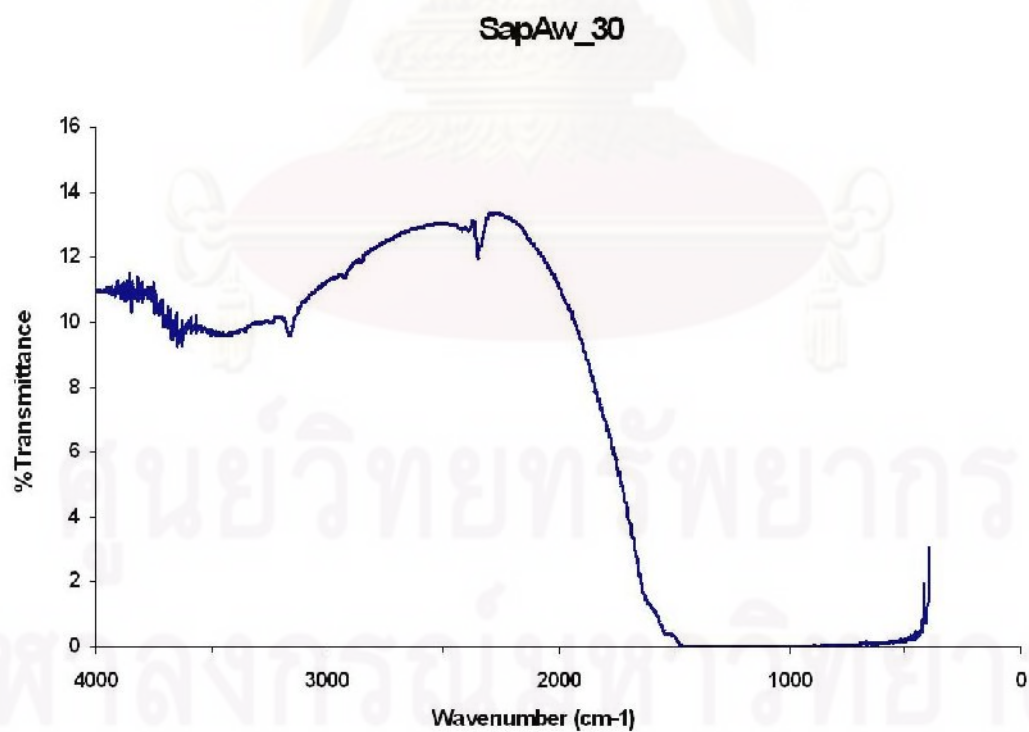


Figure B-1.30 FTIR spectra of the sample SapAw_30

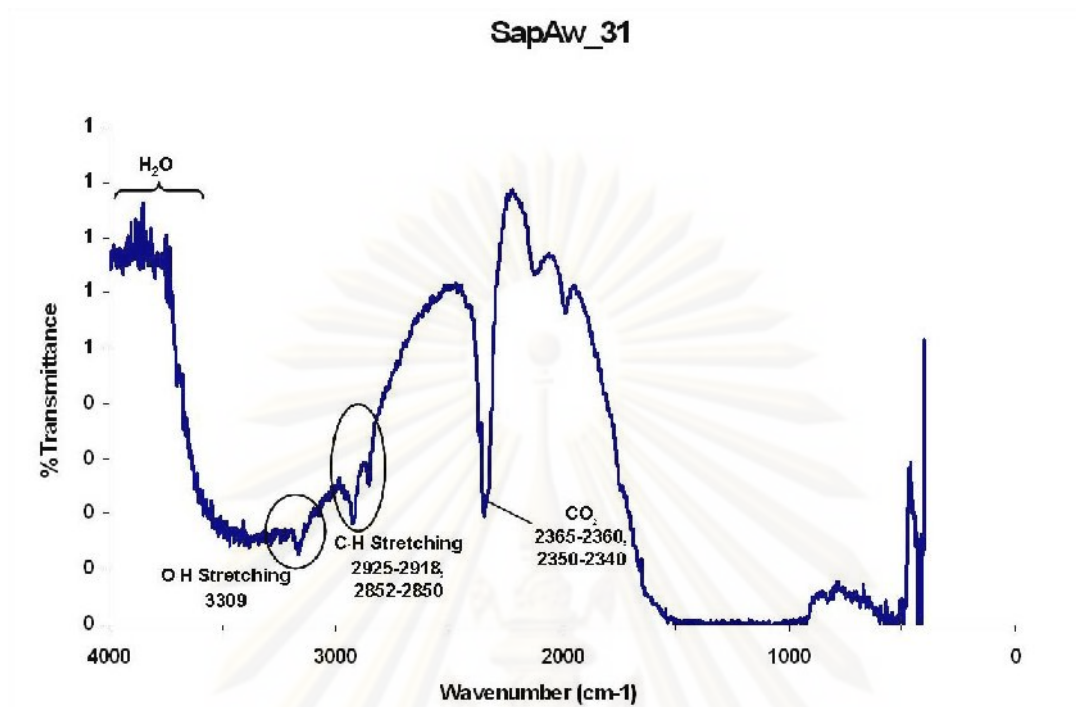


Figure B-1.31 FTIR spectra of the sample SapAw_31

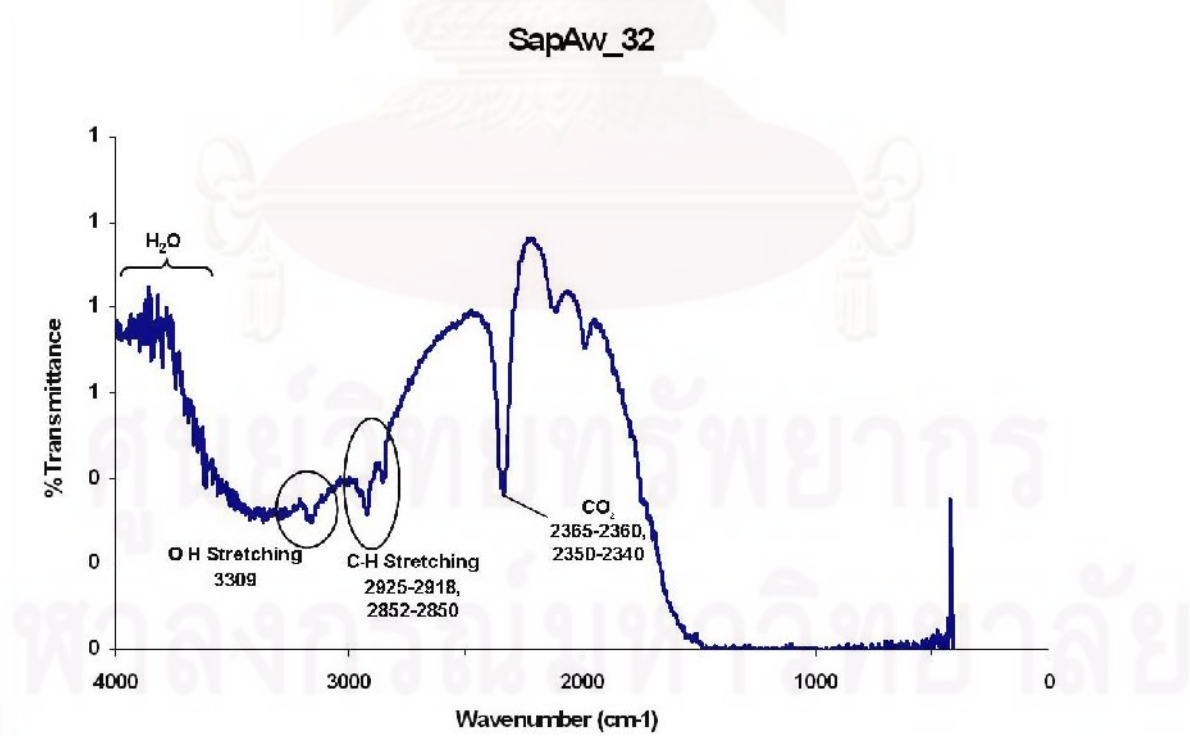


Figure B-1.32 FTIR spectra of the sample SapAw_32

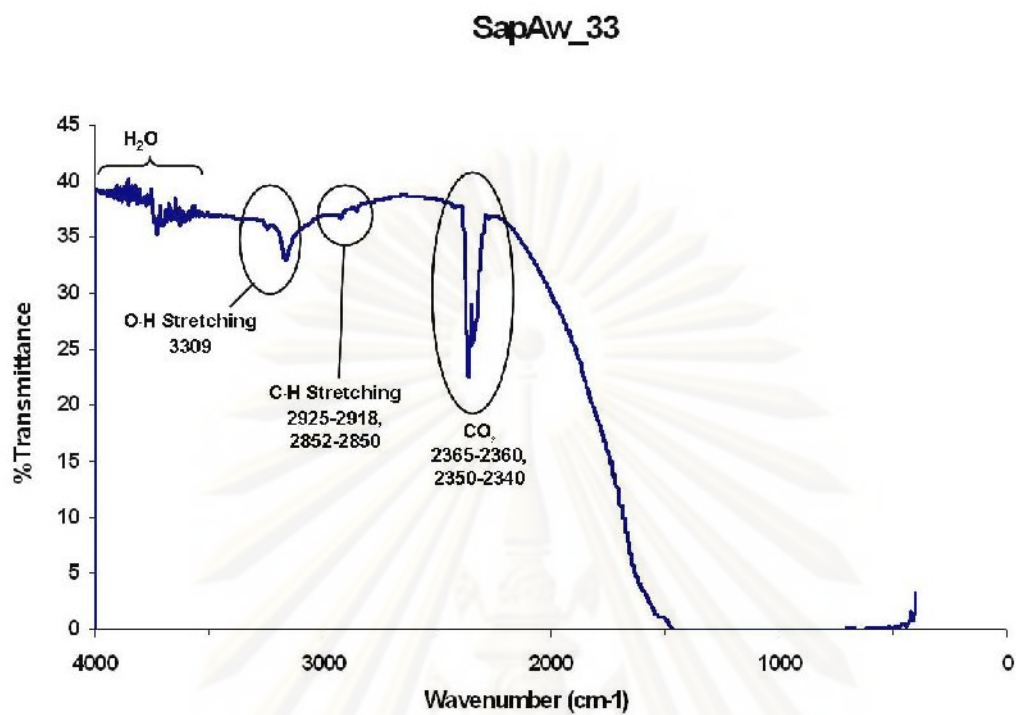


Figure B-1.32 FTIR spectra of the sample SapAw_33

ศูนย์วิทยทรัพยากร
จุฬาลงกรณ์มหาวิทยาลัย

Appendix B-2 FTIR spectra of light blue sapphire variety from Awissawella, Sri Lanka

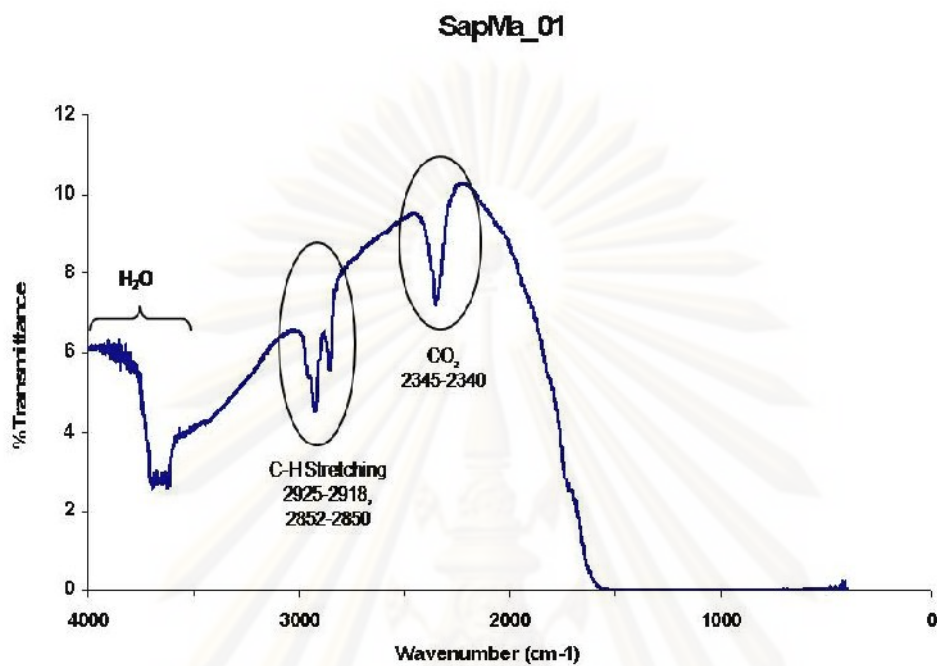


Figure B-2.1 FTIR spectra of the sample SapMa_01

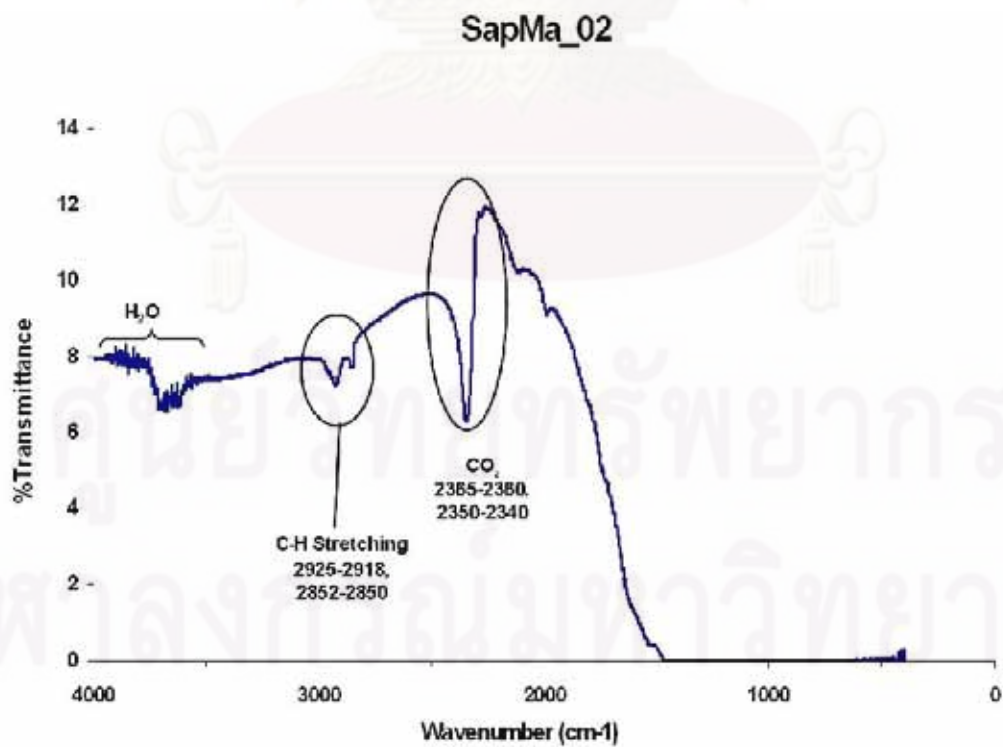


Figure B-2.2 FTIR spectra of the sample SapMa_02

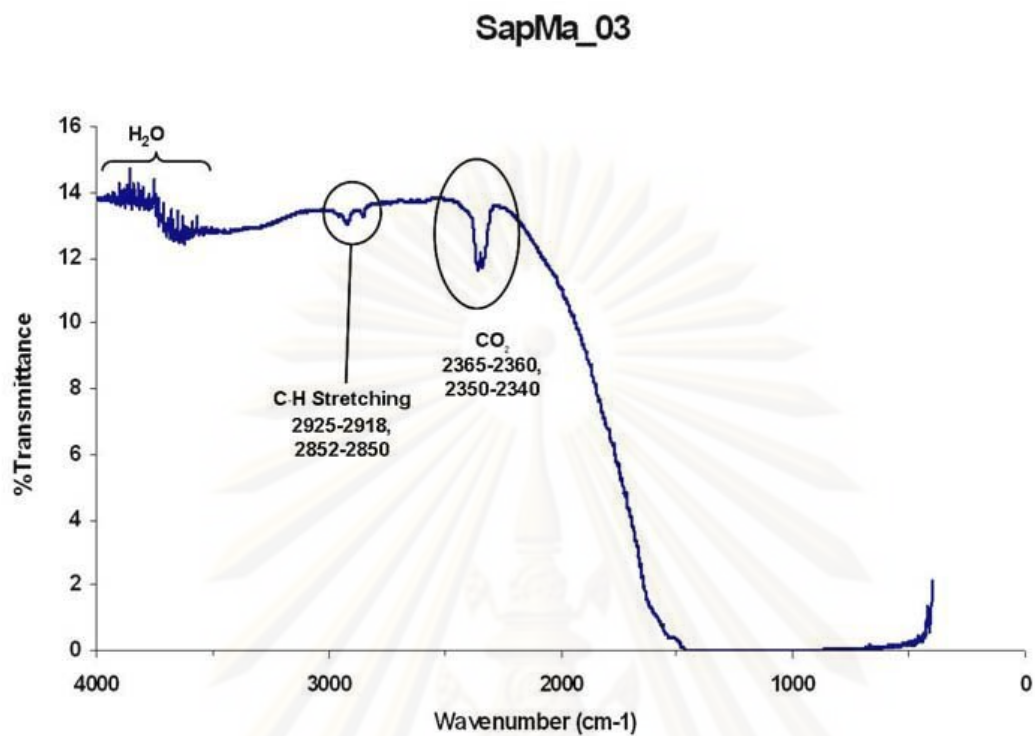


Figure B-2.3 FTIR spectra of the sample SapMa_03

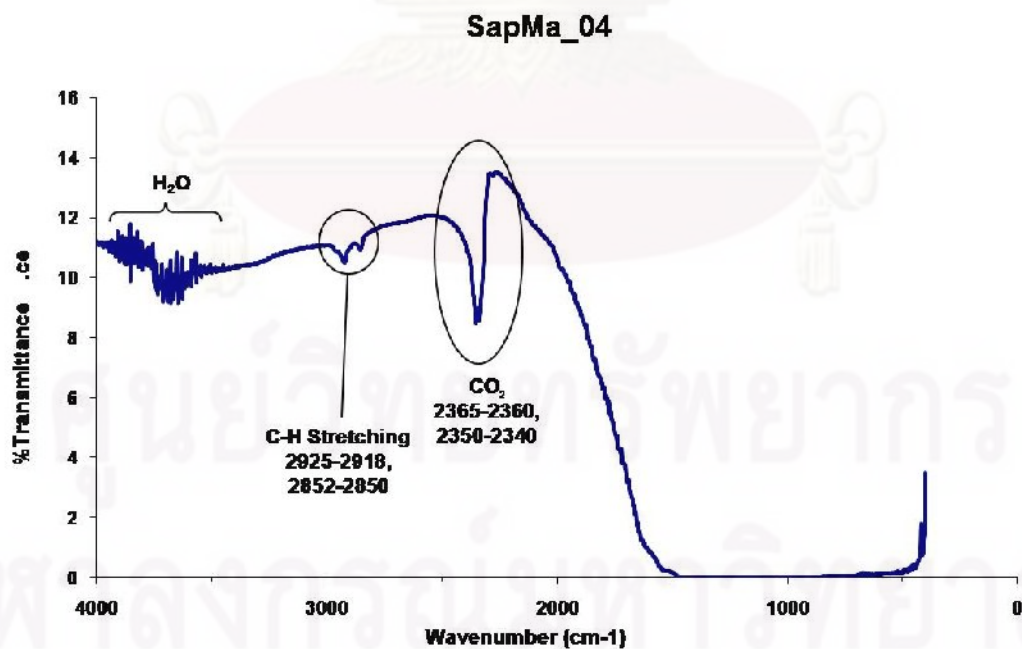


Figure B-2.4 FTIR spectra of the sample SapMa_04

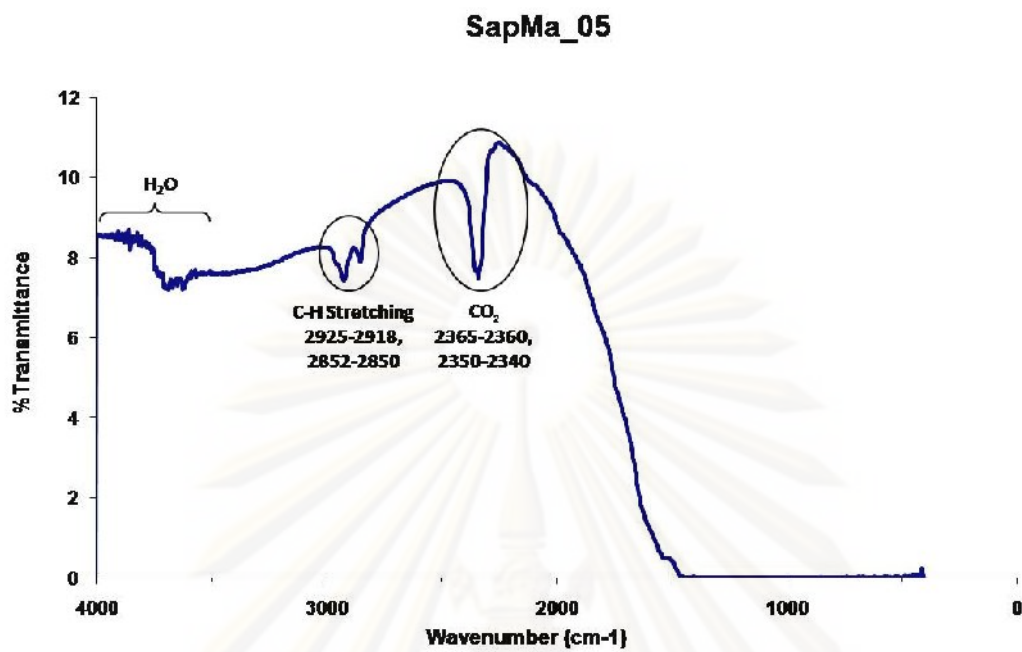


Figure B-2.5 FTIR spectra of the sample SapMa_05

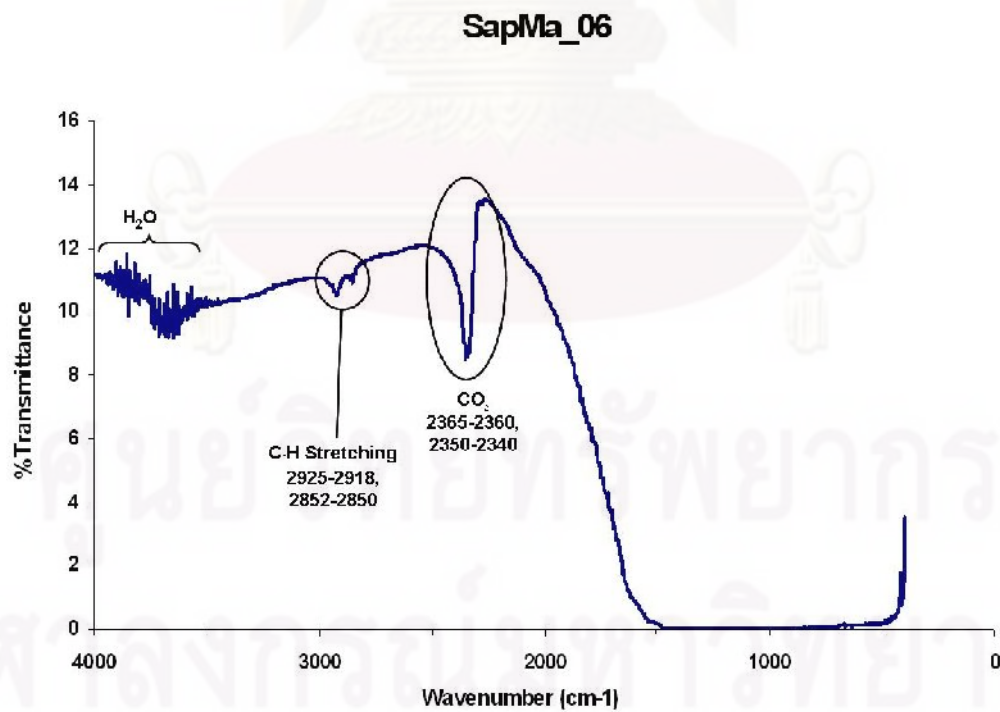


Figure B-2.6 FTIR spectra of the sample SapMa_06

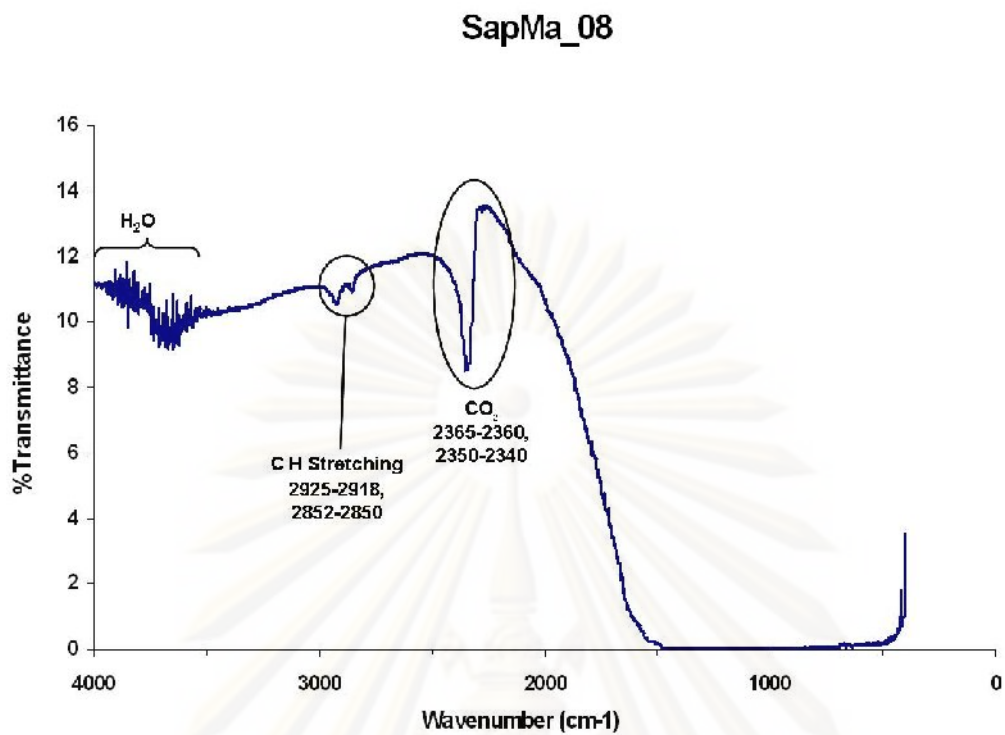


Figure B-2.7 FTIR spectra of the sample SapMa_08

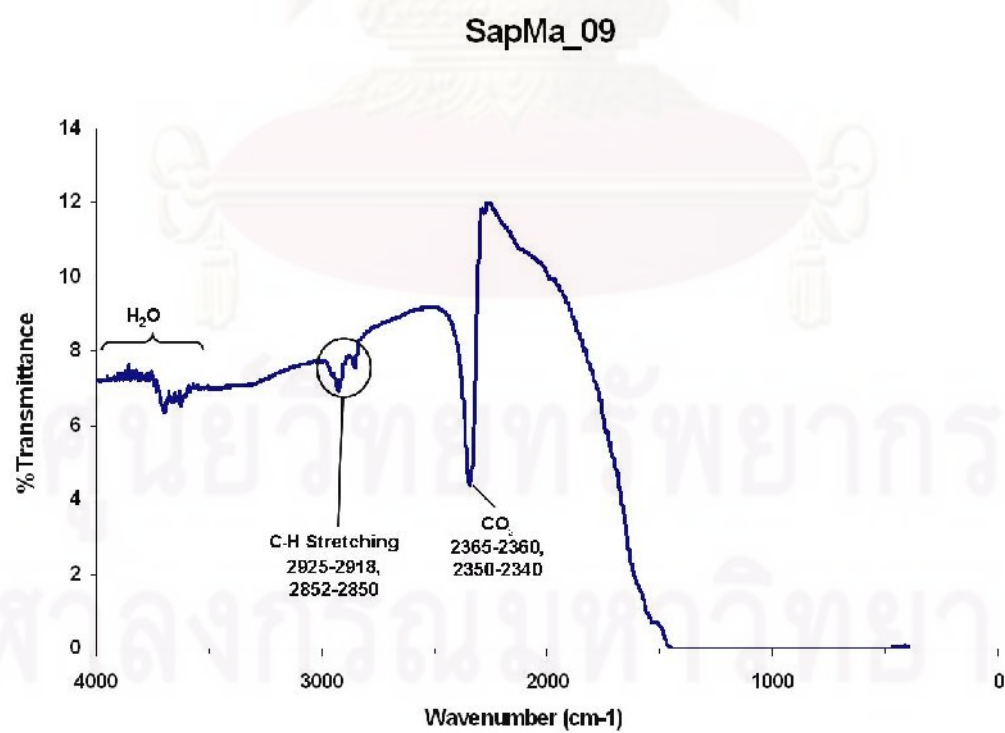


Figure B-2.8 FTIR spectra of the sample SapMa_09

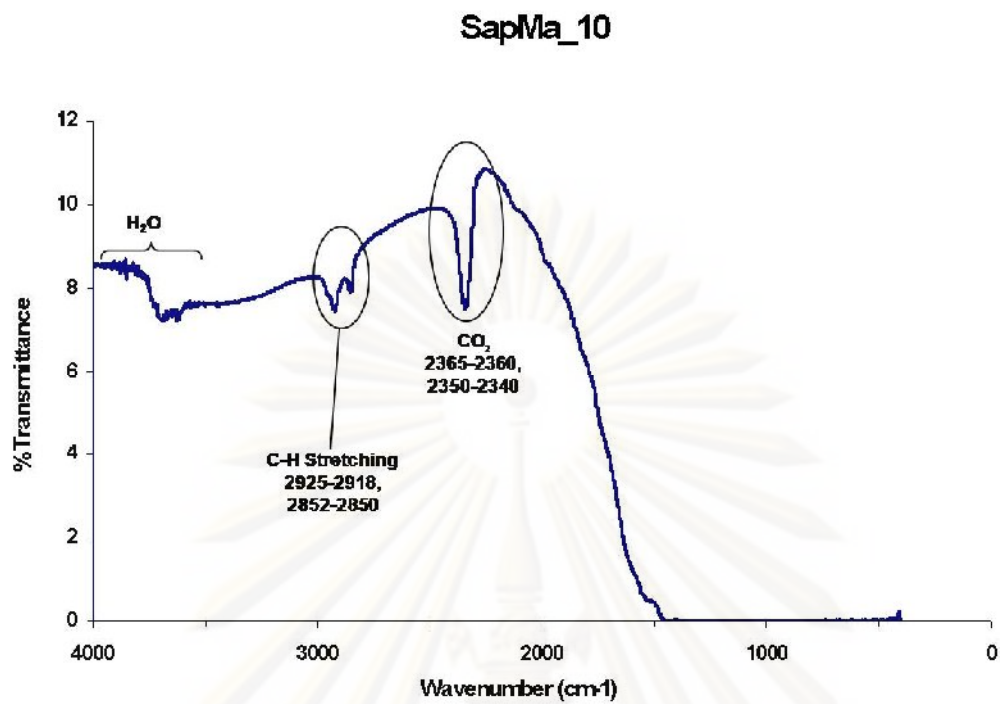


Figure B-2.9 FTIR spectra of the sample SapMa_10

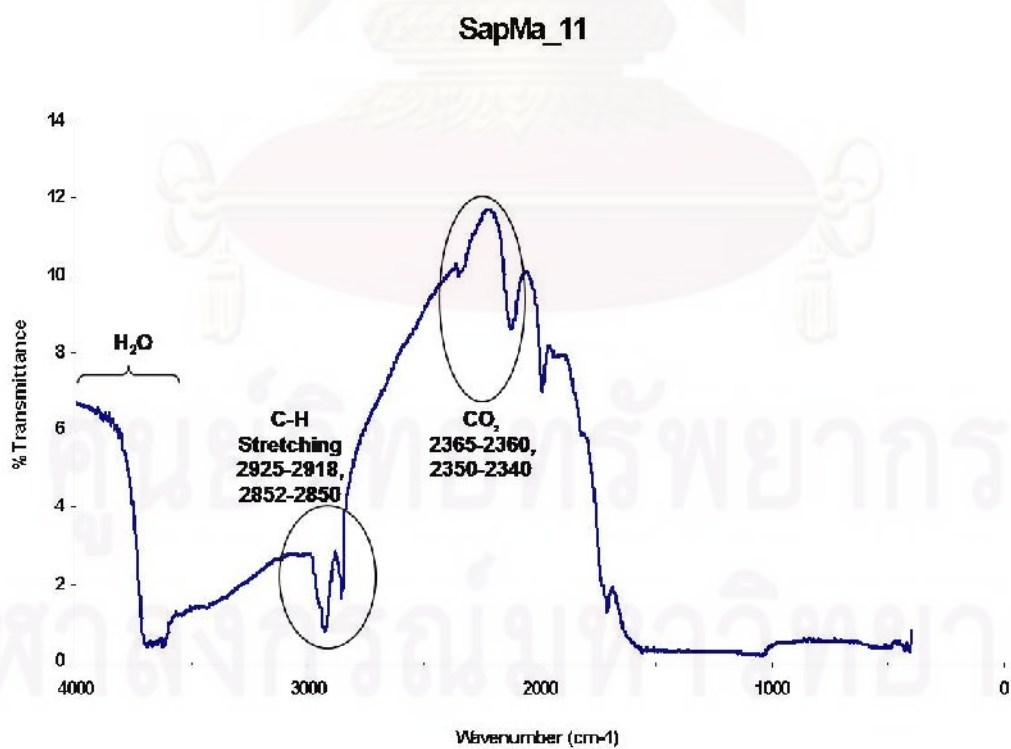


Figure B-2.10 FTIR spectra of the sample SapMa_11

SapMa_12

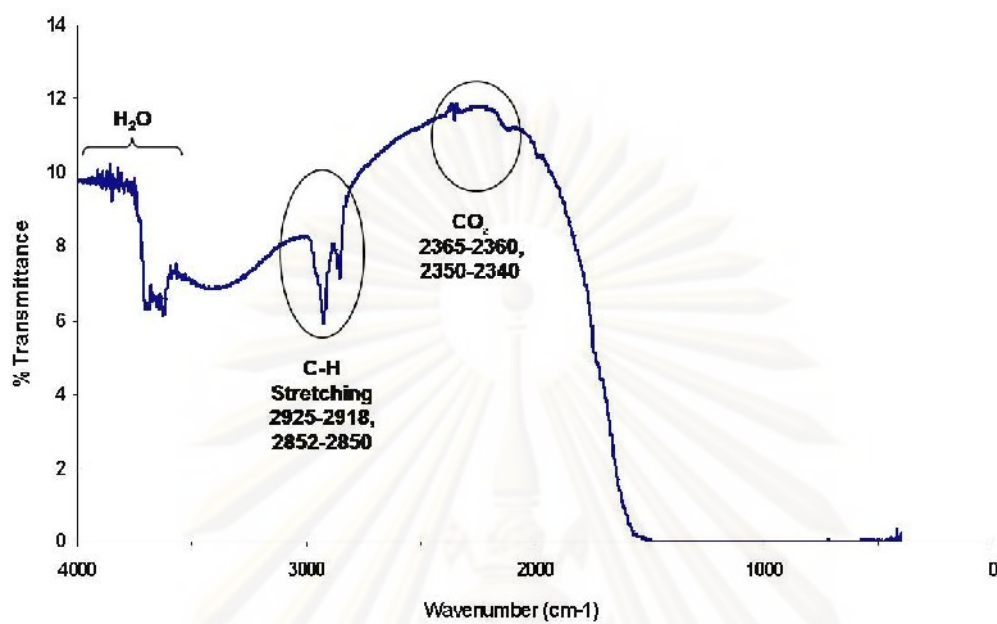


Figure B-2.11 FTIR spectra of the sample SapMa_12

SapMa_13

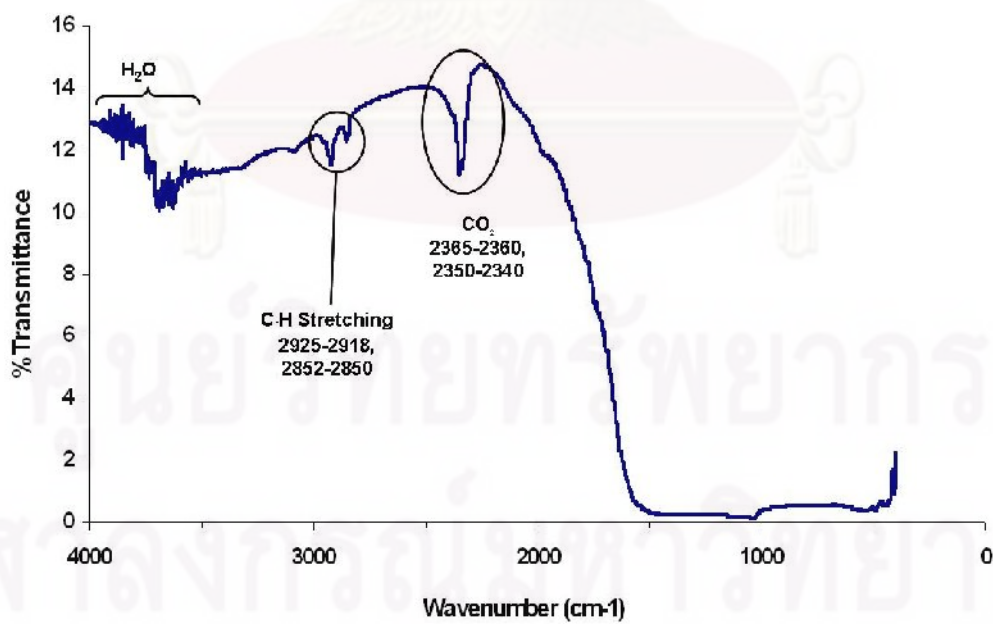


Figure B-2.12 FTIR spectra of the sample SapMa_13



APPENDIX C

ศูนย์วิทยทรัพยากร
จุฬาลงกรณ์มหาวิทยาลัย

Appendix C UV-VIS-NIR absorption spectra of unheat Awissawella corundums

Appendix C-1 UV-VIS-NIR absorption spectra of yellow sapphire variety from Awissawella

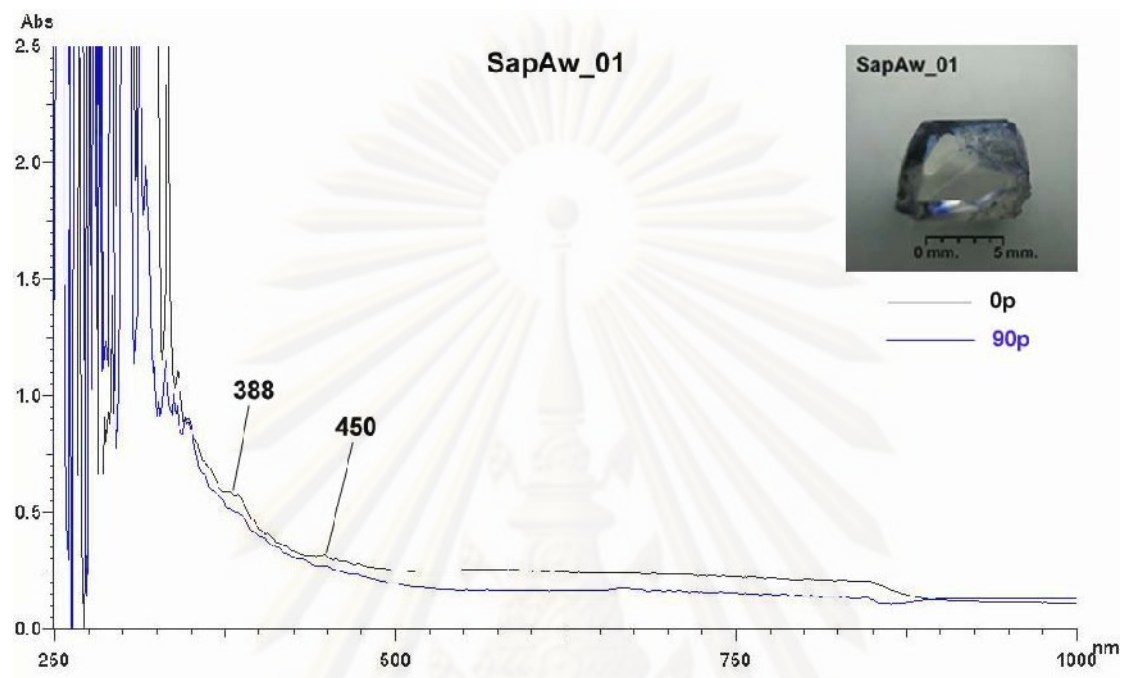


Figure C-1.1 UV-VIS-NIR absorption spectra of the sample SapAw_01

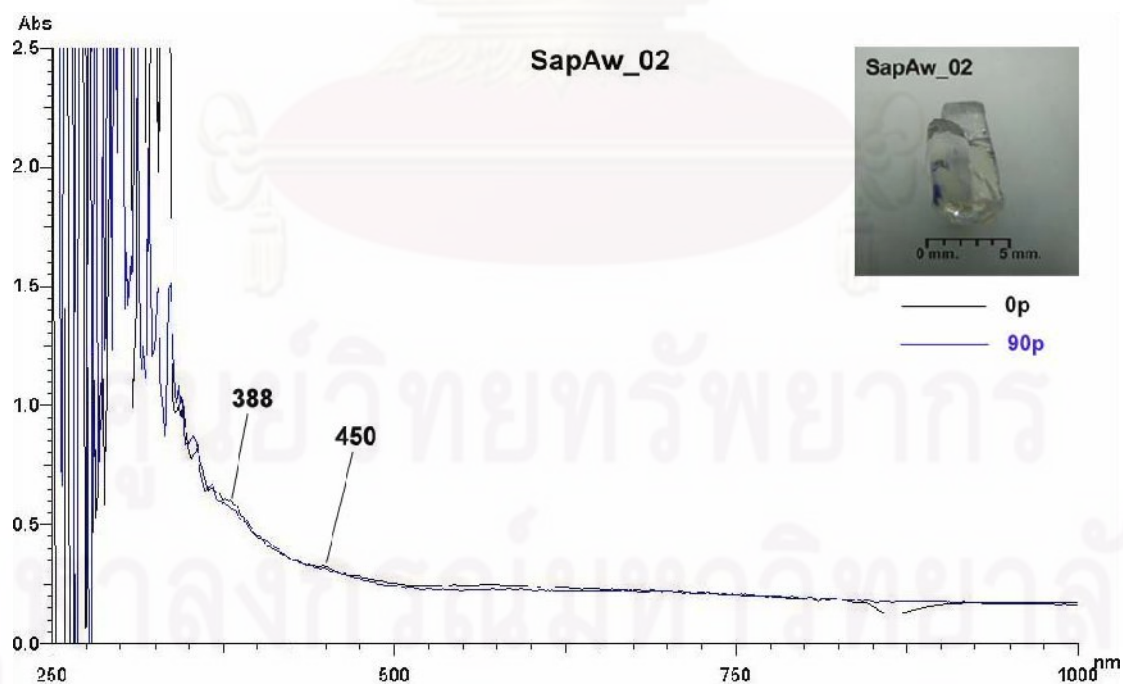


Figure C-1.2 UV-VIS-NIR absorption spectra of the sample SapAw_02

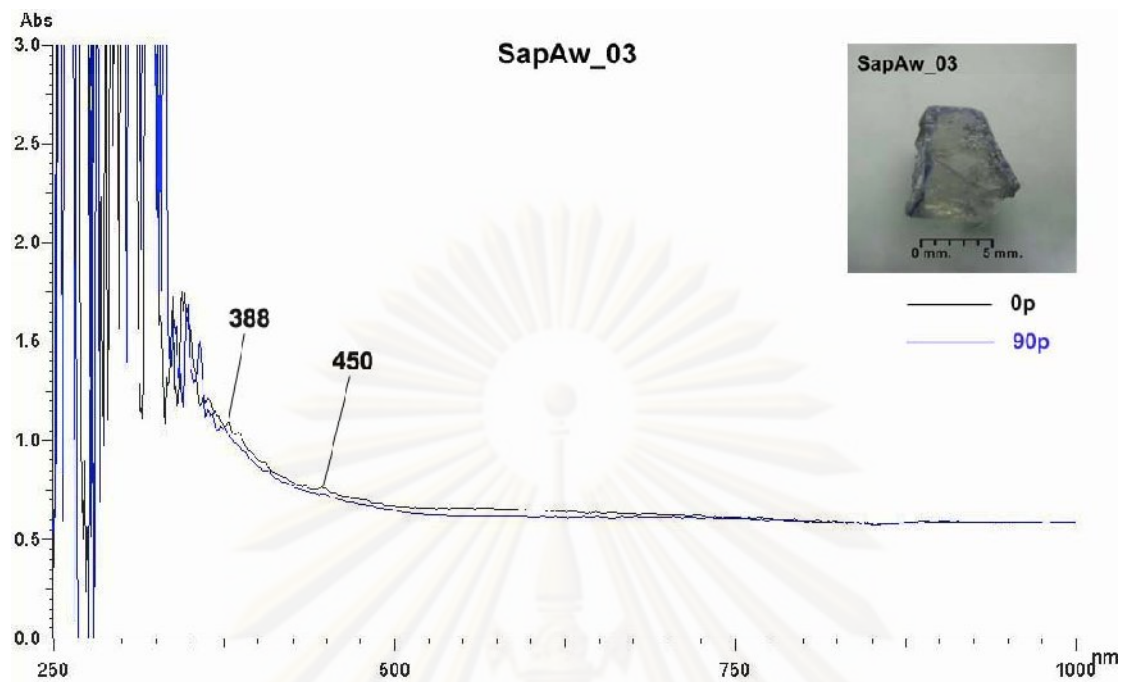


Figure C-1.3 UV-VIS-NIR absorption spectra of the sample SapAw_03

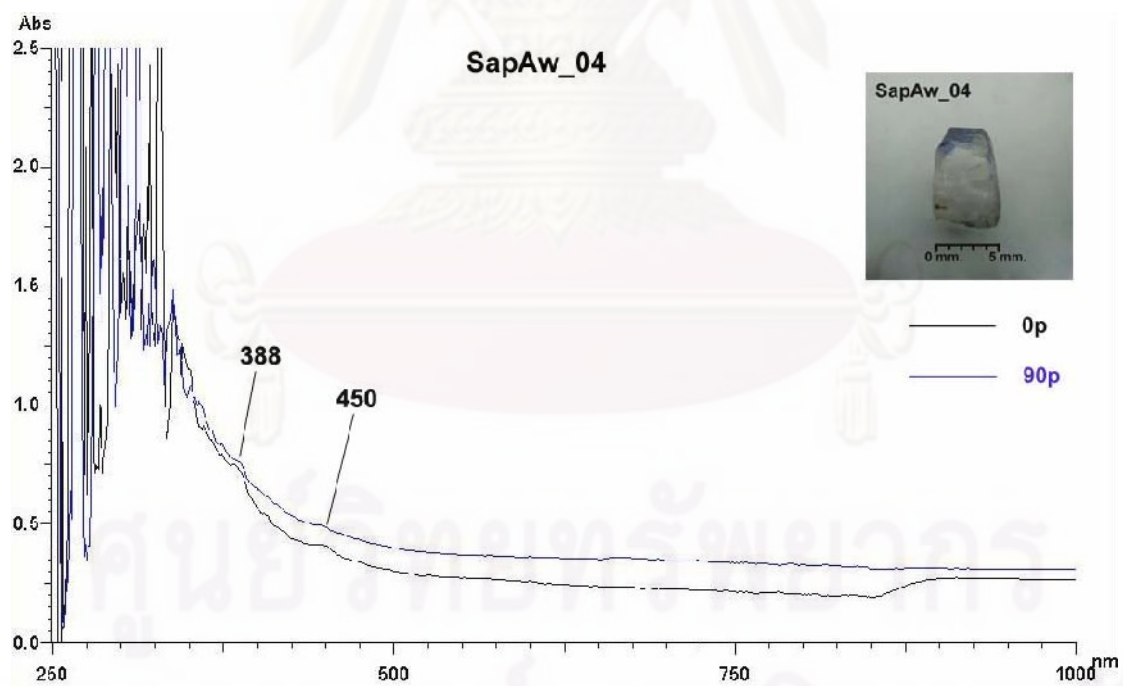


Figure C-1.4 UV-VIS-NIR absorption spectra of the sample SapAw_04

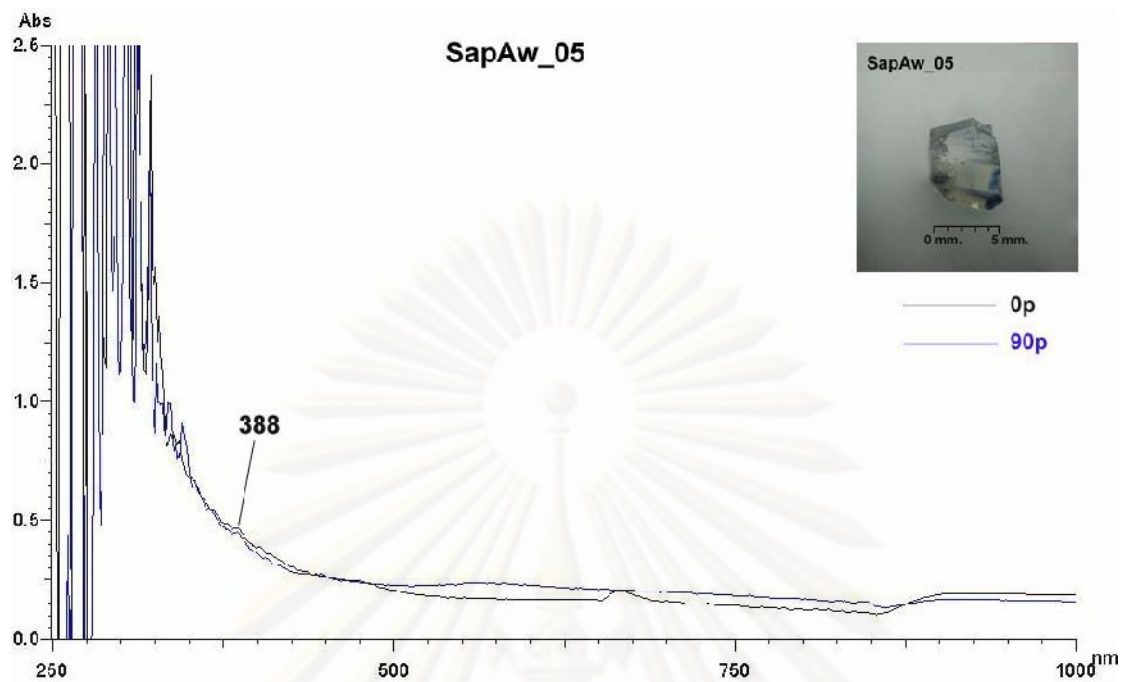


Figure C-1.5 UV-VIS-NIR absorption spectra of the sample SapAw_05

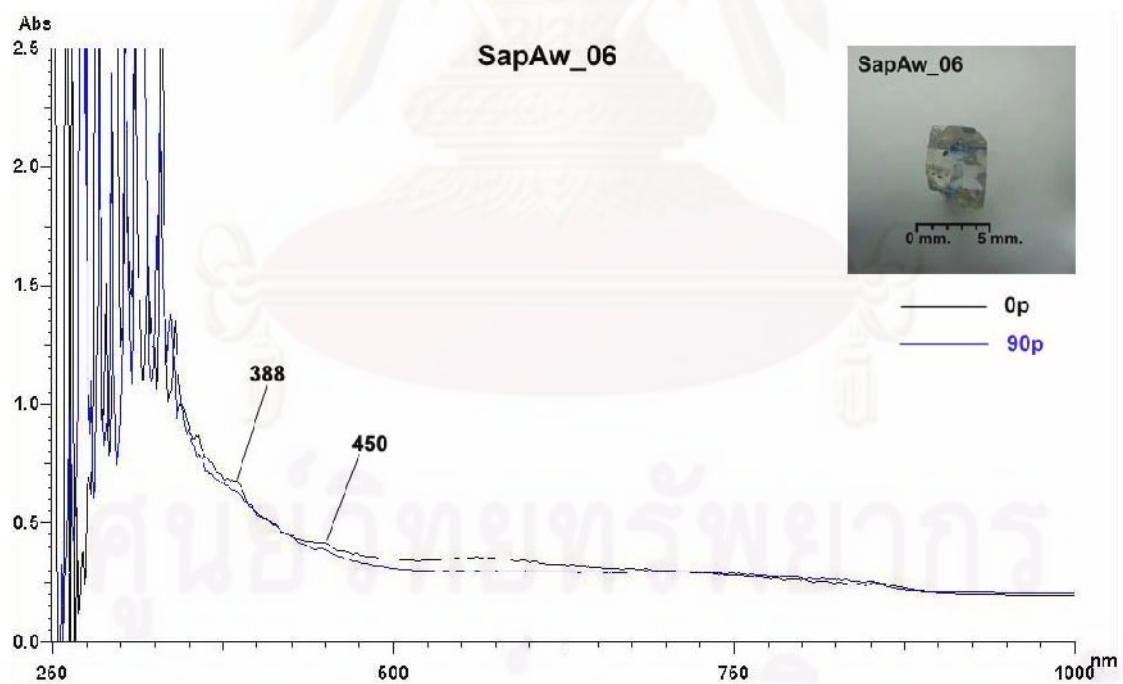


Figure C-1.6 UV-VIS-NIR absorption spectra of the sample SapAw_06

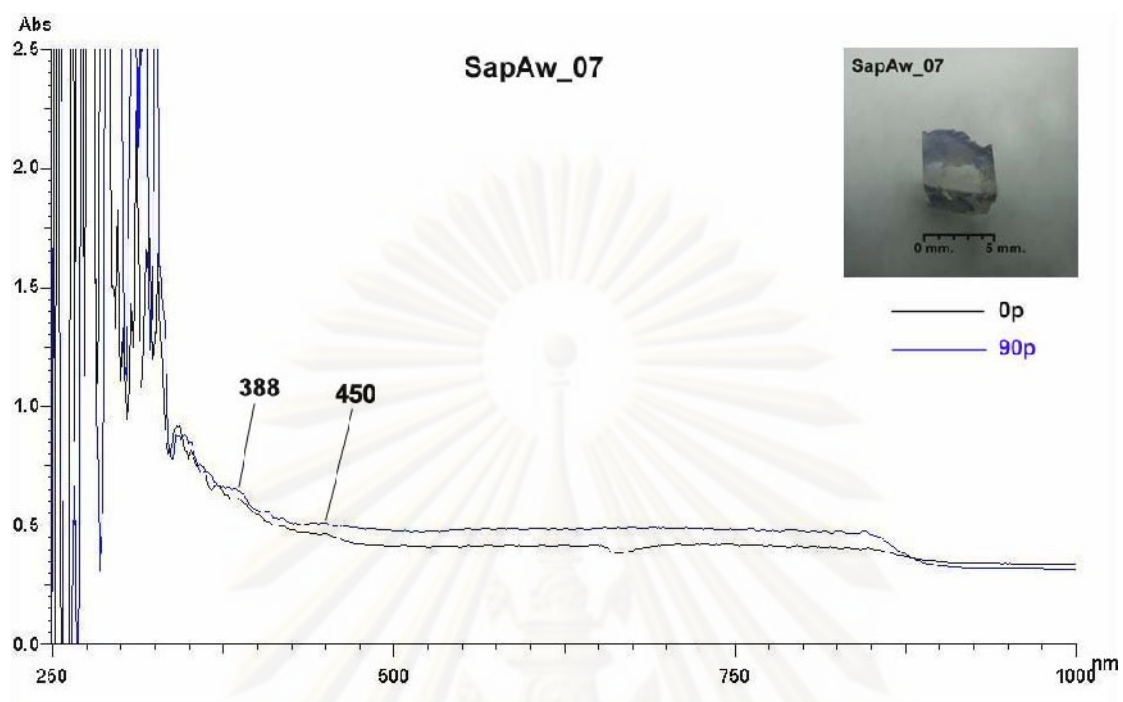


Figure C-1.7 UV-VIS-NIR absorption spectra of the sample SapAw_07

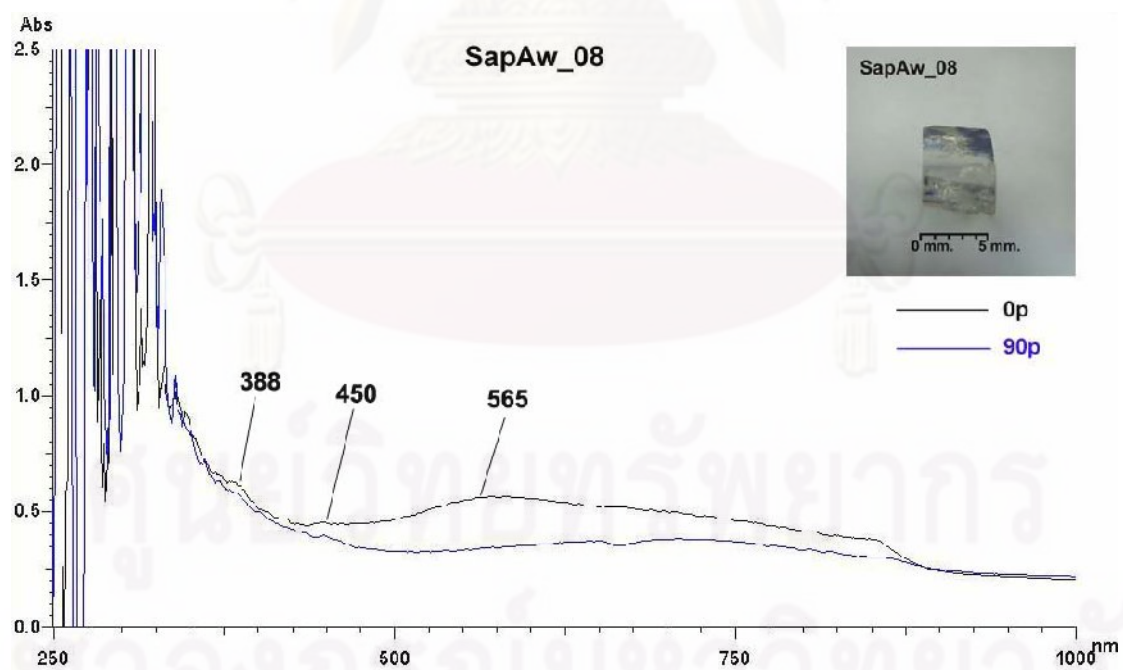


Figure C-1.8 UV-VIS-NIR absorption spectra of the sample SapAw_08

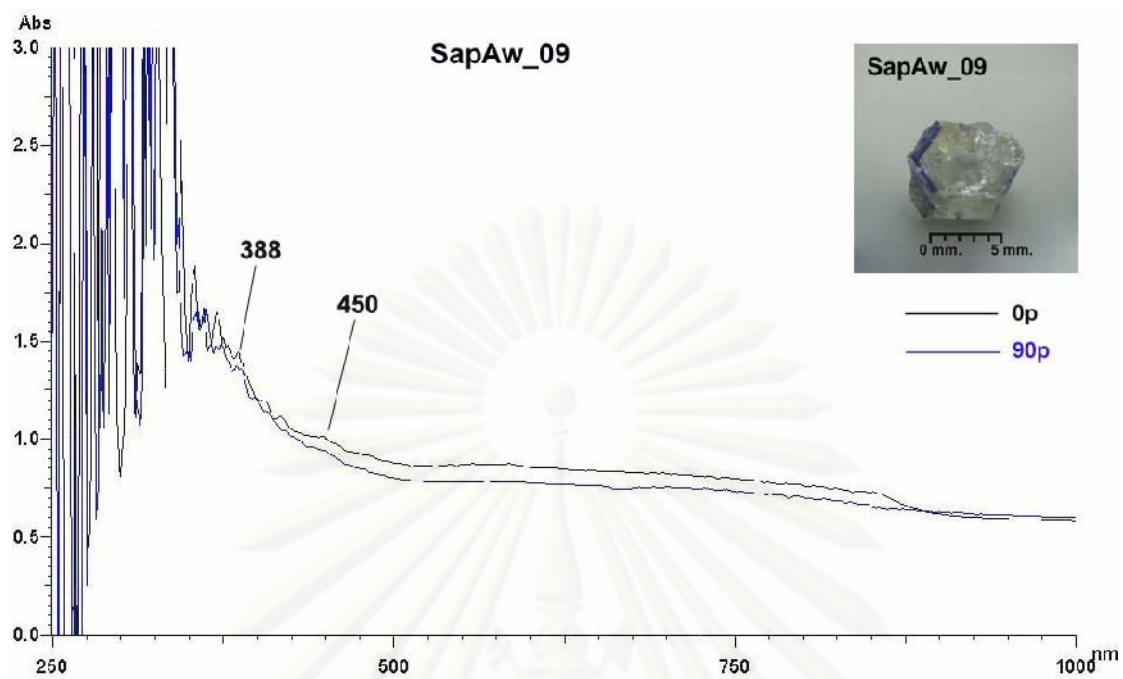


Figure C-1.9 UV-VIS-NIR absorption spectra of the sample SapAw_09

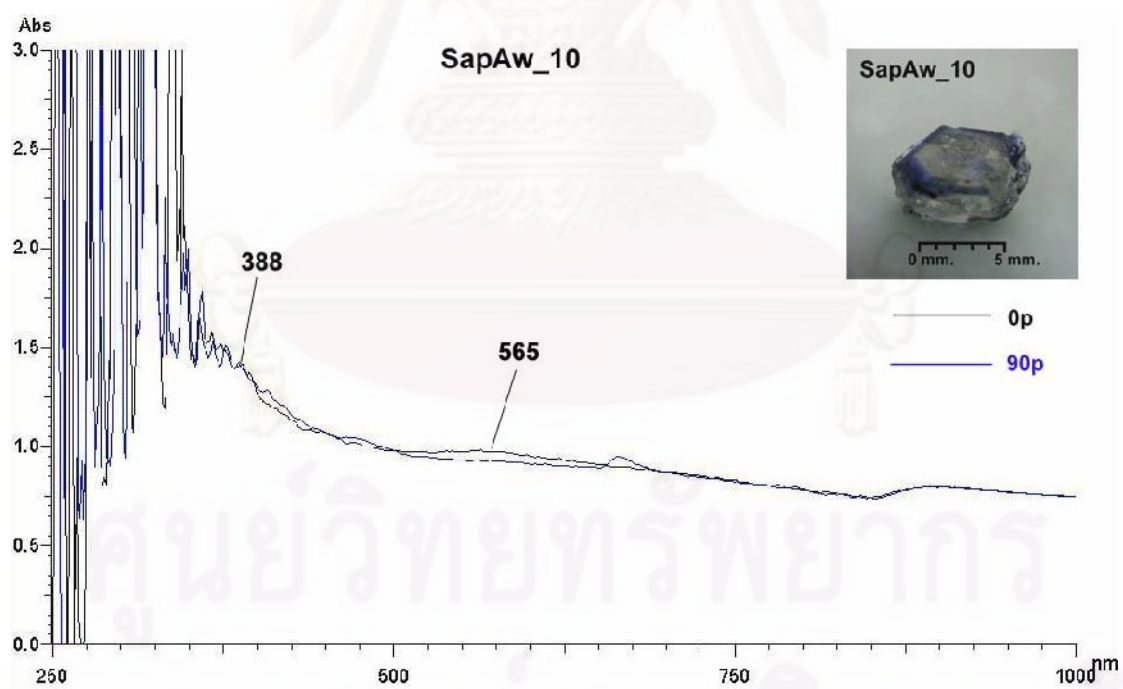


Figure C-1.10 UV-VIS-NIR absorption spectra of the sample SapAw_10

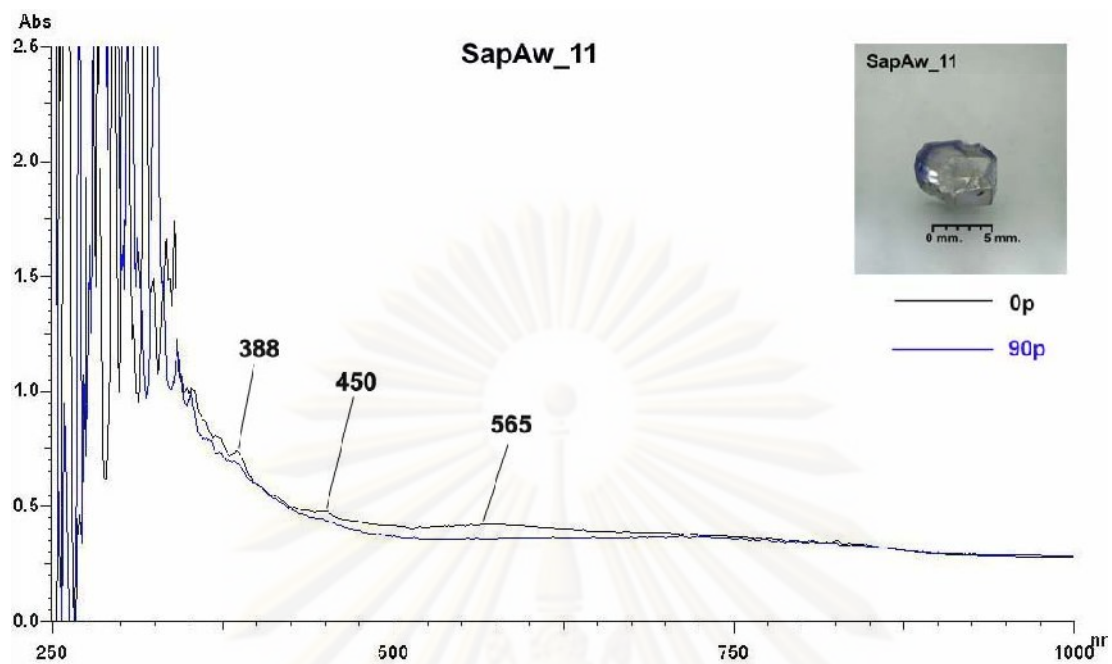


Figure C-1.11 UV-VIS-NIR absorption spectra of the sample SapAw_11

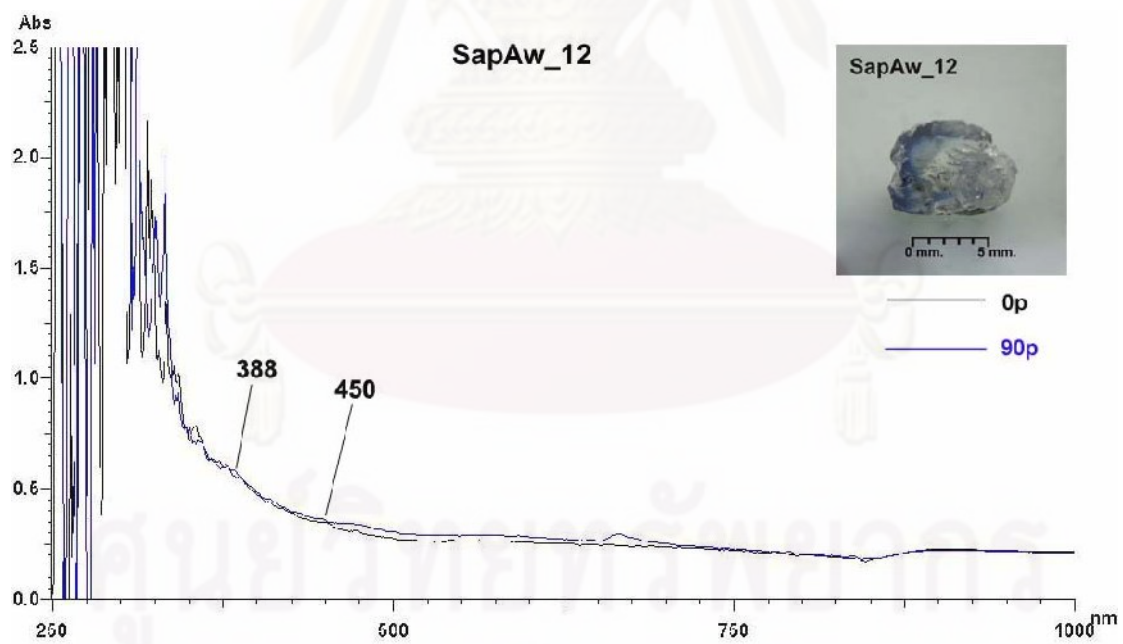


Figure C-1.12 UV-VIS-NIR absorption spectra of the sample SapAw_12

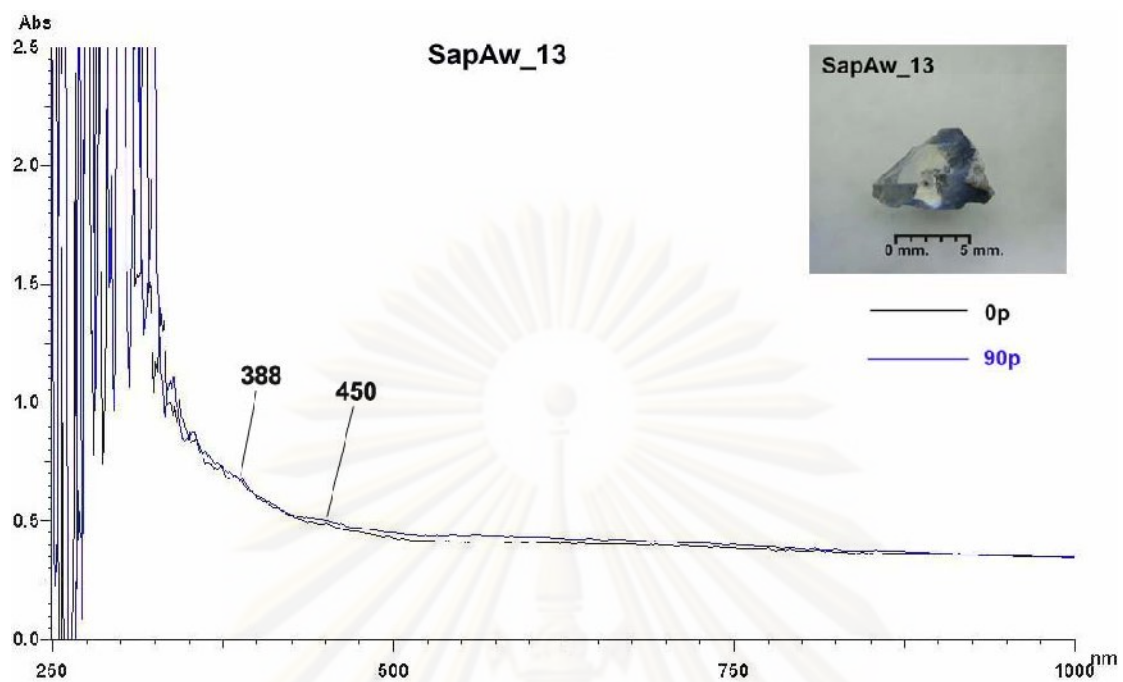


Figure C-1.13 UV-VIS-NIR absorption spectra of the sample SapAw_13

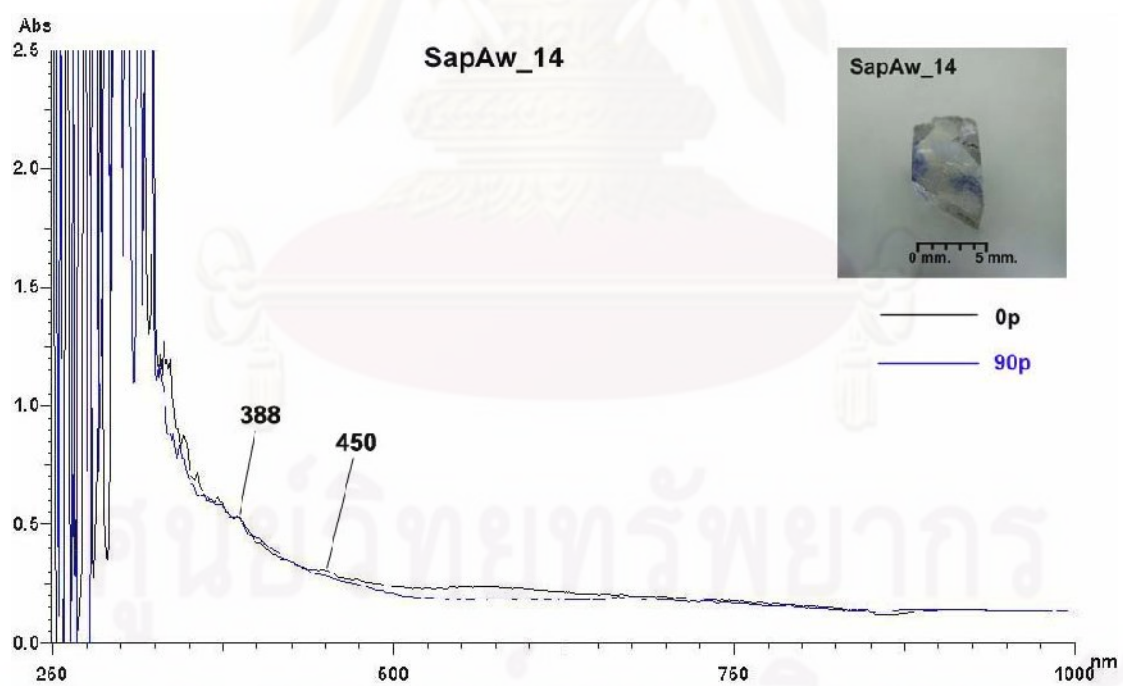


Figure C-1.14 UV-VIS-NIR absorption spectra of the sample SapAw_14

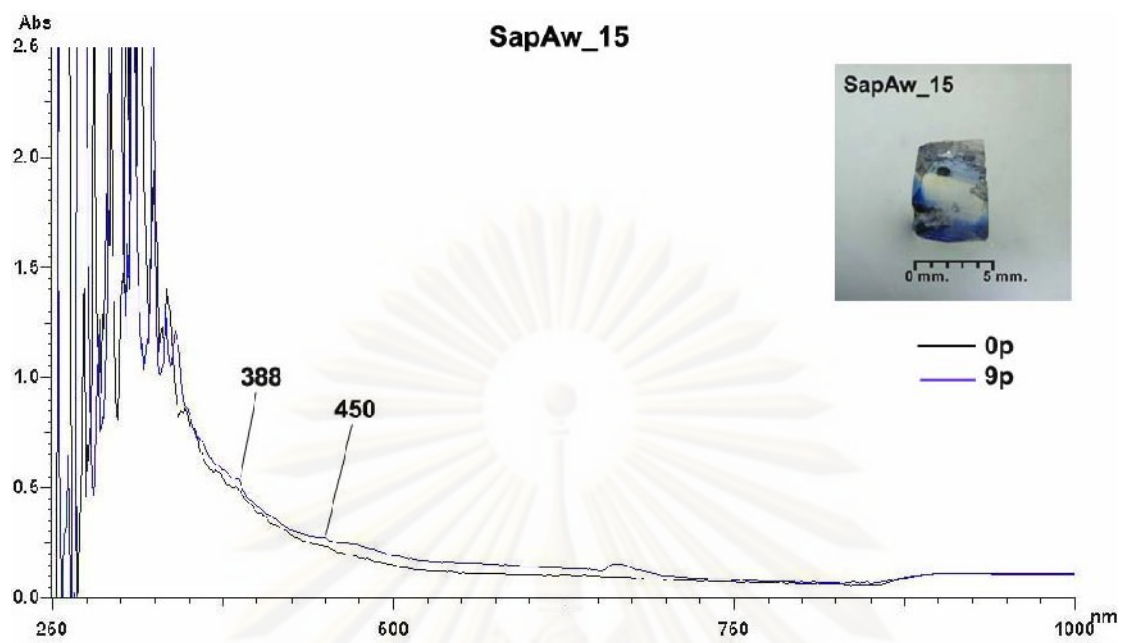


Figure C-1.15 UV-VIS-NIR absorption spectra of the sample SapAw_15

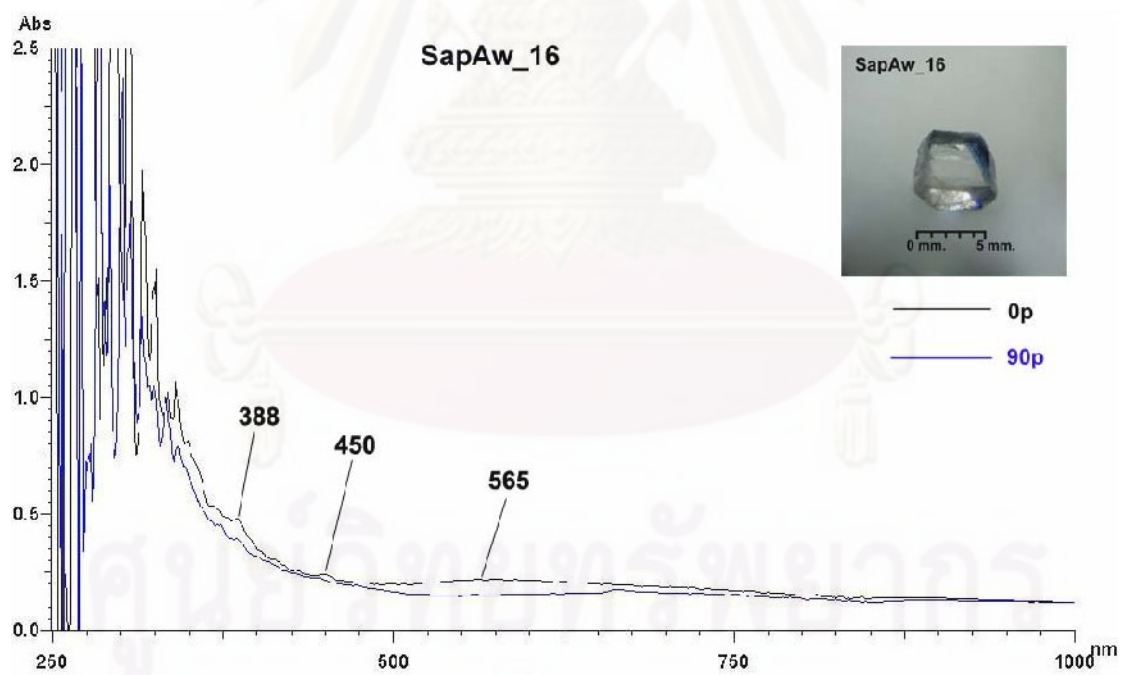


Figure C-1.16 UV-VIS-NIR absorption spectra of the sample SapAw_16

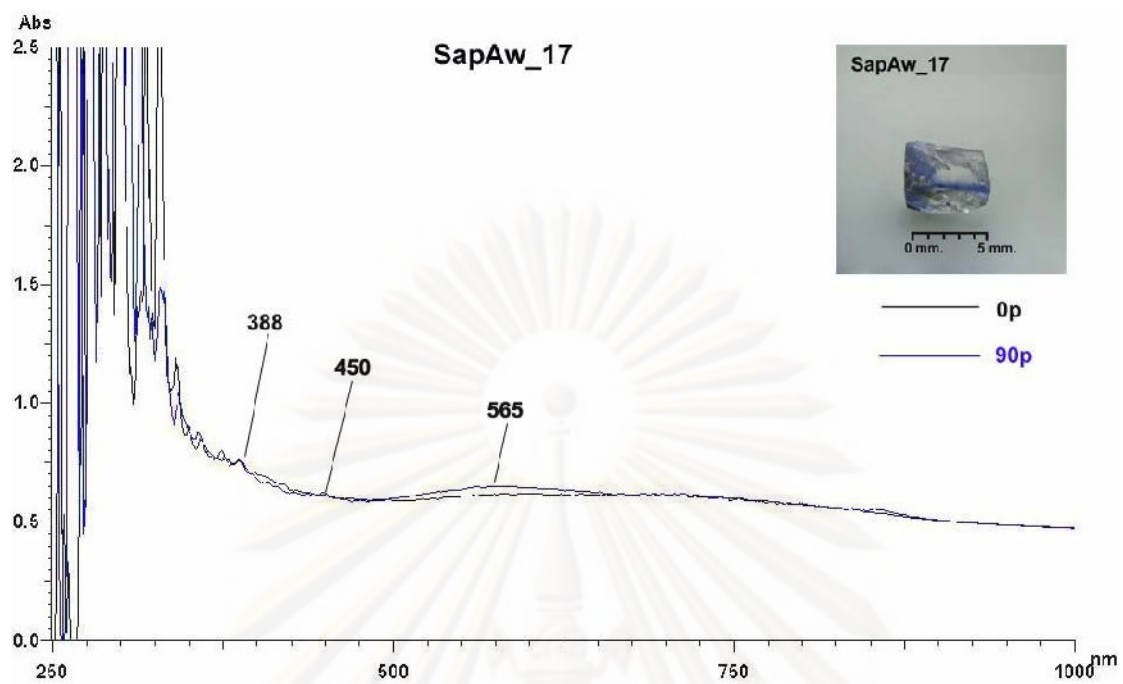


Figure C-1.17 UV-VIS-NIR absorption spectra of the sample SapAw_17

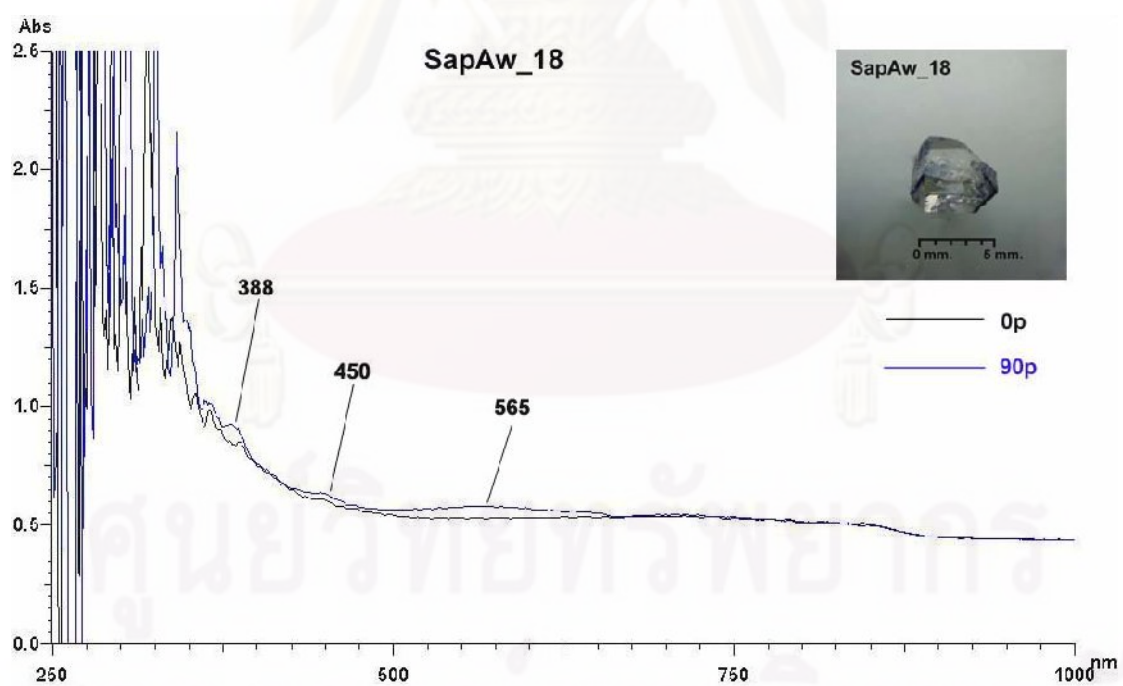


Figure C-1.18 UV-VIS-NIR absorption spectra of the sample SapAw_18

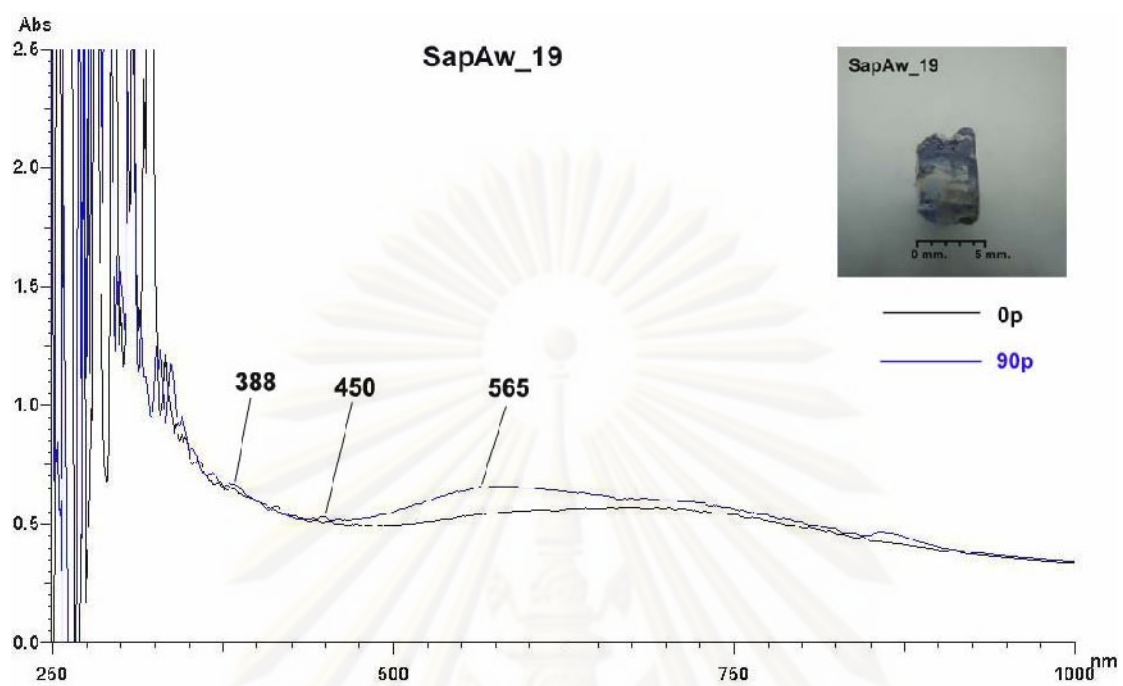


Figure C-1.19 UV-VIS-NIR absorption spectra of the sample SapAw_19

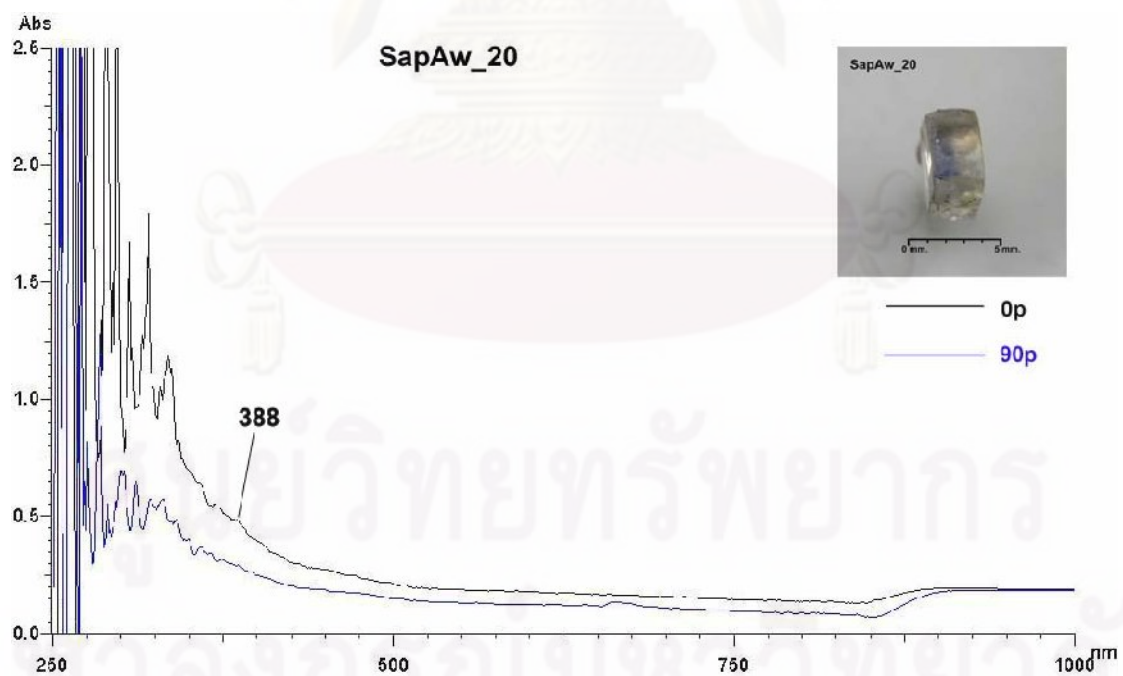


Figure C-1.20 UV-VIS-NIR absorption spectra of the sample SapAw_20

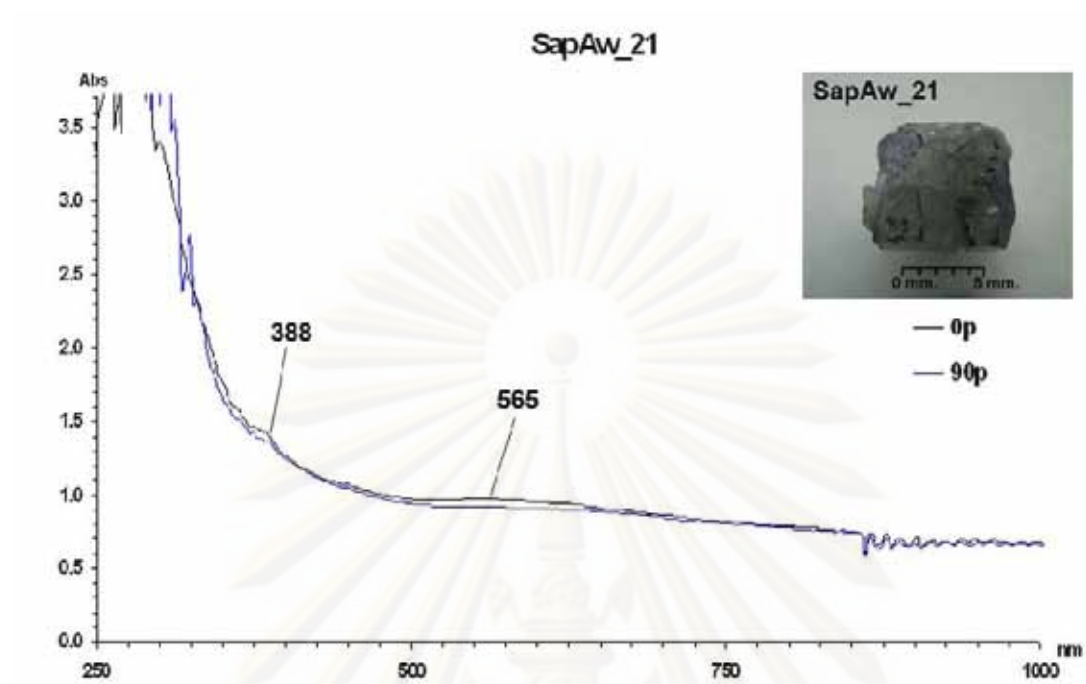


Figure C-1.21 UV-VIS-NIR absorption spectra of the sample SapAw_21

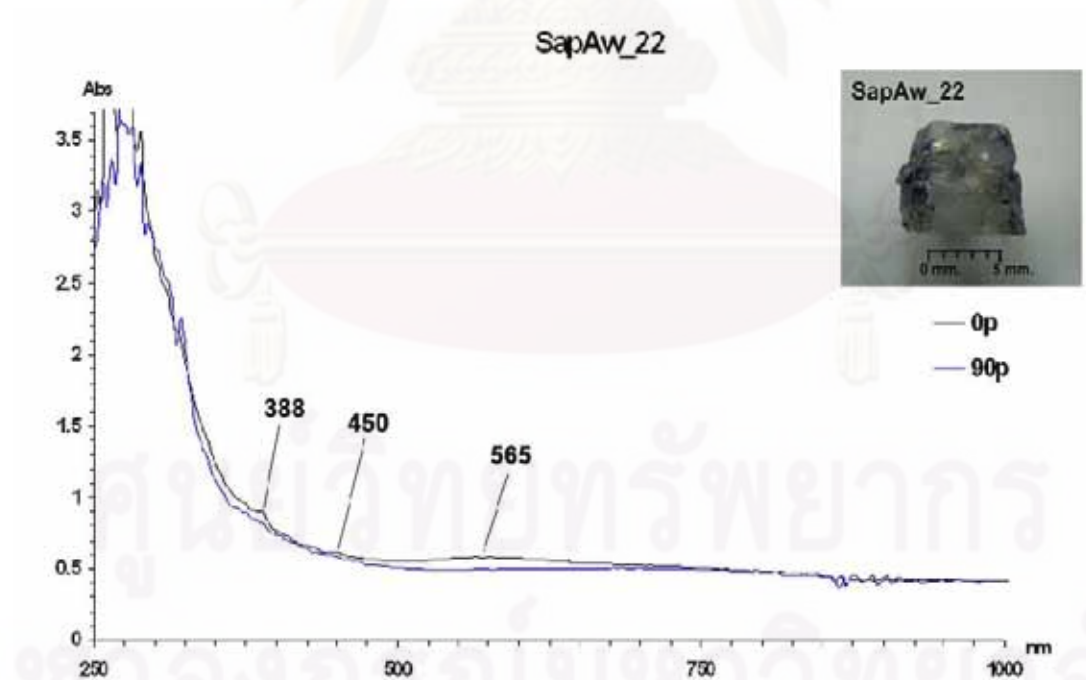


Figure C-1.22 UV-VIS-NIR absorption spectra of the sample SapAw_22

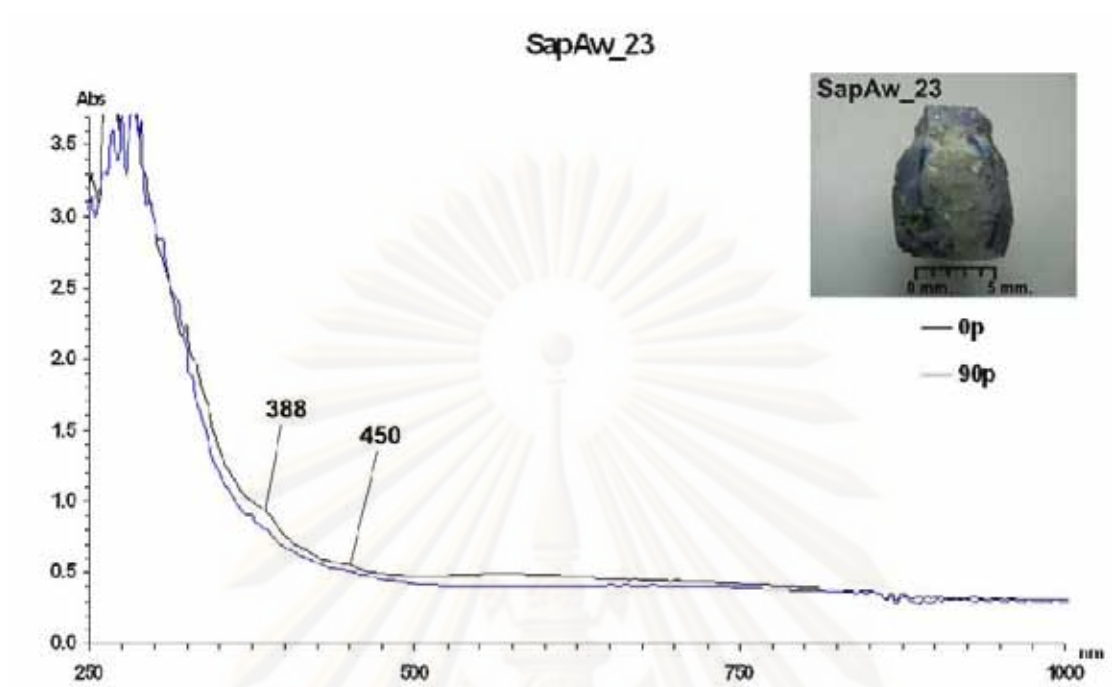


Figure C-1.23 UV-VIS-NIR absorption spectra of the sample SapAw_23

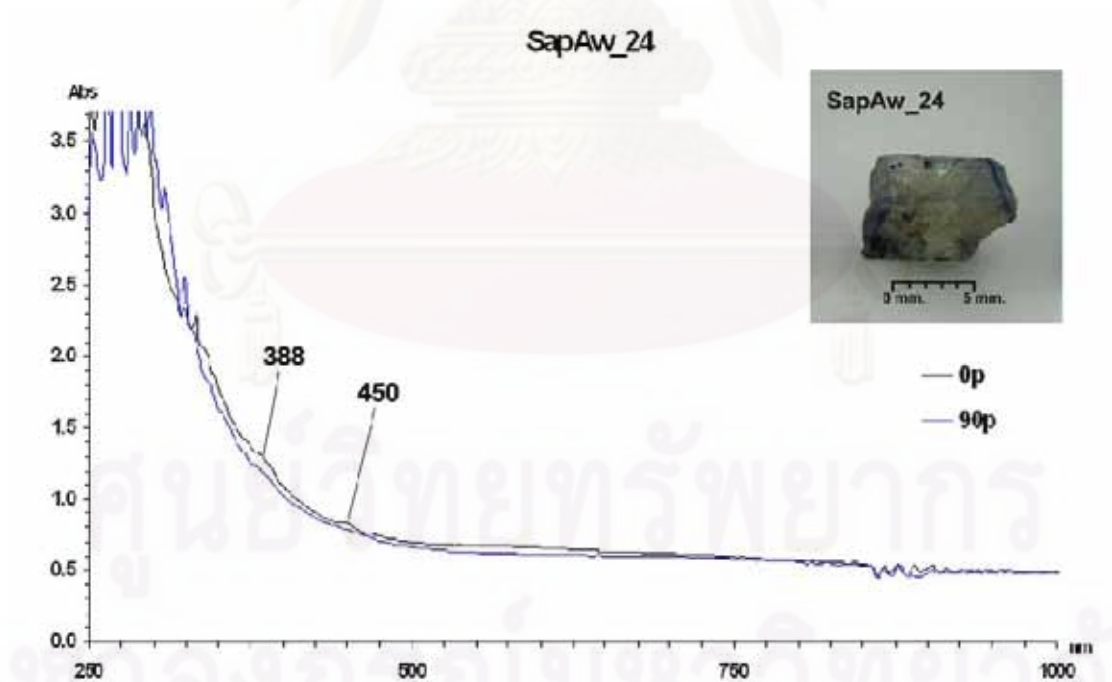


Figure C-1.24 UV-VIS-NIR absorption spectra of the sample SapAw_24

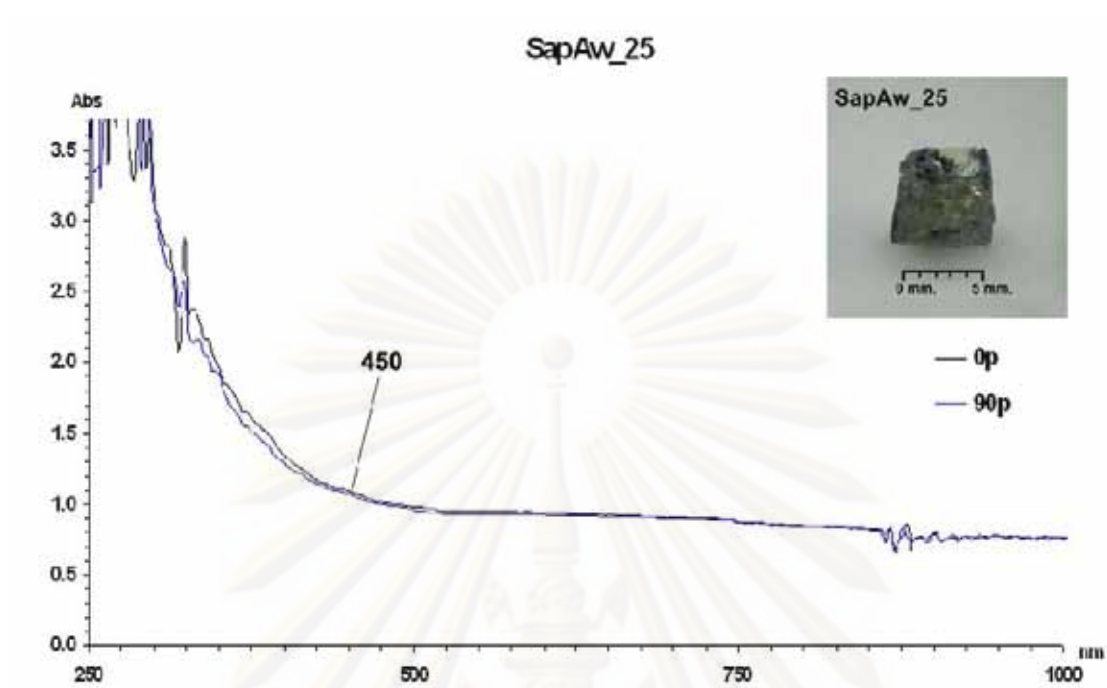


Figure C-1.25 UV-VIS-NIR absorption spectra of the sample SapAw_25

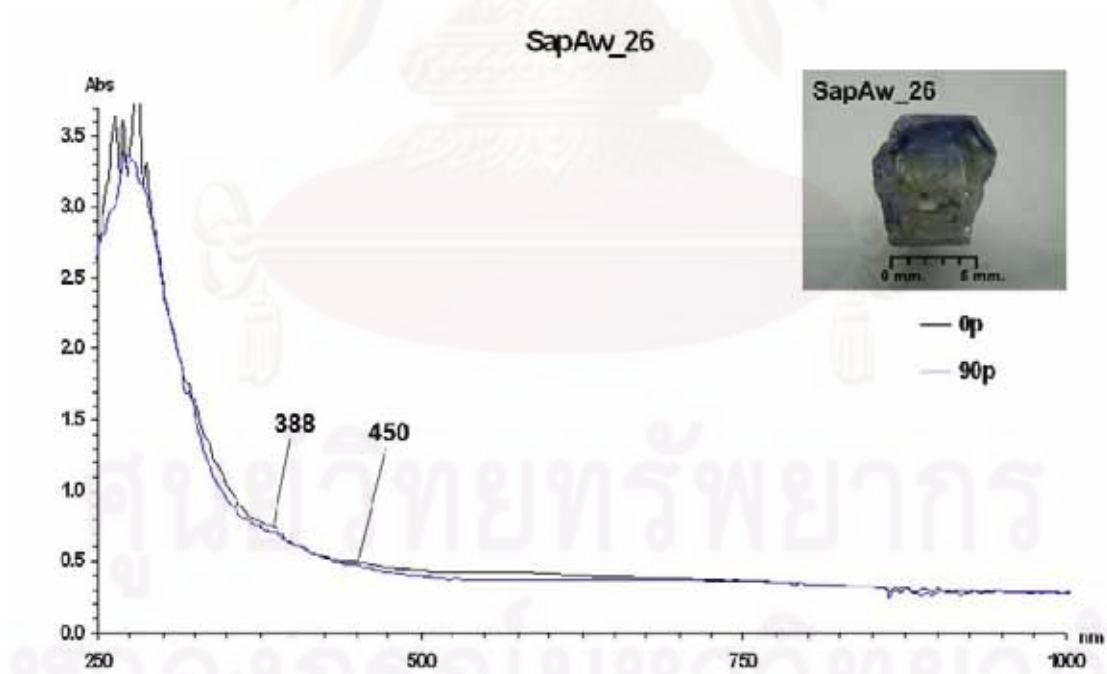


Figure C-1.26 UV-VIS-NIR absorption spectra of the sample SapAw_26

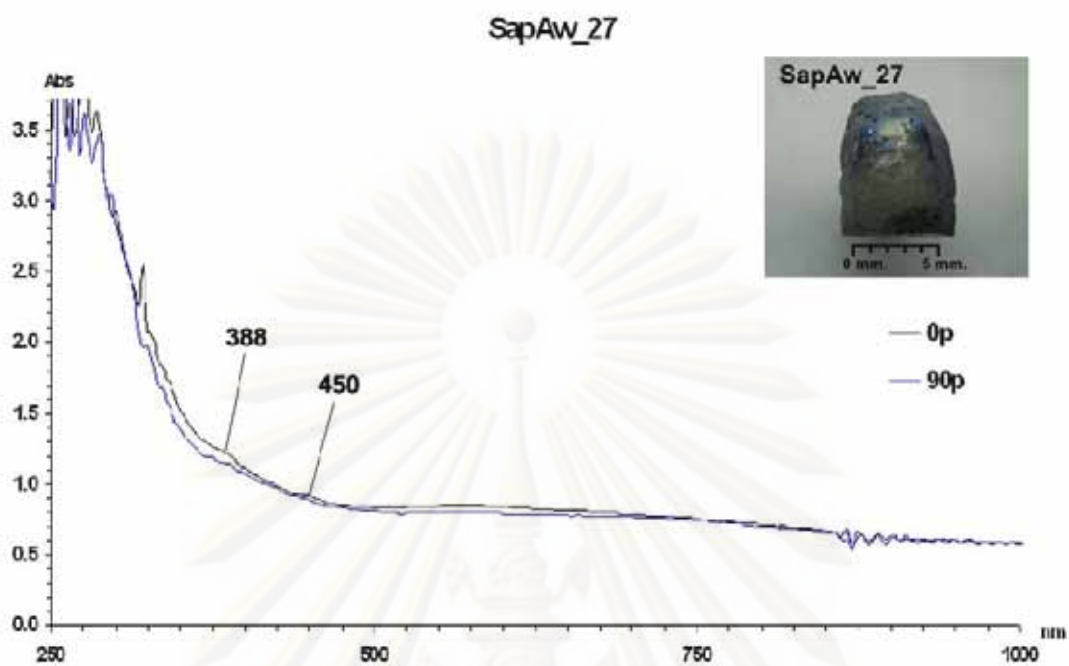


Figure C-1.27 UV-VIS-NIR absorption spectra of the sample SapAw_27

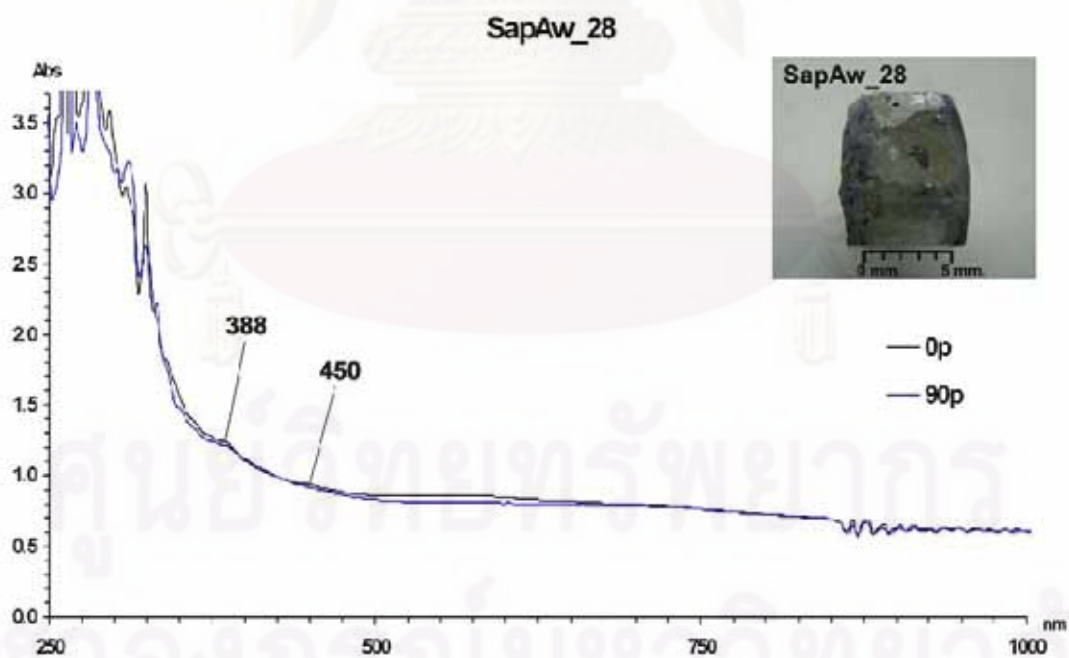


Figure C-1.28 UV-VIS-NIR absorption spectra of the sample SapAw_28

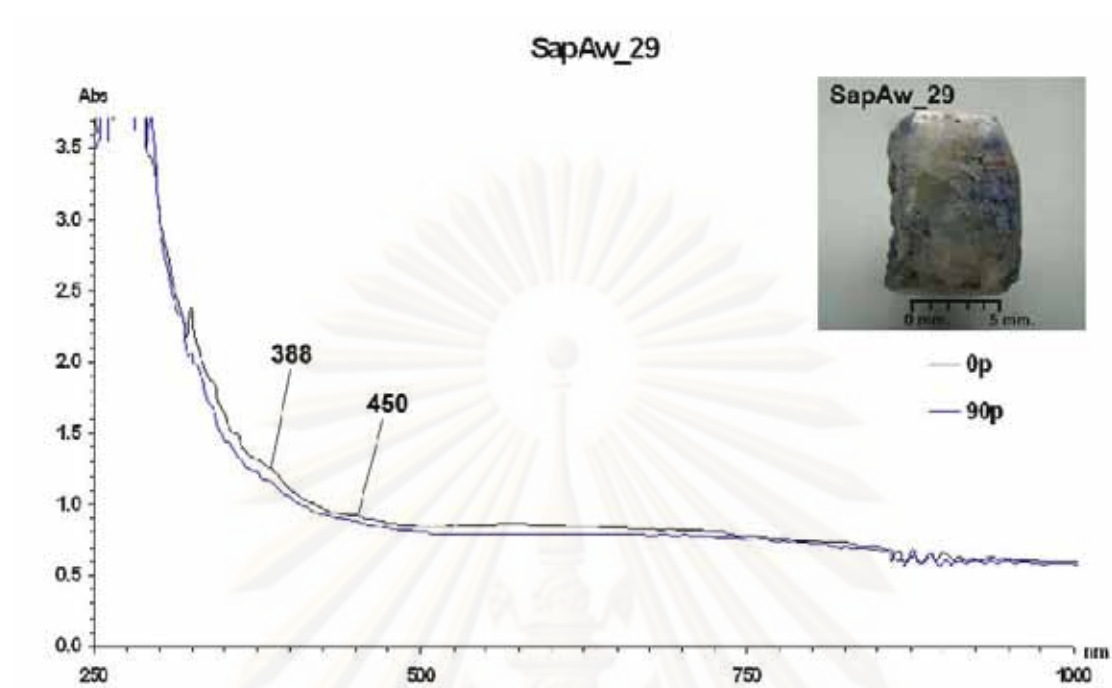


Figure C-1.29 UV-VIS-NIR absorption spectra of the sample SapAw_29

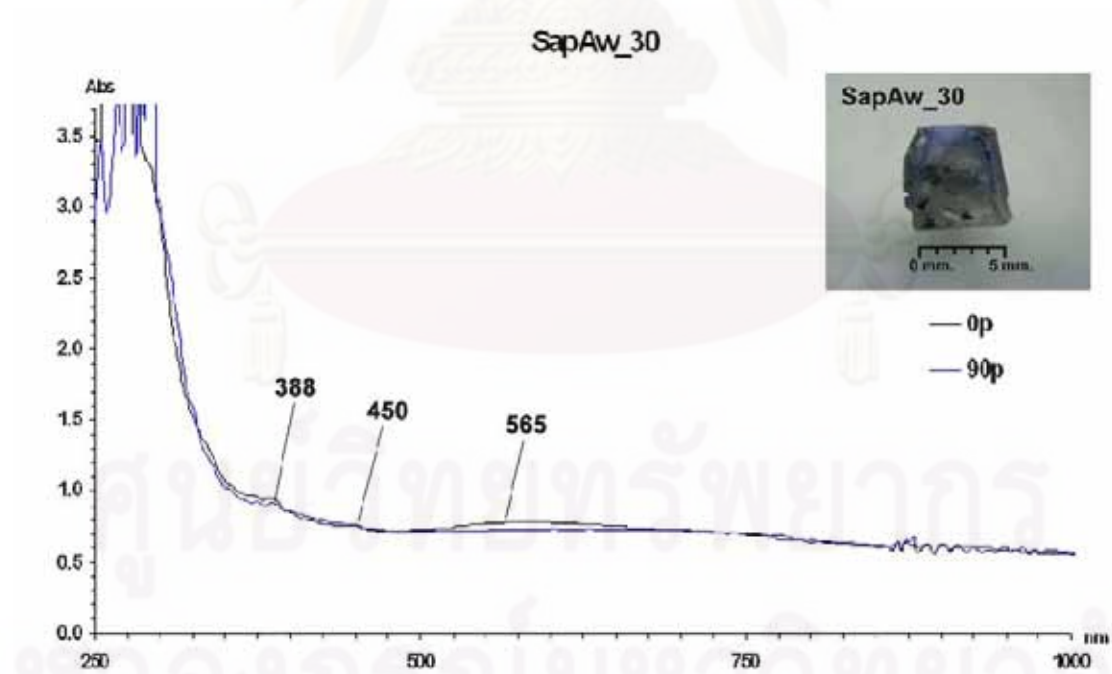


Figure C-1.30 UV-VIS-NIR absorption spectra of the sample SapAw_30

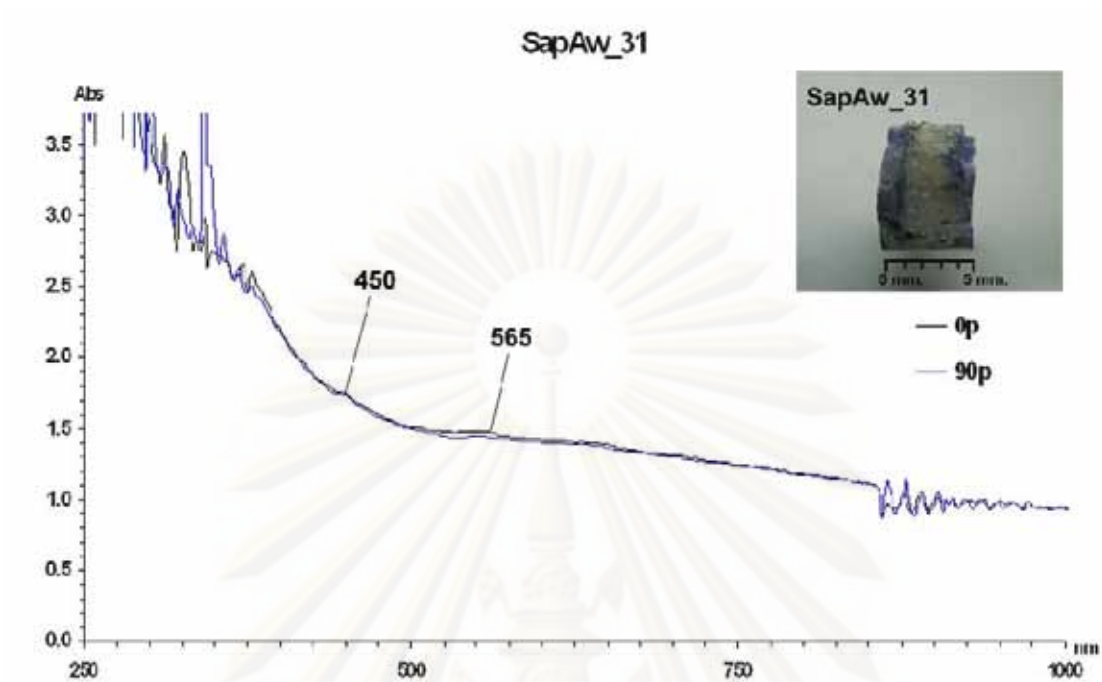


Figure C-1.31 UV-VIS-NIR absorption spectra of the sample SapAw_31

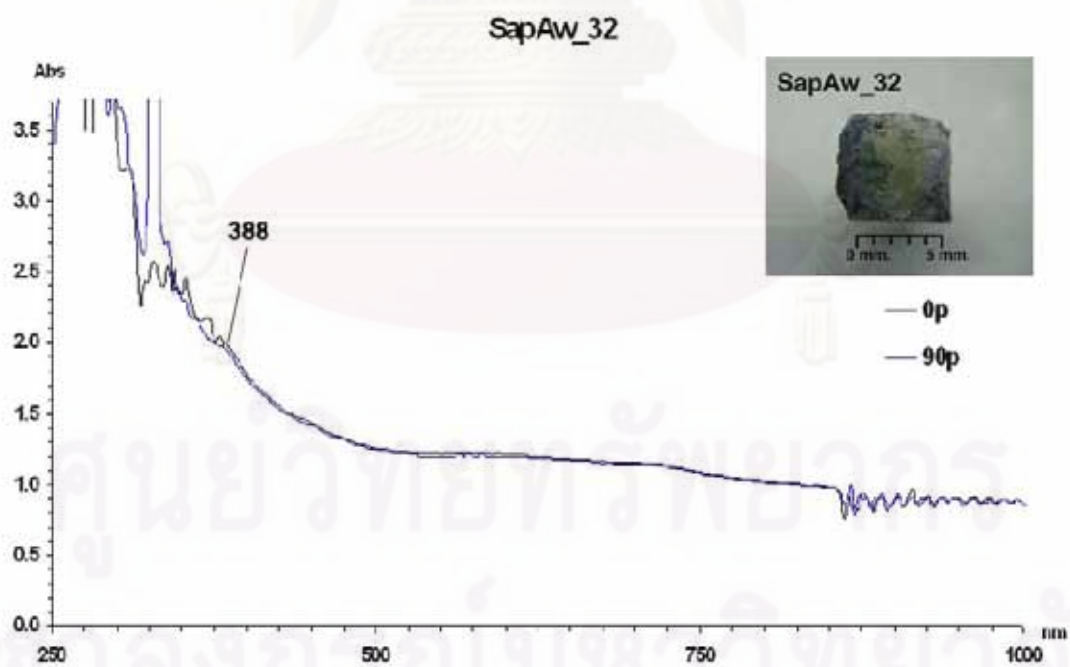


Figure C-1.32 UV-VIS-NIR absorption spectra of the sample SapAw_32

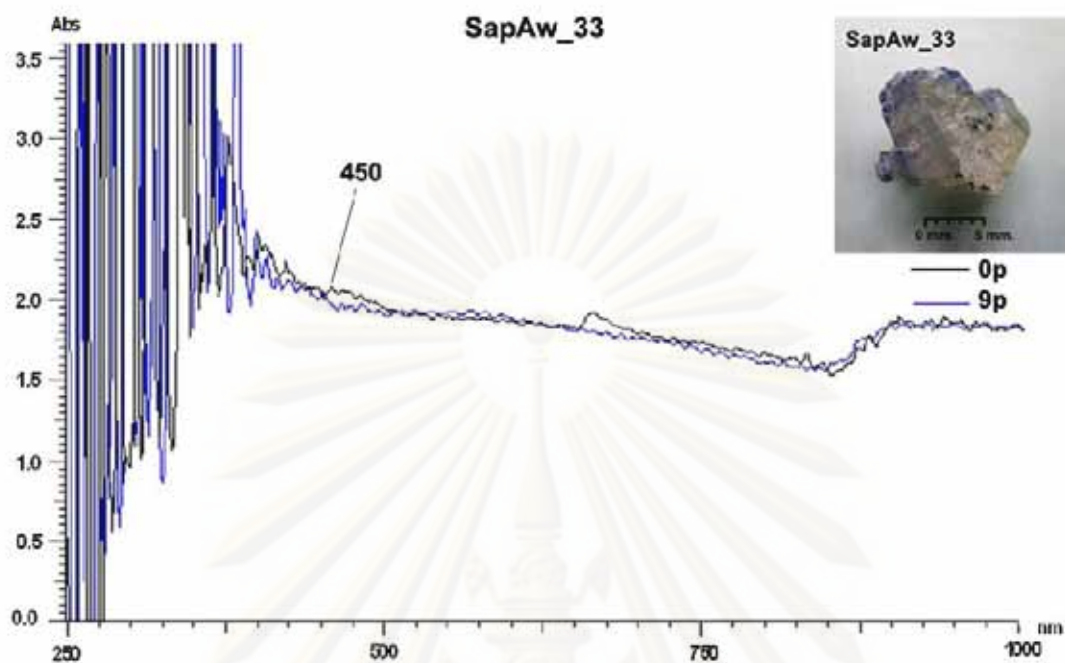


Figure C-1.33 UV-VIS-NIR absorption spectra of the sample SapAw_33 (SapAwTw_01)

ศูนย์วิทยทรัพยากร
จุฬาลงกรณ์มหาวิทยาลัย

Appendix C-2 UV-VIS-NIR absorption spectra of light blue sapphire variety from Awissawella

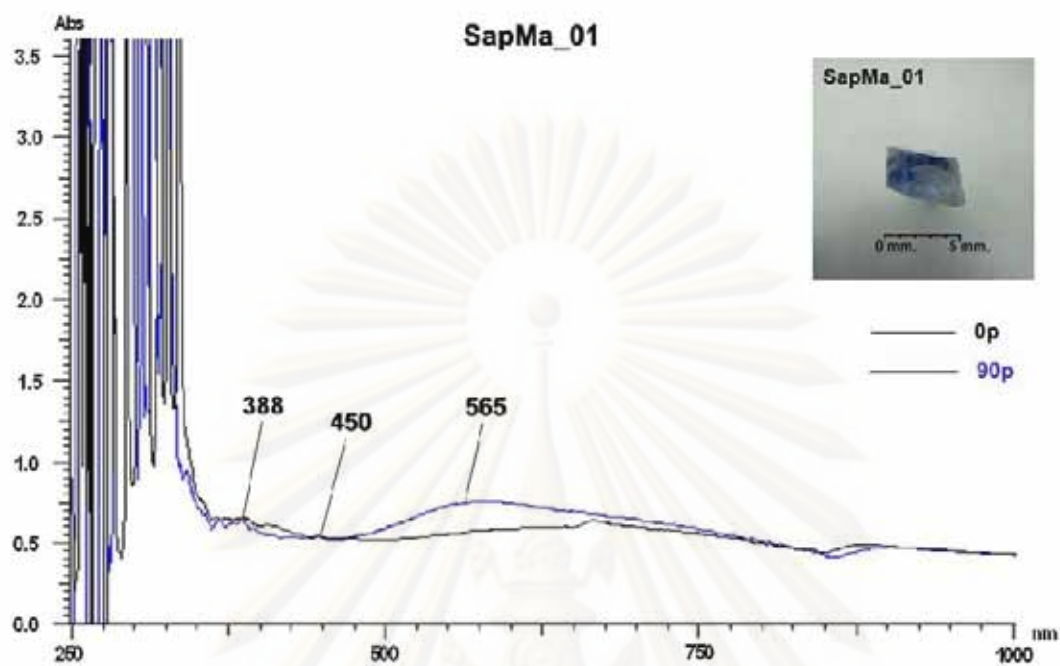


Figure C-2.1 UV-VIS-NIR absorption spectra of the sample SapMa_01

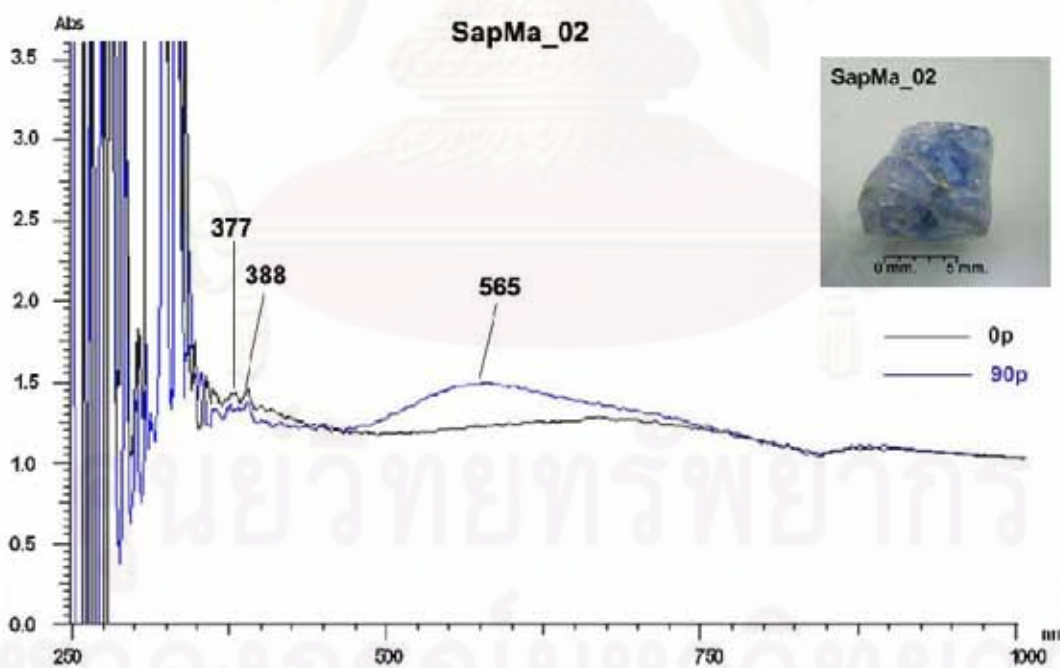


Figure C-2.2 UV-VIS-NIR absorption spectra of the sample SapMa_02

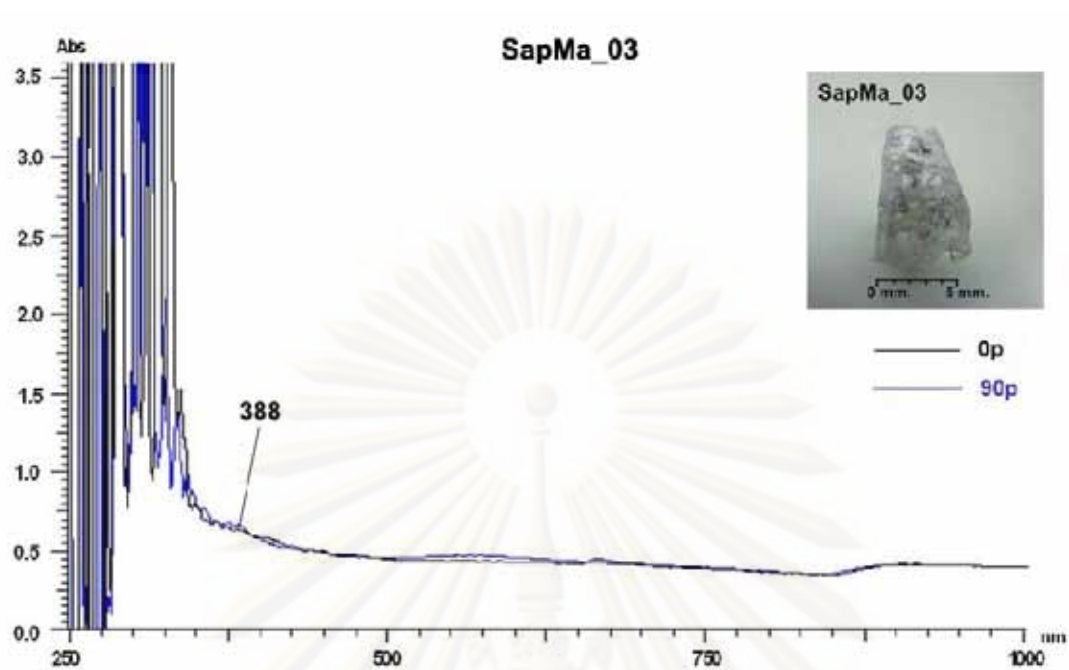


Figure C-2.3 UV-VIS-NIR absorption spectra of the sample SapMa_03

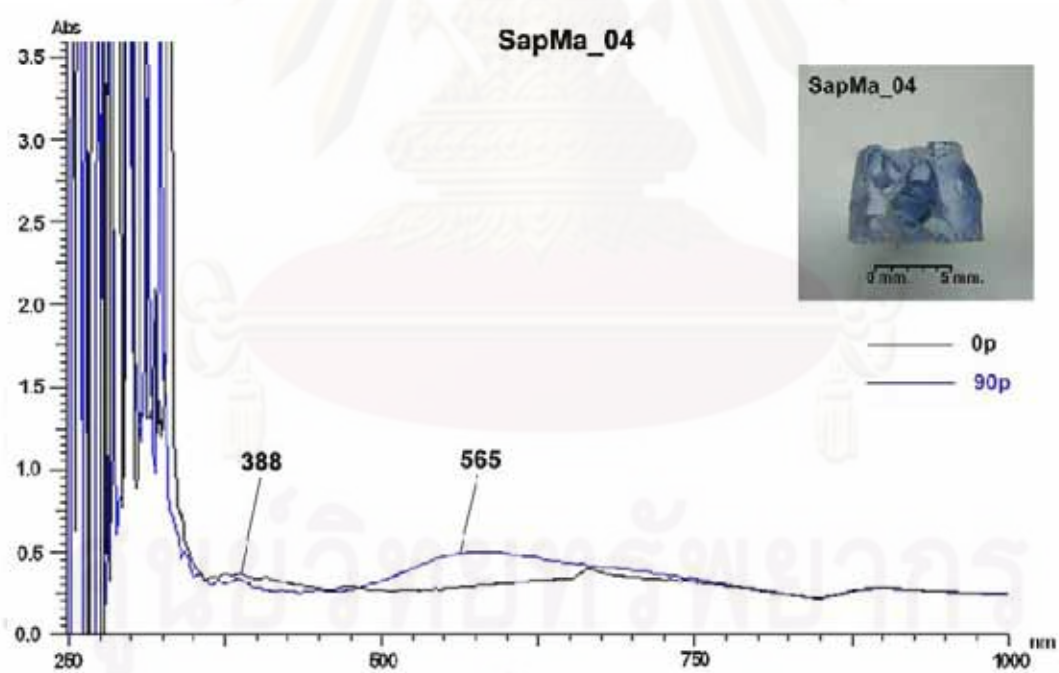


Figure C-2.4 UV-VIS-NIR absorption spectra of the sample SapMa_04

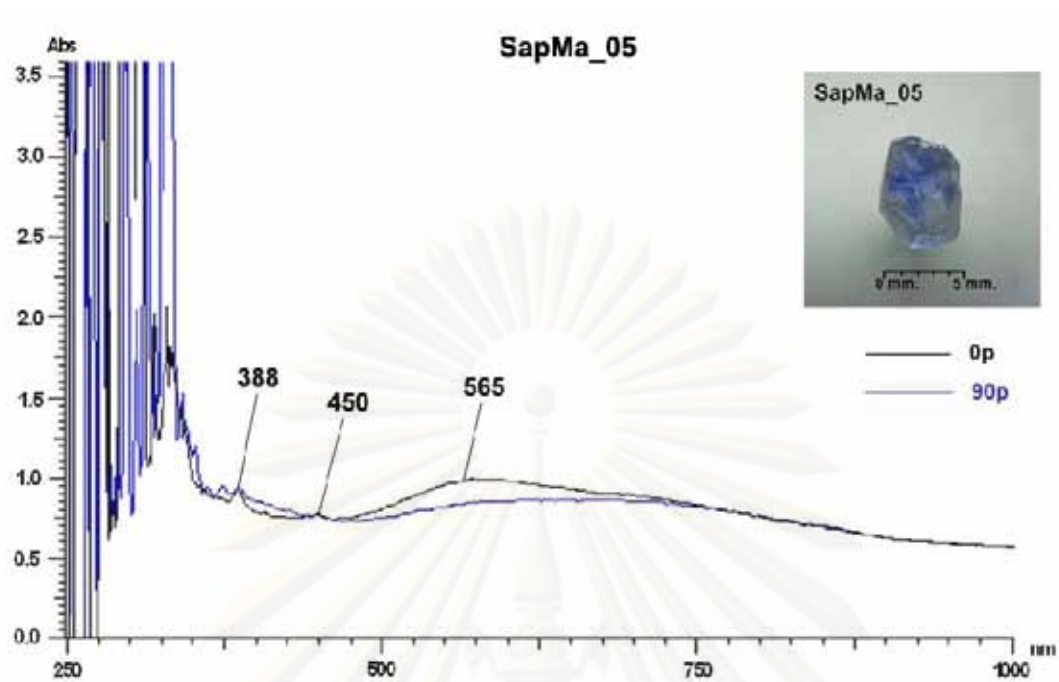


Figure C-2.5 UV-VIS-NIR absorption spectra of the sample SapMa_05

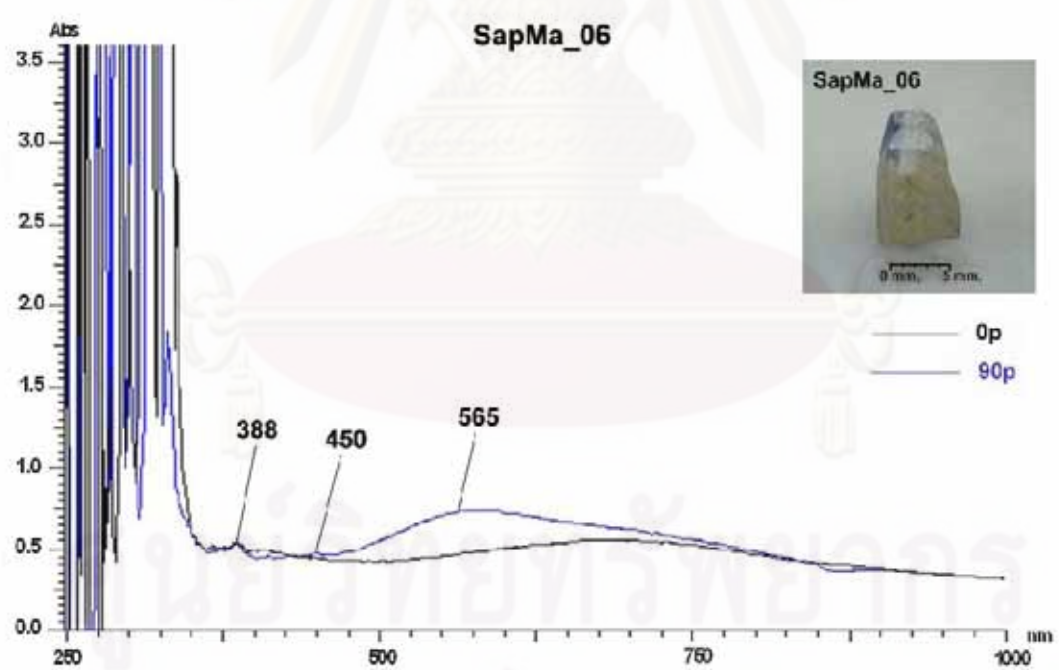


Figure C-2.6 UV-VIS-NIR absorption spectra of the sample SapMa_06

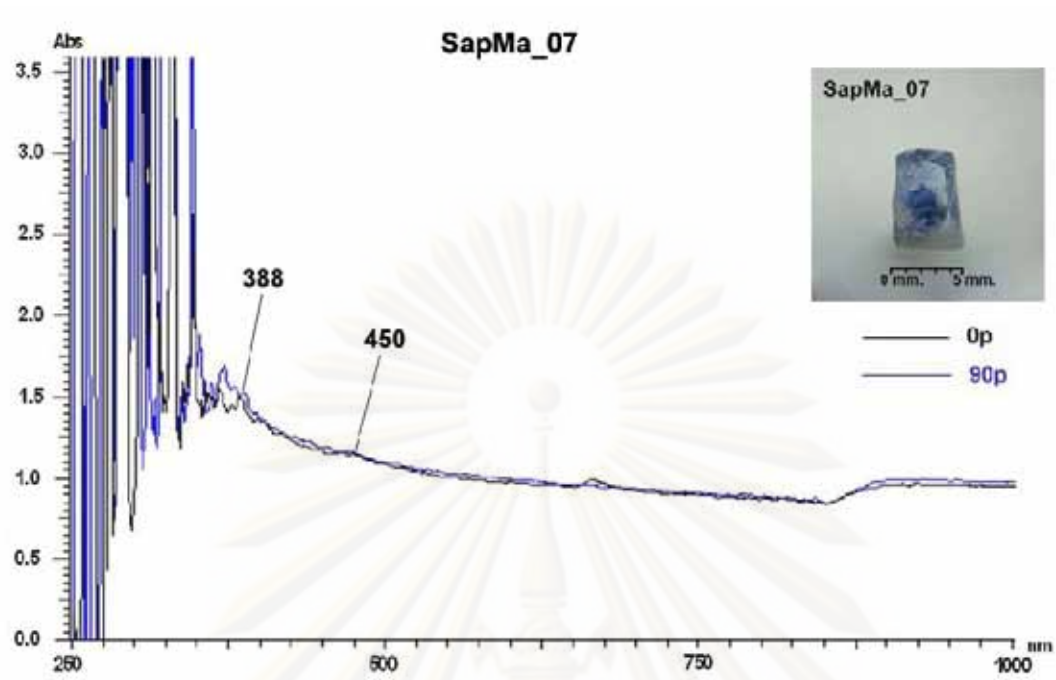


Figure C-2.7 UV-VIS-NIR absorption spectra of the sample SapMa_07



Figure C-2.8 UV-VIS-NIR absorption spectra of the sample SapMa_08

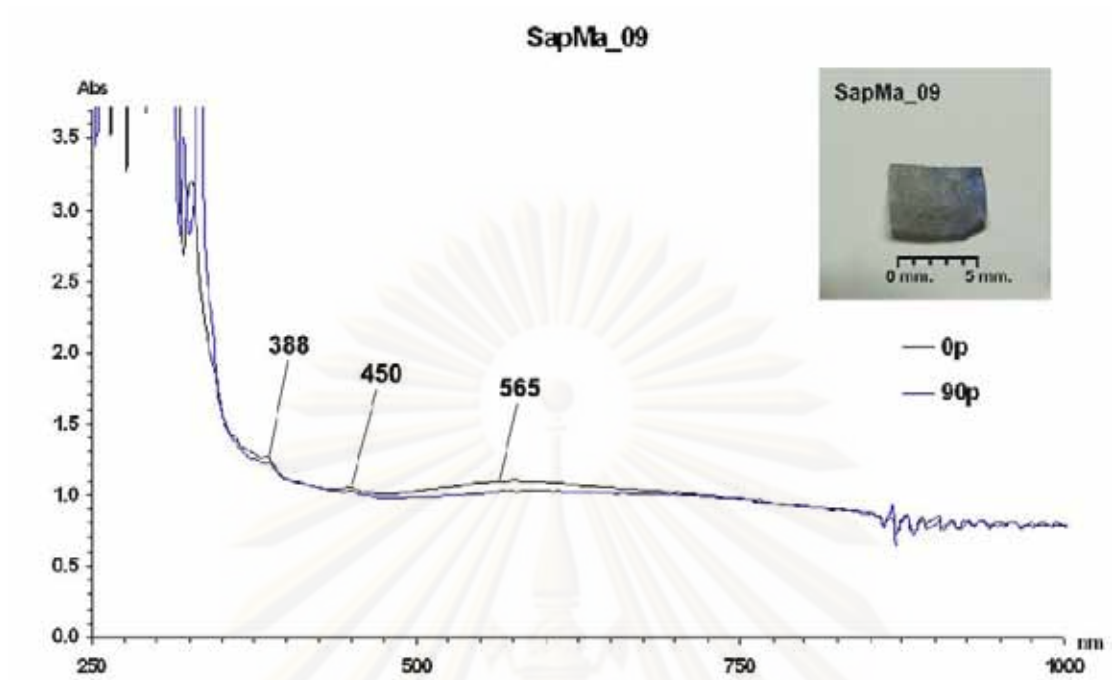


Figure C-2.9 UV-VIS-NIR absorption spectra of the sample SapMa_09

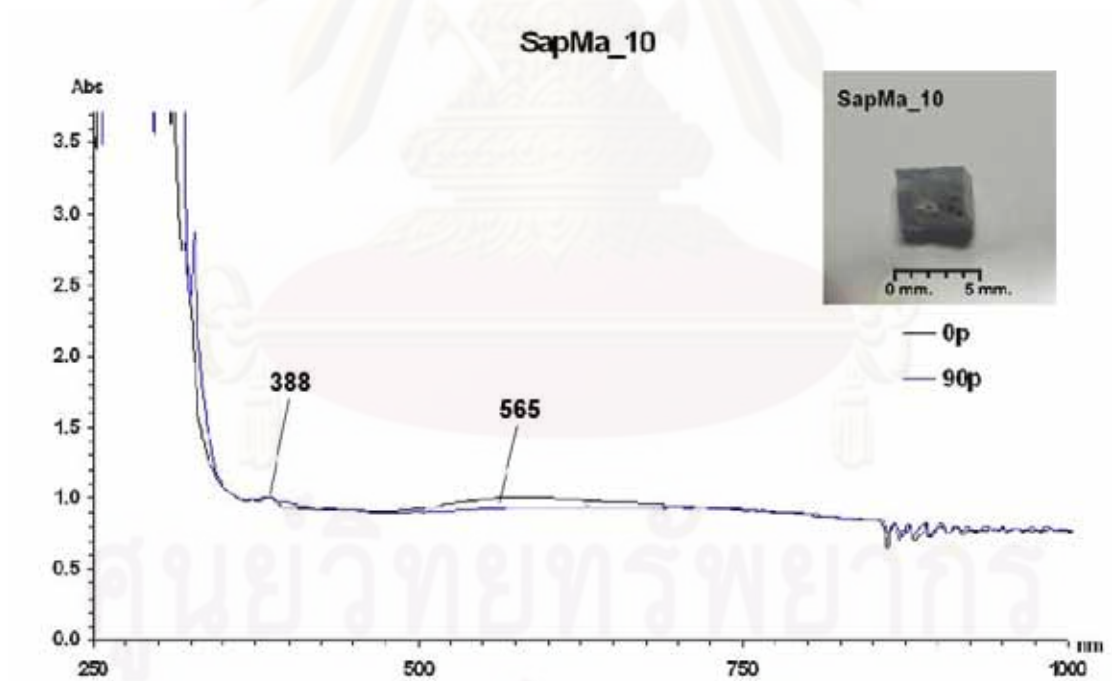


Figure C-2.10 UV-VIS-NIR absorption spectra of the sample SapMa_10

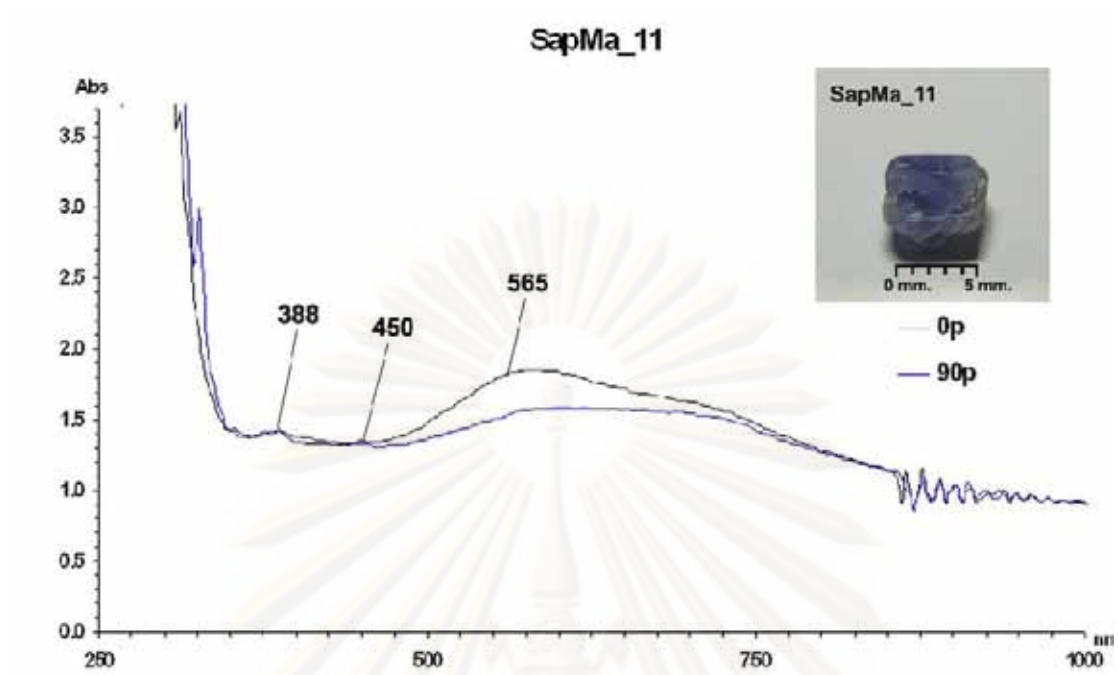


Figure C-2.11 UV-VIS-NIR absorption spectra of the sample SapMa_11

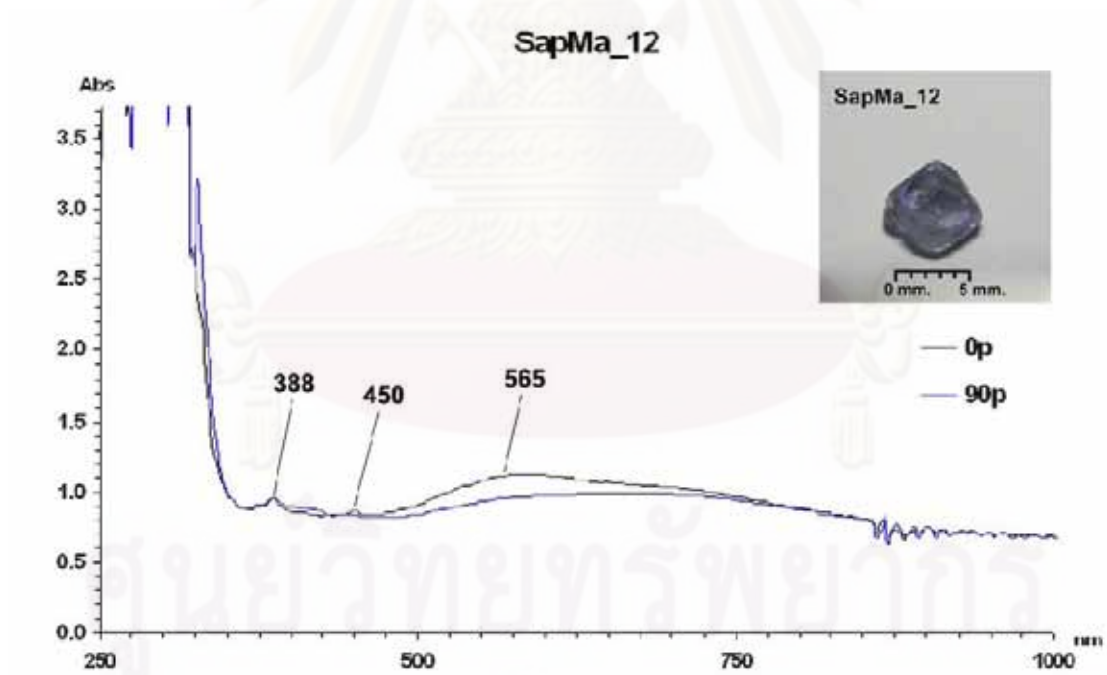


Figure C-2.12 UV-VIS-NIR absorption spectra of the sample SapMa_12

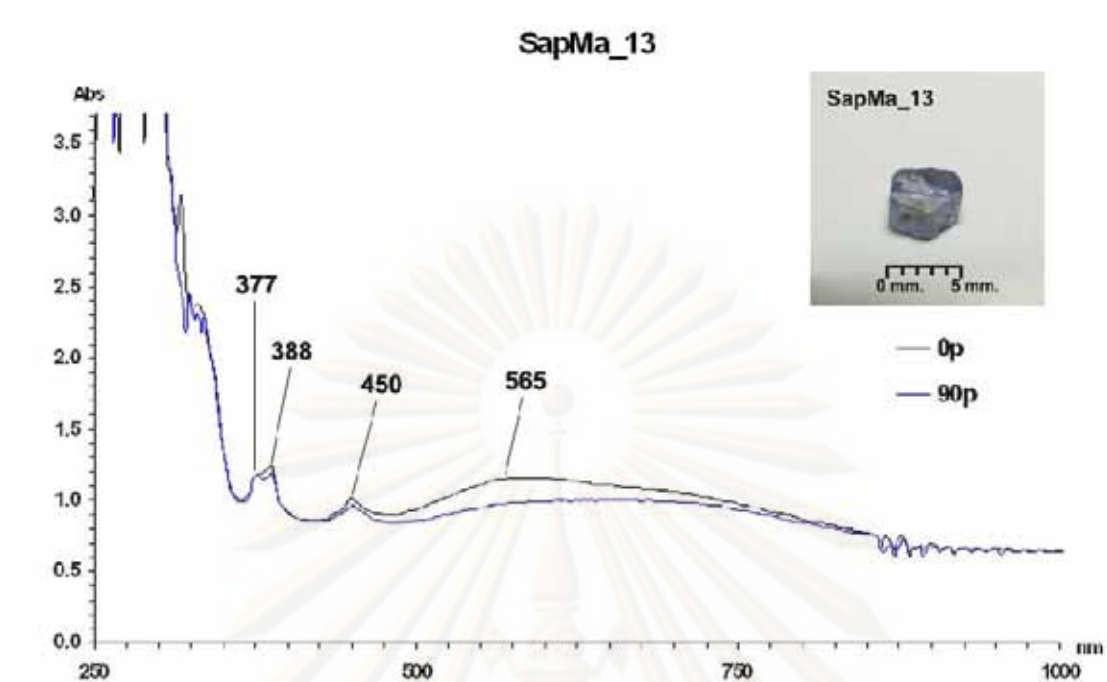


Figure C-2.13 UV-VIS-NIR absorption spectra of the sample SapMa_13

ศูนย์วิทยทรัพยากร
จุฬาลงกรณ์มหาวิทยาลัย



APPENDIX D

ศูนย์วิทยทรัพยากร
จุฬาลงกรณ์มหาวิทยาลัย

Appendix D Chemical composition of Awissawella corundums, obtained by EDXRF

Appendix D-1 Chemical composition of some Awissawella corundums by Energy Dispersive X-Ray Fluorescence, model OXFORD, ED 2000 (wt.%).

Sample	Al ₂ O ₃	Fe ₂ O ₃	TiO ₂	Cr ₂ O ₃	Ga ₂ O ₃	V ₂ O ₅	Total
SapAw_01	99.483	0.405	0.098	0.000	0.010	0.005	100.000
SapAw_02	99.543	0.399	0.043	0.000	0.010	0.005	100.000
SapAw_03	99.354	0.567	0.025	0.011	0.006	0.037	100.000
SapAw_04	99.593	0.340	0.049	0.007	0.012	0.000	100.000
SapAw_05	99.732	0.198	0.057	0.000	0.009	0.004	100.000
SapAw_06	99.779	0.125	0.069	0.018	0.007	0.002	100.000
SapAw_07	99.680	0.253	0.057	0.000	0.009	0.001	100.000
SapAw_08	99.690	0.215	0.076	0.004	0.011	0.005	100.000
SapAw_09	99.629	0.274	0.074	0.002	0.013	0.008	100.000
SapAw_10	99.389	0.519	0.066	0.012	0.010	0.006	100.000
SapAw_11	99.709	0.234	0.046	0.000	0.010	0.001	100.000
SapAw_12	99.665	0.201	0.126	0.000	0.008	0.000	100.000
SapAw_13	99.619	0.279	0.084	0.000	0.011	0.007	100.000
SapAw_14	99.595	0.307	0.071	0.017	0.010	0.000	100.000
SapAw_15	99.643	0.225	0.106	0.009	0.011	0.006	100.000
SapAw_16	99.783	0.151	0.049	0.001	0.009	0.001	99.995
SapAw_17	99.460	0.360	0.149	0.014	0.014	0.002	100.000
SapAw_18	99.465	0.299	0.223	0.000	0.009	0.004	100.000
SapAw_19	99.672	0.215	0.088	0.012	0.010	0.002	100.000
SapAw_20	99.620	0.211	0.132	0.023	0.009	0.005	100.000
SapAwTw_21	98.865	0.940	0.170	0.015	0.010	0.000	100.000
SapAwTw_22	99.175	0.757	0.048	0.009	0.008	0.004	100.000
SapMa_01	99.637	0.230	0.110	0.002	0.020	0.001	100.000
SapMa_02	99.669	0.265	0.044	0.000	0.015	0.008	100.000
SapMa_03	99.723	0.179	0.084	0.000	0.012	0.001	100.000
SapMa_04	99.657	0.258	0.061	0.000	0.018	0.006	100.000
SapMa_05	99.715	0.134	0.130	0.000	0.017	0.003	100.000
SapMa_06	99.658	0.156	0.113	0.009	0.021	0.013	99.970
SapMa_07	99.767	0.163	0.052	0.000	0.010	0.009	100.000

Appendix D-2 Chemical composition of some Awissawella corundums by Energy Dispersive X-Ray Fluorescence, model EAGLE III (wt.%).

Sample	Al ₂ O ₃	Fe ₂ O ₃	TiO ₂	Cr ₂ O ₃	Ga ₂ O ₃	V ₂ O ₅	Total
SapAw_01	99.726	0.080	0.030	0.005	0.010	0.005	100.000
SapAw_02	99.766	0.040	0.060	0.010	0.000	0.010	100.000
SapAw_03	99.211	0.315	0.055	0.005	0.005	0.010	100.000
SapAw_04	99.814	0.050	0.035	0.010	0.000	0.005	100.000
SapAw_05	99.793	0.040	0.050	0.010	0.000	0.005	100.000
SapAw_06	99.856	0.035	0.015	0.010	0.000	0.005	100.000
SapAw_07	99.824	0.045	0.025	0.010	0.000	0.005	100.000
SapAw_08	99.772	0.043	0.057	0.003	0.003	0.010	100.000
SapAw_09	99.698	0.065	0.075	0.010	0.005	0.010	100.000
SapAw_10	99.561	0.165	0.040	0.005	0.010	0.005	100.000
SapAw_11	99.804	0.040	0.040	0.000	0.010	0.005	100.000
SapAw_12	99.815	0.060	0.020	0.000	0.010	0.010	100.000
SapAw_13	99.759	0.055	0.025	0.005	0.030	0.010	100.000
SapAw_14	99.466	0.225	0.025	0.005	0.000	0.010	100.000
SapAw_15	99.805	0.035	0.050	0.000	0.010	0.005	100.000
SapAw_16	99.650	0.120	0.030	0.005	0.000	0.010	100.000
SapAw_17	99.815	0.040	0.035	0.005	0.005	0.005	100.000
SapAw_18	99.840	0.045	0.010	0.010	0.000	0.010	100.000
SapAw_19	99.418	0.080	0.200	0.010	0.020	0.000	100.000
SapAw_20	99.800	0.060	0.020	0.010	0.010	0.010	100.000
SapAw_33	99.259	0.135	0.030	0.005	0.000	0.010	100.000
SapMa_01	99.843	0.120	0.030	0.010	0.087	0.013	100.000
SapMa_02	99.781	0.063	0.033	0.003	0.007	0.007	100.000
SapMa_03	99.797	0.040	0.020	0.000	0.000	0.000	100.000
SapMa_04	99.822	0.070	0.020	0.000	0.000	0.000	100.000
SapMa_05	99.698	0.045	0.040	0.210	0.000	0.005	100.000
SapMa_06	99.561	0.055	0.035	0.000	0.010	0.005	100.000
SapMa_07	99.804	0.065	0.130	0.005	0.010	0.015	100.000



APPENDIX E

ศูนย์วิทยทรัพยากร
จุฬาลงกรณ์มหาวิทยาลัย

Appendix E Major and Trace element contents of the Awissawella corundums, obtained by EPMA

Appendix E-1 Major and trace element contents of yellow variety from Awissawella.

Samples	Areas	Point	Al ₂ O ₃	SiO ₂	TiO ₂	Cr ₂ O ₃	Ga ₂ O ₃	V ₂ O ₃	FeO	CaO	MgO	MnO	K ₂ O	Total
SapAw_01	Yellow body	Aw01-TC1-1	99.793	0.018	0.002	0.002	0.000	0.000	0.151	0.000	0.022	0.000	0.012	100.000
		Aw01-TC1-2	99.783	0.019	0.022	0.000	0.018	0.000	0.120	0.000	0.026	0.005	0.008	100.000
		Aw01-TC1-3	99.787	0.009	0.028	0.000	0.034	0.000	0.116	0.000	0.016	0.000	0.009	100.000
		Aw01-TC1-4	99.838	0.018	0.004	0.000	0.006	0.000	0.090	0.009	0.019	0.014	0.002	100.000
	Blue patches	Aw01-TB1-1	99.832	0.018	0.048	0.012	0.000	0.000	0.078	0.006	0.002	0.002	0.001	100.000
		Aw01-TB1-2	99.801	0.004	0.090	0.007	0.002	0.000	0.079	0.007	0.000	0.009	0.000	100.000
		Aw01-TB1-3	99.846	0.018	0.064	0.000	0.032	0.000	0.022	0.000	0.000	0.008	0.009	100.000
		Aw01-TB2-1	99.934	0.031	0.005	0.000	0.020	0.000	0.008	0.000	0.002	0.000	0.000	100.000
		Aw01-TB2-2	99.791	0.006	0.059	0.000	0.022	0.000	0.079	0.014	0.018	0.006	0.005	100.000
		Aw01-TB2-3	99.810	0.009	0.017	0.000	0.035	0.000	0.124	0.000	0.005	0.000	0.000	100.000
SapAw_02	Yellow body	Aw02-TC1-1	99.822	0.015	0.016	0.012	0.000	0.000	0.112	0.002	0.004	0.011	0.006	100.000
		Aw02-TC1-2	99.817	0.013	0.013	0.007	0.008	0.000	0.131	0.002	0.008	0.000	0.000	100.000
		Aw02-TC1-3	99.810	0.009	0.017	0.000	0.035	0.000	0.124	0.000	0.005	0.000	0.000	100.000
	Blue patches	Aw02-TB1-1	99.874	0.004	0.028	0.004	0.000	0.000	0.073	0.000	0.006	0.009	0.001	100.000
		Aw02-TB1-2	99.825	0.027	0.045	0.017	0.000	0.000	0.077	0.000	0.008	0.000	0.002	100.000
		Aw02-TB1-3	99.810	0.026	0.040	0.017	0.003	0.000	0.084	0.000	0.021	0.000	0.000	100.000

Appendix E-1 (Continue).

Samples	Areas	Point	Al ₂ O ₃	SiO ₂	TiO ₂	Cr ₂ O ₃	Ga ₂ O ₃	V ₂ O ₃	FeO	CaO	MgO	MnO	K ₂ O	Total
SapAw_03	Yellow body	Aw03-TC1-1	99.818	0.007	0.013	0.010	0.011	0.000	0.114	0.009	0.012	0.004	0.000	100.000
		Aw03-TC1-2	99.785	0.024	0.146	0.007	0.000	0.000	0.027	0.004	0.007	0.000	0.000	100.000
		Aw03-TC1-3	99.798	0.028	0.042	0.000	0.019	0.000	0.100	0.000	0.012	0.001	0.000	100.000
	Blue patches	Aw03-TB1-1	99.898	0.010	0.053	0.000	0.002	0.000	0.035	0.000	0.001	0.000	0.000	100.000
		Aw03-TB1-2	99.854	0.033	0.041	0.000	0.000	0.000	0.063	0.008	0.000	0.000	0.000	100.000
		Aw03-TB1-3	99.853	0.000	0.051	0.000	0.005	0.000	0.062	0.008	0.011	0.009	0.000	100.000
		Aw03-TB1-4	99.870	0.014	0.044	0.014	0.000	0.000	0.044	0.003	0.009	0.000	0.002	100.000
		Aw03-TB1-5	99.855	0.016	0.051	0.000	0.027	0.000	0.046	0.002	0.002	0.001	0.000	100.000
Aw03-TB2-1	99.823	0.009	0.049	0.006	0.002	0.000	0.090	0.004	0.004	0.001	0.011	100.000		
Aw03-TB2-2	99.850	0.025	0.048	0.008	0.011	0.000	0.047	0.009	0.000	0.000	0.001	100.000		
SapAw_04	Yellow body	Aw04-TC1-1	99.777	0.024	0.012	0.000	0.030	0.000	0.111	0.002	0.026	0.017	0.000	100.000
		Aw04-TC1-2	99.830	0.006	0.012	0.004	0.000	0.000	0.122	0.008	0.017	0.000	0.000	100.000
		Aw04-TC1-3	99.837	0.022	0.000	0.020	0.005	0.000	0.092	0.005	0.018	0.000	0.000	100.000
		Aw04-TC1-4	99.808	0.040	0.015	0.000	0.000	0.000	0.116	0.000	0.020	0.001	0.000	100.000
	Blue patches	Aw04-TB1-1	99.811	0.006	0.018	0.000	0.018	0.000	0.124	0.008	0.007	0.000	0.007	100.000
		Aw04-TB1-2	99.851	0.009	0.074	0.006	0.000	0.000	0.056	0.000	0.001	0.000	0.002	100.000
		Aw04-TB1-3	99.827	0.032	0.042	0.000	0.034	0.000	0.042	0.002	0.000	0.000	0.022	100.000
		Aw04-TB1-4	99.870	0.003	0.038	0.007	0.003	0.000	0.069	0.000	0.005	0.000	0.005	100.000
Aw04-TB1-5		99.881	0.004	0.064	0.000	0.000	0.000	0.040	0.007	0.000	0.004	0.000	100.000	

Appendix E-1 (Continue).

Samples	Areas	Point	Al ₂ O ₃	SiO ₂	TiO ₂	Cr ₂ O ₃	Ga ₂ O ₃	V ₂ O ₃	FeO	CaO	MgO	MnO	K ₂ O	Total	
SapAw_05	Yellow body	Aw05-TC1-1	99.719	0.000	0.217	0.002	0.000	0.007	0.043	0.000	0.006	0.000	0.005	100.000	
		Aw05-TC1-2	99.633	0.011	0.244	0.005	0.022	0.030	0.039	0.000	0.003	0.012	0.001	100.000	
		Aw05-TC1-3	99.802	0.001	0.062	0.000	0.011	0.000	0.105	0.009	0.009	0.000	0.000	100.000	
		Aw05-TC2-1	99.767	0.001	0.000	0.019	0.002	0.000	0.184	0.005	0.022	0.000	0.000	100.000	
		Aw05-TC2-2	99.877	0.011	0.017	0.005	0.000	0.000	0.082	0.000	0.007	0.000	0.000	100.000	
	Blue patches	Aw05-TLB1-1	99.827	0.008	0.063	0.007	0.019	0.000	0.064	0.004	0.000	0.000	0.000	0.007	100.000
		Aw05-TLB1-2	99.816	0.010	0.055	0.004	0.031	0.000	0.075	0.000	0.004	0.003	0.002	100.000	
		Aw05-TLB2-1	99.837	0.017	0.042	0.007	0.007	0.000	0.072	0.005	0.009	0.004	0.000	100.000	
		Aw05-TLB2-2	99.820	0.018	0.025	0.025	0.000	0.000	0.102	0.000	0.003	0.002	0.005	100.000	
		Aw05-TB1-1	99.849	0.034	0.017	0.000	0.000	0.000	0.076	0.000	0.014	0.005	0.004	100.000	
		Aw05-TB1-2	99.780	0.005	0.056	0.005	0.002	0.000	0.115	0.005	0.007	0.007	0.017	100.000	
SapAw_06	Yellow body	Aw06-TC1-1	99.926	0.001	0.004	0.000	0.000	0.000	0.052	0.000	0.008	0.000	0.008	100.000	
		Aw06-TC1-2	99.925	0.007	0.000	0.000	0.008	0.000	0.044	0.002	0.007	0.000	0.006	100.000	
		Aw06-TC1-3	99.848	0.000	0.030	0.019	0.001	0.000	0.079	0.007	0.016	0.000	0.000	100.000	
		Aw06-TC2-1	99.875	0.017	0.029	0.004	0.000	0.000	0.043	0.000	0.022	0.006	0.004	100.000	
		Aw06-TC2-2	99.834	0.021	0.034	0.003	0.022	0.000	0.059	0.000	0.019	0.009	0.000	100.000	
	Blue patches	Aw06-TB1-1	99.811	0.019	0.060	0.000	0.030	0.000	0.065	0.000	0.001	0.005	0.008	100.000	
		Aw06-TB1-2	99.797	0.009	0.036	0.000	0.028	0.000	0.117	0.000	0.009	0.000	0.003	100.000	
		Aw06-TB1-3	99.828	0.024	0.024	0.000	0.013	0.000	0.096	0.000	0.000	0.007	0.007	100.000	

Appendix E-1 (Continue).

Samples	Areas	Point	Al ₂ O ₃	SiO ₂	TiO ₂	Cr ₂ O ₃	Ga ₂ O ₃	V ₂ O ₃	FeO	CaO	MgO	MnO	K ₂ O	Total	
SapAw_07	Yellow body	Aw07-C1-1	99.926	0.011	0.004	0.001	0.022	0.000	0.021	0.011	0.001	0.000	0.003	100.000	
		Aw07-TC1-2	99.859	0.011	0.012	0.000	0.000	0.000	0.092	0.004	0.014	0.002	0.004	100.000	
		Aw07-TC1-3	99.826	0.021	0.029	0.000	0.030	0.000	0.084	0.000	0.008	0.000	0.002	100.000	
		Aw07-TC1-4	99.856	0.023	0.021	0.003	0.018	0.000	0.061	0.000	0.011	0.000	0.007	100.000	
	Blue patches	Aw07-TB1-1	99.809	0.003	0.051	0.018	0.018	0.000	0.086	0.000	0.016	0.000	0.000	100.000	
		Aw07-TB1-2	99.808	0.014	0.029	0.005	0.007	0.000	0.110	0.008	0.011	0.005	0.002	100.000	
		Aw07-TB1-3	99.641	0.173	0.056	0.005	0.008	0.000	0.087	0.001	0.018	0.000	0.010	100.000	
		Aw07-TB1-4	99.876	0.022	0.044	0.000	0.015	0.000	0.030	0.007	0.000	0.006	0.000	100.000	
		Aw07-TB2-1	99.844	0.018	0.037	0.000	0.027	0.000	0.066	0.007	0.000	0.001	0.000	100.000	
		Aw07-TB2-2	99.782	0.002	0.029	0.001	0.008	0.000	0.130	0.013	0.014	0.014	0.020	0.000	100.000
		Aw07-TB2-3	99.816	0.015	0.029	0.000	0.025	0.000	0.100	0.000	0.011	0.000	0.000	0.003	100.000
	SapAw_08	Yellow body	Aw08-TC1-1	99.782	0.001	0.154	0.003	0.000	0.005	0.046	0.008	0.000	0.000	0.000	100.000
			Aw08-TC1-2	99.771	0.032	0.064	0.003	0.052	0.000	0.069	0.003	0.006	0.000	0.000	100.000
Aw08-TC1-3			99.701	0.034	0.150	0.000	0.024	0.000	0.067	0.016	0.001	0.007	0.000	100.000	
Aw08-TC1-4			99.801	0.066	0.044	0.000	0.003	0.000	0.064	0.014	0.000	0.007	0.001	100.000	
Blue patches		Aw08-TB1-1	99.824	0.025	0.058	0.000	0.000	0.000	0.085	0.001	0.006	0.000	0.000	100.000	
		Aw08-TB1-2	99.820	0.050	0.057	0.000	0.013	0.000	0.049	0.007	0.004	0.000	0.000	100.000	
		Aw08-TB1-3	99.842	0.021	0.063	0.000	0.000	0.000	0.052	0.000	0.003	0.018	0.000	100.000	
		Aw08-TB1-4	99.808	0.044	0.037	0.000	0.000	0.000	0.087	0.011	0.010	0.000	0.002	100.000	

Appendix E-1 (Continue).

Samples	Areas	Point	Al ₂ O ₃	SiO ₂	TiO ₂	Cr ₂ O ₃	Ga ₂ O ₃	V ₂ O ₃	FeO	CaO	MgO	MnO	K ₂ O	Total	
SapAw_09	Yellow body	Aw09-TC1-1	99.886	0.010	0.024	0.001	0.000	0.000	0.066	0.000	0.010	0.002	0.000	100.000	
		Aw09-TC1-2	99.873	0.048	0.012	0.005	0.000	0.000	0.047	0.005	0.008	0.000	0.002	100.000	
		Aw09-TC1-3	99.785	0.033	0.026	0.003	0.041	0.000	0.079	0.002	0.020	0.008	0.002	100.000	
		Aw09-TC1-4	99.850	0.035	0.015	0.014	0.010	0.000	0.060	0.001	0.009	0.000	0.005	100.000	
	Blue patches	Aw09-TB1-1	99.821	0.022	0.043	0.000	0.000	0.000	0.102	0.006	0.006	0.000	0.000	100.000	
		Aw09-TB1-2	99.840	0.029	0.017	0.000	0.006	0.000	0.096	0.002	0.006	0.002	0.001	100.000	
		Aw09-TB1-3	99.470	0.023	0.444	0.000	0.018	0.000	0.023	0.005	0.015	0.000	0.000	100.000	
		Aw09-TB1-4	99.802	0.029	0.045	0.010	0.003	0.000	0.083	0.013	0.007	0.006	0.001	100.000	
		Aw09-TB1-5	99.821	0.029	0.083	0.004	0.012	0.000	0.039	0.000	0.011	0.000	0.000	100.000	
		Aw-09-TB2-1	99.807	0.039	0.070	0.000	0.012	0.000	0.063	0.000	0.000	0.002	0.007	100.000	
		Aw09-TB2-2	99.804	0.024	0.086	0.008	0.021	0.000	0.050	0.006	0.000	0.000	0.000	100.000	
		SapAw_10	Yellow body	Aw10-TC1-3	99.859	0.019	0.022	0.000	0.000	0.006	0.084	0.002	0.007	0.000	0.000
	Aw10-TC1-2			99.826	0.011	0.019	0.012	0.015	0.000	0.092	0.014	0.009	0.000	0.001	100.000
	Aw10-TC1-1			99.896	0.027	0.002	0.000	0.000	0.000	0.054	0.000	0.012	0.009	0.000	100.000
Blue patches	Aw10-TB1-1		99.866	0.016	0.029	0.009	0.005	0.000	0.062	0.001	0.011	0.000	0.000	100.000	
	Aw10-TB1-2		99.834	0.028	0.044	0.014	0.000	0.000	0.075	0.000	0.002	0.000	0.003	100.000	
	Aw10-TB1-3		99.874	0.023	0.023	0.000	0.000	0.000	0.062	0.000	0.011	0.001	0.007	100.000	
	Aw10-TB2-1		99.915	0.029	0.008	0.007	0.008	0.000	0.011	0.003	0.008	0.001	0.008	100.000	
	Aw10-TB2-2		99.840	0.009	0.049	0.002	0.014	0.000	0.080	0.000	0.006	0.000	0.000	100.000	
	Aw10-TB2-3		99.796	0.037	0.039	0.005	0.039	0.000	0.063	0.010	0.004	0.000	0.006	100.000	
	Aw10-TB3-1		99.812	0.019	0.090	0.001	0.001	0.000	0.067	0.005	0.004	0.000	0.000	100.000	
Aw10-TB3-2	99.821	0.017	0.067	0.000	0.024	0.000	0.051	0.005	0.004	0.000	0.010	100.000			
Aw10-TB3-3	99.831	0.006	0.093	0.000	0.003	0.000	0.052	0.012	0.000	0.003	0.000	100.000			

Appendix E-1 (Continue).

Samples	Areas	Point	Al ₂ O ₃	SiO ₂	TiO ₂	Cr ₂ O ₃	Ga ₂ O ₃	V ₂ O ₃	FeO	CaO	MgO	MnO	K ₂ O	Total	
SapAw_11	Yellow body	Aw11-TC1-1	99.750	0.042	0.009	0.000	0.000	0.000	0.166	0.007	0.020	0.000	0.006	100.000	
		Aw11-TC1-2	99.862	0.051	0.012	0.000	0.022	0.000	0.043	0.000	0.006	0.000	0.004	100.000	
		Aw11-TC1-3	99.917	0.013	0.003	0.000	0.000	0.000	0.036	0.012	0.015	0.002	0.001	100.000	
	Blue patches	Aw11-TB1-1	99.795	0.019	0.104	0.004	0.020	0.000	0.000	0.058	0.000	0.000	0.000	0.001	100.000
		Aw11-TB1-2	99.878	0.019	0.047	0.000	0.000	0.000	0.000	0.056	0.000	0.000	0.000	0.001	100.000
		Aw11-TB1-3	99.778	0.026	0.041	0.022	0.000	0.000	0.000	0.119	0.000	0.014	0.000	0.000	100.000
		Aw11-TB2-1	99.855	0.027	0.026	0.005	0.006	0.000	0.000	0.062	0.006	0.005	0.007	0.000	100.000
		Aw11-TB2-2	99.807	0.030	0.032	0.011	0.004	0.000	0.000	0.097	0.000	0.003	0.004	0.012	100.000
		Aw11-TB2-3	99.887	0.050	0.028	0.000	0.001	0.000	0.000	0.012	0.011	0.005	0.002	0.004	100.000
		Aw11-TB3-1	99.829	0.038	0.030	0.005	0.021	0.000	0.000	0.046	0.003	0.009	0.015	0.004	100.000
Aw11-TB3-2	99.852	0.015	0.051	0.016	0.023	0.000	0.000	0.038	0.003	0.000	0.001	0.000	100.000		
Aw11-TB3-3	99.827	0.023	0.035	0.000	0.029	0.000	0.000	0.060	0.007	0.014	0.000	0.004	100.000		
SapAw_12	Yellow body	Aw12-TC1-1	99.689	0.021	0.221	0.000	0.008	0.003	0.045	0.002	0.010	0.000	0.000	100.000	
		Aw12-TC1-2	99.883	0.020	0.014	0.001	0.003	0.000	0.072	0.000	0.001	0.000	0.005	100.000	
	Blue patches	Aw12-TB1-1	99.863	0.025	0.059	0.000	0.000	0.000	0.053	0.000	0.000	0.000	0.000	100.000	
		Aw12-TB1-2	99.800	0.007	0.103	0.000	0.020	0.000	0.052	0.001	0.009	0.007	0.001	100.000	
		Aw12-TB1-3	99.683	0.012	0.252	0.000	0.017	0.003	0.025	0.000	0.000	0.000	0.008	100.000	
SapAw_13	Yellow body	Aw13-TC1-1	99.817	0.025	0.027	0.000	0.008	0.000	0.102	0.000	0.022	0.000	0.000	100.000	
		Aw13-TC1-2	99.859	0.005	0.036	0.000	0.000	0.000	0.082	0.002	0.016	0.000	0.000	100.000	
		Aw13-TC1-3	99.795	0.007	0.000	0.004	0.000	0.000	0.168	0.001	0.012	0.003	0.010	100.000	
	Blue patches	Aw13-TB1-1	99.839	0.002	0.073	0.011	0.000	0.000	0.000	0.067	0.000	0.006	0.000	0.002	100.000
		Aw13-TB1-2	99.838	0.025	0.029	0.000	0.014	0.000	0.000	0.075	0.005	0.013	0.000	0.000	100.000
		Aw13-TB1-3	99.799	0.023	0.064	0.000	0.000	0.000	0.000	0.087	0.001	0.010	0.008	0.008	100.000

Appendix E-1(Continue).

Samples	Areas	Point	Al ₂ O ₃	SiO ₂	TiO ₂	Cr ₂ O ₃	Ga ₂ O ₃	V ₂ O ₃	FeO	CaO	MgO	MnO	K ₂ O	Total
SapAw_14	Yellow body	Aw14-TC1-1	99.860	0.015	0.033	0.000	0.000	0.000	0.077	0.000	0.005	0.009	0.000	100.000
		Aw14-TC1-2	99.809	0.014	0.013	0.001	0.035	0.000	0.108	0.003	0.016	0.000	0.000	100.000
		Aw14-TC1-3	99.854	0.011	0.006	0.008	0.034	0.000	0.049	0.013	0.008	0.015	0.001	100.000
		Aw14-TC1-4	99.858	0.012	0.010	0.000	0.007	0.000	0.101	0.001	0.010	0.000	0.000	100.000
	Blue patches	Aw14-TB1-1	99.879	0.020	0.039	0.000	0.011	0.000	0.037	0.002	0.006	0.002	0.003	100.000
		Aw14-TB1-2	99.793	0.031	0.050	0.000	0.001	0.000	0.107	0.000	0.010	0.008	0.000	100.000
Aw14-TB1-3		99.850	0.018	0.018	0.000	0.000	0.000	0.096	0.008	0.009	0.000	0.000	100.000	
SapAw_15	Yellow body	Aw15-TC1-1	99.861	0.029	0.013	0.000	0.013	0.000	0.067	0.006	0.008	0.000	0.002	100.000
		Aw15-TC1-2	99.842	0.006	0.017	0.004	0.003	0.000	0.097	0.004	0.016	0.010	0.000	100.000
		Aw15-TC1-3	99.894	0.005	0.002	0.008	0.012	0.000	0.064	0.000	0.003	0.012	0.000	100.000
	Blue patches	Aw15-TB1-1	99.836	0.014	0.036	0.000	0.011	0.000	0.079	0.007	0.011	0.000	0.005	100.000
		Aw15-TB1-2	99.864	0.013	0.014	0.004	0.000	0.000	0.091	0.004	0.004	0.003	0.002	100.000
		Aw15-TB1-3	99.865	0.008	0.068	0.009	0.014	0.000	0.024	0.000	0.000	0.008	0.003	100.000
		Aw15-TB2-1	99.559	0.029	0.281	0.011	0.009	0.015	0.064	0.004	0.010	0.011	0.006	100.000
		Aw15-TB2-2	99.886	0.013	0.004	0.001	0.000	0.000	0.078	0.000	0.010	0.007	0.000	100.000
Aw15-TB2-3	99.754	0.017	0.019	0.003	0.018	0.000	0.138	0.013	0.019	0.011	0.007	100.000		
SapAw_16	Yellow body	Aw16-TC1-1	99.817	0.028	0.014	0.000	0.004	0.000	0.101	0.011	0.024	0.000	0.000	100.000
		Aw16-TC1-2	99.779	0.016	0.025	0.000	0.014	0.000	0.122	0.000	0.022	0.010	0.011	100.000
		Aw16-TC1-3	99.793	0.000	0.005	0.009	0.024	0.000	0.144	0.002	0.021	0.000	0.002	100.000
		Aw16-TC2-1	99.854	0.009	0.011	0.000	0.008	0.000	0.091	0.000	0.020	0.004	0.002	100.000
		Aw16-TC2-2	99.844	0.022	0.000	0.004	0.000	0.000	0.101	0.000	0.010	0.010	0.008	100.000
		Aw16-TC2-3	99.852	0.025	0.012	0.005	0.010	0.000	0.066	0.000	0.022	0.007	0.000	100.000

Appendix E-1 (Continue).

Samples	Areas	Point	Al ₂ O ₃	SiO ₂	TiO ₂	Cr ₂ O ₃	Ga ₂ O ₃	V ₂ O ₃	FeO	CaO	MgO	MnO	K ₂ O	Total
SapAw_16	Blue patches	Aw16-TB1-1	99.947	0.000	0.015	0.025	0.002	0.000	0.000	0.004	0.006	0.000	0.000	100.000
		Aw16-TB1-2	99.850	0.016	0.044	0.000	0.036	0.000	0.050	0.000	0.004	0.000	0.000	100.000
		Aw16-TB1-3	99.882	0.007	0.004	0.003	0.036	0.000	0.034	0.012	0.009	0.006	0.005	100.000
		Aw16-TB2-1	99.888	0.003	0.039	0.000	0.000	0.000	0.054	0.000	0.005	0.000	0.010	100.000
		Aw16-TB2-2	99.905	0.009	0.025	0.000	0.009	0.000	0.041	0.003	0.004	0.004	0.000	100.000
SapAw_17	Yellow body	Aw17-TC1-1	99.799	0.024	0.012	0.011	0.000	0.000	0.139	0.004	0.010	0.000	0.000	100.000
		Aw17-TC1-2	99.815	0.013	0.049	0.008	0.000	0.000	0.094	0.003	0.007	0.000	0.010	100.000
		Aw17-TC1-3	99.833	0.006	0.013	0.007	0.006	0.000	0.110	0.006	0.006	0.003	0.008	100.000
		Aw17-TC2-1	99.744	0.024	0.034	0.010	0.040	0.000	0.125	0.000	0.020	0.000	0.003	100.000
		Aw17-TC2-2	99.811	0.019	0.014	0.000	0.016	0.000	0.116	0.006	0.017	0.000	0.000	100.000
	Blue patches	Aw17-TB1-1	99.836	0.000	0.065	0.000	0.005	0.000	0.083	0.000	0.008	0.000	0.003	100.000
		Aw17-TB1-2	99.860	0.009	0.052	0.000	0.004	0.000	0.058	0.009	0.004	0.003	0.000	100.000
		Aw17-TB1-3	99.822	0.014	0.085	0.000	0.003	0.000	0.051	0.013	0.000	0.008	0.004	100.000
		Aw17-TB2-1	99.798	0.010	0.092	0.011	0.000	0.000	0.075	0.007	0.003	0.000	0.003	100.000
		Aw17-TB2-2	99.833	0.005	0.062	0.010	0.013	0.000	0.060	0.000	0.004	0.001	0.010	100.000
	Aw17-TB2-3	99.830	0.000	0.046	0.000	0.002	0.000	0.093	0.013	0.009	0.000	0.006	100.000	
SapAw_18	Yellow body	Aw18-TC1-1	99.681	0.013	0.034	0.000	0.026	0.000	0.206	0.006	0.012	0.019	0.002	100.000
		Aw18-TC1-2	99.834	0.016	0.004	0.004	0.027	0.000	0.089	0.007	0.018	0.000	0.000	100.000
		Aw18-TC1-3	99.807	0.027	0.035	0.004	0.000	0.000	0.106	0.004	0.016	0.000	0.001	100.000
		Aw18-TC1-4	99.849	0.007	0.000	0.001	0.000	0.000	0.134	0.002	0.006	0.000	0.000	100.000
	Blue patches	Aw18-TB1-1	99.775	0.018	0.048	0.015	0.018	0.000	0.106	0.006	0.006	0.000	0.006	100.000
		Aw18-TB1-2	99.825	0.010	0.047	0.000	0.033	0.000	0.071	0.000	0.007	0.006	0.000	100.000
		Aw18-TB1-3	99.840	0.005	0.054	0.012	0.019	0.000	0.054	0.011	0.005	0.000	0.000	100.000
		Aw18-TB1-4	99.811	0.023	0.035	0.022	0.000	0.000	0.089	0.008	0.010	0.000	0.001	100.000

Appendix E-1 (Continue).

Samples	Areas	Point	Al ₂ O ₃	SiO ₂	TiO ₂	Cr ₂ O ₃	Ga ₂ O ₃	V ₂ O ₃	FeO	CaO	MgO	MnO	K ₂ O	Total
SapAw_19	Yellow body	Aw19-TC1-1	99.946	0.002	0.001	0.025	0.000	0.000	0.016	0.006	0.000	0.000	0.003	100.000
		Aw19-TC1-2	99.884	0.013	0.022	0.000	0.026	0.000	0.023	0.011	0.007	0.002	0.010	100.000
		Aw19-TC1-3	99.890	0.007	0.017	0.000	0.011	0.000	0.044	0.009	0.008	0.000	0.013	100.000
		Aw19-TC1-4	99.933	0.012	0.000	0.000	0.014	0.000	0.029	0.012	0.000	0.000	0.000	100.000
		Aw19-TC1-5	99.939	0.000	0.004	0.010	0.018	0.000	0.024	0.005	0.000	0.000	0.000	100.000
	Blue patches	Aw19-TB1-1	99.869	0.016	0.037	0.002	0.012	0.000	0.056	0.002	0.000	0.001	0.004	100.000
		Aw19-TB1-2	99.806	0.006	0.054	0.014	0.004	0.003	0.101	0.000	0.006	0.000	0.006	100.000
		Aw19-TB1-3	99.816	0.023	0.066	0.004	0.003	0.000	0.074	0.000	0.000	0.010	0.003	100.000
		Aw19-TB1-4	99.847	0.005	0.023	0.006	0.016	0.000	0.081	0.009	0.008	0.000	0.004	100.000
	SapAw_20	Yellow body	Aw20-TC1-1	99.805	0.020	0.032	0.000	0.019	0.000	0.104	0.006	0.010	0.000	0.003
Aw20-TC1-2			99.714	0.017	0.195	0.007	0.005	0.000	0.045	0.011	0.005	0.001	0.000	100.000
Aw20-TC1-3			99.777	0.035	0.066	0.000	0.000	0.000	0.104	0.005	0.009	0.000	0.004	100.000
Aw20-TC1-4			99.879	0.004	0.010	0.000	0.003	0.000	0.091	0.007	0.000	0.000	0.005	100.000
Blue patches		Aw20-TLB1-1	99.858	0.022	0.067	0.000	0.000	0.000	0.041	0.008	0.001	0.002	0.000	100.000
		Aw20-TLB1-2	99.870	0.021	0.041	0.004	0.005	0.000	0.050	0.000	0.000	0.000	0.008	100.000
		Aw20-TLB1-3	99.879	0.023	0.043	0.000	0.000	0.000	0.050	0.000	0.000	0.000	0.005	100.000
SapAw_21	Yellow body	Aw21TY1	99.867	0.005	0.022	0.000	0.009	0.000	0.067	0.000	0.011	0.000	0.000	99.981
		Aw21TY2	99.738	0.008	0.016	0.001	0.000	0.014	0.100	0.003	0.001	0.000	0.004	99.885
		Aw21TY3	99.528	0.058	0.062	0.003	0.000	0.006	0.075	0.007	0.032	0.000	0.004	99.775
		Aw21TY4	99.405	0.005	0.003	0.000	0.003	0.003	0.078	0.006	0.011	0.000	0.003	99.517
		Aw21TY5	99.868	0.011	0.012	0.000	0.004	0.001	0.097	0.003	0.008	0.002	0.000	100.006
		Aw21TY6	99.957	0.013	0.024	0.007	0.019	0.000	0.068	0.004	0.009	0.001	0.001	100.103

Appendix E-1 (Continue).

Samples	Areas	Point	Al ₂ O ₃	SiO ₂	TiO ₂	Cr ₂ O ₃	Ga ₂ O ₃	V ₂ O ₃	FeO	CaO	MgO	MnO	K ₂ O	Total
SapAw_21	Blue patches	Aw21TB1	98.727	0.016	0.046	0.000	0.022	0.000	0.083	0.002	0.015	0.000	0.004	98.915
		Aw21TB2	99.767	0.024	0.021	0.001	0.003	0.014	0.026	0.003	0.000	0.004	0.000	99.863
		Aw21TB3	99.407	0.005	0.035	0.000	0.002	0.018	0.067	0.004	0.008	0.000	0.006	99.552
		Aw21TB4	98.632	0.027	0.087	0.007	0.003	0.004	0.087	0.005	0.009	0.001	0.002	98.864
		Aw21TB5	99.987	0.010	0.065	0.004	0.002	0.001	0.104	0.001	0.001	0.000	0.010	100.185
		Aw21TB6	100.703	0.000	0.053	0.000	0.018	0.015	0.058	0.000	0.000	0.000	0.000	100.847
SapAw_22	Yellow body	Aw22TY1	100.211	0.023	0.016	0.000	0.015	0.000	0.080	0.002	0.010	0.002	0.000	100.359
		Aw22TY2	100.104	0.020	0.010	0.004	0.000	0.006	0.081	0.000	0.009	0.001	0.001	100.236
		Aw22TY3	100.495	0.014	0.016	0.003	0.005	0.013	0.083	0.002	0.000	0.004	0.001	100.636
		Aw22TY4	100.864	0.016	0.059	0.001	0.000	0.001	0.089	0.003	0.011	0.001	0.001	101.046
		Aw22TY5	100.990	0.009	0.169	0.000	0.010	0.001	0.029	0.001	0.003	0.003	0.003	101.218
		Aw22TY6	101.073	0.000	0.004	0.000	0.013	0.013	0.020	0.003	0.006	0.000	0.000	101.132
	Blue patches	Aw22TB1	101.201	0.022	0.065	0.006	0.005	0.013	0.045	0.000	0.000	0.004	0.003	101.364
		Aw22TB3	100.813	0.003	0.012	0.000	0.005	0.008	0.013	0.001	0.009	0.001	0.000	100.865
		Aw22TB4	100.918	0.012	0.028	0.000	0.004	0.006	0.022	0.001	0.005	0.002	0.002	101.000
		Aw22TB5	99.827	0.007	0.044	0.000	0.008	0.013	0.087	0.004	0.010	0.000	0.000	100.000
		Aw22TB6	101.064	0.008	0.059	0.001	0.004	0.007	0.061	0.000	0.012	0.000	0.000	101.216
		SapAw_23	Yellow body	Aw23TY1	101.136	0.008	0.011	0.001	0.005	0.003	0.078	0.002	0.009	0.000
Aw23TY2	101.143			0.009	0.020	0.000	0.011	0.000	0.104	0.001	0.012	0.005	0.001	101.306
Aw23TY3	100.516			0.000	0.030	0.000	0.009	0.003	0.123	0.002	0.016	0.000	0.002	100.701
Aw23TY4	101.130			0.006	0.023	0.006	0.008	0.012	0.115	0.000	0.011	0.000	0.000	101.311
Aw23TY5	101.074			0.027	0.006	0.003	0.000	0.000	0.094	0.002	0.015	0.001	0.003	101.225

Appendix E-1 (Continue).

Samples	Areas	Point	Al ₂ O ₃	SiO ₂	TiO ₂	Cr ₂ O ₃	Ga ₂ O ₃	V ₂ O ₃	FeO	CaO	MgO	MnO	K ₂ O	Total
SapAw_23	Blue patches	Aw23TB1	101.263	0.011	0.053	0.006	0.010	0.000	0.052	0.004	0.008	0.000	0.001	101.408
		Aw23TB2	101.002	0.006	0.075	0.000	0.000	0.000	0.048	0.005	0.000	0.000	0.001	101.137
		Aw23TB3	99.934	0.017	0.048	0.000	0.014	0.006	0.028	0.000	0.000	0.000	0.006	100.053
		Aw23TB4	100.053	0.000	0.023	0.001	0.007	0.001	0.054	0.002	0.004	0.002	0.003	100.150
		Aw23TB5	101.198	0.002	0.053	0.000	0.012	0.006	0.049	0.000	0.000	0.000	0.003	101.323
		Aw23TB6	101.071	0.015	0.036	0.004	0.006	0.019	0.032	0.004	0.000	0.000	0.005	101.192
SapAw_24	Yellow body	Aw24TY1	99.925	0.010	0.015	0.002	0.006	0.001	0.077	0.004	0.015	0.000	0.000	100.055
		Aw24TY2	99.955	0.009	0.031	0.000	0.020	0.011	0.126	0.004	0.009	0.002	0.005	100.172
		Aw24TY3	99.563	0.015	0.026	0.000	0.007	0.008	0.137	0.003	0.023	0.000	0.000	99.782
		Aw24TY4	99.122	0.009	0.020	0.002	0.006	0.000	0.076	0.000	0.014	0.000	0.002	99.251
		Aw24TY5	99.396	0.000	0.012	0.000	0.009	0.019	0.087	0.001	0.012	0.000	0.003	99.539
		Aw24TY6	99.361	0.009	0.009	0.000	0.000	0.000	0.101	0.000	0.017	0.000	0.001	99.498
	Blue patches	Aw24TB1	99.668	0.028	0.159	0.001	0.003	0.027	0.023	0.004	0.000	0.000	0.000	99.913
		Aw24TB2	99.562	0.000	0.040	0.005	0.007	0.007	0.028	0.004	0.003	0.002	0.004	99.662
		Aw24TB3	98.915	0.004	0.048	0.002	0.011	0.000	0.053	0.000	0.001	0.004	0.003	99.041
		Aw24TB4	99.157	0.018	0.046	0.004	0.012	0.016	0.042	0.002	0.003	0.000	0.002	99.302
		Aw24TB5	98.628	0.019	0.039	0.002	0.008	0.005	0.054	0.002	0.000	0.002	0.000	98.759
		Aw24TB6	99.274	0.016	0.047	0.003	0.000	0.004	0.092	0.002	0.005	0.006	0.001	99.450
SapAw_25	Yellow body	Aw25TY1	98.829	0.011	0.025	0.000	0.008	0.013	0.152	0.000	0.015	0.004	0.000	99.057
		Aw25TY2	98.948	0.006	0.027	0.000	0.000	0.019	0.092	0.003	0.025	0.000	0.000	99.120
		Aw25TY3	98.624	0.006	0.126	0.004	0.012	0.011	0.071	0.003	0.007	0.003	0.003	98.870
		Aw25TY4	98.743	0.020	0.000	0.000	0.012	0.006	0.109	0.003	0.014	0.002	0.000	98.909
		Aw25TY5	98.820	0.003	0.007	0.003	0.004	0.000	0.092	0.008	0.007	0.000	0.000	98.944

Appendix E-1 (Continue).

Samples	Areas	Point	Al ₂ O ₃	SiO ₂	TiO ₂	Cr ₂ O ₃	Ga ₂ O ₃	V ₂ O ₃	FeO	CaO	MgO	MnO	K ₂ O	Total	
SapAw_25	Blue patches	Aw25TB1	99.884	0.008	0.052	0.000	0.000	0.000	0.055	0.000	0.000	0.000	0.001	100.000	
		Aw25TB2	99.849	0.000	0.057	0.000	0.006	0.001	0.075	0.006	0.002	0.000	0.003	100.000	
		Aw25TB3	99.922	0.006	0.017	0.000	0.004	0.000	0.040	0.003	0.002	0.001	0.004	100.000	
		Aw25TB4	99.869	0.029	0.007	0.000	0.011	0.006	0.070	0.000	0.005	0.003	0.000	100.000	
SapAw_26	Yellow body	Aw26TY1	98.728	0.000	0.033	0.008	0.000	0.000	0.058	0.004	0.000	0.003	0.002	98.836	
		Aw26TY2	99.068	0.011	0.007	0.000	0.012	0.009	0.061	0.001	0.007	0.000	0.000	99.176	
		Aw26TY3	99.053	0.011	0.014	0.004	0.020	0.000	0.063	0.000	0.008	0.000	0.000	99.173	
		Aw26TY4	98.672	0.013	0.000	0.000	0.000	0.008	0.016	0.004	0.010	0.000	0.000	98.723	
		Aw26TY5	99.054	0.007	0.014	0.001	0.002	0.014	0.070	0.001	0.003	0.000	0.000	99.166	
	Blue patches	Aw26TB1	99.976	0.001	0.001	0.000	0.000	0.000	0.020	0.000	0.000	0.000	0.000	0.002	100.000
		Aw26TB2	98.916	0.000	0.059	0.000	0.014	0.017	0.065	0.000	0.009	0.002	0.000	0.000	99.082
		Aw26TB3	98.748	0.008	0.051	0.005	0.000	0.000	0.087	0.007	0.009	0.000	0.005	98.920	
		Aw26TB4	98.778	0.009	0.078	0.005	0.012	0.020	0.050	0.000	0.003	0.000	0.003	98.958	
		Aw26TB5	99.419	0.002	0.041	0.000	0.022	0.007	0.077	0.000	0.008	0.000	0.001	99.577	
SapAw_27	Yellow body	Aw27TY1	100.098	0.002	0.004	0.000	0.007	0.002	0.040	0.004	0.001	0.000	0.003	100.161	
		Aw27TY2	100.371	0.012	0.009	0.000	0.011	0.010	0.075	0.000	0.000	0.004	0.000	100.492	
		Aw27TY3	100.653	0.006	0.016	0.001	0.010	0.022	0.081	0.002	0.010	0.002	0.001	100.804	
		Aw27TY4	100.353	0.008	0.006	0.000	0.020	0.010	0.106	0.000	0.010	0.004	0.003	100.520	

Appendix E-1 (Continue).

Samples	Areas	Point	Al ₂ O ₃	SiO ₂	TiO ₂	Cr ₂ O ₃	Ga ₂ O ₃	V ₂ O ₃	FeO	CaO	MgO	MnO	K ₂ O	Total	
SapAw_27	Blue patches	Aw27TB1	100.100	0.000	0.038	0.000	0.002	0.006	0.058	0.000	0.003	0.000	0.002	100.209	
		Aw27TB2	100.977	0.025	0.009	0.000	0.000	0.000	0.062	0.000	0.004	0.000	0.002	101.079	
		Aw27TB3	99.835	0.009	0.047	0.000	0.022	0.000	0.085	0.000	0.007	0.000	0.000	100.005	
		Aw27TB4	99.535	0.019	0.049	0.000	0.011	0.016	0.061	0.005	0.005	0.000	0.000	99.701	
		Aw27TB5	100.402	0.009	0.030	0.000	0.000	0.016	0.051	0.000	0.002	0.003	0.000	100.513	
		Aw27TB6	99.919	0.008	0.017	0.004	0.005	0.011	0.056	0.006	0.002	0.000	0.003	100.031	
SapAw_28	Yellow body	Aw28TY1	99.168	0.005	0.002	0.000	0.006	0.005	0.064	0.000	0.005	0.002	0.004	99.261	
		Aw28TY2	99.344	0.015	0.023	0.005	0.000	0.013	0.113	0.010	0.009	0.000	0.000	99.532	
		Aw28TY3	99.773	0.018	0.017	0.000	0.010	0.000	0.060	0.001	0.010	0.004	0.003	99.896	
		Aw28TY4	100.050	0.003	0.012	0.008	0.010	0.011	0.066	0.001	0.016	0.000	0.000	100.177	
		Aw28TY5	99.838	0.005	0.022	0.000	0.002	0.026	0.083	0.007	0.019	0.000	0.003	100.005	
		Aw28TY6	100.313	0.006	0.008	0.006	0.012	0.000	0.036	0.003	0.003	0.007	0.000	100.394	
	Blue patches	Aw28TB1	99.179	0.000	0.064	0.001	0.000	0.018	0.018	0.055	0.004	0.000	0.000	0.002	99.323
		Aw28TB2	99.266	0.008	0.034	0.000	0.010	0.015	0.059	0.000	0.011	0.003	0.002	99.408	
		Aw28TB3	100.390	0.020	0.031	0.000	0.023	0.013	0.136	0.003	0.021	0.000	0.001	100.638	
		Aw28TB4	100.164	0.007	0.136	0.002	0.003	0.003	0.036	0.004	0.000	0.002	0.000	100.357	
		Aw28TB5	98.650	0.020	0.029	0.001	0.012	0.000	0.058	0.000	0.002	0.000	0.000	98.772	
SapAw_29	Yellow body	Aw29TY1	99.827	0.004	0.015	0.001	0.019	0.000	0.118	0.000	0.010	0.001	0.005	100.000	
		Aw29TY2	99.845	0.013	0.010	0.000	0.017	0.000	0.097	0.005	0.010	0.000	0.002	100.000	
		Aw29TY3	99.746	0.000	0.025	0.000	0.010	0.009	0.181	0.000	0.028	0.000	0.000	100.000	
		Aw29TY4	99.835	0.022	0.014	0.001	0.001	0.012	0.091	0.003	0.020	0.000	0.000	100.000	

Appendix E-1 (Continue).

Samples	Areas	Point	Al ₂ O ₃	SiO ₂	TiO ₂	Cr ₂ O ₃	Ga ₂ O ₃	V ₂ O ₃	FeO	CaO	MgO	MnO	K ₂ O	Total
SapAw_29	Blue patches	Aw29TB1	99.852	0.000	0.070	0.000	0.018	0.001	0.047	0.007	0.000	0.002	0.002	100.000
		Aw29TB2	98.431	0.016	0.125	0.003	0.000	0.000	0.038	0.003	0.000	0.002	0.000	98.618
		Aw29TB3	99.900	0.015	0.020	0.000	0.016	0.009	0.029	0.005	0.005	0.000	0.000	100.000
		Aw29TB4	98.474	0.000	0.142	0.000	0.016	0.000	0.044	0.005	0.000	0.000	0.000	98.681
		Aw29TB5	99.001	0.008	0.010	0.004	0.003	0.002	0.037	0.003	0.000	0.000	0.002	99.070
		Aw29TB6	98.984	0.007	0.092	0.000	0.000	0.014	0.050	0.002	0.008	0.000	0.001	99.158
SapAw_30	Yellow body	Aw30TY1	100.940	0.024	0.013	0.009	0.002	0.012	0.109	0.002	0.011	0.000	0.000	101.122
		Aw30TY2	100.864	0.000	0.000	0.001	0.015	0.000	0.036	0.000	0.008	0.000	0.003	100.927
		Aw30TY3	100.732	0.019	0.007	0.008	0.019	0.000	0.093	0.001	0.012	0.002	0.004	100.897
		Aw30TY4	100.589	0.010	0.024	0.000	0.012	0.001	0.137	0.005	0.023	0.000	0.003	100.804
		Aw30TY5	100.391	0.005	0.015	0.000	0.017	0.016	0.058	0.000	0.002	0.000	0.000	100.504
		Aw30TY6	101.089	0.006	0.025	0.000	0.004	0.010	0.114	0.007	0.014	0.000	0.004	101.273
	Blue patches	Aw30TB1	94.647	0.958	0.254	0.000	0.006	0.000	0.084	0.025	0.232	0.001	0.031	96.238
		Aw30TB2	100.747	0.021	0.065	0.000	0.003	0.016	0.046	0.002	0.013	0.000	0.002	100.915
		Aw30TB3	100.804	0.024	0.035	0.005	0.009	0.000	0.053	0.008	0.003	0.000	0.002	100.943
		Aw30TB4	100.583	0.028	0.056	0.004	0.008	0.001	0.063	0.004	0.024	0.000	0.000	100.771
		Aw30TB5	100.983	0.015	0.030	0.002	0.008	0.004	0.047	0.000	0.000	0.006	0.002	101.097
		Aw30TB6	100.421	0.000	0.059	0.000	0.013	0.002	0.057	0.009	0.004	0.005	0.004	100.574
		Aw30TB7	100.541	0.021	0.022	0.000	0.004	0.015	0.150	0.003	0.008	0.000	0.000	100.764

Appendix E-1 (Continue).

Samples	Areas	Point	Al ₂ O ₃	SiO ₂	TiO ₂	Cr ₂ O ₃	Ga ₂ O ₃	V ₂ O ₃	FeO	CaO	MgO	MnO	K ₂ O	Total	
SapAw_31	Yellow body	Aw31TY1	100.945	0.026	0.001	0.006	0.006	0.011	0.079	0.002	0.013	0.000	0.000	101.089	
		Aw31TY2	100.775	0.000	0.015	0.003	0.001	0.013	0.091	0.000	0.000	0.000	0.004	100.902	
		Aw31TY3	100.657	0.016	0.016	0.004	0.009	0.000	0.084	0.002	0.015	0.000	0.000	100.803	
		Aw31TY4	100.998	0.023	0.010	0.000	0.005	0.000	0.091	0.000	0.007	0.000	0.000	101.134	
		Aw31TY5	101.163	0.018	0.032	0.000	0.005	0.000	0.122	0.000	0.009	0.000	0.002	101.351	
	Blue patches	Aw31TB1	99.795	0.024	0.108	0.002	0.014	0.000	0.058	0.000	0.000	0.000	0.000	0.000	100.000
		Aw31TB2	99.805	0.004	0.145	0.003	0.000	0.005	0.032	0.006	0.000	0.000	0.000	0.000	100.000
		Aw31TB3	101.334	0.123	0.073	0.000	0.009	0.000	0.056	0.002	0.046	0.001	0.006	101.650	
		Aw31TB4	101.376	0.000	0.052	0.006	0.022	0.000	0.051	0.000	0.004	0.000	0.002	101.513	
		Aw31TB5	100.572	0.017	0.028	0.000	0.000	0.000	0.031	0.000	0.005	0.000	0.000	100.653	
		Aw31TB6	100.584	0.010	0.046	0.000	0.020	0.000	0.027	0.000	0.000	0.000	0.000	0.003	100.690
		Aw31TB7	100.261	0.000	0.052	0.014	0.016	0.000	0.060	0.001	0.000	0.003	0.000	100.407	
	SapAw_32	Yellow body	Aw32TY1	100.900	0.005	0.010	0.000	0.022	0.000	0.104	0.000	0.007	0.000	0.005	101.053
Aw32TY2			101.097	0.015	0.010	0.009	0.012	0.009	0.103	0.000	0.011	0.000	0.003	101.269	
Aw32TY3			101.116	0.013	0.000	0.002	0.000	0.000	0.098	0.000	0.006	0.000	0.001	101.236	
Aw32TY4			101.043	0.002	0.028	0.000	0.016	0.005	0.065	0.002	0.012	0.004	0.000	101.177	
Aw32TY5			100.989	0.005	0.014	0.004	0.011	0.000	0.098	0.003	0.017	0.000	0.002	101.143	
Aw32TY6			101.000	0.003	0.013	0.004	0.006	0.000	0.101	0.004	0.017	0.001	0.000	101.149	
Blue patches		Aw32TB1	100.837	0.032	0.032	0.002	0.010	0.007	0.027	0.000	0.003	0.002	0.002	100.954	
		Aw32TB2	100.737	0.019	0.150	0.005	0.017	0.000	0.056	0.000	0.001	0.000	0.001	100.986	
		Aw32TB3	99.917	0.000	0.036	0.000	0.005	0.006	0.031	0.000	0.002	0.000	0.003	100.000	
		Aw32TB4	100.907	0.000	0.056	0.001	0.002	0.020	0.058	0.002	0.000	0.001	0.000	101.047	
		Aw32TB5	100.179	0.023	0.023	0.000	0.000	0.010	0.062	0.007	0.008	0.000	0.008	100.320	
		Aw32TB6	100.165	0.011	0.037	0.001	0.010	0.010	0.069	0.001	0.006	0.002	0.002	100.314	

Appendix E-1 (Continue).

Samples	Areas	Point	Al ₂ O ₃	SiO ₂	TiO ₂	Cr ₂ O ₃	Ga ₂ O ₃	V ₂ O ₃	FeO	CaO	MgO	MnO	K ₂ O	Total	
SapAw_33	Yellow body	Aw33-TC1-1	99.825	0.023	0.000	0.000	0.053	0.000	0.047	0.007	0.030	0.000	0.016	100.000	
		Aw33-TC1-2	99.938	0.000	0.006	0.001	0.000	0.000	0.039	0.005	0.010	0.000	0.000	100.000	
		Aw33-TC1-3	99.913	0.000	0.017	0.004	0.004	0.000	0.043	0.000	0.018	0.000	0.000	100.000	
	Blue patches	Aw33-TB1-1	99.836	0.011	0.053	0.000	0.000	0.000	0.000	0.079	0.000	0.009	0.000	0.011	100.000
		Aw33-TB1-2	99.782	0.028	0.017	0.000	0.009	0.000	0.127	0.014	0.022	0.000	0.000	100.000	
		Aw33-TB1-3	99.868	0.013	0.016	0.000	0.018	0.000	0.071	0.004	0.007	0.000	0.003	100.000	
		Aw33-TB2-1	99.818	0.021	0.017	0.000	0.008	0.000	0.098	0.015	0.009	0.010	0.004	100.000	
		Aw33-TB2-2	99.913	0.000	0.005	0.000	0.014	0.000	0.067	0.000	0.000	0.001	0.000	100.000	
		Aw33-TB2-3	99.939	0.002	0.000	0.000	0.000	0.000	0.033	0.002	0.013	0.009	0.001	100.000	

Appendix E-2 Major and trace element contents of light blue variety from Awissawella.

Samples	Areas	Point	Al ₂ O ₃	SiO ₂	TiO ₂	Cr ₂ O ₃	Ga ₂ O ₃	V ₂ O ₃	FeO	CaO	MgO	MnO	K ₂ O	Total
SapMa_01	Light blue body	Ma01-TC1-1	99.695	0.021	0.127	0.000	0.019	0.000	0.108	0.007	0.002	0.015	0.005	100.000
		Ma01-TC1-2	99.695	0.067	0.089	0.000	0.000	0.000	0.112	0.000	0.022	0.004	0.009	100.000
		Ma01-TC1-3	99.732	0.048	0.068	0.005	0.000	0.000	0.117	0.009	0.006	0.007	0.008	100.000
		Ma01-TC2-1	99.777	0.045	0.036	0.002	0.009	0.000	0.114	0.007	0.007	0.000	0.003	100.000
		Ma01-TC2-2	99.846	0.016	0.024	0.000	0.001	0.000	0.107	0.000	0.006	0.000	0.000	100.000
		Ma01-TC2-3	99.726	0.020	0.095	0.000	0.009	0.000	0.106	0.012	0.017	0.006	0.008	100.000
	Blue patches	Ma01-TB1-1	99.735	0.039	0.028	0.010	0.028	0.000	0.128	0.009	0.008	0.001	0.014	100.000
		Ma01-TB1-2	99.740	0.035	0.047	0.005	0.039	0.000	0.117	0.002	0.013	0.000	0.002	100.000
		Ma01-TB1-3	99.785	0.034	0.027	0.000	0.016	0.001	0.114	0.001	0.013	0.000	0.009	100.000
SapMa_02	Light blue body	Ma02-TC1-1	99.842	0.000	0.011	0.001	0.035	0.000	0.095	0.000	0.008	0.000	0.006	100.000
		Ma02-TC1-2	99.771	0.023	0.060	0.015	0.011	0.000	0.081	0.005	0.010	0.014	0.008	100.000
		Ma02-TC1-3	99.769	0.013	0.088	0.000	0.021	0.006	0.083	0.000	0.018	0.000	0.002	100.000
	Blue patches	Ma02-TLB1-1	99.826	0.000	0.023	0.000	0.026	0.000	0.108	0.012	0.000	0.000	0.005	100.000
		Ma02-TLB1-2	99.797	0.021	0.036	0.009	0.011	0.000	0.108	0.008	0.004	0.000	0.005	100.000
		Ma02-TLB1-3	99.855	0.000	0.019	0.009	0.010	0.000	0.096	0.006	0.000	0.000	0.004	100.000
		Ma02-TLB1-4	99.841	0.001	0.020	0.000	0.018	0.000	0.098	0.005	0.002	0.005	0.010	100.000

Appendix E-2 (Continue).

Samples	Areas	Point	Al ₂ O ₃	SiO ₂	TiO ₂	Cr ₂ O ₃	Ga ₂ O ₃	V ₂ O ₃	FeO	CaO	MgO	MnO	K ₂ O	Total
SapMa_03	Light blue body	Ma03-TC1-1	99.918	0.008	0.000	0.006	0.000	0.000	0.040	0.015	0.000	0.008	0.004	100.000
		Ma03-TC1-2	99.760	0.000	0.075	0.005	0.027	0.000	0.102	0.002	0.019	0.000	0.009	100.000
		Ma03-TC2-1	99.860	0.012	0.038	0.013	0.002	0.000	0.057	0.008	0.005	0.000	0.003	100.000
		Ma03-TC2-2	99.852	0.025	0.033	0.000	0.018	0.000	0.056	0.003	0.009	0.000	0.004	100.000
		Ma03-TC2-3	99.663	0.012	0.141	0.013	0.022	0.002	0.113	0.008	0.025	0.000	0.000	100.000
SapMa_04	Light blue body	Ma04-TC1-1	99.808	0.003	0.045	0.009	0.029	0.000	0.091	0.006	0.001	0.001	0.006	100.000
		Ma04-TC1-2	99.834	0.013	0.037	0.000	0.017	0.000	0.074	0.009	0.003	0.007	0.005	100.000
		Ma04-TC1-3	99.751	0.025	0.097	0.000	0.005	0.000	0.099	0.009	0.005	0.000	0.008	100.000
	Blue patches	Ma04-TB1-1	99.727	0.005	0.081	0.009	0.018	0.000	0.129	0.006	0.010	0.011	0.003	100.000
		Ma04-TB1-2	99.854	0.003	0.018	0.016	0.006	0.000	0.093	0.000	0.001	0.002	0.005	100.000
		Ma04-TB1-3	99.760	0.022	0.050	0.011	0.003	0.000	0.119	0.001	0.019	0.011	0.003	100.000
		Ma04-TB2-1	99.831	0.004	0.008	0.005	0.006	0.000	0.104	0.006	0.007	0.022	0.006	100.000
		Ma04-TB2-2	99.832	0.011	0.013	0.010	0.000	0.000	0.100	0.000	0.009	0.010	0.013	100.000
		Ma04-TB2-3	99.809	0.007	0.024	0.000	0.057	0.000	0.084	0.002	0.011	0.006	0.000	100.000
		SapMa_05	Light blue body	Ma05-TC1-1	99.815	0.032	0.045	0.001	0.000	0.000	0.102	0.005	0.000	0.000
Ma05-TC1-2	99.722			0.059	0.068	0.010	0.026	0.000	0.090	0.002	0.023	0.000	0.000	100.000
Ma05-TC1-3	99.718			0.052	0.095	0.000	0.013	0.000	0.093	0.004	0.012	0.008	0.004	100.000
Ma05-TC2-1	99.784			0.030	0.021	0.010	0.044	0.000	0.109	0.000	0.000	0.000	0.002	100.000
Ma05-TC2-2	99.710			0.018	0.111	0.023	0.027	0.000	0.099	0.000	0.006	0.000	0.005	100.000
Ma05-TC2-3	99.744			0.048	0.069	0.000	0.020	0.000	0.106	0.001	0.009	0.000	0.003	100.000
Blue patches	Ma05-TB1-1		99.774	0.019	0.099	0.000	0.020	0.000	0.077	0.000	0.008	0.001	0.001	100.000
	Ma05-TB1-2		99.767	0.036	0.077	0.000	0.008	0.000	0.093	0.002	0.013	0.000	0.003	100.000

Appendix E-2 (Continue).

Samples	Areas	Point	Al ₂ O ₃	SiO ₂	TiO ₂	Cr ₂ O ₃	Ga ₂ O ₃	V ₂ O ₃	FeO	CaO	MgO	MnO	K ₂ O	Total	
SapMa_06	Light blue body	Ma06-TC1-1	99.796	0.022	0.017	0.000	0.016	0.000	0.130	0.000	0.016	0.000	0.002	100.000	
		Ma06-TC1-2	99.893	0.022	0.006	0.010	0.000	0.000	0.044	0.002	0.012	0.000	0.010	100.000	
		Ma06-TC1-3	99.851	0.022	0.009	0.009	0.032	0.000	0.068	0.000	0.001	0.007	0.000	100.000	
		Ma06-TC2-1	99.741	0.028	0.005	0.015	0.019	0.000	0.179	0.002	0.005	0.003	0.002	100.000	
		Ma06-TC2-2	99.780	0.032	0.024	0.006	0.000	0.000	0.122	0.012	0.012	0.002	0.009	100.000	
		Ma06-TC2-3	99.773	0.051	0.038	0.000	0.014	0.000	0.111	0.000	0.014	0.000	0.000	100.000	
	Blue patches	Ma06-TB1-1	99.779	0.030	0.029	0.015	0.033	0.000	0.099	0.002	0.010	0.000	0.002	100.000	
		Ma06-TB1-2	99.746	0.077	0.147	0.000	0.009	0.000	0.016	0.000	0.000	0.000	0.005	100.000	
		Ma06-TB1-3	99.813	0.026	0.013	0.000	0.000	0.000	0.115	0.004	0.007	0.012	0.009	100.000	
SapMa_07	Light blue body	Ma07-TC1-1	99.561	0.018	0.223	0.000	0.015	0.000	0.145	0.007	0.017	0.013	0.000	100.000	
		Ma07-TC1-2	99.748	0.031	0.065	0.003	0.016	0.000	0.107	0.003	0.021	0.001	0.004	100.000	
		Ma07-TC1-3	99.649	0.021	0.189	0.000	0.011	0.000	0.118	0.000	0.010	0.000	0.002	100.000	
		Ma07-TC2-1	99.661	0.002	0.143	0.000	0.049	0.000	0.124	0.002	0.014	0.000	0.006	100.000	
		Ma07-TC2-2	99.657	0.027	0.181	0.000	0.014	0.000	0.110	0.000	0.011	0.000	0.000	100.000	
		Ma07-TC2-3	99.657	0.009	0.168	0.000	0.026	0.000	0.126	0.000	0.014	0.000	0.000	100.000	
	Blue patches	Ma07-TB1-1	99.825	0.000	0.028	0.013	0.000	0.000	0.000	0.110	0.004	0.000	0.009	0.010	100.000
		Ma07-TB1-2	99.856	0.001	0.015	0.003	0.009	0.000	0.000	0.088	0.009	0.009	0.007	0.002	100.000
		Ma07-TB1-3	99.789	0.002	0.031	0.000	0.041	0.000	0.000	0.097	0.006	0.012	0.018	0.003	100.000

Appendix E-2 (Continue).

Samples	Areas	Point	Al ₂ O ₃	SiO ₂	TiO ₂	Cr ₂ O ₃	Ga ₂ O ₃	V ₂ O ₃	FeO	CaO	MgO	MnO	K ₂ O	Total	
SapMa_08	Light blue body	Ma08TLB1	100.625	0.000	0.044	0.000	0.000	0.022	0.076	0.002	0.009	0.000	0.006	100.784	
		Ma08TLB2	101.061	0.009	0.041	0.003	0.011	0.000	0.072	0.000	0.006	0.002	0.001	101.206	
		Ma08TLB3	100.382	0.010	0.050	0.000	0.010	0.002	0.083	0.003	0.008	0.002	0.005	100.555	
	Blue patches	Ma08TB1	100.826	0.000	0.010	0.000	0.009	0.000	0.000	0.076	0.003	0.000	0.000	0.000	100.924
		Ma08TB2	100.934	0.000	0.022	0.000	0.013	0.000	0.000	0.085	0.004	0.000	0.000	0.006	101.064
		Ma08TB3	100.522	0.003	0.090	0.002	0.004	0.007	0.106	0.006	0.009	0.001	0.005	100.755	
SapMa09	Light blue body	Ma09TLB1	100.596	0.007	0.112	0.000	0.023	0.002	0.121	0.004	0.017	0.001	0.000	100.883	
		Ma09TLB2	100.554	0.008	0.166	0.007	0.009	0.015	0.122	0.003	0.026	0.000	0.002	100.912	
		Ma09TLB3	99.969	0.012	0.089	0.001	0.008	0.000	0.176	0.007	0.035	0.005	0.001	100.303	
		Ma09TLB4	100.472	0.006	0.169	0.000	0.000	0.003	0.104	0.001	0.009	0.000	0.003	100.767	
	Blue patches	Ma09TB1	96.604	2.014	0.103	0.000	0.000	0.026	0.187	0.032	0.722	0.003	0.036	99.727	
		Ma09TB2	100.477	0.029	0.076	0.000	0.017	0.000	0.162	0.004	0.039	0.005	0.004	100.813	
		Ma09TB3	100.510	0.009	0.026	0.000	0.014	0.000	0.137	0.008	0.021	0.000	0.002	100.727	
		Ma09TB4	100.191	0.013	0.074	0.002	0.004	0.016	0.194	0.002	0.044	0.000	0.007	100.547	
SapMa10	Light blue body	Ma10TLB1	100.851	0.009	0.006	0.000	0.000	0.016	0.087	0.011	0.007	0.003	0.006	100.996	
		Ma10TLB2	101.033	0.004	0.026	0.000	0.017	0.008	0.085	0.000	0.000	0.000	0.000	101.173	
		Ma10TLB3	100.764	0.002	0.004	0.000	0.008	0.004	0.094	0.004	0.000	0.000	0.007	100.887	
	Blue patches	Ma10TB1	101.051	0.000	0.003	0.003	0.007	0.020	0.085	0.005	0.003	0.002	0.003	101.182	
		Ma10TB2	100.850	0.007	0.010	0.005	0.024	0.000	0.096	0.003	0.000	0.000	0.003	100.998	
		Ma10TB3	100.526	0.000	0.010	0.002	0.016	0.000	0.090	0.000	0.011	0.000	0.004	100.659	

Appendix E-2 (Continue).

Samples	Areas	Point	Al ₂ O ₃	SiO ₂	TiO ₂	Cr ₂ O ₃	Ga ₂ O ₃	V ₂ O ₃	FeO	CaO	MgO	MnO	K ₂ O	Total	
SapMa_11	Light blue body	Ma11TLB1	100.736	0.017	0.022	0.000	0.014	0.009	0.096	0.002	0.007	0.000	0.005	100.908	
		Ma11TLB2	100.959	0.015	0.092	0.000	0.026	0.005	0.109	0.009	0.013	0.000	0.004	101.232	
		Ma11TLB3	100.382	0.017	0.025	0.004	0.000	0.007	0.091	0.004	0.000	0.003	0.006	100.539	
		Ma11TLB4	100.708	0.009	0.023	0.003	0.008	0.000	0.079	0.005	0.003	0.001	0.003	100.842	
		Ma11TLB5	100.414	0.030	0.019	0.000	0.000	0.000	0.097	0.005	0.005	0.000	0.001	100.571	
SapMa_12	Light blue body	Ma12TLB1	99.636	0.010	0.033	0.004	0.017	0.034	0.102	0.000	0.012	0.000	0.004	99.852	
		Ma12TLB2	99.585	0.000	0.059	0.003	0.021	0.007	0.099	0.002	0.009	0.000	0.006	99.791	
		Ma12TLB3	99.701	0.005	0.023	0.003	0.016	0.013	0.106	0.000	0.007	0.000	0.001	99.875	
		Ma12TLB4	99.814	0.022	0.042	0.000	0.011	0.002	0.099	0.006	0.003	0.000	0.000	100.000	
		Ma12TLB5	99.866	0.009	0.013	0.000	0.006	0.000	0.098	0.001	0.004	0.000	0.003	100.000	
SapMa_13	Light blue body	Ma13TLB1	100.036	0.004	0.036	0.005	0.013	0.000	0.411	0.000	0.019	0.001	0.000	100.525	
		Ma13TLB2	100.041	0.007	0.036	0.001	0.016	0.002	0.375	0.007	0.013	0.000	0.006	100.504	
	Blue patches	Ma13TB1	100.667	0.002	0.021	0.001	0.000	0.000	0.000	0.327	0.003	0.007	0.003	0.000	101.031
		Ma13TB2	100.123	0.015	0.033	0.004	0.002	0.000	0.000	0.365	0.004	0.020	0.000	0.001	100.567
		Ma13TB3	100.515	0.009	0.024	0.000	0.000	0.004	0.004	0.345	0.004	0.023	0.000	0.006	100.930
		Ma13TB4	100.111	0.014	0.014	0.001	0.000	0.022	0.022	0.335	0.002	0.008	0.005	0.004	100.516
		Ma13TB5	96.096	0.029	2.340	0.003	0.000	0.028	2.077	0.003	0.164	0.002	0.005	100.747	

Appendix E-3 Atomic proportion based on 3 oxygen atoms of major and trace elements contained in Awissawella yellow variety.

Samples	Areas	Point	Elements											Total*
			Al	Si	Ti	Cr	Ga	V	Fe	Ca	Mg	Mn	K	
SapAw_01	Yellow body	Aw01-TC1-1	1.997	0.000	0.000	0.000	0.000	0.000	0.002	0.000	0.001	0.000	0.000	2.000
		Aw01-TC1-2	1.997	0.000	0.000	0.000	0.000	0.000	0.002	0.000	0.001	0.000	0.000	2.000
		Aw01-TC1-3	1.997	0.000	0.000	0.000	0.000	0.000	0.001	0.000	0.000	0.000	0.000	2.000
		Aw01-TC1-4	1.998	0.000	0.000	0.000	0.000	0.000	0.001	0.000	0.000	0.000	0.000	2.000
	Blue patches	Aw01-TB1-1	1.997	0.000	0.001	0.000	0.000	0.000	0.001	0.000	0.000	0.000	0.000	2.000
		Aw01-TB1-2	1.997	0.000	0.001	0.000	0.000	0.000	0.001	0.000	0.000	0.000	0.000	2.000
		Aw01-TB1-3	1.998	0.000	0.001	0.000	0.000	0.000	0.000	0.000	0.000	0.000	0.000	2.000
		Aw01-TB2-1	1.999	0.001	0.000	0.000	0.000	0.000	0.000	0.000	0.000	0.000	0.000	2.000
		Aw01-TB2-2	1.997	0.000	0.001	0.000	0.000	0.000	0.000	0.001	0.000	0.000	0.000	2.000
	SapAw_02	Yellow body	Aw02-TC1-1	1.998	0.000	0.000	0.000	0.000	0.000	0.001	0.000	0.000	0.000	0.000
Aw02-TC1-2			1.997	0.000	0.000	0.000	0.000	0.000	0.002	0.000	0.000	0.000	0.000	2.000
Aw02-TC1-3			1.997	0.000	0.000	0.000	0.000	0.000	0.002	0.000	0.000	0.000	0.000	2.000
Blue patches		Aw02-TB1-1	1.998	0.000	0.000	0.000	0.000	0.000	0.001	0.000	0.000	0.000	0.000	2.000
		Aw02-TB1-2	1.997	0.000	0.001	0.000	0.000	0.000	0.001	0.000	0.000	0.000	0.000	2.000
		Aw02-TB1-3	1.997	0.000	0.001	0.000	0.000	0.000	0.001	0.000	0.001	0.000	0.000	2.000
SapAw_03	Yellow body	Aw03-TC1-1	1.998	0.000	0.000	0.000	0.000	0.000	0.001	0.000	0.000	0.000	0.000	2.000
		Aw03-TC1-2	1.996	0.000	0.002	0.000	0.000	0.000	0.000	0.000	0.000	0.000	0.000	1.999
		Aw03-TC1-3	1.997	0.000	0.001	0.000	0.000	0.000	0.000	0.001	0.000	0.000	0.000	2.000

Appendix E-3 (Continue).

Samples	Areas	Point	Elements											Total*	
			Al	Si	Ti	Cr	Ga	V	Fe	Ca	Mg	Mn	K		
SapAw_03	Blue patches	Aw03-TB1-1	1.998	0.000	0.001	0.000	0.000	0.000	0.000	0.000	0.000	0.000	0.000	0.000	2.000
		Aw03-TB1-2	1.998	0.001	0.001	0.000	0.000	0.000	0.000	0.001	0.000	0.000	0.000	0.000	2.000
		Aw03-TB1-3	1.998	0.000	0.001	0.000	0.000	0.000	0.000	0.001	0.000	0.000	0.000	0.000	2.000
		Aw03-TB1-4	1.998	0.000	0.001	0.000	0.000	0.000	0.000	0.001	0.000	0.000	0.000	0.000	2.000
		Aw03-TB1-5	1.998	0.000	0.001	0.000	0.000	0.000	0.000	0.001	0.000	0.000	0.000	0.000	2.000
		Aw03-TB2-1	1.997	0.000	0.001	0.000	0.000	0.000	0.000	0.001	0.000	0.000	0.000	0.000	2.000
		Aw03-TB2-2	1.998	0.000	0.001	0.000	0.000	0.000	0.000	0.001	0.000	0.000	0.000	0.000	2.000
SapAw_04	Yellow body	Aw04-TC1-1	1.997	0.000	0.000	0.000	0.000	0.000	0.000	0.001	0.000	0.001	0.000	0.000	2.000
		Aw04-TC1-2	1.998	0.000	0.000	0.000	0.000	0.000	0.000	0.002	0.000	0.000	0.000	0.000	2.000
		Aw04-TC1-3	1.998	0.000	0.000	0.000	0.000	0.000	0.000	0.001	0.000	0.000	0.000	0.000	2.000
		Aw04-TC1-4	1.997	0.001	0.000	0.000	0.000	0.000	0.000	0.001	0.000	0.001	0.000	0.000	2.000
	Blue patches	Aw04-TB1-1	1.997	0.000	0.000	0.000	0.000	0.000	0.000	0.002	0.000	0.000	0.000	0.000	2.000
		Aw04-TB1-2	1.998	0.000	0.001	0.000	0.000	0.000	0.000	0.001	0.000	0.000	0.000	0.000	2.000
		Aw04-TB1-3	1.997	0.001	0.001	0.000	0.000	0.000	0.000	0.001	0.000	0.000	0.000	0.000	2.000
		Aw04-TB1-4	1.998	0.000	0.000	0.000	0.000	0.000	0.000	0.001	0.000	0.000	0.000	0.000	2.000
		Aw04-TB1-5	1.998	0.000	0.001	0.000	0.000	0.000	0.000	0.001	0.000	0.000	0.000	0.000	2.000
		Aw04-TB1-6	1.998	0.000	0.001	0.000	0.000	0.000	0.000	0.001	0.000	0.000	0.000	0.000	2.000
SapAw_05	Yellow body	Aw05-TC1-1	1.995	0.000	0.003	0.000	0.000	0.000	0.000	0.001	0.000	0.000	0.000	0.000	1.999
		Aw05-TC1-2	1.994	0.000	0.003	0.000	0.000	0.000	0.000	0.000	0.000	0.000	0.000	0.000	1.999
		Aw05-TC1-3	1.997	0.000	0.001	0.000	0.000	0.000	0.000	0.001	0.000	0.000	0.000	0.000	2.000
		Aw05-TC2-1	1.997	0.000	0.000	0.000	0.000	0.000	0.000	0.002	0.000	0.001	0.000	0.000	2.000
		Aw05-TC2-2	1.998	0.000	0.000	0.000	0.000	0.000	0.000	0.001	0.000	0.000	0.000	0.000	2.000

Appendix E-3 (Continue).

Samples	Areas	Point	Elements											Total*
			Al	Si	Ti	Cr	Ga	V	Fe	Ca	Mg	Mn	K	
SapAw_05	Blue patches	Aw05-TLB1-1	1.998	0.000	0.001	0.000	0.000	0.000	0.001	0.000	0.000	0.000	0.000	2.000
		Aw05-TLB1-2	1.997	0.000	0.001	0.000	0.000	0.000	0.001	0.000	0.000	0.000	0.000	2.000
		Aw05-TLB2-1	1.998	0.000	0.001	0.000	0.000	0.000	0.001	0.000	0.000	0.000	0.000	2.000
		Aw05-TLB2-2	1.997	0.000	0.000	0.000	0.000	0.000	0.001	0.000	0.000	0.000	0.000	2.000
		Aw05-TB1-1	1.998	0.001	0.000	0.000	0.000	0.000	0.001	0.000	0.000	0.000	0.000	2.000
		Aw05-TB1-2	1.997	0.000	0.001	0.000	0.000	0.000	0.001	0.000	0.000	0.000	0.000	2.000
SapAw_06	Yellow body	Aw06-TC1-1	1.999	0.000	0.000	0.000	0.000	0.000	0.001	0.000	0.000	0.000	0.000	2.000
		Aw06-TC1-2	1.999	0.000	0.000	0.000	0.000	0.000	0.001	0.000	0.000	0.000	0.000	2.000
		Aw06-TC1-3	1.998	0.000	0.000	0.000	0.000	0.000	0.001	0.000	0.000	0.000	0.000	2.000
		Aw06-TC2-1	1.998	0.000	0.000	0.000	0.000	0.000	0.001	0.000	0.001	0.000	0.000	2.000
		Aw06-TC2-2	1.998	0.000	0.000	0.000	0.000	0.000	0.001	0.000	0.000	0.000	0.000	2.000
	Blue patches	Aw06-TB1-1	1.997	0.000	0.001	0.000	0.000	0.000	0.000	0.001	0.000	0.000	0.000	2.000
		Aw06-TB1-2	1.997	0.000	0.000	0.000	0.000	0.000	0.000	0.001	0.000	0.000	0.000	2.000
		Aw06-TB1-3	1.998	0.000	0.000	0.000	0.000	0.000	0.000	0.001	0.000	0.000	0.000	2.000
	SapAw_07	Yellow body	Aw07-C1-1	1.999	0.000	0.000	0.000	0.000	0.000	0.000	0.000	0.000	0.000	0.000
Aw07-C1-2			1.998	0.000	0.000	0.000	0.000	0.000	0.001	0.000	0.000	0.000	0.000	2.000
Aw07-C1-3			1.997	0.000	0.000	0.000	0.000	0.000	0.001	0.000	0.000	0.000	0.000	2.000
Aw07-C1-4			1.998	0.000	0.000	0.000	0.000	0.000	0.001	0.000	0.000	0.000	0.000	2.000

Appendix E-3 (Continue).

Samples	Areas	Point	Elements											Total*
			Al	Si	Ti	Cr	Ga	V	Fe	Ca	Mg	Mn	K	
SapAw_07	Blue patches	Aw07-TB1-1	1.997	0.000	0.001	0.000	0.000	0.000	0.001	0.000	0.000	0.000	0.000	2.000
		Aw07-TB1-2	1.997	0.000	0.000	0.000	0.000	0.000	0.001	0.000	0.000	0.000	0.000	2.000
		Aw07-TB1-3	1.993	0.003	0.001	0.000	0.000	0.000	0.001	0.000	0.000	0.000	0.000	1.999
		Aw07-TB1-4	1.998	0.000	0.001	0.000	0.000	0.000	0.000	0.000	0.000	0.000	0.000	2.000
		Aw07-TB2-1	1.998	0.000	0.000	0.000	0.000	0.000	0.001	0.000	0.000	0.000	0.000	2.000
		Aw07-TB2-2	1.997	0.000	0.000	0.000	0.000	0.000	0.002	0.000	0.000	0.000	0.000	2.000
		Aw07-TB2-3	1.997	0.000	0.000	0.000	0.000	0.000	0.001	0.000	0.000	0.000	0.000	2.000
SapAw_08	Yellow body	Aw08-TC1-1	1.997	0.000	0.002	0.000	0.000	0.000	0.001	0.000	0.000	0.000	0.000	1.999
		Aw08-TC1-2	1.997	0.001	0.001	0.000	0.001	0.000	0.001	0.000	0.000	0.000	0.000	2.000
		Aw08-TC1-3	1.995	0.001	0.002	0.000	0.000	0.000	0.001	0.000	0.000	0.000	0.000	1.999
		Aw08-TC1-4	1.997	0.001	0.001	0.000	0.000	0.000	0.001	0.000	0.000	0.000	0.000	2.000
	Blue patches	Aw08-TB1-1	1.997	0.000	0.001	0.000	0.000	0.000	0.001	0.000	0.000	0.000	0.000	2.000
		Aw08-TB1-2	1.997	0.001	0.001	0.000	0.000	0.000	0.001	0.000	0.000	0.000	0.000	2.000
		Aw08-TB1-3	1.998	0.000	0.001	0.000	0.000	0.000	0.001	0.000	0.000	0.000	0.000	2.000
		Aw08-TB1-4	1.997	0.001	0.000	0.000	0.000	0.000	0.001	0.000	0.000	0.000	0.000	2.000
SapAw_09	Yellow body	Aw09-TC1-1	1.998	0.000	0.000	0.000	0.000	0.000	0.001	0.000	0.000	0.000	0.000	2.000
		Aw09-TC1-2	1.998	0.001	0.000	0.000	0.000	0.000	0.001	0.000	0.000	0.000	0.000	2.000
		Aw09-TC1-3	1.997	0.001	0.000	0.000	0.000	0.000	0.001	0.000	0.001	0.000	0.000	2.000
		Aw09-TC1-4	1.998	0.001	0.000	0.000	0.000	0.000	0.001	0.000	0.000	0.000	0.000	2.000

Appendix E-3 (Continue).

Samples	Areas	Point	Elements											Total*
			Al	Si	Ti	Cr	Ga	V	Fe	Ca	Mg	Mn	K	
SapAw_09	Blue patches	Aw09-TB1-1	1.997	0.000	0.001	0.000	0.000	0.000	0.001	0.000	0.000	0.000	0.000	2.000
		Aw09-TB1-2	1.998	0.000	0.000	0.000	0.000	0.000	0.001	0.000	0.000	0.000	0.000	2.000
		Aw09-TB1-3	1.991	0.000	0.006	0.000	0.000	0.000	0.000	0.000	0.000	0.000	0.000	1.998
		Aw09-TB1-4	1.997	0.000	0.001	0.000	0.000	0.000	0.001	0.000	0.000	0.000	0.000	2.000
		Aw09-TB1-5	1.997	0.000	0.001	0.000	0.000	0.000	0.001	0.000	0.000	0.000	0.000	2.000
		Aw09-TB2-1	1.997	0.001	0.001	0.000	0.000	0.000	0.001	0.000	0.000	0.000	0.000	2.000
		Aw09-TB2-2	1.997	0.000	0.001	0.000	0.000	0.000	0.001	0.000	0.000	0.000	0.000	2.000
SapAw_10	Yellow body	Aw10-TC1-3	1.998	0.000	0.000	0.000	0.000	0.000	0.001	0.000	0.000	0.000	0.000	2.000
		Aw10-TC1-2	1.998	0.000	0.000	0.000	0.000	0.000	0.001	0.000	0.000	0.000	0.000	2.000
		Aw10-TC1-1	1.998	0.000	0.000	0.000	0.000	0.000	0.001	0.000	0.000	0.000	0.000	2.000
	Blue patches	Aw10-TB3-1	1.997	0.000	0.001	0.000	0.000	0.000	0.001	0.000	0.000	0.000	0.000	2.000
		Aw10-TB3-2	1.997	0.000	0.001	0.000	0.000	0.000	0.001	0.000	0.000	0.000	0.000	2.000
		Aw10-TB3-3	1.997	0.000	0.001	0.000	0.000	0.000	0.001	0.000	0.000	0.000	0.000	2.000
		Aw10-TB1-1	1.998	0.000	0.000	0.000	0.000	0.000	0.001	0.000	0.000	0.000	0.000	2.000
		Aw10-TB1-2	1.997	0.000	0.001	0.000	0.000	0.000	0.001	0.000	0.000	0.000	0.000	2.000
		Aw10-TB1-3	1.998	0.000	0.000	0.000	0.000	0.000	0.001	0.000	0.000	0.000	0.000	2.000
		Aw10-TB2-1	1.999	0.000	0.000	0.000	0.000	0.000	0.000	0.000	0.000	0.000	0.000	2.000
Aw10-TB2-2	1.998	0.000	0.001	0.000	0.000	0.000	0.001	0.000	0.000	0.000	0.000	2.000		
Aw10-TB2-3	1.997	0.001	0.000	0.000	0.000	0.000	0.001	0.000	0.000	0.000	0.000	2.000		

Appendix E-3 (Continue).

Samples	Areas	Point	Elements											Total*		
			Al	Si	Ti	Cr	Ga	V	Fe	Ca	Mg	Mn	K			
SapAw_11	Yellow body	Aw11-TC1-1	1.996	0.001	0.000	0.000	0.000	0.000	0.000	0.002	0.000	0.001	0.000	0.000	2.000	
		Aw11-TC1-2	1.998	0.001	0.000	0.000	0.000	0.000	0.000	0.001	0.000	0.000	0.000	0.000	2.000	
		Aw11-TC1-3	1.999	0.000	0.000	0.000	0.000	0.000	0.000	0.000	0.000	0.000	0.000	0.000	2.000	
	Blue patches	Aw11-TB1-1	1.997	0.000	0.001	0.000	0.000	0.000	0.000	0.001	0.000	0.000	0.000	0.000	1.999	
		Aw11-TB1-2	1.998	0.000	0.001	0.000	0.000	0.000	0.000	0.001	0.000	0.000	0.000	0.000	2.000	
		Aw11-TB1-3	1.997	0.000	0.001	0.000	0.000	0.000	0.000	0.002	0.000	0.000	0.000	0.000	2.000	
		Aw11-TB2-1	1.998	0.000	0.000	0.000	0.000	0.000	0.000	0.001	0.000	0.000	0.000	0.000	2.000	
		Aw11-TB2-2	1.997	0.001	0.000	0.000	0.000	0.000	0.000	0.001	0.000	0.000	0.000	0.000	2.000	
		Aw11-TB2-3	1.998	0.001	0.000	0.000	0.000	0.000	0.000	0.000	0.000	0.000	0.000	0.000	2.000	
		Aw11-TB3-1	1.997	0.001	0.000	0.000	0.000	0.000	0.000	0.001	0.000	0.000	0.000	0.000	2.000	
		Aw11-TB3-2	1.998	0.000	0.001	0.000	0.000	0.000	0.000	0.000	0.000	0.000	0.000	0.000	2.000	
		Aw11-TB3-3	1.997	0.000	0.000	0.000	0.000	0.000	0.000	0.001	0.000	0.000	0.000	0.000	2.000	
	SapAw_12	Yellow body	Aw12-TC1-1	1.995	0.000	0.003	0.000	0.000	0.000	0.000	0.001	0.000	0.000	0.000	0.000	1.999
			Aw12-TC1-2	1.998	0.000	0.000	0.000	0.000	0.000	0.000	0.001	0.000	0.000	0.000	0.000	2.000
		Blue patches	Aw12-TB1-1	1.998	0.000	0.001	0.000	0.000	0.000	0.000	0.001	0.000	0.000	0.000	0.000	2.000
Aw12-TB1-2			1.997	0.000	0.001	0.000	0.000	0.000	0.000	0.001	0.000	0.000	0.000	0.000	2.000	
Aw12-TB1-3			1.995	0.000	0.003	0.000	0.000	0.000	0.000	0.000	0.000	0.000	0.000	0.000	1.999	

Appendix E-3 (Continue).

Samples	Areas	Point	Elements											Total*	
			Al	Si	Ti	Cr	Ga	V	Fe	Ca	Mg	Mn	K		
SapAw_13	Yellow body	Aw13-TC1-1	1.997	0.000	0.000	0.000	0.000	0.000	0.000	0.001	0.000	0.001	0.000	0.000	2.000
		Aw13-TC1-2	1.998	0.000	0.000	0.000	0.000	0.000	0.000	0.001	0.000	0.000	0.000	0.000	2.000
		Aw13-TC1-3	1.997	0.000	0.000	0.000	0.000	0.000	0.000	0.002	0.000	0.000	0.000	0.000	2.000
	Blue patches	Aw13-TB1-1	1.998	0.000	0.001	0.000	0.000	0.000	0.000	0.001	0.000	0.000	0.000	0.000	2.000
		Aw13-TB1-2	1.998	0.000	0.000	0.000	0.000	0.000	0.000	0.001	0.000	0.000	0.000	0.000	2.000
		Aw13-TB1-3	1.997	0.000	0.001	0.000	0.000	0.000	0.000	0.001	0.000	0.000	0.000	0.000	2.000
SapAw_14	Yellow body	Aw14-TC1-1	1.998	0.000	0.000	0.000	0.000	0.000	0.000	0.001	0.000	0.000	0.000	0.000	2.000
		Aw14-TC1-2	1.997	0.000	0.000	0.000	0.000	0.000	0.000	0.001	0.000	0.000	0.000	0.000	2.000
		Aw14-TC1-3	1.998	0.000	0.000	0.000	0.000	0.000	0.000	0.001	0.000	0.000	0.000	0.000	2.000
		Aw14-TC1-4	1.998	0.000	0.000	0.000	0.000	0.000	0.000	0.001	0.000	0.000	0.000	0.000	2.000
	Blue patches	Aw14-TB1-1	1.998	0.000	0.001	0.000	0.000	0.000	0.000	0.000	0.000	0.000	0.000	0.000	2.000
		Aw14-TB1-2	1.997	0.001	0.001	0.000	0.000	0.000	0.000	0.001	0.000	0.000	0.000	0.000	2.000
Aw14-TB1-3		1.998	0.000	0.000	0.000	0.000	0.000	0.000	0.001	0.000	0.000	0.000	0.000	2.000	
SapAw_15	Yellow body	Aw15-TC1-1	1.998	0.001	0.000	0.000	0.000	0.000	0.000	0.001	0.000	0.000	0.000	0.000	2.000
		Aw15-TC1-2	1.998	0.000	0.000	0.000	0.000	0.000	0.000	0.001	0.000	0.000	0.000	0.000	2.000
		Aw15-TC1-3	1.999	0.000	0.000	0.000	0.000	0.000	0.000	0.001	0.000	0.000	0.000	0.000	2.000
	Blue patches	Aw15-TB1-1	1.998	0.000	0.000	0.000	0.000	0.000	0.000	0.001	0.000	0.000	0.000	0.000	2.000
		Aw15-TB1-2	1.998	0.000	0.000	0.000	0.000	0.000	0.000	0.001	0.000	0.000	0.000	0.000	2.000
		Aw15-TB1-3	1.998	0.000	0.001	0.000	0.000	0.000	0.000	0.000	0.000	0.000	0.000	0.000	2.000
		Aw15-TB2-1	1.993	0.000	0.004	0.000	0.000	0.000	0.000	0.001	0.000	0.000	0.000	0.000	1.999
		Aw15-TB2-2	1.998	0.000	0.000	0.000	0.000	0.000	0.000	0.001	0.000	0.000	0.000	0.000	2.000
Aw15-TB2-3	1.997	0.000	0.000	0.000	0.000	0.000	0.000	0.002	0.000	0.000	0.000	0.000	2.000		

Appendix E-3 (Continue).

Samples	Areas	Point	Elements											Total*	
			Al	Si	Ti	Cr	Ga	V	Fe	Ca	Mg	Mn	K		
SapAw_16	Yellow body	Aw16-TC1-1	1.997	0.000	0.000	0.000	0.000	0.000	0.000	0.001	0.000	0.001	0.000	0.000	2.000
		Aw16-TC1-2	1.997	0.000	0.000	0.000	0.000	0.000	0.000	0.002	0.000	0.001	0.000	0.000	2.000
		Aw16-TC1-3	1.997	0.000	0.000	0.000	0.000	0.000	0.000	0.002	0.000	0.001	0.000	0.000	2.000
		Aw16-TC2-1	1.998	0.000	0.000	0.000	0.000	0.000	0.000	0.001	0.000	0.000	0.000	0.000	2.000
		Aw16-TC2-2	1.998	0.000	0.000	0.000	0.000	0.000	0.000	0.001	0.000	0.000	0.000	0.000	2.000
		Aw16-TC2-3	1.998	0.000	0.000	0.000	0.000	0.000	0.000	0.001	0.000	0.001	0.000	0.000	2.000
	Blue patches	Aw16-TB1-1	1.999	0.000	0.000	0.000	0.000	0.000	0.000	0.000	0.000	0.000	0.000	0.000	2.000
		Aw16-TB1-2	1.998	0.000	0.001	0.000	0.000	0.000	0.000	0.001	0.000	0.000	0.000	0.000	2.000
		Aw16-TB1-3	1.998	0.000	0.000	0.000	0.000	0.000	0.000	0.000	0.000	0.000	0.000	0.000	2.000
		Aw16-TB2-1	1.998	0.000	0.001	0.000	0.000	0.000	0.000	0.001	0.000	0.000	0.000	0.000	2.000
Aw16-TB2-2		1.999	0.000	0.000	0.000	0.000	0.000	0.000	0.001	0.000	0.000	0.000	0.000	2.000	
SapAw_17	Yellow body	Aw17-TC1-1	1.997	0.000	0.000	0.000	0.000	0.000	0.000	0.002	0.000	0.000	0.000	0.000	2.000
		Aw17-TC1-2	1.997	0.000	0.001	0.000	0.000	0.000	0.000	0.001	0.000	0.000	0.000	0.000	2.000
		Aw17-TC1-3	1.998	0.000	0.000	0.000	0.000	0.000	0.000	0.001	0.000	0.000	0.000	0.000	2.000
		Aw17-TC2-1	1.996	0.000	0.000	0.000	0.000	0.000	0.000	0.002	0.000	0.000	0.000	0.000	2.000
		Aw17-TC2-2	1.997	0.000	0.000	0.000	0.000	0.000	0.000	0.001	0.000	0.000	0.000	0.000	2.000
	Blue patches	Aw17-TB1-1	1.998	0.000	0.001	0.000	0.000	0.000	0.000	0.001	0.000	0.000	0.000	0.000	2.000
		Aw17-TB1-2	1.998	0.000	0.001	0.000	0.000	0.000	0.000	0.001	0.000	0.000	0.000	0.000	2.000
		Aw17-TB1-3	1.997	0.000	0.001	0.000	0.000	0.000	0.000	0.001	0.000	0.000	0.000	0.000	2.000
		Aw17-TB2-1	1.997	0.000	0.001	0.000	0.000	0.000	0.000	0.001	0.000	0.000	0.000	0.000	2.000
		Aw17-TB2-2	1.998	0.000	0.001	0.000	0.000	0.000	0.000	0.001	0.000	0.000	0.000	0.000	2.000
		Aw17-TB2-3	1.998	0.000	0.001	0.000	0.000	0.000	0.001	0.000	0.000	0.000	0.000	2.000	

Appendix E-3 (Continue).

Samples	Areas	Point	Elements											Total*	
			Al	Si	Ti	Cr	Ga	V	Fe	Ca	Mg	Mn	K		
SapAw_18	Yellow body	Aw18-TC1-1	1.996	0.000	0.000	0.000	0.000	0.000	0.000	0.003	0.000	0.000	0.000	0.000	2.000
		Aw18-TC1-2	1.998	0.000	0.000	0.000	0.000	0.000	0.000	0.001	0.000	0.000	0.000	0.000	2.000
		Aw18-TC1-3	1.997	0.000	0.000	0.000	0.000	0.000	0.000	0.001	0.000	0.000	0.000	0.000	2.000
		Aw18-TC1-4	1.998	0.000	0.000	0.000	0.000	0.000	0.000	0.002	0.000	0.000	0.000	0.000	2.000
	Blue patches	Aw18-TB1-1	1.997	0.000	0.001	0.000	0.000	0.000	0.000	0.001	0.000	0.000	0.000	0.000	2.000
		Aw18-TB1-2	1.998	0.000	0.001	0.000	0.000	0.000	0.000	0.001	0.000	0.000	0.000	0.000	2.000
		Aw18-TB1-3	1.998	0.000	0.001	0.000	0.000	0.000	0.000	0.001	0.000	0.000	0.000	0.000	2.000
		Aw18-TB1-4	1.997	0.000	0.000	0.000	0.000	0.000	0.000	0.001	0.000	0.000	0.000	0.000	2.000
SapAw_19	Yellow body	Aw19-TC1-1	1.999	0.000	0.000	0.000	0.000	0.000	0.000	0.000	0.000	0.000	0.000	0.000	2.000
		Aw19-TC1-2	1.998	0.000	0.000	0.000	0.000	0.000	0.000	0.000	0.000	0.000	0.000	0.000	2.000
		Aw19-TC1-3	1.999	0.000	0.000	0.000	0.000	0.000	0.000	0.001	0.000	0.000	0.000	0.000	2.000
		Aw19-TC1-4	1.999	0.000	0.000	0.000	0.000	0.000	0.000	0.000	0.000	0.000	0.000	0.000	2.000
	Blue patches	Aw19-TB1-1	1.999	0.000	0.000	0.000	0.000	0.000	0.000	0.000	0.000	0.000	0.000	0.000	2.000
		Aw19-TB1-2	1.997	0.000	0.001	0.000	0.000	0.000	0.000	0.001	0.000	0.000	0.000	0.000	2.000
		Aw19-TB1-3	1.997	0.000	0.001	0.000	0.000	0.000	0.000	0.001	0.000	0.000	0.000	0.000	2.000
		Aw19-TB1-4	1.998	0.000	0.000	0.000	0.000	0.000	0.000	0.001	0.000	0.000	0.000	0.000	2.000

Appendix E-3 (Continue).

Samples	Areas	Point	Elements										Total*	
			Al	Si	Ti	Cr	Ga	V	Fe	Ca	Mg	Mn		K
SapAw_20	Yellow body	Aw20-TC1-1	1.997	0.000	0.000	0.000	0.000	0.000	0.001	0.000	0.000	0.000	0.000	2.000
		Aw20-TC1-2	1.995	0.000	0.002	0.000	0.000	0.000	0.001	0.000	0.000	0.000	0.000	1.999
		Aw20-TC1-3	1.997	0.001	0.001	0.000	0.000	0.000	0.001	0.000	0.000	0.000	0.000	2.000
		Aw20-TC1-4	1.998	0.000	0.000	0.000	0.000	0.000	0.001	0.000	0.000	0.000	0.000	2.000
	Blue patches	Aw20-TLB1-1	1.998	0.000	0.001	0.000	0.000	0.000	0.001	0.000	0.000	0.000	0.000	2.000
		Aw20-TLB1-2	1.998	0.000	0.001	0.000	0.000	0.000	0.001	0.000	0.000	0.000	0.000	2.000
Aw20-TLB1-3		1.998	0.000	0.001	0.000	0.000	0.000	0.001	0.000	0.000	0.000	0.000	2.000	
SapAw_21	Yellow body	Aw21TY1	1.998	0.000	0.000	0.000	0.000	0.000	0.001	0.000	0.000	0.000	0.000	2.000
		Aw21TY2	1.998	0.000	0.000	0.000	0.000	0.000	0.001	0.000	0.000	0.000	0.000	2.000
		Aw21TY3	1.996	0.001	0.001	0.000	0.000	0.000	0.001	0.000	0.001	0.000	0.000	2.000
		Aw21TY4	1.998	0.000	0.000	0.000	0.000	0.000	0.001	0.000	0.000	0.000	0.000	2.000
		Aw21TY5	1.998	0.000	0.000	0.000	0.000	0.000	0.001	0.000	0.000	0.000	0.000	2.000
		Aw21TY6	1.998	0.000	0.000	0.000	0.000	0.000	0.001	0.000	0.000	0.000	0.000	2.000
	Blue patches	Aw21TB1	1.997	0.000	0.001	0.000	0.000	0.000	0.000	0.001	0.000	0.000	0.000	2.000
		Aw21TB2	1.998	0.000	0.000	0.000	0.000	0.000	0.000	0.000	0.000	0.000	0.000	2.000
		Aw21TB3	1.998	0.000	0.000	0.000	0.000	0.000	0.000	0.001	0.000	0.000	0.000	2.000
		Aw21TB4	1.996	0.000	0.001	0.000	0.000	0.000	0.000	0.001	0.000	0.000	0.000	2.000
		Aw21TB5	1.997	0.000	0.001	0.000	0.000	0.000	0.000	0.001	0.000	0.000	0.000	2.000
		Aw21TB6	1.998	0.000	0.001	0.000	0.000	0.000	0.000	0.001	0.000	0.000	0.000	2.000

Appendix E-3 (Continue).

Samples	Areas	Point	Elements											Total*
			Al	Si	Ti	Cr	Ga	V	Fe	Ca	Mg	Mn	K	
SapAw_22	Yellow body	Aw22TY1	1.998	0.000	0.000	0.000	0.000	0.000	0.001	0.000	0.000	0.000	0.000	2.000
		Aw22TY2	1.998	0.000	0.000	0.000	0.000	0.000	0.001	0.000	0.000	0.000	0.000	2.000
		Aw22TY3	1.998	0.000	0.000	0.000	0.000	0.000	0.001	0.000	0.000	0.000	0.000	2.000
		Aw22TY4	1.997	0.000	0.001	0.000	0.000	0.000	0.001	0.000	0.000	0.000	0.000	2.000
		Aw22TY5	1.996	0.000	0.002	0.000	0.000	0.000	0.000	0.000	0.000	0.000	0.000	1.999
		Aw22TY6	1.999	0.000	0.000	0.000	0.000	0.000	0.000	0.000	0.000	0.000	0.000	2.000
	Blue patches	Aw22TB1	1.997	0.000	0.001	0.000	0.000	0.000	0.001	0.000	0.000	0.000	0.000	2.000
		Aw22TB3	1.999	0.000	0.000	0.000	0.000	0.000	0.000	0.000	0.000	0.000	0.000	2.000
		Aw22TB4	1.999	0.000	0.000	0.000	0.000	0.000	0.000	0.000	0.000	0.000	0.000	2.000
		Aw22TB5	1.998	0.000	0.001	0.000	0.000	0.000	0.001	0.000	0.000	0.000	0.000	2.000
		Aw22TB6	1.998	0.000	0.001	0.000	0.000	0.000	0.001	0.000	0.000	0.000	0.000	2.000
SapAw_23	Yellow body	Aw23TY1	1.998	0.000	0.000	0.000	0.000	0.000	0.001	0.000	0.000	0.000	0.000	2.000
		Aw23TY2	1.998	0.000	0.000	0.000	0.000	0.000	0.001	0.000	0.000	0.000	0.000	2.000
		Aw23TY3	1.997	0.000	0.000	0.000	0.000	0.000	0.002	0.000	0.000	0.000	0.000	2.000
		Aw23TY4	1.998	0.000	0.000	0.000	0.000	0.000	0.001	0.000	0.000	0.000	0.000	2.000
		Aw23TY5	1.998	0.000	0.000	0.000	0.000	0.000	0.001	0.000	0.000	0.000	0.000	2.000

Appendix E-3 (Continue).

Samples	Areas	Point	Elements											Total*
			Al	Si	Ti	Cr	Ga	V	Fe	Ca	Mg	Mn	K	
SapAw_23	Blue patches	Aw23TB1	1.998	0.000	0.001	0.000	0.000	0.000	0.001	0.000	0.000	0.000	0.000	2.000
		Aw23TB2	1.998	0.000	0.001	0.000	0.000	0.000	0.001	0.000	0.000	0.000	0.000	2.000
		Aw23TB3	1.998	0.000	0.001	0.000	0.000	0.000	0.000	0.000	0.000	0.000	0.000	2.000
		Aw23TB4	1.999	0.000	0.000	0.000	0.000	0.000	0.001	0.000	0.000	0.000	0.000	2.000
		Aw23TB5	1.998	0.000	0.001	0.000	0.000	0.000	0.001	0.000	0.000	0.000	0.000	2.000
		Aw23TB6	1.998	0.000	0.000	0.000	0.000	0.000	0.000	0.000	0.000	0.000	0.000	2.000
SapAw_24	Yellow body	Aw24TY1	1.998	0.000	0.000	0.000	0.000	0.000	0.001	0.000	0.000	0.000	0.000	2.000
		Aw24TY2	1.997	0.000	0.000	0.000	0.000	0.000	0.002	0.000	0.000	0.000	0.000	2.000
		Aw24TY3	1.997	0.000	0.000	0.000	0.000	0.000	0.000	0.002	0.000	0.001	0.000	2.000
		Aw24TY4	1.998	0.000	0.000	0.000	0.000	0.000	0.001	0.000	0.000	0.000	0.000	2.000
		Aw24TY5	1.998	0.000	0.000	0.000	0.000	0.000	0.001	0.000	0.000	0.000	0.000	2.000
		Aw24TY6	1.998	0.000	0.000	0.000	0.000	0.000	0.001	0.000	0.000	0.000	0.000	2.000
	Blue patches	Aw24TB1	1.996	0.000	0.002	0.000	0.000	0.000	0.000	0.000	0.000	0.000	0.000	1.999
		Aw24TB2	1.999	0.000	0.001	0.000	0.000	0.000	0.000	0.000	0.000	0.000	0.000	2.000
		Aw24TB3	1.998	0.000	0.001	0.000	0.000	0.000	0.001	0.000	0.000	0.000	0.000	2.000
		Aw24TB4	1.998	0.000	0.001	0.000	0.000	0.000	0.001	0.000	0.000	0.000	0.000	2.000
		Aw24TB5	1.998	0.000	0.001	0.000	0.000	0.000	0.001	0.000	0.000	0.000	0.000	2.000
		Aw24TB6	1.997	0.000	0.001	0.000	0.000	0.000	0.001	0.000	0.000	0.000	0.000	2.000

Appendix E-3 (Continue).

Samples	Areas	Point	Elements											Total*
			Al	Si	Ti	Cr	Ga	V	Fe	Ca	Mg	Mn	K	
SapAw_25	Yellow body	Aw25TY1	1.997	0.000	0.000	0.000	0.000	0.000	0.002	0.000	0.000	0.000	0.000	2.000
		Aw25TY2	1.997	0.000	0.000	0.000	0.000	0.000	0.001	0.000	0.001	0.000	0.000	2.000
		Aw25TY3	1.996	0.000	0.002	0.000	0.000	0.000	0.001	0.000	0.000	0.000	0.000	2.000
		Aw25TY4	1.998	0.000	0.000	0.000	0.000	0.000	0.001	0.000	0.000	0.000	0.000	2.000
		Aw25TY5	1.998	0.000	0.000	0.000	0.000	0.000	0.001	0.000	0.000	0.000	0.000	2.000
	Blue patches	Aw25TB1	1.998	0.000	0.001	0.000	0.000	0.000	0.001	0.000	0.000	0.000	0.000	2.000
		Aw25TB2	1.998	0.000	0.001	0.000	0.000	0.000	0.001	0.000	0.000	0.000	0.000	2.000
		Aw25TB3	1.999	0.000	0.000	0.000	0.000	0.000	0.001	0.000	0.000	0.000	0.000	2.000
Aw25TB4		1.998	0.000	0.000	0.000	0.000	0.000	0.001	0.000	0.000	0.000	0.000	2.000	
SapAw_26	Yellow body	Aw26TY1	1.998	0.000	0.000	0.000	0.000	0.000	0.001	0.000	0.000	0.000	0.000	2.000
		Aw26TY2	1.998	0.000	0.000	0.000	0.000	0.000	0.001	0.000	0.000	0.000	0.000	2.000
		Aw26TY3	1.998	0.000	0.000	0.000	0.000	0.000	0.001	0.000	0.000	0.000	0.000	2.000
		Aw26TY4	1.999	0.000	0.000	0.000	0.000	0.000	0.000	0.000	0.000	0.000	0.000	2.000
		Aw26TY5	1.998	0.000	0.000	0.000	0.000	0.000	0.001	0.000	0.000	0.000	0.000	2.000
	Blue patches	Aw26TB1	2.000	0.000	0.000	0.000	0.000	0.000	0.000	0.000	0.000	0.000	0.000	2.000
		Aw26TB2	1.998	0.000	0.001	0.000	0.000	0.000	0.001	0.000	0.000	0.000	0.000	2.000
		Aw26TB3	1.997	0.000	0.001	0.000	0.000	0.000	0.001	0.000	0.000	0.000	0.000	2.000
		Aw26TB4	1.997	0.000	0.001	0.000	0.000	0.000	0.001	0.000	0.000	0.000	0.000	2.000
		Aw26TB5	1.998	0.000	0.001	0.000	0.000	0.000	0.001	0.000	0.000	0.000	0.000	2.000

Appendix E-3 (Continue).

Samples	Areas	Point	Elements											Total*	
			Al	Si	Ti	Cr	Ga	V	Fe	Ca	Mg	Mn	K		
SapAw_27	Yellow body	Aw27TY1	1.999	0.000	0.000	0.000	0.000	0.000	0.001	0.000	0.000	0.000	0.000	2.000	
		Aw27TY2	1.998	0.000	0.000	0.000	0.000	0.000	0.001	0.000	0.000	0.000	0.000	2.000	
		Aw27TY3	1.998	0.000	0.000	0.000	0.000	0.000	0.001	0.000	0.000	0.000	0.000	2.000	
		Aw27TY4	1.998	0.000	0.000	0.000	0.000	0.000	0.001	0.000	0.000	0.000	0.000	2.000	
	Blue patches	Aw27TB1	1.998	0.000	0.000	0.000	0.000	0.000	0.001	0.000	0.000	0.000	0.000	2.000	
		Aw27TB2	1.998	0.000	0.000	0.000	0.000	0.000	0.001	0.000	0.000	0.000	0.000	2.000	
		Aw27TB3	1.998	0.000	0.001	0.000	0.000	0.000	0.001	0.000	0.000	0.000	0.000	2.000	
		Aw27TB4	1.997	0.000	0.001	0.000	0.000	0.000	0.001	0.000	0.000	0.000	0.000	2.000	
		Aw27TB5	1.998	0.000	0.000	0.000	0.000	0.000	0.001	0.000	0.000	0.000	0.000	2.000	
		Aw27TB6	1.998	0.000	0.000	0.000	0.000	0.000	0.001	0.000	0.000	0.000	0.000	2.000	
	SapAw_28	Yellow body	Aw28TY1	1.999	0.000	0.000	0.000	0.000	0.000	0.001	0.000	0.000	0.000	0.000	2.000
			Aw28TY2	1.997	0.000	0.000	0.000	0.000	0.000	0.001	0.000	0.000	0.000	0.000	2.000
Aw28TY3			1.998	0.000	0.000	0.000	0.000	0.000	0.001	0.000	0.000	0.000	0.000	2.000	
Aw28TY4			1.998	0.000	0.000	0.000	0.000	0.000	0.001	0.000	0.000	0.000	0.000	2.000	
Aw28TY5			1.998	0.000	0.000	0.000	0.000	0.000	0.001	0.000	0.000	0.000	0.000	2.000	
Aw28TY6			1.999	0.000	0.000	0.000	0.000	0.000	0.000	0.000	0.000	0.000	0.000	2.000	
Blue patches		Aw28TB1	1.998	0.000	0.001	0.000	0.000	0.000	0.001	0.000	0.000	0.000	0.000	2.000	
		Aw28TB2	1.998	0.000	0.000	0.000	0.000	0.000	0.001	0.000	0.000	0.000	0.000	2.000	
		Aw28TB3	1.996	0.000	0.000	0.000	0.000	0.000	0.002	0.000	0.001	0.000	0.000	2.000	
		Aw28TB4	1.997	0.000	0.002	0.000	0.000	0.000	0.000	0.000	0.000	0.000	0.000	1.999	
		Aw28TB5	1.998	0.000	0.000	0.000	0.000	0.000	0.001	0.000	0.000	0.000	0.000	2.000	

Appendix E-3 (Continue).

Samples	Areas	Point	Elements											Total*	
			Al	Si	Ti	Cr	Ga	V	Fe	Ca	Mg	Mn	K		
SapAw_29	Yellow body	Aw29TY1	1.998	0.000	0.000	0.000	0.000	0.000	0.000	0.002	0.000	0.000	0.000	0.000	2.000
		Aw29TY2	1.998	0.000	0.000	0.000	0.000	0.000	0.000	0.001	0.000	0.000	0.000	0.000	2.000
		Aw29TY3	1.997	0.000	0.000	0.000	0.000	0.000	0.000	0.002	0.000	0.001	0.000	0.000	2.000
		Aw29TY4	1.998	0.000	0.000	0.000	0.000	0.000	0.000	0.001	0.000	0.001	0.000	0.000	2.000
	Blue patches	Aw29TB1	1.998	0.000	0.001	0.000	0.000	0.000	0.000	0.001	0.000	0.000	0.000	0.000	2.000
		Aw29TB3	1.998	0.000	0.000	0.000	0.000	0.000	0.000	0.000	0.000	0.000	0.000	0.000	2.000
		Aw29TB5	1.999	0.000	0.000	0.000	0.000	0.000	0.000	0.000	0.000	0.000	0.000	0.000	2.000
		Aw29TB6	1.997	0.000	0.001	0.000	0.000	0.000	0.000	0.001	0.000	0.000	0.000	0.000	2.000
SapAw_30	Yellow body	Aw30TY1	1.997	0.000	0.000	0.000	0.000	0.000	0.001	0.000	0.000	0.000	0.000	0.000	2.000
		Aw30TY2	1.999	0.000	0.000	0.000	0.000	0.000	0.000	0.000	0.000	0.000	0.000	0.000	2.000
		Aw30TY3	1.998	0.000	0.000	0.000	0.000	0.000	0.000	0.001	0.000	0.000	0.000	0.000	2.000
		Aw30TY4	1.997	0.000	0.000	0.000	0.000	0.000	0.000	0.002	0.000	0.001	0.000	0.000	2.000
		Aw30TY5	1.998	0.000	0.000	0.000	0.000	0.000	0.000	0.001	0.000	0.000	0.000	0.000	2.000
		Aw30TY6	1.997	0.000	0.000	0.000	0.000	0.000	0.000	0.001	0.000	0.000	0.000	0.000	2.000
	Blue patches	Aw30TB2	1.997	0.000	0.001	0.000	0.000	0.000	0.000	0.001	0.000	0.000	0.000	0.000	2.000
		Aw30TB3	1.998	0.000	0.000	0.000	0.000	0.000	0.000	0.001	0.000	0.000	0.000	0.000	2.000
		Aw30TB4	1.997	0.000	0.001	0.000	0.000	0.000	0.000	0.001	0.000	0.001	0.000	0.000	2.000
		Aw30TB5	1.998	0.000	0.000	0.000	0.000	0.000	0.000	0.001	0.000	0.000	0.000	0.000	2.000
		Aw30TB6	1.998	0.000	0.001	0.000	0.000	0.000	0.000	0.001	0.000	0.000	0.000	0.000	2.000
		Aw30TB7	1.997	0.000	0.000	0.000	0.000	0.000	0.000	0.002	0.000	0.000	0.000	0.000	2.000

Appendix E-3 (Continue).

Samples	Areas	Point	Elements											Total*
			Al	Si	Ti	Cr	Ga	V	Fe	Ca	Mg	Mn	K	
SapAw_31	Yellow body	Aw31TY1	1.998	0.000	0.000	0.000	0.000	0.000	0.001	0.000	0.000	0.000	0.000	2.000
		Aw31TY2	1.998	0.000	0.000	0.000	0.000	0.000	0.001	0.000	0.000	0.000	0.000	2.000
		Aw31TY3	1.998	0.000	0.000	0.000	0.000	0.000	0.001	0.000	0.000	0.000	0.000	2.000
		Aw31TY4	1.998	0.000	0.000	0.000	0.000	0.000	0.001	0.000	0.000	0.000	0.000	2.000
		Aw31TY5	1.997	0.000	0.000	0.000	0.000	0.000	0.002	0.000	0.000	0.000	0.000	2.000
	Blue patches	Aw31TB1	1.997	0.000	0.001	0.000	0.000	0.000	0.001	0.000	0.000	0.000	0.000	1.999
		Aw31TB2	1.997	0.000	0.002	0.000	0.000	0.000	0.000	0.000	0.000	0.000	0.000	1.999
		Aw31TB3	1.994	0.002	0.001	0.000	0.000	0.000	0.001	0.000	0.001	0.000	0.000	1.999
		Aw31TB4	1.998	0.000	0.001	0.000	0.000	0.000	0.001	0.000	0.000	0.000	0.000	2.000
		Aw31TB5	1.999	0.000	0.000	0.000	0.000	0.000	0.000	0.000	0.000	0.000	0.000	2.000
		Aw31TB6	1.998	0.000	0.001	0.000	0.000	0.000	0.000	0.000	0.000	0.000	0.000	2.000
		Aw31TB7	1.998	0.000	0.001	0.000	0.000	0.000	0.000	0.001	0.000	0.000	0.000	2.000
	SapAw_32	Yellow body	Aw32TY1	1.998	0.000	0.000	0.000	0.000	0.000	0.001	0.000	0.000	0.000	0.000
Aw32TY2			1.998	0.000	0.000	0.000	0.000	0.000	0.001	0.000	0.000	0.000	0.000	2.000
Aw32TY3			1.998	0.000	0.000	0.000	0.000	0.000	0.001	0.000	0.000	0.000	0.000	2.000
Aw32TY4			1.998	0.000	0.000	0.000	0.000	0.000	0.001	0.000	0.000	0.000	0.000	2.000
Aw32TY5			1.998	0.000	0.000	0.000	0.000	0.000	0.001	0.000	0.000	0.000	0.000	2.000
Aw32TY6			1.998	0.000	0.000	0.000	0.000	0.000	0.001	0.000	0.000	0.000	0.000	2.000
Blue patches		Aw32TB1	1.998	0.001	0.000	0.000	0.000	0.000	0.000	0.000	0.000	0.000	0.000	2.000
		Aw32TB2	1.996	0.000	0.002	0.000	0.000	0.000	0.001	0.000	0.000	0.000	0.000	1.999
		Aw32TB3	1.999	0.000	0.000	0.000	0.000	0.000	0.000	0.000	0.000	0.000	0.000	2.000
		Aw32TB4	1.998	0.000	0.001	0.000	0.000	0.000	0.001	0.000	0.000	0.000	0.000	2.000
		Aw32TB5	1.998	0.000	0.000	0.000	0.000	0.000	0.001	0.000	0.000	0.000	0.000	2.000
		Aw32TB6	1.998	0.000	0.000	0.000	0.000	0.000	0.001	0.000	0.000	0.000	0.000	2.000

Appendix E-3 (Continue).

Samples	Areas	Point	Elements											Total*
			Al	Si	Ti	Cr	Ga	V	Fe	Ca	Mg	Mn	K	
SapAw_33	Yellow body	Aw33-TC1-1	1.998	0.000	0.000	0.000	0.001	0.000	0.001	0.000	0.001	0.000	0.000	2.000
		Aw33-TC1-2	1.999	0.000	0.000	0.000	0.000	0.000	0.001	0.000	0.000	0.000	0.000	2.000
		Aw33-TC1-3	1.999	0.000	0.000	0.000	0.000	0.000	0.001	0.000	0.000	0.000	0.000	2.000
	Blue patches	Aw33-TB1-1	1.998	0.000	0.001	0.000	0.000	0.000	0.001	0.000	0.000	0.000	0.000	2.000
		Aw33-TB1-2	1.997	0.000	0.000	0.000	0.000	0.000	0.002	0.000	0.001	0.000	0.000	2.000
		Aw33-TB1-3	1.998	0.000	0.000	0.000	0.000	0.000	0.001	0.000	0.000	0.000	0.000	2.000
		Aw33-TB1-4	1.997	0.000	0.000	0.000	0.000	0.000	0.001	0.000	0.000	0.000	0.000	2.000
		Aw33-TB1-5	1.999	0.000	0.000	0.000	0.000	0.000	0.001	0.000	0.000	0.000	0.000	2.000
		Aw33-TB1-6	1.999	0.000	0.000	0.000	0.000	0.000	0.000	0.000	0.000	0.000	0.000	2.000

Appendix E-4 Atomic proportion based on 3 oxygen atoms of major and trace elements contained in Awissawella light blue variety.

Samples	Areas	Point	Elements											Total*
			Al	Si	Ti	Cr	Ga	V	Fe	Ca	Mg	Mn	K	
SapMa_01	Light blue body	Ma01-TC1-1	1.995	0.000	0.002	0.000	0.000	0.000	0.001	0.000	0.000	0.000	0.000	2.000
		Ma01-TC1-2	1.995	0.001	0.001	0.000	0.000	0.000	0.001	0.000	0.001	0.000	0.000	2.000
		Ma01-TC1-3	1.996	0.001	0.001	0.000	0.000	0.000	0.001	0.000	0.000	0.000	0.000	2.000
		Ma01-TC2-1	1.997	0.001	0.000	0.000	0.000	0.000	0.001	0.000	0.000	0.000	0.000	2.000
		Ma01-TC2-2	1.998	0.000	0.000	0.000	0.000	0.000	0.001	0.000	0.000	0.000	0.000	2.000
		Ma01-TC2-3	1.996	0.000	0.001	0.000	0.000	0.000	0.001	0.000	0.000	0.000	0.000	2.000
	Blue patches	Ma01-TB1-1	1.996	0.001	0.000	0.000	0.000	0.000	0.002	0.000	0.000	0.000	0.000	2.000
		Ma01-TB1-2	1.996	0.001	0.001	0.000	0.000	0.000	0.002	0.000	0.000	0.000	0.000	2.000
		Ma01-TB1-3	1.997	0.001	0.000	0.000	0.000	0.000	0.001	0.000	0.000	0.000	0.000	2.000
SapMa_02	Light blue body	Ma02-TC1-1	1.998	0.000	0.000	0.000	0.000	0.000	0.001	0.000	0.000	0.000	0.000	2.000
		Ma02-TC1-2	1.997	0.000	0.001	0.000	0.000	0.000	0.001	0.000	0.000	0.000	0.000	2.000
		Ma02-TC1-3	1.997	0.000	0.001	0.000	0.000	0.000	0.001	0.000	0.000	0.000	0.000	2.000
	Blue patches	Ma02-TLB1-1	1.998	0.000	0.000	0.000	0.000	0.000	0.001	0.000	0.000	0.000	0.000	2.000
		Ma02-TLB1-2	1.997	0.000	0.000	0.000	0.000	0.000	0.001	0.000	0.000	0.000	0.000	2.000
		Ma02-TLB1-3	1.998	0.000	0.000	0.000	0.000	0.000	0.001	0.000	0.000	0.000	0.000	2.000
		Ma02-TLB1-4	1.998	0.000	0.000	0.000	0.000	0.000	0.001	0.000	0.000	0.000	0.000	2.000
SapMa_03	Light blue body	Ma03-TC1-1	1.999	0.000	0.000	0.000	0.000	0.000	0.001	0.000	0.000	0.000	0.000	2.000
		Ma03-TC1-2	1.997	0.000	0.001	0.000	0.000	0.000	0.001	0.000	0.000	0.000	0.000	2.000
		Ma03-TC1-3	1.998	0.000	0.000	0.000	0.000	0.000	0.001	0.000	0.000	0.000	0.000	2.000
		Ma03-TC2-1	1.998	0.000	0.000	0.000	0.000	0.000	0.001	0.000	0.000	0.000	0.000	2.000
		Ma03-TC2-2	1.995	0.000	0.002	0.000	0.000	0.000	0.001	0.000	0.001	0.000	0.000	2.000
		Ma03-TC2-3	1.999	0.000	0.000	0.000	0.000	0.000	0.001	0.000	0.000	0.000	0.000	2.000

Appendix E-4 (Continue).

Samples	Areas	Point	Elements											Total*	
			Al	Si	Ti	Cr	Ga	V	Fe	Ca	Mg	Mn	K		
SapMa_04	Light blue body	Ma04-TC1-1	1.997	0.000	0.001	0.000	0.000	0.000	0.000	0.001	0.000	0.000	0.000	0.000	2.000
		Ma04-TC1-2	1.998	0.000	0.000	0.000	0.000	0.000	0.000	0.001	0.000	0.000	0.000	0.000	2.000
		Ma04-TC1-3	1.996	0.000	0.001	0.000	0.000	0.000	0.000	0.001	0.000	0.000	0.000	0.000	2.000
	Blue patches	Ma04-TB1-1	1.996	0.000	0.001	0.000	0.000	0.000	0.000	0.002	0.000	0.000	0.000	0.000	2.000
		Ma04-TB1-2	1.998	0.000	0.000	0.000	0.000	0.000	0.000	0.001	0.000	0.000	0.000	0.000	2.000
		Ma04-TB1-3	1.996	0.000	0.001	0.000	0.000	0.000	0.000	0.002	0.000	0.000	0.000	0.000	2.000
		Ma04-TB2-1	1.998	0.000	0.000	0.000	0.000	0.000	0.000	0.001	0.000	0.000	0.000	0.000	2.000
		Ma04-TB2-2	1.998	0.000	0.000	0.000	0.000	0.000	0.000	0.001	0.000	0.000	0.000	0.000	2.000
		Ma04-TB2-3	1.997	0.000	0.000	0.000	0.000	0.001	0.000	0.001	0.000	0.000	0.000	0.000	2.000
SapMa_05	Light blue body	Ma05-TC1-1	1.997	0.001	0.001	0.000	0.000	0.000	0.000	0.001	0.000	0.000	0.000	0.000	2.000
		Ma05-TC1-2	1.996	0.001	0.001	0.000	0.000	0.000	0.000	0.001	0.000	0.001	0.000	0.000	2.000
		Ma05-TC1-3	1.996	0.001	0.001	0.000	0.000	0.000	0.000	0.001	0.000	0.000	0.000	0.000	2.000
		Ma05-TC2-1	1.997	0.001	0.000	0.000	0.000	0.000	0.000	0.001	0.000	0.000	0.000	0.000	2.000
		Ma05-TC2-2	1.996	0.000	0.001	0.000	0.000	0.000	0.000	0.001	0.000	0.000	0.000	0.000	2.000
		Ma05-TC2-3	1.996	0.001	0.001	0.000	0.000	0.000	0.000	0.001	0.000	0.000	0.000	0.000	2.000
	Blue patches	Ma05-TB1-1	1.997	0.000	0.001	0.000	0.000	0.000	0.000	0.001	0.000	0.000	0.000	0.000	2.000
		Ma05-TB1-2	1.996	0.001	0.001	0.000	0.000	0.000	0.000	0.001	0.000	0.000	0.000	0.000	2.000

Appendix E-4 (Continue).

Samples	Areas	Point	Elements											Total*	
			Al	Si	Ti	Cr	Ga	V	Fe	Ca	Mg	Mn	K		
SapMa_06	Light blue body	Ma06-TC1-1	1.997	0.000	0.000	0.000	0.000	0.000	0.000	0.002	0.000	0.000	0.000	0.000	2.000
		Ma06-TC1-2	1.998	0.000	0.000	0.000	0.000	0.000	0.000	0.001	0.000	0.000	0.000	0.000	2.000
		Ma06-TC1-3	1.998	0.000	0.000	0.000	0.000	0.000	0.000	0.001	0.000	0.000	0.000	0.000	2.000
		Ma06-TC2-1	1.996	0.000	0.000	0.000	0.000	0.000	0.000	0.002	0.000	0.000	0.000	0.000	2.000
		Ma06-TC2-2	1.997	0.001	0.000	0.000	0.000	0.000	0.000	0.002	0.000	0.000	0.000	0.000	2.000
		Ma06-TC2-3	1.996	0.001	0.000	0.000	0.000	0.000	0.000	0.001	0.000	0.000	0.000	0.000	2.000
	Blue patches	Ma06-TB1-1	1.997	0.001	0.000	0.000	0.000	0.000	0.000	0.001	0.000	0.000	0.000	0.000	2.000
		Ma06-TB1-2	1.995	0.001	0.002	0.000	0.000	0.000	0.000	0.000	0.000	0.000	0.000	0.000	1.999
		Ma06-TB1-3	1.997	0.000	0.000	0.000	0.000	0.000	0.000	0.001	0.000	0.000	0.000	0.000	2.000
SapMa_07	Light blue body	Ma07-TC1-1	1.993	0.000	0.003	0.000	0.000	0.000	0.000	0.002	0.000	0.000	0.000	0.000	1.999
		Ma07-TC1-2	1.996	0.001	0.001	0.000	0.000	0.000	0.000	0.001	0.000	0.001	0.000	0.000	2.000
		Ma07-TC1-3	1.994	0.000	0.002	0.000	0.000	0.000	0.000	0.002	0.000	0.000	0.000	0.000	1.999
		Ma07-TC2-1	1.995	0.000	0.002	0.000	0.001	0.000	0.000	0.002	0.000	0.000	0.000	0.000	2.000
		Ma07-TC2-2	1.995	0.000	0.002	0.000	0.000	0.000	0.000	0.001	0.000	0.000	0.000	0.000	1.999
		Ma07-TC2-3	1.995	0.000	0.002	0.000	0.000	0.000	0.000	0.002	0.000	0.000	0.000	0.000	1.999
	Blue patches	Ma07-TB1-1	1.998	0.000	0.000	0.000	0.000	0.000	0.000	0.001	0.000	0.000	0.000	0.000	2.000
		Ma07-TB1-2	1.998	0.000	0.000	0.000	0.000	0.000	0.000	0.001	0.000	0.000	0.000	0.000	2.000
		Ma07-TB1-3	1.997	0.000	0.000	0.000	0.000	0.000	0.000	0.001	0.000	0.000	0.000	0.000	2.000

Appendix E-4 (Continue).

Samples	Areas	Point	Elements											Total*
			Al	Si	Ti	Cr	Ga	V	Fe	Ca	Mg	Mn	K	
SapMa_08	Light blue body	Ma08TLB1	1.998	0.000	0.001	0.000	0.000	0.000	0.001	0.000	0.000	0.000	0.000	2.000
		Ma08TLB2	1.998	0.000	0.001	0.000	0.000	0.000	0.001	0.000	0.000	0.000	0.000	2.000
		Ma08TLB3	1.998	0.000	0.001	0.000	0.000	0.000	0.001	0.000	0.000	0.000	0.000	2.000
	Blue patches	Ma08TB1	1.999	0.000	0.000	0.000	0.000	0.000	0.001	0.000	0.000	0.000	0.000	2.000
		Ma08TB2	1.998	0.000	0.000	0.000	0.000	0.000	0.001	0.000	0.000	0.000	0.000	2.000
		Ma08TB3	1.997	0.000	0.001	0.000	0.000	0.000	0.001	0.000	0.000	0.000	0.000	2.000
SapMa_09	Light blue body	Ma09TLB1	1.996	0.000	0.001	0.000	0.000	0.000	0.002	0.000	0.000	0.000	0.000	2.000
		Ma09TLB2	1.995	0.000	0.002	0.000	0.000	0.000	0.002	0.000	0.001	0.000	0.000	2.000
		Ma09TLB3	1.995	0.000	0.001	0.000	0.000	0.000	0.002	0.000	0.001	0.000	0.000	2.000
		Ma09TLB4	1.995	0.000	0.002	0.000	0.000	0.000	0.001	0.000	0.000	0.000	0.000	1.999
	Blue patches	Ma09TB2	1.995	0.000	0.001	0.000	0.000	0.000	0.002	0.000	0.001	0.000	0.000	2.000
		Ma09TB3	1.997	0.000	0.000	0.000	0.000	0.000	0.002	0.000	0.001	0.000	0.000	2.000
SapMa_10	Light blue body	Ma10TLB1	1.998	0.000	0.000	0.000	0.000	0.000	0.001	0.000	0.000	0.000	0.000	2.000
		Ma10TLB2	1.998	0.000	0.000	0.000	0.000	0.000	0.001	0.000	0.000	0.000	0.000	2.000
		Ma10TLB3	1.998	0.000	0.000	0.000	0.000	0.000	0.001	0.000	0.000	0.000	0.000	2.000
	Blue patches	Ma10TB1	1.998	0.000	0.000	0.000	0.000	0.000	0.001	0.000	0.000	0.000	0.000	2.000
		Ma10TB2	1.998	0.000	0.000	0.000	0.000	0.000	0.001	0.000	0.000	0.000	0.000	2.000
		Ma10TB3	1.998	0.000	0.000	0.000	0.000	0.000	0.001	0.000	0.000	0.000	0.000	2.000

Appendix E-4 (Continue).

Samples	Areas	Point	Elements											Total*	
			Al	Si	Ti	Cr	Ga	V	Fe	Ca	Mg	Mn	K		
SapMa_11	Light blue body	Ma11TLB1	1.998	0.000	0.000	0.000	0.000	0.000	0.000	0.001	0.000	0.000	0.000	0.000	2.000
		Ma11TLB2	1.996	0.000	0.001	0.000	0.000	0.000	0.000	0.001	0.000	0.000	0.000	0.000	2.000
		Ma11TLB3	1.998	0.000	0.000	0.000	0.000	0.000	0.000	0.001	0.000	0.000	0.000	0.000	2.000
		Ma11TLB4	1.998	0.000	0.000	0.000	0.000	0.000	0.000	0.001	0.000	0.000	0.000	0.000	2.000
		Ma11TLB5	1.998	0.001	0.000	0.000	0.000	0.000	0.000	0.001	0.000	0.000	0.000	0.000	2.000
SapMa_12	Light blue body	Ma12TLB1	1.997	0.000	0.000	0.000	0.000	0.000	0.000	0.001	0.000	0.000	0.000	0.000	2.000
		Ma12TLB2	1.997	0.000	0.001	0.000	0.000	0.000	0.000	0.001	0.000	0.000	0.000	0.000	2.000
		Ma12TLB3	1.998	0.000	0.000	0.000	0.000	0.000	0.000	0.001	0.000	0.000	0.000	0.000	2.000
		Ma12TLB4	1.997	0.000	0.001	0.000	0.000	0.000	0.000	0.001	0.000	0.000	0.000	0.000	2.000
		Ma12TLB5	1.998	0.000	0.000	0.000	0.000	0.000	0.000	0.001	0.000	0.000	0.000	0.000	2.000
SapMa_13	Light blue body	Ma13TLB1	1.994	0.000	0.000	0.000	0.000	0.000	0.000	0.005	0.000	0.000	0.000	0.000	2.000
		Ma13TLB2	1.994	0.000	0.000	0.000	0.000	0.000	0.000	0.005	0.000	0.000	0.000	0.000	2.000
	Blue patches	Ma13TB1	1.995	0.000	0.000	0.000	0.000	0.000	0.000	0.004	0.000	0.000	0.000	0.000	2.000
		Ma13TB2	1.994	0.000	0.000	0.000	0.000	0.000	0.000	0.005	0.000	0.001	0.000	0.000	2.000
		Ma13TB3	1.994	0.000	0.000	0.000	0.000	0.000	0.000	0.004	0.000	0.001	0.000	0.000	2.000
		Ma13TB4	1.995	0.000	0.000	0.000	0.000	0.000	0.000	0.004	0.000	0.000	0.000	0.000	2.000



APPENDIX F

ศูนย์วิทยทรัพยากร
จุฬาลงกรณ์มหาวิทยาลัย

Appendix F Triangular diagram of atomic proportions between Mg, Ti and Fe of Awissawella corundums

Appendix F-1 Triangular diagram of yellow sapphire variety from Awissawella, Sri Lanka. Data points were performed analyses by EPMA (JEOL Electron Probe Micro-Analyzer, model JXA-8100)

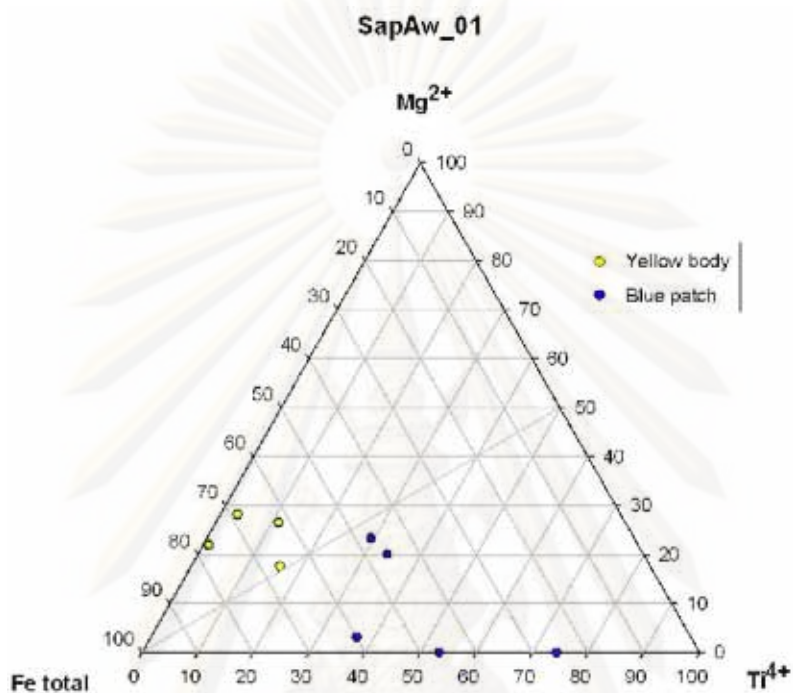


Figure F-1.1 Triangular diagram showing atomic proportions between Mg, Fe and Ti of SapAw_01 (color code gY2/3).

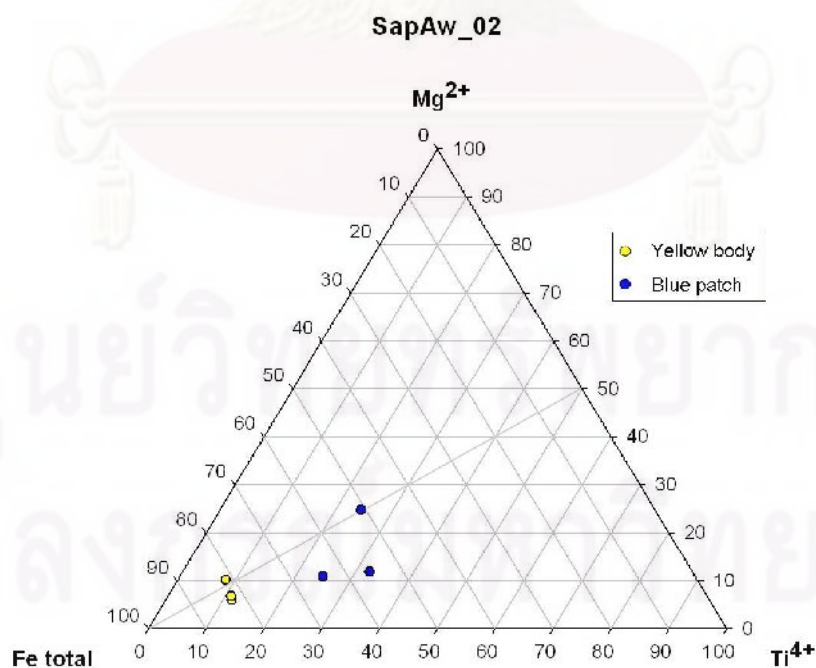


Figure F-1.2 Triangular diagram showing atomic proportions between Mg, Fe and Ti of SapAw_02 (color code YG/GY2/1).

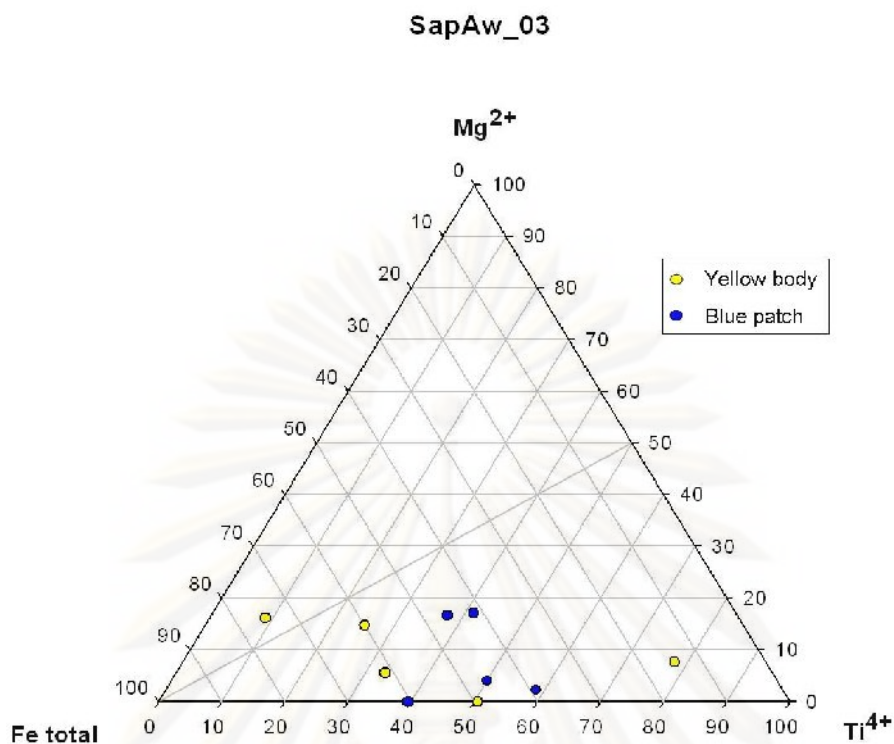


Figure F-1.3 Triangular diagram showing atomic proportions between Mg, Fe and Ti of SapAw_03 (color code YG/GY2/1).

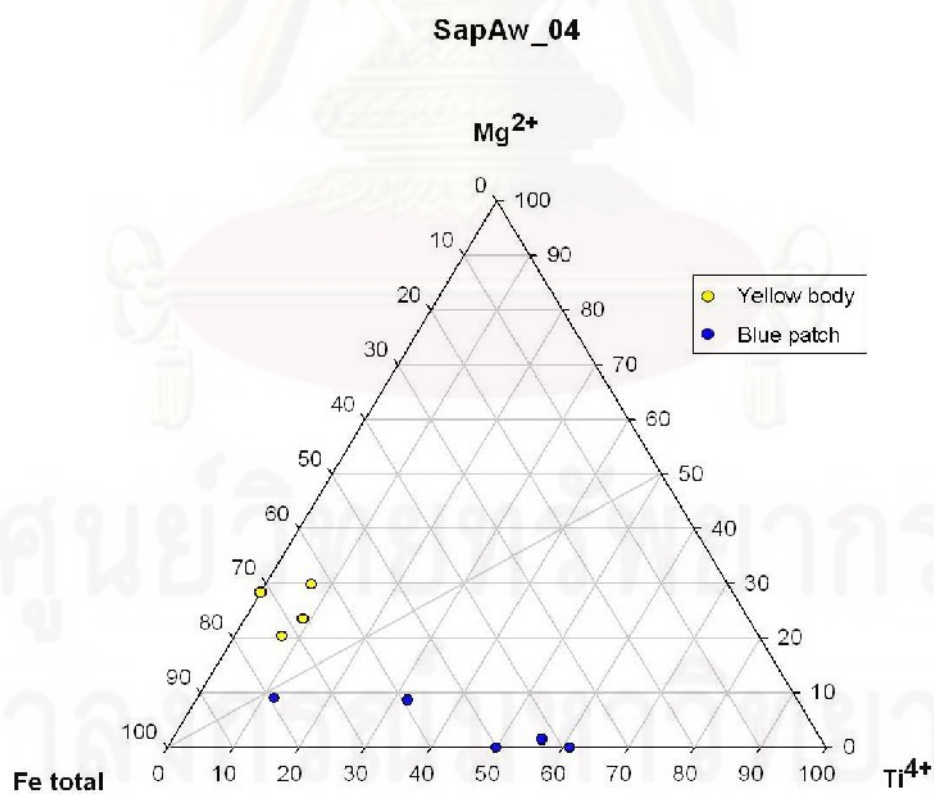


Figure F-1.4 Triangular diagram showing atomic proportions between Mg, Fe and Ti of SapAw_04 (color code Y2/2).

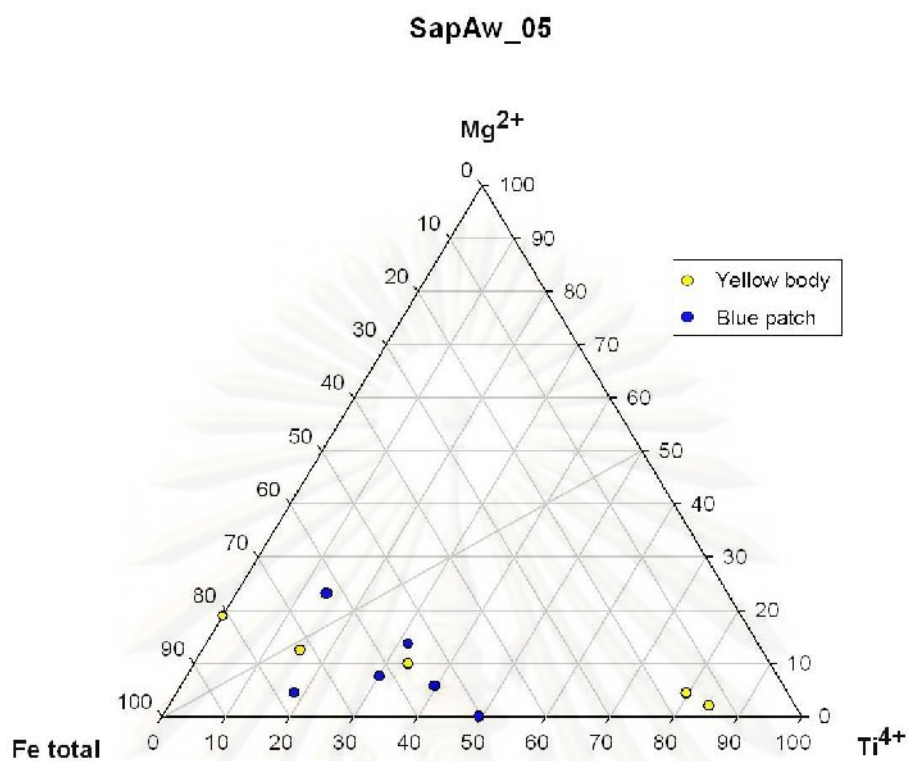


Figure F-1.5 Triangular diagram showing atomic proportions between Mg, Fe and Ti of SapAw_05 (color code gY2/3).

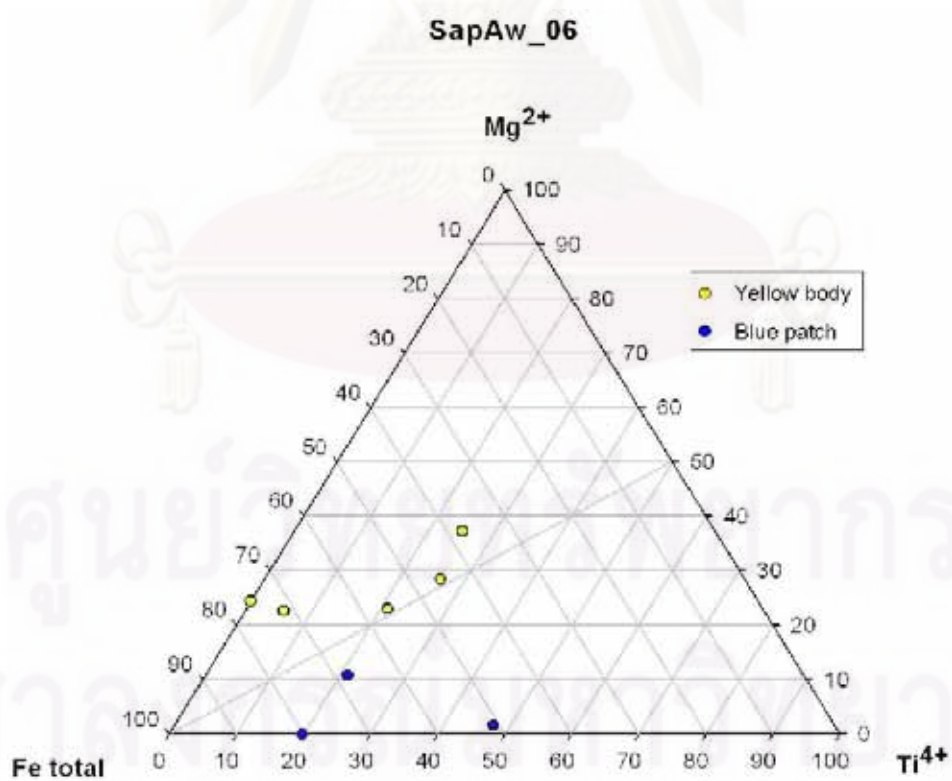


Figure F-1.6 Triangular diagram showing atomic proportions between Mg, Fe and Ti of SapAw_06 (color code Y2/2).

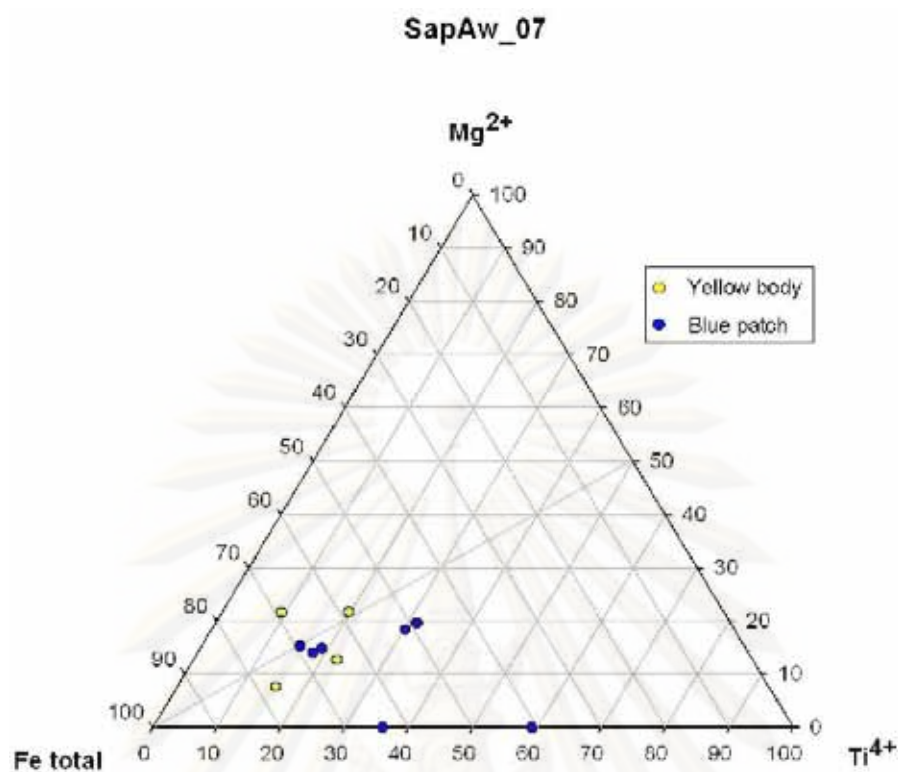


Figure F-1.7 Triangular diagram showing atomic proportions between Mg, Fe and Ti of SapAw_07 (color code YG/GY2/1).

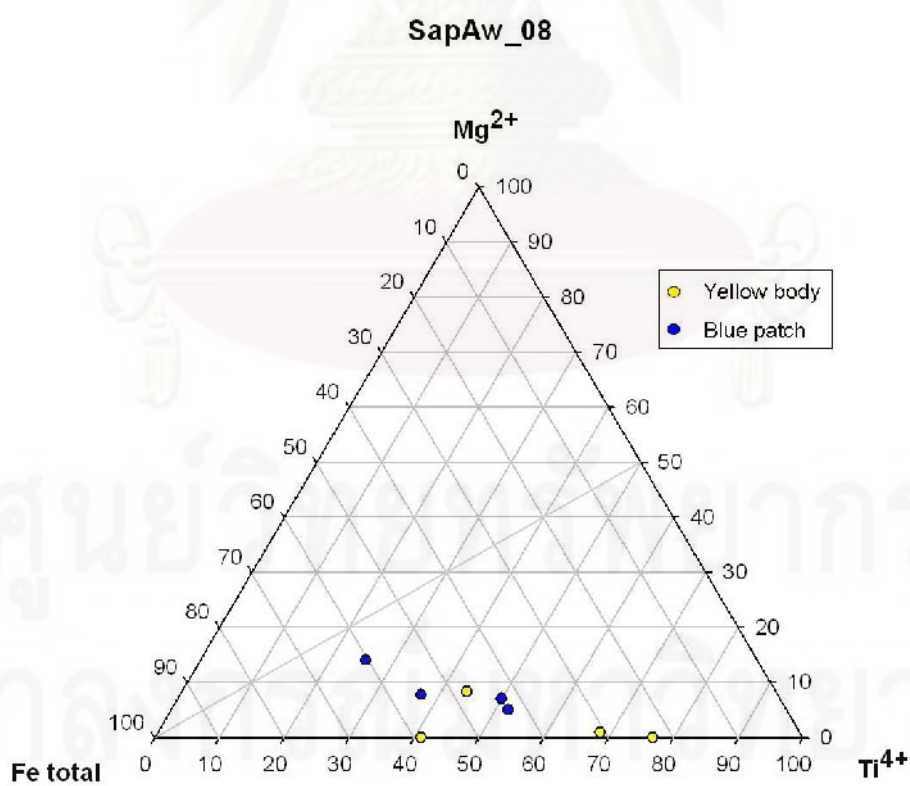


Figure F-1.8 Triangular diagram showing atomic proportions between Mg, Fe and Ti of SapAw_08 (color code gY2/3).

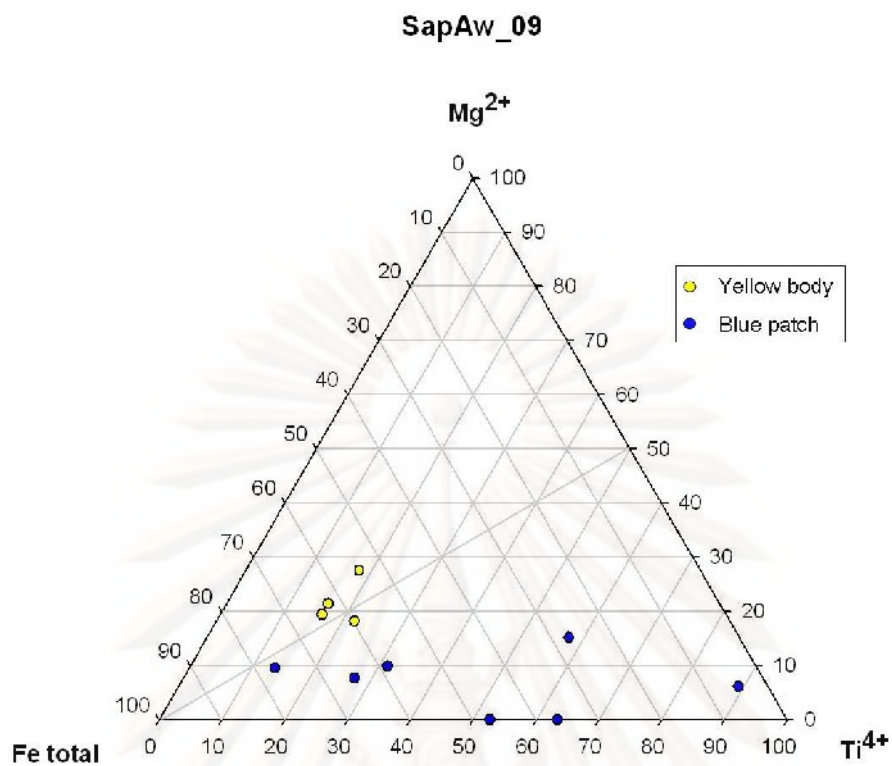


Figure F-1.9 Triangular diagram showing atomic proportions between Mg, Fe and Ti of SapAw_09 (color code YG/GY2/1).

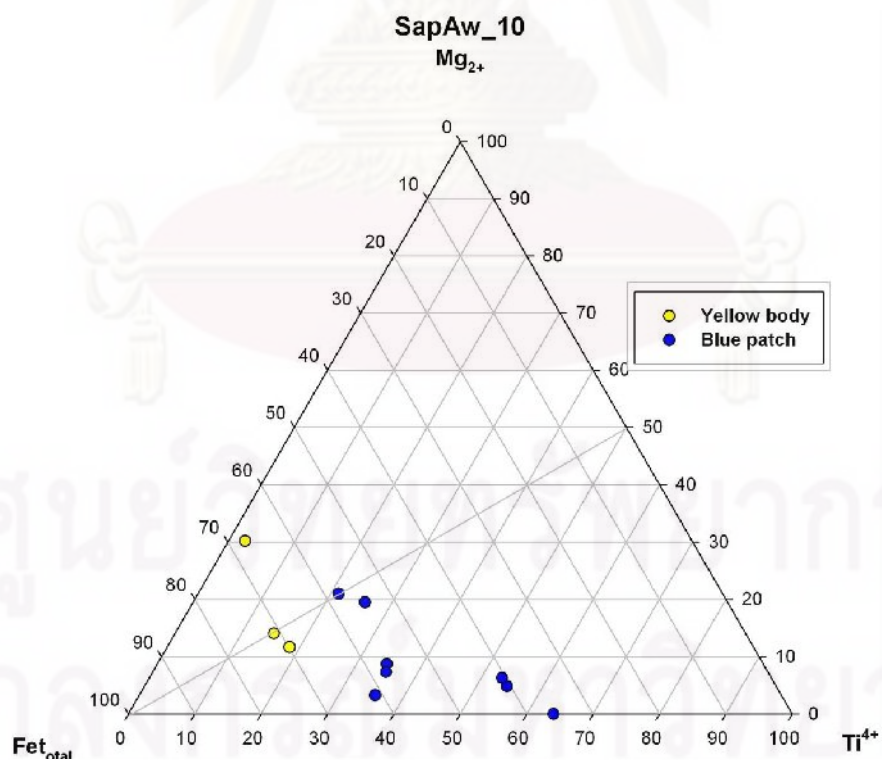


Figure F-1.10 Triangular diagram showing atomic proportions between Mg, Fe and Ti of SapAw_10 (color code gY2/3).

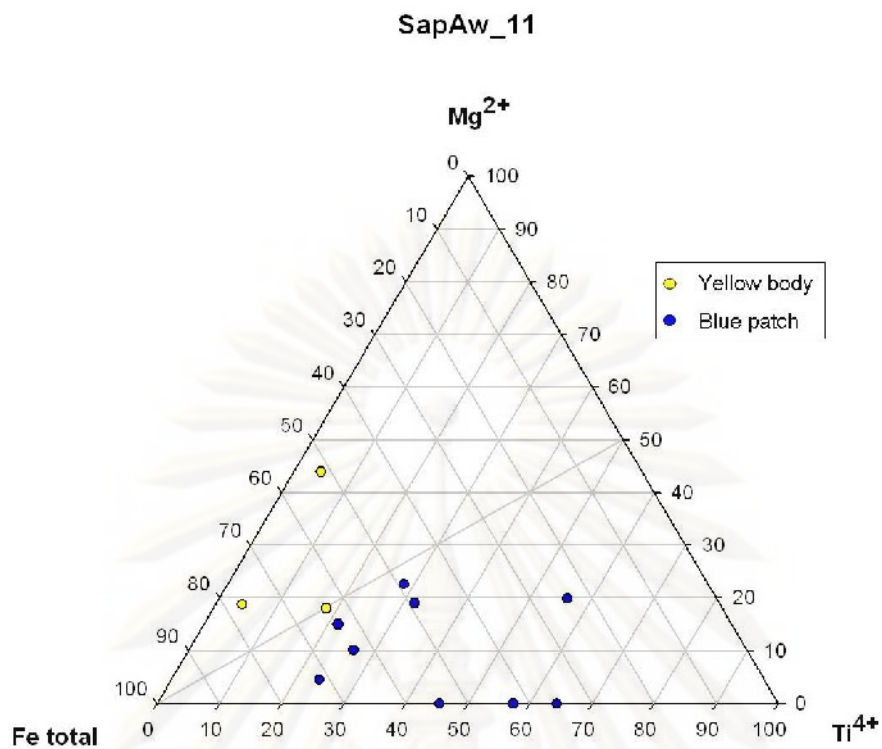


Figure F-1.11 Triangular diagram showing atomic proportions between Mg, Fe and Ti of SapAw_11 (color code gY3/4).

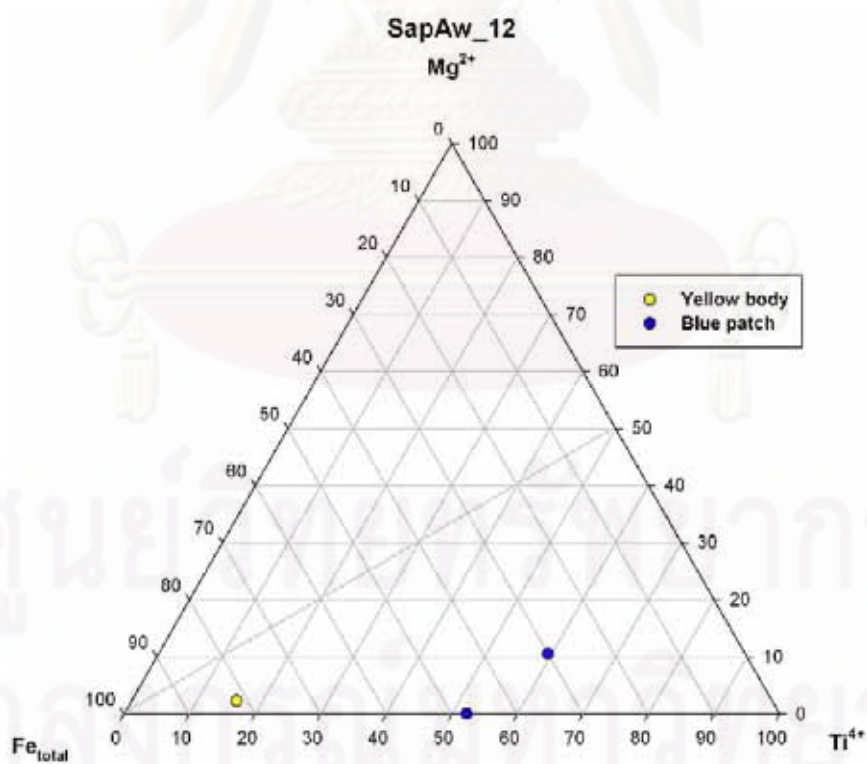


Figure F-1.12 Triangular diagram showing atomic proportions between Mg, Fe and Ti of SapAw_12 (color code Y2/2).

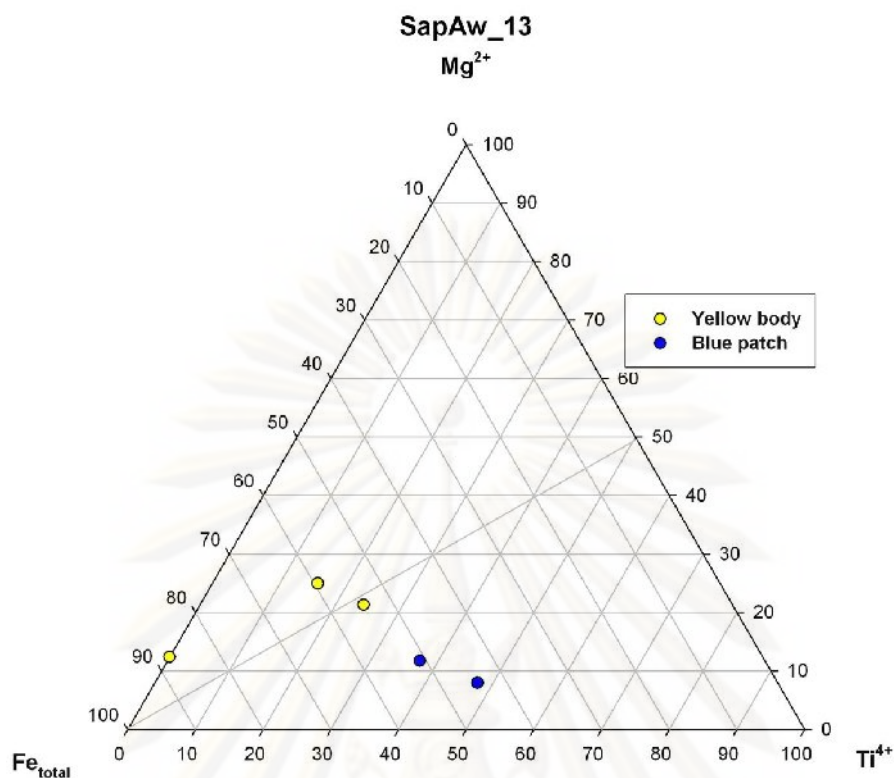


Figure F-1.13 Triangular diagram showing atomic proportions between Mg, Fe and Ti of SapAw_13 (color code Y2/2).

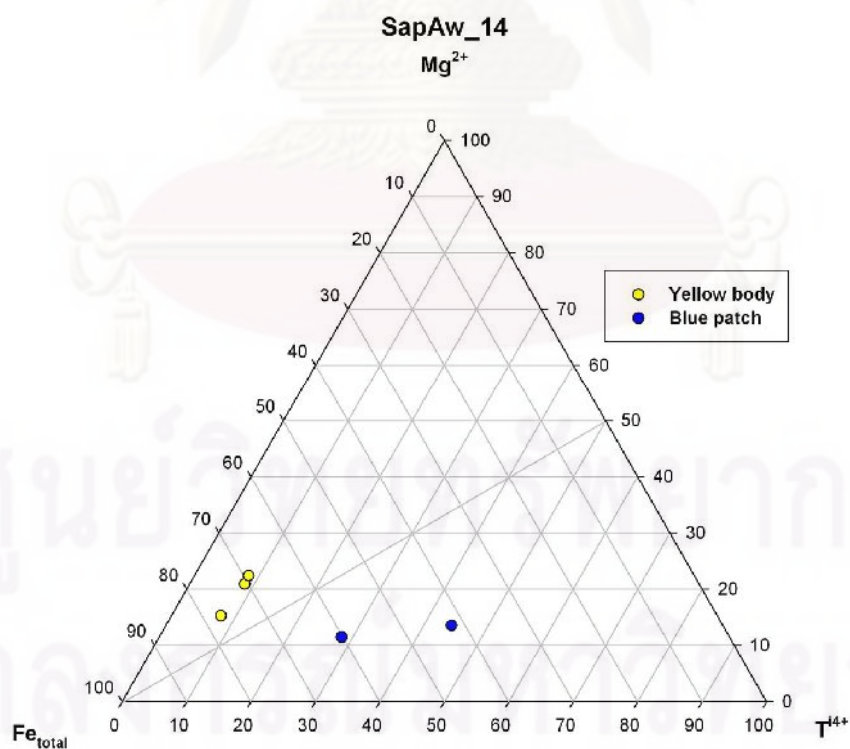


Figure F-1.14 Triangular diagram showing atomic proportions between Mg, Fe and Ti of SapAw_14 (color code Y3/5).

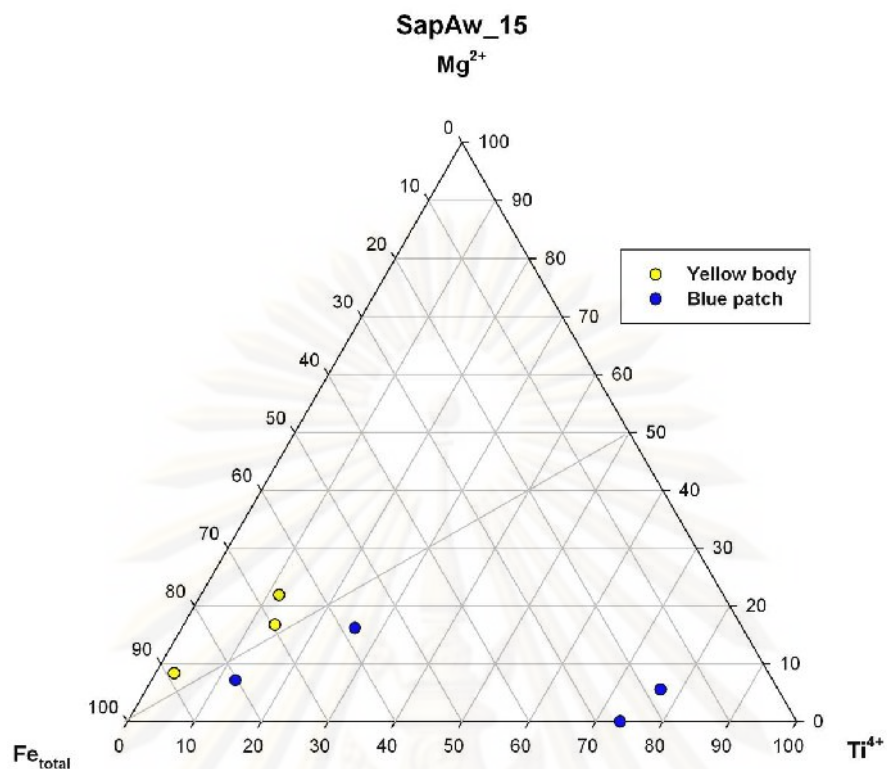


Figure F-1.15 Triangular diagram showing atomic proportions between Mg, Fe and Ti of SapAw_15 (color code Y3/3).

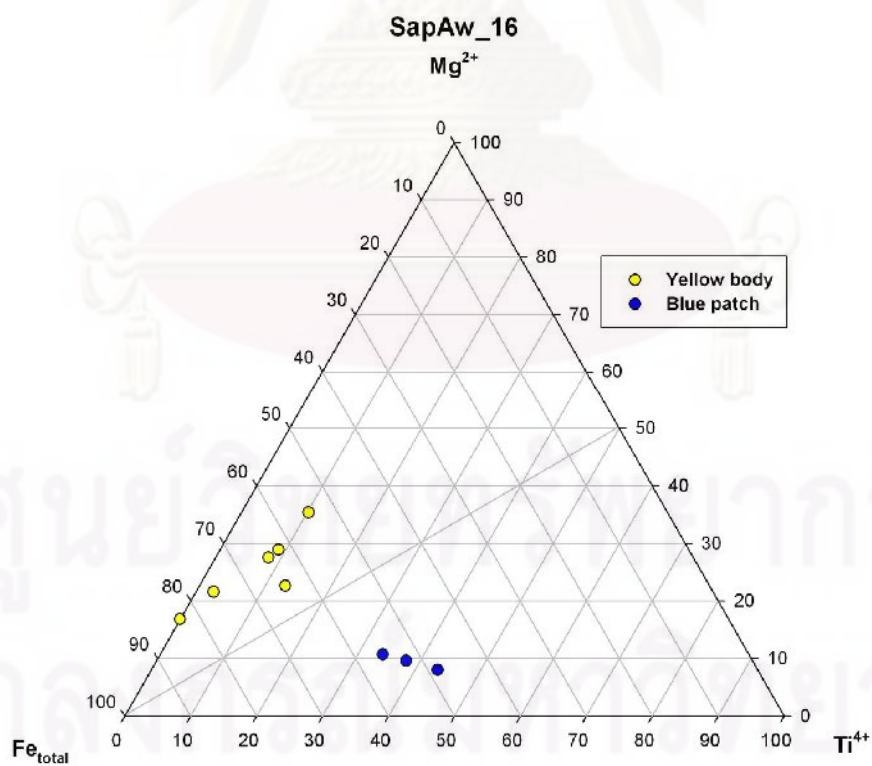


Figure F-1.16 Triangular diagram showing atomic proportions between Mg, Fe and Ti of SapAw_16 (color code YG/GY2/1).

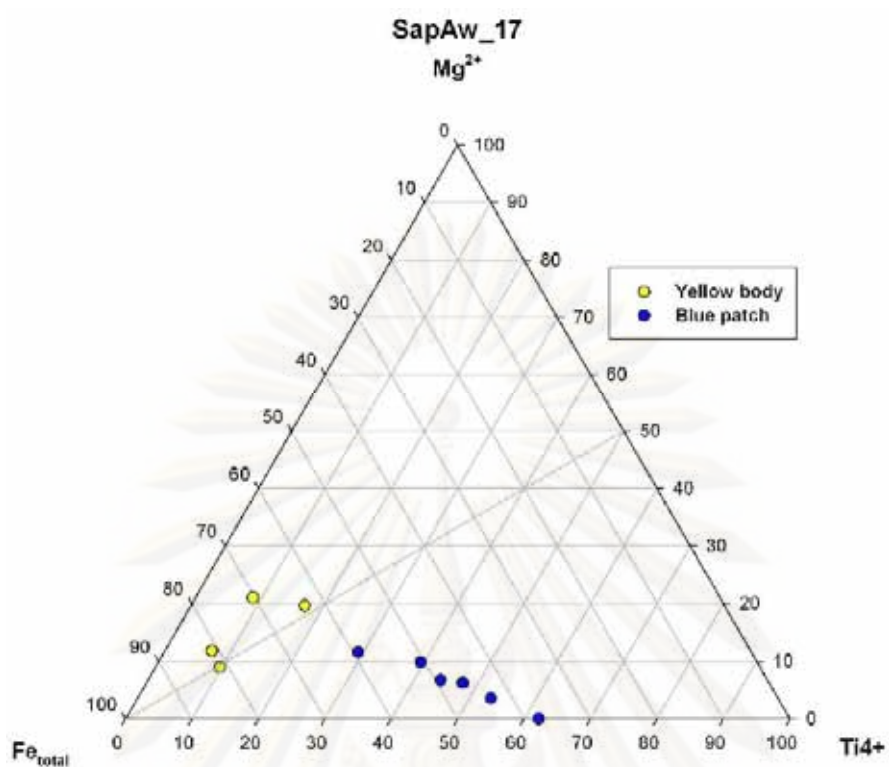


Figure F-1.17 Triangular diagram showing atomic proportions between Mg, Fe and Ti of SapAw_17 (color code YG/GY2/1).

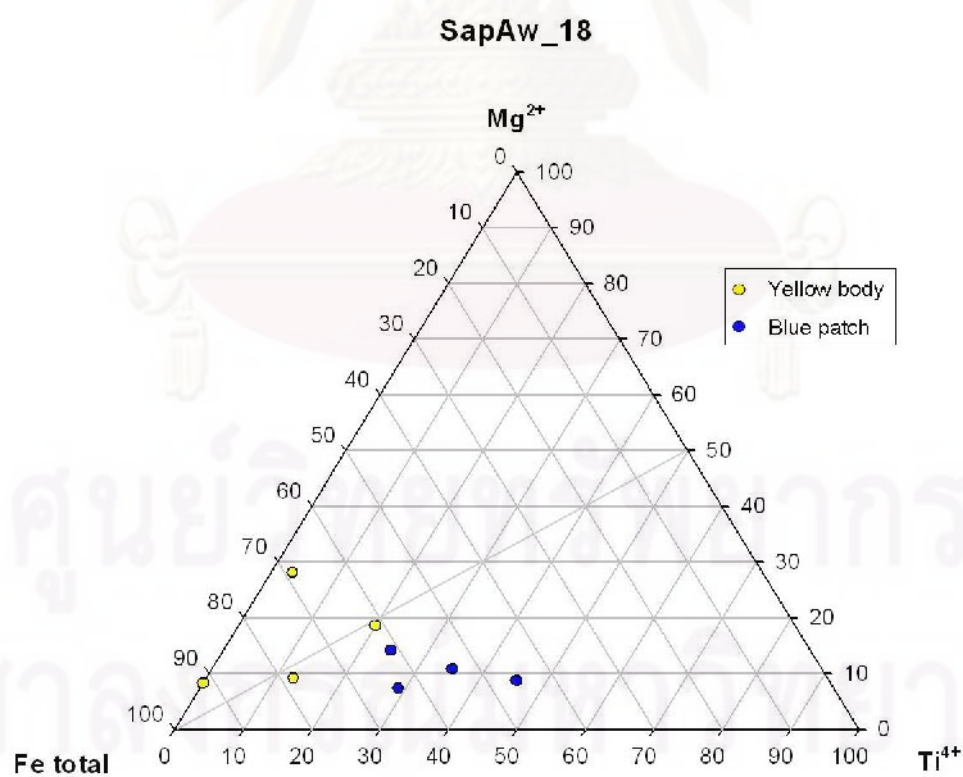


Figure F-1.18 Triangular diagram showing atomic proportions between Mg, Fe and Ti of SapAw_18 (color code gY3/4).

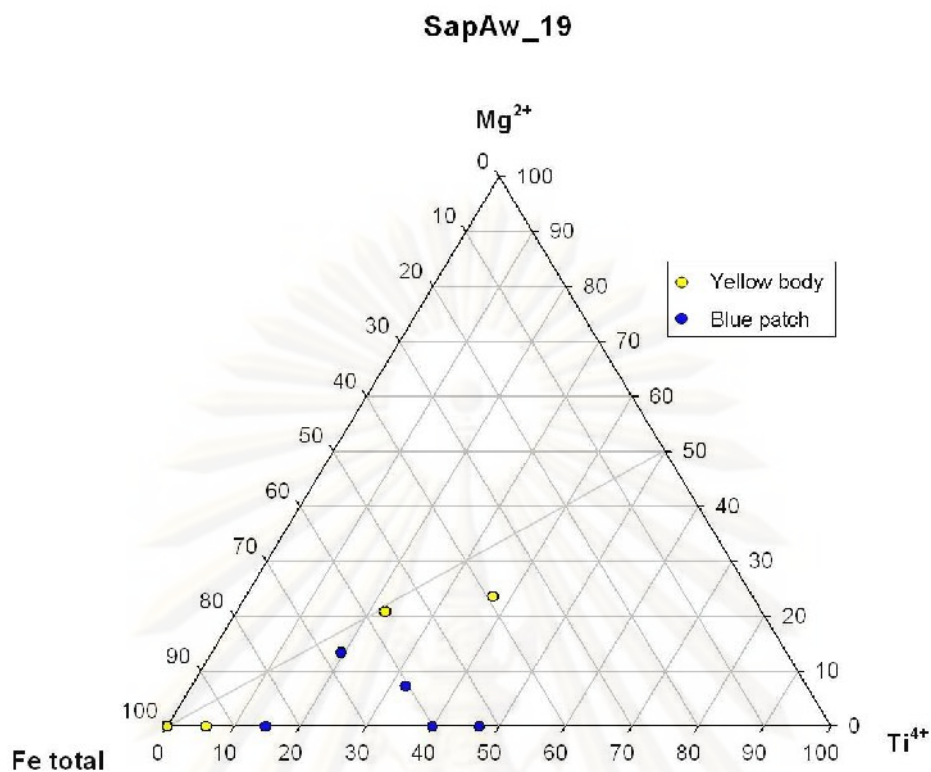


Figure F-1.19 Triangular diagram showing atomic proportions between Mg, Fe and Ti of SapAw_19 (color code Y3/3).

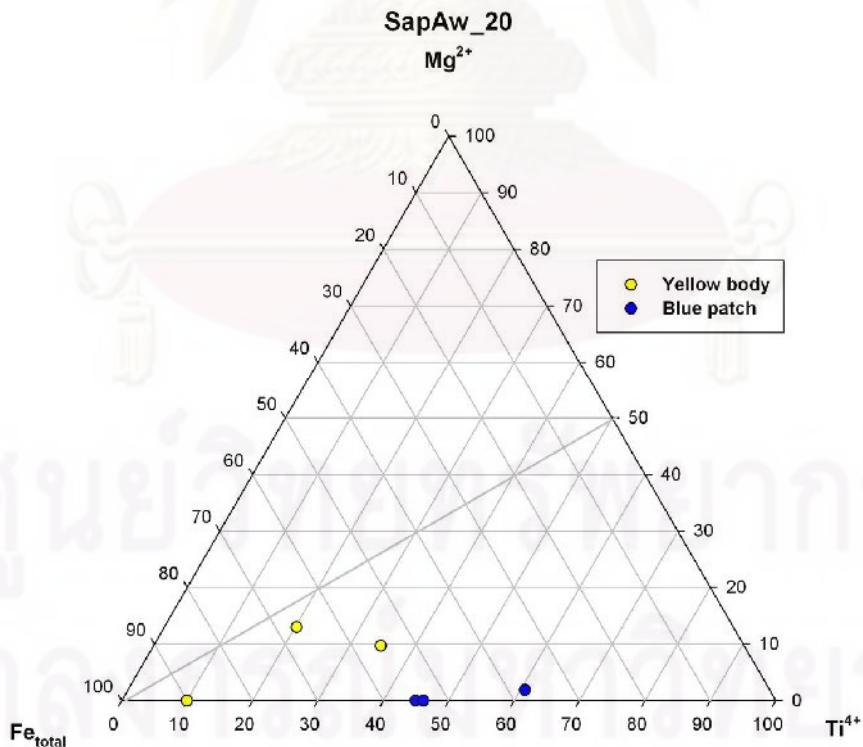


Figure F-1.20 Triangular diagram showing atomic proportions between Mg, Fe and Ti of SapAw_20 (color code gY2/3).

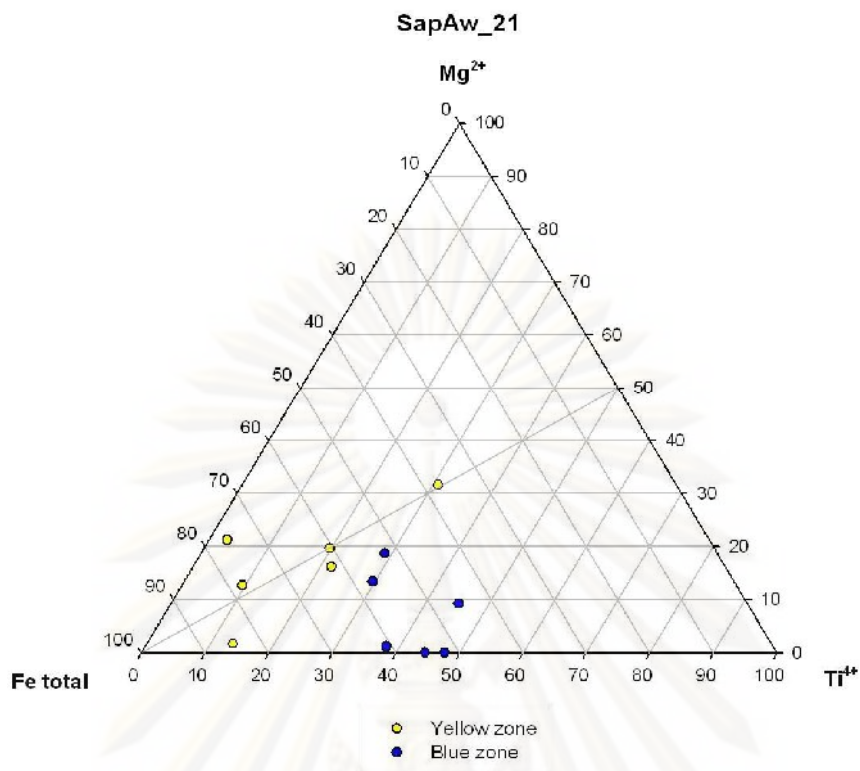


Figure F-1.21 Triangular diagram showing atomic proportions between Mg, Fe and Ti of SapAw_21 (color code YG/GY2/1).

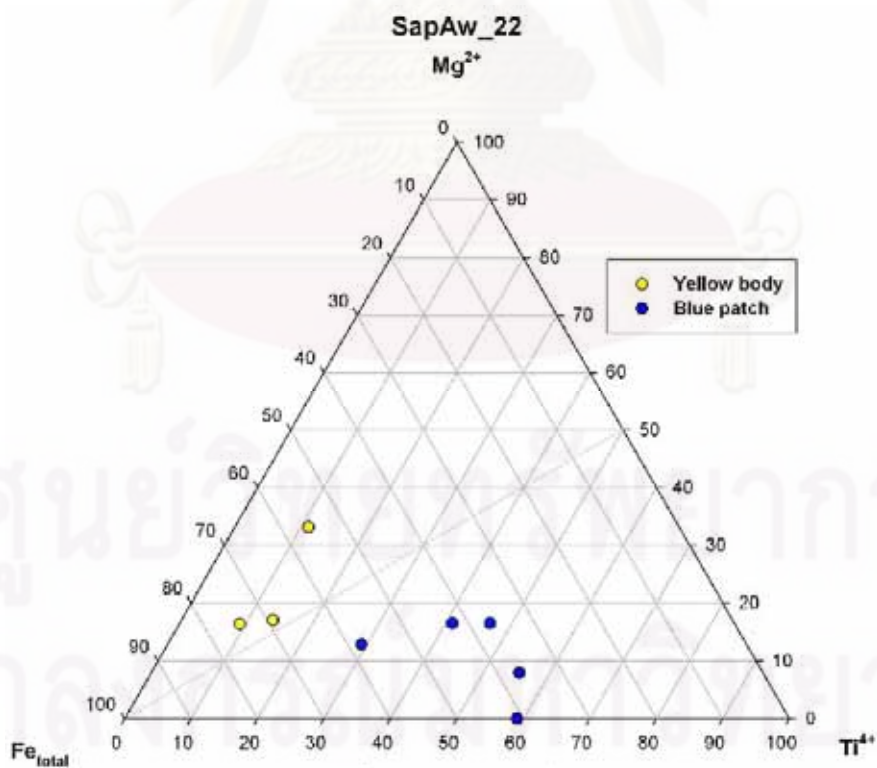


Figure F-1.22 Triangular diagram showing atomic proportions between Mg, Fe and Ti of SapAw_22 (color code YG/GY2/1).

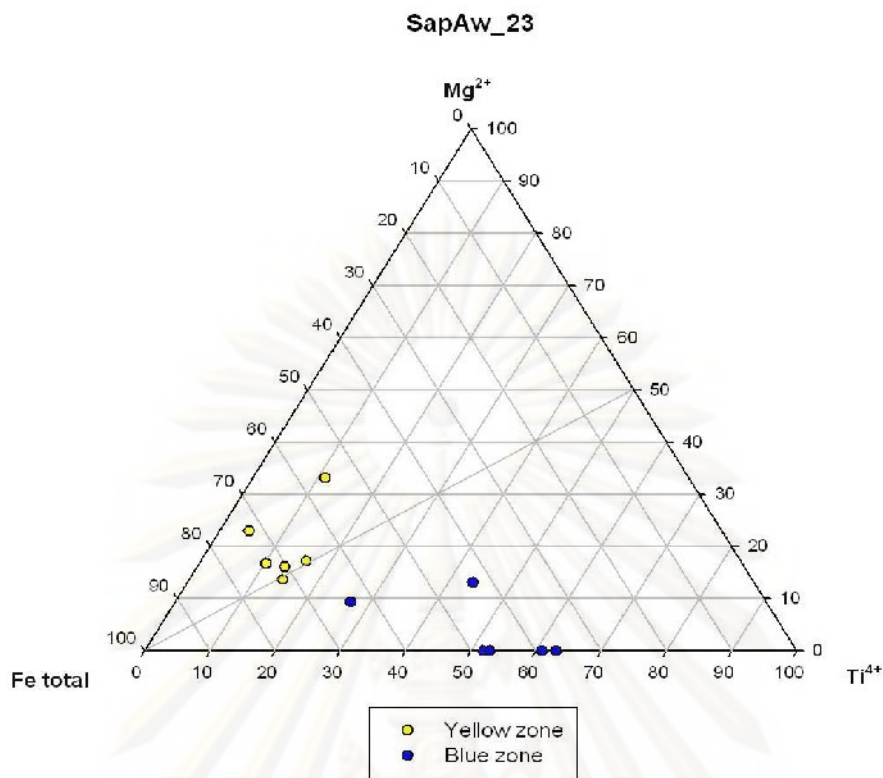


Figure F-1.23 Triangular diagram showing atomic proportions between Mg, Fe and Ti of SapAw_23 (color code YG/GY2/1).

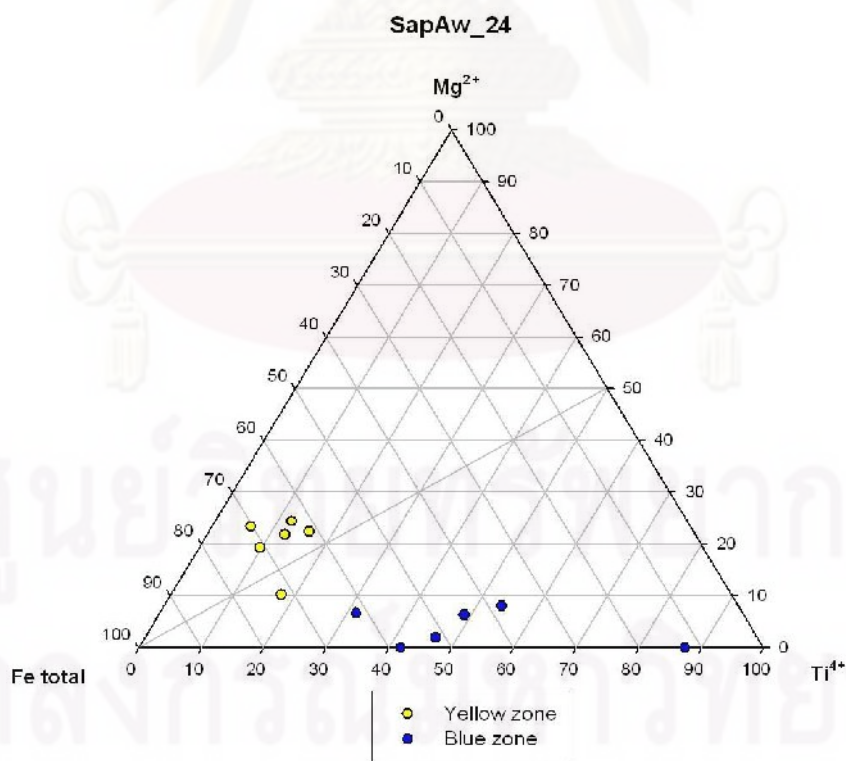


Figure F-1.24 Triangular diagram showing atomic proportions between Mg, Fe and Ti of SapAw_24 (color code Y2/2).

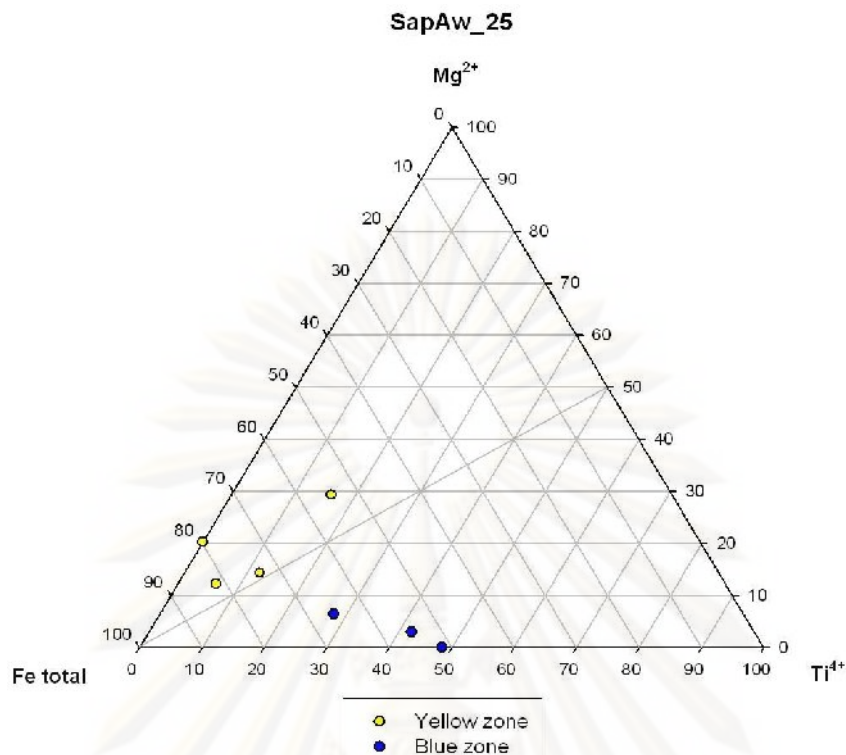


Figure F-1.25 Triangular diagram showing atomic proportions between Mg, Fe and Ti of SapAw_25 (color code YG/GY2/1).

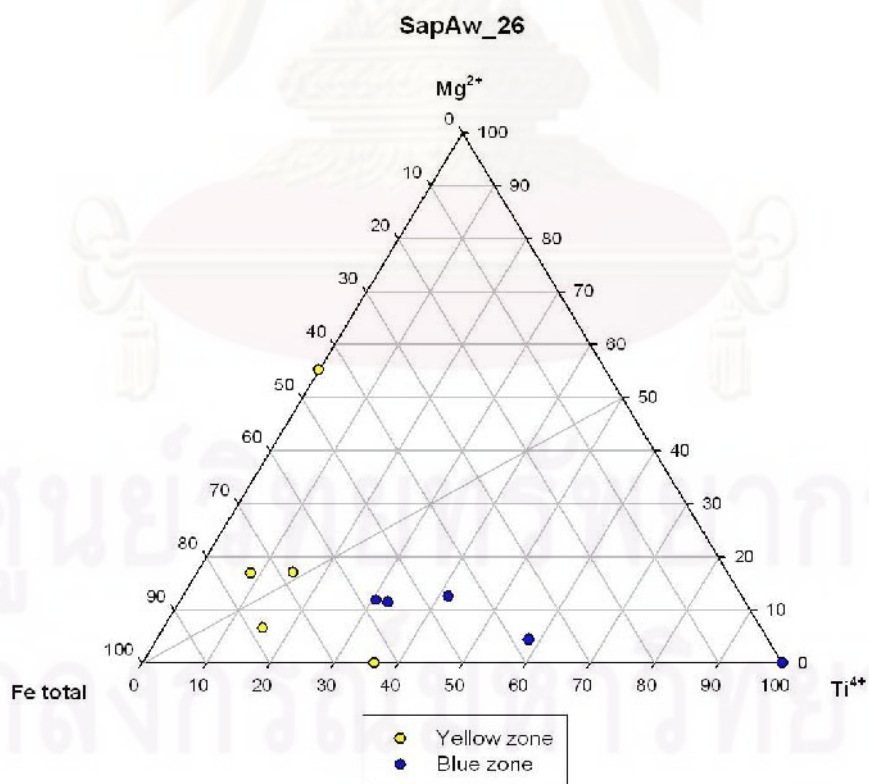


Figure F-1.26 Triangular diagram showing atomic proportions between Mg, Fe and Ti of SapAw_26 (color code Y2/2).

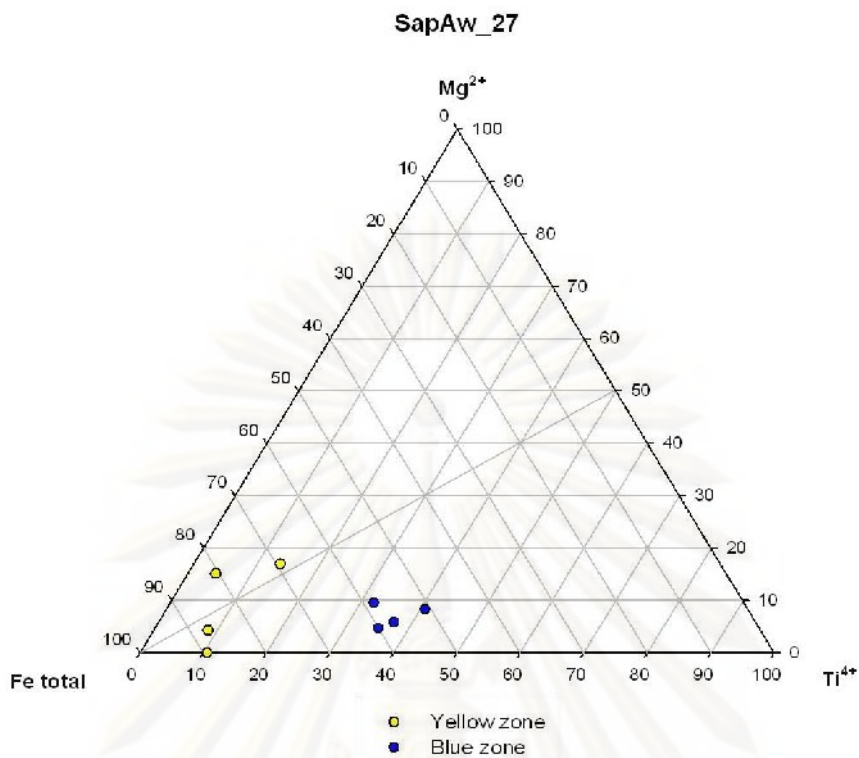


Figure F-1.27 Triangular diagram showing atomic proportions between Mg, Fe and Ti of SapAw_27 (color code YG/GY2/1).

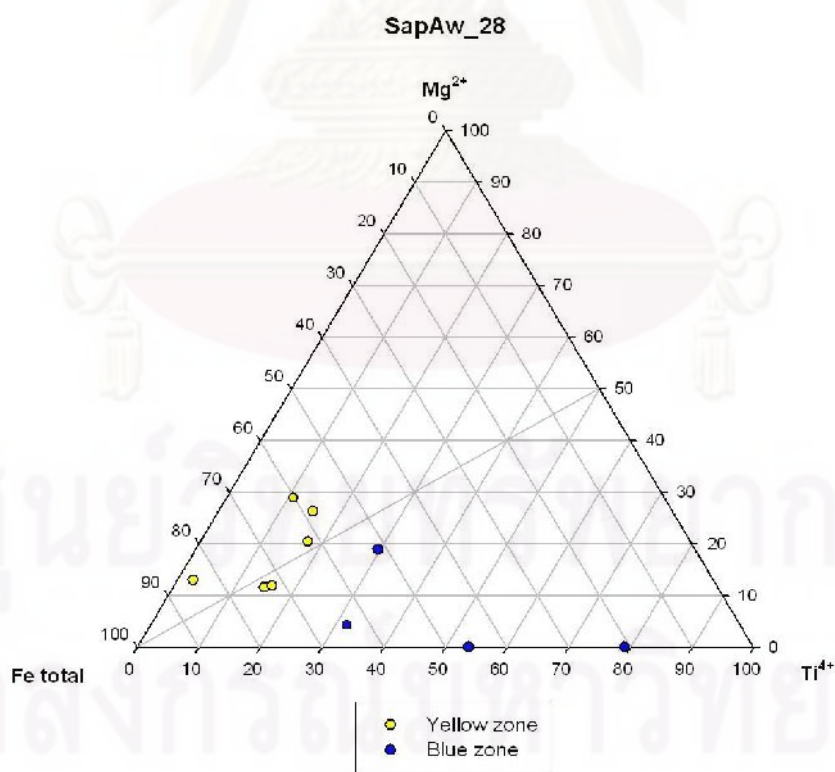


Figure F-1.28 Triangular diagram showing atomic proportions between Mg, Fe and Ti of SapAw_28 (color code Y2/2).

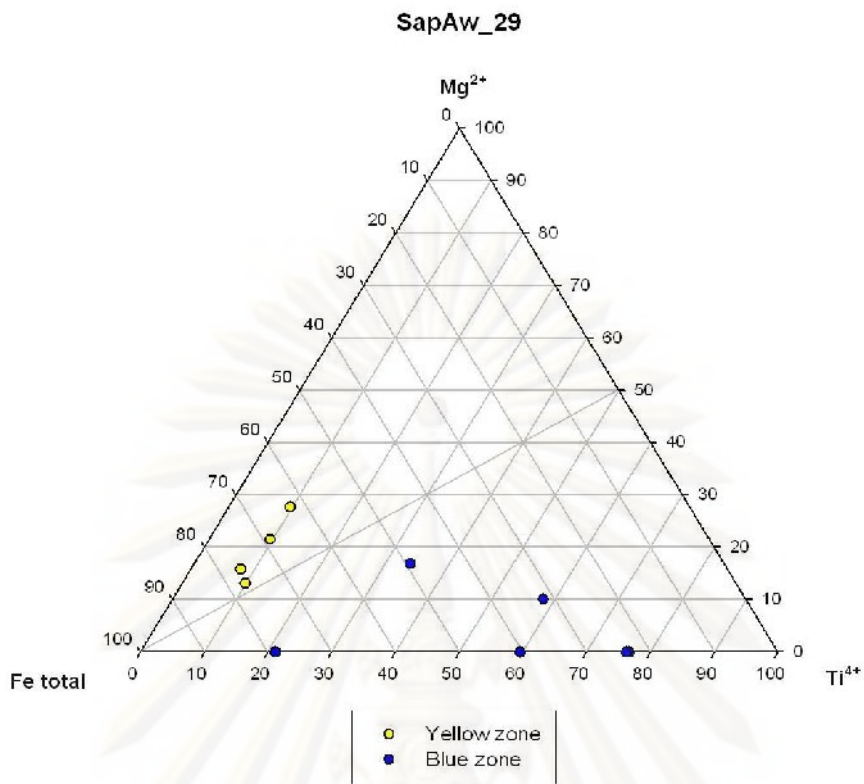


Figure F-1.29 Triangular diagram showing atomic proportions between Mg, Fe and Ti of SapAw_29 (color code YG/GY2/1).

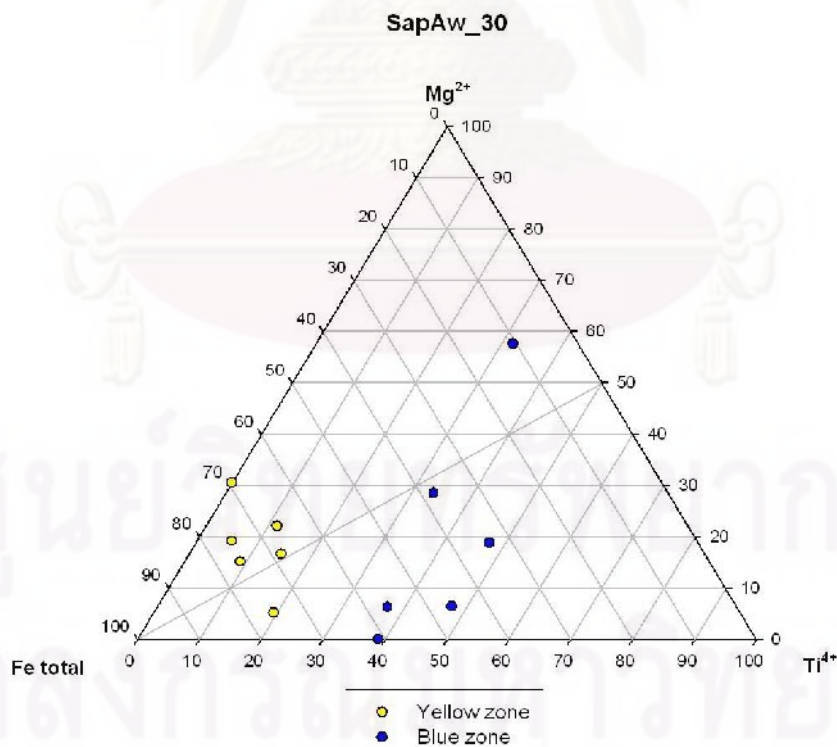


Figure F-1.30 Triangular diagram showing atomic proportions between Mg, Fe and Ti of SapAw_30 (color code Y2/2).

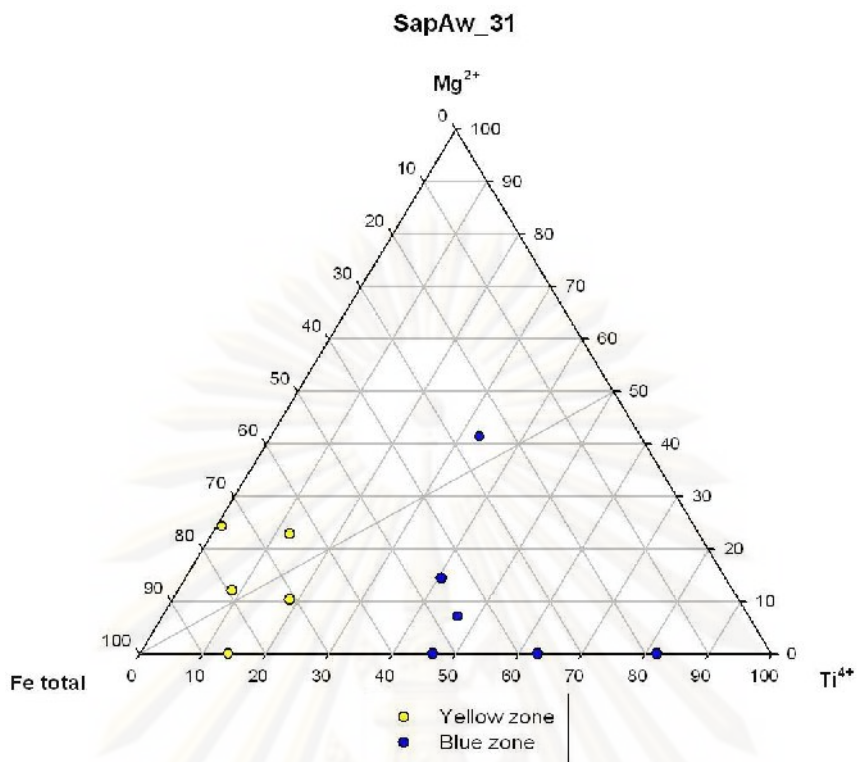


Figure F-1.31 Triangular diagram showing atomic proportions between Mg, Fe and Ti of SapAw_31 (color code YG/GY2/1).

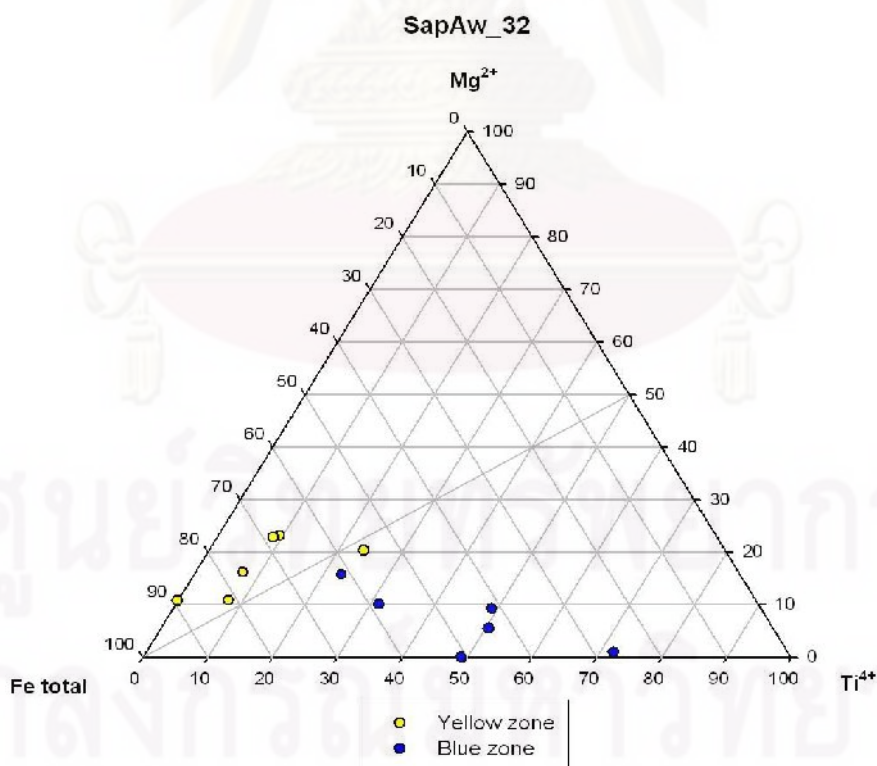


Figure F-1.32 Triangular diagram showing atomic proportions between Mg, Fe and Ti of SapAw_32 (color code Y2/2).

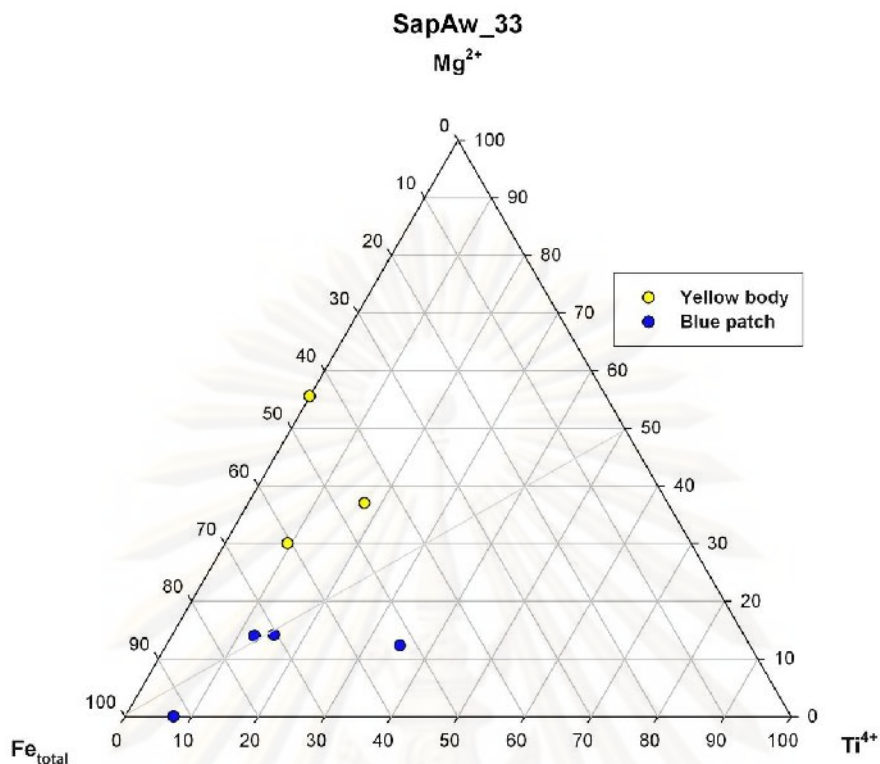


Figure F-1.33 Triangular diagram showing atomic proportions between Mg, Fe and Ti of SapAw_33 (SapTwAw_01) (color code YG/GY2/1).

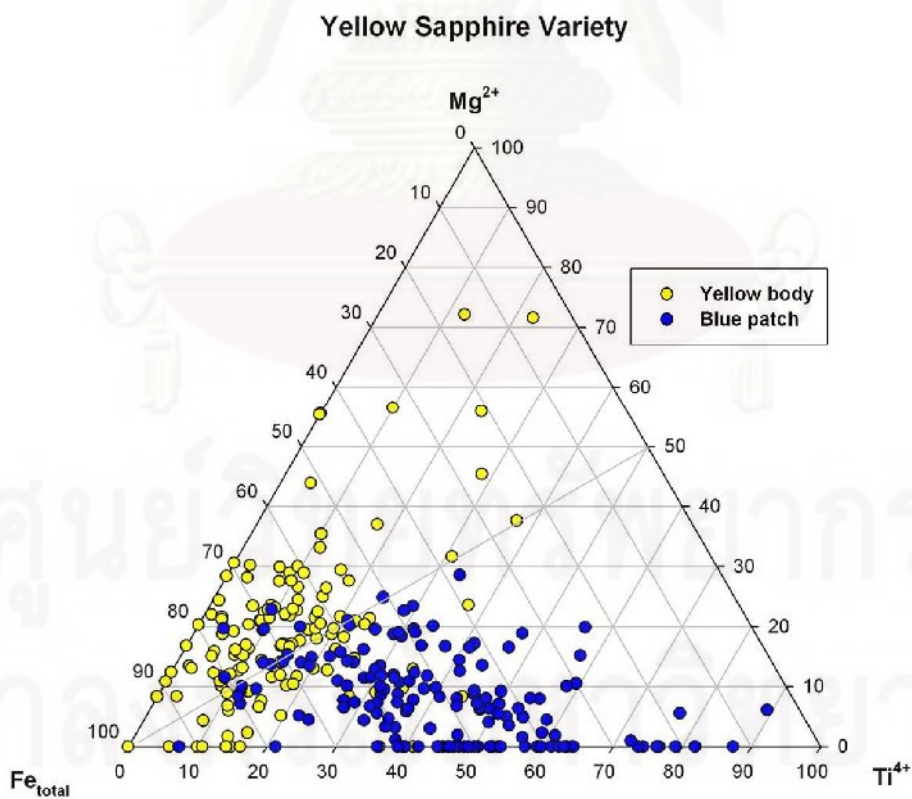


Figure F-1.34 Mg-Fe-Ti ternary diagram of Awissawella corundums in yellow variety; that are plotted based on trace analyses in different color zones.

Appendix F-2 Triangular diagram of light blue sapphire variety from Awissawella, Sri Lanka. Data points were performed analyses by EPMA (JEOL Electron Probe Micro-Analyzer, model JXA-8100)

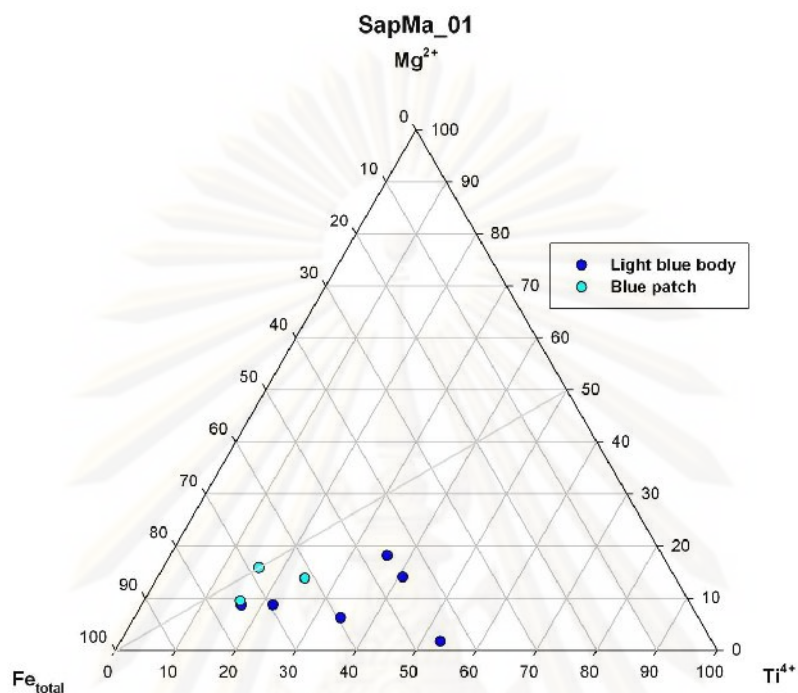


Figure F-2.1 Triangular diagram showing atomic proportions between Mg, Fe and Ti of SapMa_01 (color code B2/2).

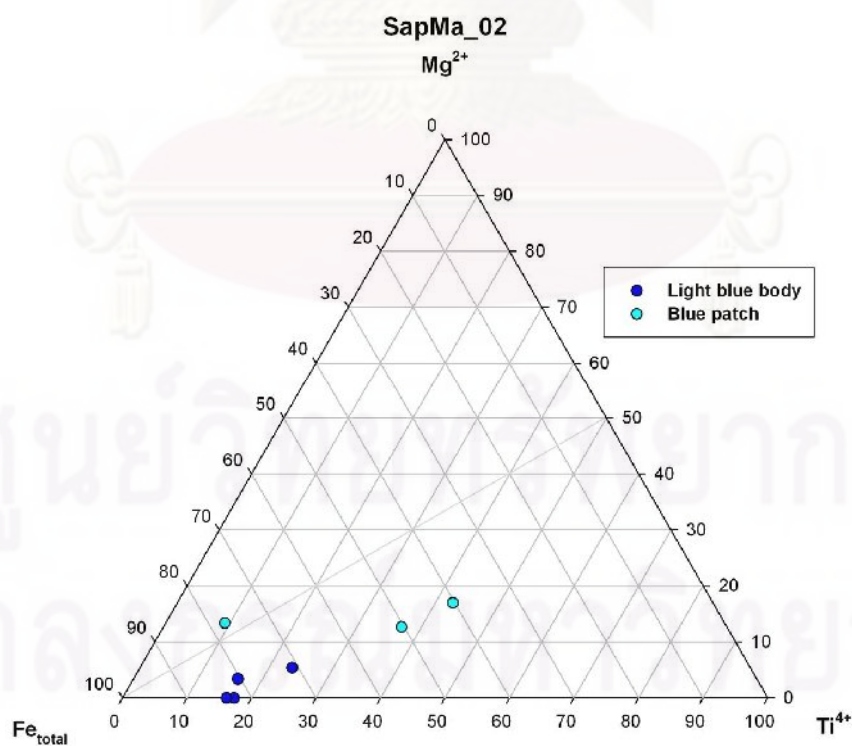


Figure F-2.2 Triangular diagram showing atomic proportions between Mg, Fe and Ti of SapMa_02 (color code vB3/3).

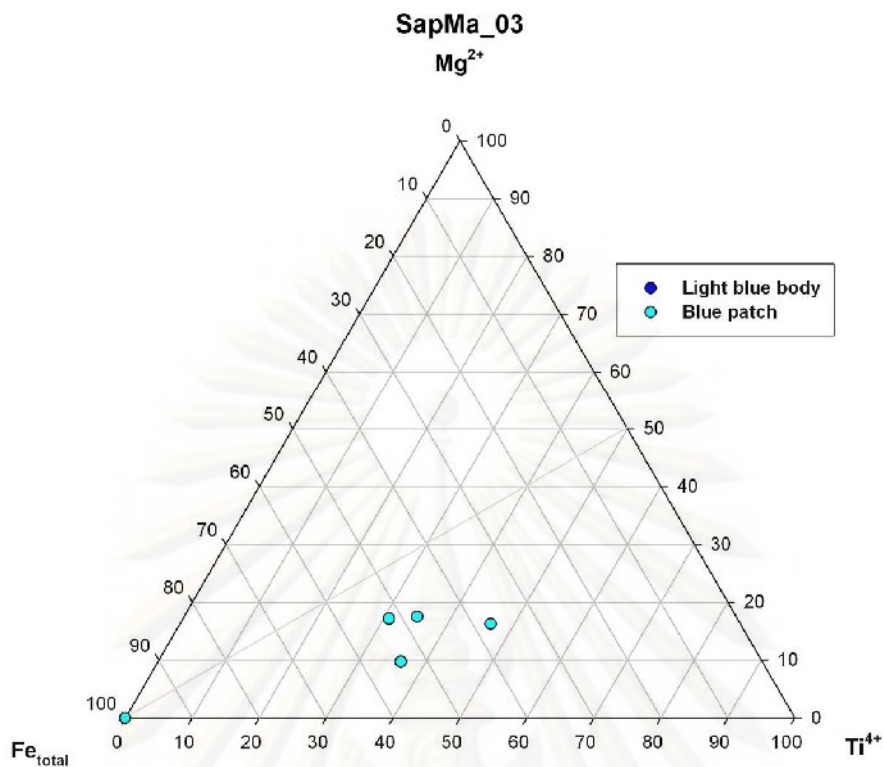


Figure F-2.3 Triangular diagram showing atomic proportions between Mg, Fe and Ti of SapMa_03 (color code B3/1).

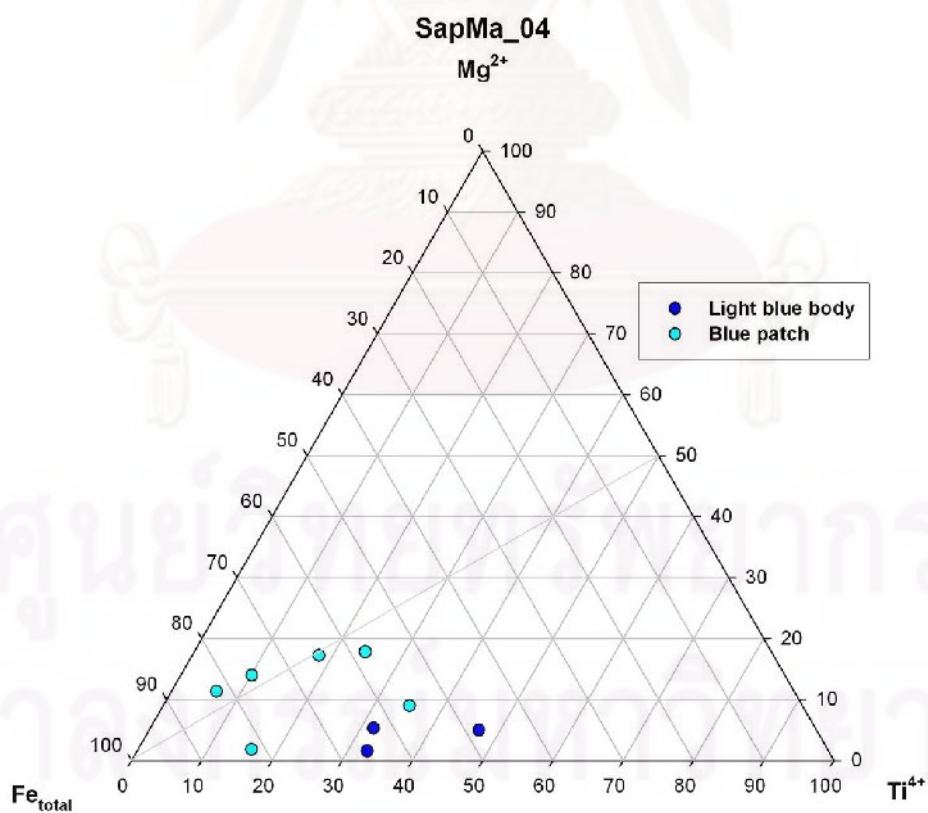


Figure F-2.4 Triangular diagram showing atomic proportions between Mg, Fe and Ti of SapMa_04 (color code B3/1).

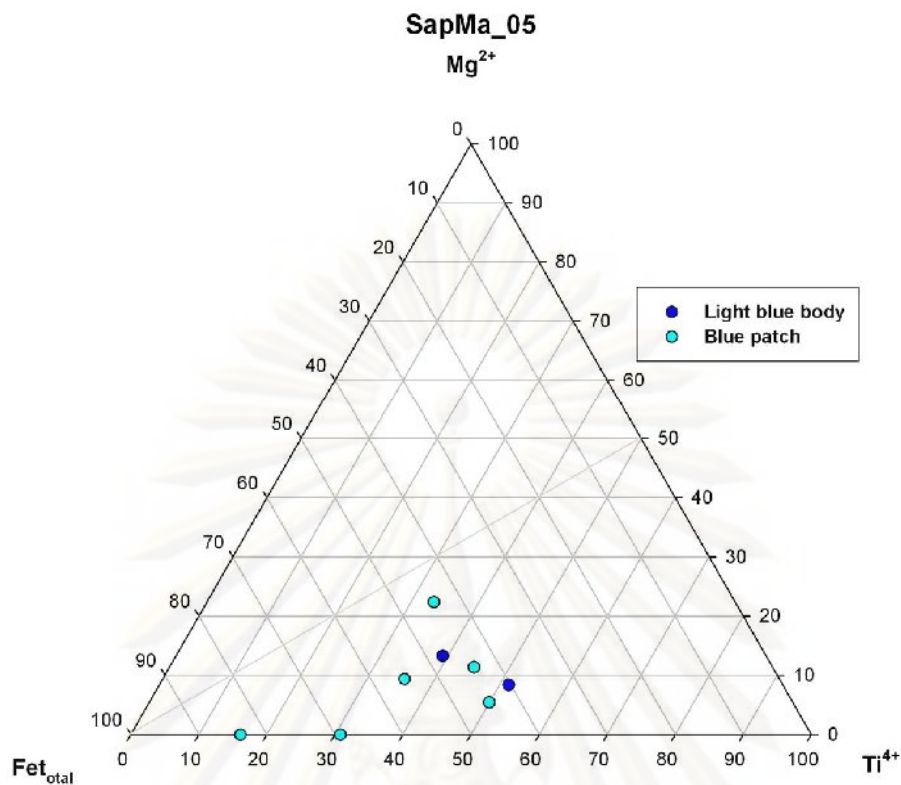


Figure F-2.5 Triangular diagram showing atomic proportions between Mg, Fe and Ti of SapMa_05 (color code B5/2).

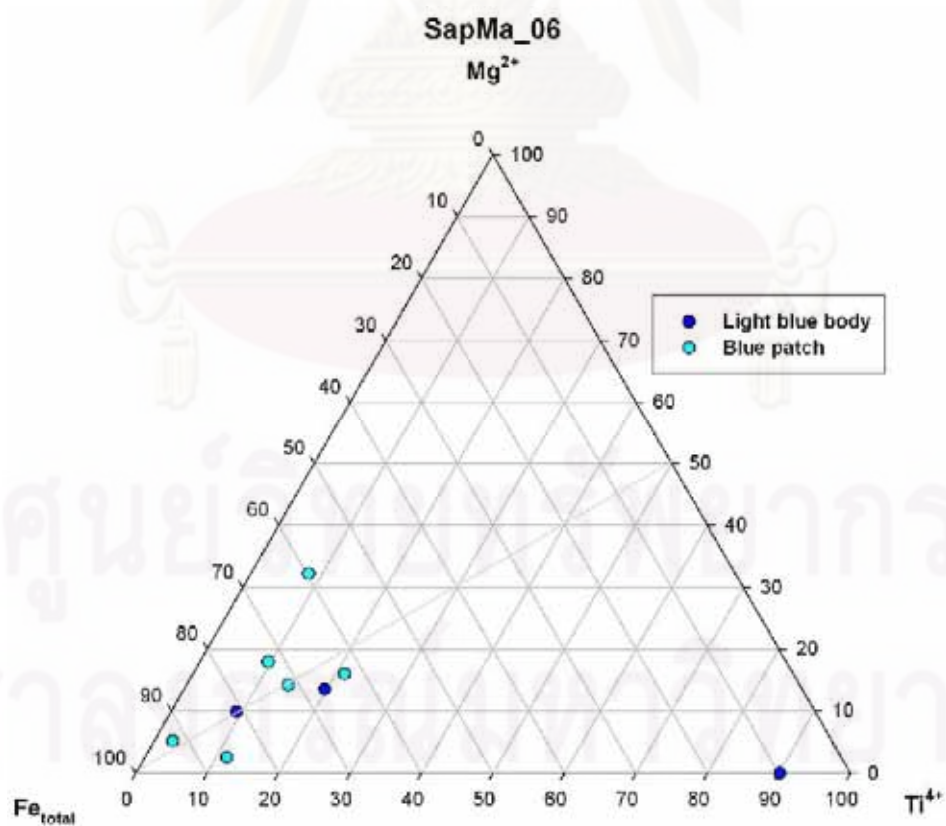


Figure F-2.6 Triangular diagram showing atomic proportions between Mg, Fe and Ti of SapMa_06 (color code B2/2).

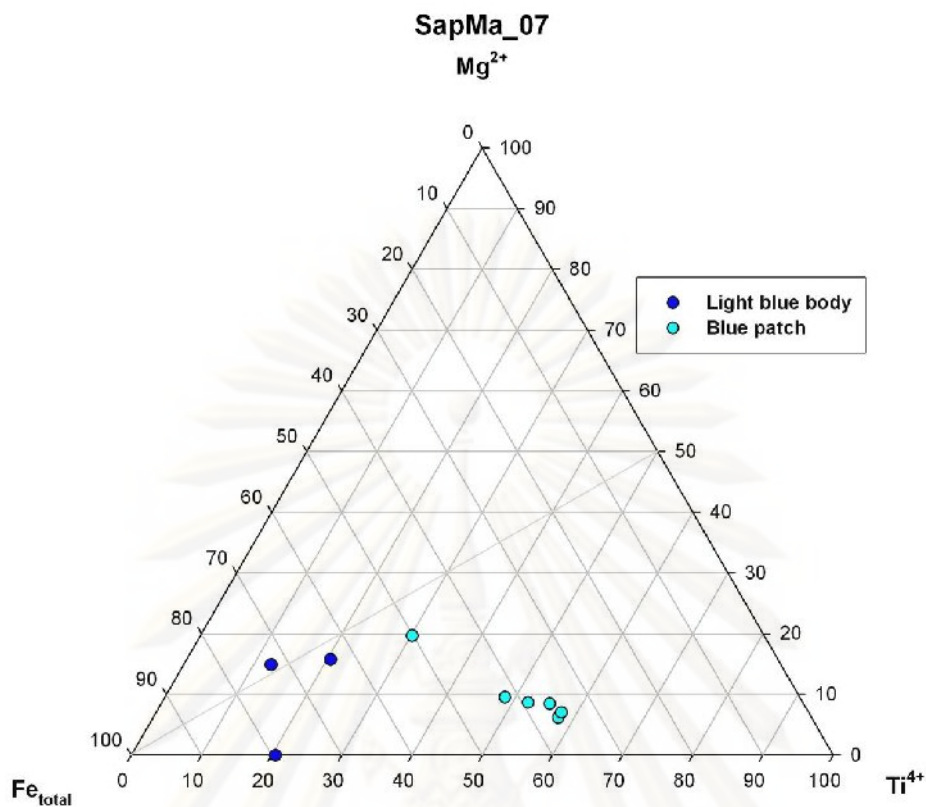


Figure F-2.7 Triangular diagram showing atomic proportions between Mg, Fe and Ti of SapMa_07 (color code B3/3).

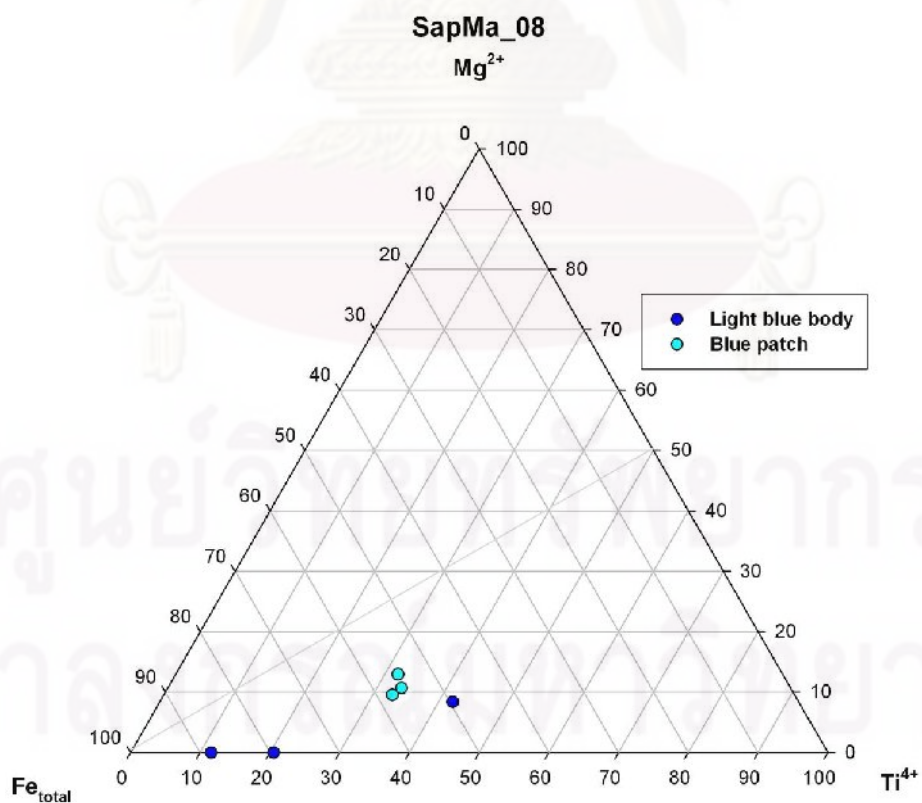


Figure F-2.8 Triangular diagram showing atomic proportions between Mg, Fe and Ti of SapMa_08 (color code B3/3).

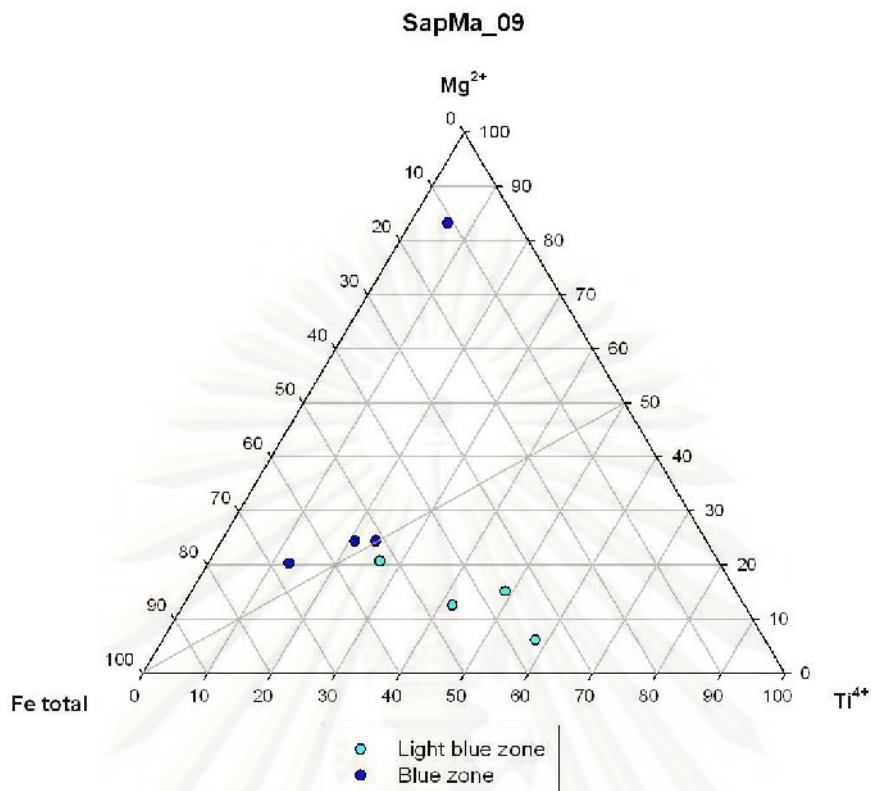


Figure F-2.9 Triangular diagram showing atomic proportions between Mg, Fe and Ti of SapMa_09 (color code B2/2).

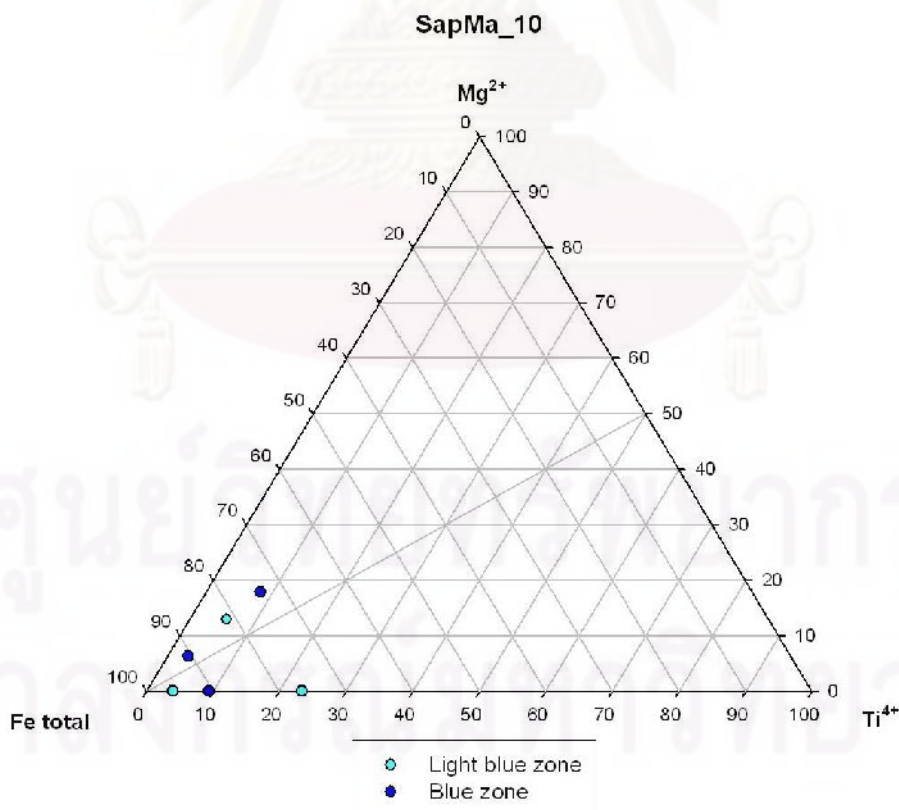


Figure F-2.10 Triangular diagram showing atomic proportions between Mg, Fe and Ti of SapMa_10 (color code B4/2).

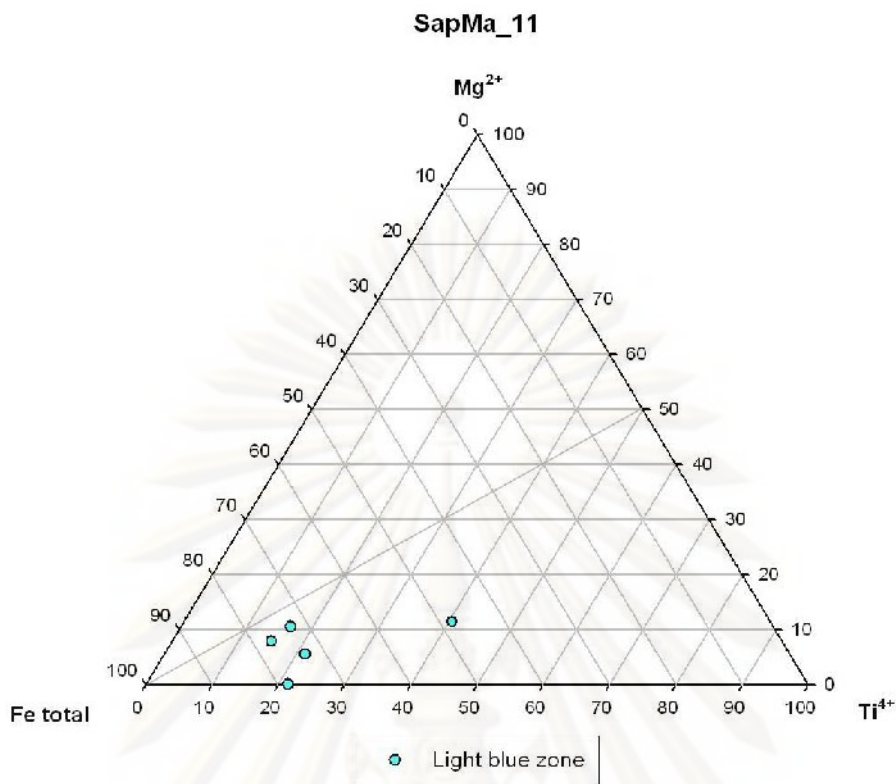


Figure F-2.11 Triangular diagram showing atomic proportions between Mg, Fe and Ti of SapMa_11 (color code vB3/4).

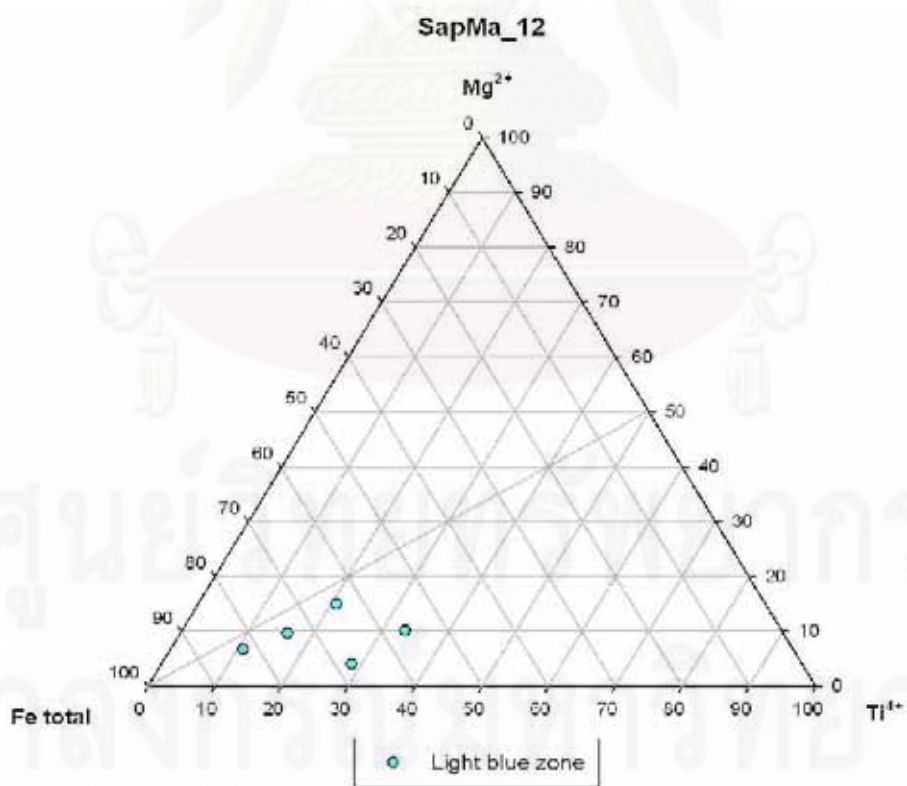


Figure F-2.12 Triangular diagram showing atomic proportions between Mg, Fe and Ti of SapMa_12 (color code vB3/3).

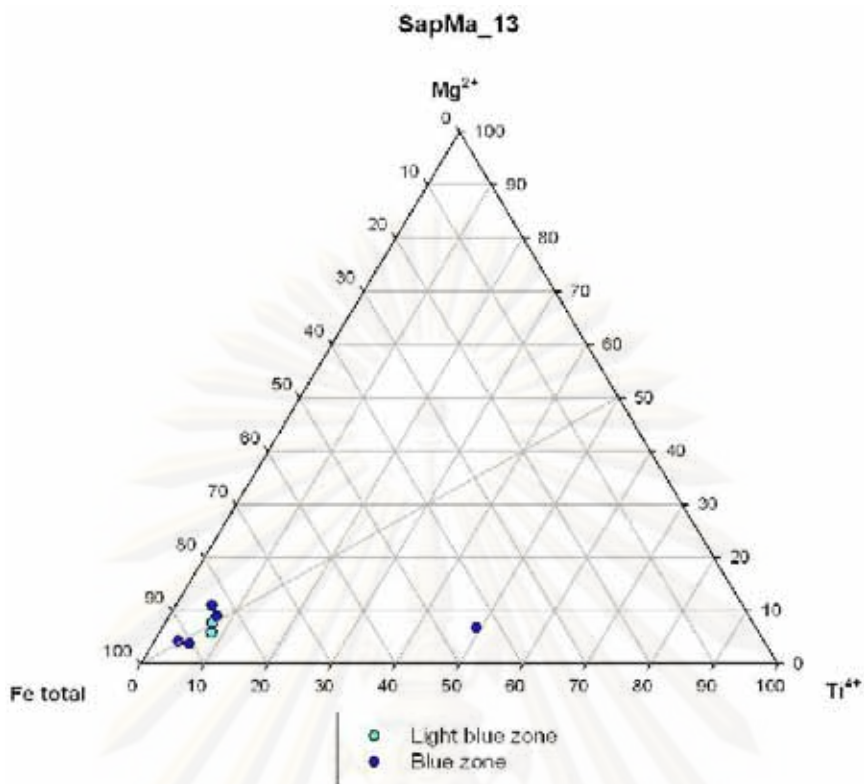


Figure F-2.13 Triangular diagram showing atomic proportions between Mg, Fe and Ti of SapMa_13 (color code vB4/3).

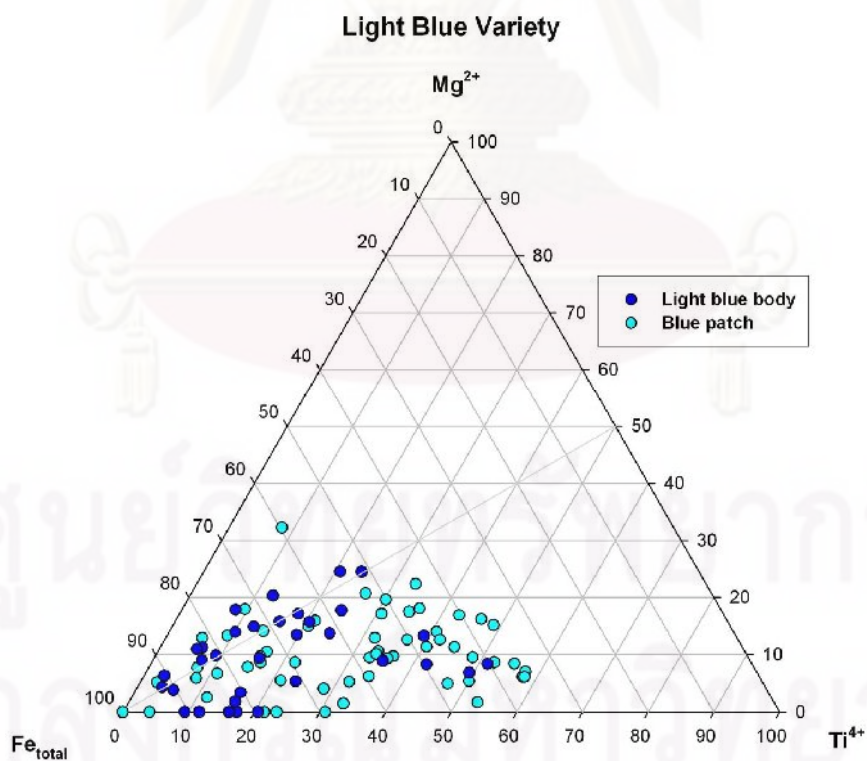


Figure F-2.14 Mg-Fe-Ti ternary diagram of Awissawella corundums in blue variety; that are plotted based on trace analyses in different color zones.



APPENDIX G

ศูนย์วิทยทรัพยากร
จุฬาลงกรณ์มหาวิทยาลัย

Appendix G UV-VIS-NIR & FTIR spectra after heat treatment of Awissawella corundums

Appendix G-1 UV-VIS-NIR spectra of Awisawella corundums after heat in oxidizing atmosphere

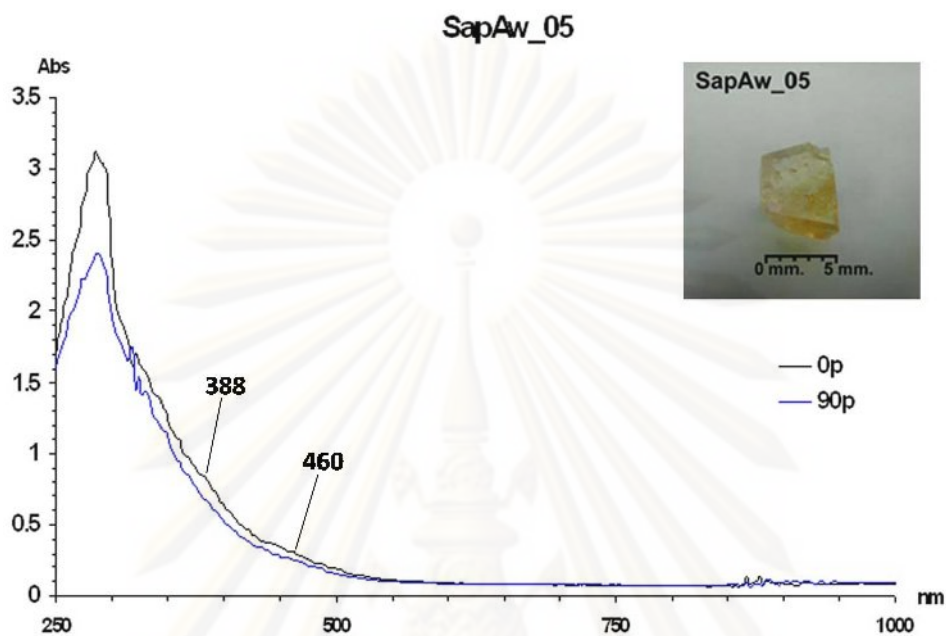


Figure G-1.1 UV-VIS spectra of the sample SapAw_05 measured after heating experiment at 1,650°C in O₂ atmosphere for 10 hours soaking time.

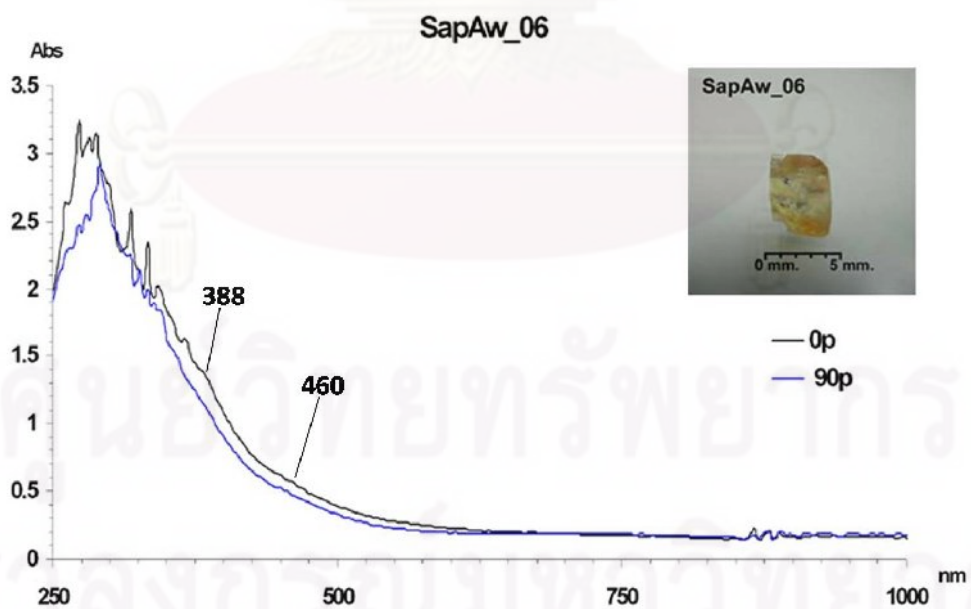


Figure G-1.2 UV-VIS spectra of the sample SapAw_06 measured after heating experiment at 1,650°C in O₂ atmosphere for 10 hours soaking time.

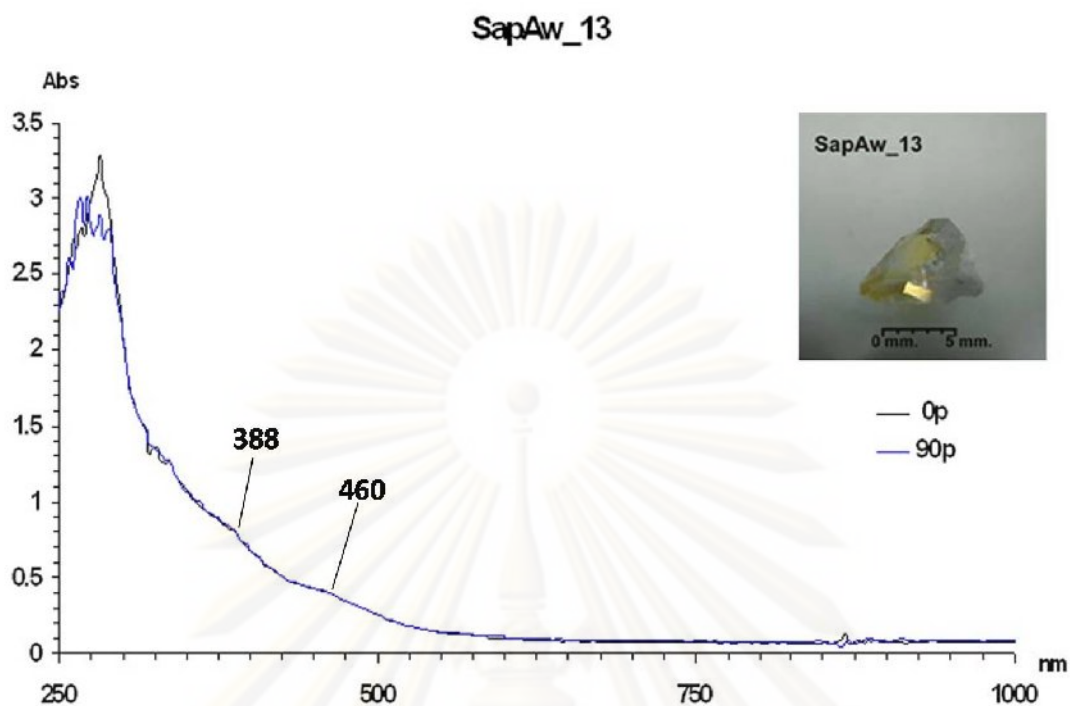


Figure G-1.3 UV-VIS spectra of the sample SapAw_13 measured after heating experiment at 1,650°C in O₂ atmosphere for 10 hours soaking time.

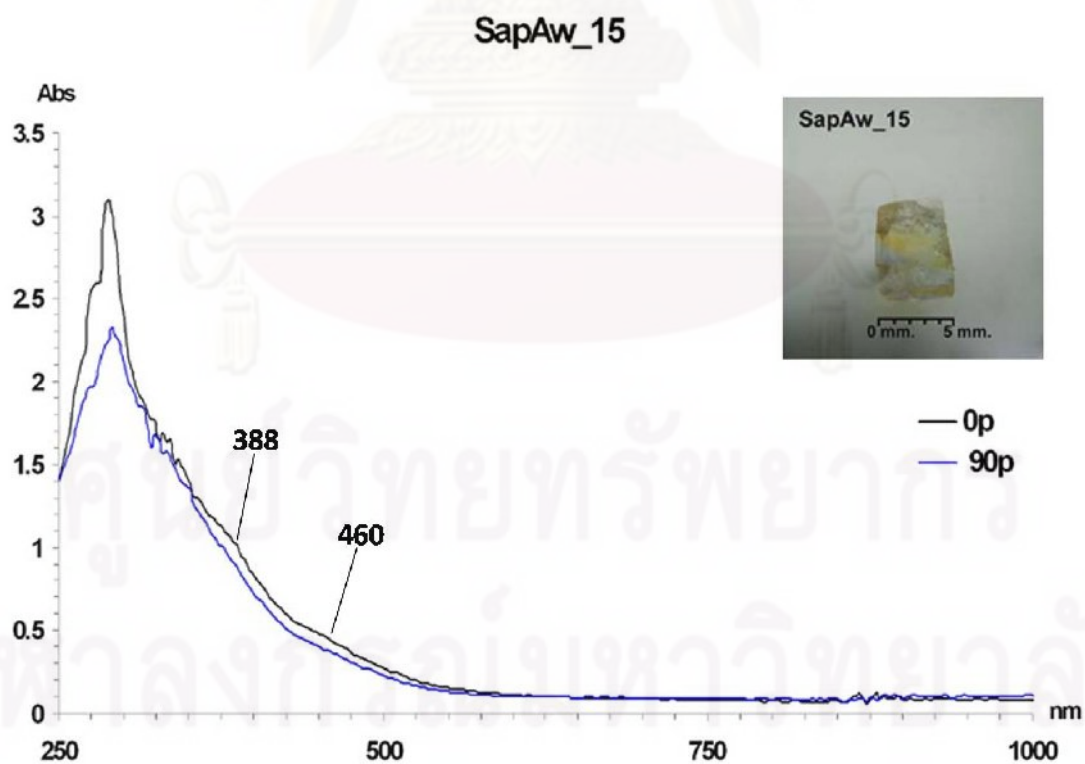


Figure G-1.4 UV-VIS spectra of the sample SapAw_15 measured after heating experiment at 1,650°C in O₂ atmosphere for 10 hours soaking time.

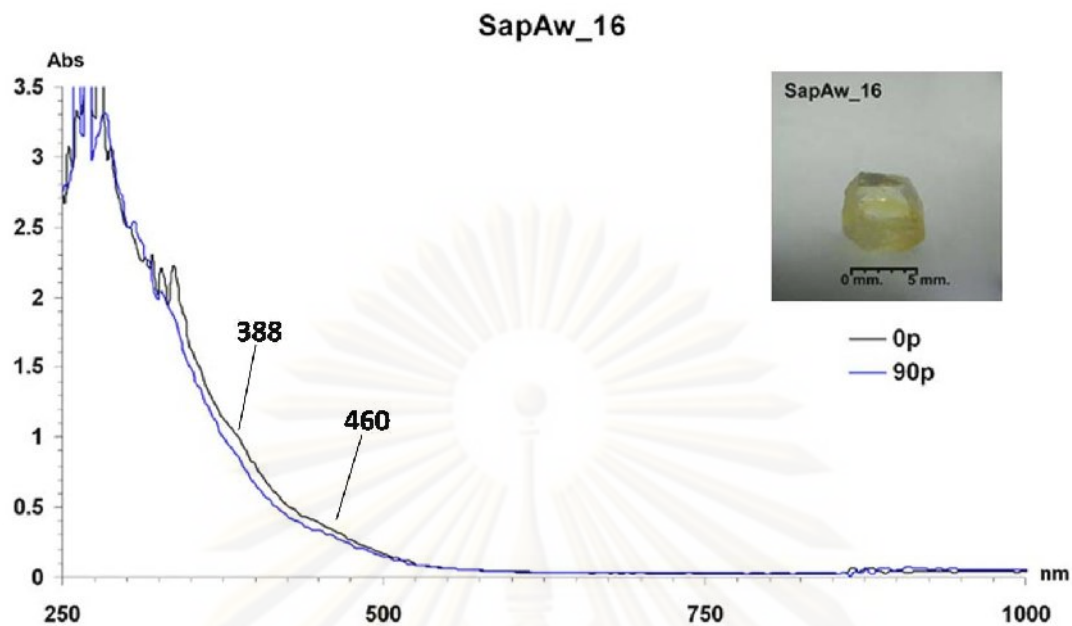


Figure G-1.5 UV-VIS spectra of the sample SapAw_16 measured after heating experiment at 1,650°C in O₂ atmosphere for 10 hours soaking time.

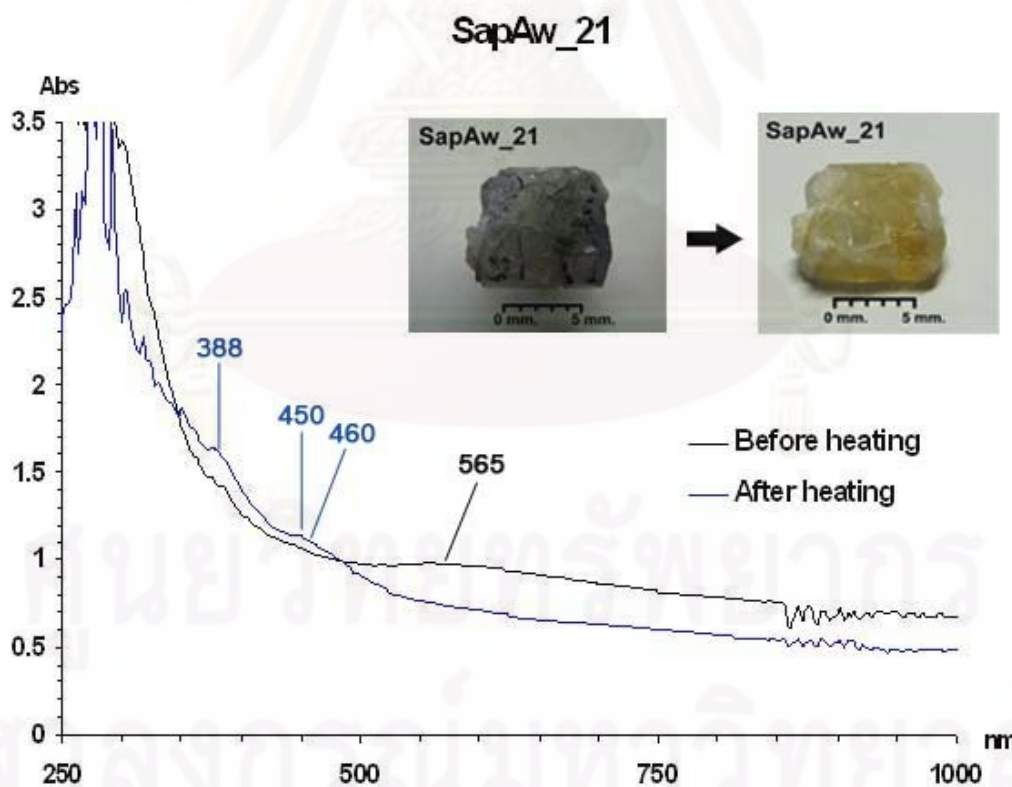


Figure G-1.6 UV-VIS spectra of the sample SapAw_21 measured before and after heating experiment at 1,650°C in O₂ atmosphere for 10 hours soaking time.

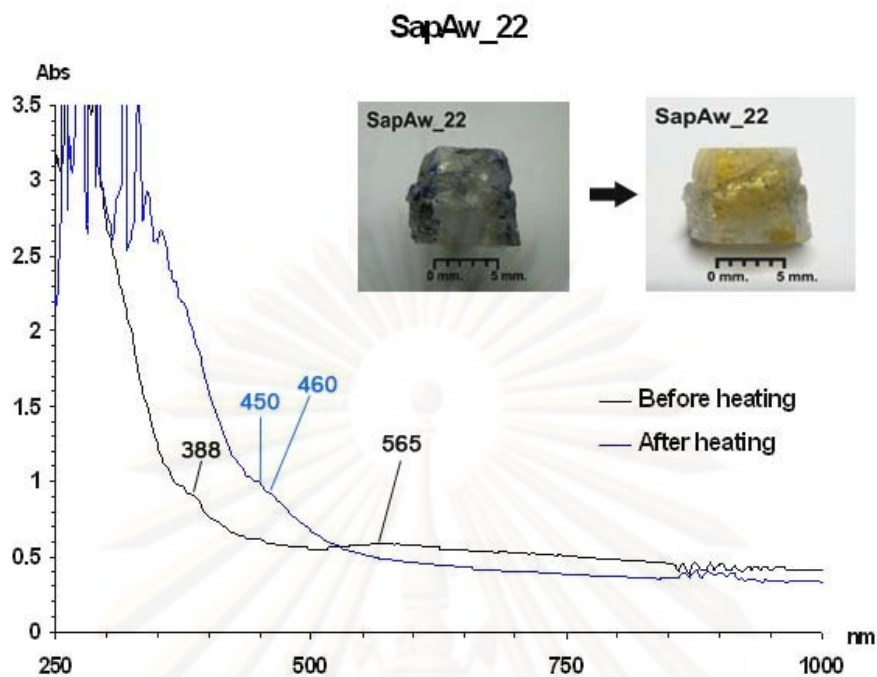


Figure G-1.7 UV-VIS spectra of the sample SapAw_22 measured before and after heating experiment at 1,650°C in O₂ atmosphere for 10 hours soaking time.

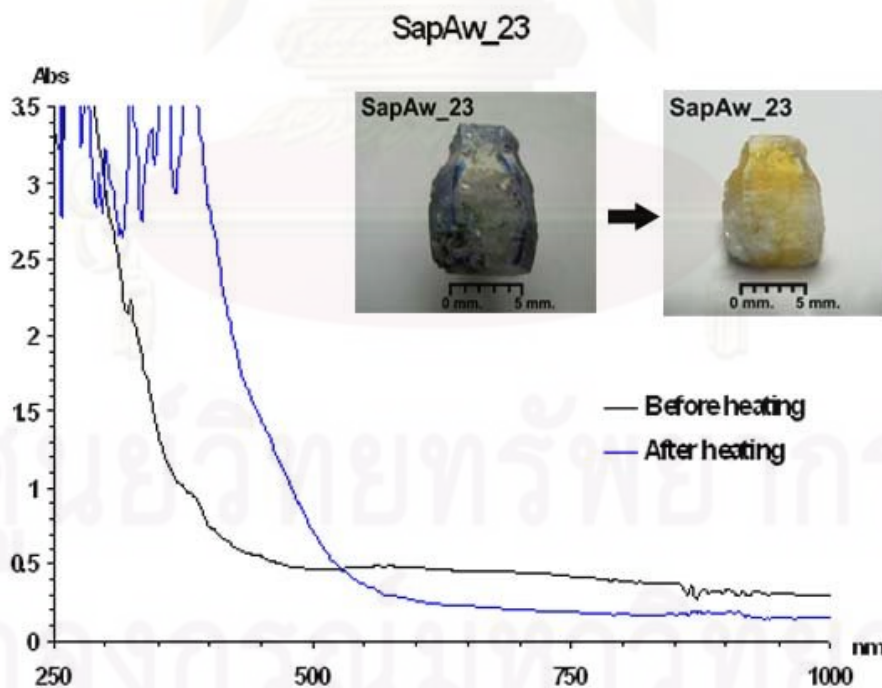


Figure G-1.8 UV-VIS spectra of the sample SapAw_23 measured before and after heating experiment at 1,650°C in O₂ atmosphere for 10 hours soaking time.

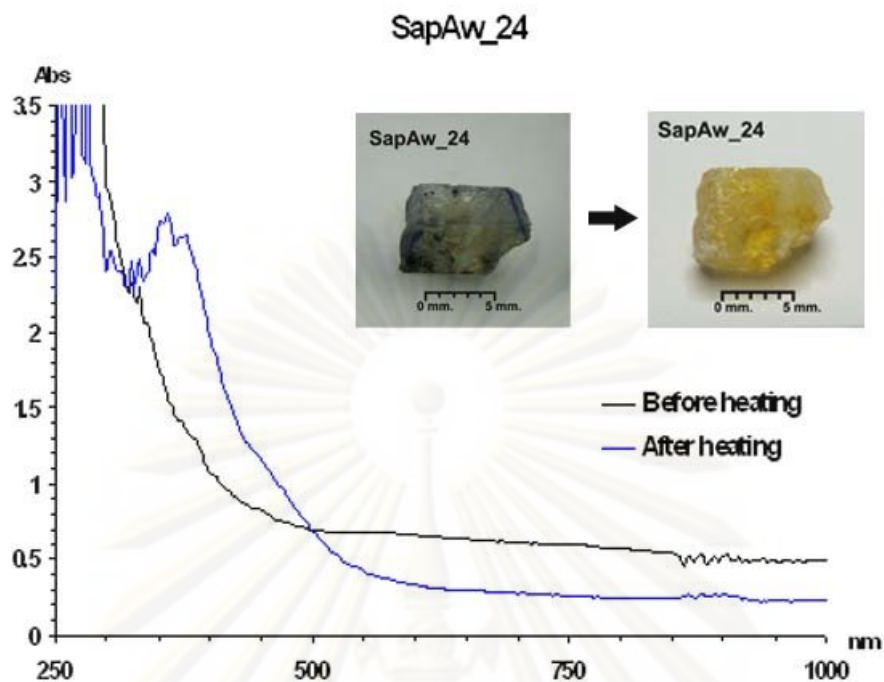


Figure G-1.9 UV-VIS spectra of the sample SapAw_24 measured before and after heating experiment at 1,650°C in O₂ atmosphere for 10 hours soaking time.

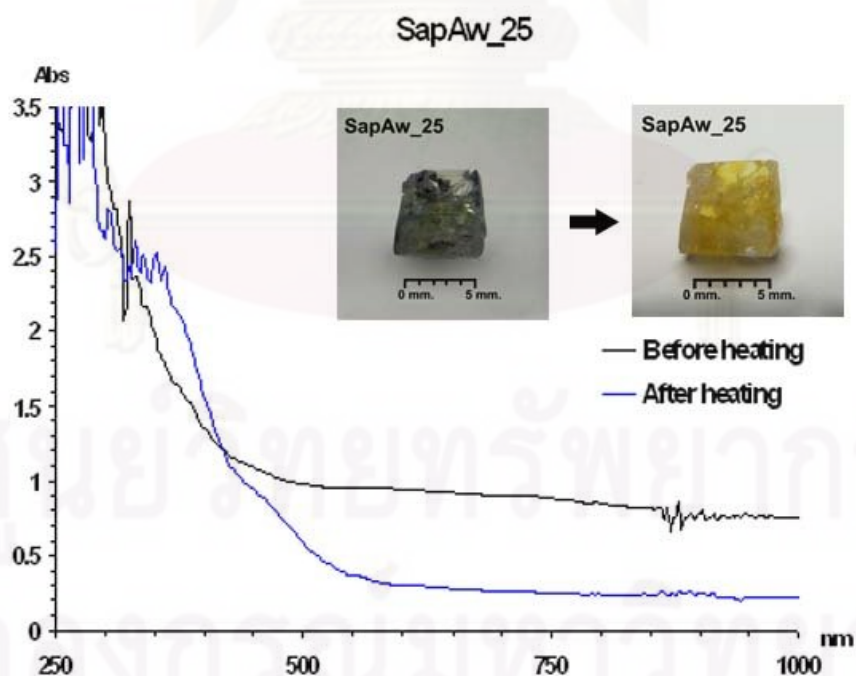


Figure G-1.10 UV-VIS spectra of the sample SapAw_25 measured before and after heating experiment at 1,650°C in O₂ atmosphere for 10 hours soaking time.

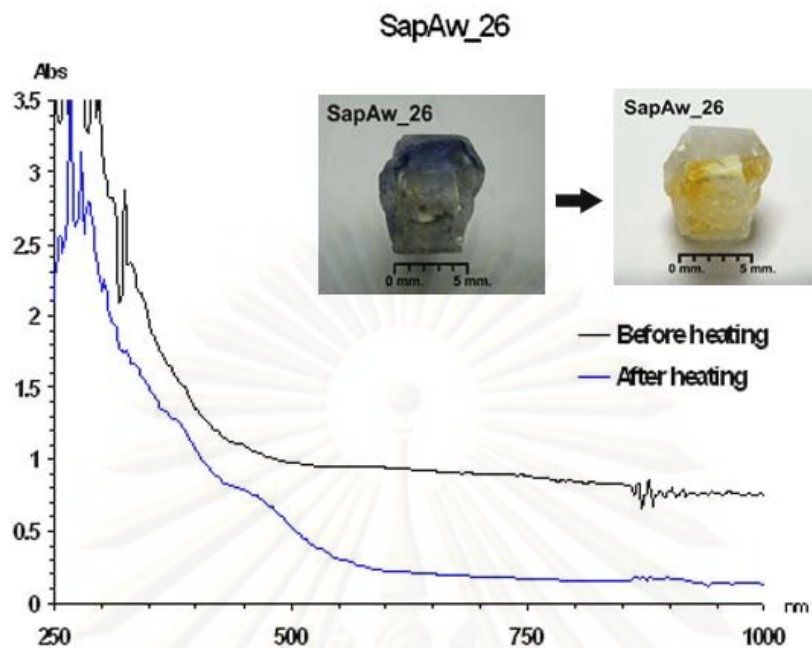


Figure G-1.11 UV-VIS spectra of the sample SapAw_26 measured before and after heating experiment at 1,650°C in O₂ atmosphere for 10 hours soaking time.

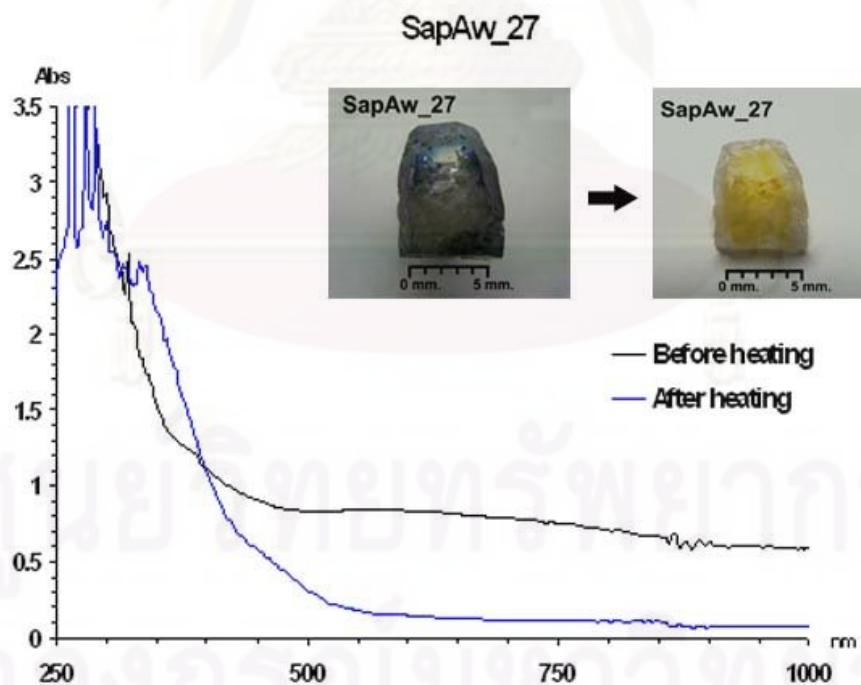


Figure G-1.12 UV-VIS spectra of the sample SapAw_27 measured before and after heating experiment at 1,650°C in O₂ atmosphere for 10 hours soaking time.

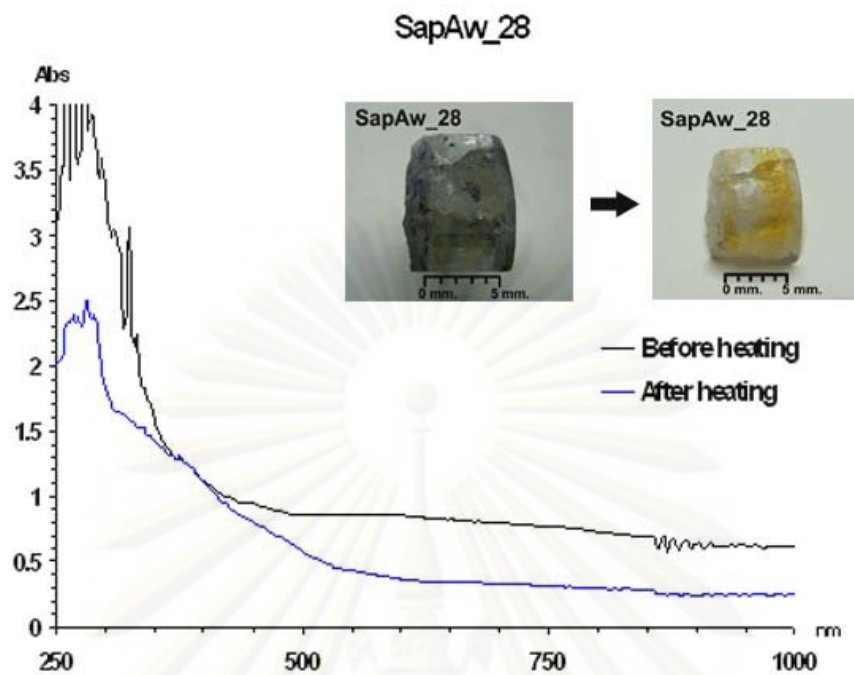


Figure G-1.13 UV-VIS spectra of the sample SapAw_28 measured before and after heating experiment at 1,650°C in O₂ atmosphere for 10 hours soaking time.

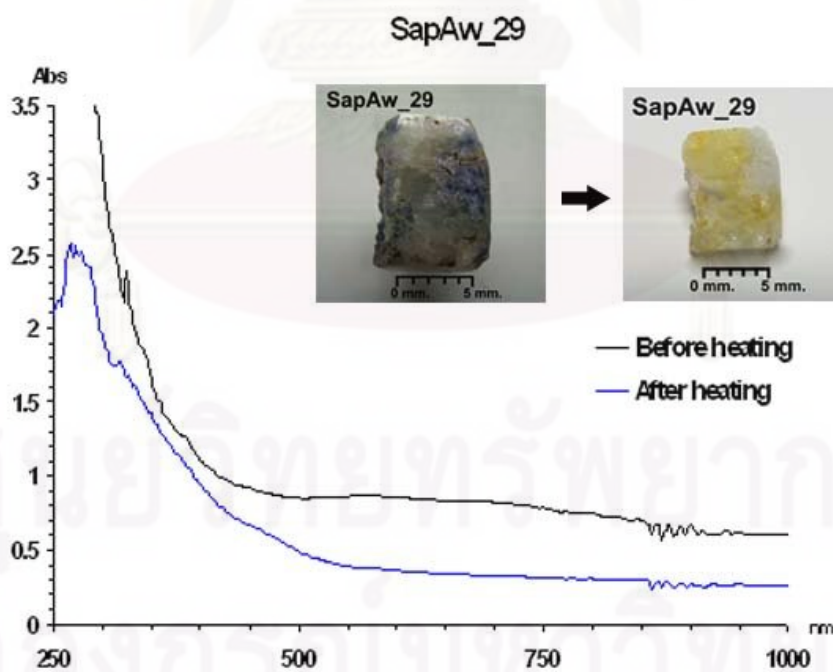


Figure G-1.14 UV-VIS spectra of the sample SapAw_29 measured before and after heating experiment at 1,650°C in O₂ atmosphere for 10 hours soaking time.

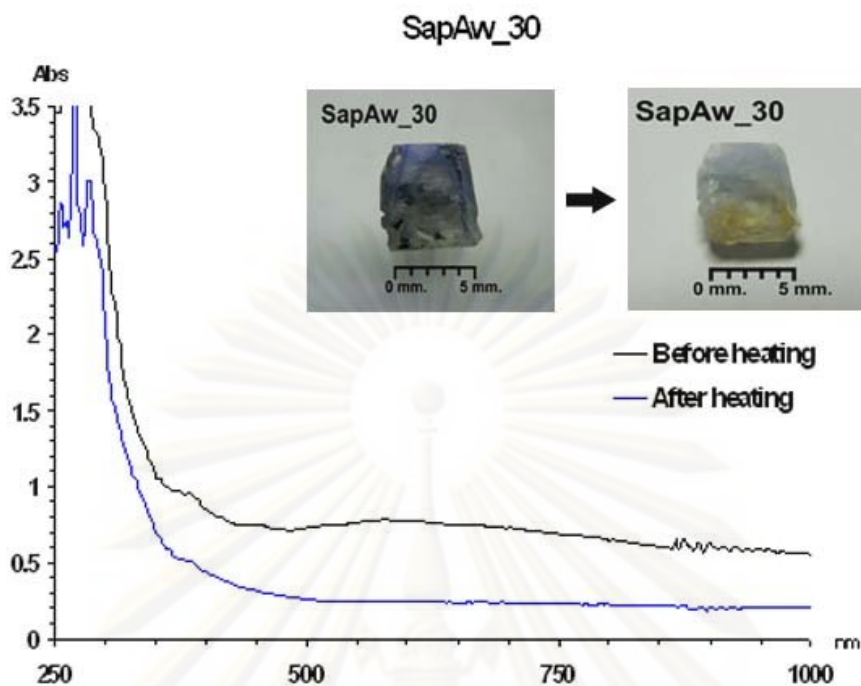


Figure G-1.15 UV-VIS spectra of the sample SapAw_30 measured before and after heating experiment at 1,650°C in O₂ atmosphere for 10 hours soaking time.

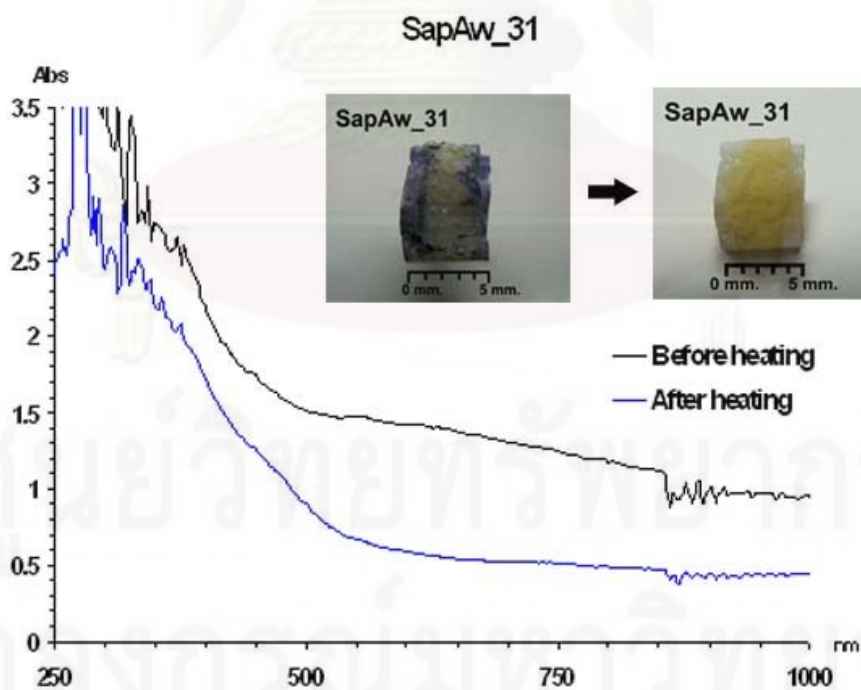


Figure G-1.16 UV-VIS spectra of the sample SapAw_31 measured before and after heating experiment at 1,650°C in O₂ atmosphere for 10 hours soaking time.

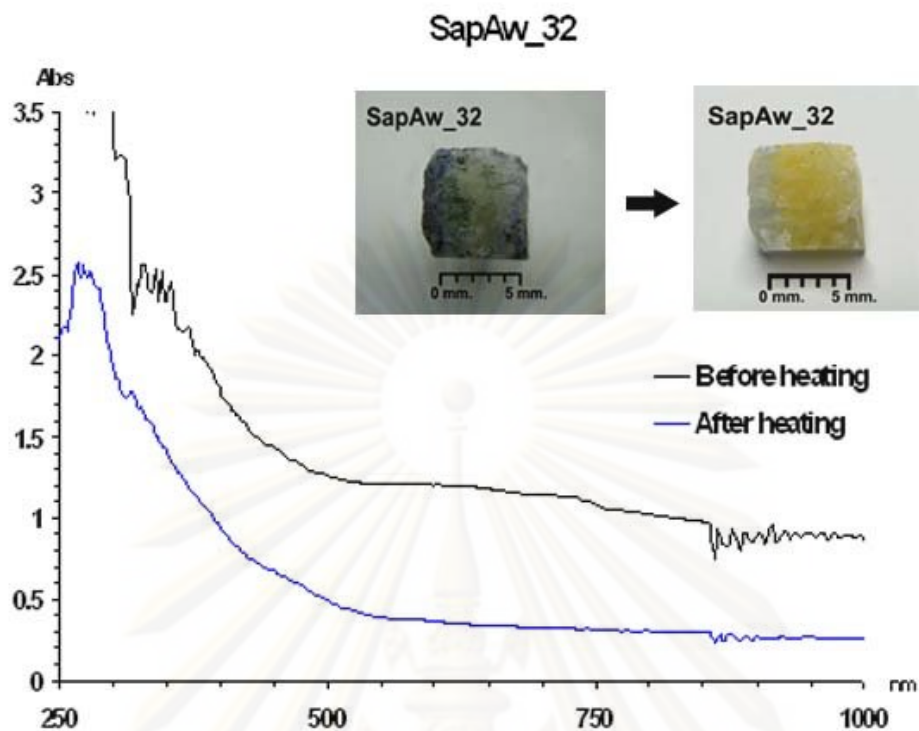


Figure G-1.17 UV-VIS spectra of the sample SapAw_32 measured before and after heating experiment at 1,650°C in O₂ atmosphere for 10 hours soaking time.

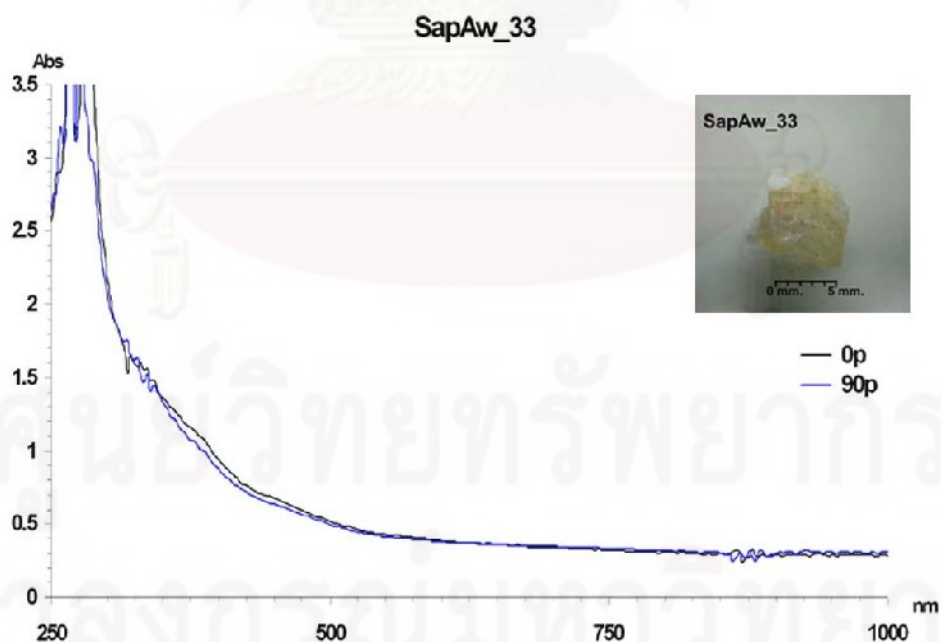


Figure G-1.18 UV-VIS spectra of the sample SapAw_33 measured before and after heating experiment at 1,650°C in O₂ atmosphere for 10 hours soaking time.

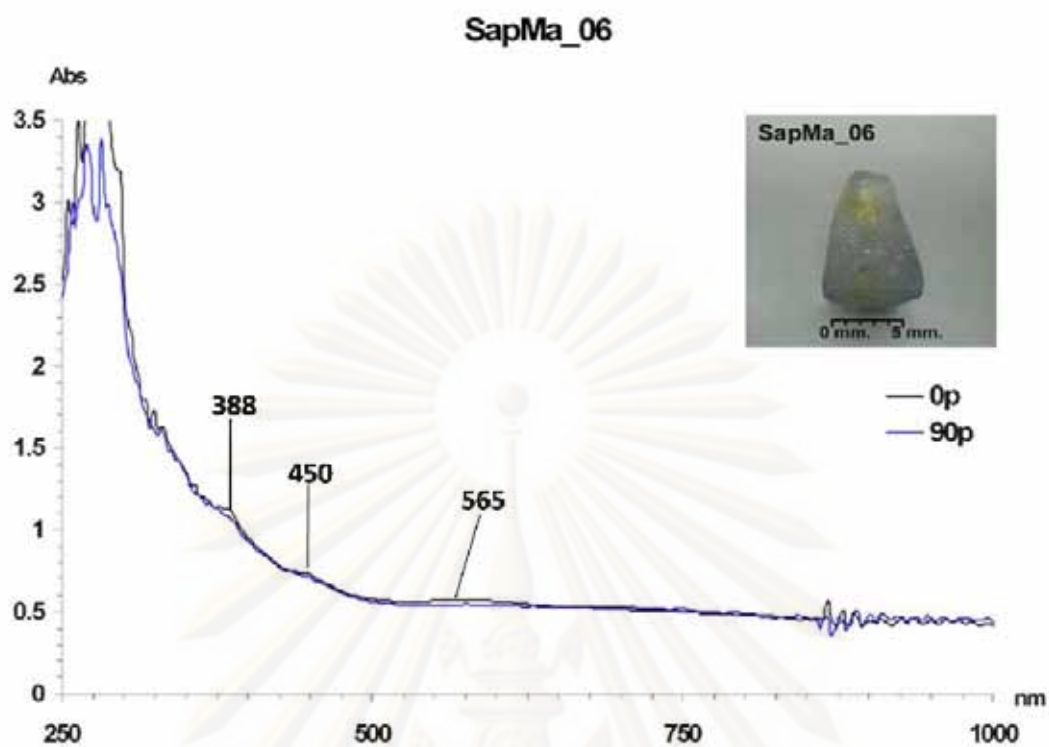


Figure G-1.19 UV-VIS spectra of the sample SapMa_06 measured after heating experiment at 1,650°C in O₂ atmosphere for 10 hours soaking time.

Appendix G-2 UV-VIS-NIR spectra of Awisawella corundums after heat in reducing atmosphere

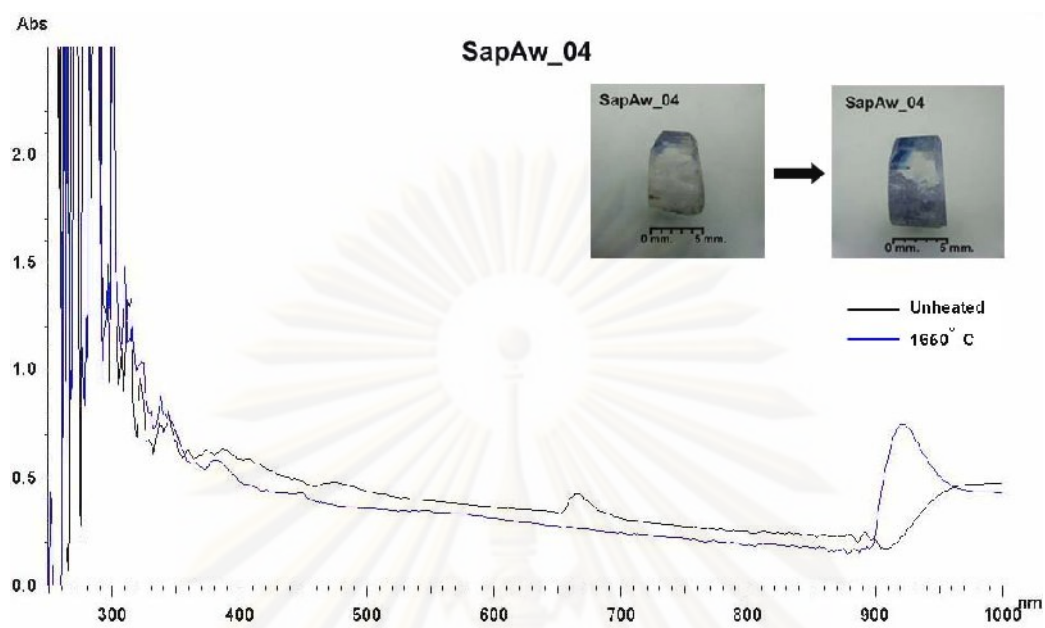


Figure G-2.1 UV-VIS spectra of the sample SapAw_04 measured before and after heating experiment at 1,650°C in N₂ atmosphere for 5 hours soaking time.

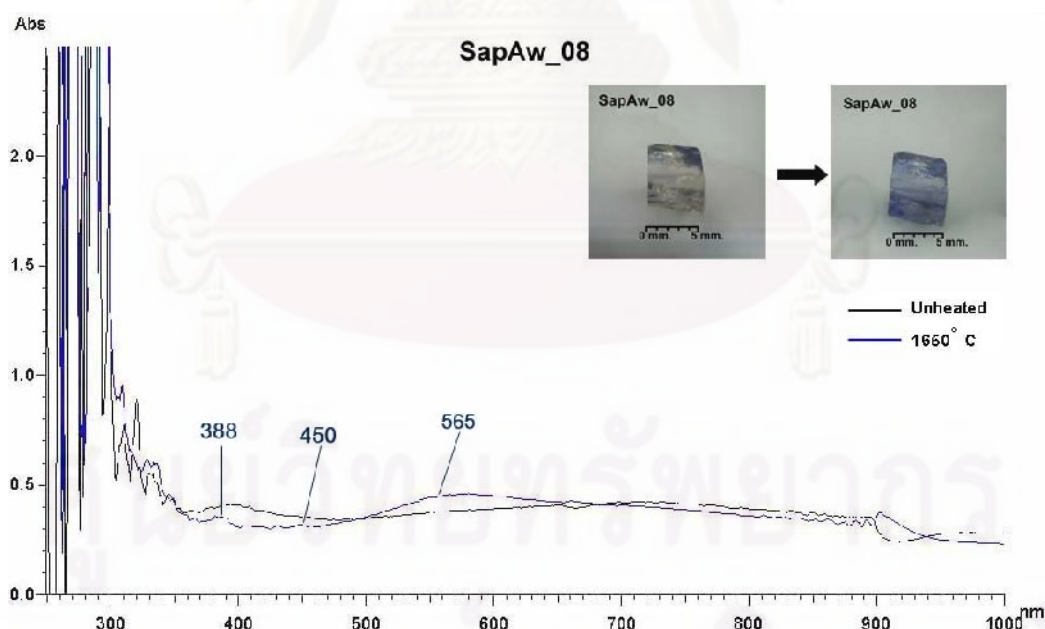


Figure G-2.2 UV-VIS spectra of the sample SapAw_08 measured before and after heating experiment at 1,650°C in N₂ atmosphere for 5 hours soaking time.

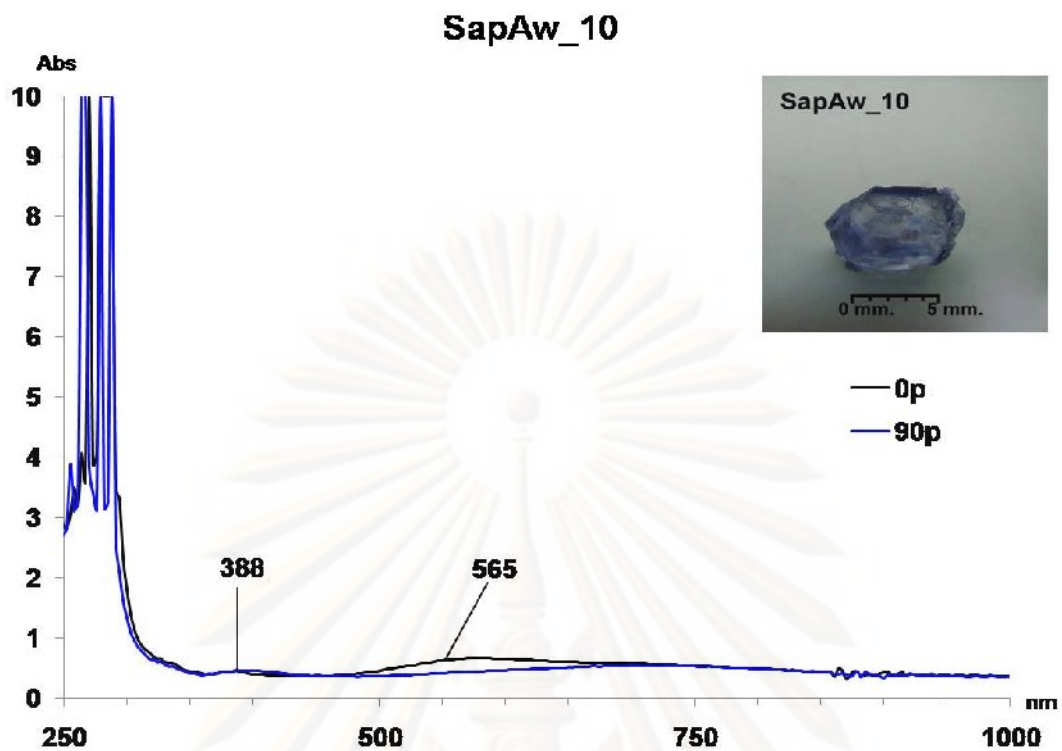


Figure G-2.3 UV-VIS spectra of the sample SapAw_10 measured after heating experiment at 1,650°C in N₂ atmosphere for 5 hours soaking time.

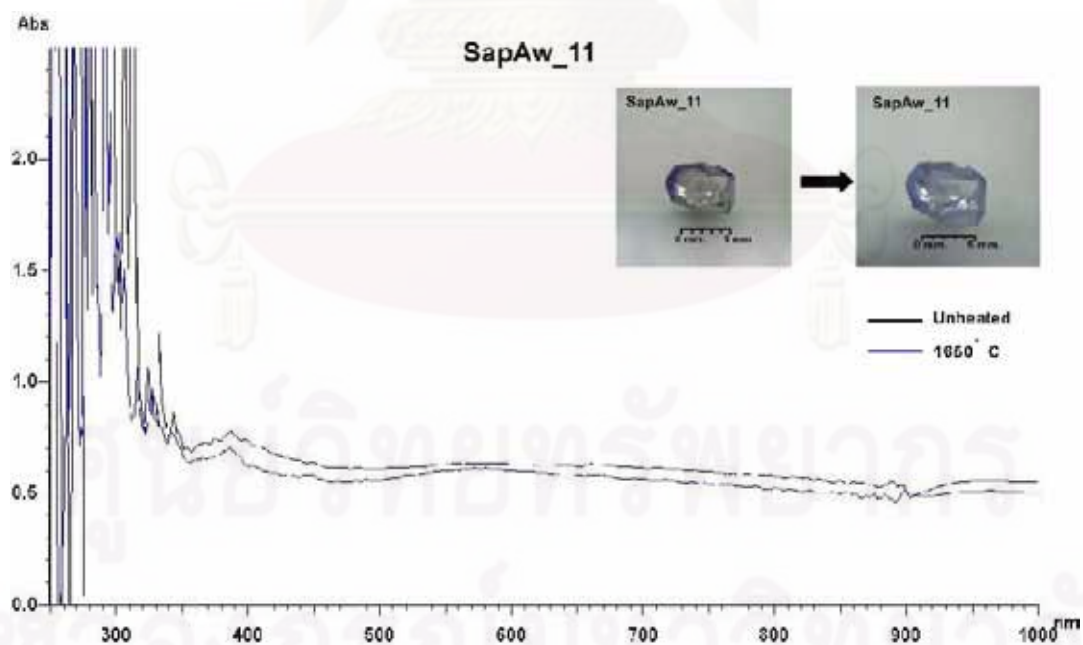


Figure G-2.4 UV-VIS spectra of the sample SapAw_11 measured before and after heating experiment at 1,650°C in N₂ atmosphere for 5 hours soaking time.

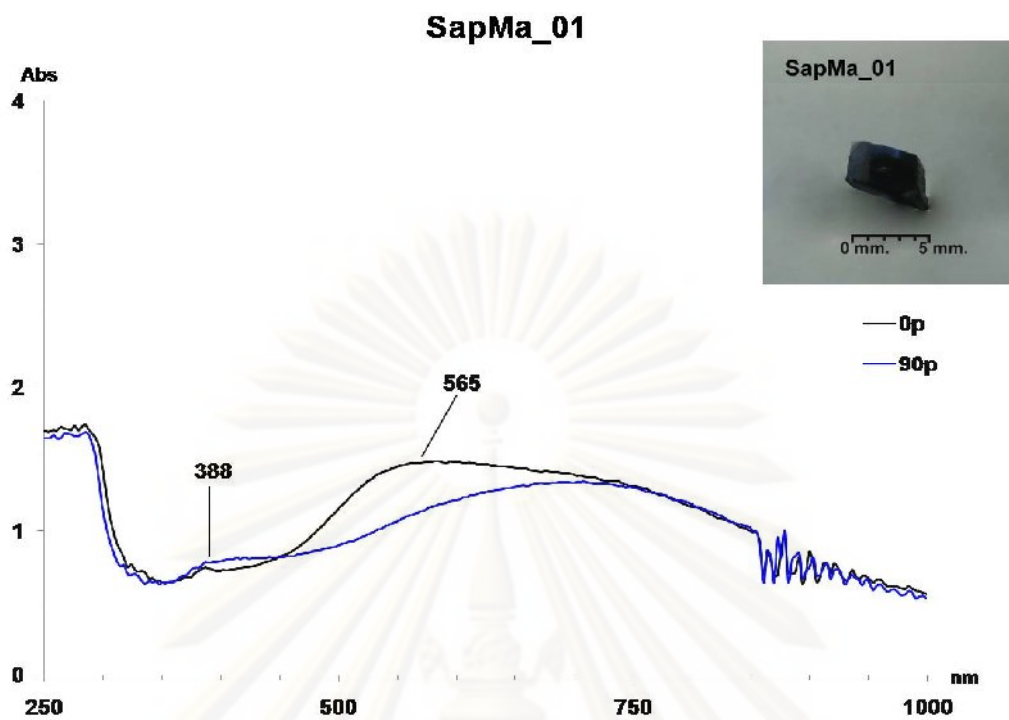


Figure G-2.5 UV-VIS spectra of the sample SapMa_01 measured after heating experiment at 1,650°C in N₂ atmosphere for 5 hours soaking time.

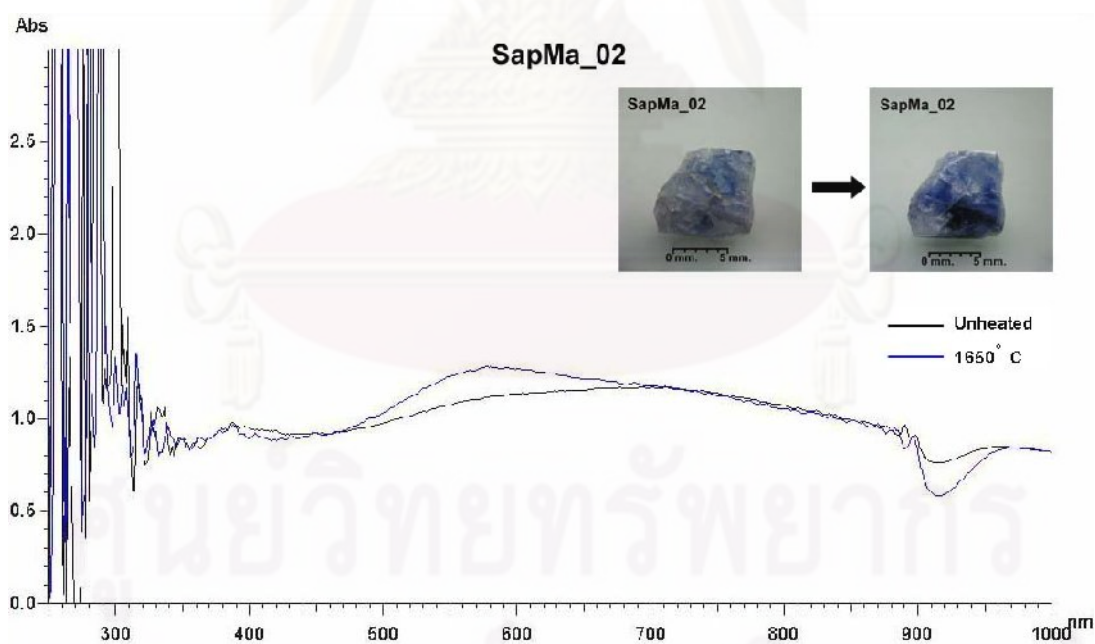


Figure G-2.6 UV-VIS spectra of the sample SapMa_02 measured before and after heating experiment at 1,650°C in N₂ atmosphere for 5 hours soaking time.

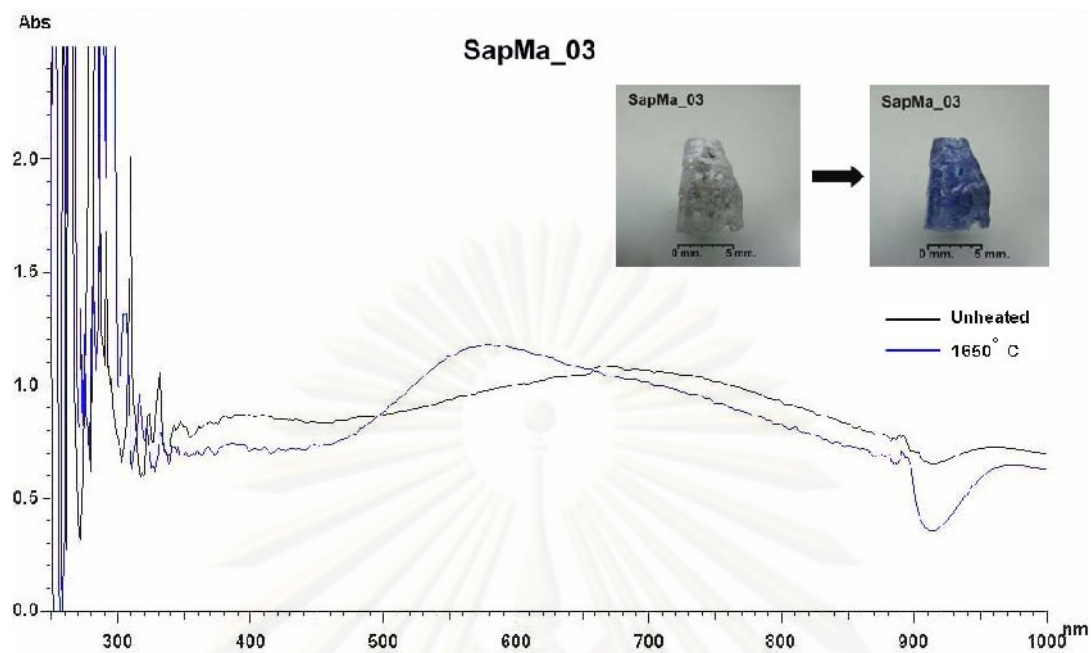


Figure G-2.7 UV-VIS spectra of the sample SapMa_03 measured before and after heating experiment at 1,650°C in N₂ atmosphere for 5 hours soaking time.

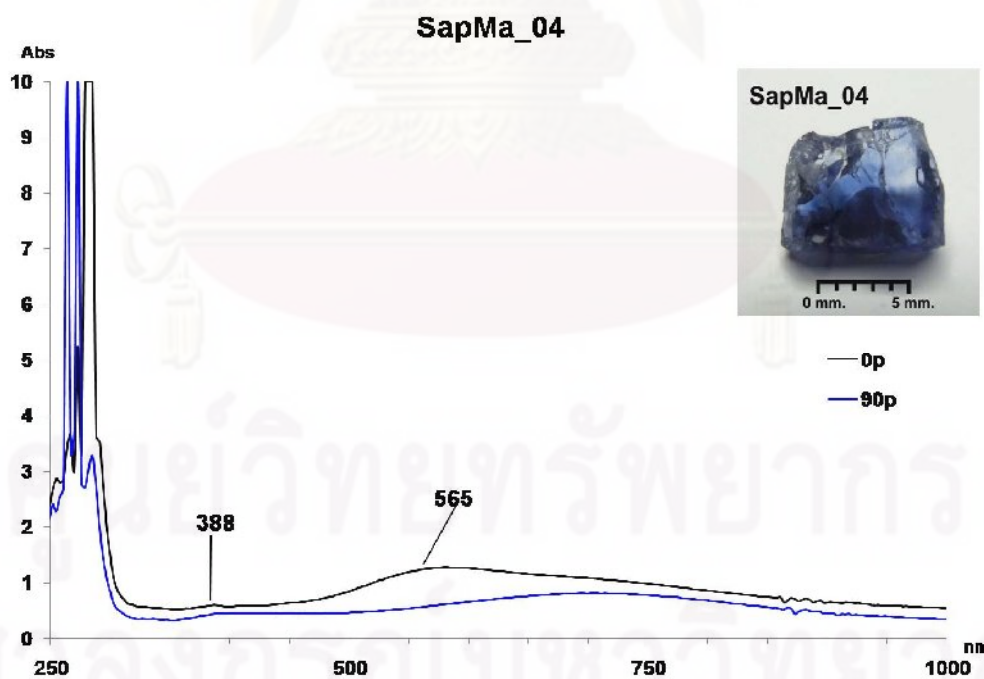


Figure G-2.8 UV-VIS spectra of the sample SapMa_04 measured after heating experiment at 1,650°C in N₂ atmosphere for 5 hours soaking time.

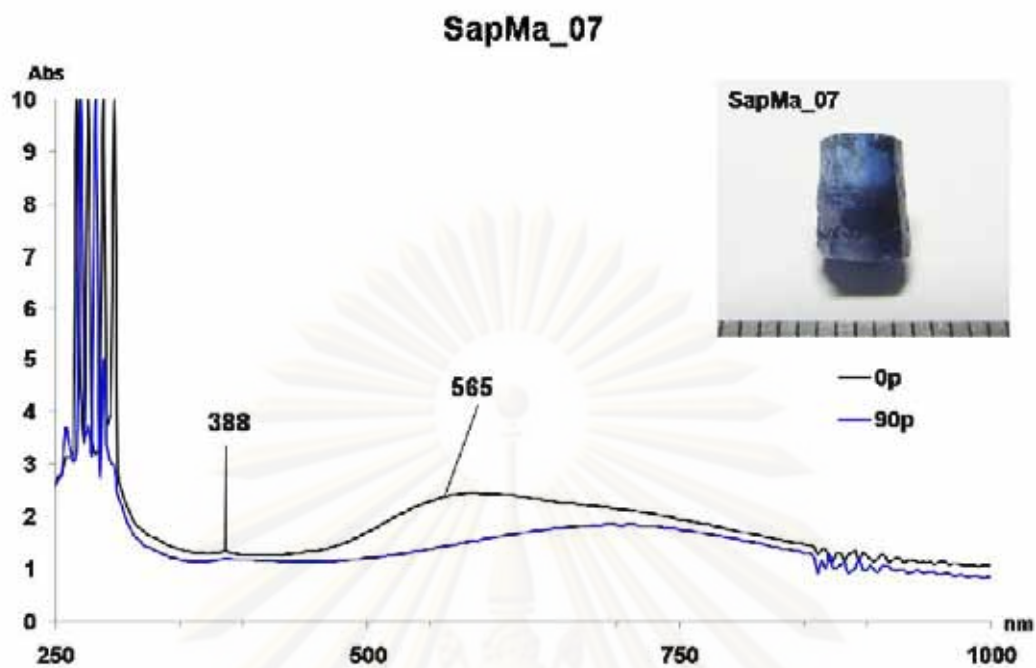


Figure G-2.9 UV-VIS spectra of the sample SapMa_07 measured after heating experiment at 1,650°C in N₂ atmosphere for 5 hours soaking time.

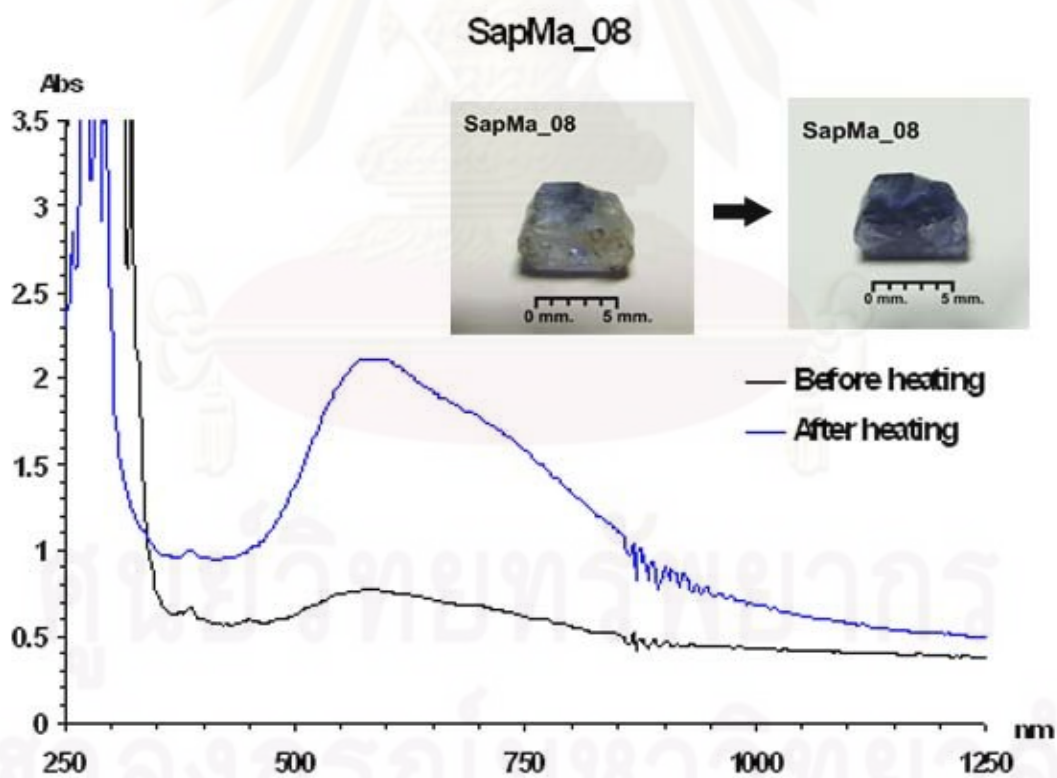


Figure G-2.10 UV-VIS spectra of the sample SapMa_08 measured before and after heating experiment at 1,650°C in N₂ atmosphere for 5 hours soaking time.

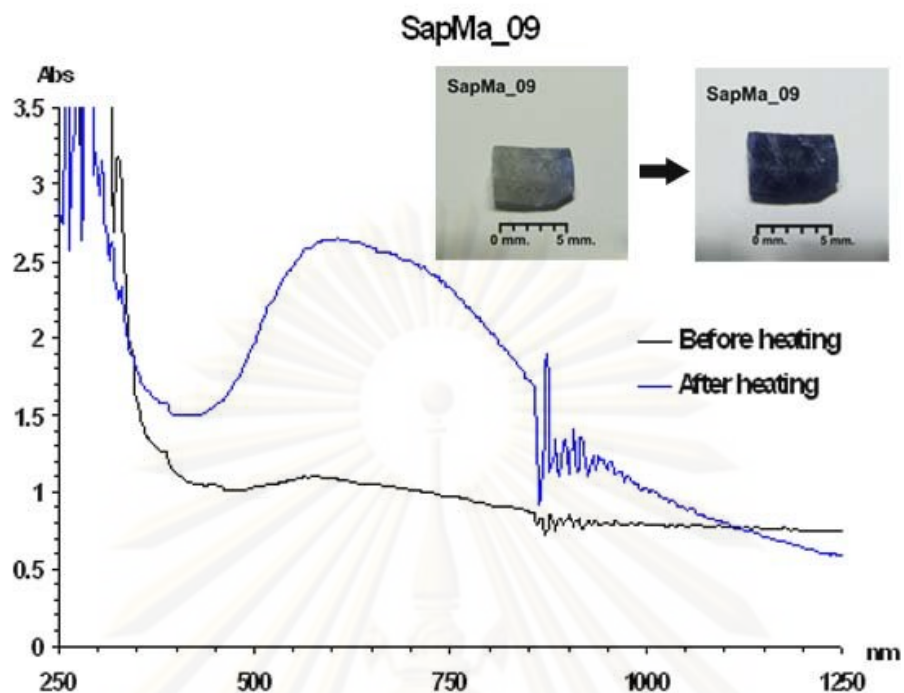


Figure G-2.11 UV-VIS spectra of the sample SapMa_09 measured before and after heating experiment at 1,650°C in N₂ atmosphere for 5 hours soaking time.

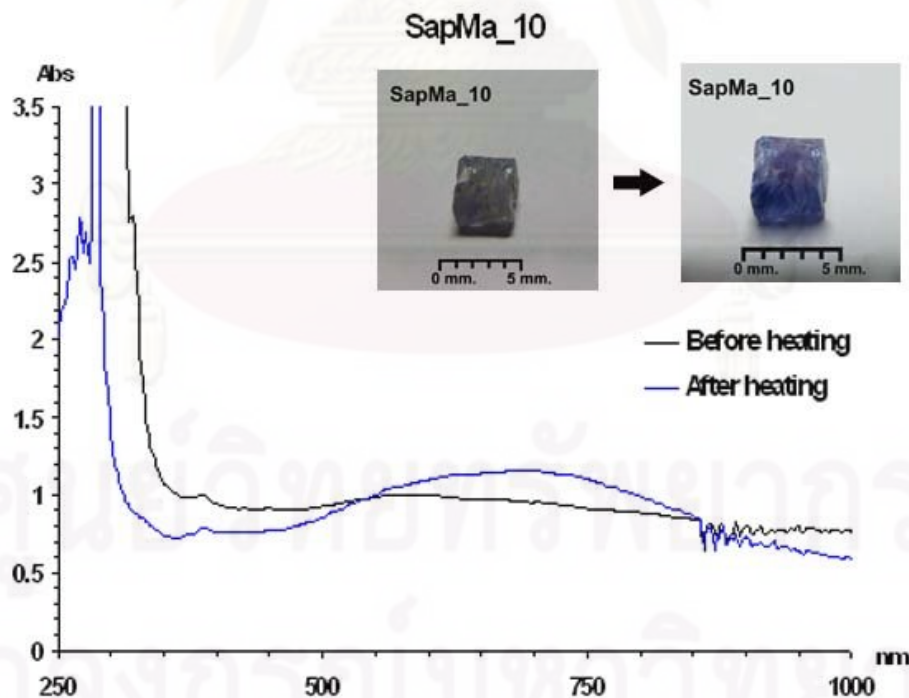


Figure G-2.12 UV-VIS spectra of the sample SapMa_10 measured before and after heating experiment at 1,650°C in N₂ atmosphere for 5 hours soaking time.

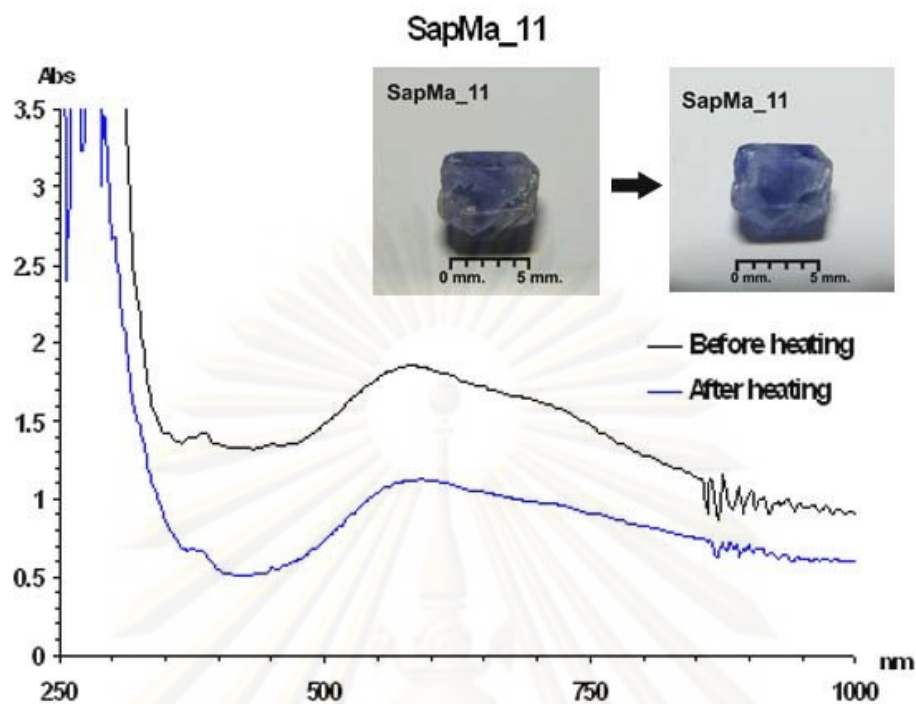


Figure G-2.13 UV-VIS spectra of the sample SapMa_11 measured before and after heating experiment at 1,650°C in N₂ atmosphere for 5 hours soaking time.

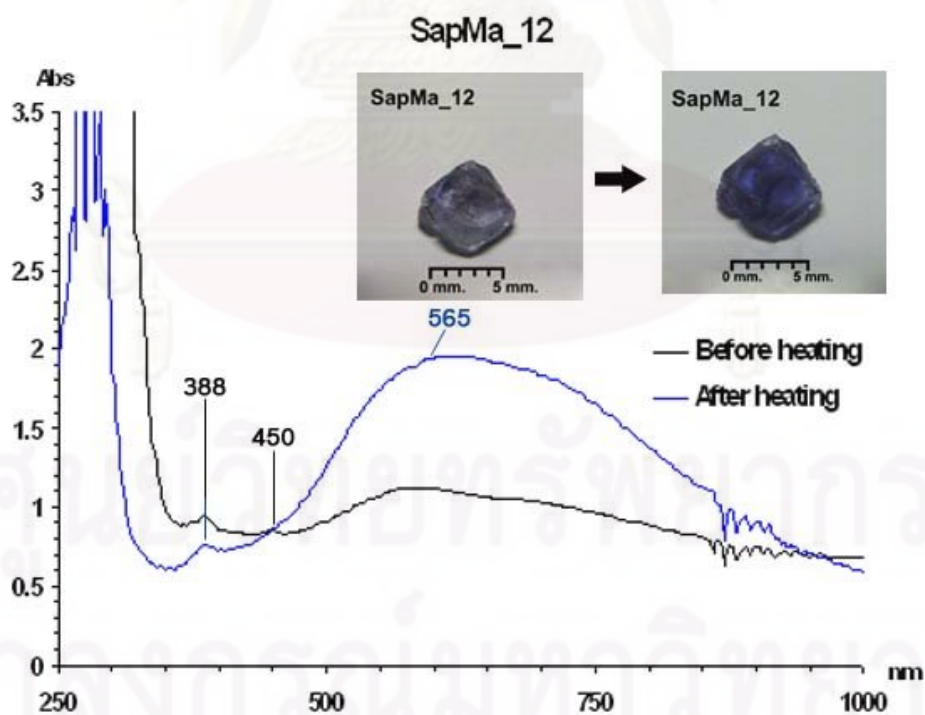


Figure G-2.14 UV-VIS spectra of the sample SapMa_12 measured before and after heating experiment at 1,650°C in N₂ atmosphere for 5 hours soaking time.

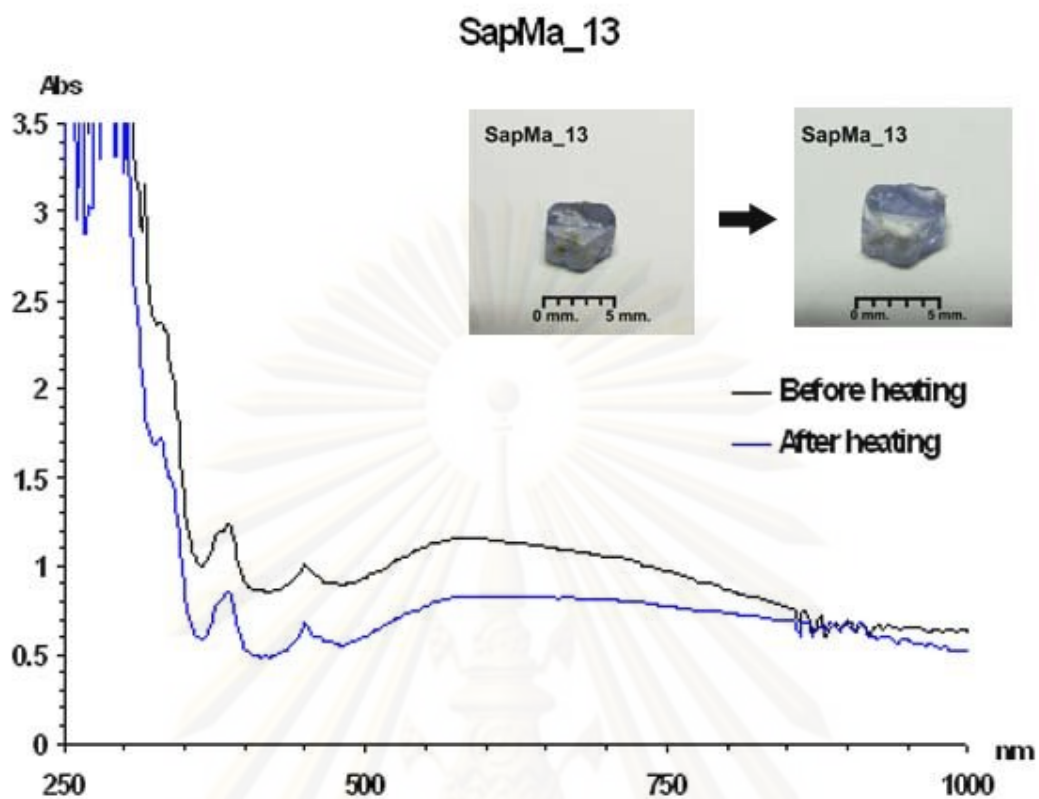


Figure G-2.15 UV-VIS spectra of the sample SapMa_13 measured before and after heating experiment at 1,650°C in N₂ atmosphere for 5 hours soaking time.

Appendix G-3 FTIR spectra of Awisawella corundums after heat treatment

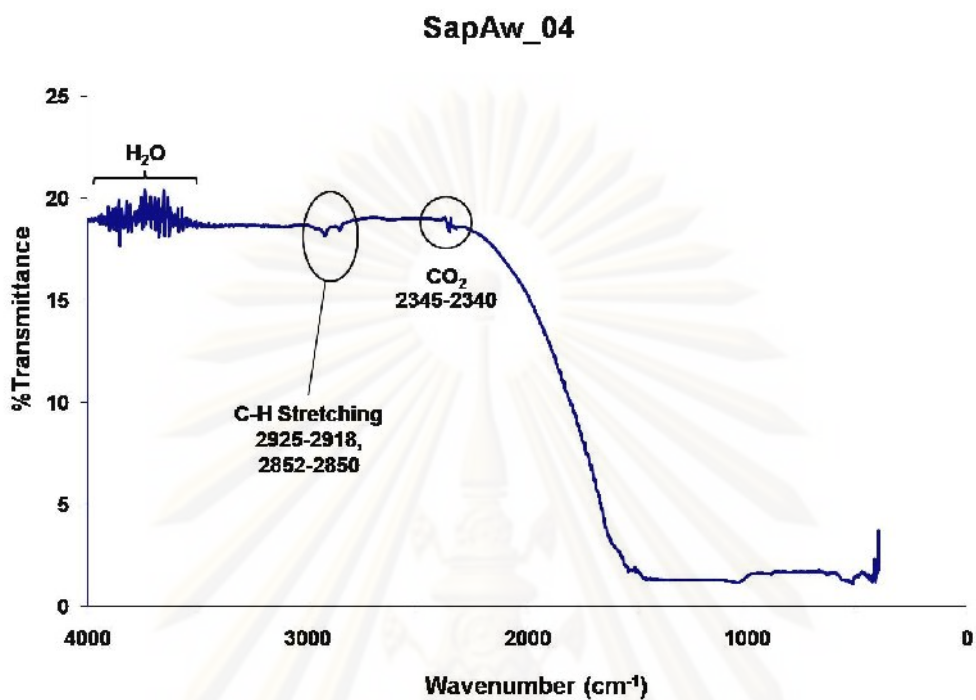


Figure G-3.1 FTIR spectra of the sample SapAw_04 of yellow variety after heating in reducing environment at 1,650°C.

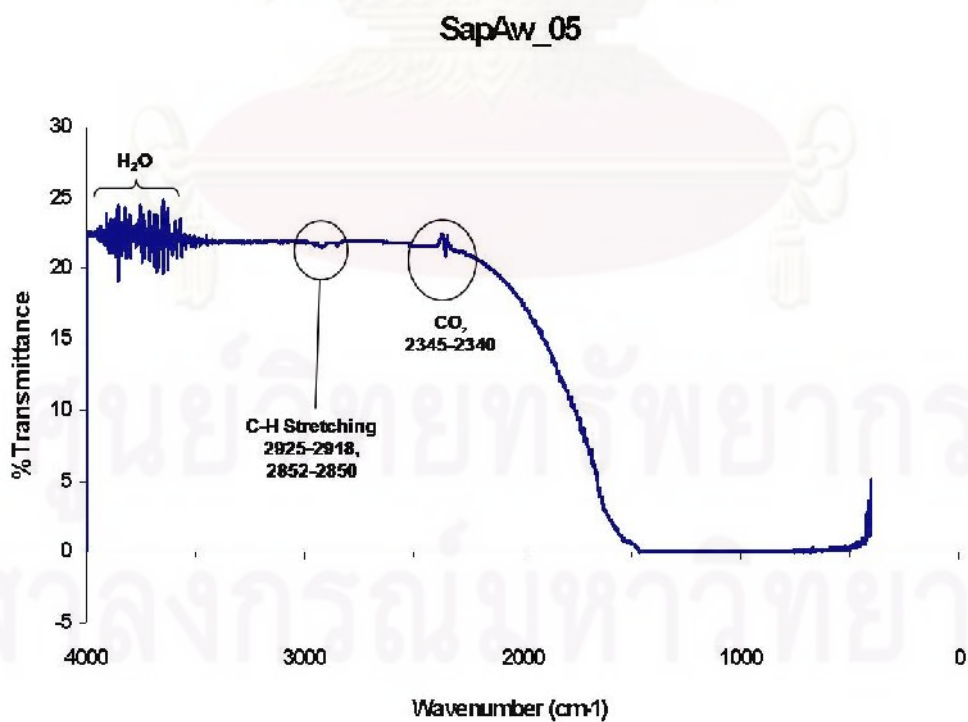


Figure G-3.2 FTIR spectra of the sample SapAw_05 of yellow variety after heating in oxidizing environment at 1,650°C.

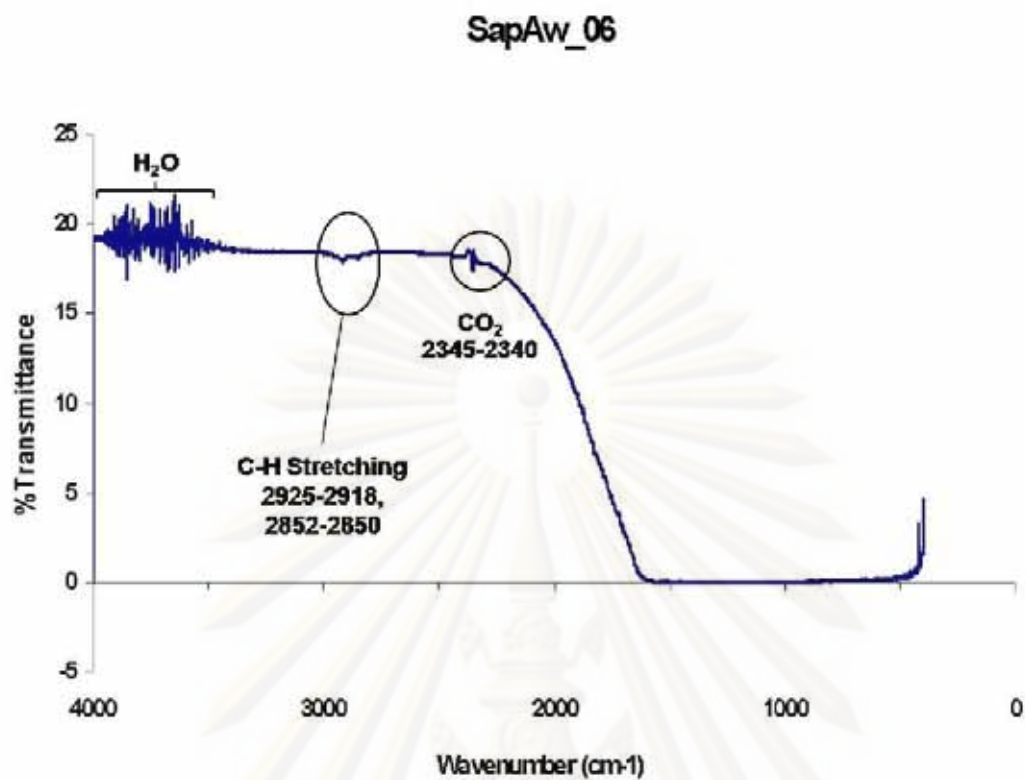


Figure G-3.3 FTIR spectra of the sample SapAw_06 of yellow variety after heating in oxidizing environment at 1,650°C.

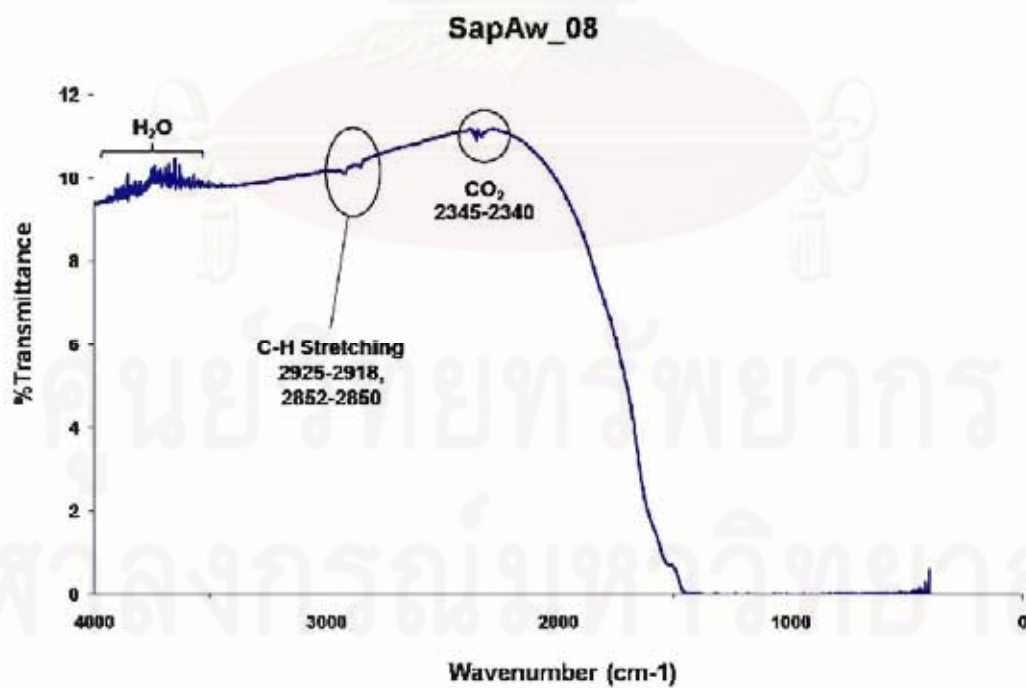


Figure G-3.4 FTIR spectra of the sample SapAw_08 of yellow variety after heating in reducing environment at 1,650°C.

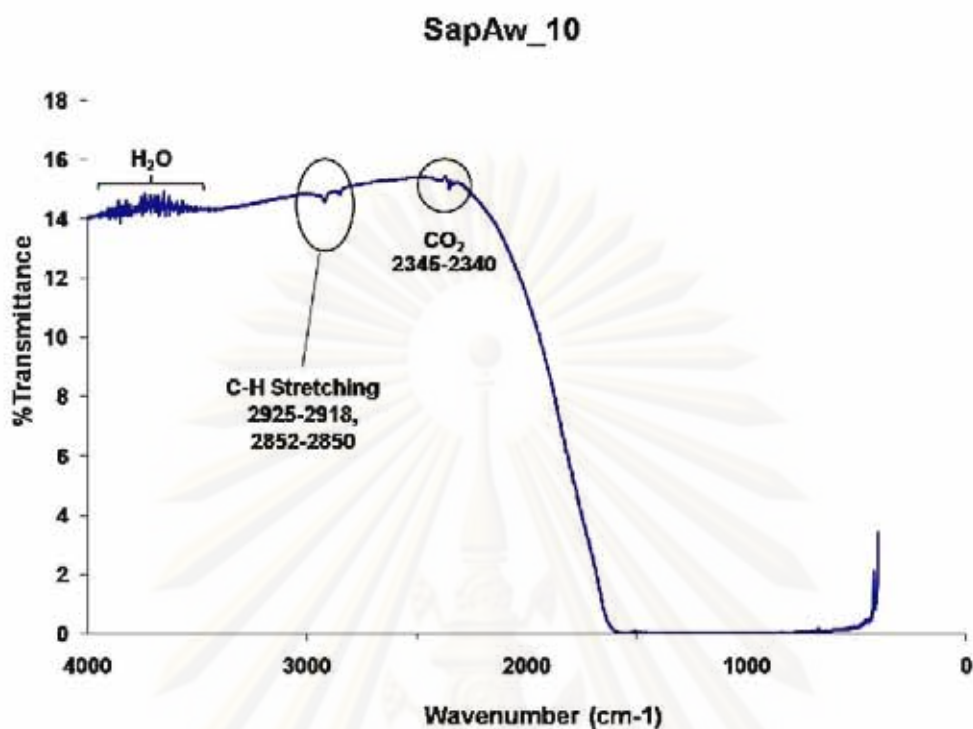


Figure G-3.5 FTIR spectra of the sample SapAw_10 of yellow variety after heating in reducing environment at 1,650°C.

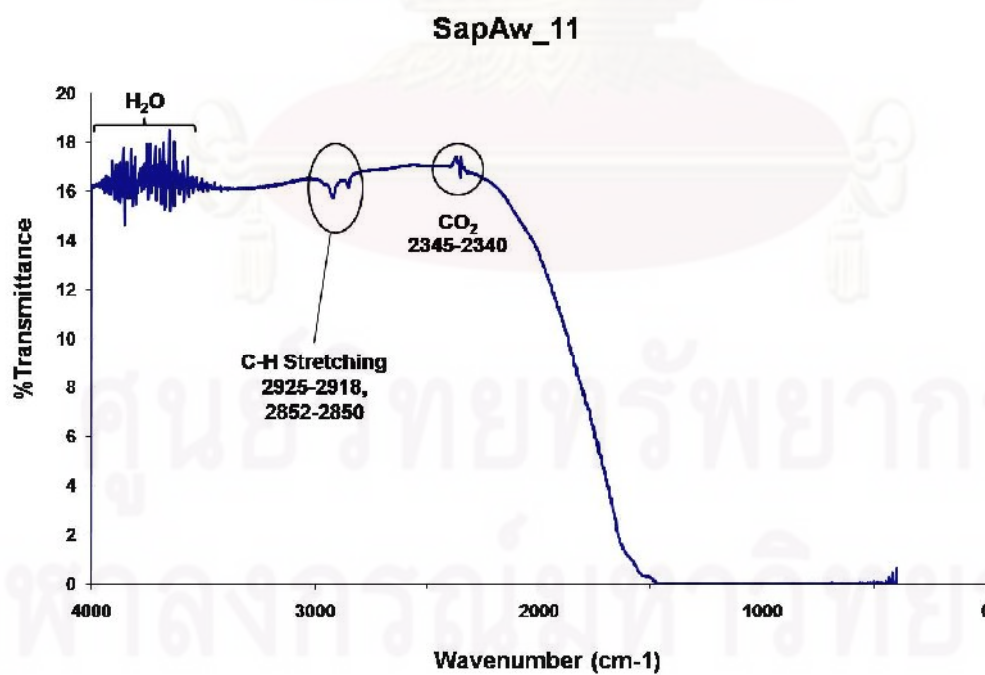


Figure G-3.6 FTIR spectra of the sample SapAw_11 of yellow variety after heating in reducing environment at 1,650°C.

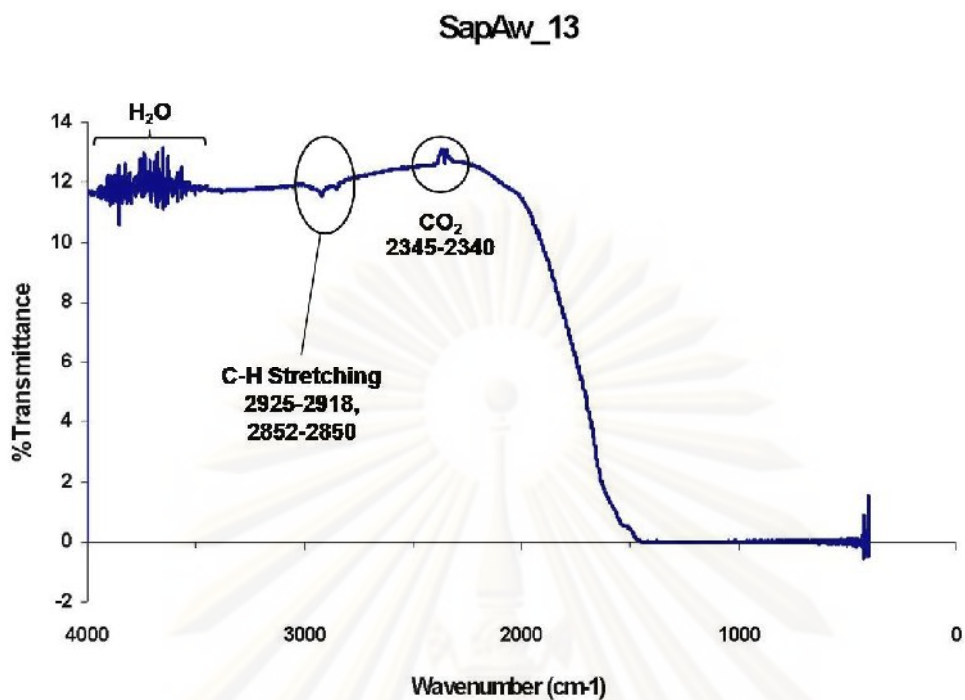


Figure G-3.7 FTIR spectra of the sample SapAw_13 of yellow variety after heating in oxidizing environment at 1,650°C.

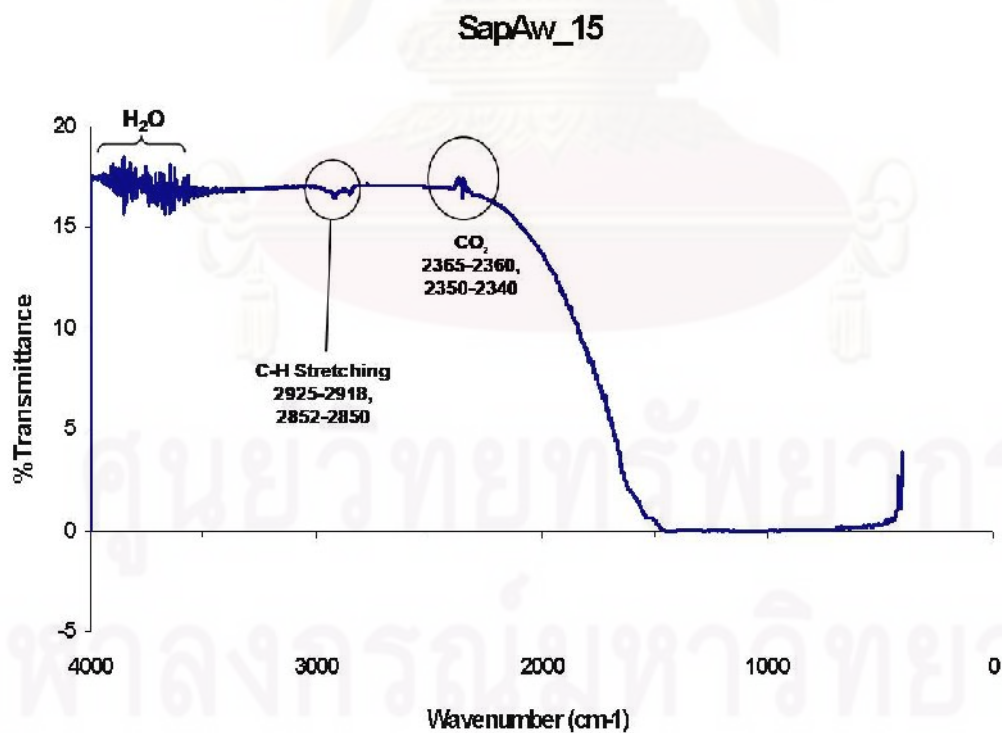


Figure G-3.8 FTIR spectra of the sample SapAw_15 of yellow variety after heating in oxidizing environment at 1,650°C.

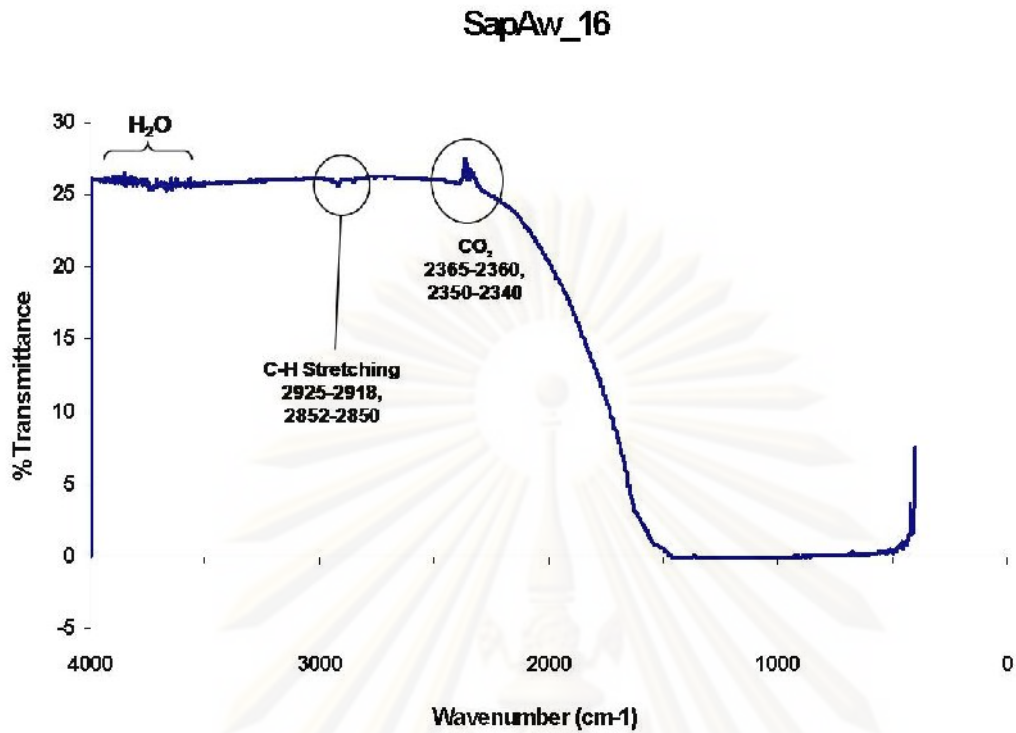


Figure G-3.9 FTIR spectra of the sample SapAw_16 of yellow variety after heating in oxidizing environment at 1,650°C.

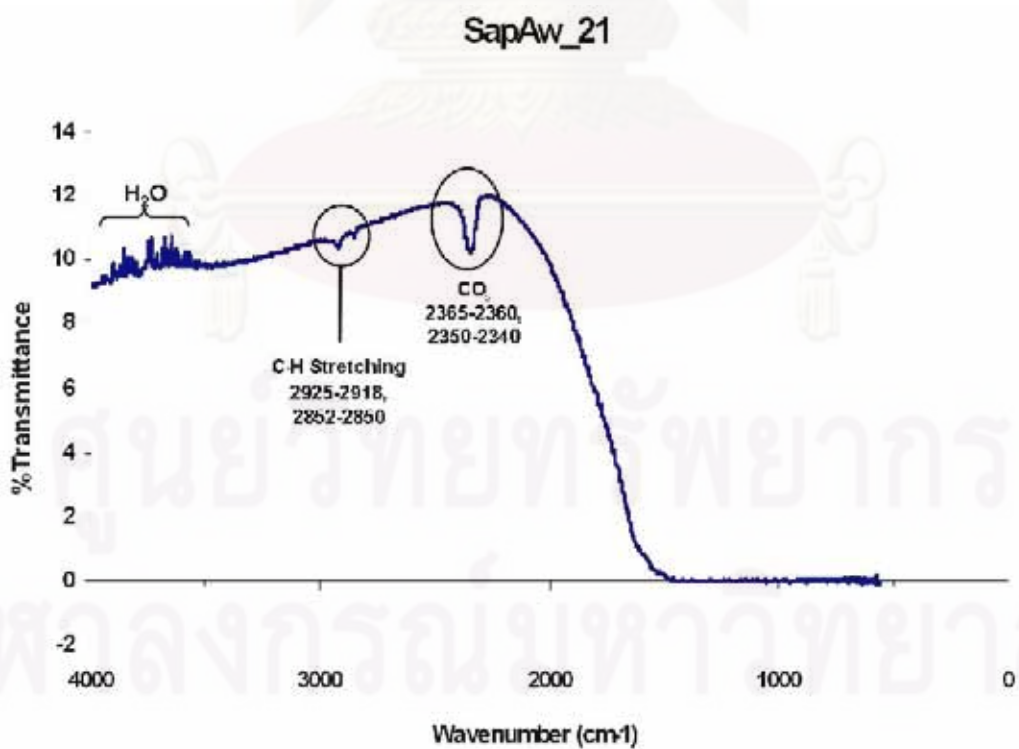


Figure G-3.10 FTIR spectra of the sample SapAw_21 of yellow variety after heating in oxidizing environment at 1,650°C.

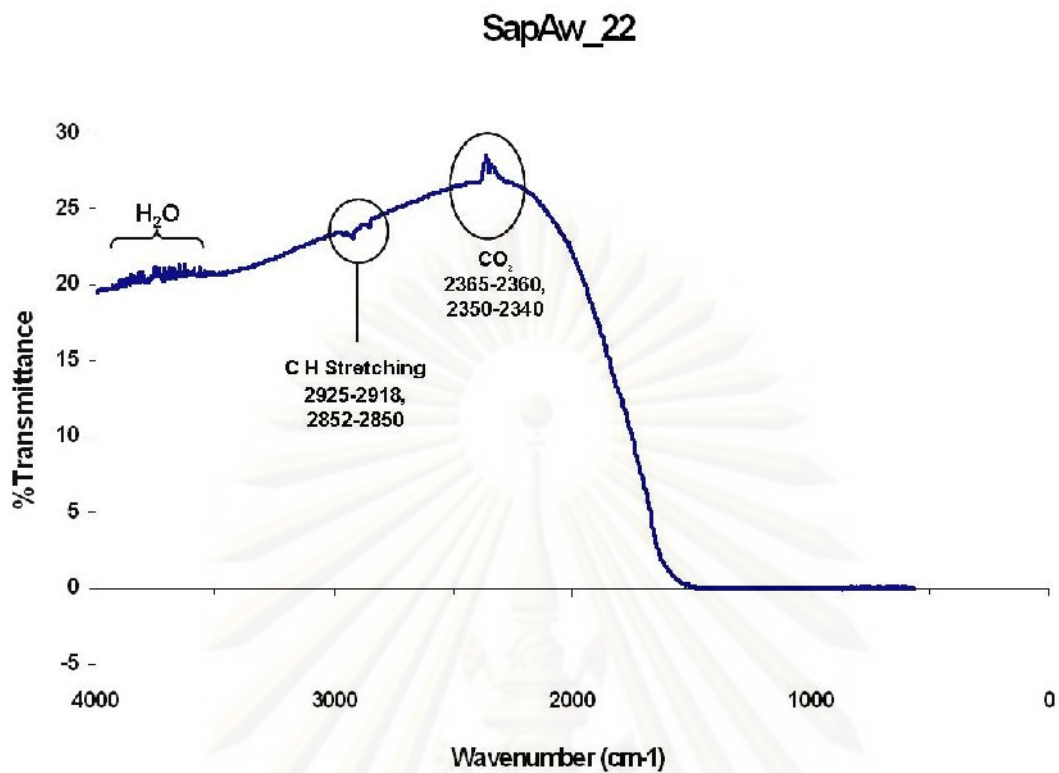


Figure G-3.11 FTIR spectra of the sample SapAw_22 of yellow variety after heating in oxidizing environment at 1,650°C.

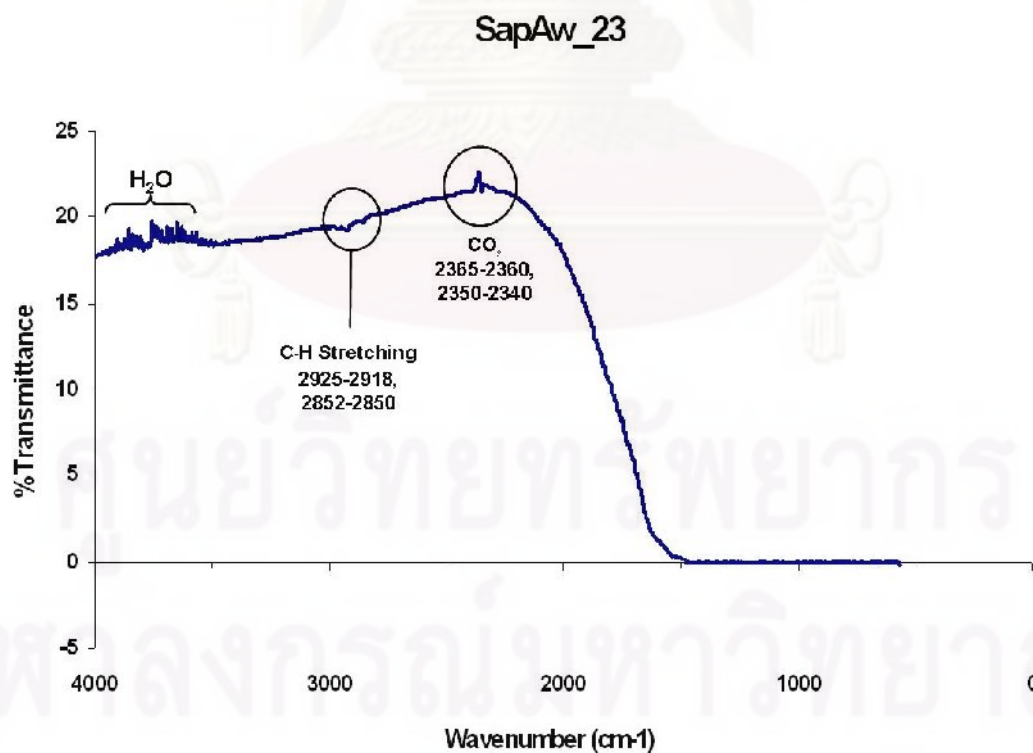


Figure G-3.12 FTIR spectra of the sample SapAw_23 of yellow variety after heating in oxidizing environment at 1,650°C.

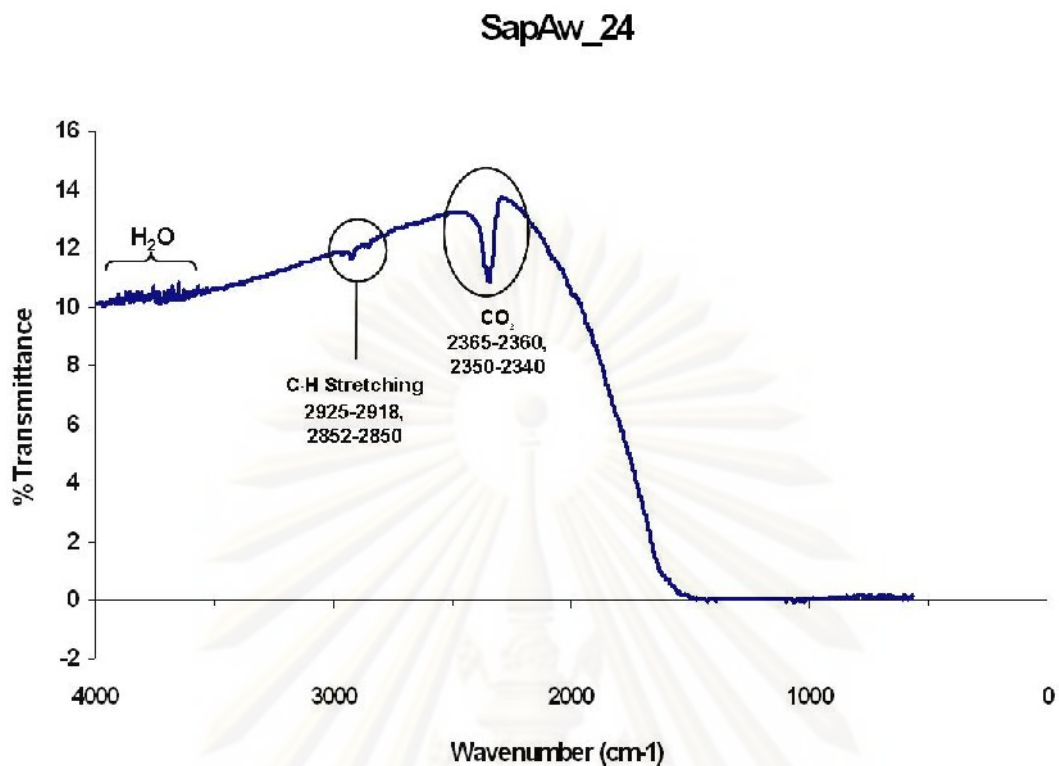


Figure G-3.13 FTIR spectra of the sample SapAw_24 of yellow variety after heating in oxidizing environment at 1,650°C.

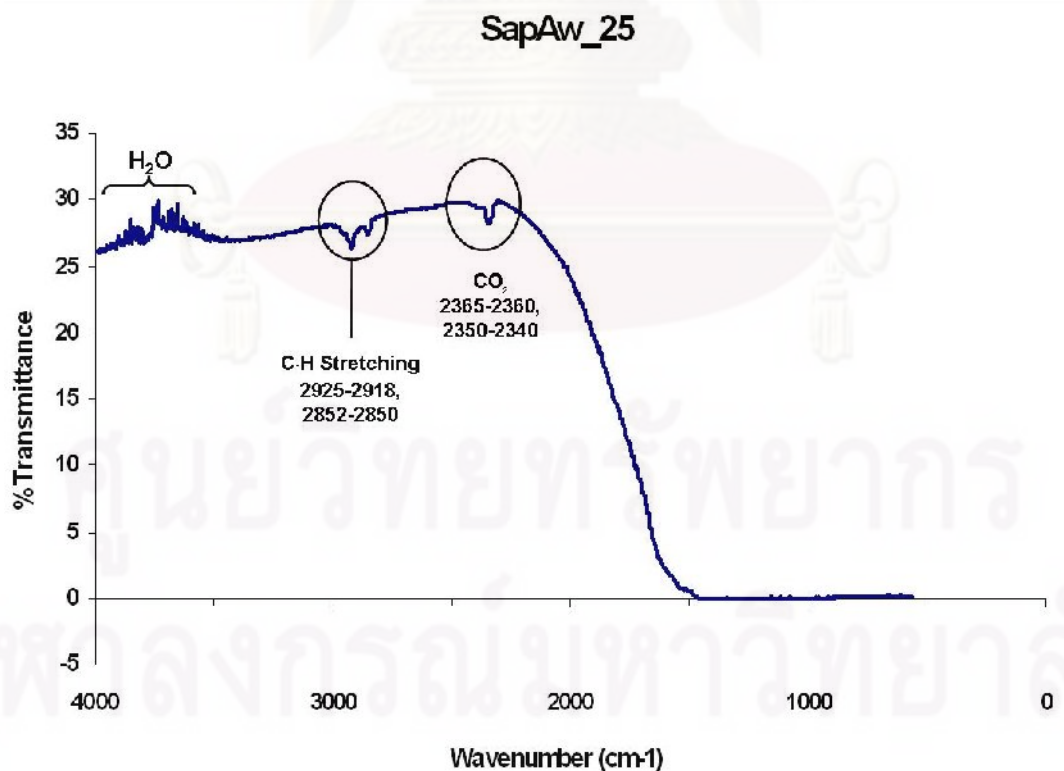


Figure G-3.14 FTIR spectra of the sample SapAw_25 of yellow variety after heating in oxidizing environment at 1,650°C.

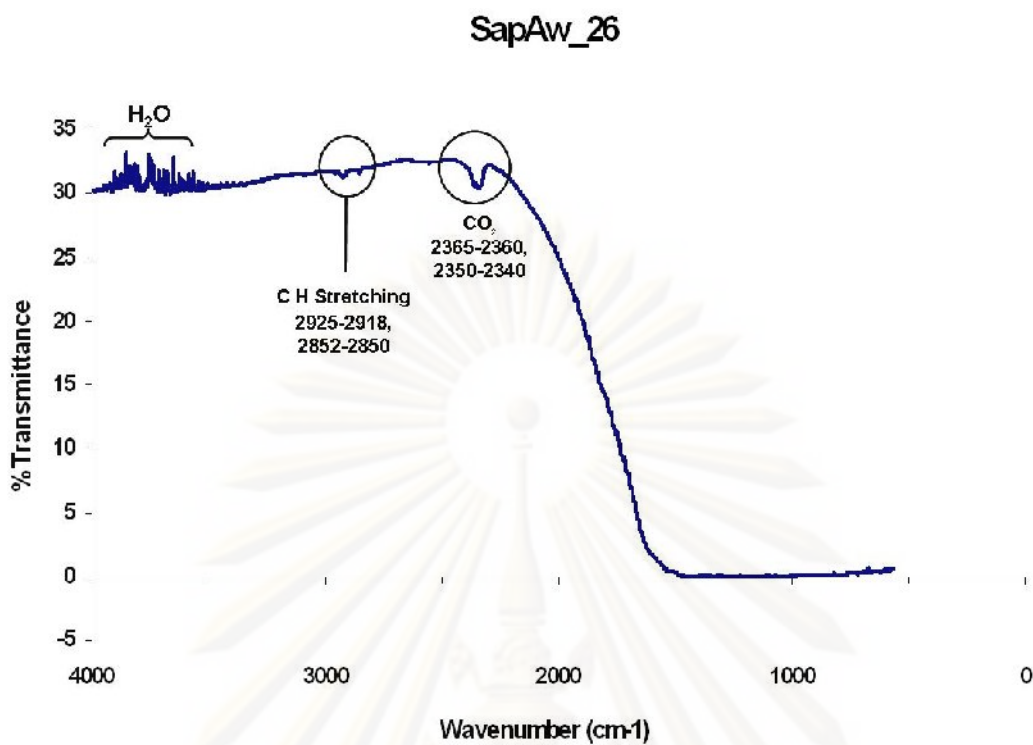


Figure G-3.15 FTIR spectra of the sample SapAw_26 of yellow variety after heating in oxidizing environment at 1,650°C.

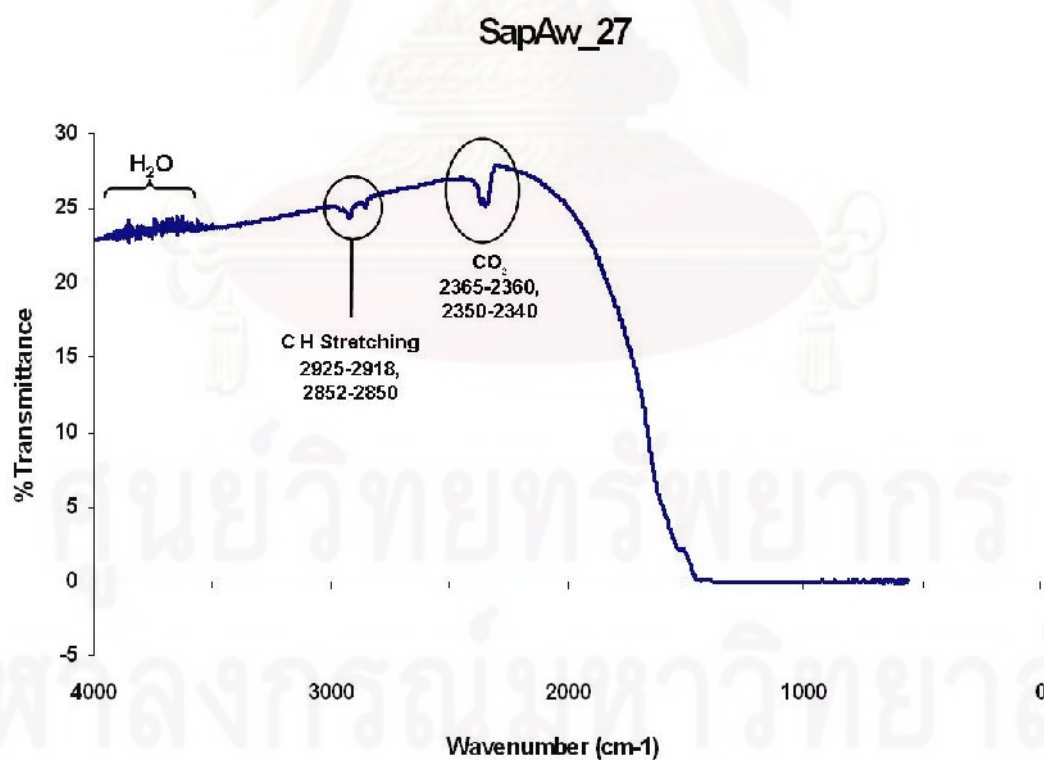


Figure G-3.16 FTIR spectra of the sample SapAw_27 of yellow variety after heating in oxidizing environment at 1,650°C.

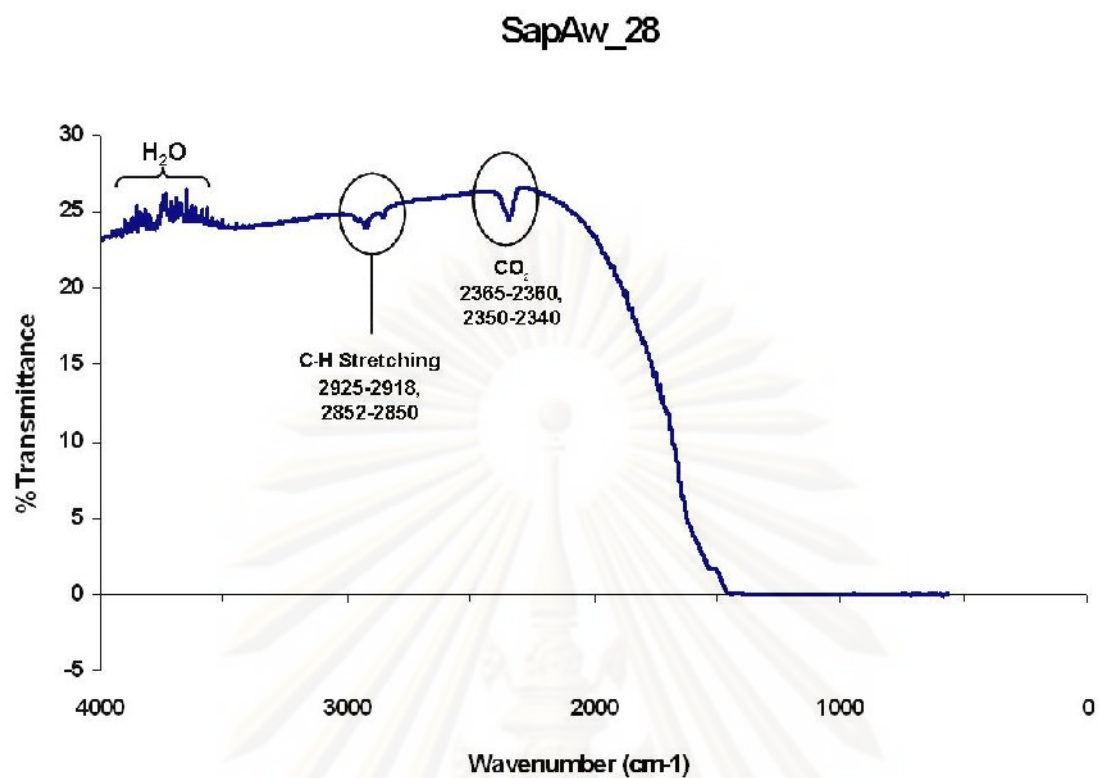


Figure G-3.17 FTIR spectra of the sample SapAw_28 of yellow variety after heating in oxidizing environment at 1,650°C.

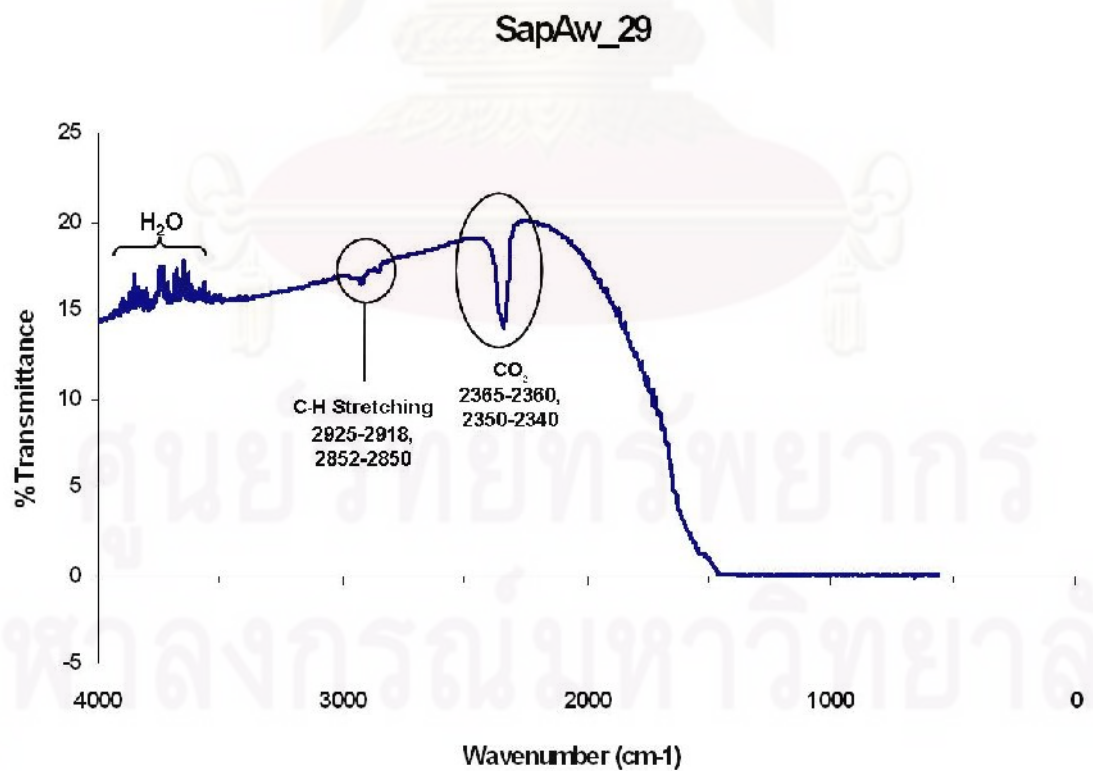


Figure G-3.18 FTIR spectra of the sample SapAw_29 of yellow variety after heating in oxidizing environment at 1,650°C.

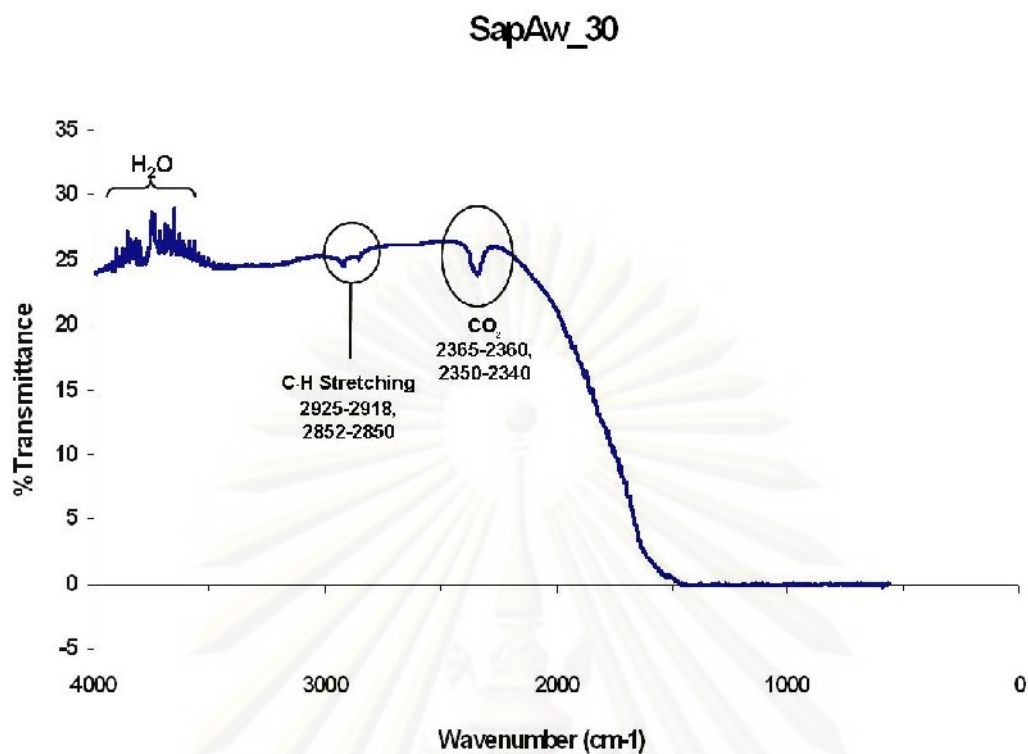


Figure G-3.19 FTIR spectra of the sample SapAw_30 of yellow variety after heating in oxidizing environment at 1,650°C.

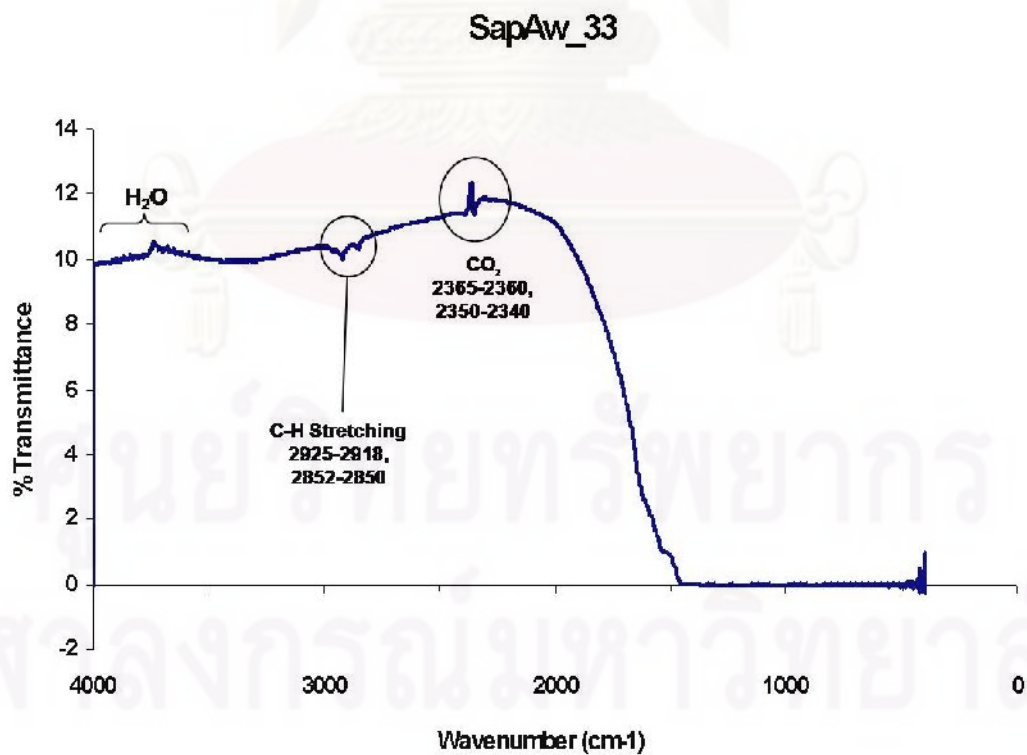


Figure G-3.20 FTIR spectra of the sample SapAw_33 of yellow variety after heating in oxidizing environment at 1,650°C.

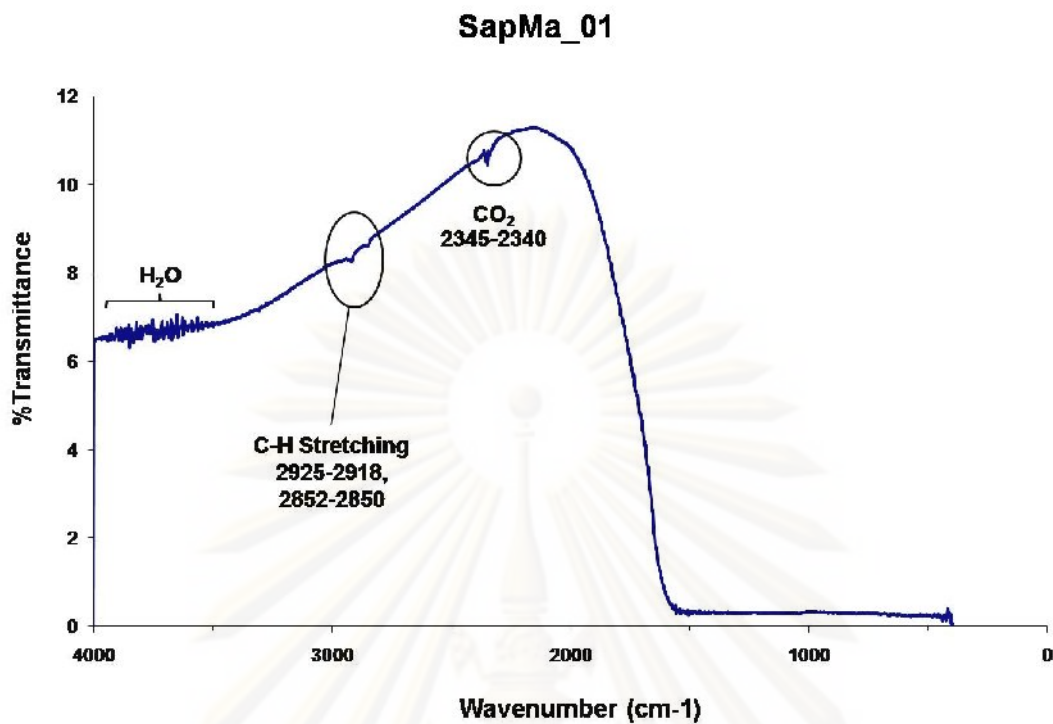


Figure G-3.21 FTIR spectra of the sample SapMa_01 of light blue variety after heating in reducing environment at 1,650°C.

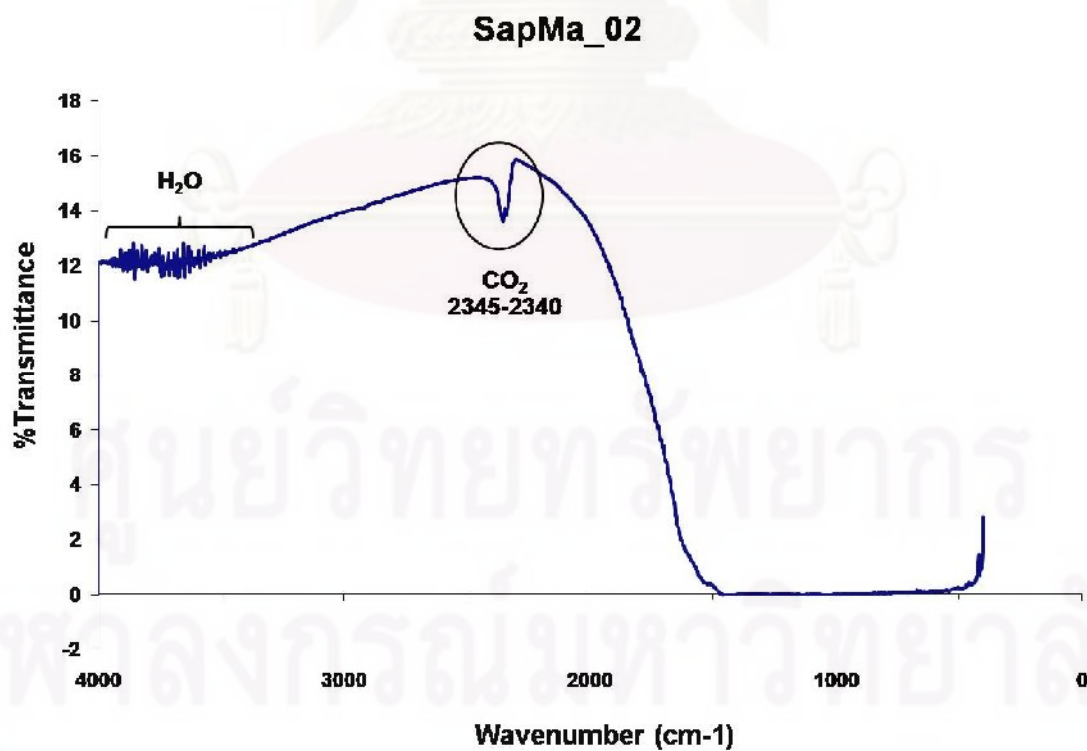


Figure G-3.22 FTIR spectra of the sample SapMa_02 of light blue variety after heating in reducing environment at 1,650°C.

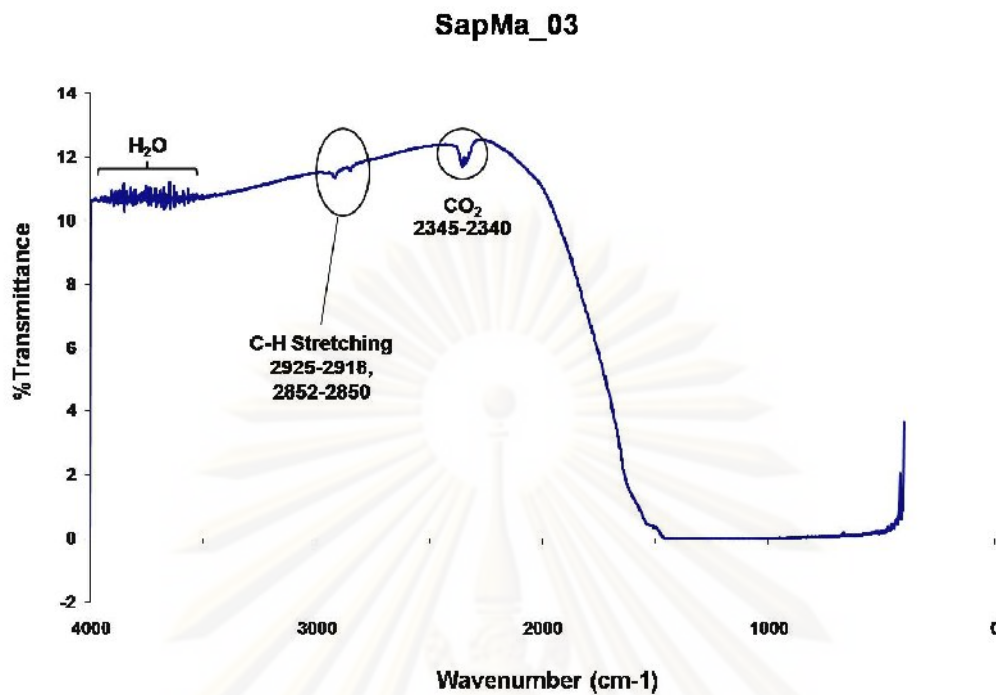


Figure G-3.23 FTIR spectra of the sample SapMa_03 of light blue variety after heating in reducing environment at 1,650°C.

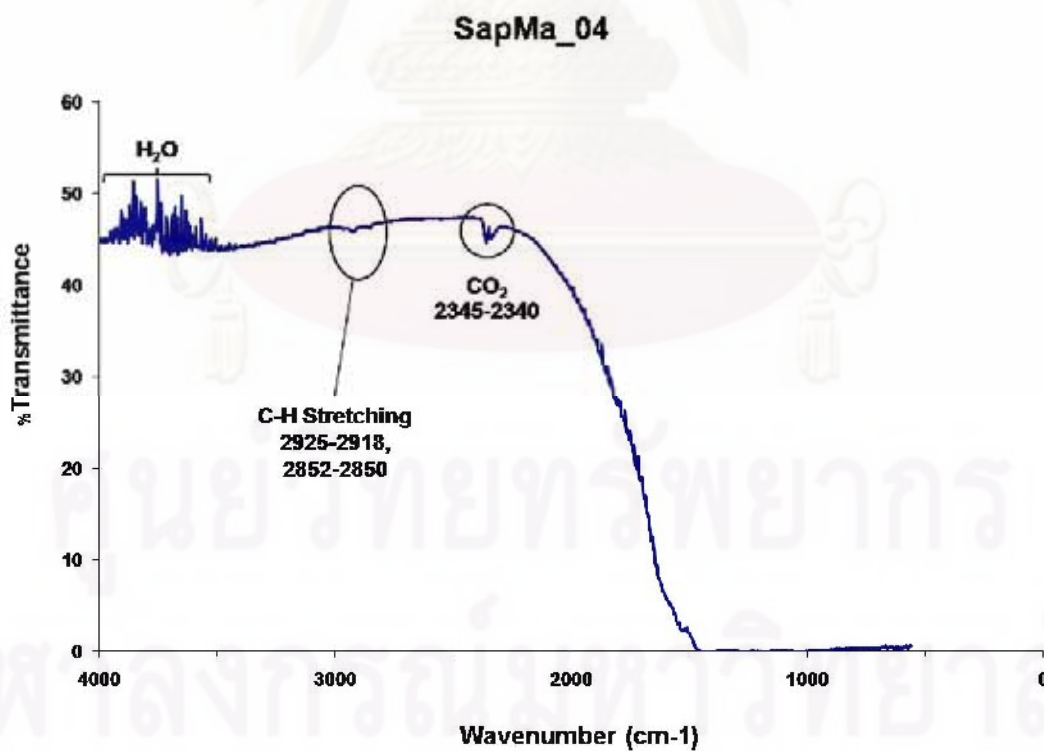


Figure G-3.24 FTIR spectra of the sample SapMa_04 of light blue variety after heating in reducing environment at 1,650°C.

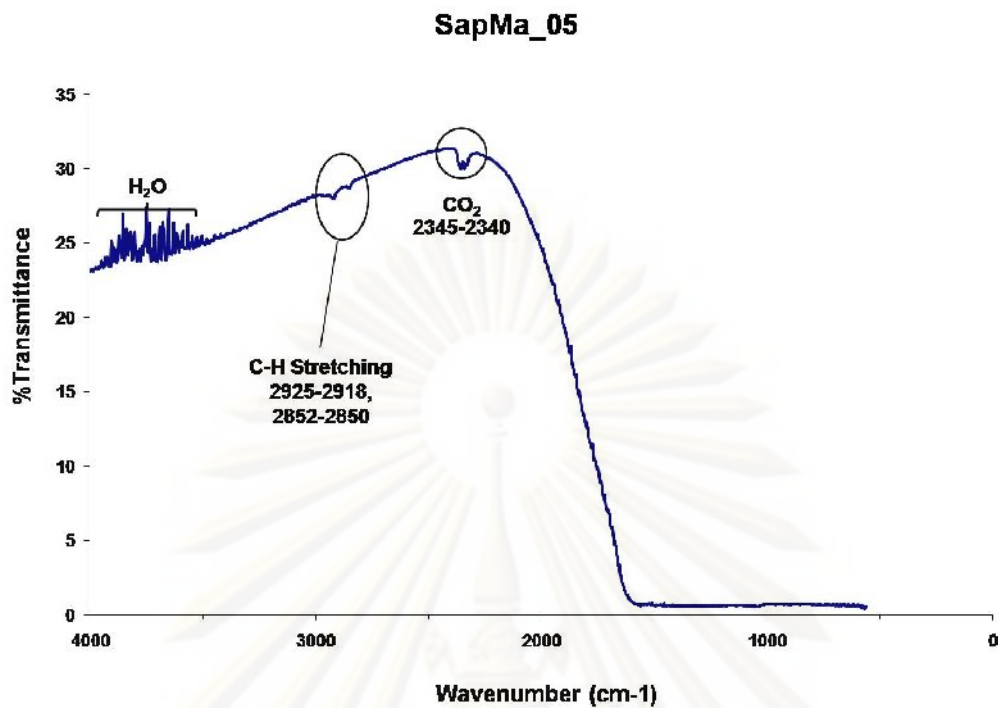


Figure G-3.25 FTIR spectra of the sample SapMa_05 of light blue variety after heating in reducing environment at 1,650°C.

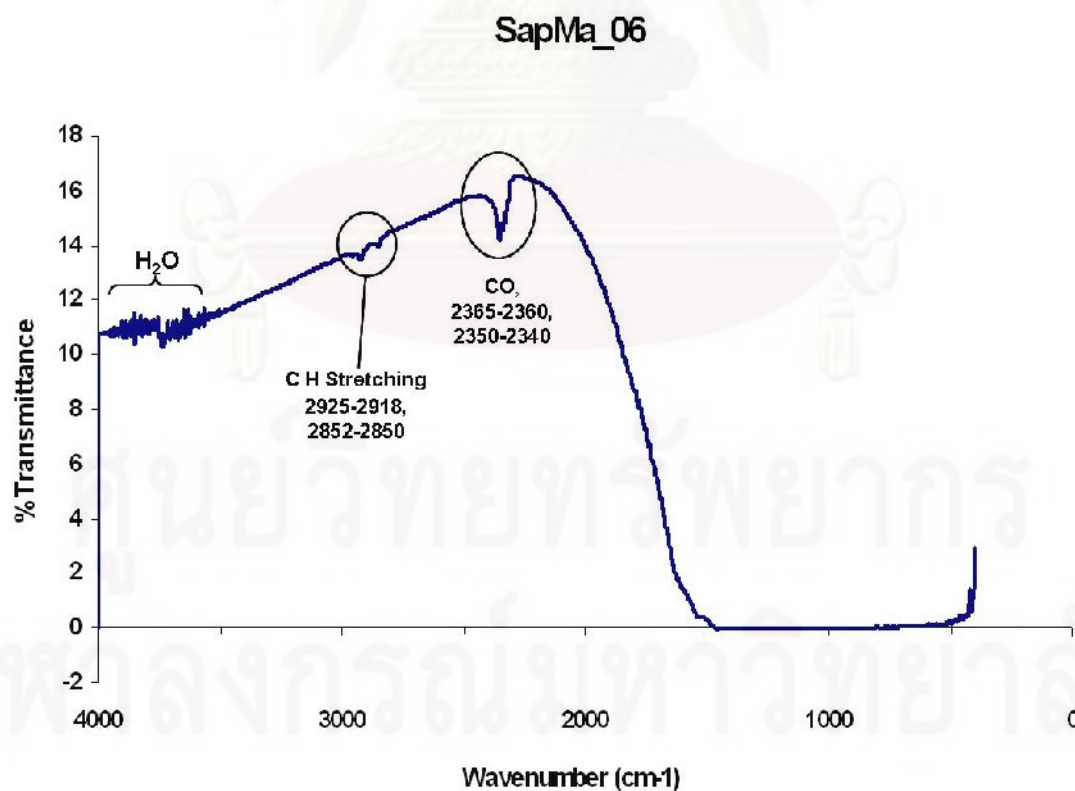


Figure G-3.26 FTIR spectra of the sample SapMa_06 of light blue variety after heating in oxidizing environment at 1,650°C.

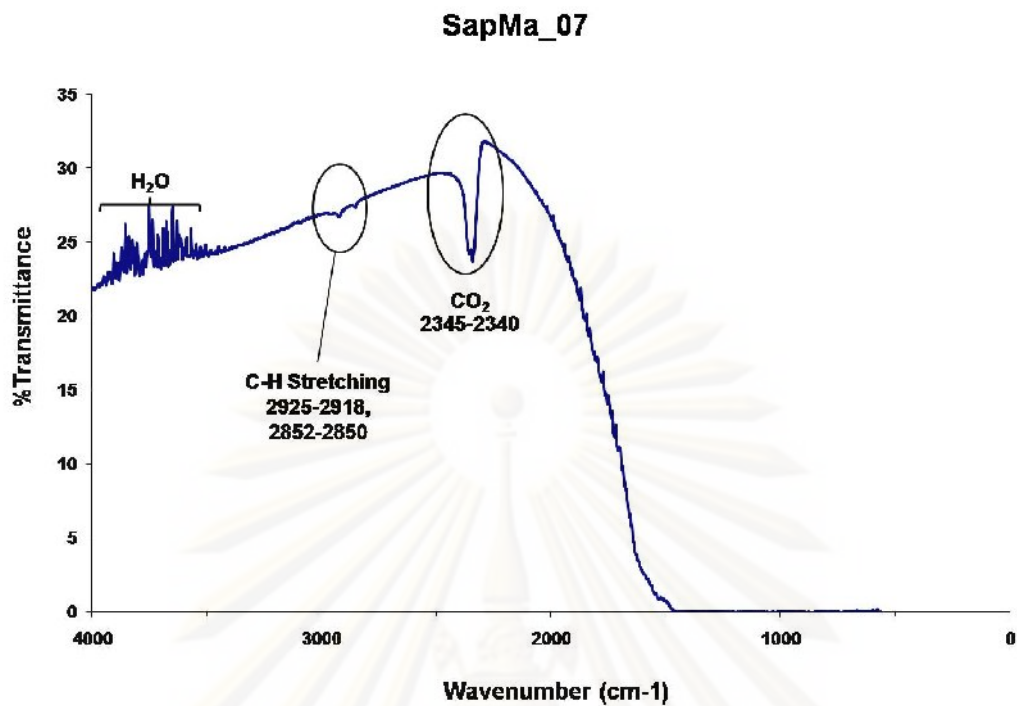


Figure G-3.27 FTIR spectra of the sample SapMa_07 of light blue variety after heating in reducing environment at 1,650°C.

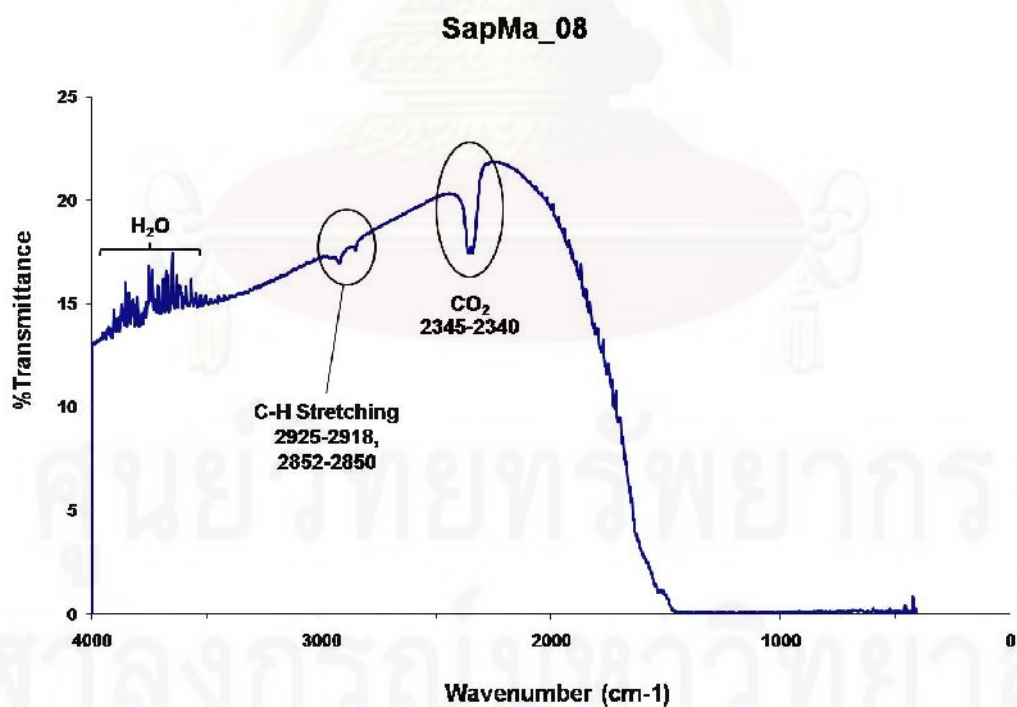


Figure G-3.28 FTIR spectra of the sample SapMa_08 of light blue variety after heating in reducing environment at 1,650°C.

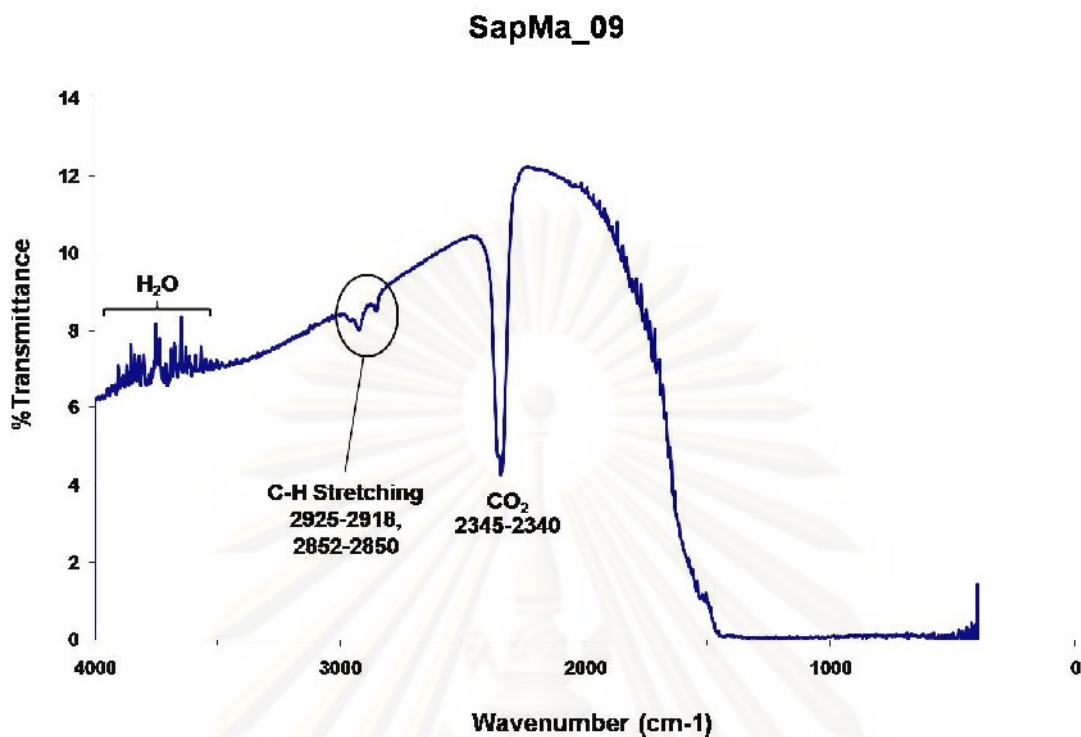


Figure G-3.29 FTIR spectra of the sample SapMa_09 of light blue variety after heating in reducing environment at 1,650°C.

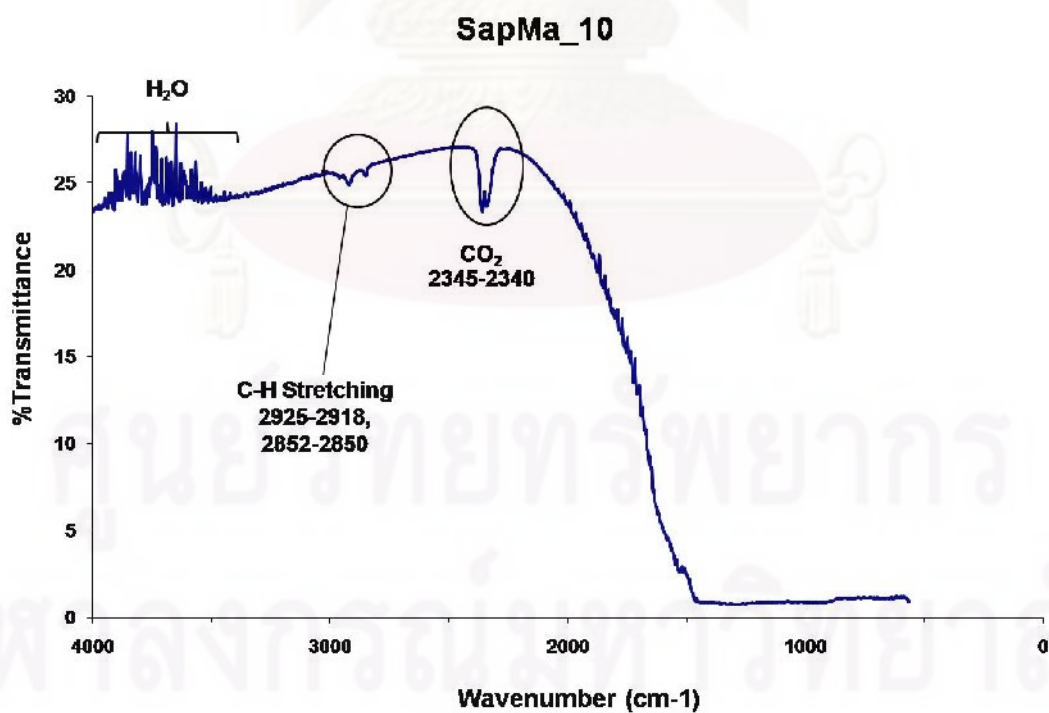


Figure G-3.30 FTIR spectra of the sample SapMa_10 of light blue variety after heating in reducing environment at 1,650°C.

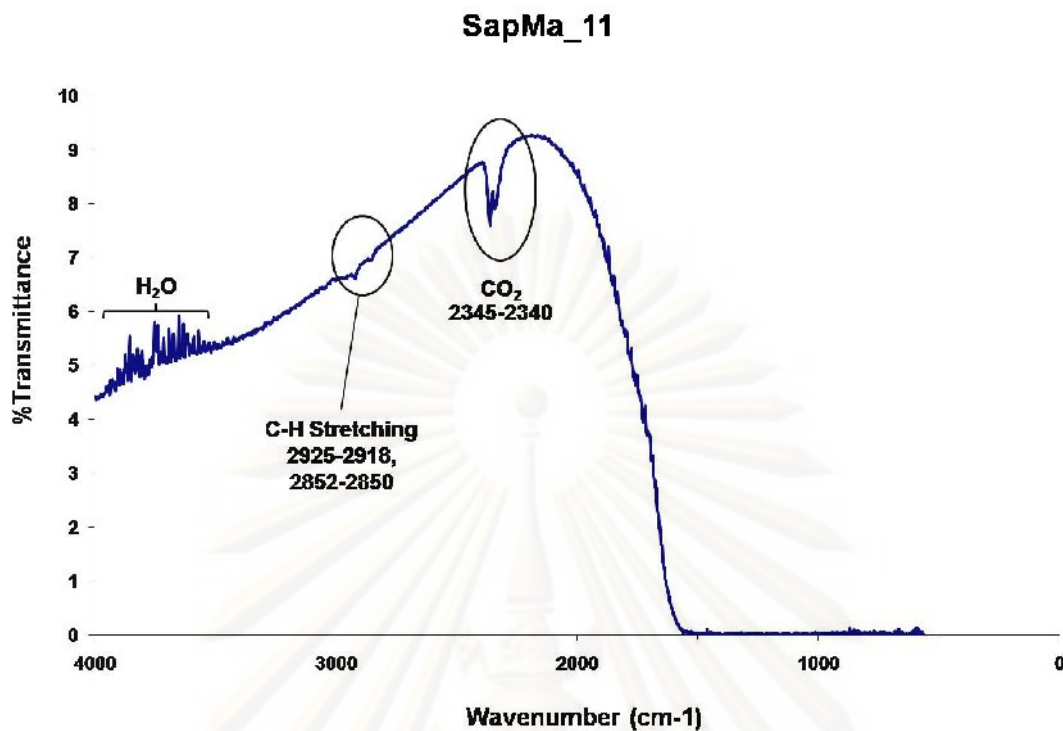


Figure G-3.31 FTIR spectra of the sample SapMa_11 of light blue variety after heating in reducing environment at 1,650°C.

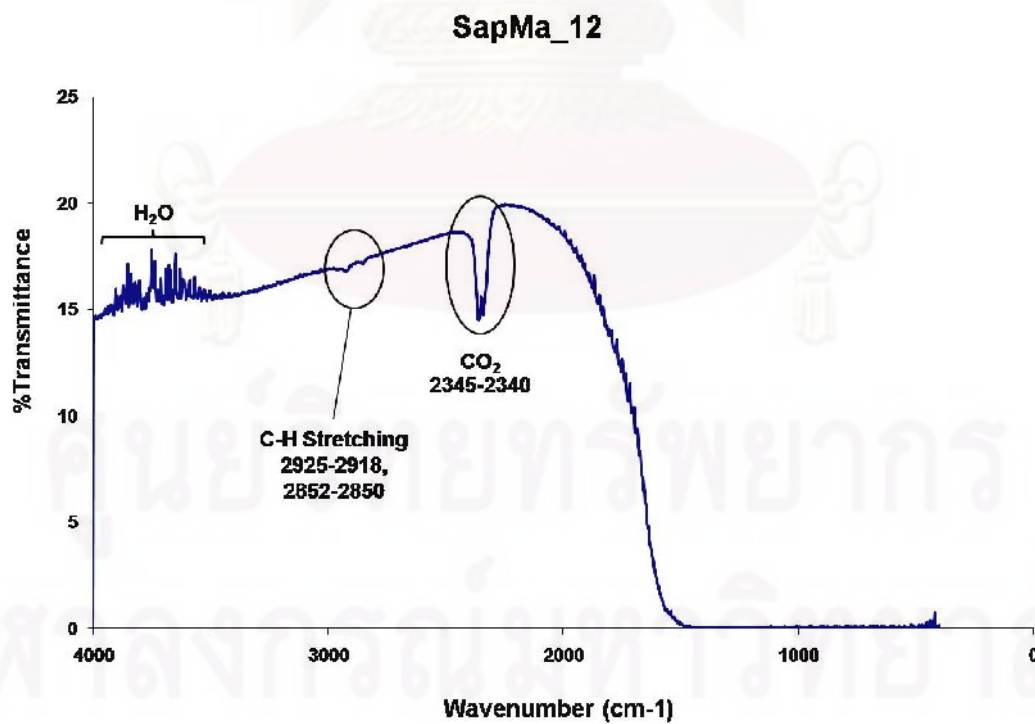


Figure G-3.32 FTIR spectra of the sample SapMa_12 of light blue variety after heating in reducing environment at 1,650°C.

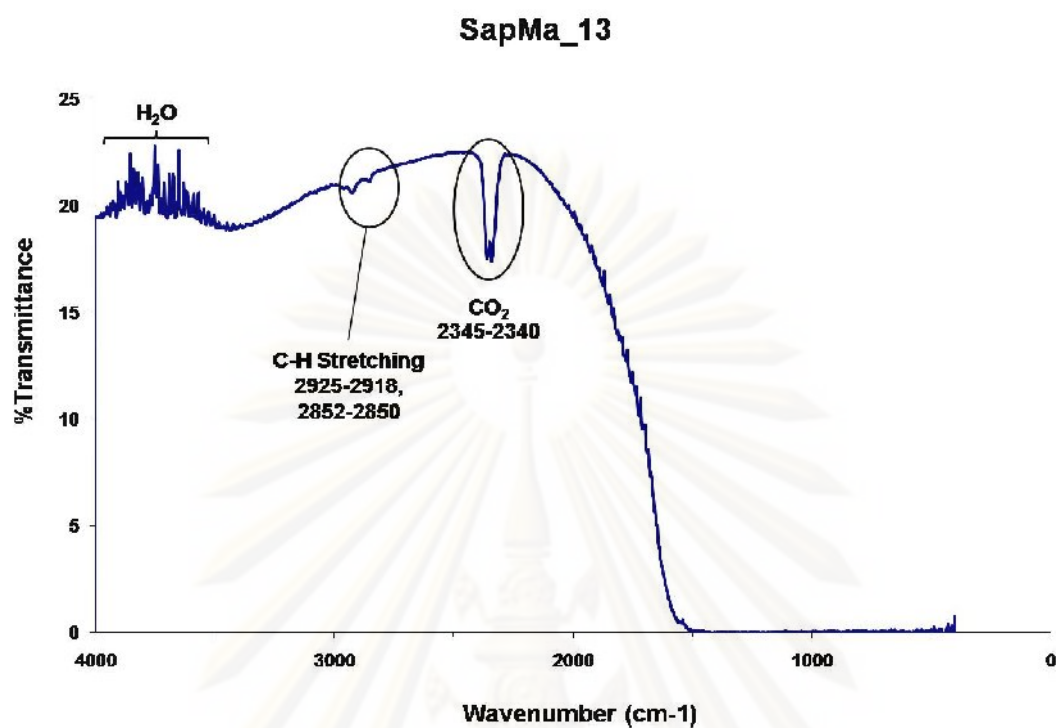


Figure G-3.33 FTIR spectra of the sample SapMa_13 of light blue variety after heating in reducing environment at 1,650°C.

BIOGRAPHY

Miss Nattaphanee Buadee was born in May 13, 1982, at Pichit Province. She graduated with a bachelor degree in gemology from the Department of Geology, Faculty of Science, Chiang Mai University in 2001. At present, she studies in a Master program in geology at Chulalongkorn University.



ศูนย์วิทยทรัพยากร
จุฬาลงกรณ์มหาวิทยาลัย